

Some pages of this thesis may have been removed for copyright restrictions.

If you have discovered material in AURA which is unlawful e.g. breaches copyright, (either yours or that of a third party) or any other law, including but not limited to those relating to patent, trademark, confidentiality, data protection, obscenity, defamation, libel, then please read our [Takedown Policy](#) and [contact the service](#) immediately

SOFT β -ADRENOCEPTOR AGONISTS FOR TOPICAL
USE IN PSORIASIS

USE IN PSORIASIS

by

HARDYAL SINGH GILL

A thesis submitted for the degree of
Doctor of Philosophy

at

University of Aston in Birmingham

November 1994

The pH-rate profile for the hydrolysis of soft-drug pro-drugs... The individual rate constants for the degradation and the pH-rate profile... The pK_a of 7.40 is in excellent agreement with that determined... satisfactory convergence was achieved. The soft-drug... efficient and, over the... At lower values, the largely protonated species... However, above pH 7, chemical degradation was rapid so that a dose...

This copy of the thesis has been supplied on condition that anyone who consults it is understood to recognise that its copyright rests with its author and that no quotation from the thesis and no information derived from it may be published without the author's prior written consent.

UNIVERSITY OF ASTON IN BIRMINGHAM
SOFT β -ADRENOCEPTOR AGONISTS FOR TOPICAL
USE IN PSORIASIS

Hardyal Singh Gill
Doctor of Philosophy, 1994

SUMMARY

Psoriasis is characterised by epidermal proliferation and inflammation resulting in the appearance of elevated erythematous plaques. The ratio of c-AMP/c-GMP is decreased in psoriatic skin and when the epidermal cell surface receptors are stimulated by β -adrenergic agonists, intracellular ATP is transformed into c-AMP, thus restoring the c-AMP/c-GMP levels. This thesis describes a series of β -adrenoceptor agonists for topical delivery based upon the soft-drug approach. Soft drugs are defined as biologically active, therapeutically useful chemical compounds (drugs) characterised by a predictable and controllable *in vivo* destruction (metabolism) to non-toxic moieties, after they achieve their therapeutic role. The *N*-substituent can accommodate a broad range of structures and here the alkoxycarbonyl ethyl group has been used to provide metabolic susceptibility. The increased polarity of the dihydroxy acid, expected after metabolic conversion of the soft-drug, ethyl *N*-[2'-(3",4"-dihydroxyphenyl)-2'-hydroxyethyl]-3-aminopropionate, should eliminate agonist activity. Further, to prevent oxidation and enhance topical delivery, the catechol hydroxyl groups have been esterified to produce a pro-soft-drug which generates the soft-drug in enzymic systems.

The chemical hydrolysis of the pro-soft-drug proceeded *via* the formation of the dipivaloyloxy acid and it failed to generate the active dihydroxy ester soft-drug. In contrast, in the presence of porcine liver carboxyesterase, the hydrolysis of the pro-soft drug proceeded *via* the formation of the required active soft-drug. This compound, thus, has the appropriate kinetic features to enable it to be evaluated further as a drug for the treatment of psoriasis.

The pH rate-profile for the hydrolysis of soft-drug indicated a maximum stability at pH ~ 4.0. The individual rate constants for the degradation and the pK_a were analysed by non-linear regression. The pK_a of 7.40 is in excellent agreement with that determined by direct titration (7.43) and indicates that satisfactory convergence was achieved. The soft-drug was poorly transported across a silicone membrane; it was also air-sensitive due to oxidation of the catechol group. The transport of the pro-soft-drug was more efficient and, over the donor pH range 3-8, increased with pH. At lower values, the largely protonated species was not transported. However, above pH 7, chemical degradation was rapid so that a donor pH of 5-6 was optimum.

The β -adrenergic agonist activity of these compounds was tested *in vitro* by measuring chronotropic and inotropic responses in the guinea pig atria and relaxation of guinea pig trachea precontracted with acetylcholine (10^{-5} M). The soft-drug was a full agonist on the tracheal preparation but was less potent than isoprenaline. Responses of the soft-drug were competitively antagonised by propranolol (10^{-6} M). The soft-drug produced an increase in force and rate of the isolated atrial preparation. The propyl analogue was equally potent with ED_{50} of 6.52×10^{-7} M. In contrast, at equivalent doses, the dihydroxy acid showed no activity; only a marginal effect was observed on the tracheal preparation.

For the pro-soft-drug, responses were of slow onset in both preparations, with a slowly developing relaxation of the tracheal preparation at high concentrations (10^{-5} M). This is consistent with *in vitro* results where the dipivaloyl groups are hydrolysed more readily than the ethyl ester to give the active soft-drug. These results confirm the validity of the pro-soft-drug approach to the delivery of β -adrenoceptor agonists.

Keywords: Acetylcholine, Chemical and enzymatic hydrolysis, Chronotropic and inotropic responses, Cyclic-AMP, Diffusion, Epidermal proliferation, Guinea pig trachea and atria, Inflammation, Isoprenaline, Oxidation, Permeation, pH Rate-profile, Pro-soft-drug, Prodrug, Propranolol, Silicone membrane, Soft-drug.

ACKNOWLEDGEMENTS

I would like to thank Dr. William J. Irwin and Dr. Sally Freeman for their advice, guidance, encouragement and active support throughout the duration of this work.

My thanks are also extended to my fellow postgraduate friends and colleagues, lecturers and staff especially Dr. Ghouse Baig, Dr. John Gardiner, Mrs. Karen Farrow, Kevin Ward, Dr. William Fraser, Dr. Anne Routledge, Dr. Washington Ayuko, Mark Philip Wallis, Kenneth Charles Ross, Ian David Spiers, Miss Nayna Chouhan, Mandeep Mudhar, Dr. Mohammed Fiaz, Dr. Saghir Akhtar, Bhupinder Singh Bains, Onkar Singh, Parmjit Singh, Shamraiz Iqbal, Miss Sukhavinder Chouhan, Zahid, David Bozward, Miss Udkhar Singh Gill, Javid Yusuf Awan, Dr. Subhash Banerjee, Martin Gosling, Chris Bache, Victor Meidan, Mrs. Annette Phipps, Miss Tracey Dalton, Jim Eyles, Miss Alison Tookey, Sarbjit Singh Saini, Miss Debbie Stagg, Miss Barbara Conway, Andrew Walsh, Miss Kuldip Kaur, Miss Vanessa Moore, Miss Pam Blake, Mrs. Alaco Millard, Mrs. Ann White, Mrs. Joyce Rich, Stan Curry, Alan, Shamraiz, Onkar Singh, Bhupinder Singh Bains, Naik M. Pashtoonmal, Dr. Naman Baker, Miss Teresa Pepper, Miss Geeta Sood, at Aston University for their companionship and co-operation throughout my stay.

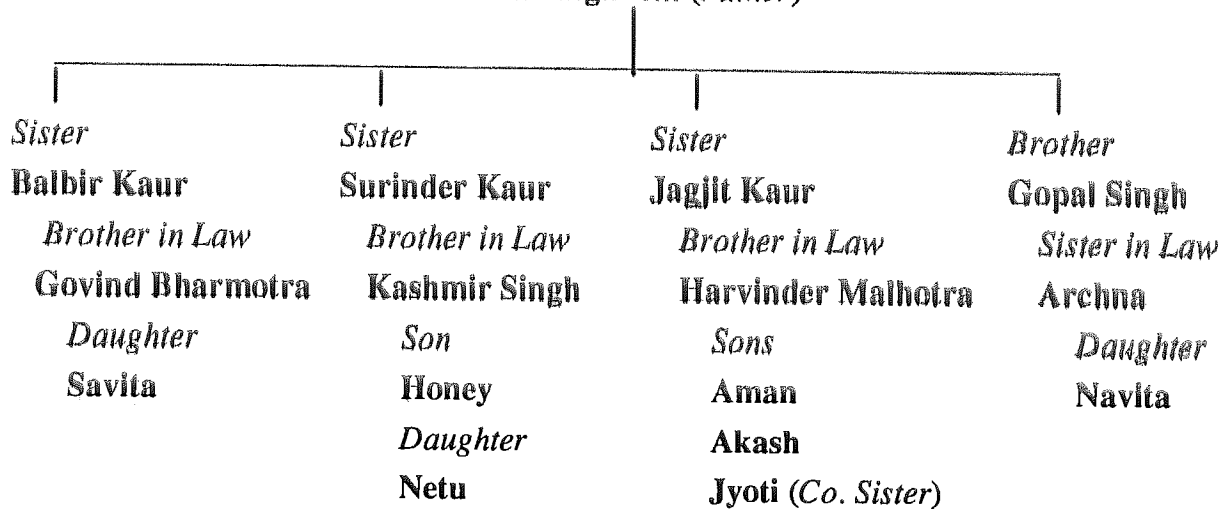
My sincere thanks to Dr. Keith Wilson and Mr. Alan Richardson for testing the biological activity of the compounds and Mr. Graham Smith for the art work. I also convey my thanks to Professor Michael Tisdale, Head of Department, for providing me with research facilities at Aston University.

My special thanks go to THE GOVERNMENT OF INDIA for providing me with financial support for the work, especially I wish to thank Mr. S. Mukherji, Student Welfare Officer, for providing me with financial and emotional support throughout my Ph.D. and a travel grant to present my work at 208th American Chemical Society Conference at Washington D.C., USA.

In conclusion, I wish to thank my parents and family for their support, encouragement and profound patience, particularly during the preparation of this manuscript, and my mother for her love and confidence, always.

Dedicated to my Family

Swarn Kaur (*Mother*)
Bawa Singh Gill (*Father*)



Title page	1
Summary	2
Acknowledgements	3
Dedication	4
Contents	5
List of figures	13
List of tables in text	19
List of tables in appendix	21
List of schemes	23
Abbreviations	24
CHAPTER ONE	
INTRODUCTION- PSORIASIS	26
1.1 Psoriasis	27
1.1.1 Different forms of psoriasis	27
1.1.2 Pathogenesis of psoriasis	28
1.1.3 Cell cycle	29
1.1.4 Inflammatory mediators in psoriasis	31
1.1.5 Role of c-AMP in psoriasis	31
1.2 Drugs used in psoriasis	35
1.2.1 Topical therapy and ultraviolet light	35
1.2.1.1 Dithranol	35
1.2.1.2 Coal tar phototherapy	36
1.2.1.3 Topical corticosteroids	36
1.2.1.4 The vitamin D analogues	38
1.2.1.5 6-Aminonicotinamide	38
1.2.1.6 Ultraviolet phototherapy	38
1.2.2 Systemic therapy	39
1.2.2.1 Immuno-suppressant	39
1.2.2.2 Methotrexate	39
1.2.2.3 Hydroxyurea	40
1.2.2.4 Razoxane	40
1.2.2.5 6-Thioguanine	40
1.2.2.6 The vitamin A derivatives (retinoids)	41
1.3 β -Adrenoceptor agonists	43
1.3.1 Adrenoreceptors	43

1.3.2 Sub-classification of β -receptors	43
1.3.3 Ligand-binding sites of β -adrenoceptor	44
1.3.4 Mechanism of action of β -adrenoceptor agonists	46
1.3.5 Chemical basis of β -adrenoceptor stimulation	47
1.3.6 Structure-activity relationship of β -adrenoceptor agonists	48
1.3.6.1 Effect of modification of the catechol group	48
1.3.6.2 Effect of the β -hydroxyl group	49
1.3.6.3 Effect of α -substitution on the side-chain	50
1.3.6.4 Effect of <i>N</i> -substitution	50
1.3.6.5 Effect of polar side-chain	52
1.3.6.6 Conformational requirement for β -adrenoceptor agonists	54
1.4 Aims and objectives of the present study	55
1.4.1 New therapeutic approaches <i>via</i> stimulation of adenylate cyclase	55
1.4.2 The design of β -adrenoceptor agonists for psoriasis	55
1.4.2.1 Deactivation of β -adrenoceptor activity by loss of the basic centre at nitrogen	56
1.4.2.2 Deactivation of β -adrenoceptor activity by dramatic polarity change in the <i>N</i> -substitution	58
1.4.3 Soft and prodrugs	59
1.4.4 Prodrugs in which the catechol hydroxyl groups are protected	63
1.4.5 Potential biolabile soft drugs of β -adrenoceptor agonists	64

CHAPTER TWO

RESULTS AND DISCUSSION (SYNTHESIS OF SOFT β -ADRENOCEPTOR AGONISTS)

2.1 Introduction	67
2.2 Attempted synthesis of amino acid esters (50 , <i>n</i> =1, R= ethyl)	68
2.3 Synthesis of phenyl amino acid esters (50 , <i>n</i> =2, R=methyl and ethyl)	74
2.4 Synthesis of catechol amino acid esters (74 , R=methyl, ethyl, <i>n</i> -propyl, <i>n</i> -butyl)	79
2.5 Synthesis of acyl prodrugs of the catechol amino acids (106 , R= ethyl, R'= CH ₃ CO) and (107 , R= ethyl, R'= Bu ^t CO)	98
2.5.1 Prodrugs of ethyl <i>N</i> -[2'-(3'',4''-dihydroxyphenyl)-2'-hydroxyethyl]-3-aminopropionate (74 , R=ethyl)	98
2.6 Comparison of δ_H values obtained for dipivaloyl ethyl ester (107), dihydroxy ethyl ester (74 , R=Et) and dihydroxy acid (74 , R=H) by ¹ H NMR spectroscopy	108

CHAPTER THREE

SYNTHESIS OF SOFT β -ADRENOCEPTOR AGONISTS	110
-EXPERIMENTAL (CHEMISTRY)	
3.1 Introduction	111
3.1.1 Correlated spectroscopy in ^1H NMR (^1H - ^1H COSY)	111
3.1.2 Distortionless Enhancement by Polarisation Transfer in ^{13}C NMR (^{13}C DEPT)	112
3.2 Synthesis of alkyl esters of 3-bromopropionate	114
3.2.1 Propyl 3-bromopropionate (68 , R= n-Pr)	114
3.2.2 Butyl 3-bromopropionate (68 , R= n-Bu)	114
3.3 Synthesis of alkyl esters of <i>N</i> -benzyl-3-aminopropionate	115
3.3.1 Methyl <i>N</i> -benzyl-3-aminopropionate (64 , R= Me)	115
3.3.2 Ethyl <i>N</i> -benzyl-3-aminopropionate (64 , R= Et)	116
3.3.3 Propyl <i>N</i> -benzyl-3-aminopropionate (64 , R= n-Pr)	116
3.3.4 Butyl <i>N</i> -benzyl-3-aminopropionate (64 , R= n-Bu)	117
3.4 Synthesis of α -chloroacetophenone analogues	117
3.4.1 3,4-Dihydroxy- α -chloroacetophenone (75)	117
3.4.2 1,2-Diacetoxybenzene (108)	118
3.4.3 3,4-Dimethoxy- α -chloroacetophenone (84)	118
3.4.4 Attempted synthesis of 3,4-dibenzyloxy- α -chloroacetophenone (80)	118
3.4.5 3,4-(1',1',3',3'-Tetra- <i>t</i> -butyldisiloxane)dioxy- α -chloroacetophenone (93)	119
3.4.6 3,4-Diphenylmethylenedioxy- α -chloroacetophenone (102)	120
3.4.7 3,4-Diacetoxy- α -chloroacetophenone (109)	120
3.4.8 3,4-dipivaloyloxy- α -chloroacetophenone (113)	120
3.5 Product (53) isolated from the reaction between ethyl bromoacetate and 1-phenyl-2-aminoethanol	121
3.6 Reactions of α -chloroacetophenone with esters of amino acids (excluding esters of <i>N</i> -benzyl-3-aminopropionate)	123
3.6.1 Methyl <i>N</i> -(benzoylmethyl)proline (59)	123
3.6.2 Ethyl <i>N</i> -(benzoylmethyl)-3-piperidine carboxylate (61)	124
3.6.3 Ethyl aminoethanoate (55)	125
3.6.4 Ethyl <i>N</i> -benzoylmethyl aminoethanoate (56)	125
3.7 Synthesis of esters of <i>N</i> -(substituted) benzoylmethyl- <i>N</i> -benzyl-3-aminopropionate	126
3.7.1 Ethyl <i>N</i> -(benzoylmethyl)- <i>N</i> -benzyl-3-aminopropionate (65 , R= Et)	126
3.7.2 Ethyl <i>N</i> -[(3',4'-diacetoxybenzoyl)methyl]- <i>N</i> -benzyl-3-amino propionate (110)	126

3.7.3	Ethyl <i>N</i> -[(3',4'-dimethoxybenzoyl)methyl]- <i>N</i> -benzyl-3-aminopropionate (85)	127
3.7.4	Ethyl <i>N</i> -{[3,4-(1',1',3',3'-tetra- <i>t</i> -butyldisiloxane)dioxybenzoyl]-methyl}- <i>N</i> -benzyl-3-aminopropionate (96)	127
3.7.5	Ethyl <i>N</i> -[(3',4'-diphenylmethylenedioxy)benzoylmethyl]- <i>N</i> -benzyl-3-aminopropionate (103 , R= Et)	128
3.7.6	Methyl <i>N</i> -[(3',4'-diphenylmethylenedioxy)benzoylmethyl]- <i>N</i> -benzyl-3-aminopropionate (103 , R= Me)	129
3.7.7	Propyl <i>N</i> -[(3',4'-diphenylmethylenedioxy)benzoylmethyl]- <i>N</i> -benzyl-3-aminopropionate (103 , R= n-Pr)	129
3.7.8	Butyl <i>N</i> -[(3',4'-diphenylmethylenedioxy)benzoylmethyl]- <i>N</i> -benzyl-3-aminopropionate (103 , R= n-Bu)	130
3.7.9	Ethyl <i>N</i> -[(3',4'-dipivaloyloxybenzoyl)methyl]- <i>N</i> -benzyl-3-aminopropionate (114)	131
3.8	Synthesis of alkyl <i>N</i> -[(2'-hydroxy-2'-(substituted) phenylethyl]- <i>N</i> -benzyl-3-aminopropionate	132
3.8.1	Ethyl <i>N</i> -(2'-hydroxy-2'-phenylethyl)- <i>N</i> -benzyl-3-aminopropionate (66 , R= Et)	132
3.8.2	Ethyl <i>N</i> -[2'-(3'',4''-dimethoxyphenyl)-2'-hydroxyethyl]- <i>N</i> -benzyl-3-aminopropionate (86)	133
3.8.3	Ethyl <i>N</i> -{2'-[3'',4''-(1''',1''',3''',3'''-tetra- <i>t</i> -butyldisiloxane)dioxyphenyl]-2'-hydroxyethyl}- <i>N</i> -benzyl-3-aminopropionate (97)	133
3.8.4	Methyl <i>N</i> -[2'-(3'',4''-diphenylmethylenedioxyphenyl)-2'-hydroxyethyl]- <i>N</i> -benzyl-3-aminopropionate (104 , R= Me)	134
3.8.5	Ethyl <i>N</i> -[2'-(3'',4''-diphenylmethylenedioxyphenyl)-2'-hydroxyethyl]- <i>N</i> -benzyl-3-aminopropionate (104 , R= Et)	135
3.8.6	Propyl <i>N</i> -[2'-(3'',4''-diphenylmethylenedioxyphenyl)-2'-hydroxyethyl]- <i>N</i> -benzyl-3-aminopropionate (104 , R= n-Pr)	136
3.8.7	Butyl <i>N</i> -[2'-(3'',4''-diphenylmethylenedioxyphenyl)-2'-hydroxyethyl]- <i>N</i> -benzyl-3-aminopropionate (104 , R= n-Bu)	136
3.8.8	Ethyl <i>N</i> -[2'-(3'',4''-dipivaloyloxyphenyl)-2'-hydroxyethyl]- <i>N</i> -benzyl-3-aminopropionate (115)	137
3.9	Synthesis of esters of <i>N</i> -[(2'-hydroxy-2'-(substituted) phenylethyl]-3-aminopropionate	139
3.9.1	Ethyl <i>N</i> -(2'-hydroxy-2'-phenylethyl)-3-aminopropionate (50 , R=Et)	139
3.9.2	Methyl <i>N</i> -(2'-hydroxy-2'-phenylethyl)-3-aminopropionate (50 , R=Me)	140
3.9.3	Ethyl <i>N</i> -[2'-(3'',4''-dimethoxyphenyl)-2'-hydroxyethyl]-3-aminopropionate (87)	141

3.9.4	Ethyl <i>N</i> -[2'-(3'',4''-diphenylmethylenedioxyphenyl)-2'-hydroxyethyl]-3-aminopropionate (105 , R= Et)	141
3.9.5	Ethyl <i>N</i> -{2'-[3'',4''-(1''',1''',3''',3'''-tetra- <i>t</i> -butyldisiloxane)dioxyphenyl]-2'-hydroxyethyl}-3-aminopropionate (98)	142
3.9.6	Ethyl <i>N</i> -[2'-(3'',4''-dihydroxyphenyl)-2'-hydroxyethyl]-3-aminopropionate (74 , R= Et)	142
3.9.7	Methyl <i>N</i> -[2'-(3'',4''-dihydroxyphenyl)-2'-hydroxyethyl]-3-aminopropionate (74 , R= Me)	144
3.9.8	Propyl <i>N</i> -[2'-(3'',4''-dihydroxyphenyl)-2'-hydroxyethyl]-3-aminopropionate (74 , R= <i>n</i> -Pr)	144
3.9.9	Butyl <i>N</i> -[2'-(3'',4''-dihydroxyphenyl)-2'-hydroxyethyl]-3-aminopropionate (74 , R= <i>n</i> -Bu)	145
3.9.10	Ethyl <i>N</i> -[2'-(3'',4''-dipivaloyloxyphenyl)-2'-hydroxyethyl]-3-aminopropionate (107)	146
3.9.11	Synthesis of <i>N</i> -[2'-(3'',4''-hydroxyphenyl)-2'-hydroxyethyl]-3-aminopropionic acid (74 , R= H)	147

CHAPTER FOUR

HPLC OF β -ADRENOCEPTOR AGONISTS	148
4.1 Introduction	149
4.2 Materials	151
4.3 Instrumentation (High-performance liquid chromatography)	151
4.4 Experimental	151
4.5 Result and Discussion	152
4.5.1 Selection of UV wavelength	152
4.5.2 Choice of stationary phase	153
4.5.3 Choice of mobile phase	154
4.5.4 Analysis of soft-drugs, their prodrugs and their analogues	154
4.5.4.1 Choice of mobile phase for alkyl <i>N</i> -(2'-hydroxy-2'-phenylethyl)-3-aminopropionate (50 , R= Et, Me)	155
4.5.4.2 Choice of mobile phase for ethyl <i>N</i> -[2'-(3'',4''-dihydroxyphenyl)-2'-hydroxyethyl]-3-aminopropionate (74 , R= Et)	159
4.5.4.3 Choice of mobile phase for ethyl <i>N</i> -[2'-(3'',4''-dipivaloyloxyphenyl)-2'-hydroxyethyl]-3-aminopropionate (107)	162
4.5.4.4 Choice of mobile phase for propyl <i>N</i> -[2'-(3'',4''-dihydroxyphenyl)-2'-hydroxyethyl]-3-aminopropionate (74 , R= Pr)	164
4.6 Summary	166

CHAPTER FIVE

DEGRADATION KINETICS OF SOFT β -ADRENOCEPTOR AGONISTS

168

5.1	Introduction	169
5.2	Experimental	172
5.2.1	Chemical hydrolysis of ethyl <i>N</i> -[2'-(3'',4''-dihydroxyphenyl)-2'-hydroxyethyl]-3-aminopropionate (74 , R= Et), ethyl <i>N</i> -[2'-(3'',4''-dipivaloyloxyphenyl)-2'-hydroxyethyl]-3-aminopropionate (107) and the unsubstituted phenyl- analogue (50 , R=Et) from pH 2.0-11.0 at 50 °C	172
5.2.2	Enzyme hydrolysis of ethyl <i>N</i> -[2'-(3'',4''-dihydroxyphenyl)-2'-hydroxyethyl]-3-aminopropionate (74 , R= Et) and ethyl <i>N</i> -[2'-(3'',4''-dipivaloyloxyphenyl)-2'-hydroxyethyl]-3-aminopropionate (107) with porcine liver carboxyesterase at pH 7.4 at 37 °C	173
5.2.3	Determination of dissociation constant (pK_a value) of ethyl <i>N</i> -[2'-(3'',4''-dipivaloyloxyphenyl)-2'-hydroxyethyl]-3-aminopropionate (107) and their analogues (50 , R=Et, Me) by potentiometric titrations	174
5.2.4	Determination of degradation profile of ethyl <i>N</i> -[2'-(3'',4''-dipivaloyloxyphenyl)-2'-hydroxyethyl]-3-aminopropionate (107) in chemical [pD 8.57 (pH 8.17)] and enzyme medium (porcine liver carboxyesterase, pH 7.4) at 37 °C	174
5.3	Results and discussion	175
5.3.1	Chemical hydrolysis of ethyl <i>N</i> -(2'-phenyl-2'-hydroxyethyl)-3-aminopropionate (50 , R= Et) in phosphate-citrate buffer containing 10% acetonitrile from pH 2.0 to 11.0 at 50 °C	175
5.3.2	Chemical hydrolysis of ethyl <i>N</i> -[2'-(3'',4''-dihydroxyphenyl)-2'-hydroxyethyl]-3-aminopropionate hydrochloride (74 , R=Et) in phosphate-citrate buffer containing 10% acetonitrile from pH 2.0 to 11.0 at 50 °C	177
5.3.3	Chemical hydrolysis of ethyl <i>N</i> -[2'-(3'',4''-dipivaloyloxyphenyl)-2'-hydroxyethyl]-3-aminopropionate hydrochloride (107) in phosphate-citrate buffer containing 10% acetonitrile from pH 2.0 to 11.0 at 50 °C	178
5.3.4	Calculation of rate-constants (pH-rate profile) and pK_a	181
5.3.4.1	Calculation of rate-constants and pK_a for ethyl <i>N</i> -(2'-hydroxy-2'-phenylethyl)-3-aminopropionate (50 , R=Et)	181
5.3.4.2	Calculation of rate constants and pK_a for ethyl <i>N</i> -[2'-(3'',4''-dihydroxyphenyl)-2'-hydroxyethyl]-3-aminopropionate (74 , R=Et)	184
5.3.4.3	Calculation of rate constants and pK_a for ethyl <i>N</i> -[2'-(3'',4''-dipivaloyloxyphenyl)-2'-hydroxyethyl]-3-aminopropionate (107)	186

5.3.5	Enzyme hydrolysis of β -adrenoceptor agonists with porcine liver carboxyesterase in phosphate-citrate buffer at pH 7.4 at 37 °C	188
5.3.5.1	Enzymatic hydrolysis of ethyl <i>N</i> -[2'-(3'',4''-dihydroxyphenyl)-2'-hydroxyethyl]-3-aminopropionate HCl (74 , R=Et) in phosphate-citrate buffer at pH 7.4 and 37 °C with PLCE	189
5.3.5.2	Enzymatic hydrolysis of ethyl <i>N</i> -[2'-(3'',4''-dipivaloyloxyphenyl)-2'-hydroxyethyl]-3-aminopropionate HCl (107) in phosphate-citrate buffer at pH 7.4 and 37 °C with PLCE	190
5.3.6	Determination of dissociation constants (pK_a)	192
5.3.6.1	Determination of ionization constant (pK_a) of ethyl <i>N</i> -(2'-hydroxy-2'-phenylethyl)-3-aminopropionate (50 , R=Et)	193
5.3.6.2	Determination of ionization constant (pK_a) of methyl <i>N</i> -(2'-hydroxy-2'-phenylethyl)-3-aminopropionate (50 , R=Me)	194
5.3.6.3	Determination of ionization constant (pK_a) of ethyl <i>N</i> -[2'-(3'',4''-dipivaloyloxyphenyl)-2'-hydroxyethyl]-3-aminopropionate (107)	194
5.3.6.4	Determination of ionization constant (pK_a) of ephedrine base and hydrochloride salt in water and 10% MeCN in water	194
5.3.7	Determination of degradation profile of ethyl <i>N</i> -[2'-(3'',4''-dipivaloyloxyphenyl)-2'-hydroxyethyl]-3-aminopropionate (107) in enzyme medium (PLCE) at pH 7.4 and 37 °C	196
5.4	Conclusions	201
CHAPTER SIX		
DEGRADATION PATHWAYS OF SOFT β-ADRENOCEPTOR AGONISTS		
6.1	Introduction	203
6.2	Experimental	206
6.3	Results and Discussion	207
6.3.1	Chemical hydrolysis studies of ethyl <i>N</i> -[2'-(3'',4''-dipivaloyloxyphenyl)-2'-hydroxyethyl]-3-aminopropionate (107) at pD 8.57 (pH 8.17) and 37 °C by ¹ H-NMR spectroscopy	207
6.3.1.1	Products from and mechanism of chemical hydrolysis	207
6.3.1.2	Products from and mechanism of hydrolysis of ethyl <i>N</i> -[2'-(3'',4''-dipivaloyloxyphenyl)-2'-hydroxyethyl]-3-aminopropionate (107) in phosphate-citrate buffer at pH 7.4 at 37 °C, containing 10% acetonitrile in the presence of porcine liver carboxyesterase	225
6.3.1.3	Rearrangement of catechol esters in ethyl <i>N</i> -[2'-(3'',4''-dipivaloyloxyphenyl)-2'-hydroxyethyl]-3-aminopropionate (107)	228

6.3.2	Chemical hydrolysis studies of ethyl <i>N</i> -[2'-(3",4"-dihydroxyphenyl)-2'-hydroxyethyl]-3-aminopropionate (74 , R= Et) at pD 8.57 (pH 8.17) and 37 °C by ¹ H-NMR spectroscopy	230
6.4	Conclusions	236
CHAPTER SEVEN		
PERCUTANEOUS ABSORPTION STUDIES OF β-ADRENOCEPTOR AGONISTS		
7.1	Introduction	239
7.2	Experimental	241
	7.2.1 Preparation of membranes	241
	7.2.2 Franz-type diffusion cells	242
	7.2.3 Preparation of test vehicles	242
	7.2.4 Permeation procedure	243
7.3	Results and discussion	244
	7.3.1 Percutaneous absorption of ethyl <i>N</i> -[2'-(3",4"-dihydroxyphenyl)-2'-hydroxyethyl]-3-aminopropionate (74 , R=Et)	244
	7.3.2 Percutaneous absorption of ethyl <i>N</i> -[2'-(3",4"-dipivaloyloxyphenyl)-2'-hydroxyethyl]-3-aminopropionate (107)	245
	7.3.2.1 Percutaneous absorption of ethyl <i>N</i> -[2'-(3",4"-dipivaloyloxyphenyl)-2'-hydroxyethyl]-3-aminopropionate (107) at buffered pH 3.0-8.0 in 10% propylene glycol in water	247
7.4	Conclusions	251
CHAPTER EIGHT		
BIOLOGICAL ACTIVITY OF SOFT-DRUGS AND PRO-SOFT-DRUG		
8.1	Introduction	253
	8.1.1 Effect of β-adrenoceptor agonists on trachea	253
	8.1.2 Effect of β-adrenoceptor agonists on heart	253
8.2	Experimental	253
	8.2.1 Guinea pig trachea	253
	8.2.2 Guinea pig atria	254
8.3	Results and discussion	254
CHAPTER NINE		
CONCLUSION		
		258
REFERENCES		
		263
APPENDICES		
		280
	Posters presented	295

LIST OF FIGURES

1.1	Diagram of proliferative (germinative) cell cycle.	30
1.2	Cyclic AMP cascade.	33
1.3	Fluorinated corticosteroids used topically in psoriasis.	37
1.4	Primary structure and topological model of the β -adrenoceptor.	45
1.5	Model of the ligand-binding site of the β -adrenergic receptor.	46
1.6	Adenylate cyclase activation by β -adrenoceptor agonists.	47
1.7	A proposed chemical basis for β -adrenoceptor stimulation.	47
1.8	Catalysis of cyclic-AMP formation by catecholamines.	53
1.9	Schematic diagram of the attachment of isoprenaline to the β -adrenoreceptor.	58
1.10	Schematic illustration of the prodrug concept.	60
2.1	^1H - ^1H COSY spectrum of compound (53).	69
2.2	^1H - ^1H COSY spectrum of butyl <i>N</i> -[2'-(3'',4''-diphenylmethylenedioxyphenyl)-2'-hydroxyethyl]- <i>N</i> -benzyl-3-aminopropionate (104 , R= butyl).	91
2.4	^1H -NMR and ^{13}C -NMR assignments of ethyl <i>N</i> -[2'-(3'',4''-dihydroxyphenyl)-2'-hydroxyethyl]-3-aminopropionate as its hydrochloride salt (74 , R= ethyl) in (D_2O).	94
2.3	^1H - ^1H COSY spectrum of ethyl <i>N</i> -[2'-(3'',4''-dihydroxyphenyl)-2'-hydroxyethyl]-3-aminopropionate (74 , R= ethyl).	95
2.5	^1H -NMR and ^{13}C -NMR assignments of ethyl <i>N</i> -[2'-(3'',4''-dihydroxyphenyl)-2'-hydroxyethyl]-3-aminopropionate as its hydrochloride salt (74 , R=ethyl) in (MeOH-d_4).	96
2.6a	^1H - ^1H COSY spectrum of ethyl <i>N</i> -[2'-(3'',4''-dipivaloyloxyphenyl)-2'-hydroxyethyl]-3-aminopropionate (107).	105
2.6b	Expansion of ^1H - ^1H COSY spectrum of ethyl <i>N</i> -[2'-(3'',4''-dipivaloyloxyphenyl)-2'-hydroxyethyl]-3-aminopropionate (107).	106
2.7	^1H -NMR and ^{13}C -NMR assignments of ethyl <i>N</i> -[2'-(3'',4''-dipivaloyloxyphenyl)-2'-hydroxyethyl]-3-aminopropionate (107) in (CDCl_3).	107
3.1	Typical COSY spectrum obtained from 1,3-dinitrobenzene.	112
3.2	A diagram of the ^{13}C NMR and ^{13}C DEPT spectrum (D_2O) of ethyl <i>N</i> -[2'-(3'',4''-dihydroxyphenyl)-2'-hydroxyethyl]-3-aminopropionate (74 , R= Et).	113
4.1	Typical HPLC chromatogram of a two-component mixture.	150
4.2	UV spectrum of ethyl <i>N</i> -[2'-(3'',4''-dihydroxyphenyl)-2'-hydroxyethyl]-3-aminopropionate (74 , R=Et) in chloroform (200-350 nm).	152

4.3	UV spectrum of ethyl <i>N</i> -[2'-(3'',4''-dipivaloyloxyphenyl)-2'-hydroxyethyl]-3-aminopropionate (107) in chloroform (190-450 nm).	153
4.4	HPLC chromatogram of [A= ethyl <i>N</i> -(2'-hydroxy-2'-phenylethyl)-3-amino- propionate (50 , R= Et)] in 40% methanol in water mobile phase. [B=acid; (50 , R=H)].	156
4.5	HPLC chromatogram of [A= methyl <i>N</i> -(2'-hydroxy-2'-phenylethyl)-3-amino- propionate (50 , R= Me)] in 30% methanol in water mobile phase. [B=acid; (50 , R=H)].	157
4.6	Calibration graph for ethyl <i>N</i> -(2'-hydroxy-2'-phenylethyl)-3-aminopropionate (50 , R=Et) in 15% acetonitrile in water mobile phase.	158
4.7	HPLC chromatogram of ethyl <i>N</i> -(2'-hydroxy-2'-phenylethyl)-3-amino- propionate (50 , R=Et) in 15% acetonitrile in water mobile phase. [B=acid; (50 , R=H)].	159
4.8	HPLC chromatogram of [A= ethyl <i>N</i> -[2'-(3'',4''-dihydroxyphenyl)-2'-hydroxy- ethyl]-3-aminopropionate (74 , R= Et)] in 4% acetonitrile mobile phase. [B=acid; (74 , R=H)].	160
4.9	Calibration graph for ethyl <i>N</i> -[2'-(3'',4''-dihydroxyphenyl)-2'-hydroxyethyl]- 3-aminopropionate (74 , R= Et) in 4% acetonitrile in water mobile phase.	161
4.10	HPLC chromatogram of [A= ethyl <i>N</i> -[2'-(3'',4''-dipivaloyloxyphenyl)-2'- hydroxyethyl]-3-aminopropionate (107)] in 30% acetonitrile mobile phase. [B=dipivaloyl acid; (120 , R=H)].	163
4.11	Calibration graph for ethyl <i>N</i> -[2'-(3'',4''-dipivaloyloxyphenyl)-2'-hydroxyethyl]- 3-aminopropionate (107) in 30% acetonitrile in water mobile phase.	163
4.12	HPLC chromatogram of [A= propyl <i>N</i> -[2'-(3'',4''-dihydroxyphenyl)-2'-hydroxy- ethyl]-3-aminopropionate (74 , R= Pr)] in 10% acetonitrile mobile phase. [B=acid; (74 , R=H)].	165
4.13	Calibration graph for propyl <i>N</i> -[2'-(3'',4''-dihydroxyphenyl)-2'-hydroxyethyl]- 3-aminopropionate (74 , R= Pr) in 10% acetonitrile in water.	166
5.1	Postulated hydrolysis pathway of triester (107).	171
5.2	Chemical hydrolysis of ethyl <i>N</i> -(2'-hydroxy-2'-phenylethyl)-3-aminopropionate (50 , R=Et) in phosphate-citrate buffer pH 5.0 without any co-solvent.	175
5.3	Chemical hydrolysis of ethyl <i>N</i> -(2'-hydroxy-2'-phenylethyl)-3-aminopropionate (50 , R= Et) in phosphate-citrate buffer pH 2.0 to 11.0 in 10% acetonitrile in water at 50 °C.	176
5.4	Chemical hydrolysis of ethyl <i>N</i> -[2'-(3'',4''-dihydroxyphenyl)-2'-hydroxyethyl]- 3-aminopropionate (74 , R= Et) in phosphate-citrate buffer pH 2.0 to 11.0 at 50 °C.	177
5.5	Hydrolysis of ethyl <i>N</i> -[2'-(3'',4''-dipivaloyloxyphenyl)-2'-hydroxyethyl]-3- aminopropionate (107) in different solvents included in phosphate-citrate buffer at pH 9.0 at 50 °C.	179

5.6	Chemical hydrolysis of ethyl <i>N</i> -[2'-(3'',4''-dipivaloyloxyphenyl)-2'-hydroxyethyl]-3-aminopropionate (107) in aqueous phosphate-citrate buffer, pH 2.0 to 11.0 containing 10% acetonitrile at 50 °C.	180
5.7	Hydrolysis rate constants of ethyl <i>N</i> -(2'-hydroxy-2'-phenylethyl)-3-aminopropionate (50 , R=Et) dependent upon pH.	183
5.8	Hydrolysis rate constants of ethyl <i>N</i> -[2'-(3'',4''-dihydroxyphenyl)-2'-hydroxyethyl]-3-aminopropionate (74 , R=Et) dependent upon pH.	185
5.9	Hydrolysis rate constants of ethyl <i>N</i> -[2'-(3'',4''-dipivaloyloxyphenyl)-2'-hydroxyethyl]-3-aminopropionate (107) dependent upon pH.	187
5.10	Enzyme hydrolysis of ethyl <i>N</i> -[2'-(3'',4''-dihydroxyphenyl)-2'-hydroxyethyl]-3-aminopropionate (74 , R=Et) with and without PLCE at pH 7.4 and 37 °C.	189
5.11	Hydrolysis of ethyl <i>N</i> -[2'-(3'',4''-dipivaloyloxyphenyl)-2'-hydroxyethyl]-3-aminopropionate (107 , 80 μM) in buffer solution pH 7.4 at 37 °C with PLCE.	190
5.12	Enzyme hydrolysis of ethyl <i>N</i> -[2'-(3'',4''-dipivaloyloxyphenyl)-2'-hydroxyethyl]-3-aminopropionate HCl (107) without PLCE at pH 7.4 and 37 °C.	191
5.13	Potentiometric titration run of ethyl <i>N</i> -(2'-hydroxy-2'-phenylethyl)-3-aminopropionate (50 , R=Et) with 0.1 M HCl.	193
5.14	Half-lives of pro-soft-drug (107) and <i>in situ</i> generated soft-drug (74 , R=Et) in enzyme hydrolysis in buffer containing 10% acetonitrile at pH 7.4 and 37 °C.	197
5.15	Kinetic profile of pro-soft-drug (107) and <i>in situ</i> generated soft-drug (74 , R=Et) in enzyme hydrolysis in buffer containing 10% acetonitrile at pH 7.4 and 37 °C.	197
5.16	Half-lives of pro-soft-drug (107) and <i>in situ</i> generated soft-drug (74 , R=Et) in enzyme hydrolysis in buffer containing 10% acetonitrile at pH 7.4 and 37 °C.	198
5.17	Kinetic profile of pro-soft-drug (107) and <i>in situ</i> generated soft-drug (74 , R=Et) in enzyme hydrolysis in buffer containing 10% acetonitrile at pH 7.4 and 37 °C.	198
5.18	Chemical and enzymatic hydrolysis of pro-soft-drug (107).	199
6.1	HPLC chromatogram shows the formation of unknown peak [B= dipivaloyl carboxylic acid (120)] in the chemical hydrolysis of ethyl <i>N</i> -[2'-(3'',4''-dipivaloyloxyphenyl)-2'-hydroxyethyl]-3-aminopropionate (107 , A) at pH 4.0 after 582 hours.	204
6.2	HPLC chromatogram shows very little or no formation of unknown peak [B= dipivaloyl carboxylic acid (120)] in the esterase catalysed hydrolysis of ethyl <i>N</i> -[2'-(3'',4''-dipivaloyloxyphenyl)-2'-hydroxyethyl]-3-aminopropionate (107 , A).	204
6.3	Assignments of ethyl <i>N</i> -[2'-(3'',4''-dipivaloyloxyphenyl)-2'-hydroxyethyl]-3-aminopropionate (107) by ¹ H-NMR [D ₂ O, pD 8.57-CD ₃ CN (8:2, v/v)].	208
6.4a	¹ H-NMR spectrum of ethyl <i>N</i> -[2'-(3'',4''-dipivaloyloxyphenyl)-2'-hydroxyethyl]-3-aminopropionate (107) in buffer pD 8.57 (pH 8.17) in 20% CD ₃ CN in D ₂ O.	209

6.4b	Expansion of aromatic region of ethyl <i>N</i> -[2'-(3",4"-dipivaloyloxyphenyl)-2'-hydroxyethyl]-3-aminopropionate (107) in buffer pD 8.57 (pH 8.17) in 20% CD ₃ CN in D ₂ O.	210
6.5	Assignments of <i>N</i> -[2'-(3",4"-dipivaloyloxyphenyl)-2'-hydroxyethyl]-3-amino propionic acid (120) by ¹ H-NMR [D ₂ O, pD 8.57-CD ₃ CN (8:2, v/v)].	211
6.6	Assignments of <i>N</i> -[2'-(3",4"-dihydroxyphenyl)-2'-hydroxyethyl]-3-amino-propionic acid (74 , R=H) by ¹ H-NMR [D ₂ O, pD 8.57-CD ₃ CN (8:2, v/v)].	211
6.7a	¹ H-NMR spectrum of ethyl <i>N</i> -[2'-(3",4"-dipivaloyloxyphenyl)-2'-hydroxy-ethyl]-3-aminopropionate (107) in buffer pD 8.57 (pH 8.17) in 20% CD ₃ CN in D ₂ O after 24 hrs.	213
6.7b	Expansion of aromatic region of ethyl <i>N</i> -[2'-(3",4"-dipivaloyloxyphenyl)-2'-hydroxyethyl]-3-aminopropionate (107) in buffer pD 8.57 (pH 8.17) in 20% CD ₃ CN in D ₂ O after 24 hrs.	214
6.8a	¹ H-NMR spectrum of ethyl <i>N</i> -[2'-(3",4"-dipivaloyloxyphenyl)-2'-hydroxy-ethyl]-3-aminopropionate (107) in buffer pD 8.57 (pH 8.17) in 20% CD ₃ CN in D ₂ O after 70 hrs.	215
6.8b	Expansion of aromatic region of ethyl <i>N</i> -[2'-(3",4"-dipivaloyloxyphenyl)-2'-hydroxyethyl]-3-aminopropionate (107) in buffer pD 8.57 (pH 8.17) in 20% CD ₃ CN in D ₂ O after 70 hrs.	216
6.9a	¹ H-NMR spectrum of ethyl <i>N</i> -[2'-(3",4"-dipivaloyloxyphenyl)-2'-hydroxy-ethyl]-3-aminopropionate (107) in buffer pD 8.57 (pH 8.17) in 20% CD ₃ CN in D ₂ O after 300 hrs.	217
6.9b	Expansion of aromatic region of ethyl <i>N</i> -[2'-(3",4"-dipivaloyloxyphenyl)-2'-hydroxyethyl]-3-aminopropionate (107) in buffer pD 8.57 (pH 8.17) in 20% CD ₃ CN in D ₂ O after 300 hrs.	218
6.10a	Hydrolysis of triester (107) in potassium phosphate buffer (pD 8.57) in 20% acetonitrile at 37 °C by ¹ H-NMR spectroscopy over 70 hrs.	221
6.10b	Hydrolysis of triester (107) in potassium phosphate buffer (pD 8.57) in 20% acetonitrile at 37 °C by ¹ H-NMR spectroscopy over 300 hrs.	222
6.11a	Hydrolysis of triester (107): formation of the dipivaloyloxy acid (120) and the dihydroxy acid (74 , R=H). After 70 h the proportions of (107), (120) and (74 , R=H) were 58, 29 and 13% respectively by ¹ H-NMR spectroscopy.	222
6.11b	Hydrolysis of triester (107): formation of the dipivaloyloxy acid (120) and the dihydroxy acid (74 , R=H). After 300 h the proportions of (107), (120) and (74 , R=H) were 9, 23 and 68% respectively by ¹ H-NMR spectroscopy.	223
6.12	Enzyme hydrolysis of triester (107) in 10% acetonitrile in phosphate-citrate buffer at pH 7.4 and 37 °C with 6.29 U of porcine liver carboxyesterase.	225
6.13	Half-life of dihydroxy ethyl ester (74 , R= Et) formed in the reaction mixture by the hydrolysis of triester HCl (107) in 10% acetonitrile in phosphate-citrate buffer at pH 7.4 at 37 °C with 6.29 U of porcine liver carboxyesterase.	226

6.14	Assignments of ethyl <i>N</i> -[2'-(3",4"-dihydroxyphenyl)-2'-hydroxyethyl]-3-amino propionate (74 , R= Et) in ¹ H-NMR [D ₂ O, pD 8.57-CD ₃ CN (9:1, v/v)].	230
6.15a	¹ H-NMR spectrum of ethyl <i>N</i> -[2'-(3",4"-dihydroxyphenyl)-2'-hydroxyethyl]-3-aminopropionate (74 , R= Et) in buffer pD 8.57 (pH 8.17) in 10% CD ₃ CN in D ₂ O.	232
6.15b	Expansion of aromatic region of ethyl <i>N</i> -[2'-(3",4"-dihydroxyphenyl)-2'-hydroxyethyl]-3-aminopropionate (74 , R= Et) in buffer pD 8.57 (pH 8.17) in 10% CD ₃ CN in D ₂ O.	233
6.16	¹ H-NMR spectrum of ethyl <i>N</i> -[2'-(3",4"-dihydroxyphenyl)-2'-hydroxyethyl]-3-aminopropionate (74 , R= Et) in buffer pD 8.57 (pH 8.17) in 10% CD ₃ CN in D ₂ O after 5 hrs.	234
6.17	Hydrolysis of ethyl <i>N</i> -[2'-(3",4"-dihydroxyphenyl)-2'-hydroxyethyl]-3-aminopropionate (74 , R= Et) at pH 8.17 (pD 8.57) in potassium phosphate buffer in 10% acetonitrile at 37 °C by ¹ H-NMR spectroscopy.	235
6.18	Hydrolysis of ethyl <i>N</i> -[2'-(3",4"-dihydroxyphenyl)-2'-hydroxyethyl]-3-aminopropionate (74 , R= Et) in pH 8.17 (pD 8.57) and formation of dihydroxyacid (74 , R=H) in potassium phosphate buffer in 10% acetonitrile at 37 °C by ¹ H-NMR spectroscopy.	235
7.1	The time course for absorption for the simple flux obtained by plotting the cumulative amount of diffusant crossing unit area of membrane (M) as a function of time.	240
7.2	Schematic representation of a Franz-type diffusion cell.	242
7.3	Transport of ethyl <i>N</i> -[2'-(3",4"-dihydroxyphenyl)-2'-hydroxyethyl]-3-aminopropionate (74 , R=Et) through the silicone membrane at pH 6.5 in the donor compartment. Receiving compartment contains 10% propylene glycol in water at pH 3.0.	244
7.4	Transport of ethyl <i>N</i> -[2'-(3",4"-dipivaloyloxyphenyl)-2'-hydroxyethyl]-3-amino propionate (107) through the silicone membrane in 10% propylene glycol in water at pH 6.5 in receiving compartment (pH 7.0 in the donor compartment).	245
7.5	Transport of ethyl <i>N</i> -[2'-(3",4"-dipivaloyloxyphenyl)-2'-hydroxyethyl]-3-amino propionate (107) through the silicone membrane in 10% propylene glycol in water at pH 3.0 in receiving compartment (pH 7.0 in the donor compartment).	246
7.6	Permeation of ethyl <i>N</i> -[2'-(3",4"-dipivaloyloxyphenyl)-2'-hydroxyethyl]-3-aminopropionate (107) across the silicone membrane at different pH (non-buffered) in 10% propylene glycol in water in the donor compartment.	246
7.7	Silicone membrane transport of ethyl <i>N</i> -[2'-(3",4"-dipivaloyloxyphenyl)-2'-hydroxyethyl]-3-aminopropionate (107) at buffered pH 3.0-5.0 in 10% propylene glycol in water in the donor compartment.	248
7.8	Silicone membrane transport of ethyl <i>N</i> -[2'-(3",4"-dipivaloyloxyphenyl)-2'-hydroxyethyl]-3-aminopropionate (107) at buffered pH 6.0-8.0 in 10% propylene glycol in water in the donor compartment.	248
7.9	Silicone membrane transport of ethyl <i>N</i> -[2'-(3",4"-dipivaloyloxyphenyl)-2'-hydroxyethyl]-3-aminopropionate (107) at different buffered pH in 10% propylene glycol in water in the donor compartment.	249

- 7.10 Permeation of ethyl *N*-[2'-(3'',4''-dipivaloyloxyphenyl)-2'-hydroxyethyl]-3-aminopropionate (**107**) increases as the percentage of unionized triester increases in the donor compartment. 250
- 8.1 The soft-drug (**74**, R=Et) was a full agonist on the trachea preparations but was less potent than isoprenaline [ED₅₀ of 4.07 (± 0.49) × 10⁻⁷ M compared with 2.68 (± 0.37) × 10⁻⁷ M for isoprenaline]. 256
- 8.2 Responses to the soft-drug (**74**, R=Et) was competitively antagonised by propranolol (10⁻⁶ M) and, in the presence of propranolol, the ED₅₀ of the drug was 8.8 (± 0.9) × 10⁻⁶ M. 256
- 8.3 The maximal response of acid (**74**, R=H) was significantly less than the agonist (**74**, R=Et) and was attained at a concentration of 3 × 10⁻⁴ M whereas with the soft drug the maximum response was achieved at a concentration of 10⁻⁵ M [ED₅₀ of 2.95 (± 0.9) × 10⁻⁵ M]. 257
- 8.4 The maximum relaxation of guinea pig trachea by soft-drug (**74**, R=Et) at a concentration of 3 × 10⁻⁵ M, isoprenaline at a concentration of 3 × 10⁻⁵ M and dihydroxy acid (**74**, R=H) at a concentration of 3 × 10⁻⁴ M. 257

LIST OF TABLES IN TEXT

1.1	Cell cycle time: in normal and in psoriatic epidermis.	30
1.2	Anti-inflammatory steroids used for topical application in psoriasis.	37
1.3	α - and β -Receptor agonists and antagonists.	43
1.4	β_1 and β_2 -Receptor antagonists.	44
1.5	Influence of catechol function on β -agonist activity.	49
1.6	Effect of α -methyl substitution on α - and β -receptor activities of 5'-(2-amino-1-hydroxyethyl)-2'-hydroxy alkanesulfonamides.	50
1.7	Effect of <i>N</i> -substitution on α - and β -activity of DL-norepinephrine.	51
1.8	Effect of <i>N</i> -substitution on β -receptor stimulant activity of norepinephrine.	52
1.9	Isoprenaline analogues with β -adrenoceptor agonist activity.	57
1.10	Drugs which require bioactivation to form active compounds.	61
2.1	Chemical shifts of dipivaloyl ethyl ester (107), dihydroxy ethyl ester (74 , R=Et) and dihydroxy acid (74 , R=H) by ¹ H NMR spectroscopy.	109
4.1	Mathematical parameters and their typical values in HPLC.	150
4.2	Chromatographic data for ethyl <i>N</i> -(2'-hydroxy-2'-phenylethyl)-3-aminopropionate (50 , R= Et) and methyl <i>N</i> -(2'-hydroxy-2'-phenylethyl)-3-aminopropionate (50 , R= Me) in 30 and 40% methanol in water mobile phase.	156
4.3	Chromatographic data for ethyl <i>N</i> -(2'-hydroxy-2'-phenylethyl)-3-aminopropionate (50 , R= Et) and acid (50 , R= H) in 15% acetonitrile in water mobile phase.	157
4.4	Statistical data for ethyl <i>N</i> -(2'-hydroxy-2'-phenylethyl)-3-aminopropionate (50 , R=Et), showing standard deviation and coefficient of variation in calibration curve (n=3).	158
4.5	Chromatographic data for ethyl <i>N</i> -[2'-(3'',4''-dihydroxyphenyl)-2'-hydroxyethyl]-3-aminopropionate (74 , R= Et) in 4% acetonitrile mobile phase.	160
4.6	Statistical data for ethyl <i>N</i> -[2'-(3'',4''-dihydroxyphenyl)-2'-hydroxyethyl]-3-aminopropionate (74 , R= Et), showing standard deviation and coefficient of variation in calibration curve (n=3).	161
4.7	Chromatographic data for ethyl <i>N</i> -[2'-(3'',4''-dipivaloyloxyphenyl)-2'-hydroxyethyl]-3-aminopropionate (107) in 30% acetonitrile in water mobile phase.	162
4.8	Statistical data for ethyl <i>N</i> -[2'-(3'',4''-dipivaloyloxyphenyl)-2'-hydroxyethyl]-3-aminopropionate (107), showing standard deviation and coefficient of variation in calibration curve (n=3).	164
4.9	Chromatographic data for propyl <i>N</i> -[2'-(3'',4''-dihydroxyphenyl)-2'-hydroxyethyl]-3-aminopropionate (74 , R= Pr) in 10% acetonitrile in water.	164

4.10	Statistical data for propyl <i>N</i> -[2'-(3'',4''-dihydroxyphenyl)-2'-hydroxyethyl]-3-aminopropionate (74 , R= Pr), showing standard deviation and coefficient of variation in calibration curve (n=3).	165
4.11	HPLC solvent systems used for soft β -adrenoceptor agonist, prodrug of soft β -adrenoceptor agonist and their analogues.	167
5.1	Examples of prodrugs developed for topical use.	170
5.2	Rate constants of ethyl <i>N</i> -(2'-hydroxy-2'-phenylethyl)-3-aminopropionate (50 , R= Et) from pH 2.0 to 11.0 in 10% acetonitrile in water at 50 °C.	176
5.3	Rate constants of ethyl <i>N</i> -[2'-(3'',4''-dihydroxyphenyl)-2'-hydroxyethyl]-3-aminopropionate (74 , R= Et) from pH 2.0 to 11.0 in 10% acetonitrile in water at 50 °C.	178
5.4	Rate constants of ethyl <i>N</i> -[2'-(3'',4''-dipivaloyloxyphenyl)-2'-hydroxyethyl]-3-aminopropionate (107) from pH 2.0 to 11.0 in 10% acetonitrile in water at 50 °C.	180
5.5	Individual rate constants and pK _a calculated by NONREG and FIGP programs in the hydrolysis of ethyl <i>N</i> -(2'-hydroxy-2'-phenylethyl)-3-aminopropionate (50 , R= Et).	182
5.6	Individual rate constants and pK _a calculated by NONREG and FIGP programs in the hydrolysis of ethyl <i>N</i> -[2'-(3'',4''-dihydroxyphenyl)-2'-hydroxyethyl]-3-aminopropionate (74 , R=Et).	184
5.7	Individual rate constants and pK _a calculated by NONREG and FIGP programs in the hydrolysis of ethyl <i>N</i> -[2'-(3'',4''-dipivaloyloxyphenyl)-2'-hydroxyethyl]-3-aminopropionate (107).	186
5.8	Enzyme hydrolysis of ethyl <i>N</i> -[2'-(3'',4''-dihydroxyphenyl)-2'-hydroxyethyl]-3-aminopropionate (74 , R=Et) with and without PLCE at pH 7.4 and 37 °C.	189
5.9	Hydrolysis data of ethyl <i>N</i> -[2'-(3'',4''-dipivaloyloxyphenyl)-2'-hydroxyethyl]-3-aminopropionate (107 , 80 μ M) in buffer solution pH 7.4 at 37 °C with PLCE.	191
5.10	Potentiometric titration of ethyl <i>N</i> -(2'-hydroxy-2'-phenylethyl)-3-aminopropionate (50 , R=Et) (19.5 mg) with HCl (0.1 M).	193
5.11	The pK _a values of analogue (50 , R ₁ =Me, R ₂ =H), analogue (50 , R ₁ =Et, R ₂ =H), and Et) pro-soft-drug (107 , R ₁ =Et, R ₂ =Bu ^t COO).	195
5.12	Rate data for the alkaline and enzymatic hydrolysis of various benzoate esters at 37 °C.	200
6.1	Chemical shifts and coupling constants of aromatic protons in catechol derivatives.	208
6.2	Calculation of % of ethyl <i>N</i> -[2'-(3'',4''-dipivaloyloxyphenyl)-2'-hydroxyethyl]-3-aminopropionate (107) and hydrolysis product <i>N</i> -[2'-(3'',4''-dipivaloyloxyphenyl)-2'-hydroxyethyl]-3-aminopropionic acid (120) and <i>N</i> -[2'-(3'',4''-dihydroxyphenyl)-2'-hydroxyethyl]-3-aminopropionic acid (74 , R=H) by integration in ¹ H-NMR.	220

6.3	Chemical shift and coupling constants of aromatic protons of ethyl <i>N</i> -[2'-(3",4"-dihydroxyphenyl)-2'-hydroxyethyl]-3-aminopropionate (74 , R= Et) and dihydroxy acid (74 , R=H).	231
6.4	Calculation of % of ethyl <i>N</i> -[2'-(3",4"-dihydroxyphenyl)-2'-hydroxyethyl]-3-aminopropionate (74) and hydrolysis product <i>N</i> -[2'-(3",4"-dihydroxyphenyl)-2'-hydroxyethyl]-3-aminopropionic acid (74 , R=H) by integration in ¹ H-NMR.	231
7.1	Permeation data for ethyl <i>N</i> -[2'-(3",4"-dipivaloyloxyphenyl)-2'-hydroxyethyl]-3-aminopropionate (107) across the silicone membrane at different pH (non-buffered) in 10% propylene glycol in water in the donor compartment.	247
7.2	Silicone membrane transport data of ethyl <i>N</i> -[2'-(3",4"-dipivaloyloxyphenyl)-2'-hydroxyethyl]-3-aminopropionate (107) at different buffered pH in 10% propylene glycol in water in the donor compartment.	249
7.3	Percentage of ionized and unionized ethyl <i>N</i> -[2'-(3",4"-dipivaloyloxyphenyl)-2'-hydroxyethyl]-3-aminopropionate (107) at different buffered pH in 10% propylene glycol in water in the donor compartment.	250
8.1	The ED ₅₀ of isoprenaline, soft drugs (74 , R=Et, Pr), soft drug (74 , R=Et) with propranolol and metabolite (74 , R=H).	254

LIST OF TABLES IN APPENDIX

5.1A	Preparation of McIlvaine buffers.	281
5.2A	Potentiometric titration of methyl <i>N</i> -(2'-hydroxy-2'-phenylethyl)-3-aminopropionate HCl (50 , R=Me, 129.92 mg) with KOH (0.1 M) in 10% acetonitrile in water.	281
5.3A	Potentiometric titration of ethyl <i>N</i> -[2'-(3",4"-dipivaloyloxyphenyl)-2'-hydroxyethyl]-3-aminopropionate HCl (107 , 180.80 mg) with KOH (0.1 M) in 10% acetonitrile in water.	282
5.4A	Potentiometric titration of ephedrine HCl (105.35 mg) with KOH (0.1 M) in water.	282
5.5A	Potentiometric titration of ephedrine HCl (100.85 mg) with KOH (0.1 M) in 10% acetonitrile in water.	283
5.6A	Potentiometric titration of ephedrine (83.5 mg) with HCl (0.1 M) in 10% acetonitrile in water.	284
5.7A	Enzymatic hydrolysis of ethyl <i>N</i> -[2'-(3",4"-dipivaloyloxyphenyl)-2'-hydroxyethyl]-3-aminopropionate HCl (107) with 6.29 U of PLCE at pH 7.4. Hydrolysis was monitored by HPLC using 30% acetonitrile in water as mobile phase [I]. The same experiment was repeated and monitored in 4% acetonitrile in water [II].	285
5.8A	Enzymatic hydrolysis of <i>in situ</i> generated soft-drug (74 , R=Et) by the enzymatic hydrolysis of pro-soft-drug (107) [mobile phase is 4% MeCN in water].	285
5.9A	Enzymatic hydrolysis of ethyl <i>N</i> -[2'-(3",4"-dipivaloyloxyphenyl)-2'-hydroxyethyl]-3-aminopropionate HCl (107) with 6.29 U of PLCE at pH 7.4. Hydrolysis was monitored by HPLC using 30% acetonitrile in water as mobile phase [I]. The same experiment was repeated and monitored in 4% acetonitrile in water [II].	286

5.10A	Enzymatic hydrolysis of <i>in situ</i> generated soft-drug (74 , R=Et) by the enzymatic hydrolysis of pro-soft-drug (107) [mobile phase is 4% MeCN in water].	286
6.1A	Calculation of % of ethyl <i>N</i> -[2'-(3'',4''-dipivaloyloxyphenyl)-2'-hydroxyethyl]-3-aminopropionate (107) and hydrolysis products <i>N</i> -[2'-(3'',4''-dipivaloyloxyphenyl)-2'-hydroxyethyl]-3-aminopropionic acid (120) and <i>N</i> -[2'-(3'',4''-dihydroxyphenyl)-2'-hydroxyethyl]-3-aminopropionic acid (74 , R=H) by integration in ¹ H-NMR.	287
6.1B	Calculation of % of (107) and hydrolysis product (120) and (74 , R=H) by integration in ¹ H-NMR.	288
6.1C	Calculation of % of (107) and hydrolysis product (120) and (74 , R=H) by integration in ¹ H-NMR.	289
6.2A	Calculation of % of ethyl <i>N</i> -[2'-(3'',4''-dihydroxyphenyl)-2'-hydroxyethyl]-3-aminopropionate (74 , R=Et) and hydrolysis product <i>N</i> -[2'-(3'',4''-dihydroxyphenyl)-2'-hydroxyethyl]-3-aminopropionic acid (74 , R=H) by integration in ¹ H-NMR.	290
7.1A	Transport of ethyl <i>N</i> -[2'-(3'',4''-dipivaloyloxyphenyl)-2'-hydroxyethyl]-3-aminopropionate (107) through the silicone membrane in 10% propylene glycol in water at pH 6.5 in receiving compartment.	290
7.2A	Transport of ethyl <i>N</i> -[2'-(3'',4''-dipivaloyloxyphenyl)-2'-hydroxyethyl]-3-aminopropionate (107) through the silicone membrane in 10% propylene glycol in water at pH 3.0 in receiving compartment.	291
7.3A	Cumulative transport data for ethyl <i>N</i> -[2'-(3'',4''-dipivaloyloxyphenyl)-2'-hydroxyethyl]-3-aminopropionate (107) across the silicone membrane at different pH in the donor compartment [flux in (μmol/cm ² /h)].	291
7.4A	Silicone membrane transport data of ethyl <i>N</i> -[2'-(3'',4''-dipivaloyloxyphenyl)-2'-hydroxyethyl]-3-aminopropionate (107) at buffered pH 3.0 in 10% propylene glycol in water in the donor compartment.	292
7.5A	Silicone membrane transport data of ethyl <i>N</i> -[2'-(3'',4''-dipivaloyloxyphenyl)-2'-hydroxyethyl]-3-aminopropionate (107) at buffered pH 4.0 in 10% propylene glycol in water in the donor compartment.	292
7.6A	Silicone membrane transport data of ethyl <i>N</i> -[2'-(3'',4''-dipivaloyloxyphenyl)-2'-hydroxyethyl]-3-aminopropionate (107) at buffered pH 5.0 in 10% propylene glycol in water in the donor compartment.	293
7.7A	Silicone membrane transport data of ethyl <i>N</i> -[2'-(3'',4''-dipivaloyloxyphenyl)-2'-hydroxyethyl]-3-aminopropionate (107) at buffered pH 6.0 in 10% propylene glycol in water in the donor compartment.	293
7.8A	Silicone membrane transport data of ethyl <i>N</i> -[2'-(3'',4''-dipivaloyloxyphenyl)-2'-hydroxyethyl]-3-aminopropionate (107) at buffered pH 7.0 in 10% propylene glycol in water in the donor compartment.	294
7.9A	Silicone membrane transport data of ethyl <i>N</i> -[2'-(3'',4''-dipivaloyloxyphenyl)-2'-hydroxyethyl]-3-aminopropionate (107) at buffered pH 8.0 in 10% propylene glycol in water in the donor compartment.	294

LIST OF SCHEMES

1.1	Mechanism of deactivation of β -adrenoceptor agonist activity by loss of the basic centre at nitrogen.	56
1.2	Mechanism of deactivation of β -adrenoceptor agonist activity by rapid hydrolysis of potential biolabile glycolamide ester soft-drugs.	65
2.1	Formation of compound (53) due to acylation of hydroxyl group in compound (51).	70
2.2	Synthetic route for phenyl amino acid esters (50 , $n=2$, R= methyl and ethyl).	74
2.3	Synthesis of alkyl 3-bromopropionate (R= n-Pr and n-Bu).	75
2.4	A possible route of decomposition of alkyl <i>N</i> -(benzoylmethyl)- <i>N</i> -benzyl-3-aminopropionate (65).	76
2.5	Mass spectrum (CI, NH ₃) fragmentation of ethyl <i>N</i> -(2'-hydroxy-2'-phenylethyl)-3-aminopropionate (50 , R=ethyl).	78
2.6	Proposed synthetic route for catechol amino acid esters (74 , R=Me, Et, n-Pr, n-Bu).	79
2.7	Mechanism showing why the 4-benzyloxy group is cleaved more readily than the 3-benzyloxy group.	81
2.8	Mechanism of 1-hydroxybenzotriazole catalysis.	85
2.9	Mass spectrum (CI, NH ₃) fragmentation pattern of ethyl <i>N</i> -{2'-[3'',4''-(1''',1''',3''',3'''-tetra- <i>t</i> -butyldisiloxane)dioxyphenyl]-2'-hydroxyethyl}- <i>N</i> -benzyl-3-aminopropionate (97).	87
2.10	Mass spectrum (CI, NH ₃) fragmentation pattern of butyl <i>N</i> -[2'-(3'',4''-diphenylmethylenedioxyphenyl)-2'-hydroxyethyl]- <i>N</i> -benzyl-3-aminopropionate (104 , R= n-Bu).	92
2.11	Mass spectrum (FAB) fragmentation pattern of ethyl <i>N</i> -[2'-(3'',4''-dihydroxyphenyl)-2'-hydroxyethyl]-3-aminopropionate (74 , R= ethyl).	96
2.12	Mass spectral fragmentation (CI, NH ₃) and EI pattern of ethyl <i>N</i> -[2'-(3'',4''-dipivaloyloxyphenyl)-2'-hydroxyethyl]-3-aminopropionate (107).	107
6.1	Possible routes of hydrolysis of ethyl <i>N</i> -[2'-(3'',4''-dipivaloyloxyphenyl)-2'-hydroxyethyl]-3-aminopropionate (107).	205
6.2	Mechanism of chemical hydrolysis of triester (107) in potassium phosphate buffer in D ₂ O (pH 8.17, pD 8.57-acetonitrile (8:2 v/v) at 37 °C by ¹ H-NMR spectroscopy.	224
6.3	Hydrolysis of triester HCl (107) in phosphate-citrate buffer (10% acetonitrile) pH 7.4 at 37 °C with 6.29 U of porcine liver carboxyesterase by HPLC analysis.	227
6.4	Oxidation of dihydroxy acid (74 , R=H).	228
6.5	Rearrangement of the pivaloyloxy group in the catechol ring. Isomeric degradation intermediates are not detected by HPLC or ¹ H-NMR spectroscopy.	229

6.6	Intramolecular hydrogen bonding with neighbouring hydroxyl group assists the rapid hydrolysis of mono pivaloyl group in catechol.	229
6.7	Mechanism of chemical hydrolysis of dihydroxy ethyl ester (74, R= Et) in potassium phosphate buffer (10% acetonitrile) pH 8.17 (pD 8.57) at 37 °C by ¹ H-NMR spectroscopy.	236
6.8	Major products in the chemical and enzyme hydrolysis of triester (107).	237

ABBREVIATIONS

%	=	percentage
AUFS	=	absorbance unit full scale
¹ H NMR	=	proton nuclear magnetic resonance
¹³ C NMR	=	carbon nuclear magnetic resonance
cm	=	centimetres
COSY	=	correlated spectroscopy
DEPT	=	distortionless enhancement by polarisation transfer
DMF	=	dimethylformamide
DMSO	=	dimethylsulphoxide
fmol	=	femtomoles (10 ⁻¹⁵)
g	=	grammes
h	=	hours
HPLC	=	high performance liquid chromatography
Hz	=	hertz
IR	=	infra-red
KBr	=	potassium bromide
ln	=	natural logarithm (to base 2)
log	=	logarithm (to base 10)
m.p.	=	melting point
mg	=	milligrammes
MHz	=	megahertz
min	=	minutes
ml	=	millilitres

mmol	=	millimoles
mol	=	moles
MTX	=	methotrexate
μl	=	microlitres
μg	=	microgrammes
μmol	=	micromoles
PBS	=	phosphate buffered saline
PG	=	propylene glycol
pK _a	=	log ₁₀ dissociation constant
PLCE	=	Porcine liver carboxyesterase
pmol	=	picomoles (10 ⁻¹²)
psi	=	pressure per square inch
PUVA	=	psoralen plus UV-A
r	=	correlation coefficient
R _f	=	relative front
rpm	=	revolution per minute
SAR	=	structure-activity relationship
sem	=	standard error of the mean
THF	=	tetrahydrofuran
6-TG	=	6-thioguanine
t _L	=	lag time
t _R	=	retention time
UV	=	ultra-violet
v/v	=	volume in volume
°C	=	degrees Celsius

CHAPTER ONE

INTRODUCTION-PSORIASIS

1.1 PSORIASIS

Dermatological disorders affect some 20% of the UK population with psoriasis being one of the most prevalent with a 2 to 6% incidence nationwide. Psoriasis¹ is characterized by epidermal proliferation and inflammation resulting in the appearance of elevated erythematous plaques, which in severe cases may involve the entire body surface. Psoriasis occurs most commonly on the skin of the extensor surfaces of the elbows and knees, but may affect any part of the body including scalp and genitalia, however it is uncommon on the face. The erythema is due to proliferation of dermal blood vessels, but this effect, and the accumulation of lymphocytes and histocytes in the dermal papillae are probably secondary to the changes in the epidermis.

The aetiology of psoriasis is multifactorial with a genetic predisposition combining with environmental trigger-factors to initiate the production of skin lesions. The most important triggering and aggravating factor in psoriasis is psychological stress. Hormonal and/or immunological processes may be influenced by stress, but any theories linking these processes with psoriasis are, at this time, speculative considering the lack of understanding of the biological effects of stress.

The progress of the disease often follows a cycle of remission and exacerbation and the aim of the therapy is to ameliorate the symptoms of psoriasis rather than exercise a total cure. Thus, chronic therapy usually involves a course of treatment followed by a period free from medication.

1.1.1 Different forms of psoriasis

Psoriasis exists in several different clinical forms.

i) *Eczematous Psoriasis*: This is characterised by erythematous, usually sharply marginated, plaques that often have silvery scales in hairy areas and severe dandruff, often with marginated plaques. Pitting of finger nails and nail separation, without evidence of fungus, occurs.

ii) *Generalised Pustular Psoriasis*: The clinical manifestation involved with this form is eruption of sterile, superficial pustules resulting from neutrophil accumulation, often in association with psoriatic lesions and causing severe disability. Generalised pustular psoriasis is classified as:

Acute generalised pustular psoriasis
 Generalised pustular psoriasis of pregnancy
 Circinate and annular pustular psoriasis
 Juvenile and infantile pustular psoriasis
 Palmoplantar psoriasis

Two forms, generalised pustular psoriasis and palmoplantar psoriasis, may be distinguished, the localised variant is usually limited to the palms and soles (palmoplantar psoriasis) whereas the less common widespread form (generalised pustular psoriasis) affects the entire body surface. The latter entity (von Zumbusch psoriasis) is one of the most severe and disabling forms of psoriasis.

iii) *Arthropathica Psoriasis*: When psoriasis is associated with rheumatoid arthritis, the condition is called arthropathica psoriasis.

iv) *Chronic Plaque Psoriasis*: This is the most common form, also known as psoriasis vulgaris, affecting some 90% of psoriatic patients. It is characterised by the sharply defined erythematous plaques, usually distributed fairly symmetrical and most commonly affecting the knees, elbows and lumbar region. The size of the lesion varies from coin-sized to large assemblies of coalescent lesions (psoriasis geographica).

v) *Guttate Psoriasis*: This form is characterised by small 'drop-like' lesions distributed over most of the body surface, particularly the trunk and the limbs. It is most commonly seen in children, often following an episode of stress or a streptococcal throat infection, and usually resolves with minimal therapy in the course of six to twelve weeks.

vi) *Erythrodermic Psoriasis*: This exfoliative form involves the entire skin surface, with generalised erythema and scaling replacing the characteristic psoriatic lesion. It may lead to systemic complications, notably thermal irregularity, dehydration and protein-loss with renal and cardiac failure in extreme cases.

1.1.2 Pathogenesis of psoriasis

The clinical manifestation of psoriasis is marked by extensive scaling and a thickened epidermis. The investigations of van Scott² suggested and quantified the concept of 'hyperplasia of psoriasis' based on the finding of a 27-fold increase in the mitotic rate of psoriatic keratinocytes, together with a decreased epidermal turnover time as compared with normal skin.

An uncontrolled cellular proliferation of epidermal cells was therefore regarded as the primary disorder in psoriasis. In psoriasis there is increased mitosis and shortened transit times to decrease cell cycle time. More recent work, however, suggests that the increased epidermal turnover in psoriasis is not due to any major alteration in the cell cycle time, but is the result of a large proliferative cell population (germinative compartment) and an increase in the proportion of these cells recruited to the active cycling phase.³

1.1.3 Cell cycle

The cell cycle can be divided into four main phases:

- G₁ interphase
- S or DNA synthesis phase
- G₂ resting phase
- M or mitotic phase

After the M phase, which consists of nuclear division (mitosis) and cytoplasmic division (cytokinesis), the daughter cells begin interphase of the new cycle. Interphase starts with the G₁ phase, in which the biosynthetic activities of the cell, which proceed very slowly during mitosis, resume at a high rate. In most cells, the DNA in the nucleus is replicated during only a limited portion of interphase; this period of DNA synthesis is called the S-phase of the cell cycle. Between the end of the M phase and the beginning of DNA synthesis, there is usually an interval, known as the G₁ phase (G= gap); a second interval, known as the G₂ phase, separates the end of DNA synthesis from the beginning of the next M phase. The S phase begins when DNA synthesis starts, and ends when the DNA content of the nucleus has doubled and the chromosomes have replicated (each chromosome now consists of two identical sister chromatids). The cell then enters the G₂ phase, which continues until mitosis starts, initiating the M phase. Cytokinesis terminates the M phase and marks the beginning of the interphase of the next cell cycle. Interphase is thus composed of successive G₁, S and G₂ phases and it normally comprises 90% or more of the cell cycle. A typical cell cycle with its four successive phases is illustrated in Figure 1.1.

The cell cycle also includes the possibility for a G₀ population. The G₀ population represents the potential proliferative cells in a resting or inactive state that can be induced to enter into the active cycling state by specific stimuli. However, G₀ cells cannot be identified by available histologic techniques and thus cannot be separated from G₁ cells microscopically. If G₀ cells are present within a defined germinative cell population, then the growth fraction (GF) will be less than unity. The GF is the ratio of actively proliferating cells per total number of cells in the defined proliferative compartment, that is, the basal cell layer.

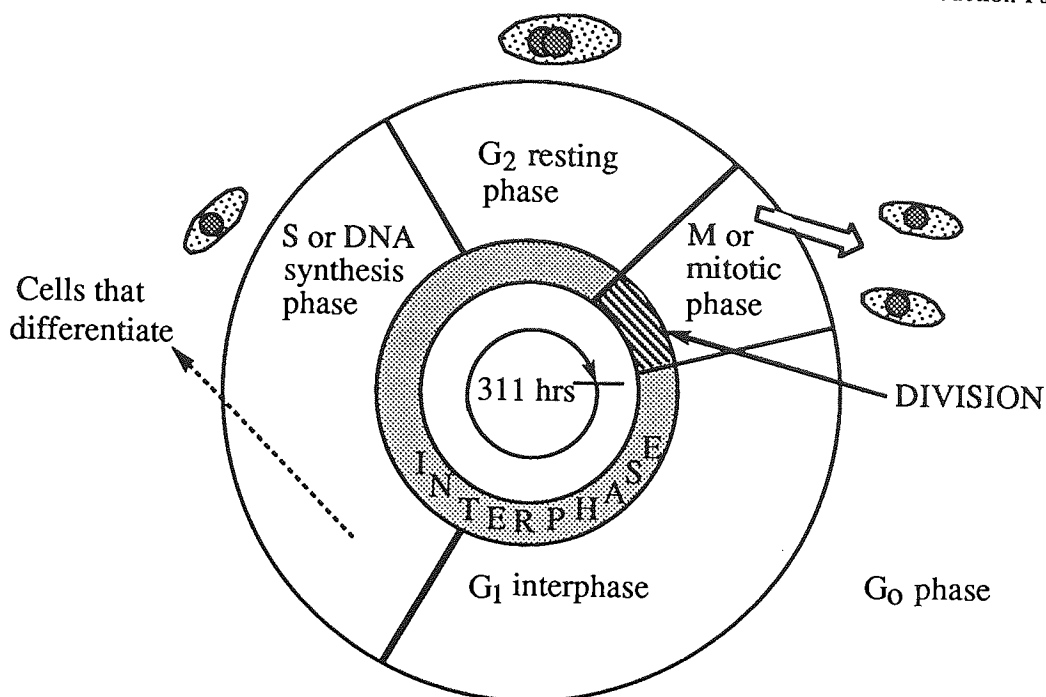


Figure 1.1: Diagram of the proliferative (germinative) cell cycle. The G_0 phase represents a potential population of cells in a 'resting' state that can be stimulated to re-enter the cell cycle by various triggers.

Psoriasis appears to involve at least three proliferative defects in the transformation of normal to psoriatic epidermis. The most significant kinetic change is due to the reduction of cell cycle (CC) duration from 311 to 36 hr (Table 1.1). The other two changes are a doubling of the proliferative cell population and an increase in the GF from 60 to 100%. The psoriatic epidermis produces 35,000 new cells per mm^2 per day in a proliferative compartment containing 52,000 cells, while the parallel values in normal epidermis are 1246 new cells per mm^2 per day with 27,000 cells.

	Duration (hr)				
	S	G_2	M	G_1	CC (total)
Normal Skin	14	10	1	286	311
Psoriatic Skin	8.5	4	0.3	23	36

Table 1.1: Cell cycle time: in normal and in psoriatic epidermis.

Early work with guinea-pig and adult human epidermis suggested that the elevation of intracellular c-AMP inhibits proliferation of cells at the G_1 and G_2 phase of the cell cycle, but not at the S phase.⁴

In psoriasis, the number of proliferating cells in lesional and uninvolved skin is, respectively, 12- and 2-fold greater than normal.⁵ Thus, in psoriasis, homeostatic restraint is defective throughout the entire epidermis.

1.1.4 Inflammatory mediators in psoriasis

One of the most prominent features of the psoriatic lesion is the accumulation of polymorphonuclear leucocytes (PMNL's) in the upper region of the epidermis where they form characteristic Munro's microabscesses and spongioform pustules.⁶ Hammarstrom and coworkers⁷ in 1975, first introduced the possibility that arachidonic acid metabolism may play a possible role in the pathogenesis of psoriasis. Arachidonic acid is an unsaturated, long-chain, fatty acid (5,8,11,14-eicosatetraenoic acid), which has been shown to be a bioprecursor for prostaglandins.

Arachidonic acid and its metabolites are elevated in psoriatic lesional epidermis and may be important to the pathogenesis of psoriasis. The enzyme phospholipase A₂, responsible for the cleavage of arachidonic acid from the cell membranes, is inhibited by c-AMP.⁴ Prostaglandin E₂, generated from arachidonic acid, is not an effective stimulator of adenylate cyclase in psoriatic epidermis.⁸ Prostaglandin E stimulates adenylate cyclase whereas prostaglandin F activates guanylate cyclase. Therefore, prostaglandins E and F are antagonists in their effect on the system of cyclic nucleotides. Perhaps a defective c-AMP generating cascade could explain the increase in the phospholipase A₂ activity in psoriasis. Also, arachidonic acid and other fatty acids are known inhibitors of adenylate cyclase,⁹ thus further interfering with c-AMP regulation.

1.1.5 Role of c-AMP in psoriasis

A defect in the cyclic nucleotide system in the epidermis, reflected by an imbalance in the ratio of c-AMP to c-GMP, has been proposed to play a central role in the pathogenesis of psoriasis.¹⁰ Normal human epidermis contains approximately 0.2-0.4 pmol of cyclic-AMP/ μ g of DNA. Cyclic-GMP is also present in the dermis but in much smaller amounts, ranging from 5 to 7 fmol/ μ g of DNA, and shows a statistically significant two-fold increase in the lesional epidermis.¹¹

Voorhees *et al*¹² suggested that the ratio of the two cyclic nucleotides c-AMP and c-GMP control skin glycogen metabolism. The ratio of c-AMP/c-GMP was found to be decreased in psoriatic skin, and this was presumed to be the cause of increased cellular proliferation and decreased glycogenolysis in psoriatic skin. The mean glycogen content ($\mu \pm \sigma$) in the normal skin is 35 ± 6.9 mg/100g of wet weight of the tissue. The mean glycogen content of the psoriatic skin is 108.6 ± 43.7 mg/100g of wet weight of tissue.¹⁰ Royer *et al*.¹³ found that c-AMP formation was significantly lower in psoriatic than in normal skin. Cyclic-AMP formation in lesional psoriatic epidermis is 25% of that in uninvolved skin. In the cell, cyclic nucleotide metabolism is important in the regulation of such diverse functions as hormone action, neuronal function, growth and differentiation, muscular contraction, cell product

secretion, and immune responses. Sutherland and Rall¹⁴ gave the name 'second messenger' to c-AMP after showing that hormones (such as catecholamines), sometimes called 'chemical messengers', first interact with liver cell membranes to release c-AMP which then subsequently activate the phosphorylase enzyme responsible for glycogen breakdown.

When the epidermal cell surface receptors are stimulated by any of the five known types of agonist (β -adrenergic agonists, prostaglandins, histamine, adenosine and cholera toxin, Figure 1.2) intracellular ATP is transformed into c-AMP *via* a GTP-coupling protein: adenylate cyclase complex. The c-AMP which is not degraded to AMP by cyclic nucleotide phosphodiesterase (PDE), is free to activate c-AMP-dependent protein kinase (PK) which in turn transfers the terminal phosphate of the ATP to a series of cellular proteins. The biological effects of these phosphorylations are dependent on the amount and type of proteins available, which are probably determined by the state of cellular activity or differentiation.¹⁵

Figure 1.2 is a simplified diagram of this proposed c-AMP cascade. Perturbations of the cell membranes or surface receptors result in the activation of adenylate cyclase through a membrane coupling system. Adenylate cyclase subsequently catalyses the production of intracellular c-AMP. The level of c-AMP is determined by the balance of this production with its breakdown catalysed by cyclic nucleotide phosphodiesterase. Any increase in c-AMP results in the activation of protein kinase, which then phosphorylates cellular protein.

Activation of protein kinase leads to the phosphorylation of a wide variety of protein substrates. Phosphorylation of membrane proteins may control membrane ionic conductance. An increased membrane permeability to Ca^{2+} may cause inhibition of adenylate cyclase and activation of guanylate cyclase. The physiological role of these protein phosphorylations remains unknown, but they could be the molecular mediators of c-AMP effects in the human epidermis. Any defect in the entire cascade could result in altered cell function.

In addition to a decreased ability of the cell surface to activate adenylate cyclase in psoriasis and decrease c-AMP transfer by gap junction, increased activity of c-AMP phosphodiesterase (c-AMP-PDE) might explain the lower c-AMP synthesizing capacity of psoriatic epidermis. A defective c-AMP cascade is related to this weakened restraint of proliferation and is important in the pathogenesis of psoriasis. Normally, the epidermis is maintained by a low level of cell proliferation sufficient to provide new cells to replace those shed from normal, undamaged skin. β -Adrenergic agonists such as catecholamines¹⁶ stimulate c-AMP production in a variety of epidermal tissue preparations.¹⁷ This response is decreased with the addition of β -antagonists (propranolol) but not with α -antagonists.

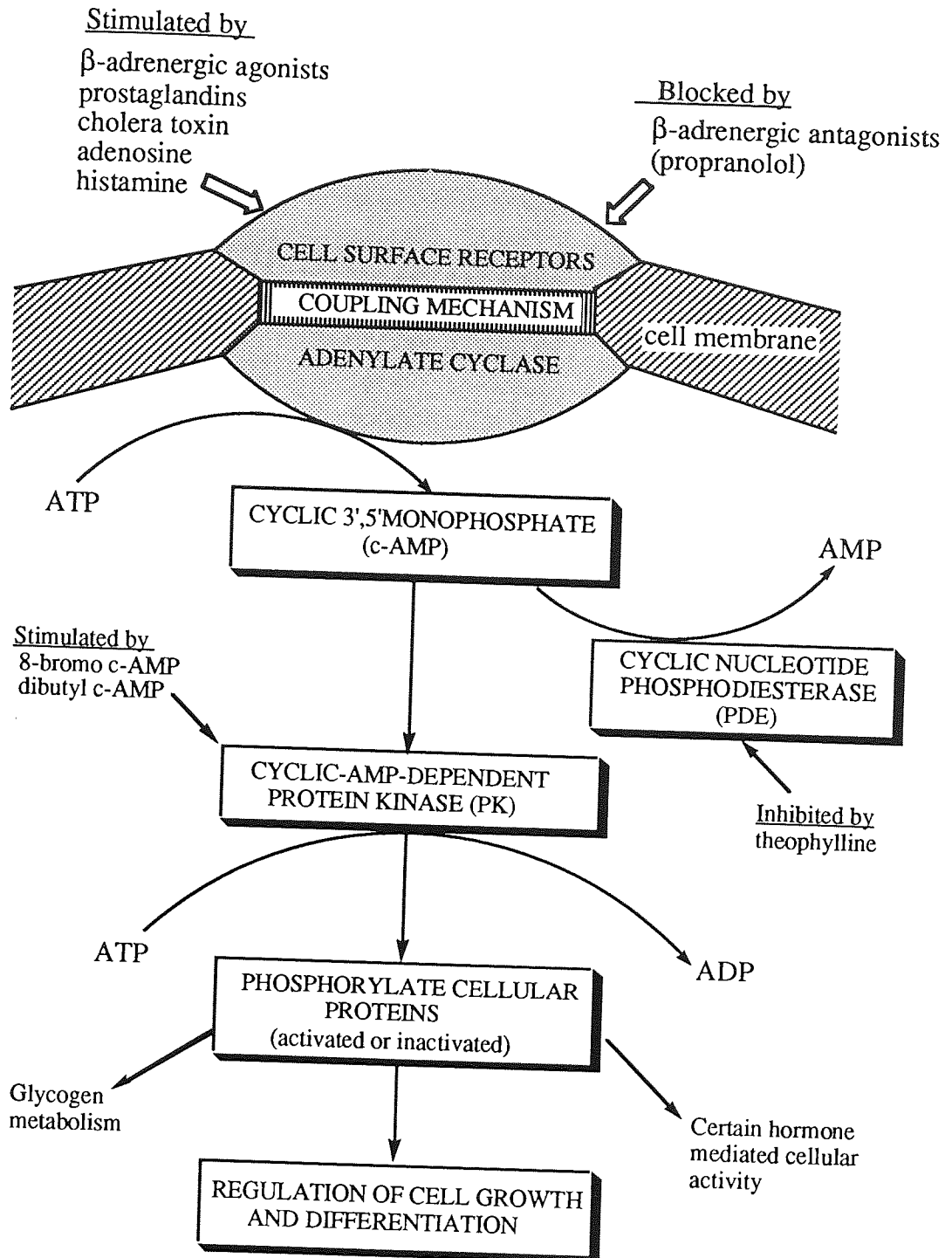


Figure 1.2: Cyclic-AMP cascade

In addition to regulation, proliferation and differentiation, c-AMP interacts with other aspects of cellular metabolism. Cyclic-AMP elevation is associated with glycogen breakdown in muscle tissue. Topical isoprenaline reduces the elevated glycogen content of lesional psoriatic epidermis.¹⁰ It is likely that c-AMP regulates glycogen metabolism in the epidermis as it does in other tissues. Glycolysis is increased in psoriatic plaques¹⁸ and is inhibited in the epidermis by c-AMP analogues and elevating agents.¹⁹

This view is supported by the finding that psoriasis is aggravated by lithium carbonate, antimalarials or β -adrenoceptor blocking drugs which decrease c-AMP.²⁰ The local application of β -adrenoceptor blocking drugs produces psoriasiform-lesions in guinea pigs,²¹ and, in latent psoriasis, β -antagonists greatly increase epidermal proliferation.²² Topical application of propranolol to the guinea-pig skin causes thickening of the skin with histological changes which strikingly resemble psoriasis in man. These findings suggest that propranolol has a direct pharmacological effect on the skin. The presence of β -adrenergic blocking agents may interfere with the normal homeostasis of the epidermis.

Compared to normal skin, uninvolved psoriatic skin has a greater proliferation response 48 hrs after propranolol injection, saline injection and or stripping. Despite the fact that tape stripping was the strongest stimulus for proliferation, propranolol was most effective in differentiating uninvolved psoriatic skin from the normal skin.²² This possible selectivity suggests that the propranolol may be biochemically altering a defective modulator of epidermopoiesis in uninvolved psoriatic skin. Tutton and Helme²³ found that propranolol shortened cell cycle time in the crypts of rat jejunum. Winchurch and Mardiney²⁴ have shown that propranolol enhances antigen-induced lymphocyte blastogenesis. Both of these effects are mediated by the β -adrenergic blocking properties of propranolol.

Drugs which increase c-AMP levels, such as sympathomimetics or inhibitors of cyclic nucleotide phosphodiesterase, inhibit epidermal mitosis. Thus a topical application of the β -adrenoceptor agonist isoprenaline has been reported to be an effective treatment for psoriasis and causes a concomitant reduction in glycogen content of the lesion to normal levels.¹⁰ The topical application of 0.1% isoprenaline sulphate in white vaseline was found to significantly decrease the glycogen content and scaliness of psoriatic skin, and cause remission of psoriasis. Isoprenaline *in vitro* stimulates adenylate cyclase to give c-AMP²⁵, and isoprenaline *in vivo* in psoriatic patients may decrease cell turnover by increasing the c-AMP/c-GMP ratio.

Inhibitors of cyclic nucleotide phosphodiesterase such as papaverine and Ro 20-1724 [4-(3'-butoxy-4'-methoxybenzyl)-2-imidazolidinone] have also been shown to be beneficial in psoriasis.²⁶ Papaverine inhibits both cyclic AMP-phosphodiesterase (c-AMP-PDE) and c-GMP-PDE whereas Ro 20-1724 inhibits c-AMP-PDE only, but both agents improve psoriasis lesions. Papaverine and Ro 20-1724 significantly increase the accumulation of c-AMP in incubated slices of involved or uninvolved psoriatic epidermis. Ro 20-1724 increased c-AMP accumulation to a greater extent than papaverine. Selective inhibition of c-AMP hydrolysis by Ro 20-1724 is responsible for its greater effectiveness in elevating c-AMP levels in slices of psoriatic epidermis. Both compounds are equally effective in inhibiting *in vitro* c-AMP-PDE activity.

Inflammation is a prominent feature of psoriatic skin lesions, and suppression of the inflammatory response is likely to be beneficial. β -Adrenoceptor agonists suppress inflammation by a multiplicity of actions including inhibition of mediator release, inhibition of leucocyte activity and a direct suppression of increased vascular permeability. For example, topical application of fenoterol (β -adrenergic agonist) suppresses increased vascular permeability induced by histamine²⁷ and locally injected terbutaline suppresses antigen-induced flares in sensitive subjects.²⁸ Further, the wheal and erythema reaction caused by intracutaneous application of histamine can be inhibited by applying fenoterol. The inhibitory effect of β -adrenergic stimulants on the histamine-induced reaction of the skin is due to the influence on the c-AMP system and the mast cells.²⁷

Salbutamol applied topically appears to have a potency similar to hydrocortisone as an anti-inflammatory agent.²⁹ Inhibition of histamine-release is accomplished partly by increasing the cellular level of c-AMP. Anti-inflammatory steroids stimulate adenylate cyclase to convert adenosine triphosphate to c-AMP, and β -adrenergic agonists stimulate adenylate cyclase at the β -adrenergic receptor. Salbutamol is relatively specific selectively stimulating β -adrenergic receptors. Salbutamol has significant topical anti-inflammatory activity and is very effective in the prevention of local inflammation. Both inflammation and proliferation are suppressed by topical application of salbutamol thus selective β_2 -adrenoceptor agonists might be effective in psoriasis. The β -adrenoceptors in the mast cells may be involved in the action of salbutamol in inflammation. The β -blocking agent propranolol interferes with the ability of salbutamol to inhibit inflammation.²⁹

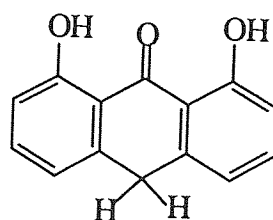
1.2 DRUGS USED IN PSORIASIS

The treatment options are many, involving topical, systemic and conditional approaches, and vary with disease severity.

1.2.1 Topical therapy and ultraviolet light

1.2.1.1 *Dithranol*

The hydroxy-anthracene derivatives, the active principles of 'Goa powder', have had an important place in the treatment of psoriasis since 1868. Dithranol or anthralin (**1**) is 1,8-dihydroxy-anthr-9-one which is used in a concentration of 0.1-3.0% as a cream or in petrolatum. It is also given in combination with salicylic acid and urea.



(1)

Dithranol inhibits glucose-6-phosphate dehydrogenase, an enzyme within the pentose phosphate shunt of the glycolytic pathway. The levels of this enzyme are elevated in psoriasis³⁰ and treatment of psoriatic lesions with anthralin results in its return to baseline values.³¹ The most important side-effect associated with dithranol is staining and irritation of the uninvolved skin.³² Dithranol in Lassar's paste is used most successfully for in-patient treatment but it stains both skin and clothing to such an extent that patient compliance is poor when used as an out-patient therapy. Proprietary dithranol containing products are more acceptable. They can be used in 'short contact regimes' being applied to the psoriatic plaques and left for up to one hour, before washing off. This method reduces dithranol burning and staining.

1.2.1.2 Coal tar phototherapy:

In 1925 Goeckerman³³ introduced the concept of combining ultraviolet radiation with coal tar. Tar products are derived either from shale (ichthammol), wood or coal. Ichthammol has less efficacy than wood tar which is not as potent as coal tar. Cade oil, derived from Juniper trees, is useful for treating thickened scalp psoriasis. Coal tar is a thick, blackish liquid obtained by the destructive distillation of bituminous coal. It contains benzene, toluene, naphthalene, anthracene, xylene, phenol, cresols, pyridine and quinoline. It has antipruritic, antiseptic and keratoplastic activity. Coal tar, in its crude state, can be used but patient compliance is very poor. Purified coal tar preparations improve compliance and as they are less of an irritant than dithranol they may be tolerated on sites where dithranol is unsuitable. Tar is used as a 1-5% ointment for the treatment of psoriasis. The tar is thought to act by depressing the rate of mitosis of the epidermal cells and to act synergistically with ultraviolet light.³⁴ They are often given in combination with corticosteroids, or other drugs. Adverse reactions associated with coal tar are primary irritation, folliculitis, and tar acne as well as allergic reactions. Phototoxic reactions from crude coal tar may be seen in patients who have not been warned against sun exposure during the summer.

1.2.1.3 Topical corticosteroids:

Some fluorinated corticosteroids with good percutaneous absorption characteristics have recently been synthesised and evaluated in animal models of inflammation and psoriasis with encouraging results, some of the compounds having activity comparable with that of hydrocortisone³⁵ (Table 1.2). Triamcinolone (2), dexamethasone (3), betamethasone (4), fluocinide (5) and betamethasone-17-valerate (6) are commonly used topical fluorinated corticosteroids with good percutaneous penetration (Figure 1.3).

Substances	Concentration (%)
Triamcinolone (2)	0.025 - 0.05
Dexamethasone (3)	0.1
Betamethasone-17-valerate (6)	0.1
Fluocinolone acetonide (Fluocinide) (5)	0.01 - 0.2

Table 1.2 : Anti-inflammatory steroids used for topical application in psoriasis.

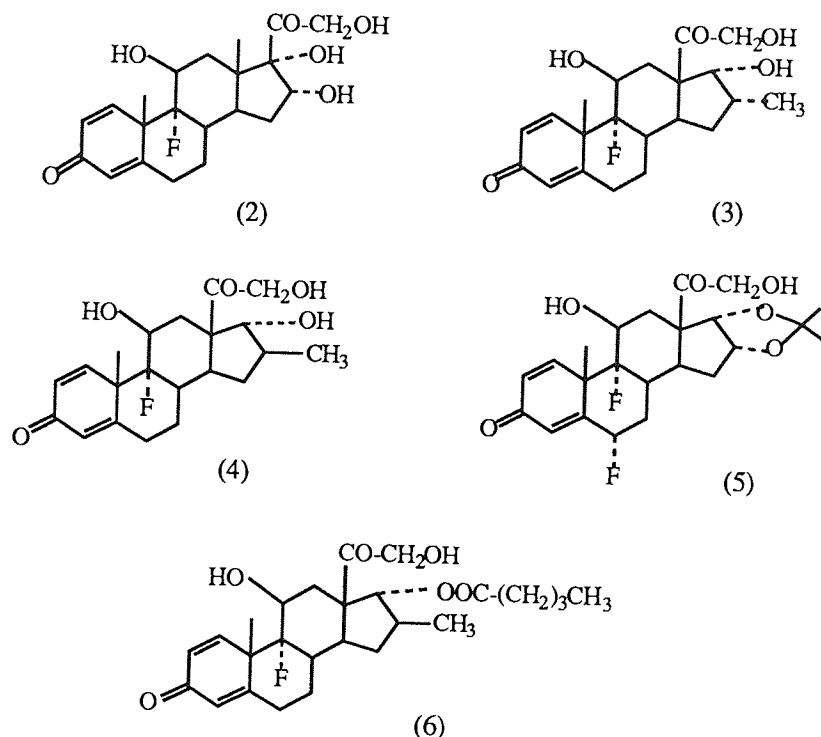


Figure 1.3: Fluorinated corticosteroids used topically in psoriasis

Fried and Sabo in 1953 synthesized fluorinated corticosteroids and these steroids have much more penetration and mineralocorticoid activity.³⁶ Prodrugs are used to enhance absorption eg. acetamide, acetate, valerate. These steroids are used in concentrations of 0.01-0.1% in cream, lotion and ointment (Table 1.2, Figure 1.3).

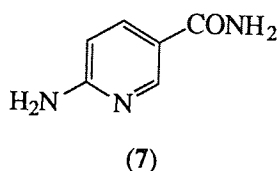
Hydrocortisones and the fluorinated derivatives are used in psoriasis due to their vasoconstrictor and anti-inflammatory effects, and reduce epidermal cell turnover; but their long-term side effects prohibit their prolonged use in extensive psoriasis. They are, however, useful for treating small areas, the scalp and the flexures. Side-effects associated with corticosteroids are many and include acne, perioral dermatitis, rosacea, striae, atrophy, purpura, glaucoma, allergic contact dermatitis, plasma cortisol suppression, Cushing's syndrome and cataracts.³⁷

1.2.1.4 *The vitamin D analogues:*³⁸

The vitamin D analogue, calcipotriol, inhibits cell proliferation and stimulates differentiation of keratinocytes correcting the abnormal cell turnover that characterises psoriasis. Unlike naturally occurring vitamin D, it has less effect on calcium metabolism, so the risks of hypercalcaemia and hypercalciuria are reduced. It is available as a 0.005% ointment as a smooth, soft white cream. Side-effects associated with calcipotriol are transient irritation, dermatitis, pruritus, aggravation of psoriasis, photosensitivity.

1.2.1.5 *6-Aminonicotinamide:*

In 1975, Zackheim³⁹ introduced 6-aminonicotinamide (7, 6-AN) for the topical treatment of psoriasis as a cream or solution. Nicotinamide (niacinamide) analogues constitute a new class of compounds found to clear psoriatic lesions by topical application.



Nicotinamide adenine dinucleotide (NAD) and NAD phosphate (NADPH) play a key role in many important metabolic processes by acting as hydrogen and electron transfer agents. 6-AN can substitute for nicotinamide, to give 6-AN-NADP which blocks the glycolytic pentose phosphate pathway (hexose monophosphate shunt) at two points.⁴¹ This prevents the formation of ribose needed for the formation of RNA and DNA.⁴⁰ However, 6-AN is toxic and teratogenic.⁴² The principal limiting factors were oral complications, eighth nerve (auditory) damage and CNS toxicity.

1.2.1.6 *Ultraviolet phototherapy:*

Ultraviolet radiation⁽⁴³⁻⁴⁴⁾ in psoriasis causes a decrease in DNA synthesis in the hyperproliferative cells, which influences the return of more normal cell kinetics. Ultraviolet-B (UVB) may decrease macromolecular synthesis in all psoriatic cells or there may be selective inhibition or killing of a smaller population of highly proliferative cells. Wave length (λ) of broad band UVB is from 290-320 nm, narrow band UVB is 312 ± 2 nm and UVA from 320-400 nm.⁽⁴⁵⁻⁴⁶⁾ The major acute side effects of phototherapy are the manifestation of inflammation, redness, swelling, heat and pain. There is a potential risk of skin cancer. The narrow band UVB has less burning and carcinogenic potential than broad band UVB.

1.2.2 SYSTEMIC THERAPY

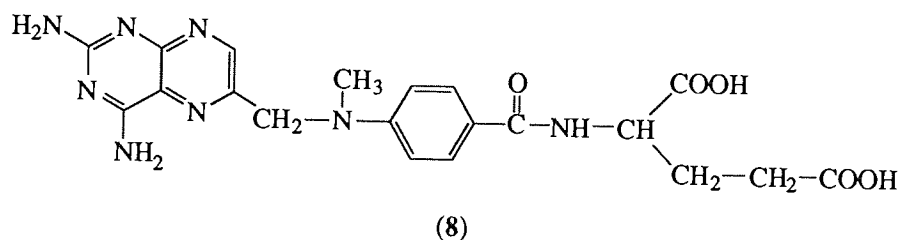
Systemic therapeutic regimens are usually reserved for severe recalcitrant cases of psoriasis and include the use of vitamin A analogues, anti-metabolites and steroids.

1.2.2.1 *Immuno-suppressant:*⁴⁷

Cyclosporin is highly effective in severe psoriasis refractory to other treatments. It is a lipophilic orally active cyclic peptide. Its exact mechanism of action is not fully understood, but one possibility is that it inhibits epidermal hyperproliferation by suppressing T-lymphocyte activity in the dermis and epidermis of psoriatic skin. Side effects associated with cyclosporin are renal and hepatic dysfunction, hypertension, tremor, GI disturbances, lymphoproliferative disorders, burning sensations (feet and hands), fatigue, muscle weakness or cramp.

1.2.2.2 *Methotrexate:*

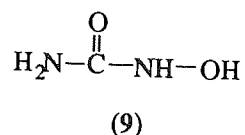
Gubner⁴⁸ noted the rapid clearing of the psoriatic skin lesions in a patient with rheumatoid arthritis who was treated with aminopterin, which was later replaced by a more stable derivative methotrexate. Methotrexate (**8**, MTX, 4-amino-10-methyl pteroyl-glutamic acid), a structural analogue of folic acid, is a potent inhibitor of the enzyme dihydrofolate reductase which catalyses the formation of dihydro- and tetrahydro-folic acid from folic acid.



Tetrahydrofolic acid is the precursor of N⁵,N¹⁰methylene tetrahydrofolic acid, an essential cofactor in the conversion of deoxyuridylic to thymidylic acid, which is required for the synthesis of DNA. There may also be direct inhibition of thymidylate synthetase by MTX. In humans, MTX appears to inhibit DNA synthesis and results in cell death if MTX is present during the S-phase of the cell cycle. Methotrexate is given as an intravenous or intramuscular injection. It is used for psoriatic erythroderma, psoriatic arthritis, acute pustular psoriasis (von Zumbusch type) and localized pustular psoriasis. The main side effect of MTX is hepatotoxicity.⁴⁹

1.2.2.3 *Hydroxyurea:*

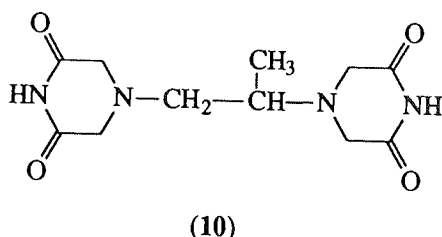
In 1970, Leavell and Yarbro⁵⁰ introduced hydroxyurea (9) in the treatment of psoriasis.



Hydroxyurea inhibits DNA synthesis,⁵¹ without significantly inhibiting RNA or protein synthesis. It is used for psoriasis vulgaris, generalized pustular psoriasis, chronic palmoplantar pustular psoriasis and erythrodermic psoriasis. Its principal toxic effects are on the bone marrow. Levels of haemoglobin, white cells, and platelets may all be depressed. The bone marrow rapidly becomes megaloblastic,⁵² reflected in marked macrocytosis in the peripheral blood.

1.2.2.4 *Razoxane:*

Razoxane [10, (+/-) 1,2-bis(3',5'-dioxopiperazin-1'-yl) propane] is a derivative of the chelating agent ethylenediamine tetra acetic acid (EDTA).



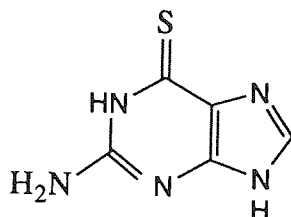
Razoxane was given orally in 125 mg tablets three times daily for two consecutive days each week. Razoxane has a potent bone-marrow-suppressive effect resulting in the depletion of the circulating neutrophil polymorphs. These cells play an important role in the pathogenesis of psoriasis, and it could be argued that a reduction in their levels may contribute to the antipsoriatic effect of the drug.

All types of cutaneous psoriasis are responsive to treatment with razoxane, including palmoplantar, and generalized pustular psoriasis.⁵³ Adverse side effects of razoxane include bone marrow suppression, neutropenia and anemia. It is no longer used as a therapy.

1.2.2.5 *6-Thioguanine:*

In 1964, Demis⁵⁴ and co-workers, treated several immunologic and dermatologic diseases with 6-thioguanine (11, 6-TG, 2-amino-6-thiopurine). The beneficial effect of the purine analogues 6-TG and 6-mercaptopurine (6-MP) on psoriasis is likely to be due to inhibition of DNA synthesis. This is believed to be secondary to inhibition of purine ring biosynthesis and nucleotide interconversion.⁵⁵ 6-Thioguanine is commercially available as 40 mg scored

tablets (Burroughs-Wellcome). The usual dosage for psoriasis is 40-80 mg per day for an average-sized adult. The principal toxicity from 6-TG is haematopoietic.

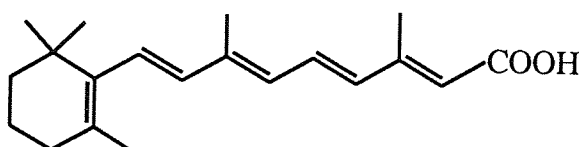


(11)

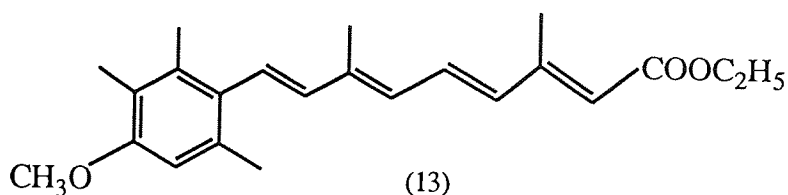
1.2.2.6 The vitamin A derivatives (retinoids):

Studies of vitamin A deficiencies induced in animals have shown epithelial changes such as hyperkeratosis of the skin and squamous metaplasia of mucous membranes.⁵⁶ These observations led to the conclusion that vitamin A is an 'anti-keratinising factor'.⁵⁷ Vitamin A (12, retinoic acid) was used for the first time in dermatology by Stuetgen⁵⁸ who showed that its topical application was beneficial in the treatment of hyperkeratoses. The combination of oral and topical administration of retinoic acid was promising for the treatment of psoriasis.⁵⁹

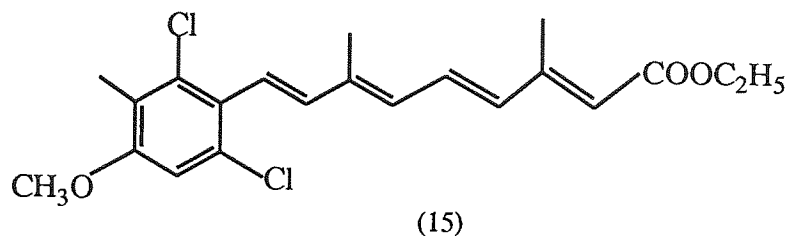
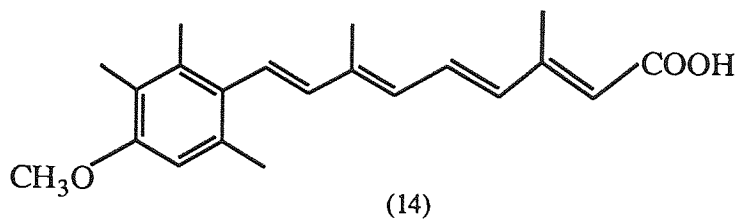
Etretinate (13), an ester analogue of retinoic acid, is used in the treatment of generalized pustular psoriasis, localized guttate psoriasis, recalcitrant pustular psoriasis, palmoplantar psoriasis, erythrodermic and arthropathic psoriasis. It is given orally at a dose of 1 mg/kg body weight per day. Other analogues used are Ro 10-1670 (14, the free acid analogue of 13), and Ro 12-7554 (15).



(12)



(13)



Retinoids show a strong keratolytic activity and lead to restoration of a normal epidermis including reappearance of the granular layer, disappearance of parakeratosis, and reduction of psoriasiform acanthosis.⁶⁰ A decrease of the labeling index for [³H]-thymidine incorporation and a prolonged time of DNA synthesis in human epidermis is also observed.⁶¹ However, retinoids also cause an increase in the serum lipids which is associated with the subsequent development of coronary artery disease. Hypertriglyceridemia in excess of 1000 mg/dl may result in acute pancreatitis.

The vitamin A derivative, acitretin, is used by dermatologists in hospital practice for severe, extensive, refractory psoriasis. It is available as 10 mg and 25 mg capsules. Side effects associated with acitretin are dryness, erosion of mucosa, erythema, pruritus, alopecia, hepatotoxicity, change in serum lipids, nausea, headache, drowsiness, sweating and calcification (long term therapy).

The majority of these treatments are only moderately effective or are associated with undesirable levels of toxicity, and no ideal regimen exists. Attempts to circumvent systemic toxicity by the topical administration of antiproliferative agents have met with limited success. Problems due to percutaneous absorption, particularly following long-term treatment, limit the dose of the drug that may be safely applied to the skin. These deficiencies with the currently available topical medication warrant the development of more effective topical antipsoriatic drugs.

1.3 β -ADRENOCEPTOR AGONISTS

1.3.1 Adrenoreceptors

Adrenoreceptors are classified into α - and β - types depending upon their action on different parts of the tissue.⁶² The classification of α - and β - types is well-accepted and highly selective agonists and antagonists of α - and β -receptors have been developed. In general, adrenergic contraction of smooth muscle is mediated by the α -receptors, and stimulation of heart muscle and relaxation of smooth muscle by the β -receptors (Table 1.3).

α -Receptor		β -Receptor	
Agonists	Antagonists	Agonists	Antagonists
Fenoxazoline	Chlorpromazine	Cyclobutyl-	Butoxamine
Methoxamine	Ergotamine	Noradrenaline	Dichloro isoprenaline
Naphazoline	Indoramine	Dobutamine	
Oxymetazoline	Phenoxybenzylamine	Ethyl noradrenaline	Labetalol
Tetrahydrozoline	Phentolamine	Hexaprenaline	Metoprolol
Tramazoline	Piperoxane	Isoetharine	Pindolol
Tymazoline	Thymoxamine	Isoprenaline	Practolol
Xylometazoline	Yohimbine	<i>N-t</i> -Butyl-noradrenaline	Propranolol
		Trimetoquinol	Sotolol

Table 1.3: α - and β -Receptor agonists and antagonists

Trimetoquinol is a cyclic catecholamine which lacks the *N*-alkyl amino ethanol side chain. Trimetoquinol produces its effects by stimulating β -receptor. Although it lacks β -hydroxyl group, it is about equipotent with isoprenaline.

1.3.2 Sub-classification of β -receptors

Lands and co-workers⁶² classified β -receptors into two distinctively different groups according to the responses of different organs to catecholamines. Lands concluded that there were two types of β -receptors which he defined as β_1 (acting on the heart and smooth intestine muscle) and β_2 (in lungs and blood vessels, vascular smooth muscle, bronchi, uterus and arteries in the skeletal muscle). β_1 -Receptors activate lipolysis and β_2 -receptors may be concerned with glycogenolysis (Table 1.4). There are many papers from both pharmacological and biochemical research groups suggesting that tissues contain a majority of one subtype of β -receptor. For example, atrial tissue contains an excess (4:1) of β_1 -receptors⁶³ while bronchial tissue contains an excess (3:1) of β_2 -receptors, suggesting that absolute tissue selectivity of drug action by β_1 - or β_2 -specific ligands is not possible. These results were confirmed by Heitz and coworkers⁶⁴ in human left atrium and ventricle (ratio

approximately 2:1), however Purdy and co-worker⁶⁵ have shown that bovine coronary artery contains a homogeneous population of β_1 -receptors.

β -Receptor antagonists			
β_1 -Receptor	β_2 -Receptor	Non-specific antagonists	Antagonists for β_1 , β_2 and α
Acebutalol	Butoxamine	Penbutolol	Labetalol
Atenolol	α -Methyldichloro-	Pindolol	
Metoprolol	isoprenaline	Propranolol	
Practolol		Sotolol	

Table 1.4: β_1 and β_2 -Receptor antagonists

1.3.3 Ligand-binding sites of β -adrenoceptor

A wide variety of hormone and neurotransmitter receptors mediate their actions through interaction with guanine nucleotide-binding regulatory proteins (G proteins). Receptors of this class respond to a structurally diverse range of agonists, including small molecules such as biogenic amines, peptides and larger proteins such as thyrotropin.

Hydropathicity analysis of the primary structures of these proteins suggests⁶⁶ that they contains seven transmembrane α -helices (Figure 1.4). β -Adrenoceptor ligands are protonated amines, suggesting that the binding pocket of the receptor should contain an acidic counterion for the amine moiety. Substitution of Asp and Glu residues located within the hydrophobic area of the β -adrenoceptor with the neutral amino acids, did not effect the binding properties of the receptor, but replacement of Asp¹¹³ in the third hydrophobic region with an Asn or a Glu residue resulted in a dramatic decrease in the affinity of the receptor both for agonists and antagonists.⁶⁷ This Asp¹¹³ residue is preserved in all other G protein-coupled receptors that bind with the biogenic amine.

A combination of genetic and biochemical analysis suggested that the catechol hydroxyl groups of agonists interact with side chains of the Ser residues at position 204 and 207 in the fifth transmembrane helix of the receptor.⁶⁸ Substitution of each of these Ser residues with an Ala, which removes the hydroxyl group from the amino acid side chain, decreases the affinity of the receptor for β -adrenoceptor agonist, without affecting antagonist affinity. Similar effects were observed when the catechol hydroxyl groups of the agonist isoprenaline were substituted with hydrogen atoms, suggesting that Ser²⁰⁴ and Ser²⁰⁷ interact with the catechol hydroxyl groups of agonist ligands. There is specific hydrogen bonding between the *meta*-hydroxyl group of the agonist and the side chain of Ser²⁰⁴ in the β -adrenoceptor, and a second specific interaction between the *para*-hydroxyl group of the ligand and Ser²⁰⁷ in the receptor.

Similar mutagenesis studies have provided evidence for an interaction of the agonist (perhaps involving the phenyl ring) with the side chain of Phe²⁹⁰ in the sixth transmembrane helix of the β -adrenoceptor and for other ligand interactions involving residues in helix 2, 4 and 7.⁶⁹⁻⁷¹

Thus a model has emerged for the ligand-binding site of the β -adrenoceptor in which the ligand is bound within the hydrophobic core of the protein, by interaction with the transmembrane helices by specific molecular interactions between amino acid residues in the receptor and functional groups on the ligand. On the basis of the seven transmembrane helical bundle model for the β -adrenoceptor, the residues shown by genetic experiments to be important for ligand binding (Asp¹¹³, Ser²⁰⁷, Ser²⁰⁴ and Phe²⁹⁰) are located on the membrane-spanning helices buried approximately 30-40% (>11 Å) of the way into the bilayer.⁷²

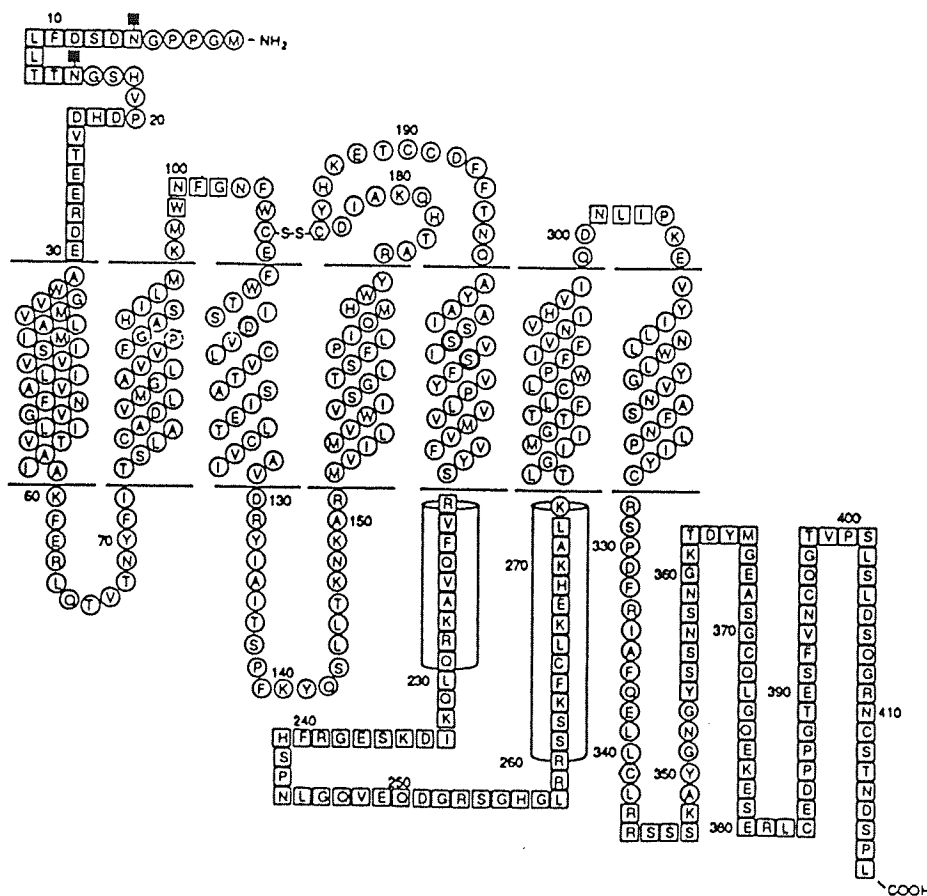


Figure 1.4: Primary structure and topological model for the β -adrenoceptor.

The receptor sequence is arranged according to the seven transmembrane helical model, with the extracellular face of the membrane at the top and the cytoplasmic region at the bottom. The single letter amino acid code is used, with residues numbered beginning at the *N*-terminus. Amino acid residues shown in squares could be deleted without affecting ligand binding or protein folding. The solid boxes are attached to the two Asn residues near the *N*-terminus that serve as glycosylation sites. The postulated disulfide bond between Cys¹⁰⁶ and Cys¹⁸⁴ is shown. Asp¹¹³, Ser²⁰⁴, Ser²⁰⁷ and Phe²⁹⁰ residues involved in ligand binding to the receptor, are encircled in bold.

Figure 1.5 represents a hypothetical working model for receptor-ligand interactions. The ligand is postulated to intercalate into the hydrophobic core of the receptor, having specific points of contact with amino acid residues on several of the hydrophobic helices. The amine substituents of the agonist and antagonist interact with the carboxylate side chain of Asp¹¹³ in helix III. The agonist catechol hydroxyl groups appear to be anchored by hydrogen bonds to the hydroxyl side chains of Ser²⁰⁴ and Ser²⁰⁷ in helix V, whereas antagonists do not interact with these Ser residues. The aromatic group interacts with Phe²⁸⁹ and Phe²⁹⁰ in helix VI.

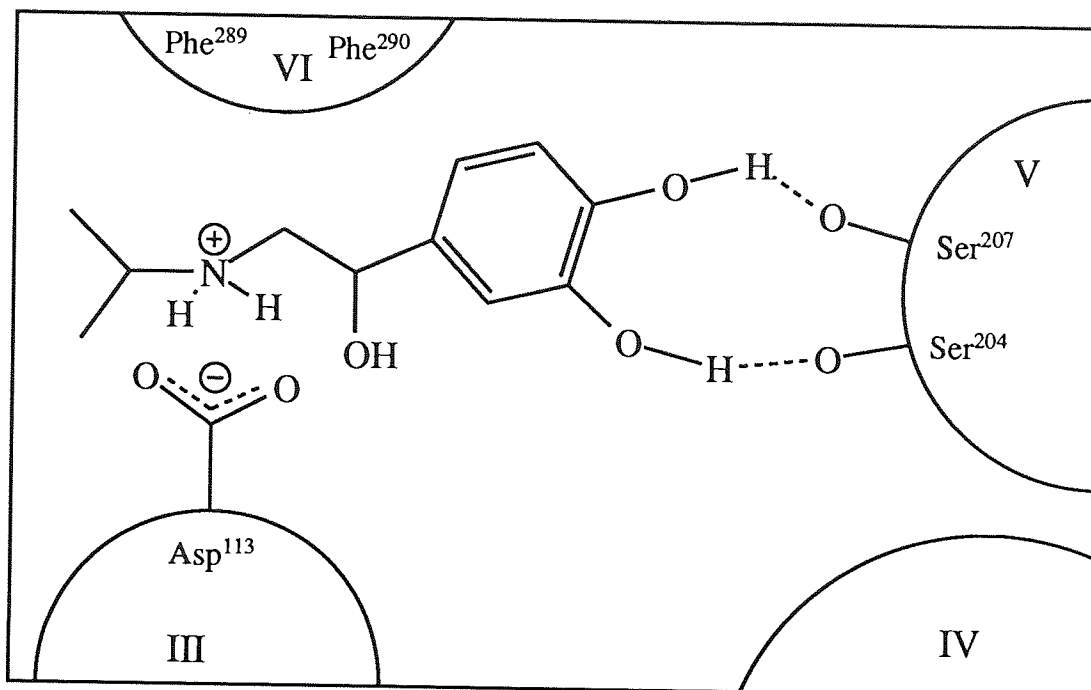


Figure 1.5: Model of the ligand-binding site of the β -adrenergic receptor. Isoprenaline is shown interacting with several of the transmembrane helices. The side chains of Asp¹¹³ in helix III and of Ser²⁰⁴ and Ser²⁰⁷ in helix V are shown in their postulated interaction with the functional moieties of the β -adrenoceptor agonist.

The binding of a ligand to its specific receptor triggers a signal transduction cascade *via* activation of a G protein, which acts as an intermediate to stimulate or inhibit one of many specific effector systems. Effector enzymes and ion channels that are coupled to G protein-mediated pathways include adenylyl and guanylyl cyclases, phospholipases A and C, Ca²⁺ and K⁺ channels, and phosphodiesterases (Figure 1.6).

1.3.4 Mechanism of action of β -adrenoceptor agonists

β -Adrenoceptor agonists bind with the β -receptor and activate the enzyme adenylyl cyclase which catalyses the formation of c-AMP from ATP.⁽⁷³⁻⁷⁵⁾ c-AMP regulates the phosphorylation of a membrane protein which in turn may control membrane ionic conductance. An increased membrane permeability to Ca²⁺ may cause inhibition of adenylyl cyclase and activation of guanylate cyclase, which catalyses the formation of 3',5'-c-GMP. The level of c-AMP is controlled by its formation utilising adenylyl cyclase and its metabolism to 5'-AMP catalysed by cyclic nucleotide phosphodiesterase (PDE) (Figure 1.6).

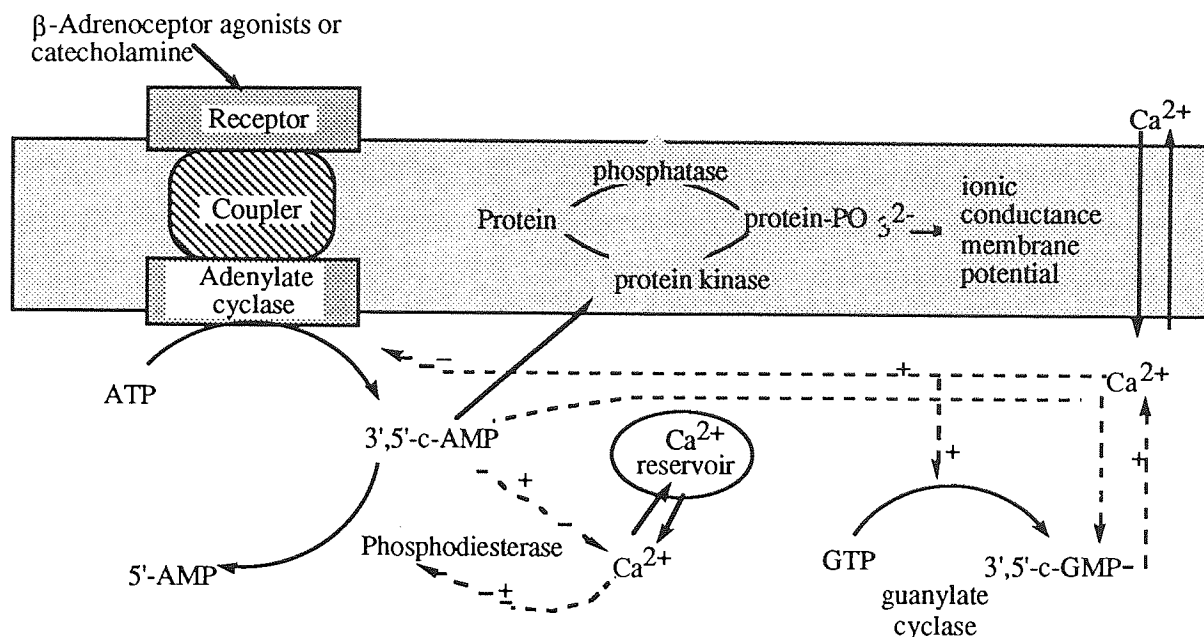


Figure 1.6: Adenylate cyclase activation by β -adrenoceptor agonists

1.3.5 Chemical basis for β -adrenoceptor stimulation

Larsen⁷⁶ proposed a model for the interaction of a β -agonist at the β -receptor based on the formation of a quinone methide intermediate involving a nucleophile on the receptor (Figure 1.7). The quinone methide (**18**) is generated from the β -adrenoceptor agonist (**16**) by activation of the benzylic hydroxyl group by an electrophile (E^+), followed by elimination of the activated hydroxyl group from (**17**). The quinone methide then reacts with the receptor to yield (**19**), this presumably being the activation step. This mechanism is able to explain why the *p*-hydroxyl group in catechol is more important than the *m*-hydroxyl group (see section 1.3.6.1, effect of modification of the catechol group). This hypothesis is no longer accepted due to the following reasons:

- 1) Compound (**18**) loses chirality before coupling to receptor implying chirality does not play any role in contrast to what is actually observed.
- 2) Compound (**19**) forms a covalent bond with the receptor. β -Adrenergic activity of most compounds is reversible, therefore covalent coupling between agonist and receptor is unlikely.

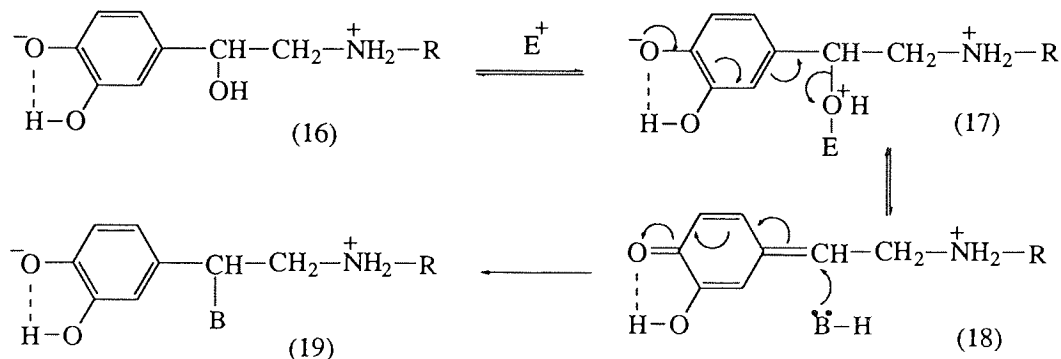
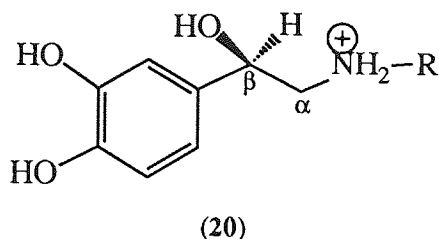


Figure 1.7: A proposed chemical basis for β -adrenoceptor stimulation

1.3.6 Structure-activity relationship of β -adrenoceptor agonists

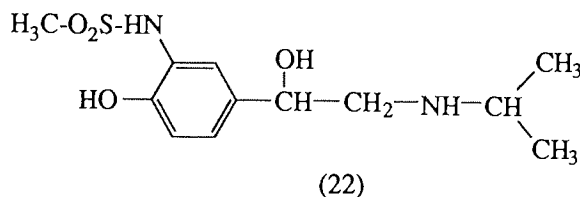
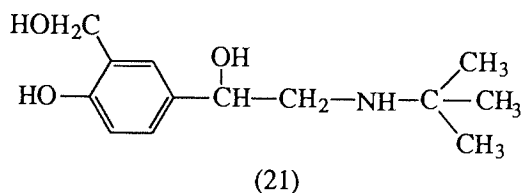
Since the pharmacological properties of β -adrenoceptor agonists (20) are well known and their structure-activity-relationship has been reviewed,⁷⁷ only a brief account is given here in order to clarify the subsequent work. The requirements for β -adrenoceptor agonists are summarised as:



- a) an aromatic six-membered ring system.
- b) an ethylamino side-chain.
- c) a hydroxyl group on the β -carbon and an *R*-configuration at the β -carbon atom.
- d) a cationic nitrogen atom with primary or secondary substitution.

1.3.6.1 Effect of modification of the catechol group

A catechol group is very important for β -agonistic activity. In the catechol substituent, the *p*-hydroxyl group is more important than the *m*-hydroxyl group. The latter may be replaced by other groups such as HOCH₂- (salbutamol, 21), CH₃SO₂NH- (soterenol, 22), H₂NCONH- (carbuterol, 23) and CH₃SO₂CH₂CH₂- (sulfonterol, 24), but the *p*-hydroxyl group cannot be replaced.



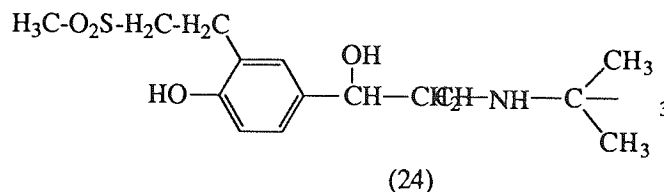
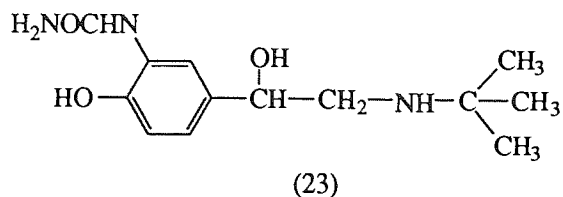


Table 1.5 shows that deletion of either phenolic group from isopropyl norepinephrine (No. 1 in Table 1.5) or its analogues leads to compounds with negligible activity at the β -receptor.

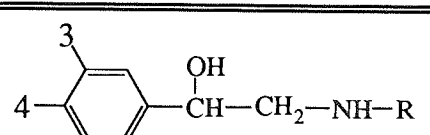
					
Substituents group				Relative Activity	
No.	4	3	R	Vasodepressor	Bronchodilator
1.	HO	HO	C ₃ H ₇ ⁱ	100	100
2.	H	HO	C ₃ H ₇ ⁱ	1.3	1.2
3.	HO	H	C ₃ H ₇ ⁱ	0.1	Very weak
4.	HO	HO	C ₂ H ₅	50	—
5.	H	HO	C ₂ H ₅	Inactive	—
6.	HO	H	C ₂ H ₅	Inactive	—
7.	HO	HO	C ₃ H ₇	20	—
8.	H	HO	C ₃ H ₇	Inactive	—
9.	HO	H	C ₃ H ₇	Inactive	—

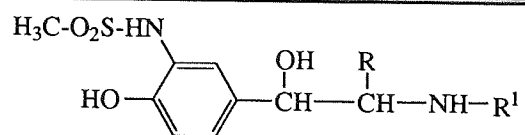
Table 1.5: Influence of catechol function on β -agonist activity

1.3.6.2 Effect of the β -hydroxyl group

A hydroxyl group on the β -carbon with R-configuration is important for β -agonistic activity. Removal of the β -hydroxyl group reduces activity considerably.^{78,79} The S-enantiomers are relatively inert. The β -hydroxyl group is very important for generating optimum agonist activity at both the α - and β -receptors.

1.3.6.3 Effect of α -substitution on the side-chain

Introduction of α -alkyl groups into the ethylamine side-chain reduces activity. The α -propyl and isopropyl analogues are at least 1000 times less active, and the α -methyl and ethyl analogues about 10 times less active than isoprenaline as bronchodilators in anaesthetised guinea-pig.⁸⁰ α -Methyl substitution reduces the α - and β -receptor activity considerably, as shown in Table 1.6

				
R	R ¹	Relative Stimulant Activity		
		α -Receptor	β -Receptor	
		Rat Seminal Vesicle	Rat Uterus	Guinea Pig Trachea
H	H	7.8	0.003	0.005
Me*	H	1.9	0.002	0.001
H	Me	12	0.001	0.03
Me*	Me	1.0	0.005	0.02
H	CH(Me)CH ₂ C ₆ H ₃ (O ₂ CH ₂)-3,4	—	4.0	4.0
Me*	CH(Me)CH ₂ C ₆ H ₃ (O ₂ CH ₂)-3,4	—	0.04	0.04
Norepinephrine		1.0	—	—
Isopropyl norepinephrine		—	1.0	1.0

* = Erythro racemates

Table 1.6: Effect of α -methyl substitution on α - and β -receptor activities of 5'-(2-amino-1-hydroxyethyl)-2'-hydroxy alkanesulfonamides

1.3.6.4 Effect of *N*-substitution

Lengthening the isopropyl chain in isoprenaline gives less potent compounds, but additional branching as in the *tert*-butyl homologue, increases activity. Table 1.7 shows a decrease in α -activity and an increase in β -activity with increasing size of the *N*-substituent.

The *N*-isopropyl or *N*-*t*-butyl substituents confer optimum activity and in a variety of *N*-substitution patterns the presence of the $-\text{C}(\text{CH}_3)_2-$ function adjacent to the nitrogen is very important for high activity (Table 1.7). Addition of further hydrocarbon bulk alone does not increase activity but introduction of a hydroxyl group in the *N*-phenyl alkyl series, increases the β -receptor activity considerably (Table 1.8). It has been suggested that the phenyl group in those compounds contributes to specific binding with the receptor and that the phenolic group reinforces this effect by hydrogen bonding or by interaction with a basic centre in the receptor.

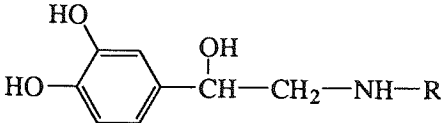
					
R	α -Receptor (Rat Vas Deferens)			β -Receptor (Calf Trachea)	
	i.a.	pD ₂	pA ₂	i.a.	pD ₂
H	1	5.4		1	5.8
CH ₃	1	5.9		1	6.7
C ₂ H ₅	0.9	5.2		1	7.2
C ₃ H ₇	0.3	3.3		—	—
C ₃ H ₇ ⁱ	0.6	3.0		1	7.5
C ₄ H ₉ ^t	0		3.0	1	7.6
CHMeCH ₂ Ph	0		4.4		
CMe ₂ CH ₂ Ph	0		5.9		

Table 1.7: Effect of *N*-substitution on α - and β - activity of DL-norepinephrine

The potency of the compounds is expressed as pD₂ obtained from log dose-response curves following intravenous injections into pithed rats.

$$pD_2 = -\log [IC_{50}]$$

The concentration of agonist giving rise to half the maximal response is equal to IC₅₀. The antagonists can be characterized by a pA₂ value which is the negative logarithm of the molar concentration of antagonist. The potency of an antagonist can be determined from the agonist response in the absence ([D]₀ = IC₅₀) and presence ([D]_A = IC₅₀) of antagonist. When the concentration of antagonist (2[A]) is such that [D]_A = 2[D]₀

$$pA_2 = -\log (2[D]_0)$$

The intrinsic activity (i.a.) of the compound is obtained from the maximal response it produces as a fraction of the maximal response to a full agonist (with i.a.=1). For active agonists producing the maximal potential response, the value of i.a. is 1; for dualists, 1 > i.a. > 0; for antagonists without agonist activity, i.a.=0.

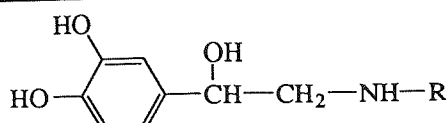
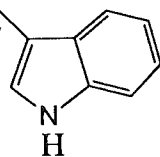
		
No.	R	Relative Bronchodilator Activity
1.	CH ₃	40
2.	C ₂ H ₅	25
3.	CH(CH ₃) ₂	100
4.	C(CH ₃) ₃	170
5.	CH ₂ (CH ₂) ₃ CH ₃	25
6.	Cyclopentyl	70
7.	CH ₂ CH ₂ C ₆ H ₅	10
8.	CH ₂ CH ₂ C ₆ H ₄ -OH(<i>p</i>)	50
9.	CH(CH ₃)CH ₂ C ₆ H ₅	100
10.	CH(CH ₃)CH ₂ C ₆ H ₄ -OH(<i>p</i>)	800
11.	CH(CH ₃)CH ₂ 	750

Table 1.8: Effect of *N*-substitution on β -receptor stimulant activity of norepinephrine

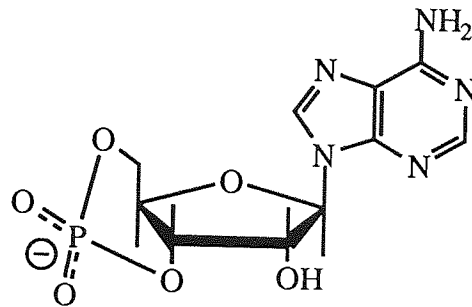
The presence of a cationic nitrogen atom appears very important for activity since carbon isosteres of catecholamines have drastically reduced activity.⁸¹ Furthermore, optimum activity is associated with primary and secondary amines, and conversion to tertiary or quaternary centres makes the compound inactive.

1.3.6.5 Effect of polar side-chain:

Bloom and Goldman⁸² proposed the *dynamic receptor* hypothesis which states that the formation of c-AMP (**25**) involves nucleophilic attack by the ribose 3-hydroxy group on the innermost phosphate atom of ATP with expulsion of a pyrophosphate residue (Figure 1.8). β -Stimulants are supposed to catalyse this reaction because their cationic head neutralises the negative charge on the α -phosphate anion, thus increasing the electrophilic character of the phosphorus atom. As a result, the rate of nucleophilic displacement by the ribose 3-hydroxy group is enhanced. Thus the absolute requirement for β -agonism is a cation correctly aligned with the appropriate phosphate group in ATP and the role of other functional groups in β -stimulants is to increase the likelihood of this event.

The potency-enhancing effect of the catechol function is attributed to chelation with Mg^{2+} bound to the β - and γ - phosphate groups in ATP, and that of non-polar N-substituents binding with the adenine moiety.

β -Receptor agonists may interact with the β -receptor through a quinone methide intermediate (Figure 1.7). Based on the receptor binding mechanism, the presence of anionic sites in the side-chain inhibits the binding of β -adrenoceptor agonists with the receptor and thus reduces their activity.



(25)

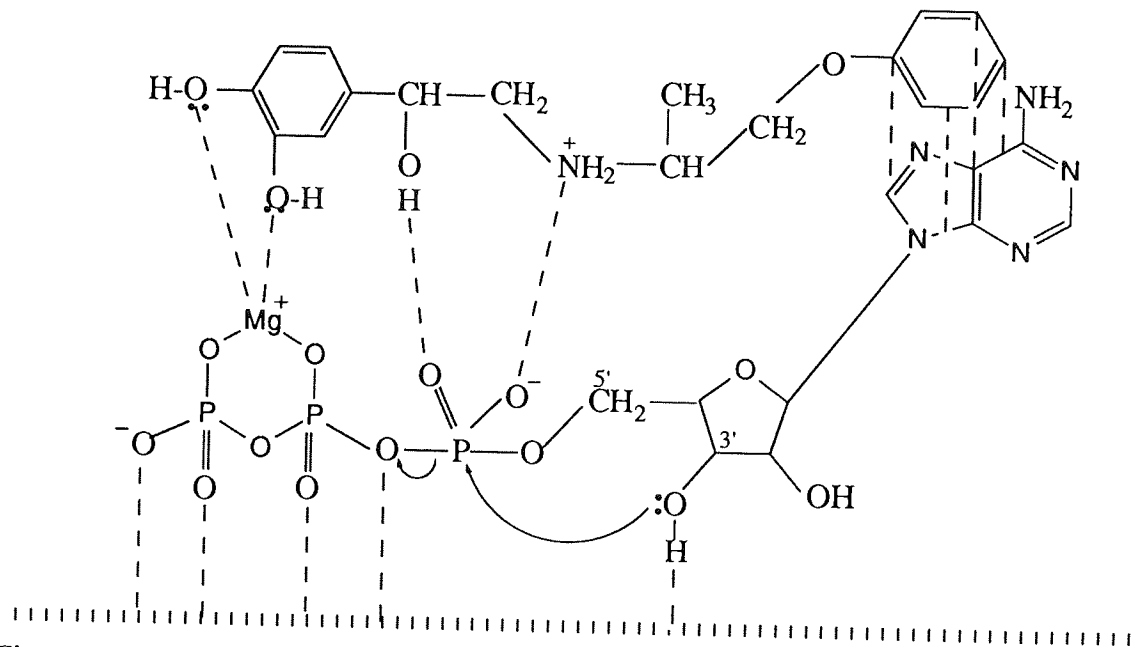
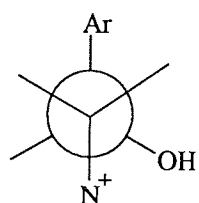


Figure 1.8: Catalysis of cyclic-AMP formation by catecholamines

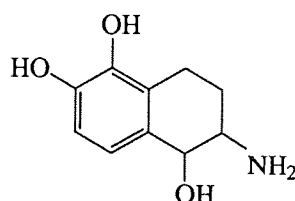
1.3.6.6 Conformational requirement for β -adrenoceptor agonists:

The general structural requirements for agonist activity at α - or β - receptors are similar, but there are differences, notably in the effects of *N*-alkyl substitution and, to a lesser extent, α -methyl substitution. X-Ray crystallography of norepinephrine, epinephrine and dopamine indicates that compounds exist in the antiperiplanar conformation where the phenyl and ammonium groups are *trans* (26). However, there is no necessary relationship between the conformation of a molecule in solution or in a crystalline state and that adopted when bound to the receptor.⁸³⁻ⁱ

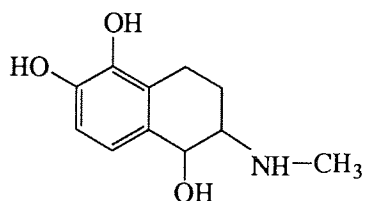
A further approach to the analysis of conformational requirements for drug activity has been in the design of rigid tetraline derivatives of noradrenaline (27), adrenaline (28) and isoprenaline (29).⁸³⁻ⁱⁱ All of these compounds showed strong direct β -stimulating activity on tracheal muscle. Activity of the *trans* isomer about the C (1) - C (2) bond was ten times more potent in bronchorelaxing and chronotropic action than the *cis* isomer.



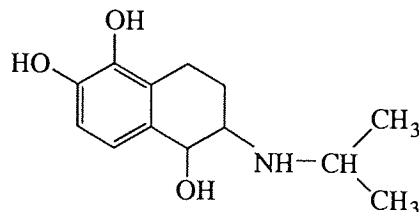
(26)



(27)



(28)



(29)

1.4 AIMS AND OBJECTIVES OF THE PRESENT STUDY

1.4.1 New therapeutic approaches *via* stimulation of adenylate cyclase

As β -adrenoceptor agonists are known to possess anti-inflammatory and anti-proliferative properties, a therapeutic benefit in inflammatory dermatitis of an acute or chronic nature, and in inflammatory proliferative disease such as psoriasis, could be anticipated. The most popular therapies for the treatment of psoriasis, including retinoids, PUVA and corticosteroids, augment the β -adrenoceptor agonist-mediated increase in c-AMP in pig skin *in vitro*. Low doses of β -adrenoceptor agonists might therefore prove to be a useful adjunct with other drugs in the treatment of inflammatory and proliferative skin disease.

Based on the earlier discussion, antipsoriatic drugs may possibly be developed due to their influence on the cyclic nucleotides in three ways:

- stimulation of adenylate cyclase,
- administration of c-AMP or dibutyl c-AMP,
- inhibition of c-AMP-degradation by phosphodiesterases.

The simultaneous use of more than one of the above mentioned pathways may provide a greater possibility of success.

It may be possible, therefore, to develop a new therapeutic approach in psoriasis *via* the stimulation of adenylate cyclase by β -adrenoceptor agonists.

1.4.2 The design of β -adrenoceptor agonists for psoriasis

For a β -adrenoceptor agonist to be useful clinically in the treatment of inflammatory and proliferative skin disease, it is a pre-requisite that activity be restricted to the percutaneous layers, and that no untoward cardiovascular effects occur as a consequence of systemic absorption. As the drug enters into the blood stream, it needs to be hydrolysed or metabolised into an inactive moiety. β -Adrenoceptor activity can be terminated in two ways:

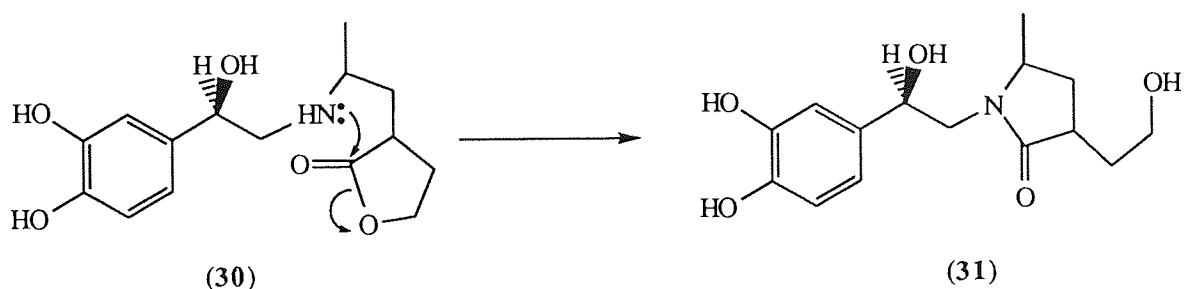
- Loss of the basic centre at nitrogen (eg. -NH- to -N-CO-)
- Dramatic polarity change in the *N*-substitution

1.4.2.1 Deactivation of β -adrenoceptor activity by loss of the basic centre at nitrogen

A further deactivation process includes the synthesis of molecules designed to undergo inactivation in a controlled manner. O-Acyl prodrugs of β -adrenoceptor antagonists have been reported.⁸⁴ These compounds undergo a facile O-to-N acyl rearrangement in aqueous systems to provide stable and inactive amide derivatives. Based on this, suitable derivatives of β -adrenoceptor agonists may afford a means to accomplish the required inactive metabolite transformation. The known structure-activity-relationship indicates that sufficient structural tolerance is available for this approach.

For example, the indole analogue of isoprenaline (**33**) (Table 1.9) is a potent β -adrenoceptor agonist, comparable to the parent compound (**32**) in terms of bronchodilator activity (Table 1.8). A large structural variation of the *N*-alkyl group is allowed without compromising activity so that the corresponding coumaran-2-one derivative (**34**) and aliphatic lactone analogue (**30**) should also exhibit activity. Subsequent nucleophilic attack by the amine at the carbonyl group of each molecule may lead to a ring-opening reaction with the concomitant formation of a pyrrolidinone (**31**) (Scheme 1.1).

Conversion of the secondary amine (**30**) to a non-basic cyclic tertiary amide (**31**) in this manner will prevent association with the β -receptor and abolish β -adrenoceptor agonist activity as required. Acyl reactivity may be controlled by both electronic and steric properties of the lactone ring, thus the coumaran-2-one derivative (**34**) should be more reactive than the aliphatic lactone (**30**) due to the enhanced reactivity of the leaving group, whereas steric effects, to reduce deactivation rates, may be invoked by the introduction of suitable alkyl substituents. Initially, model compounds of general structure (**35**, **36**, **37**) could be synthesised in order to assess the nature of the cyclisation reaction and the effect of varying substituents on the rate of the reaction. We did not explore this area.



Scheme 1.1: Mechanism of deactivation of β -adrenoceptor agonist activity by loss of the basic centre at nitrogen.

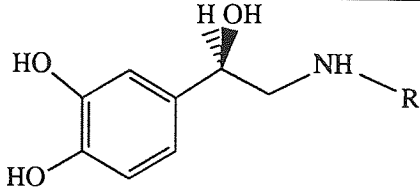
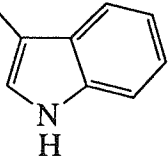
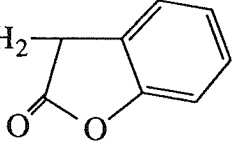
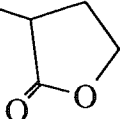
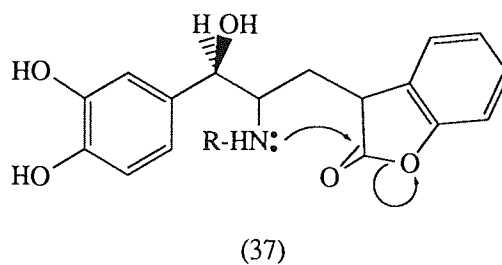
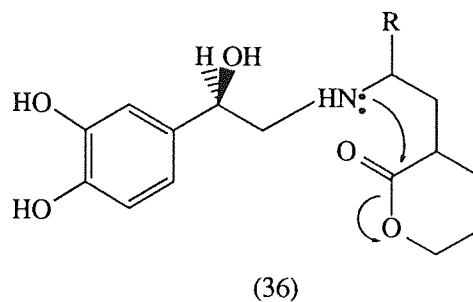
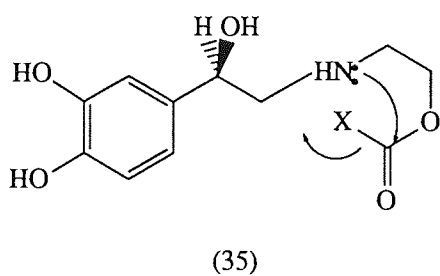
		
R	Class of compounds	Compound No.
-CH(CH ₃) ₂	Isoprenaline	32
-CH(CH ₃)-CH ₂ 	Indole derivative	33
-CH(CH ₃)-CH ₂ 	Coumaran-2-one derivative	34
-CH(CH ₃)-CH ₂ 	Aliphatic lactone derivative	30

Table 1.9: Isoprenaline analogues with β -adrenoceptor agonist activity

1.4.2.2 Deactivation of β -adrenoceptor activity by dramatic polarity change in the *N*-substitution

Although some structural flexibility is permitted, the presence of a primary or secondary amine is crucial and molecules encompassing tertiary or quaternary centres are inactive as β -adrenoceptor agonists. For hydrogen bonding, protonation of the nitrogen centre is a prerequisite for association with the β -receptor (Figure 1.5). Thus, any chemical or biological transformation resulting in the conversion of a primary or secondary amine to the corresponding tertiary or quaternary congener or dramatic change in the polarity of *N*-substitution (protonated nitrogen binds with the anionic site of Asp¹¹³, see section 1.3.3 ligand-binding sites of β -adrenoreceptor), should result in the abolition of the activity of a β -adrenoceptor agonist. β -Adrenoceptor agonists have five different sites⁸⁵ for attachments as shown in Figure 1.9.

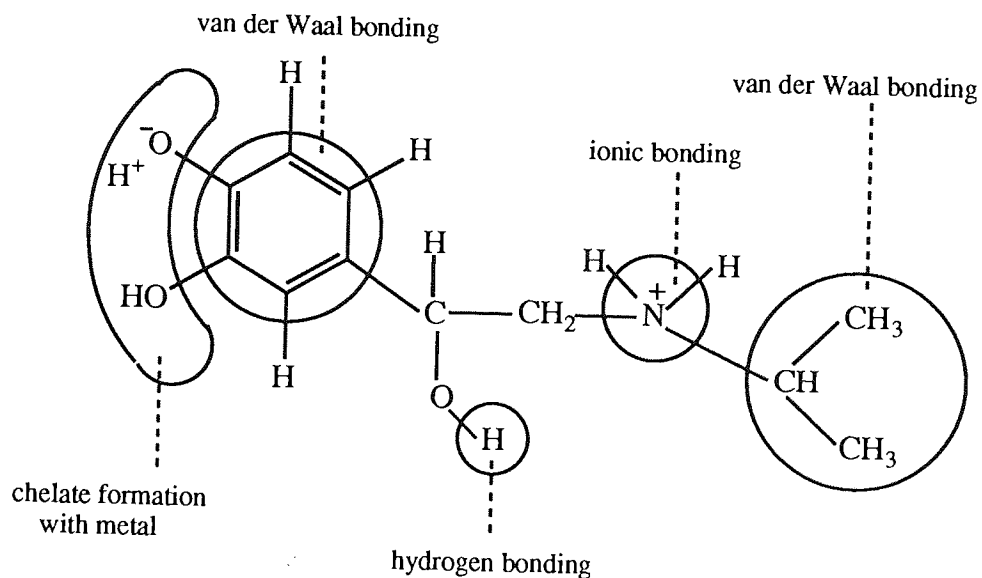


Figure 1.9: Schematic diagram of the attachment of isoprenaline to the β -adrenoreceptor

As discussed earlier (section 1.3.6.5, the effect of the polar side-chain on the activity of β -receptor agonists), the formation of anionic sites in the β -receptor agonists may hinder the interaction of the cationic nitrogen with the anionic side chain of Asp¹¹³ in helix III of the receptor and reduce the β -adrenoreceptor activity (see 1.3.3 ligand-binding sites of the β -adrenoreceptor) (Figure 1.5) (see Chapter eight, Section 8.3).

In this project, the search for a topically active β -adrenergic agonist for use in skin disease was undertaken. To limit systemic effects, the soft drug approach was considered appropriate. Soft drugs are defined as biologically active, therapeutically useful chemical compounds (drugs) characterised by a predictable and controllable *in vivo* destruction (metabolism) to non-toxic moieties, after they achieve their therapeutic role.⁸⁶ The required agent should not produce any untoward cardiovascular side-effects when applied topically.

Esterification is the most common modification in the design of soft-drugs. The predominance of carboxylic acid and hydroxyl groups in drug molecules, together with the abundance of cutaneous and other hydrolytic enzymes makes esterification an excellent soft-drug type for dermal delivery. The synthesis of ester soft-drugs has two advantages:

- They are readily hydrolysed by esterases which are present in the blood
- Hydrolysis by esterases in blood the soft-drug inactive in the blood stream, thereby minimising the cardiovascular side-effects which are the main cause of the problems associated with the use of β -adrenoceptor agonists in psoriasis.

1.4.3 Soft and prodrugs

The 'soft-drug' approach to drug design, involves the predictable *in vivo* detoxification of an active drug after therapeutic activity, in order to minimize systemic toxicity. In contrast the 'prodrug' concept involves the controlled *in vivo* bioactivation of a previously inactive species, prior to eliciting a pharmacological response.⁸⁷

Prodrugs are divided into two classes:

1. Carrier linked prodrugs
2. Bioprecursors

Carrier linked prodrugs

The drug molecule, whose usefulness is limited by its poor bioavailability (due to the presence of hydrophilic groups), is chemically modified by the attachment of a carrier group or promoiety to form a prodrug, from which the parent drug is generated *in vivo*. Prodrug design can thus be considered as conferring a transient chemical cover to alter or eliminate undesirable properties of the parent drug molecule (Figure 1.10)

A well designed prodrug should satisfy the following four criteria:⁸⁷

1. It should be biologically inactive.
2. Both the prodrug and its promoiety released *in vivo* must be non-toxic.
3. The chemical linkage between the parent drug molecule and the carrier moiety must be bioreversible.
4. The prodrug should be sufficiently stable to allow its formulation into an appropriate dosage form.

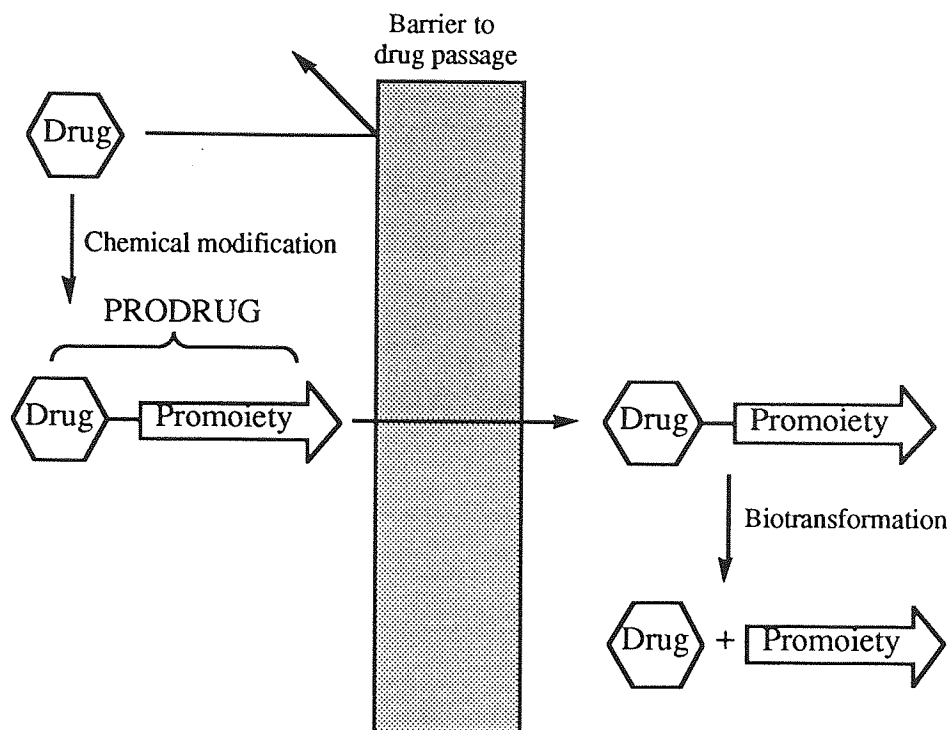
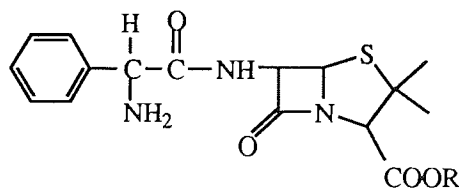


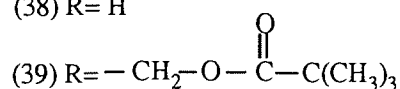
Figure 1.10: Schematic illustration of the prodrug concept.

An illustrative example of prodrug design taking these criteria into account is found in orally active ampicillin prodrugs. Ampicillin (38) is highly polar and is present in a zwitterionic form at the pH of the gastrointestinal tract; it therefore possesses low lipophilicity. It is absorbed to the extent of 30-40% following oral administration, and the unabsorbed drug destroys the intestinal flora resulting in the possibility of adverse side effects. A number of prodrugs with increased lipophilicity have been prepared by esterification of the free carboxylic group of ampicillin, notable among these are pivampicillin (39), bacampicillin (40) and talampicillin (41)⁽⁸⁸⁻⁹⁰⁾. These prodrugs are almost completely absorbed and cleaved by non-specific esterases in the body, releasing the free ampicillin.

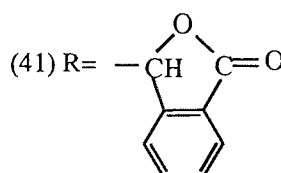
The by-products of cleavage are formaldehyde and pivaloic acid for pivampicillin (39), and acetaldehyde, ethanol and carbon dioxide in the case of bacampicillin (40). The latter three compounds are natural human metabolites.



(38) R= H



(40) R= $-\text{CH}(\text{CH}_3)-\text{O}-\overset{\text{O}}{\parallel}{\text{C}}-\text{OC}_2\text{H}_5$



The prodrug approach has been successfully applied to a wide variety of drugs and various goals achieved through the use of this concept include:

1. Enhanced bioavailability and biomembrane passage, eg. dipivefrin⁹¹
2. Enhanced site-specific drug delivery, eg. doxifluridine⁹²
3. Prolongation of drug action, eg. fluphenazine decanoate ester⁹³
4. Decreased side effects and toxicity, eg. fenbufen^{94,95}
5. Improvement of drug formulation, eg. vidarabine⁹⁶

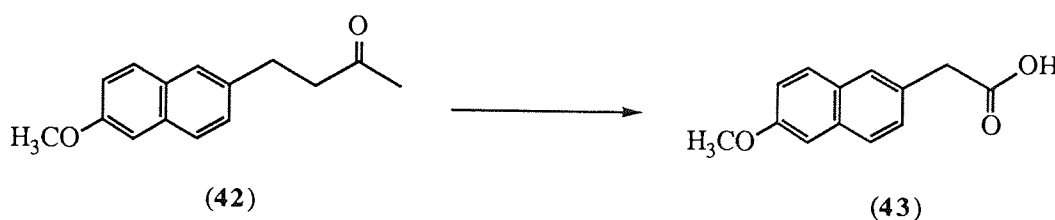
Drugs	Active metabolite
Acetanilide	Paracetamol
Imipramine	Desmethyl imipramine
Chloral hydrate	Trichloroethanol
L-DOPA	Dopamine

Table 1.10: Drugs which require bioactivation to form active compounds.

Bioprecursors

Bioprecursors (or metabolic precursors) do not have a temporary linkage between the active molecule and the carrier group, but they result from a molecular modification of the active molecule itself. This modification generates a new compound, able to be a substrate for a metabolising enzyme, the metabolite being the active molecule.

For example, nabumetone⁹⁷ (42) has been shown to have a wide spectrum of anti-inflammatory activity in animals and humans and is free from gastric irritant properties. Metabolic studies revealed that this drug is converted into the active metabolite, 6-methoxy-2-naphthylacetic acid⁹⁸ (43).



Metabolic reactions are divided into two groups:

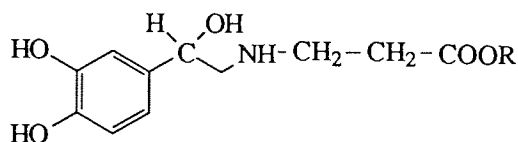
1. Phase I reactions which involves the transformation of specific group in a substrate molecule and creation of a new functional group.
2. Phase II reactions which involves conjugation of the functional groups thus creating solubilising moieties.⁹⁹

The bioprecursors belong exclusively to the phase I products and results from oxidation and reduction reactions. These reactions follows some general rules, and therefore, they can often be forecasted. Taking into account the common metabolic pathways, one can imagine the design of a given molecule so that it will be converted *in vivo* into the desired compound by one or more of the phase I reactions.

Design of β -adrenoceptor agonists based on soft-drug approach

To design β -adrenoceptor agonists and to limit their systemic effects, we have adopted the soft-drug approach. The *N*-substituent can accommodate a broad range of structures, so, here, we have used the alkoxy-carbonyl-ethyl group. The increased polarity of the dihydroxy acid (**74**, R=H), expected after metabolic conversion of the soft-drug (**74**, R=Et), should eliminate agonist activity (Section 1.4.2.2). Further, to prevent oxidation and enhance topical delivery we have sought to esterify the catechol hydroxyl groups to produce a pro-soft-drug (**107**) which generates the soft-drug (**74**, R=Et) in enzymic systems.

Utilising the soft-drug concept, soft-drugs (**74**, R= Me, Et) have been synthesized for their use in psoriasis. However, soft-drug (**74**, R=Et) is hydrophilic and has poor penetration across the membrane, therefore its lipophilic pro-soft drug (**107**) has been synthesized.

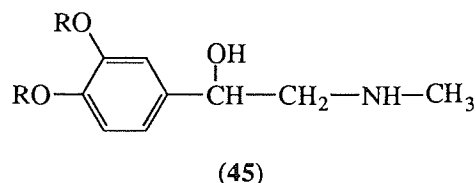
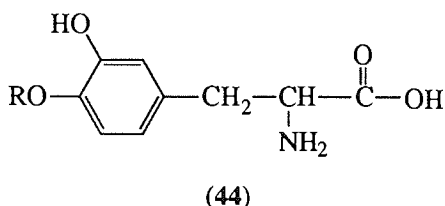


(74)

1.4.4 Prodrugs in which the catechol hydroxyl groups are protected

*L-3-(3'-Hydroxy-4'-pivaloyloxyphenyl)alanine: a monopivaloyloxy ester prodrug of L-dopa*⁹²

L-Dopa (**44**, R= H) has a short half-life *in vivo* resulting in wide interdose variation in drug levels. The fluctuation of plasma L-dopa levels may be responsible in part for some problems, namely dyskinesia and wearing-off phenomenon, that occur during chronic L-dopa therapy for Parkinson's disease. Many L-dopa prodrugs have been prepared in an effort to solve these problems but non of them has led to an agent clinically more useful than L-dopa itself. Prodrug, L-3-(3'-hydroxy-4'-pivaloyloxyphenyl)alanine [**44**, R= (CH₃)₃C-CO-], produced a sustained L-dopa plasma level and good L-dopa bioavailability after oral dosing in rats and dogs.



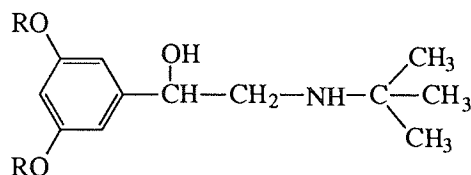
Dipivefrin: a dipivaloyloxy ester prodrug of epinephrine

Epinephrine (**45**, R=H) has long been used for the treatment of elevated intraocular pressure in patients with chronic open-angle glaucoma¹⁰⁰ although its corneal absorption is poor because of its high polarity and rapid metabolic degradation. The development of prodrug, dipivefrin [**45**, R= (CH₃)₃C-CO-], has led to improved ocular delivery of epinephrine. This dipivaloate ester prodrug is much more lipophilic than epinephrine and the esterification of the metabolically susceptible phenolic hydroxyl groups affords a delay in metabolism. These properties, coupled with a sufficiently high susceptibility to undergo enzymatic hydrolysis in the eye during and after absorption, are responsible for the approximate 20 times greater anti-glaucoma activity of the prodrug in comparison with the parent drug upon local administration in humans.⁽¹⁰¹⁻¹⁰⁴⁾

In addition, because lower doses of the prodrug can be used, untoward cardiac side-effects due to epinephrine absorption from the tear duct are decreased. Dipivefrin also has a longer duration of action than epinephrine, because the metabolism of the epinephrine, which involves a methylation of the phenolic OH groups, is delayed or prolonged as it cannot occur until the prodrug has undergone conversion to epinephrine.

*Ibuprofen: a diisobutyryl ester prodrug of terbutaline*⁹²

Terbutaline (46, R= H) is a selective β_2 -agonist, used to lower the intraocular pressure in the eye. The prodrug approach was used to reduce the systemic absorption of terbutaline when applied ocularly. Ibuprofen [46, R= (CH₃)₂CH-CO-], the diisobutyryl ester of terbutaline, was found to be almost 100 times more potent than the parent drug in lowering the intraocular pressure in rabbits. This, coupled with a longer duration of action, suggests that both the topical dose and the dosing frequency of ibuprofen can be reduced, thereby reducing systemic side-effects.



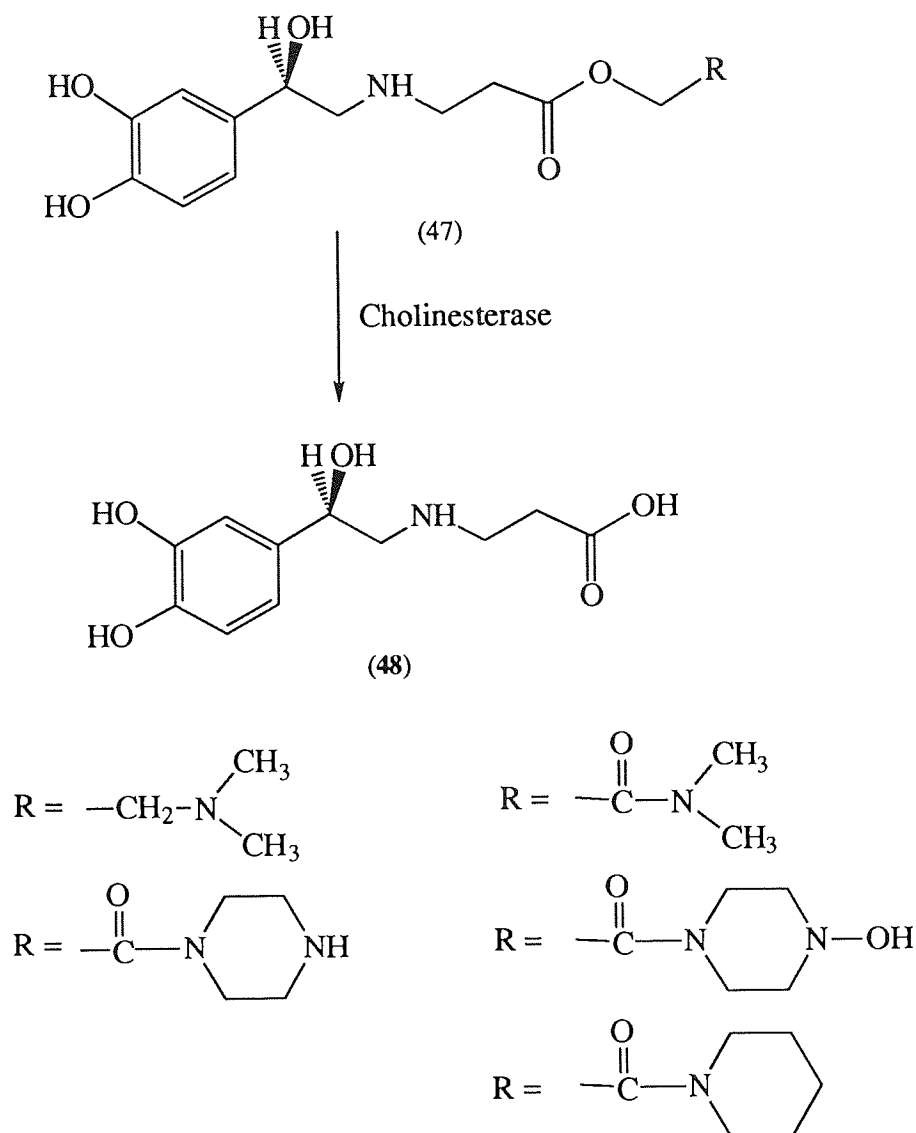
(46)

1.4.5 Potential biolabile soft-drugs of β -adrenoceptor agonists

Nielson and Bundgaard^{105,106} discovered that esters of *N,N*-disubstituted glycolamides act as potentially useful biolabile prodrugs for carboxylic acids. These esters have high susceptibility to undergo enzymatic hydrolysis in plasma and at the same time, these derivatives are stable in aqueous solutions. Furthermore, it is feasible to obtain ester derivatives with almost any desired water solubility or lipophilicity with retainment of marked lability to enzymatic hydrolysis.

The benzoate esters of various substituted 2-hydroxyacetamides (glycolamides) were found to be hydrolysed extremely rapidly in human plasma, the half-lives of hydrolysis being less than 5 seconds in 50% plasma solutions for some *N,N*-disubstituted glycolamide esters (Table 5.12, page 200, compound 13, 17 and 18). The rapid rate of hydrolysis could be largely attributed to cholinesterase (also called pseudocholinesterase) present in the plasma. From a study of a variety of substituted glycolamide and related esters, the most prominent structural requirement needed for a rapid rate of hydrolysis was found to be the glycolamide ester structure combined with the presence of two substituents on the amide nitrogen atom. These derivatives show structural similarity with benzoylcholine, a good substrate for cholinesterase.

On the basis of the above findings, the glycolamide ester derivatives (47) could be potential biolabile soft-drugs (Scheme 1.2). As soon as these biolabile soft-drugs enter into the blood stream, they will undergo hydrolysis by the pseudocholinesterases present in the blood to yield the inactive promoiety (48) so that the untoward cardiovascular side-effects can be eliminated.



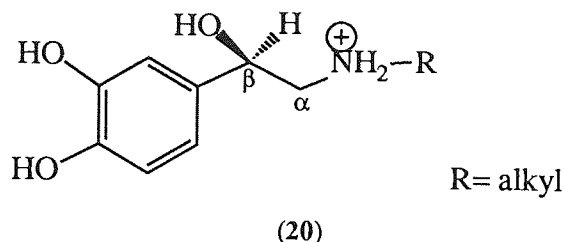
Scheme 1.2: Mechanism of deactivation of β -adrenoceptor agonist activity by rapid hydrolysis of potential biolabile glycolamide ester soft-drugs.

CHAPTER TWO

RESULTS AND DISCUSSION (SYNTHESIS OF SOFT β -ADRENOCEPTOR AGONISTS)

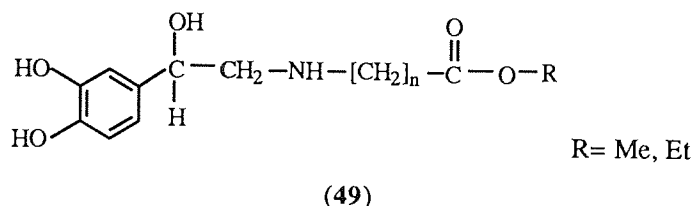
2.1 INTRODUCTION

As discussed in chapter one (section 1.3.6), the basic structure of β -adrenoceptor agonists is summarised as:

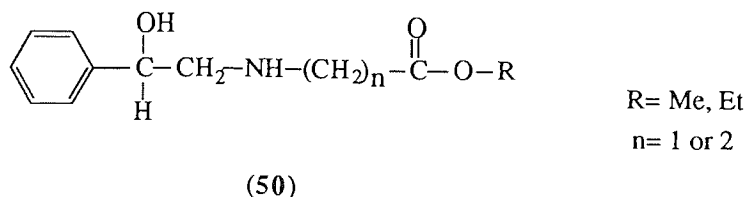


The most important side-effect associated with β -adrenoceptor agonists is their effect on the heart. Here β -adrenoceptor agonists are being developed for topical use in psoriasis. To design a β -adrenoceptor agonist which can be used in psoriasis, it is a pre-requisite that activity be restricted to the cutaneous layers, and that no untoward cardiovascular effects occur. As the drug enters into the blood stream, it should be hydrolysed or metabolised into an inactive moiety. Our proposal is to minimise β -adrenoceptor activity by the introduction of an anionic site near the amino group (see section 1.4.2.1 and 1.4.2.2).

Based on this idea, a carboxylate ester group was introduced, with a 1 or 2 carbon atom. This derivative should hydrolyse to give a carboxylate anion in the blood, which we believe will be devoid of β -adrenoceptor activity (see section 1.4.2.2). The first part of this project sets out to explore the synthesis of β -adrenoceptor agonists with the general structure (49, $n = 1$ or 2).



The catechol group is nucleophilic as well as being prone to oxidation in the presence of light and air, which may make the chemistry complex. Therefore, prior to the incorporation of the catechol group, which is important for β -adrenergic activity, the model compounds (50), without the 3,4-dihydroxy substituents, were considered.



2.2 ATTEMPTED SYNTHESIS OF AMINO ACID ESTERS (50, n=1, R=ETHYL):

The most direct method towards the preparation of (50, n=1, R= ethyl) is to react 1-phenyl-2-aminoethanol (51) with ethyl 2-bromoethanoate (52). However, the reaction was not selective at nitrogen and only complex molecule (53) was isolated. Compound (53) was derived from two molecules of 1-phenyl-2-amino ethanol (51) and four molecules of ethyl 2-bromoethanoate (52). Its structure was assigned by ^1H NMR, ^1H - ^1H COSY (correlated spectroscopy), ^{13}C NMR DEPT and elemental analysis.

The ^{13}C NMR spectrum of (53) had 12 aromatic carbon atoms, of which 10 are aromatic C-H (two quaternary carbon atoms at δ_{C} 136.8 and 141.7 are absent in the ^{13}C NMR DEPT), which shows that there are two phenyl rings in the molecule. ^{13}C NMR shows that there are 4 ester C=O groups at δ_{C} 167.2, 169.3 and 171.7 (2 equivalent). These were absent in the ^{13}C NMR DEPT which confirms that they are quaternary carbon atoms.

The alkyl region in the ^{13}C NMR spectrum shows 9 peaks in the alkyl region. The peak at δ_{C} 14.1 is for the three $-\text{CH}_3$ groups (peak phased positive in ^{13}C NMR DEPT). Two other peaks at δ_{C} 70.4 and 80.8 (both peaks phased positive in ^{13}C NMR DEPT) are for C-H groups in the molecule. ^1H NMR shows two doublet of doublet patterns at δ_{H} 4.62 and 5.58, which is characteristic for the $(-\text{CH}_2-\text{C}-\text{H})$ group in the molecule. Integration of the peaks in the ^1H NMR spectrum at δ_{H} 4.18 and 1.26 shows that there are 3 ethyl ester groups. The remaining 7 peaks in the alkyl region phased negative in ^{13}C NMR DEPT which confirms that they are all $-\text{CH}_2-$ carbons.

The ^1H NMR spectrum was further assigned with the help of a ^1H - ^1H COSY spectrum. The peak at δ_{H} 4.67 (dd) [Ph-C(OH)- $\underline{\text{H}}$] has a cross-peak connection to the signal at δ_{H} 2.60 (dd) [Ph-C(OH)- $\underline{\text{C}}\text{H}_\text{A}\text{H}_\text{B}$ -], which is further connected (dashed lines) by a cross-peak to the signal from multiplet at δ_{H} 3.13-3.21 [Ph-C(OH)- $\text{C}\text{H}_\text{A}\underline{\text{H}}_\text{B}$ - and Ph-CH- $\text{C}\text{H}_\text{A}\underline{\text{H}}_\text{B}$ -]. The peak at δ_{H} 5.56 (dd) (Ph- $\underline{\text{C}}\text{H}$ -OOC) has a cross-peak connection to the signal at δ_{H} 2.80 (dd) [Ph-CH- $\underline{\text{C}}\text{H}_\text{A}\text{H}_\text{B}$ -], which is further connected (dashed lines) by a cross-peak to the signal from multiplet at δ_{H} 3.13-3.21 [Ph-C(OH)- $\text{C}\text{H}_\text{A}\underline{\text{H}}_\text{B}$ - and Ph-CH- $\text{C}\text{H}_\text{A}\underline{\text{H}}_\text{B}$ -]. The peak at δ_{H} 3.45 (dd) has a cross-peak connection to the peak at δ_{H} 3.82 (dd) with ($J_{\text{gem}} = 17.3$ Hz) consistent with methylene protons ($-\underline{\text{C}}\text{H}_2-\text{COOC}_2\text{H}_5$). See ^1H - ^1H COSY spectrum (Figure 2.1). On the basis of the above NMR experiments, the structure of the molecule was drawn (53).

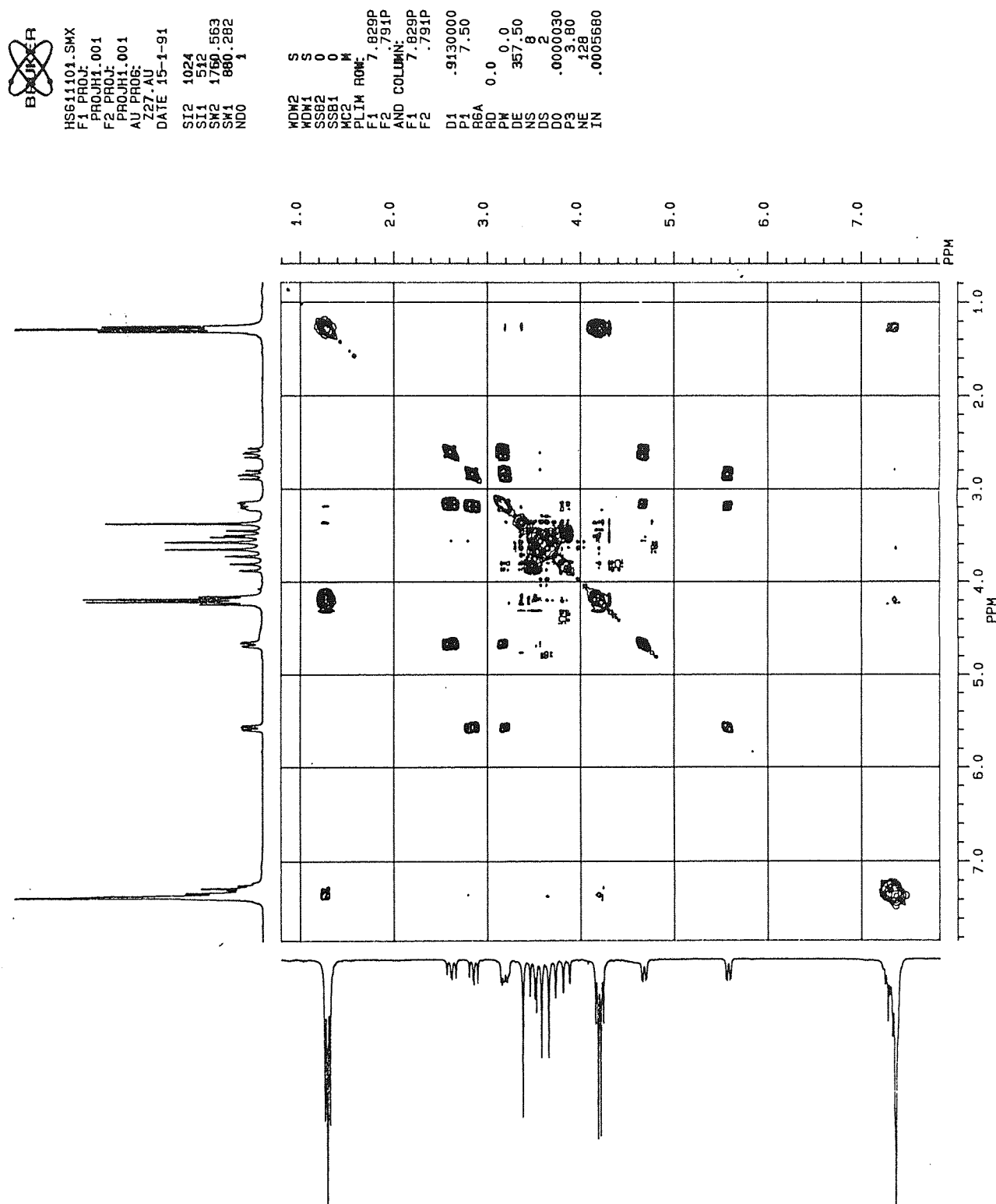
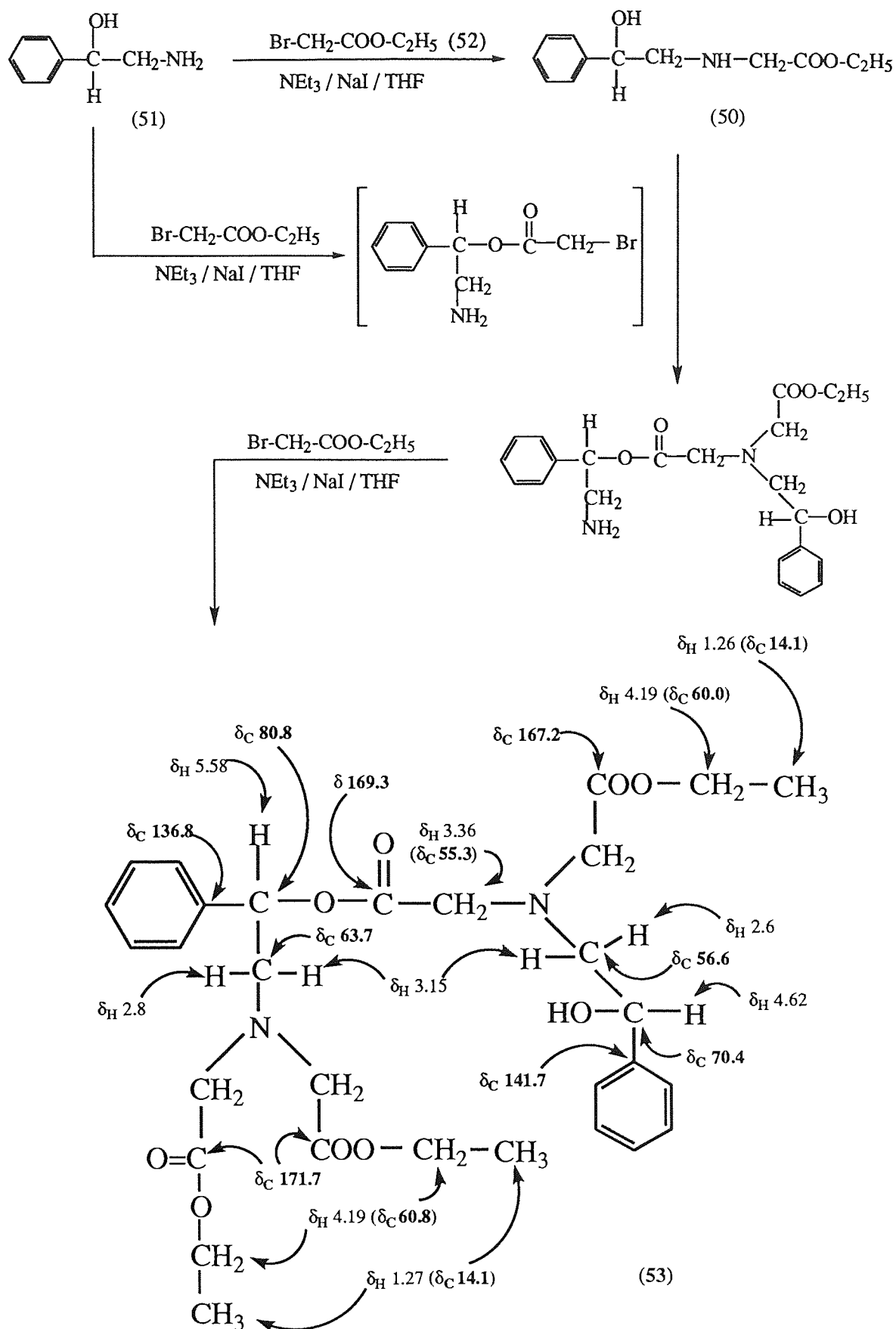


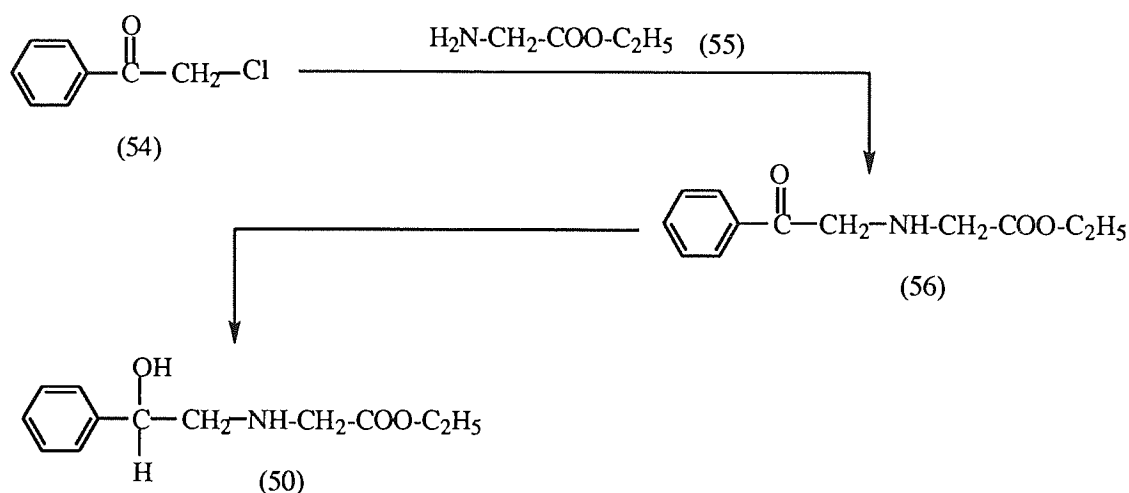
Figure 2.1: ^1H - ^1H COSY spectrum of compound (53).



Scheme 2.1: Formation of compound (53) due to acylation of hydroxyl group in compound (51)

This first experiment showed that it is difficult to get monosubstitution at the amine and there is also a problem with acylation of the hydroxy group,¹⁰⁷ in which two product molecules joined together to form (53) (Scheme 2.1). Both hydrogen atoms in the primary amine (51) are substituted, which suggest that there is a need to protect the primary amino group.

An alternative approach to (50) *via* the preparation and subsequent reduction of the keto compound (56) was pursued. α -Chloroacetophenone (54) was heated under reflux with ethyl 2-aminoethanoate (55) in ethanol,¹⁰⁸ however the desired product, ethyl *N*-(benzoylmethyl)-2-aminoethanoate (56) could not be isolated and the reaction turned dark brown. This may be due either to ethanol acting as a nucleophile in the reaction or alternatively product (56) could be heat-sensitive.



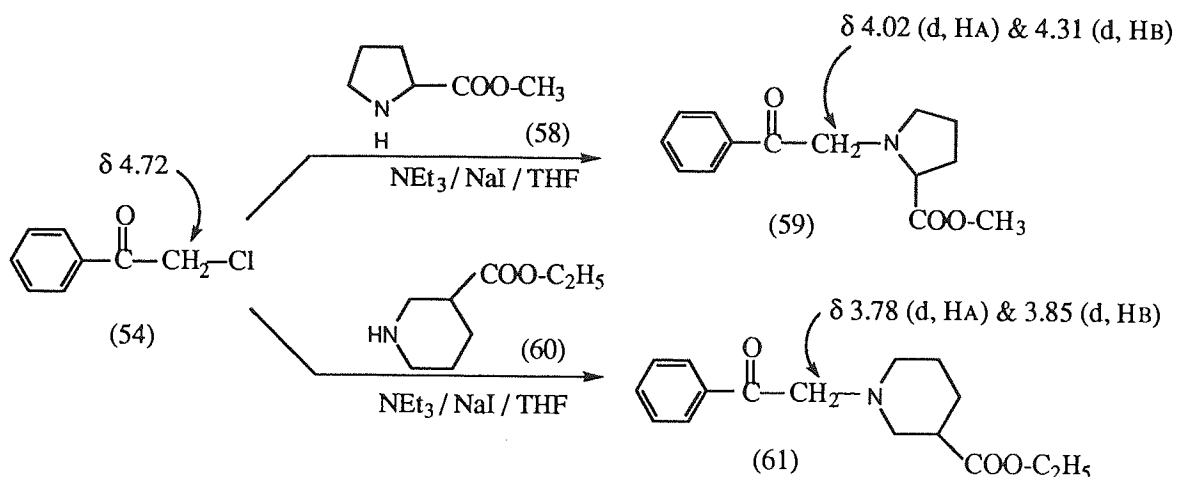
Under milder conditions, α -chloroacetophenone (54) was coupled with ethyl 2-aminoethanoate (55) in the presence of triethylamine as a base and a catalytic amount of sodium iodide (chloride is displaced by iodide to give α -iodoacetophenone, which is more susceptible to nucleophilic attack).¹⁰⁹ The product (56) was isolated by flash column chromatography on silica gel eluting with ethyl acetate. The peak in the ^1H NMR spectrum at δ_{H} 4.72 for $-\text{CO}-\text{CH}_2-\text{Cl}$ disappeared and a new peak at δ_{H} 4.21 consistent with $-\text{CO}-\text{CH}_2-\text{N}-$ was evident. Other peaks in the ^1H NMR spectrum, supporting the formation of (56) included δ_{H} 1.28 (t, $J_{\text{HH}}=7.1$ Hz) for ($-\text{CH}_3$), 3.55 (s) for ($-\text{N}-\text{CH}_2-\text{COO}$) and 4.20 (q, $J_{\text{HH}}=7.1$ Hz) for ($-\text{COO}-\text{CH}_2-$).

If the reaction mixture was left overnight, compound (**56**) changed into unidentified mixture of compounds, possibly including a lactone or resulting from intramolecular reaction of the ester and ketone function. Even after purification, compound (**56**) decomposed, therefore alternative methods to synthesise the β -hydroxyl compounds (**50**, $n=1$) were, thus, explored.

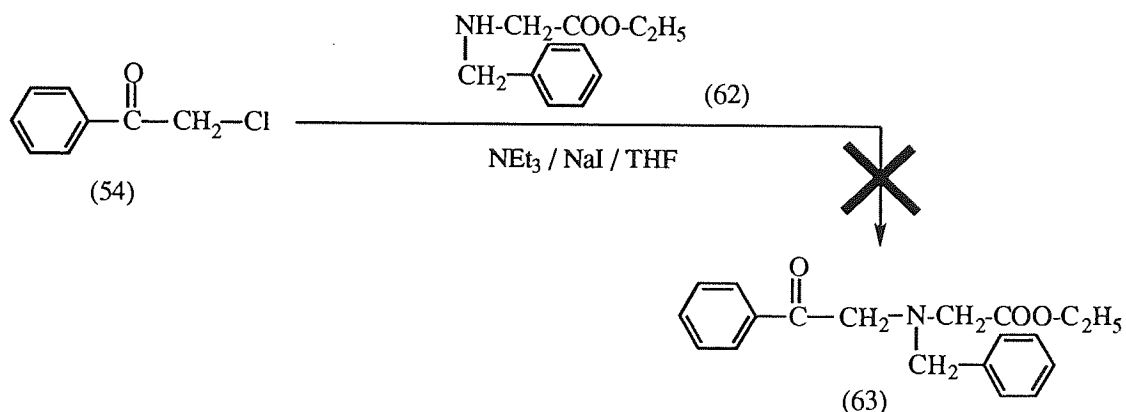
To overcome such problems, one possibility was to utilise an *N*-protected analogue of ethyl 2-aminoethanoate. To test that protection of the amino group is required, some cyclic secondary amines were reacted with α -chloroacetophenone.

The methyl ester of proline (**58**) was reacted with α -chloroacetophenone (**54**) in dry THF with sodium iodide and triethylamine¹⁰⁹ to form methyl *N*-(benzoylmethyl)proline (**59**). Disappearance of the peak at δ_{H} 4.72 for $-\text{CO}-\text{CH}_2-\text{Cl}$ and appearance of peaks at δ_{H} 4.02 (d, $J_{\text{gem}}=17.2$ Hz, 1H) for $(-\text{CO}-\text{CH}_A\text{H}_B-\text{N}-)$ and 4.31 (d, $J_{\text{gem}}=17.2$ Hz, 1H) for $(-\text{CO}-\text{CH}_A\text{H}_B-\text{N}-)$ confirms the formation of methyl *N*-(benzoylmethyl)proline (**59**). The ^1H NMR spectrum of (**59**) also included δ_{H} 3.64 (s, 3H) for (OCH_3) , and the ^{13}C NMR spectrum showed peaks at δ_{C} 196.8 and 174.1 for $(\text{C}=\text{O}$ keto) and $(\text{C}=\text{O}$ ester), respectively.

Similarly, treatment of ethyl 3-piperidine carboxylate (**60**) with α -chloroacetophenone gave ethyl *N*-(benzoylmethyl)-3-piperidine carboxylate (**61**). Peaks in the ^1H NMR spectrum of (**61**) included δ_{H} 3.78 (d, $J_{\text{gem}}=16.5$ Hz, 1H) for $(-\text{CO}-\text{CH}_A\text{H}_B-\text{N}-)$ and 3.85 (d, $J_{\text{gem}}=16.5$ Hz, 1H) for $(-\text{CO}-\text{CH}_A\text{H}_B-\text{N}-)$, and in the ^{13}C NMR spectrum δ_{C} 196.2 for $(\text{C}=\text{O}$ keto) and 172.8 for $(\text{C}=\text{O}$ ester) which confirmed the formation of ethyl *N*-(benzoylmethyl)-3-piperidine carboxylate (**61**). Both reactions proceeded cleanly and there was only the desired product formed in the reaction, in contrast to the synthesis of ethyl *N*-(benzoylmethyl)-2-aminoethanoate (**56**). Therefore, it was considered appropriate to protect ethyl 2-aminoethanoate as a secondary amine by using ethyl *N*-benzyl-2-aminoethanoate. Subsequently, the *N*-benzyl group could be removed by hydrogenation.

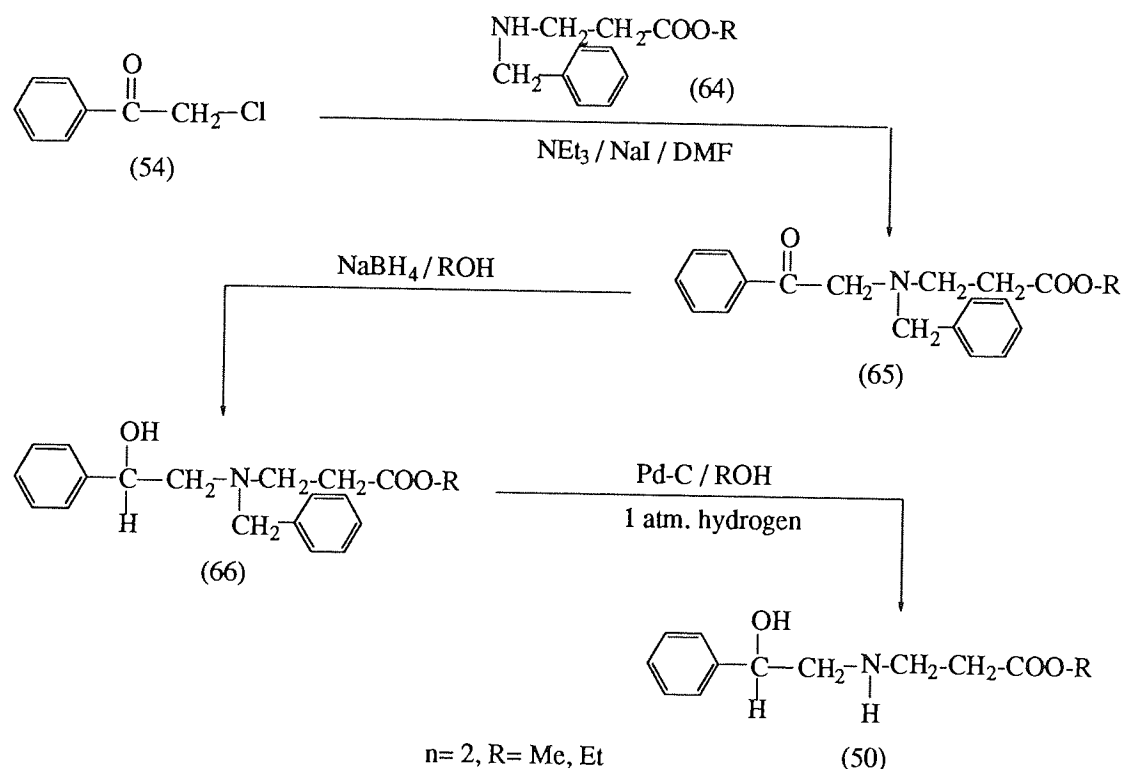


α -Chloroacetophenone (54) was reacted with ethyl *N*-benzyl 2-aminoethanoate (62) in dry THF with triethylamine and a catalytic amount of sodium iodide. However, ethyl *N*-(benzylmethyl)-*N*-benzyl-2-aminoethanoate (63) was not isolated from the reaction mixture which turned dark brown. This could be due to the instability of (63) which may react to give a 6-membered cyclic lactone, suggesting that compounds of structure type (50, $n=1$) are not stable. The attempted synthesis of this class of compound was terminated and for subsequent syntheses the chain length between the amino and carboxylate groups was increased to two carbon atoms (50, $n=2$).



2.3 SYNTHESIS OF PHENYL AMINO ACID ESTERS (50, $n=2$, R=METHYL AND ETHYL)

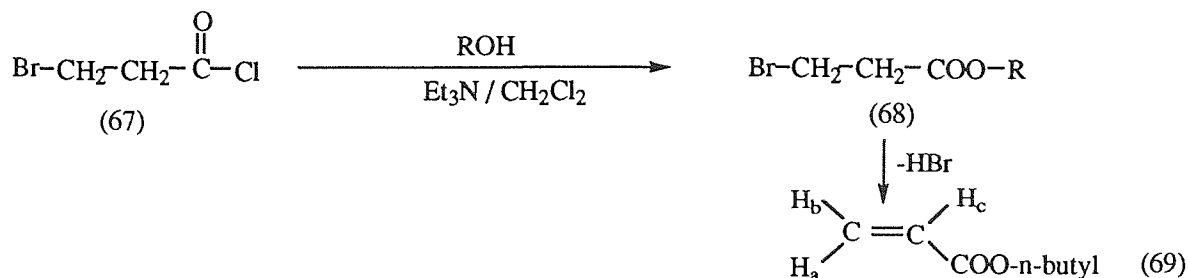
The strategy for the preparation of esters (50, $n=2$, R=methyl and ethyl) is shown in Scheme 2.2. The key step is the reaction between alkyl *N*-benzyl-3-aminopropionate (64) and α -chloroacetophenone (54) to give (65), with subsequent reduction of the keto group to give (66) and final removal of the *N*-benzyl group to give (50).



Scheme 2.2: Synthetic route for phenyl amino acid esters (50, $n=2$, R= methyl and ethyl).

It was anticipated that alkyl *N*-benzyl-3-aminopropionates (64) could be prepared from the reaction of alkyl 3-bromopropionates with benzylamine. Methyl and ethyl 3-bromopropionate (68, R=methyl and ethyl) were commercially available, whereas the propyl and butyl esters of 3-bromopropionate, required for later chemistry, were prepared as shown in Scheme 2.3.

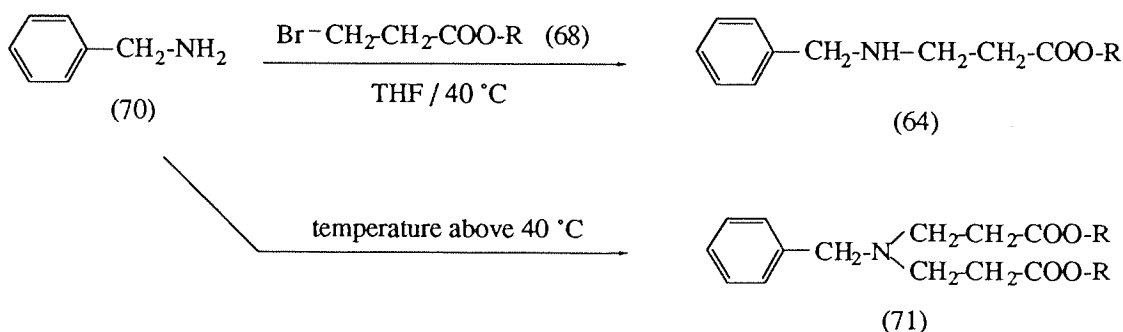
A solution of 3-bromopropionyl chloride (67) in dichloromethane was reacted with either *n*-propanol or *n*-butanol in the presence of triethylamine. The products (68, R=*n*-Pr and *n*-Bu) were isolated by flash column chromatography. Appearance of a peak at $\sim 1738 \text{ cm}^{-1}$ in the IR spectrum and a peak in the ^{13}C NMR spectrum at $\delta_{\text{C}} \sim 172.7$ for (C=O ester) supported the formation of the alkyl 3-bromopropionate (68, R=*n*-Pr and *n*-Bu). These compounds were fully characterised by ^1H and ^{13}C NMR spectroscopy.



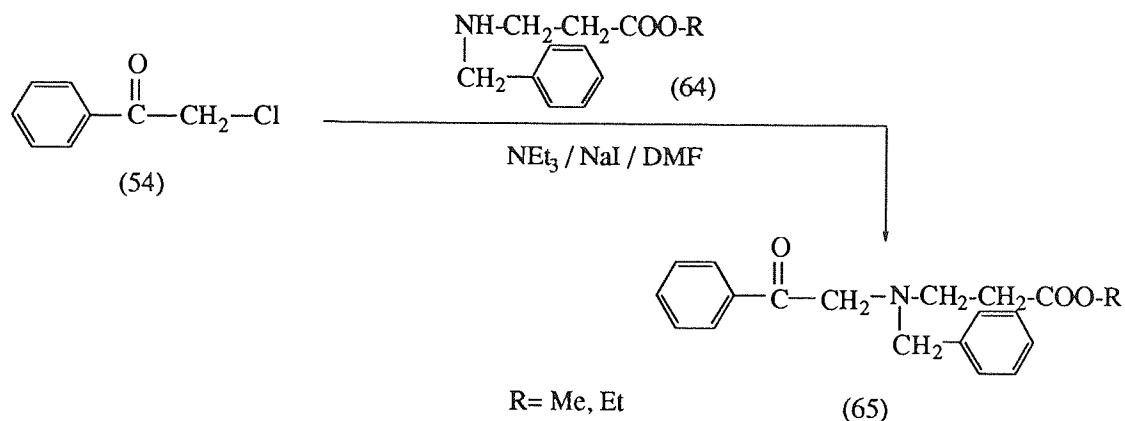
Scheme 2.3: Synthesis of alkyl 3-bromopropionate (R= n-Pr and n-Bu).

The n-butyl ester (**68**, R= n-Bu) was contaminated with 15% of the alkene (**69**, R= n-Bu) which presumably arises by elimination of HBr from the product (**68**). The presence of the alkene (**69**) was shown by ^1H NMR which included peaks at δ_{H} 5.76 (dd for H_a), 6.08 (dd for H_c) and 6.37 (dd for H_b), and ^{13}C NMR peaks at δ_{C} 128.5 for ($\text{CH}_2=\underline{\text{C}}\text{H-COO-}$) and 130.3 for ($\underline{\text{C}}\text{H}_2=\text{CH-COO-}$).

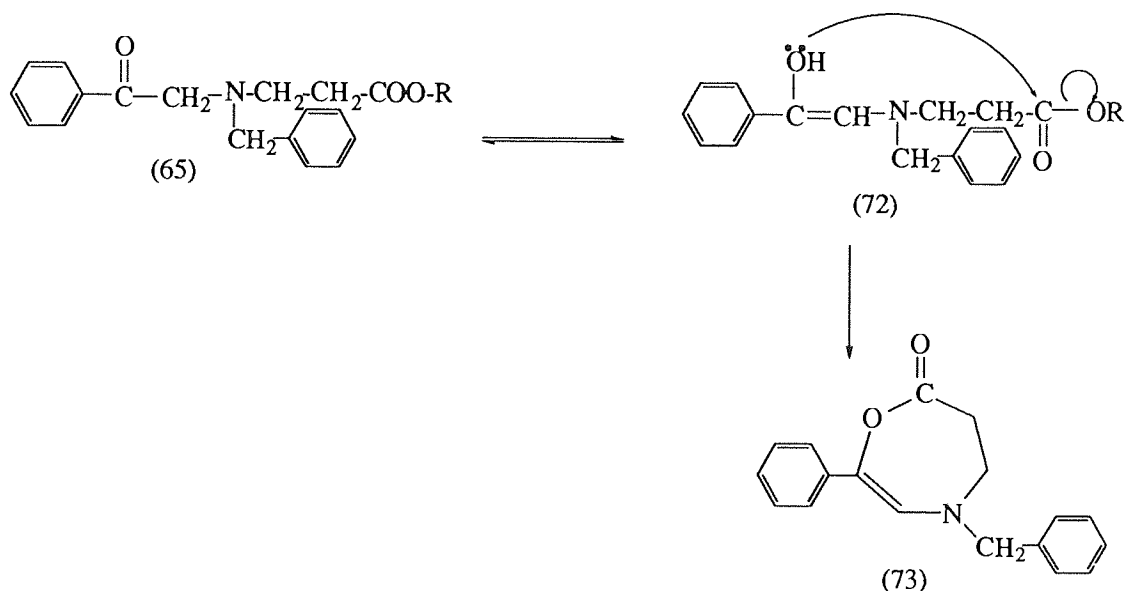
Benzylamine (**70**) was heated with the alkyl 3-bromopropionates (**68**, R= Me, Et, n-Pr, n-Bu) in THF¹¹⁰ at 40 °C to give alkyl *N*-benzyl-3-aminopropionates (**64**, R= Me, Et, n-Pr, n-Bu). These compounds were isolated as thick colourless oils by flash chromatography and were characterised by ^1H , ^{13}C NMR and IR spectroscopy. Formation of each compound was supported by ^1H NMR spectroscopy with a peak at $\delta_{\text{H}} \sim 2.9$ (t, $J_{\text{HH}} \sim 6.5$ Hz, 2H) for ($-\text{N}-\underline{\text{C}}\text{H}_2\text{-CH}_2-$), by ^{13}C NMR spectroscopy with a peak at $\delta_{\text{C}} \sim 44.5$ for ($-\text{N}-\underline{\text{C}}\text{H}_2\text{-CH}_2$) and IR spectroscopy with an absorption at ~ 3330 cm^{-1} for ($-\text{NH}-$). It was important that the reaction mixture was not heated above 40 °C, otherwise disubstituted tertiary amines (**71**) were formed.



Treatment of the alkyl *N*-benzyl-3-aminopropionate (**64**, R= Me, Et) with α -chloroacetophenone (**54**) in dry DMF in the presence of sodium iodide and triethylamine afforded alkyl *N*-(benzoylmethyl)-*N*-benzyl-3-aminopropionate (**65**, R= Me, Et). Transformation was confirmed by the disappearance of a peak in the ^1H NMR spectrum at δ_{H} 4.72 for $-\text{CO-CH}_2\text{-Cl}$ and appearance of a peak at $\delta_{\text{H}} \sim 3.90$ (s, 2H) for ($-\text{CO-CH}_2\text{-N-}$). Formation of (**65**, R= Me, Et) was further supported by ^{13}C NMR spectroscopy with peaks at δ_{C} 193.0 and 172.0 for ($\text{C}=\text{O}$ keto) and ($\text{C}=\text{O}$ ester) respectively. These compounds were fully characterised by ^1H and ^{13}C NMR spectroscopy.

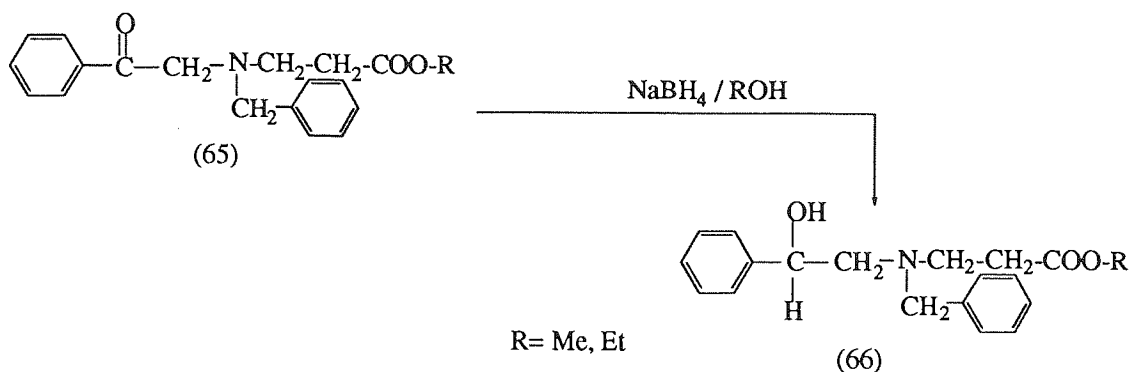


Compounds (65, $\text{R} = \text{Me, Et}$) were unstable. This is possibly attributable to the presence of the keto group which can tautomerise to the enol form (72). The enol form could react with the ester group to give the cyclic lactone (73, Scheme 2.4) or alternatively it may undergo an aldol condensation reaction.¹⁰⁷

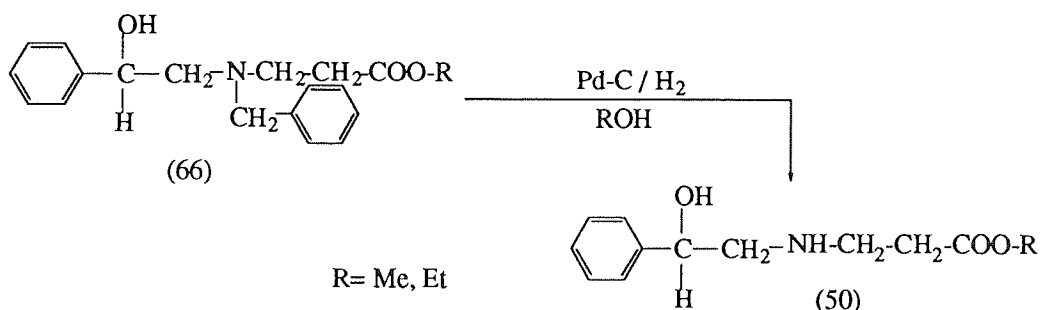


Scheme 2.4: A possible route of decomposition of alkyl N -(benzoylmethyl)- N -benzyl-3-aminopropionate (65).

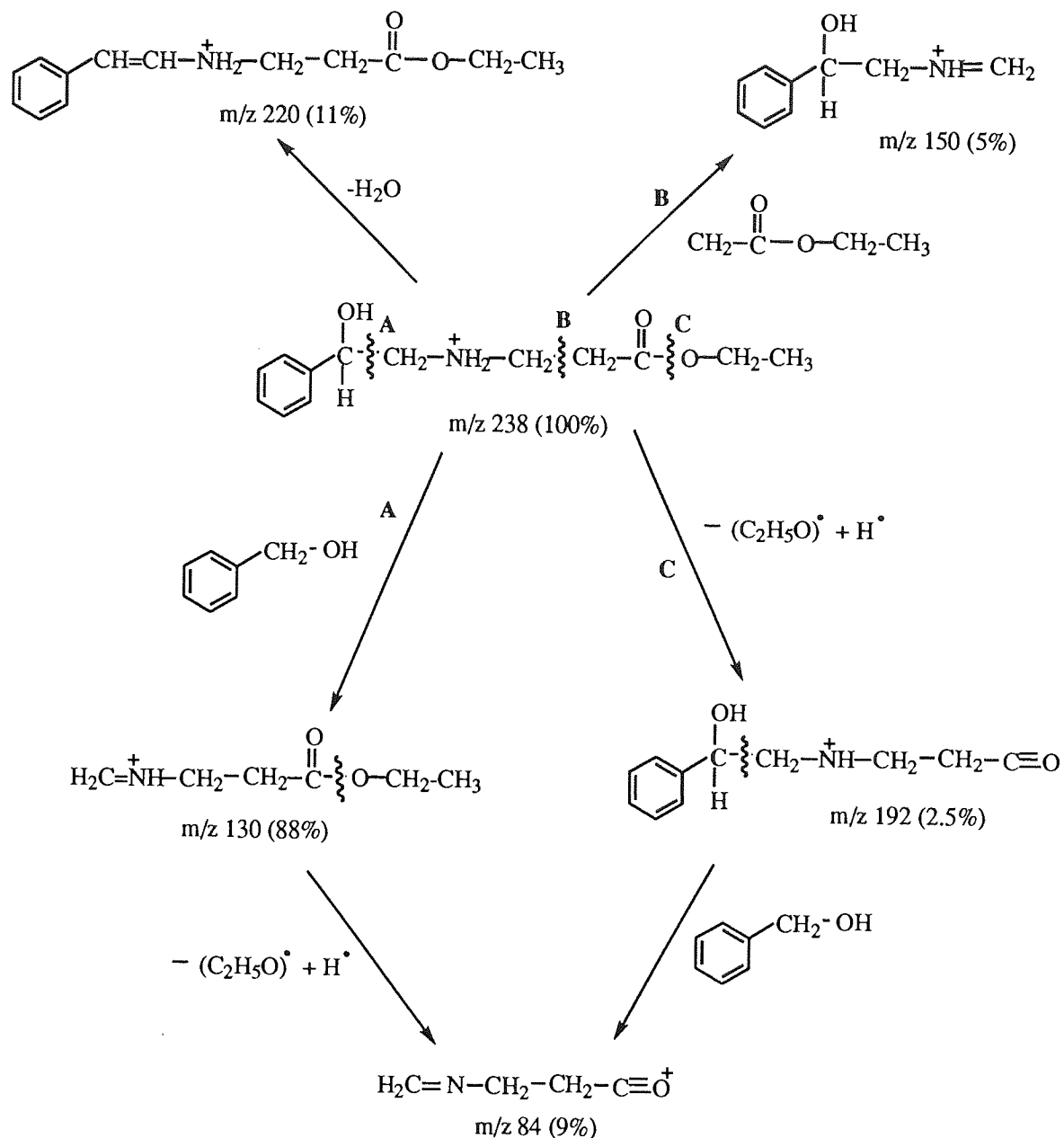
However, the keto group of (65) can readily be reduced (*in situ*) with sodium borohydride in the appropriate alcohol (methanol or ethanol)¹⁰⁹ at room temperature to yield alkyl N -[(2'-hydroxy-2'-phenyl)ethyl]- N -benzyl-3-aminopropionate (66, $\text{R} = \text{Me, Et}$). The transformation was confirmed by ^1H and ^{13}C NMR spectroscopy with the disappearance of the ketone carbonyl peak at $\delta_{\text{C}} 193.0$ and the appearance of new peaks at $\delta_{\text{C}} 69.9$ and $\delta_{\text{H}} 4.67$ (dd, $J_{\text{HH}} = 3.8$ and $J_{\text{HH}} = 9.7$ Hz) for $[-\text{C}(\text{OH})\text{H}-\text{CH}_2-\text{N}-]$. In contrast with the keto compounds (65), the hydroxy derivatives (66) were more stable.



The *N*-benzyl groups of compounds (66, R= Me, Et) were then removed by hydrogenation catalysed by 10% palladium on activated charcoal in the appropriate alcohol (methanol or ethanol)¹⁰⁹ to give the alkyl *N*-(2'-phenyl-2'-hydroxyethyl)-3-aminopropionates (50, R=Et, Me) as solids.



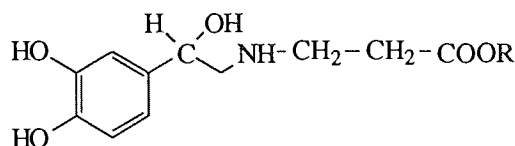
The compounds were characterised by ^1H , ^{13}C NMR and IR spectroscopy, elemental analysis and mass spectrometry. Integration of the aromatic residues decreased to five protons in the ^1H NMR spectrum and four aromatic carbon atom peaks were observed in the ^{13}C NMR spectrum, which confirms the debenzylation and formation of alkyl *N*-(2'-phenyl-2'-hydroxyethyl)-3-aminopropionate (50). Other peaks in the ^1H and ^{13}C NMR spectra, which support the formation of (50, R= Me, Et), include $\delta_{\text{H}} \sim 2.45$ (t, $J_{\text{HH}} \sim 6.5$ Hz, 2H) for $-\text{CH}_2\text{-COO-}$ and ~ 4.65 (dd, $J_{\text{HH}} \sim 3.5$, $J_{\text{HH}} \sim 9.0$, 1H) for $-\text{C}(\text{OH})\text{-H}$, and $\delta_{\text{C}} \sim 71.5$ for $-\text{C}(\text{OH})\text{-H}$ and 172.5 for $(-\text{COO-})$. The IR spectrum showed broad absorbances at ~ 3400 cm^{-1} for $(-\text{OH}$ and $-\text{NH-})$ and ~ 1730 cm^{-1} for $(-\text{COO-})$. The mass spectrum fragmentation for compound (50, R= Et) is shown in Scheme 2.5.



Scheme 2.5: Mass spectrum (CI, NH_3) fragmentation of ethyl *N*-(2'-phenyl-2'-hydroxyethyl)-3-aminopropionate (**50**, R=ethyl).

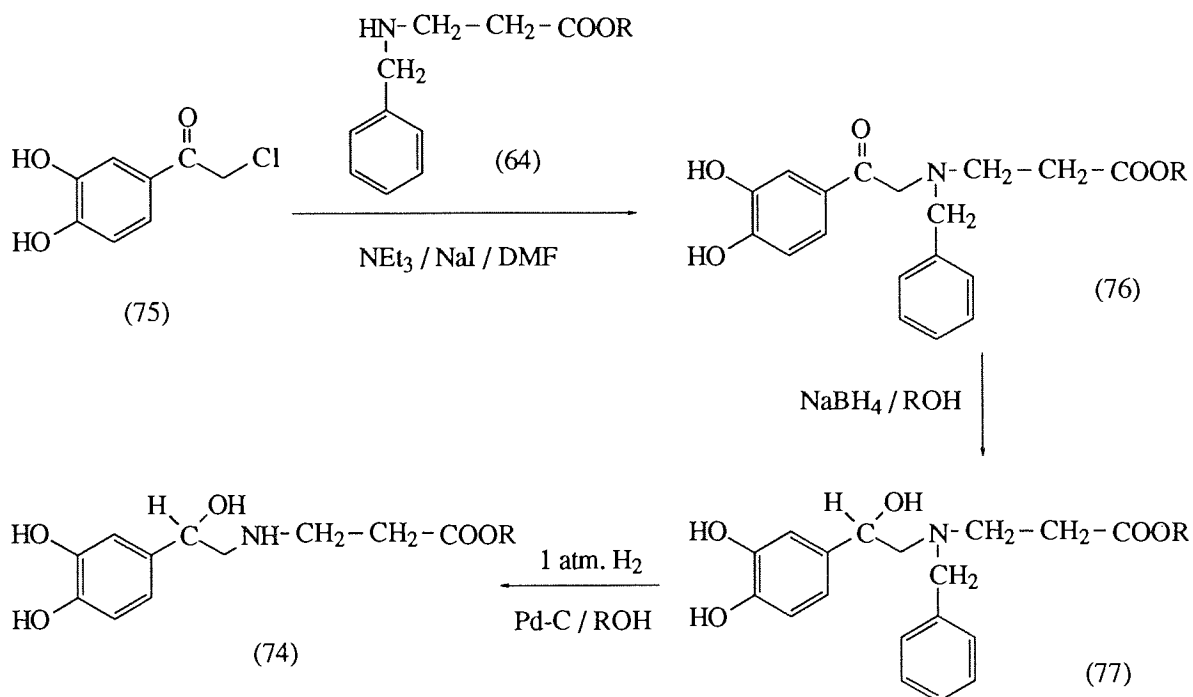
2.4 SYNTHESIS OF CATECHOL AMINO ACID ESTERS (74, R=METHYL, ETHYL, n-PROPYL, n-BUTYL)

Having successfully prepared two amino acid esters (50, $n=2$, R=Me, Et) as model compounds, the syntheses of the analogous catechol derivatives with 3,4-dihydroxy substituents (74, R= Me, Et, n-Pr, n-Bu) were attempted.



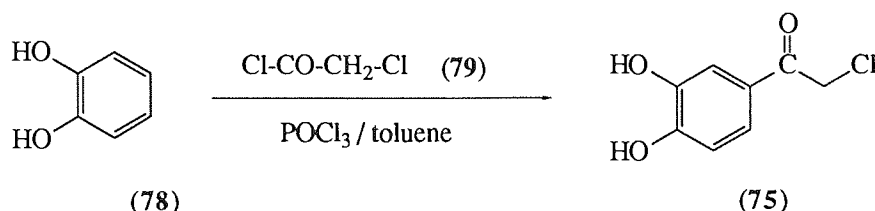
(74)

Using the model chemistry developed for the phenyl analogues, it was anticipated that the catechol amino acids esters (74, R=Me, Et, n-Pr, n-Bu) could be prepared by a similar method outlined in Scheme 2.6. Because the catechol group is light- and air-sensitive, it may make the chemistry more difficult, due to oxidation of the catechol ring. Alternatively the phenolic groups of the catechol ring could react as nucleophiles.

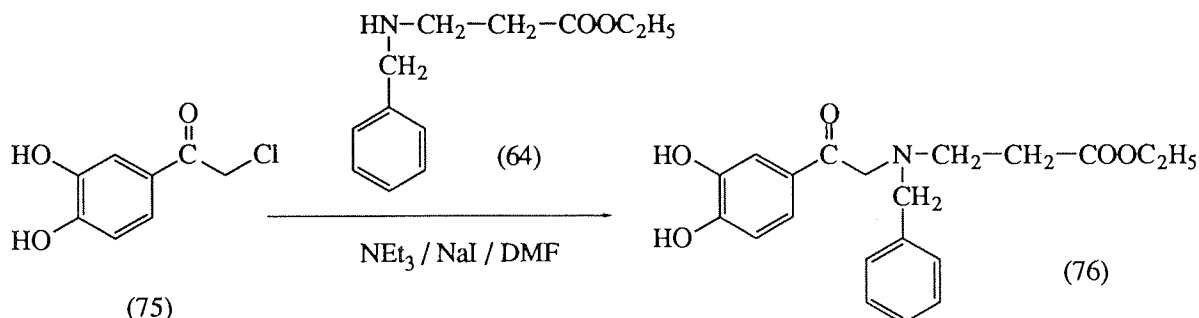


Scheme 2.6: Proposed synthetic route for catechol amino acid esters (74, R=Me, Et, n-Pr, n-Bu)

This route first required the preparation of 3,4-dihydroxy- α -chloroacetophenone (**75**) which was achieved by the Friedel-Crafts acylation reaction of catechol (**78**) with chloroacetyl chloride (**79**).¹¹¹ The appearance of a peak in the ^1H NMR spectrum at δ_{H} 4.67 (s, 2H) for $-\text{CO}-\text{CH}_2-\text{Cl}$, and aromatic protons at δ_{H} 6.92 (d, $J_{\text{ortho}}=8.3$ Hz, 1H, H₅-aromatic), 7.40 (dd, $J_{\text{ortho}}=8.3$, $J_{\text{meta}}=2.1$ Hz, 1H, H₆-aromatic) and 7.52 (d, $J_{\text{meta}}=2.1$ Hz, 1H, H₂-aromatic) confirms the formation of 3,4-dihydroxy- α -chloroacetophenone (**75**). The coupling constants being typical of a 1,3,4-tri-substituted aromatic ring.

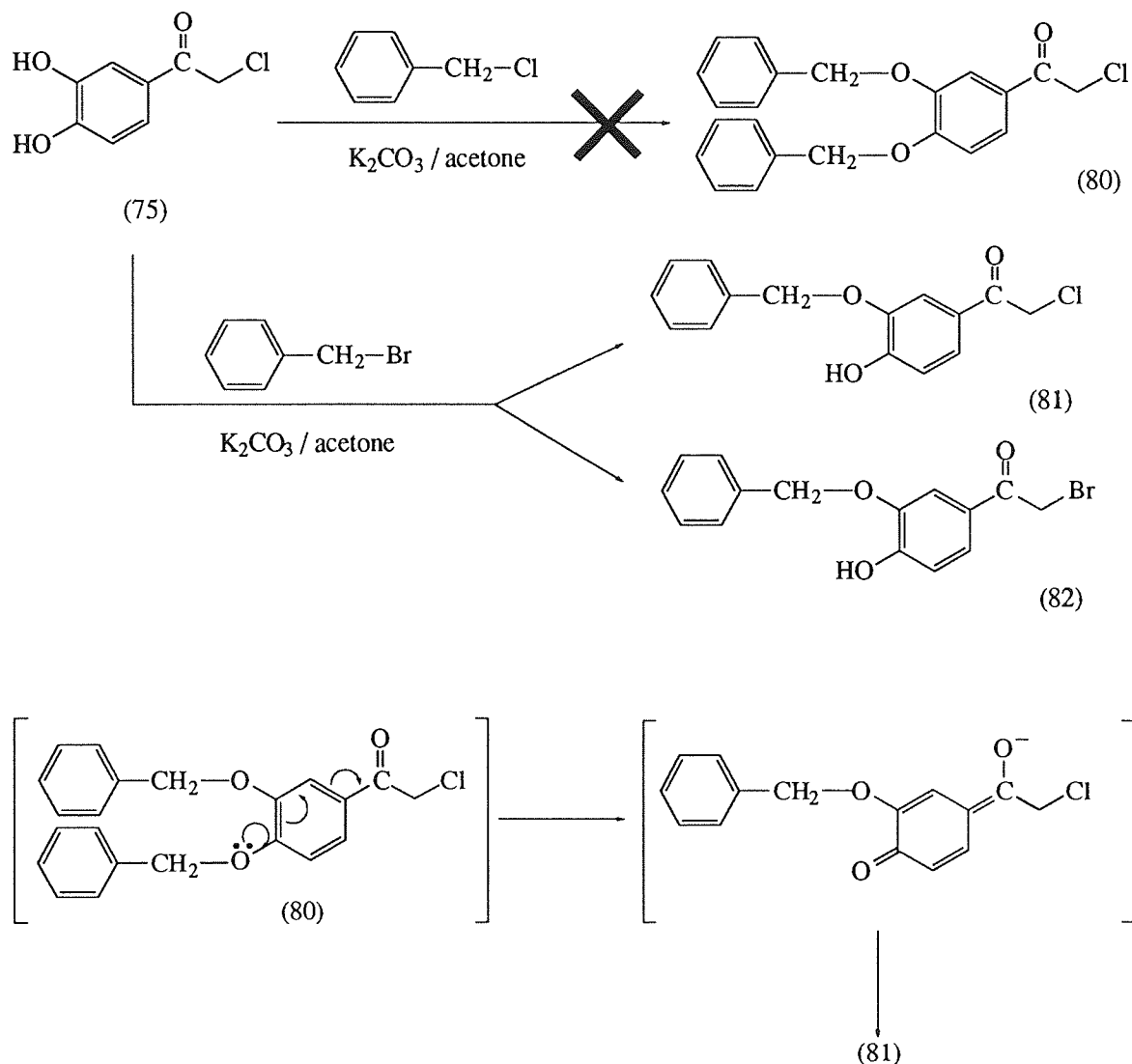


Based on the reaction conditions for the preparation of the phenyl analogue (**65**), 3,4-dihydroxy- α -chloroacetophenone (**75**) was allowed to react with ethyl *N*-benzyl-3-aminopropionate (**64**), however, the required compound (**76**) was not isolated and the reaction mixture turned dark brown. This may be due either to oxidation of the catechol ring or to the phenolic groups reacting as nucleophiles. The hydroxyl groups on the catechol ring should therefore be protected before reaction with the amine (**64**).



The first protection strategy was to convert the phenolic hydroxyl groups into benzyl ethers which ultimately should be removed by hydrogenation. 3,4-Dihydroxy- α -chloroacetophenone (**75**) was treated with benzyl chloride in dry acetone with finely powdered potassium carbonate and potassium iodide.¹¹² The reaction proceeded slowly and gave many products from which the required compound (**80**) could not be isolated. In another reaction, benzyl bromide was used instead of benzyl chloride/KI. The compound isolated was not the desired 3,4-dibenzyloxy- α -chloroacetophenone (**80**); instead, only the 3-hydroxyl group was benzylated to give 3-benzyloxy-4-hydroxy- α -chloroacetophenone (**81**) contaminated with ~35% 3-benzyloxy-4-hydroxy- α -bromoacetophenone (**82**) arising from halide exchange.

There are two peaks in the ^1H NMR spectrum at δ_{H} 4.45 (s, 35%) for $-\text{CH}_2\text{-Br}$ and 4.65 (s, 65%) for $-\text{CH}_2\text{-Cl}$. Other peaks in the ^1H NMR spectrum included δ_{H} 5.20 (s, 2H) for $-\text{O-CH}_2\text{-Ph}$ and 5.78 (br s) for $-\text{OH}$. Absorbances in the IR spectrum included 3505 cm^{-1} for (OH) and 1687 cm^{-1} for (C=O) .

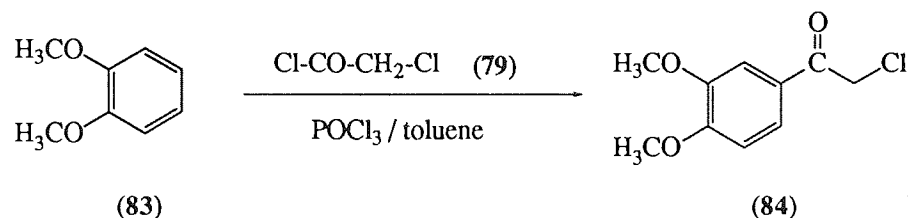


Scheme 2.7: Mechanism showing why the 4-benzyloxy group is cleaved more readily than the 3-benzyloxy group.

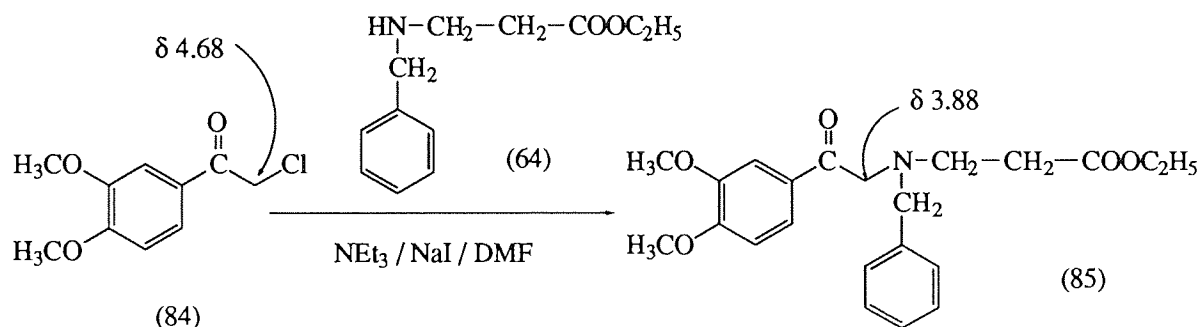
Halide exchange may arise from reaction of the potassium bromide by-product with either (75) to give 3,4-dihydroxy- α -bromoacetophenone, which after benzylation gives (82), or alternatively with (81) to give (82). The lack of further benzylation of either (81) or (82) could be attributed to a steric problem of having two benzyloxy groups *ortho* to each other, or alternatively to the ease with which the 4-benzyl group cleaves due to the stability of both the benzyl carbonium ion and the resonance stabilised phenoxide anion (Scheme 2.7).

Benzylation was therefore unsuitable as a method of protection, and attention was turned to methyl ethers.

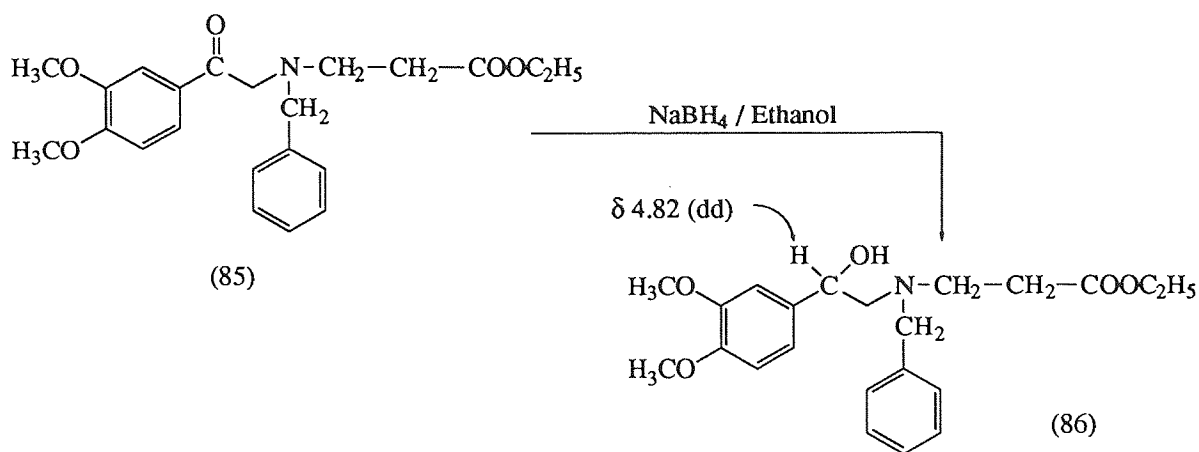
1,2-Dimethoxybenzene (**83**) was acylated with chloroacetyl chloride to yield 3,4-dimethoxy- α -chloroacetophenone (**84**).¹¹¹ The appearance of peaks in the ^1H NMR spectrum at δ 3.95 (s, 3H) for $-\text{OCH}_3$, 3.97 (s, 3H) for $-\text{OCH}_3$, and 4.68 (s, 2H) for $-\text{CH}_2\text{-Cl}$ and a absorbance in the IR spectrum at 1689 cm^{-1} for $(\text{C}=\text{O})$ support the formation of 3,4-dimethoxy- α -chloroacetophenone (**84**).



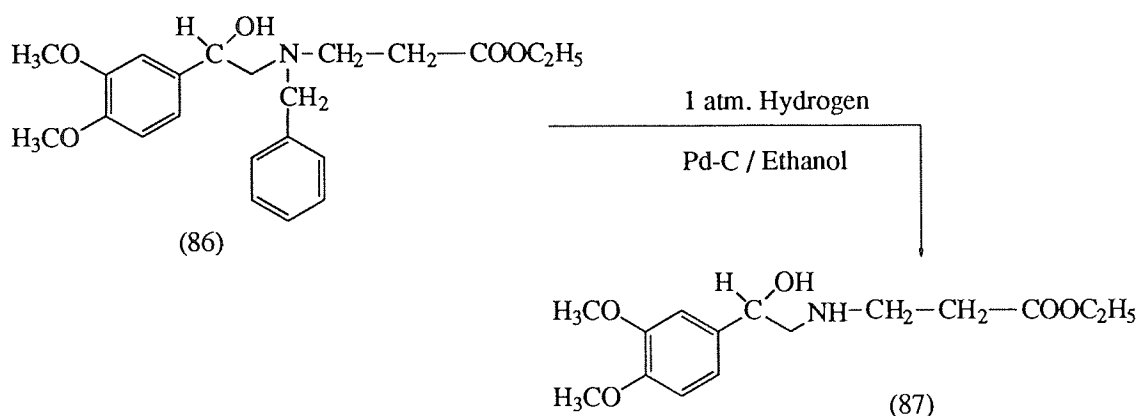
3,4-Dimethoxy- α -chloroacetophenone (**84**) was coupled with ethyl *N*-benzyl-3-aminopropionate (**64**) in dry DMF, sodium iodide and triethylamine. The product, ethyl *N*-[(3',4'-dimethoxybenzoyl)methyl]-*N*-benzyl-3-aminopropionate (**85**), was isolated as the free base by flash chromatography in a yield of 88%. The disappearance of a peak in the ^1H NMR spectrum at δ_{H} 4.68 for $-\text{CO-CH}_2\text{-Cl}$ and appearance of peaks at δ_{H} 3.88 (s, 2H) for $-\text{CO-CH}_2\text{-N-}$ and 3.81 (s, 2H) for $-\text{N-CH}_2\text{-Ph}$ confirms the formation of ethyl *N*-[(3',4'-dimethoxybenzoyl)methyl]-*N*-benzyl-3-aminopropionate (**85**).



Ethyl *N*-[(3',4'-dimethoxybenzoyl)methyl]-*N*-benzyl-3-aminopropionate (**85**) was reduced with sodium borohydride in ethanol¹⁰⁹ at room temperature to yield ethyl *N*-[2'-(3'',4''-dimethoxyphenyl)-2'-hydroxyethyl]-*N*-benzyl-3-aminopropionate (**86**). The reduction was confirmed by the appearance of a peak in the ^1H NMR spectrum at δ 4.82 (dd, $J_{\text{HH}}=8.3$, $J_{\text{HH}}=4.0$ Hz, 1H) for $-\text{C}(\text{OH})\text{-H}$.

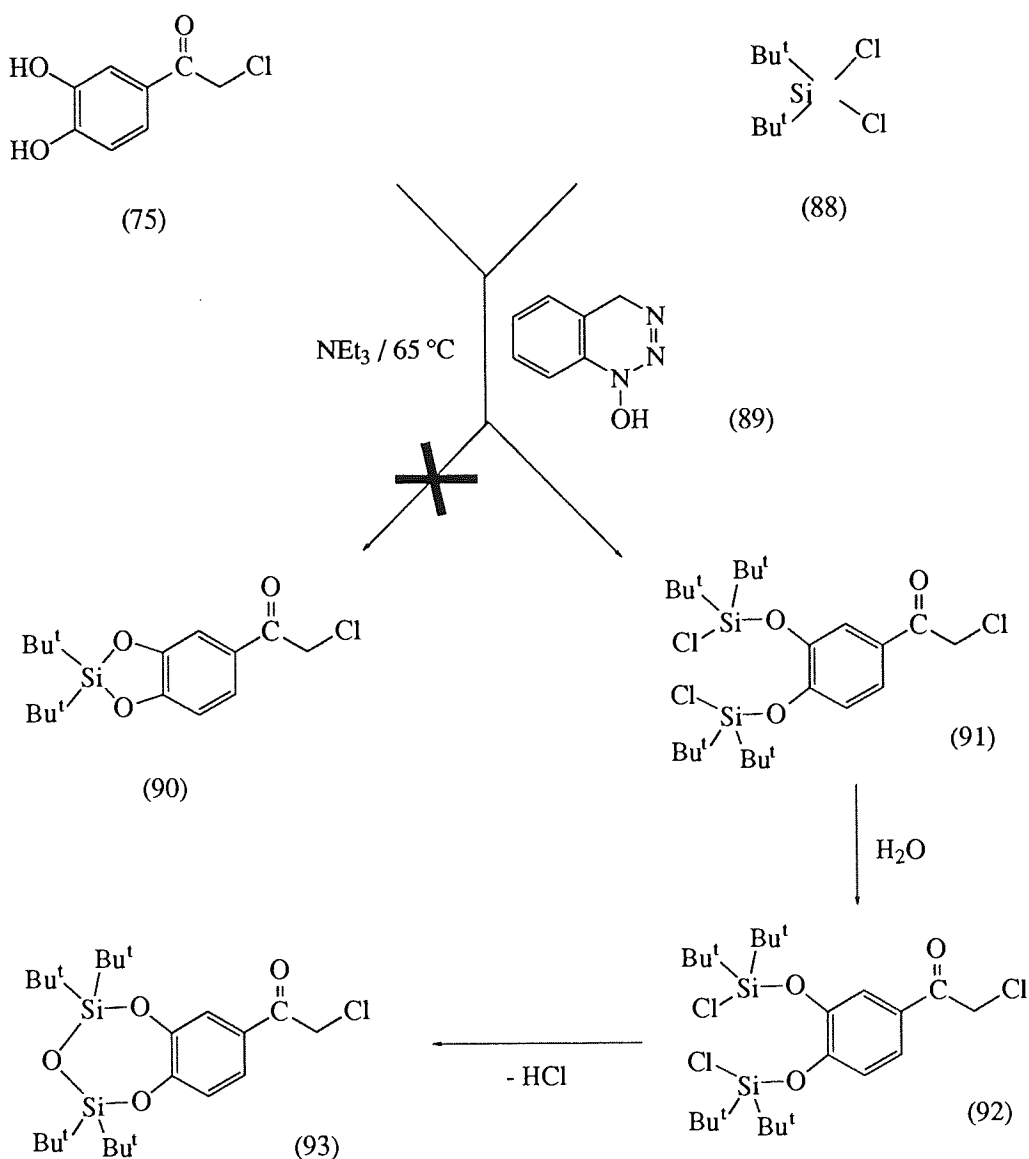


The *N*-benzyl group of compound (86) was removed by hydrogenation, catalysed by 10% palladium on activated charcoal in ethanol,¹⁰⁹ to give ethyl *N*-[2'-(3",4"-dimethoxyphenyl)-2'-hydroxyethyl]-3-aminopropionate (87). The deprotection was confirmed by ¹H NMR spectroscopy with the decrease in integration to three aromatic protons and disappearance of peaks for the methylene of the benzyl group. The product also showed an absorbance in the IR spectrum at 3313 cm^{-1} for (-NH-).

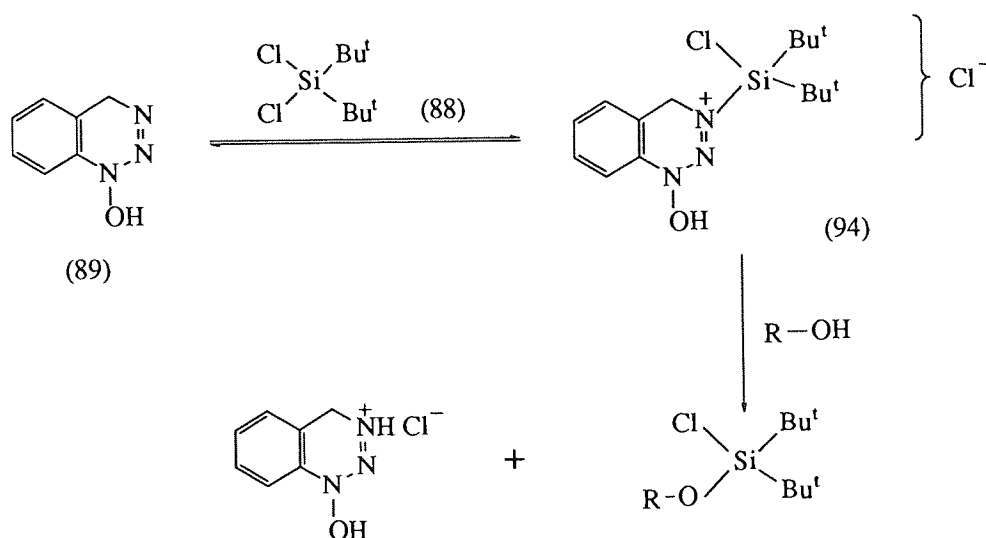


Demethylation¹¹³ of compound (87) to the 3,4-dihydroxy derivative (74, R=Et) requires Lewis acids (for example, boron tribromide) or trimethylsilyl iodide, which may attack other reactive groups in the molecule like -OH, -NH- and ester. Therefore, although this sequence has shown that the target compound may be obtained, the protection of the hydroxyl groups by methyl ethers is not an appropriate strategy. Attention was therefore turned to more labile protection groups, initially utilising the di(*t*-butylsilyl) substituent.

3,4-Dihydroxy- α -chloroacetophenone (**75**) was treated with di-*t*-butyl dichlorosilane (**88**) in dry acetonitrile in the presence of triethylamine and 1-hydroxybenzotriazole (**89**).¹¹⁴ The required product di-(*t*-butyl)silyldioxy- α -chloroacetophenone (**90**) was not formed, but the compound 3,4-(1',1',3',3'-tetra-*t*-butyldisiloxane)dioxy- α -chloroacetophenone (**93**) was isolated by flash chromatography in a 40% yield. Proton NMR peaks at δ_{H} 1.10 (s, 36H) for $(\text{CH}_3)_3\text{C-Si}$ and 4.68 (s, 2H) for $-\text{CO-CH}_2\text{-Cl}$; carbon NMR peaks at δ_{C} 21.3 for $(\text{CH}_3)_3\text{C-Si}$, 27.9 for $(\text{CH}_3)_3\text{C-Si}$, 45.7 for $-\text{CO-CH}_2\text{-Cl}$ and 193.3 for $(\text{C}=\text{O})$; and IR (KBr) peaks at 1698 cm^{-1} for $(\text{C}=\text{O})$ and 1319 cm^{-1} for (Si-O-C) support this structural assignment. Formation of compound (**93**) was further confirmed by mass spectral analysis.

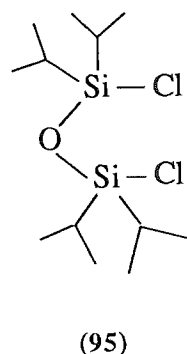


The cyclic compound (93) must arise from the reaction of 2 molecules of di-*t*-butyl dichlorosilane (88) with one molecule of 3,4-dihydroxy- α -chloroacetophenone (75), with subsequent hydrolysis of (91) to (92) and liberation of HCl to give (93). There are two proposals for the mechanism of action of 1-hydroxybenzotriazole; i) the amine functions as a proton acceptor, and ii) the amine forms a complex (94) with the silyl chloride, which subsequently reacts with the alcohol to form the silyl ether. The 1-hydroxy group is electron donating which facilitates formation of a charged intermediate (94) and in this way reaction with alcohols is accelerated (Scheme 2.8).

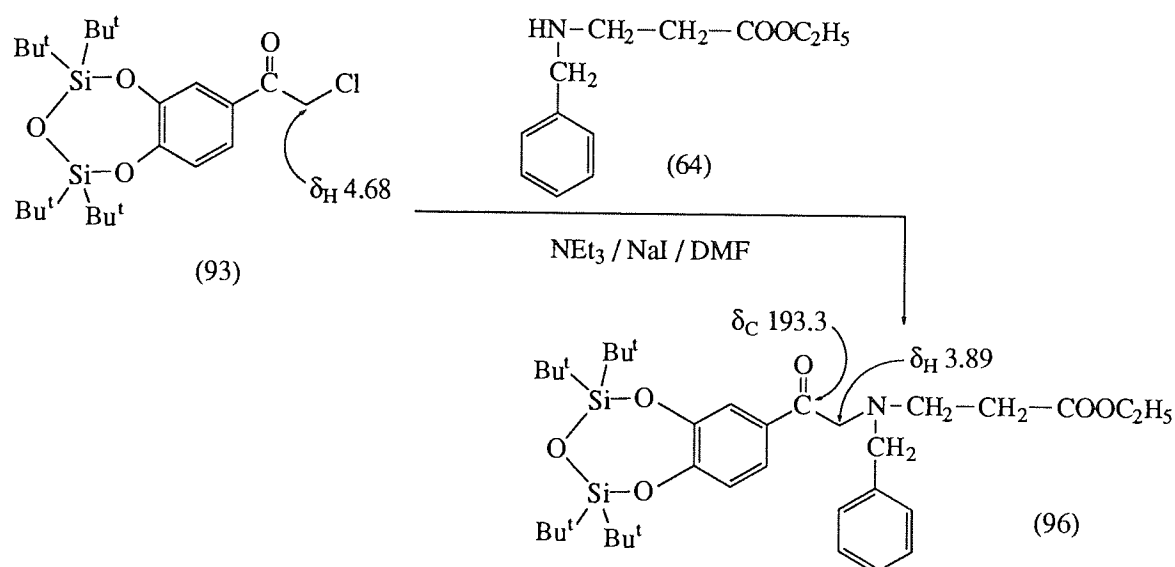


Scheme 2.8: Mechanism of 1-hydroxybenzotriazole catalysis.

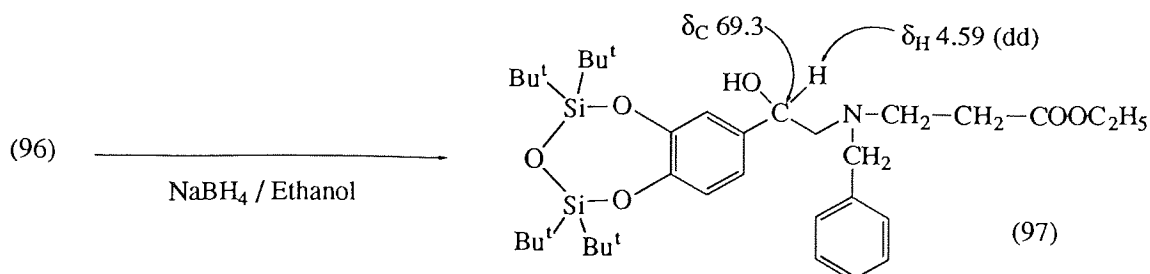
It should be noted that a more direct route to prepare compounds of type (93) would be to react 3,4-dihydroxy- α -chloroacetophenone (75) with 1,3-dichloro-1,1,3,3-tetraisopropyl disiloxane (95) which is commercially available for the protection of 1,2-diols.

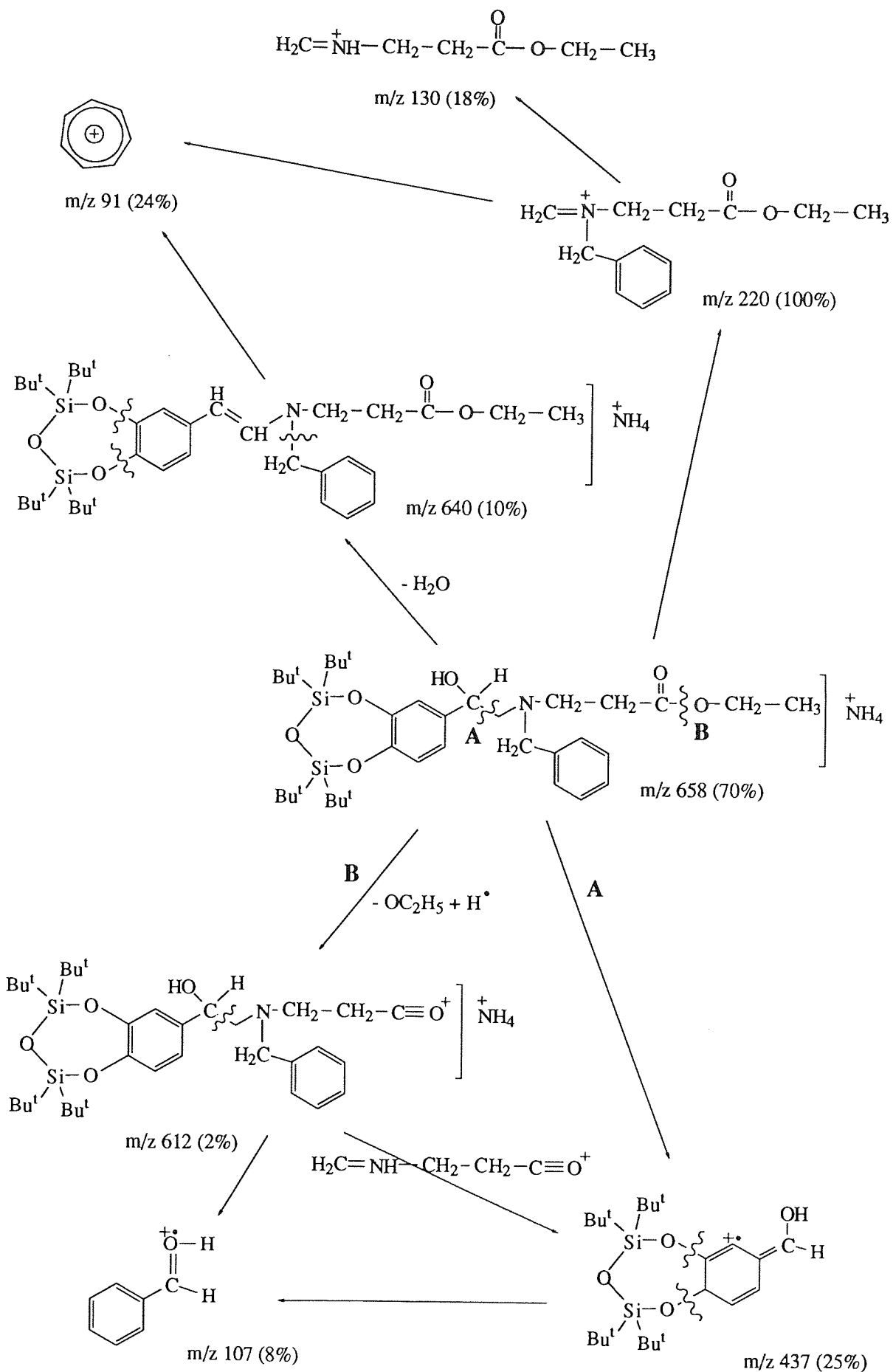


Although the desired compound (**90**) was not formed, the product obtained (**93**) may still be a useful intermediate. 3,4-(1',1',3',3'-Tetra-*t*-butyldisiloxane)dioxy- α -chloroacetophenone (**93**) was coupled with ethyl *N*-benzyl-3-aminopropionate (**64**) in dry DMF, sodium iodide and triethylamine. The desired product, ethyl *N*-{[3,4-(1',1',3',3'-tetra-*t*-butyldisiloxane)dioxybenzoyl]methyl}-*N*-benzyl-3-aminopropionate (**96**) was isolated by flash chromatography in a yield of 82%. Coupling was confirmed by the absence of a peak in the ^1H NMR spectrum at δ_{H} 4.68 (s, 2H) for $-\text{CO}-\text{CH}_2-\text{Cl}$ and the appearance of a peak at δ 3.89 (s, 2H) for $-\text{CO}-\text{CH}_2-\text{N}-$. Peaks in the ^{13}C NMR spectrum included δ_{C} 59.2 for $(-\text{CO}-\underline{\text{C}}\text{H}_2-\text{N}-)$ and 193.3 for $(-\text{C}\text{O}-\text{CH}_2-\text{N}-)$ absorbances in the IR spectrum at 1680 cm^{-1} for $(\text{C}=\text{O}$ keto) and 1729 cm^{-1} for $(\text{C}=\text{O}$ ester) also support the formation of compound (**96**).



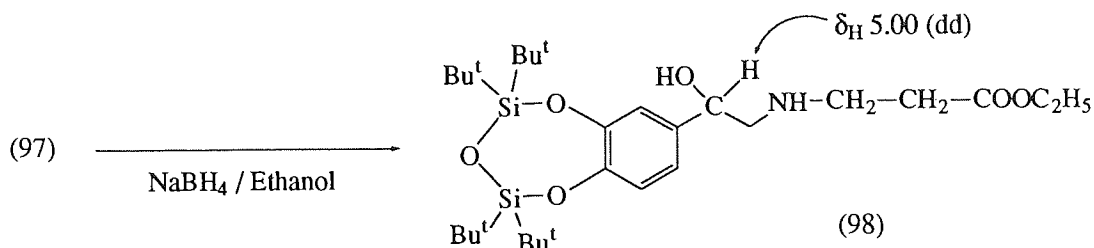
Ethyl *N*-{[3,4-(1',1',3',3'-tetra-*t*-butyldisiloxane)dioxybenzoyl]methyl}-*N*-benzyl-3-aminopropionate (**96**) was reduced with sodium borohydride in ethanol¹⁰⁹ at room temperature to give ethyl *N*-{2'-[3",4"-(1"',1"',3"',3"'-tetra-*t*-butyldisiloxane)dioxyphenyl]-2'-hydroxyethyl}-*N*-benzyl-3-aminopropionate (**97**). Reduction was confirmed by the disappearance of a peak in the ^{13}C NMR spectrum at δ_{C} 193.3 for $(\text{C}=\text{O}$ keto) and appearance of a peak at δ_{C} 69.3 for $-\text{C}(\text{OH})-\text{H}$. Transformation was further supported by disappearance of an IR stretch at 1680 cm^{-1} for $(\text{C}=\text{O}$ keto) and appearance in the ^1H NMR spectrum of a peak at δ 4.59 (dd, $J_{\text{gem}}=9.5$, $J_{\text{HH}}=3.7$ Hz, 1H) for $-\text{C}(\text{OH})-\underline{\text{H}}$. The structure was also supported by elemental analysis and mass spectroscopy. The mass spectral fragmentation pattern for (**97**) is shown in Scheme 2.9.



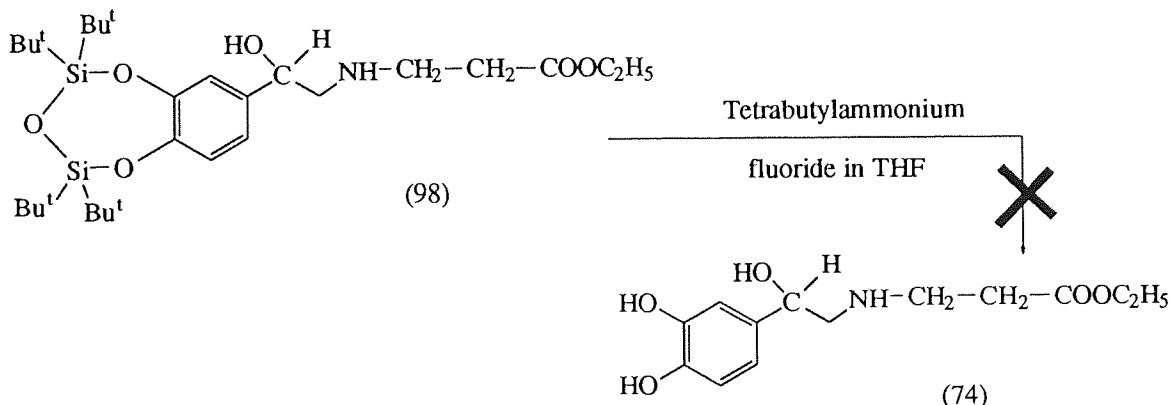


Scheme 2.9: Mass spectrum (CI, NH_3) fragmentation pattern of ethyl *N*-(2'-[3'',4''-(1''',1''',3''',3''')-tetra-*t*-butylidisiloxane]dioxiphenyl)-2'-hydroxyethyl)-*N*-benzyl-3-aminopropionate (97)

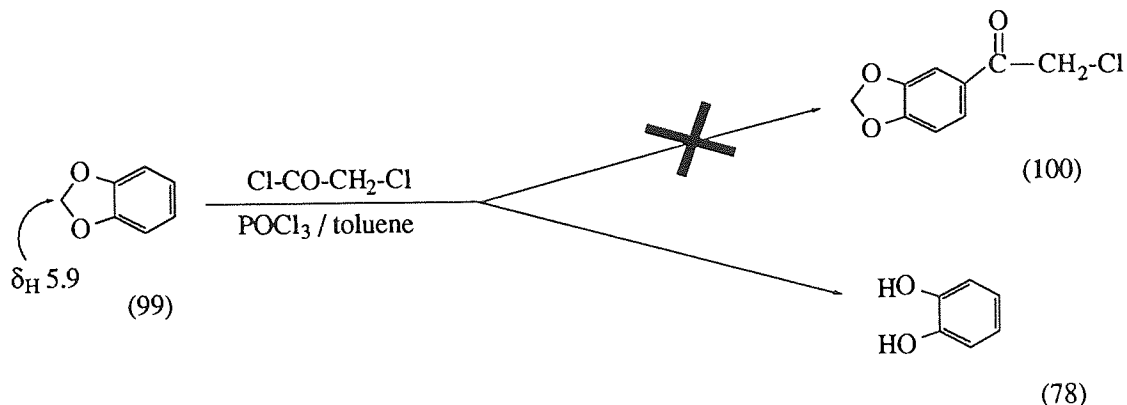
The *N*-benzyl group of compound (97) was removed by hydrogenation catalysed by 10% palladium on activated charcoal in ethanol¹⁰⁹ to give ethyl *N*-{2'-[3'',4''-(1''',1''',3''',3'''-tetra-*t*-butyldisiloxane)dioxyphenyl]-2'-hydroxyethyl}-3-aminopropionate (98). Deprotection was confirmed by ¹H NMR spectroscopy with the decrease in integration to three aromatic protons, and disappearance of peaks for an *N*-benzyl group. Other peaks in the ¹H NMR spectrum included δ_{H} 1.08 (s) for [(CH₃)₃C-Si] and 5.00 (dd, 1H, $J_{\text{HH}}=9.8$, 1Hz) for [-C(OH)-H], and in the ¹³C NMR spectrum δ_{C} 69.4 for [-C(OH)-H].



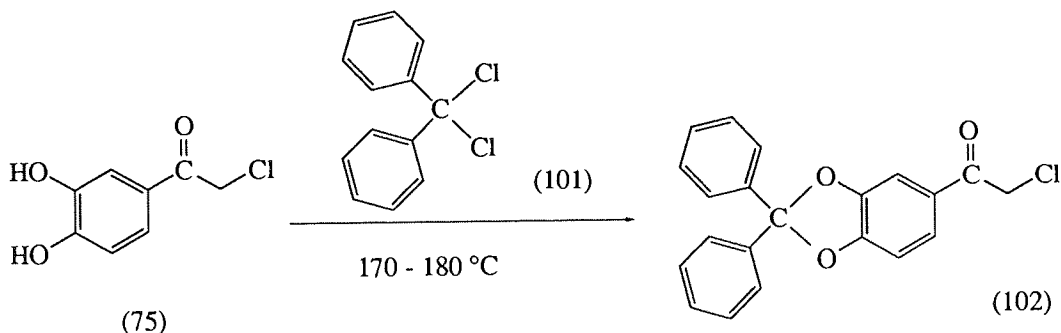
Silyl groups are usually readily removed by fluoride anions,¹¹⁵ however treatment of ethyl *N*-{2'-[3'',4''-(1''',1''',3''',3'''-tetra-*t*-butyldisiloxane)dioxyphenyl]-2'-hydroxyethyl}-3-aminopropionate (98) with tetrabutylammonium fluoride in THF, resulted in its oxidation to a dark residue. Despite various modifications, this could not be improved, therefore, it is not an appropriate protecting group for the synthesis of soft-drugs of structure (74), and attention was turned to acetal protection of the catechol ring.



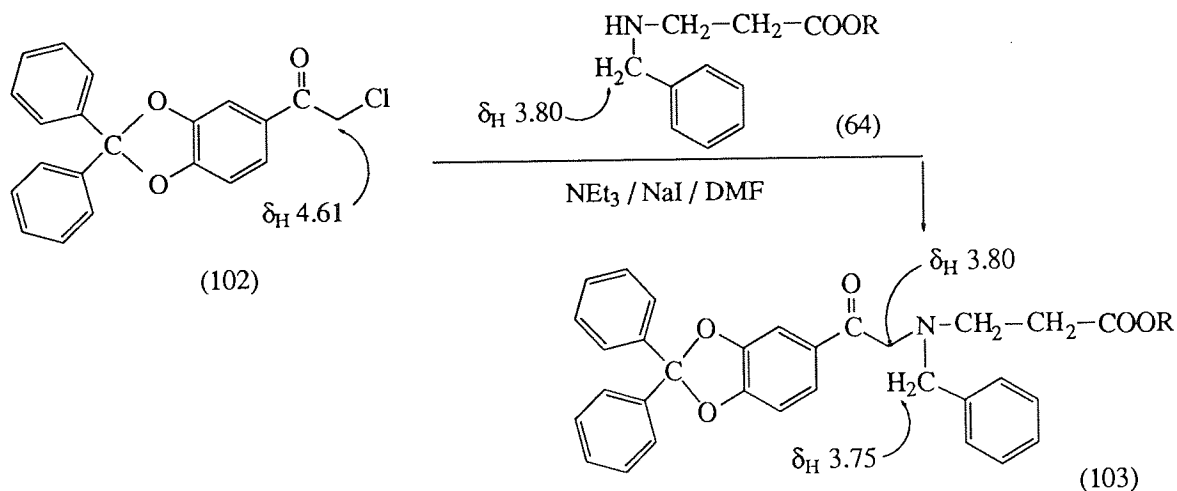
1, 2-(Methylenedioxy)benzene (99) was treated with chloroacetyl chloride in toluene.¹¹¹ The desired compound (100) was not formed, instead catechol (78) was isolated. This is due to cleavage of the methylenedioxy group by the acid generated in the Friedel-Crafts acylation reaction. It was therefore considered that protection of the 1,2-diols to an acetal should occur after the acylation reaction. Also, the diphenylmethylene acetal, which could be removed by hydrogenolysis as well as acid catalysed hydrolysis, was evaluated.



3,4-Dihydroxy- α -chloroacetophenone (**75**) was heated with dichlorodiphenylmethane (**101**) at 170-180 °C¹¹⁶ to give 3,4-diphenylmethylenedioxy- α -chloroacetophenone (**102**). Protection was confirmed by the appearance of a quaternary carbon in the ¹³C NMR spectrum at δ_{C} 117.0 for (Ph_2C), together with peaks at δ_{C} 45.6 for ($-\text{CH}_2\text{-Cl}$) and 193.0 (C=O). The peak in the ¹H NMR spectrum at δ_{H} 4.61 (s) for $-\text{CH}_2\text{-Cl}$ and the absorption in the IR spectrum at 1697 cm^{-1} for (C=O) together with the absence of an $-\text{OH}$ stretch also supports structure (**102**).

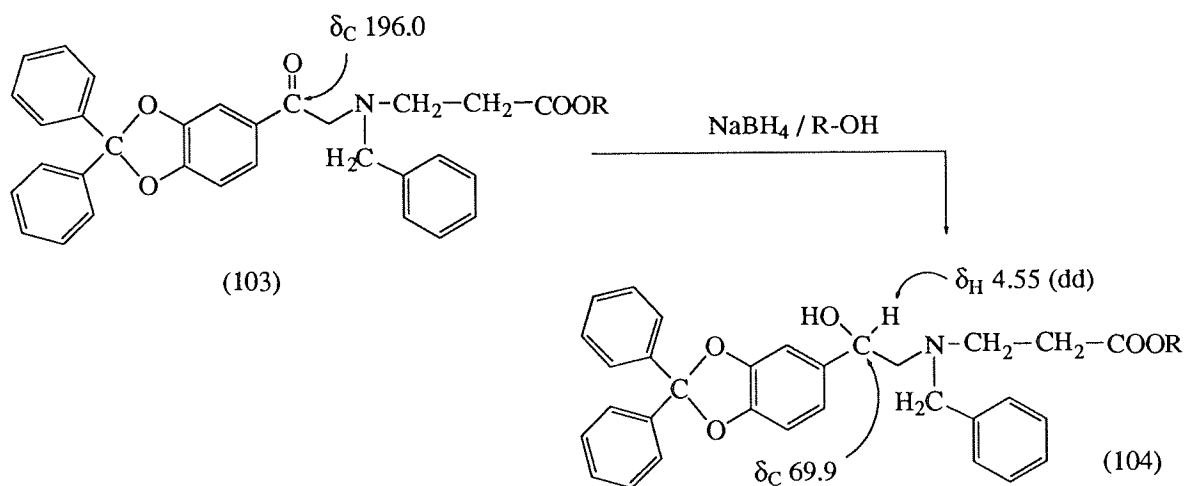


Proceeding towards the synthesis of the soft-drugs, 3,4-diphenylmethylenedioxy- α -chloroacetophenone (**102**) was coupled with alkyl *N*-benzyl-3-aminopropionates (**64**, R= Me, Et, n-Pr, n-Bu) in dry DMF, sodium iodide and triethylamine. The products, alkyl *N*-[(3',4'-diphenylmethylenedioxy)benzoylmethyl]-*N*-benzyl-3-aminopropionates (**103**, R= Me, Et, n-Pr, n-Bu), were isolated by flash chromatography as pale yellow oils.



The compounds (**103**, R= Me, Et, n-Pr, n-Bu) were characterised by ^1H and ^{13}C NMR spectroscopy and IR spectrometry. The structures were confirmed by disappearance of a peak in the ^1H NMR spectrum at δ_{H} 4.61 (s, 2H, -CO-CH₂-Cl) for starting material (**102**) and appearance of a peak at δ_{H} ~3.80 (s, 2H) for (CO-CH₂-N-). Other peaks which support the formation of (**103**) include δ_{H} ~3.75 (s, 2H) for (-N-CH₂-Ph); δ_{C} ~58.0 for (-N-CH₂-Ph), ~59.4 for (-CO-CH₂-N-), ~117.9 for (Ph₂C-), ~196.0 for (C=O keto) and ~172.0 for (C=O ester); IR (neat) peaks at ~1730 cm⁻¹ for (C=O ester) and ~1680 cm⁻¹ for (C=O keto).

The alkyl *N*-[(3',4'-diphenylmethylenedioxy)benzoylmethyl]-*N*-benzyl-3-aminopropionates (**103**, R= Me, Et, n-Pr, n-Bu) were reduced with sodium borohydride in the appropriate alcohol (methanol, ethanol, n-propanol or n-butanol)¹⁰⁹ at room temperature to yield alkyl *N*-[2'-(3'',4''-diphenylmethylenedioxyphenyl)-2'-hydroxyethyl]-*N*-benzyl-3-aminopropionates (**104**, R= Me, Et, n-Pr, n-Bu).



These reductions were confirmed by ^{13}C NMR spectroscopy with the disappearance of the carbonyl ester peak at δ_{C} 196.0 and the appearance of a peak at δ_{C} 69.9 for -C(OH)-H. ^1H NMR peak at δ_{H} 4.55 (dd, $J_{\text{HH}}=9.0$, $J_{\text{HH}}=4.8$ Hz, 1H) for [-C(OH)-H] and IR (KBr) peak at ~3400 cm⁻¹ (broad s) for (-OH and -NH-) also supports the formation of product (**104**). In the ^1H NMR spectrum, peaks were assigned with the help of a ^1H - ^1H COSY spectrum. For the n-butyl analogue (**104**, R= n-Bu) (Figure 2.2) the signal for the methyl protons at δ_{H} 0.90 (t, -CH₃) has a cross-peak connecting it (dashed lines) to the signal from the methylene protons at δ_{H} 1.34 (sextet, -CH₂-CH₃), which showed connectivity to the methylene protons at δ_{H} 1.57 (pentet, -CH₂-CH₂-CH₃), which in turn was connected to the methylene protons at δ_{H} 4.05 (quartet, -COO-CH₂-). The signal for the benzylic protons at δ_{H} 3.46 (d, -CH_AH_B-Ph) has a cross-peak connecting it (dashed lines) to the signal from benzylic protons at δ_{H} 3.81 (d, -CH_AH_B-Ph).

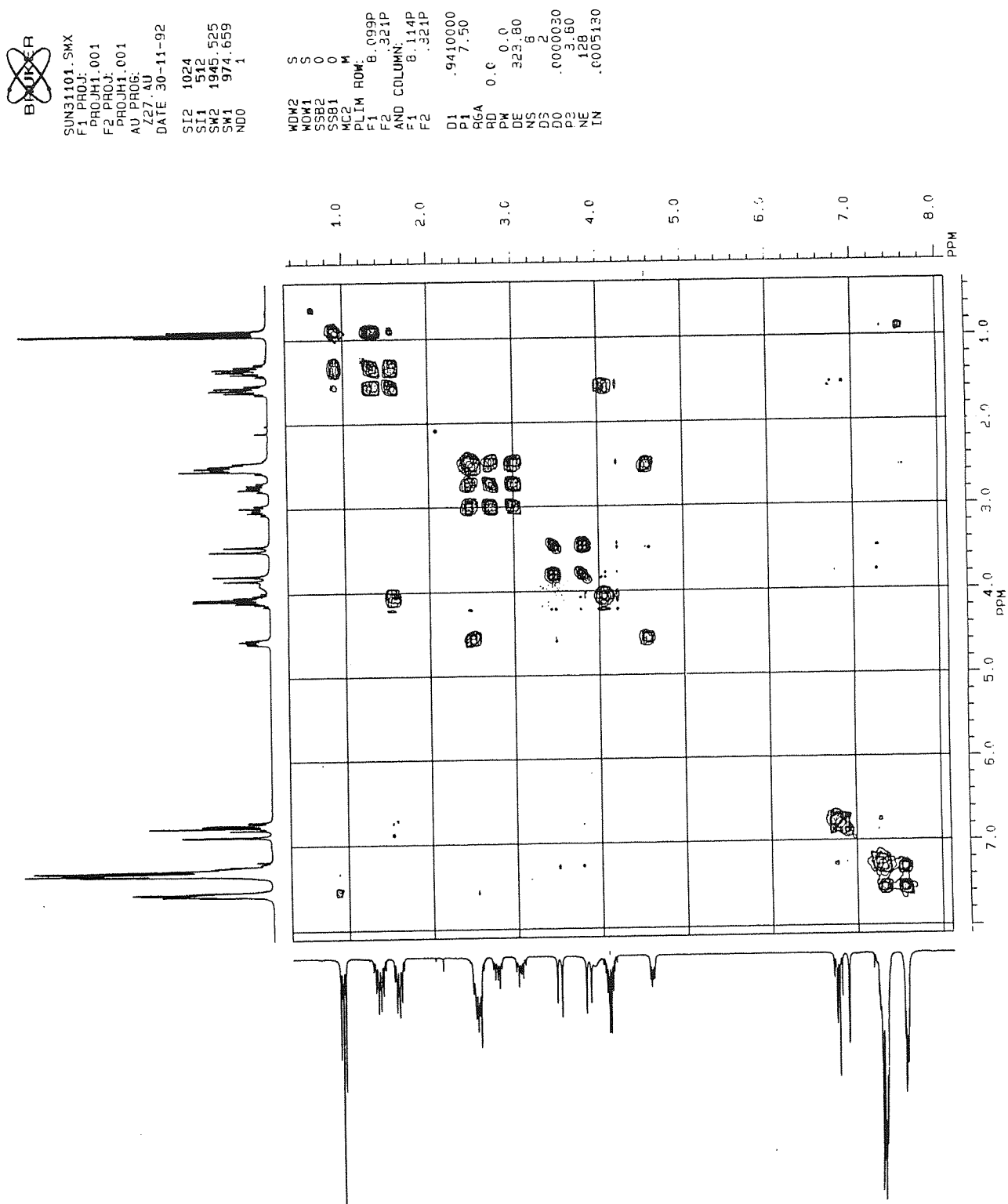
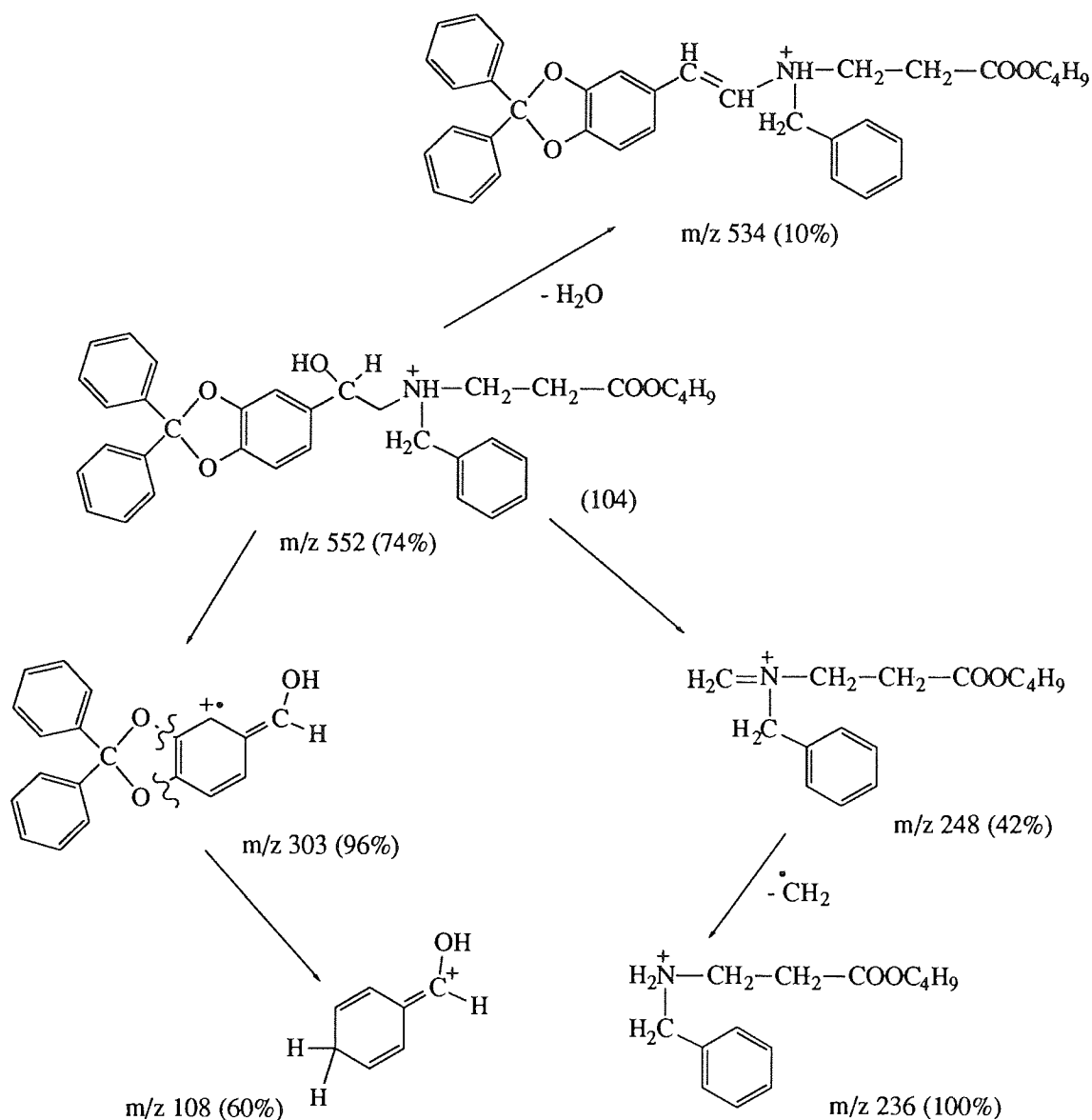


Figure 2.2: ^1H - ^1H COSY spectrum of butyl *N*-[2'-(3'',4''-diphenylmethylenedioxyphenyl)-2'-hydroxyethyl]-*N*-benzyl-3-aminopropionate (**104**, R= n-Bu)

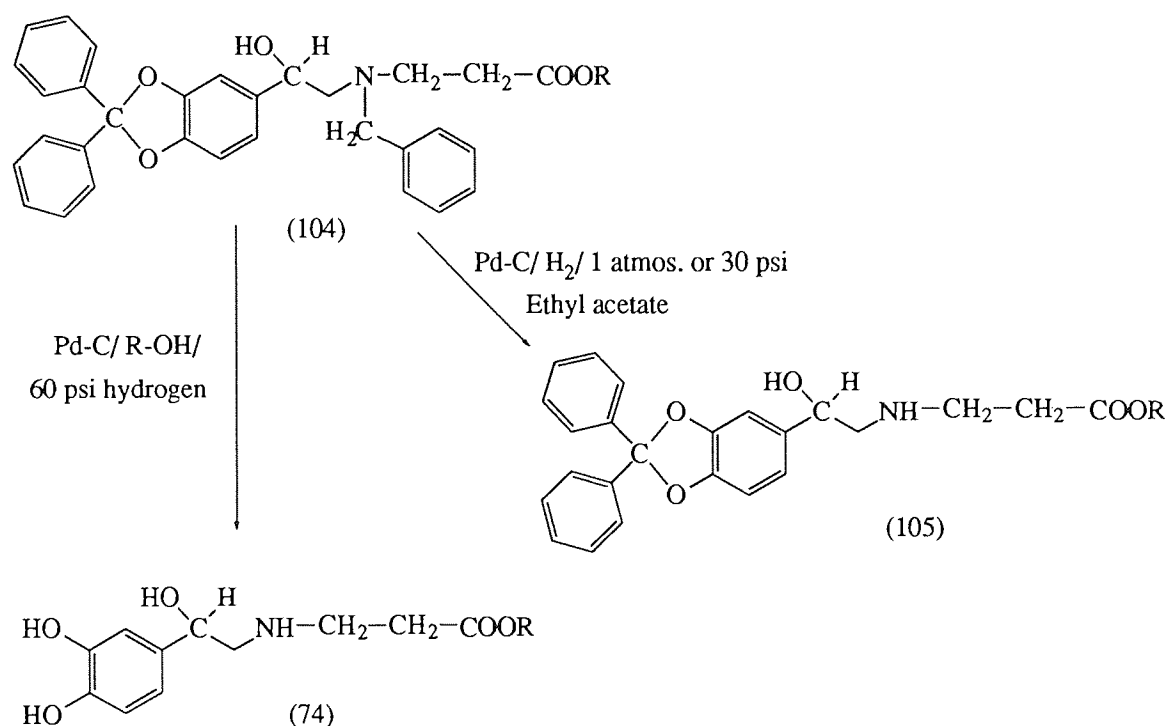


Scheme 2.10: Mass spectrum (CI, NH_3) fragmentation pattern of butyl *N*-[2'-(3'',4''-diphenylmethylenedioxyphenyl)-2'-hydroxyethyl]-*N*-benzyl-3-aminopropionate (**104**, $R = n\text{-Bu}$)

The signal at δ_{H} 4.55 (dd) for $[-\text{C}(\text{OH})-\underline{\text{H}}]$ has a cross-peak connection to the multiplet at δ_{H} 2.41-2.59, which shows that $[-\text{HC}(\text{OH})-\underline{\text{C}}\text{H}_2-\text{N}-]$ is part of the multiplet. The signals at δ_{H} 2.70 and 2.76 (dt) show a cross-peak connection to the signals at δ_{H} 2.98 and 3.03 (dt). The signals from both sets of peaks are further connected to the signals from the multiplet at δ_{H} 2.41-2.59, which shows that $(-\text{CH}_2-\text{COO}-)$ is part of the multiplet at δ_{H} 2.41-2.59. This shows that the peaks at δ_{H} 2.70 and 2.76 (dt) correspond to one proton for $(-\text{N}-\underline{\text{C}}\text{H}_\text{A}\text{H}_\text{B}-\text{CH}_2-)$ and the peaks at δ_{H} 2.98 and 3.03 (dt) corresponds to the second proton for $(-\text{N}-\text{C}\text{H}_\text{A}\underline{\text{H}}_\text{B}-\text{CH}_2-)$. The $^1\text{H}-^1\text{H}$ COSY spectrum for compound (**104**, $R = n\text{-Bu}$) is shown in Figure 2.2. The structure of (**104**, $R = n\text{-Bu}$) was also supported by elemental analysis and by mass spectrometry. The mass spectral fragmentation pattern of (**104**, $R = n\text{-Bu}$) is shown in Scheme 2.10.

The diphenylmethylene group can be removed by hydrogenation at 60 psi under hydrogen atmosphere at room temperature. It is advantageous to use the diphenylmethylene group for the protection of the catechol, because in the final step, both the diphenylmethylene and *N*-benzyl protecting groups can be removed in one step by hydrogenation at 60 psi, though removal of the *N*-benzyl group requires only 1 atmosphere pressure of hydrogen. The *N*-benzyl group of esters (**66**, R= Me, Et) were readily removed by hydrogenation at 1 atmosphere at room temperature in the presence of 10% palladium on activated charcoal catalyst.¹⁰⁹ Under these conditions the *N*-benzyl group was removed from (**104**, R=Et), however the diphenylmethylene group was not removed to give ethyl *N*-[2'-(3",4"-diphenylmethylenedioxyphenyl)-2'-hydroxyethyl]-3-aminopropionate (**105**, R=Et). Transformation was confirmed by the disappearance of benzyl peak in ¹H NMR at $\delta_{\text{H}} \sim 3.50$ (d, $J_{\text{HH}}=13.5$ Hz, 1H) for (-N-CH_AH_B-Ph) and ~ 3.85 (d, $J_{\text{HH}}=13.5$ Hz, 1H) for (-N-CH_AH_B-Ph), and decrease in integration of aromatic protons to 13 H. The ¹³C NMR spectrum with a peak at $\delta_{\text{C}} 116.5$ for Ph₂C- shows that the diphenylmethylene group is still intact.

When the hydrogen pressure was increased to 30 psi the diphenylmethylene protecting group was still not removed. Therefore, the hydrogen pressure was increased to 60 psi and, after 18 hrs, compound (**104**, R= Et) was converted to compound (**74**, R= Et). The catechol product was highly oxygen (air)-sensitive; however, the rate of oxidation could be decreased by making the hydrochloride salt.



Compound (**74**, R= Et) was characterised as its hydrochloride salt by ^1H NMR, ^1H - ^1H COSY and ^{13}C NMR spectroscopy, IR spectrometry, elemental analysis and mass spectrometry. The peaks in the ^1H NMR (D_2O) spectrum at δ_{H} 1.27 (t, $J_{\text{HH}}=7.1$ Hz, 3H) for (- CH_3) and 4.21 (q, $J_{\text{HH}}=7.1$ Hz, 2H) for (- $\text{COO}-\text{CH}_2-$) confirmed the presence of an ethyl ester. Other peaks which support the formation of (**74**, R= Et) include δ_{H} 4.96 (dd, $J_{\text{HH}}=8.5$, $J_{\text{HH}}=4.8$, 1H) for [-C(OH)- $\underline{\text{H}}$], 2.89 (t, $J_{\text{HH}}=6.7$ Hz, 2H) for (- $\text{CH}_2-\text{COO}-$), 3.28-3.36 (m, 2H) for [-HC(OH)- $\underline{\text{CH}_2}$ -N-] and 3.36-3.52 (m, 2H) for (-N- $\underline{\text{CH}_2}$ - $\underline{\text{CH}_2}$ -). Assignment of the peaks in the ^1H NMR spectrum at δ_{H} 2.89 (t), 3.28-3.36 (m) and 3.36-3.52 (m) were made with the help of a ^1H - ^1H COSY spectrum (Figure 2.3 for **74**, R=Et). The signal from peak at δ_{H} 4.96 [dd, C(OH)- $\underline{\text{H}}$] has a cross-peak connection to the peak at δ_{H} 3.28-3.36, now assigned as [-HC(OH)- $\underline{\text{CH}_2}$ -N-]. The signal from the peak at δ_{H} 2.89 (t, - $\text{CH}_2-\text{COO}-$) has a cross-connection to the signal from δ_{H} 3.36-3.52 (m), now assigned as (-N- $\underline{\text{CH}_2}$ - $\underline{\text{CH}_2}$ -).

The ^{13}C NMR assignments were confirmed by the ^{13}C DEPT experiment in which the quaternary carbons at δ_{C} 133.3, 145.5, 145.6 (aromatic C) and 173.7 ($\text{COO}-$) were absent. In the ^{13}C DEPT, the methyl and methine carbons were phased upright [14.5 for (- CH_3), 69.5 for -HC(OH)-] and all of the methylene carbons phase downwards in the spectrum. The ^1H NMR spectrum of compound (**74**, R=Et) was also recorded in $\text{MeOH}-d_4$ which showed better resolution than the spectrum recorded in D_2O . The ^1H and ^{13}C NMR assignments of compound (**74**, R= Et) in D_2O and $\text{MeOH}-d_4$ are shown in Figures 2.4 and 2.5 respectively. The IR (KBr) spectrum showed a broad peak at 3404 cm^{-1} for (-OH), a strong broad peak at 3315 cm^{-1} for (- N^+H_2-) and a peak at 1731 cm^{-1} for (C=O ester). The structure was also supported by elemental analysis and by mass spectrometry. The mass spectral fragmentation pattern is shown in Scheme 2.11.

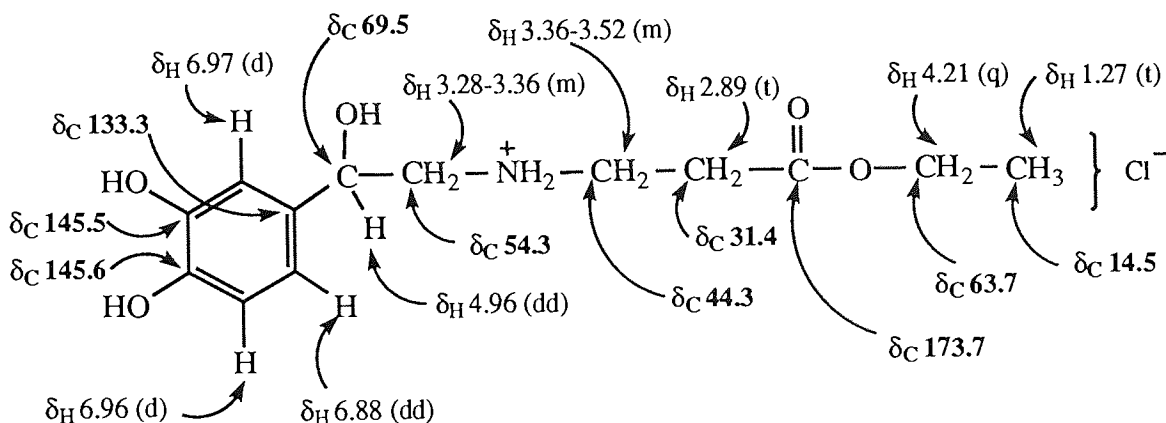


Figure 2.4: ^1H -NMR and ^{13}C -NMR assignments of ethyl *N*-[2'-(3'',4'')-dihydroxyphenyl]-2'-hydroxyethyl]-3-aminopropionate as its hydrochloride salt (**74**, R= Et) in (D_2O). All OH and NH have exchanged with D_2O .

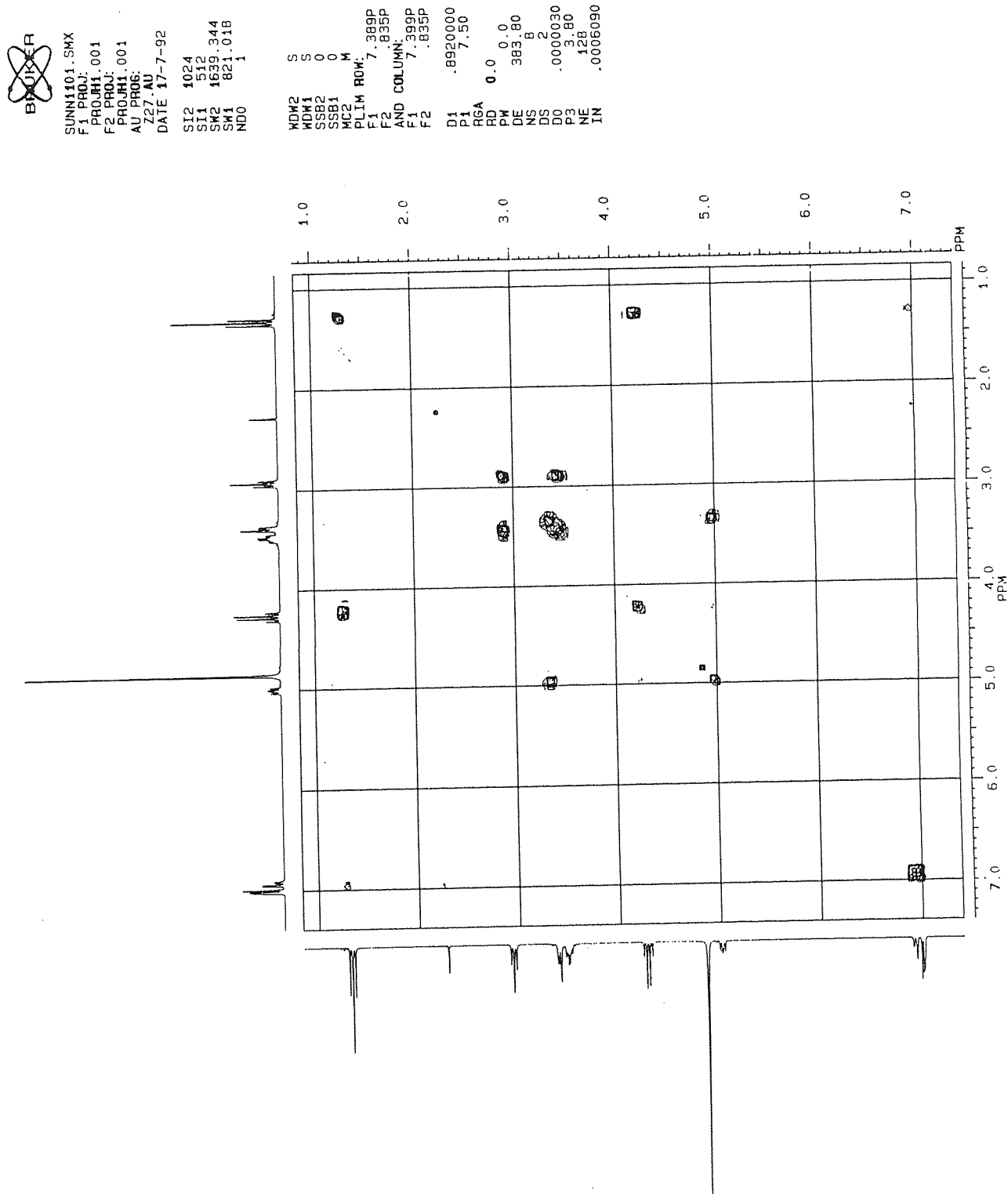


Figure 2.3: ^1H - ^1H COSY spectrum of ethyl *N*-[2'-(3'',4''-dihydroxyphenyl)-2'-hydroxyethyl]-3-aminopropionate (74, R=Et)

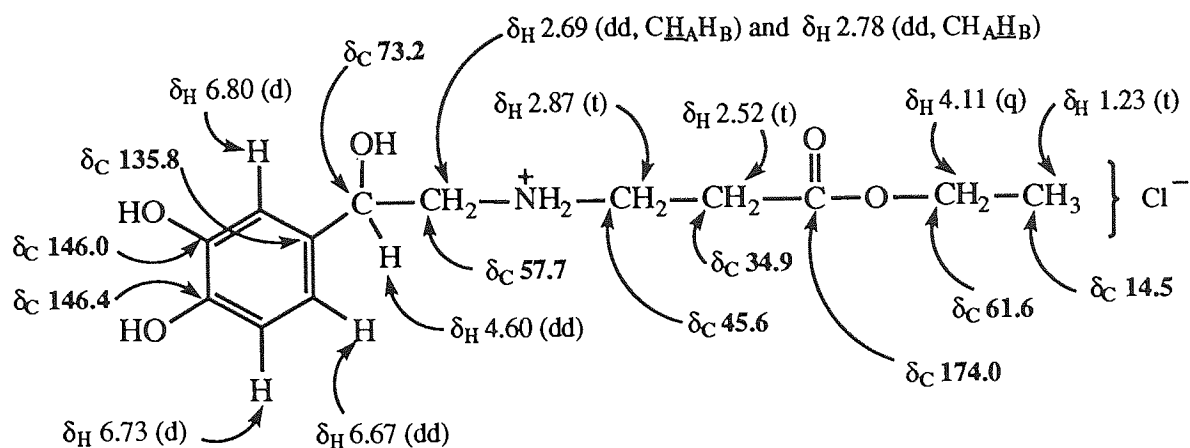
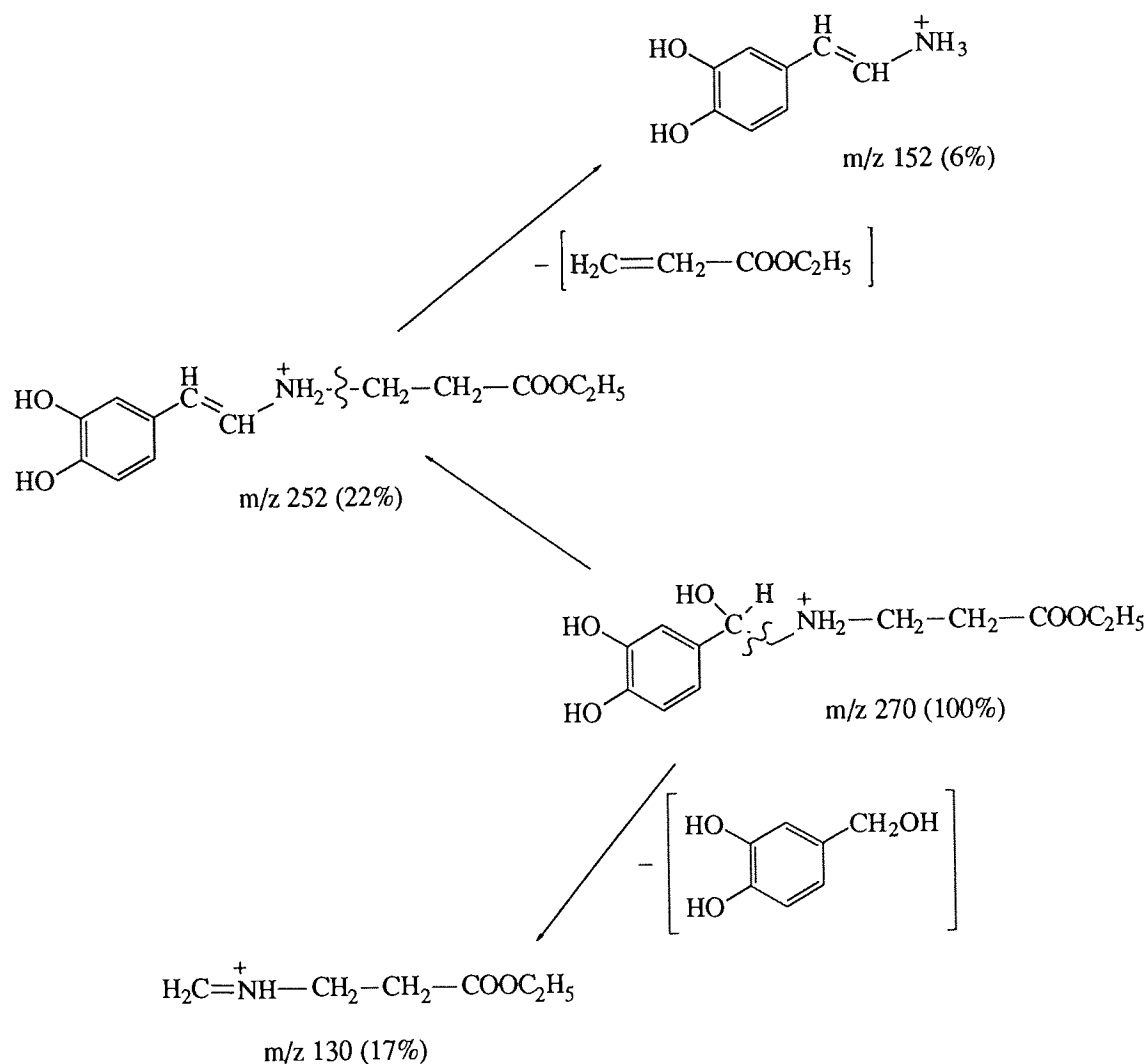


Figure 2.5: ^1H -NMR and ^{13}C -NMR assignments of ethyl *N*-[2'-(3'',4''-dihydroxyphenyl)-2'-hydroxyethyl]-3-aminopropionate as its hydrochloride salt (**74**, R=ethyl) in MeOH-d_4 . All OH and NH have exchanged with MeOH-d_4 .



Scheme 2.11: Mass spectrum (FAB) fragmentation pattern of ethyl *N*-[2'-(3'',4''-dihydroxyphenyl)-2'-hydroxyethyl]-3-aminopropionate (**74**, R=ethyl).

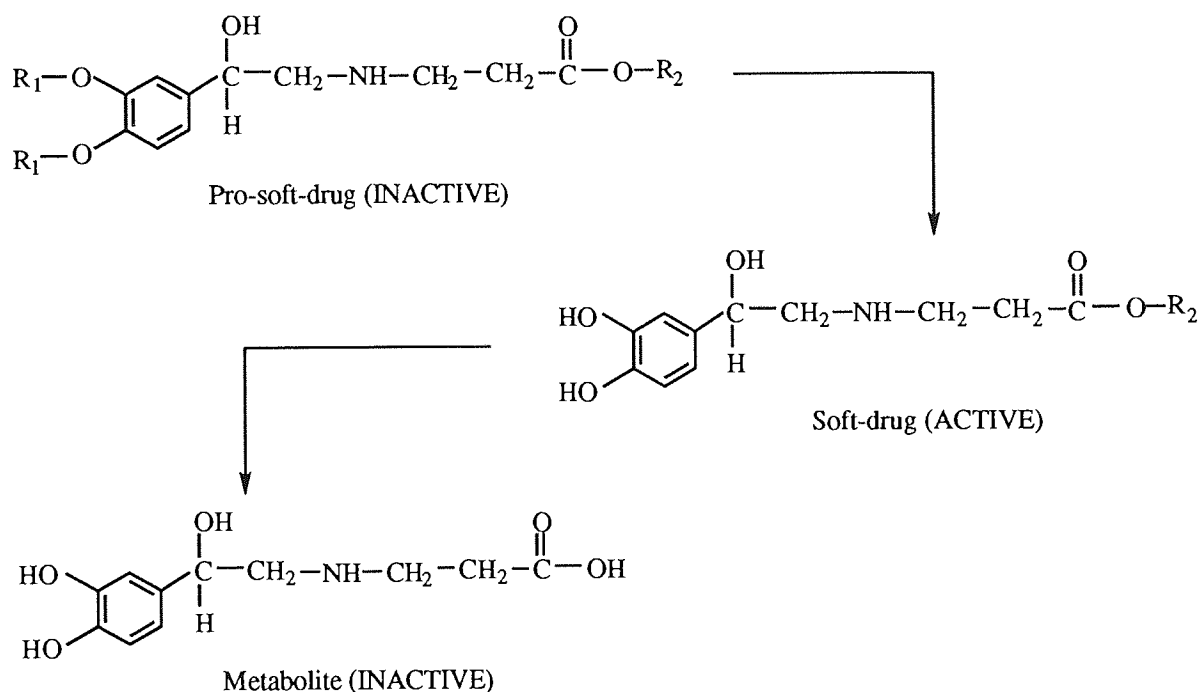
A solution of propyl *N*-[2'-(3'',4''-diphenylmethylenedioxyphenyl)-2'-hydroxyethyl]-*N*-benzyl-3-aminopropionate (**104**, R= n-Pr) in *n*-propanol was subjected to an atmosphere of hydrogen at 60 psi at room temperature in the presence of 10% palladium on charcoal catalyst. After 24 hr, the reaction mixture contained starting material and propyl *N*-[2'-(3'',4''-diphenylmethylenedioxyphenyl)-2'-hydroxyethyl]-3-aminopropionate (**105**, R= n-Pr). After a further 48 hrs, the reaction mixture contained 10% (**105**, R= n-Pr) and 90% propyl *N*-[2'-(3'',4''-dihydroxyphenyl)-2'-hydroxyethyl]-3-aminopropionate (**74**, R=n-Pr). Complete deprotection was confirmed by the absence of a peak in the ^{13}C NMR spectrum at δ_{C} 116.0 for [(Ph) $_2$ C], absence of peaks in the ^1H NMR spectrum at δ_{H} 3.42 (d, $J_{\text{gem}}=13.5$ Hz, 1H) for (-N-CH $_A$ H $_B$ -Ph) and 3.77 (d, $J_{\text{gem}}=13.5$ Hz, 1H) for (-N-CH $_A$ H $_B$ -Ph), and by a decrease in the integration of aromatic protons from 18 H to 3 H in the ^1H NMR spectrum. Peaks which support the formation of compound (**74**, R= n-Pr) included δ_{H} 2.43 (t, $J_{\text{HH}}=6.5$ Hz, 2H) for (-CH $_2$ -COO-), 2.59 (dd, $J_{\text{gem}}=12.1$, $J_{\text{HH}}=4.8$ Hz, 1H) for [-C(OH)-CH $_A$ H $_B$ -N-], 2.67 (dd, $J_{\text{gem}}=12.1$, $J_{\text{HH}}=4.8$ Hz, 1H) for [-C(OH)-CH $_A$ H $_B$ -N-] and 4.49 (dd, $J_{\text{HH}}=8.3$, $J_{\text{HH}}=4.8$ Hz, 1H) for [-C(OH)-H]; δ_{C} 57.6 for [-C(OH)-CH $_2$ -N-], 67.3 for (COO-CH $_2$ -), 73.0 for [C(OH)-H] and 174.0 for (-COO-).

A solution of butyl *N*-[2'-(3'',4''-diphenylmethylenedioxyphenyl)-2'-hydroxyethyl]-*N*-benzyl-3-aminopropionate (**104**, R= n-Bu) in *n*-butanol was subjected to hydrogenation at room temperature at 60 psi hydrogen atmosphere in the presence of 10% palladium on charcoal catalyst. After 24 hr, the reaction mixture contained starting material (**104**, R= n-Bu) and butyl *N*-[2'-(3'',4''-diphenylmethylenedioxyphenyl)-2'-hydroxyethyl]-3-aminopropionate (**105**, R= n-Bu). After hydrogenation for 96 hrs, the reaction mixture still contained 70% (**105**, R= n-Bu) and 30% butyl *N*-[2'-(3'',4''-dihydroxyphenyl)-2'-hydroxyethyl]-3-aminopropionate (**74**, R= n-Bu). Deprotection was confirmed by ^1H NMR spectroscopy (CDCl $_3$) with peaks at δ_{H} 8.70 (broad s, 1H) for phenolic (OH) and δ_{H} 9.10 (broad s, 1H) for phenolic (OH), coupled with a decrease in integration of the aromatic protons. Other peaks which support the formation of compound (**74**, R= n-Bu) includes δ_{H} 0.88 (t, $J_{\text{HH}}=7.3$ Hz, 3H) for (CH $_3$), 2.80 (t, $J_{\text{HH}}=7.1$ Hz, 2H) for (-CH $_2$ -COO-) and 4.85 (dd, $J_{\text{HH}}=7.9$, $J_{\text{HH}}=4.0$ Hz, 1H) for [-C(OH)-H].

The hydrogenation of the propyl and butyl esters (**104**, R= n-Pr and n-Bu) in *n*-propanol and *n*-butanol was not complete even after 72 and 96 hrs respectively. This is probably because of the decrease in solubility of hydrogen gas in *n*-propanol and *n*-butanol when compared with methanol and ethanol.

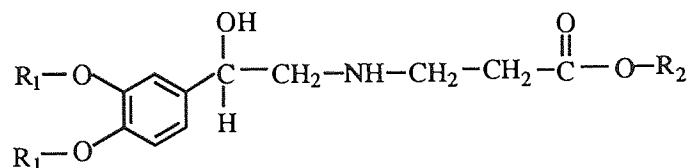
2.5 SYNTHESIS OF ACYL PRODRUGS OF THE CATECHOL AMINO ACIDS (106, R= ETHYL, R'= CH₃CO) AND (107, R= ETHYL, R'= Bu^tCO):

Compounds (74, R= Me, Et, Pr) have been prepared, however, they suffer from the presence of free catechol hydroxyl groups which are susceptible to oxidation. They are also expected to be substrates for catechol-O-methyltransferase (COMT) which may limit biological activity. Furthermore polar compounds typically show poor percutaneous absorption profiles. One promising approach to optimise the efficacy of these compounds is to prepare prodrugs.⁸⁷ Prodrugs need to undergo a biotransformation reaction to the drug, for example hydrolysis, prior to exhibiting their pharmacological effects. Indeed, here a pro-soft-drug is required. Prodrugs could be used to alter the properties of certain drugs: to increase their usefulness and to decrease or at least alter their toxicity (see section 1.4.3 for a more detailed account of the prodrug concept).



2.5.1 Prodrugs of ethyl *N*-[2'-(3'',4''-dihydroxyphenyl)-2'-hydroxyethyl]-3-aminopropionate (74, R=ethyl)

The synthesis of prodrugs of the soft-drug (74) is explored, to optimise its activity profile and topical delivery. This involved attempts to synthesise compounds in which the phenolic groups are protected with acetyl (106, R₁= H₃C-CO-) and pivaloyl [107, R₁= (H₃C)₃C-CO-] residues.

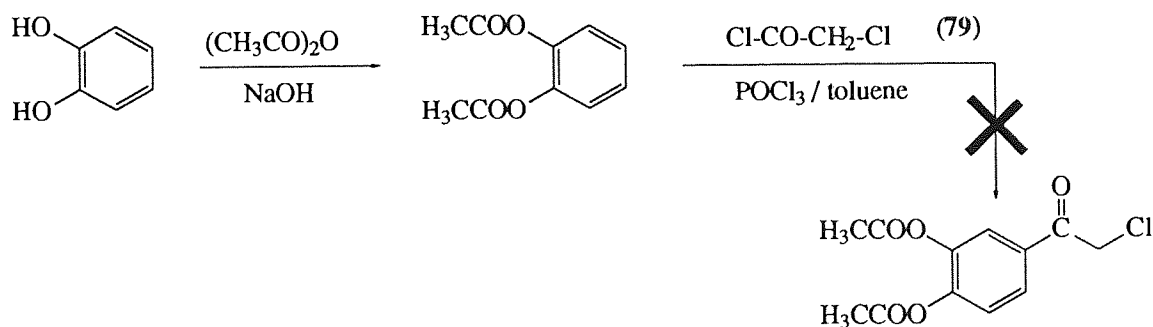
(74, $R_1 = H$, $R_2 = Et$)

Acetyl prodrug (**106**) $R_2 = Et$ and $R_1 = H_3C-CO-$

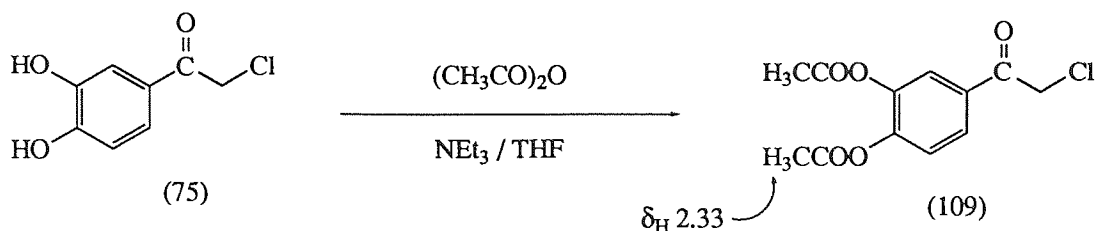
Pivaloyl prodrug (**107**) $R_2 = Et$ and $R_1 = (H_3C)_3C-CO-$

Attempted synthesis of the acetyl prodrug (106):

Catechol (**78**) was acetylated with acetic anhydride in 3 M sodium hydroxide, to yield 1,2-diacetoxybenzene (**108**).¹¹⁷ Transformation was confirmed by the 1H NMR spectrum with a peak at δ_H 2.29 (s, 6H) for the two acetyl groups. However, the Friedel-Crafts acylation reaction of 1,2-diacetoxybenzene with chloroacetyl chloride in toluene to give (**109**) was not successful. In contrast, catechol with two electron-donating hydroxyl groups, is very reactive towards electrophilic aromatic substitution.

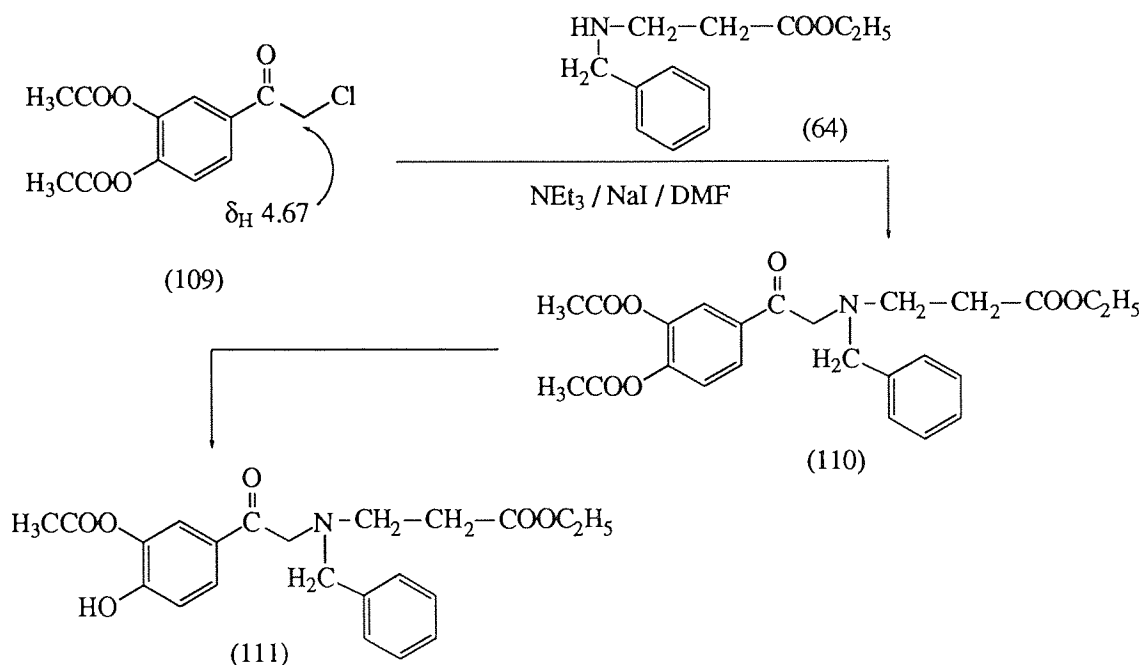


An alternative route to (**109**) was therefore considered. 3,4-Dihydroxy- α -chloroacetophenone (**75**) was acetylated with acetic anhydride in dry THF in the presence of triethylamine, to yield 3,4-diacetoxy- α -chloroacetophenone (**109**). Transformation was confirmed by the appearance in the 1H NMR spectrum of a peak at δ_H 2.33 (s, 6H) for the two acetyl groups and absence of signals for the aromatic -OH groups. Other peaks which support the formation of compound (**109**) include 4.67 (s, 2H) for (-CO-CH₂-Cl). The IR (KBr) spectrum for (**109**) shows peaks at 1769 cm^{-1} for (C=O ester) and 1706 cm^{-1} for (C=O keto).



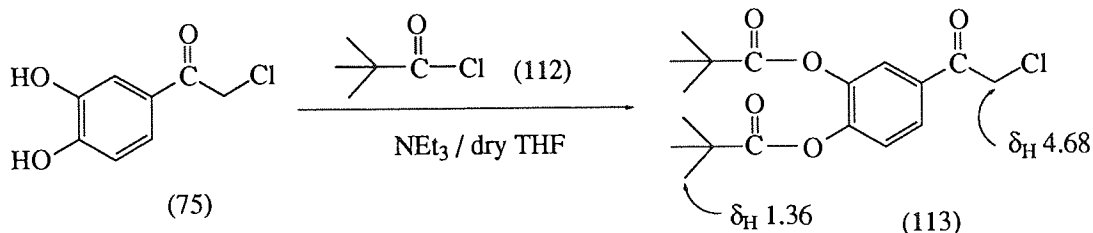
3,4-Diacetoxy- α -chloroacetophenone (**109**) was coupled with ethyl *N*-benzyl-3-aminopropionate (**64**) in dry DMF, sodium iodide and triethylamine. The product ethyl *N*-[(3',4'-diacetoxybenzoyl)methyl]-*N*-benzyl-3-aminopropionate (**110**) was isolated by flash column chromatography. Coupling was confirmed by the disappearance of a peak in the ^1H NMR spectrum at δ 4.67 (s, 2H) for (-CO-CH₂-Cl) and appearance of a peak at δ 3.85 (s, 2H) for (-CO-CH₂-N-). Other peaks in the ^1H NMR spectrum for (**110**) include δ 2.30 (s, 3H) for (H₃CCOO-), 2.31 (s, 3H) for (H₃CCOO-), 3.78 (s, 2H) for (-N-CH₂-Ph) and 3.85 (s, 2H) for (-CO-CH₂-N).

However, compound (**110**) was not stable as it readily lost an acetyl group to give (**111**), shown by the decrease in integration in the ^1H NMR spectrum of acetyl protons at δ 2.30. Compound (**111**) was also prone to oxidation as the product turned dark brown. The 4-acetoxy substituent of (**110**) is likely to be most susceptible to hydrolysis because of the ability of the electron-donating 4-hydroxyl group in the product (**111**) to be stabilised by donation of electrons to the keto group. Therefore, alternative derivatisation of the catechol group was investigated utilising the more hindered pivaloyl chloride.



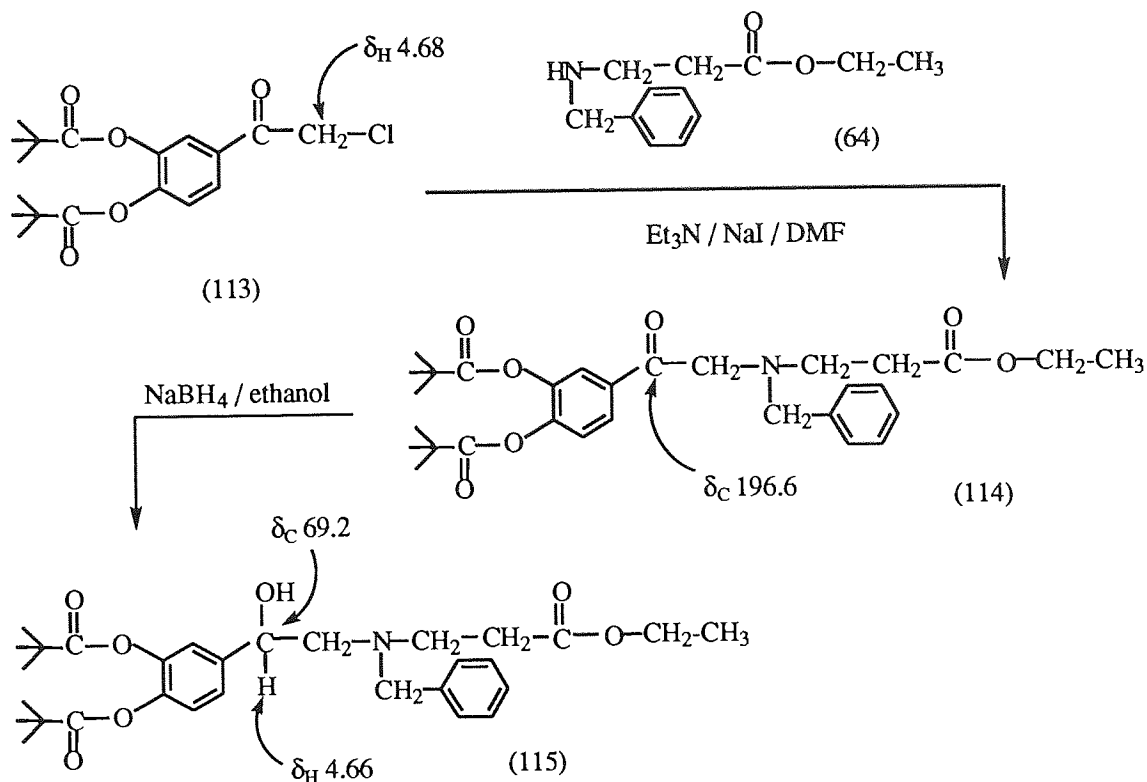
Synthesis of pivaloyl prodrug (107):

3,4-Dihydroxy- α -chloroacetophenone (**75**) was coupled with pivaloyl chloride (**112**) in dry THF in the presence of triethylamine to yield 3,4-dipivaloyloxy- α -chloroacetophenone (**113**). The appearance of peaks in the ^1H NMR spectrum at δ_{H} 1.36 (s, 9H) for (Bu^tCOO) and 1.37 (s, 9H) for (Bu^tCOO -) and in the ^{13}C NMR spectrum at δ 27.1 for [$-\text{C}(\underline{\text{C}}\text{H}_3)_3$] and 39.2 for [$-\underline{\text{C}}(\text{CH}_3)_3$] confirms the formation of compound (**113**). Formation of compound (**113**) was further supported by mass spectral fragmentation and elemental analysis.



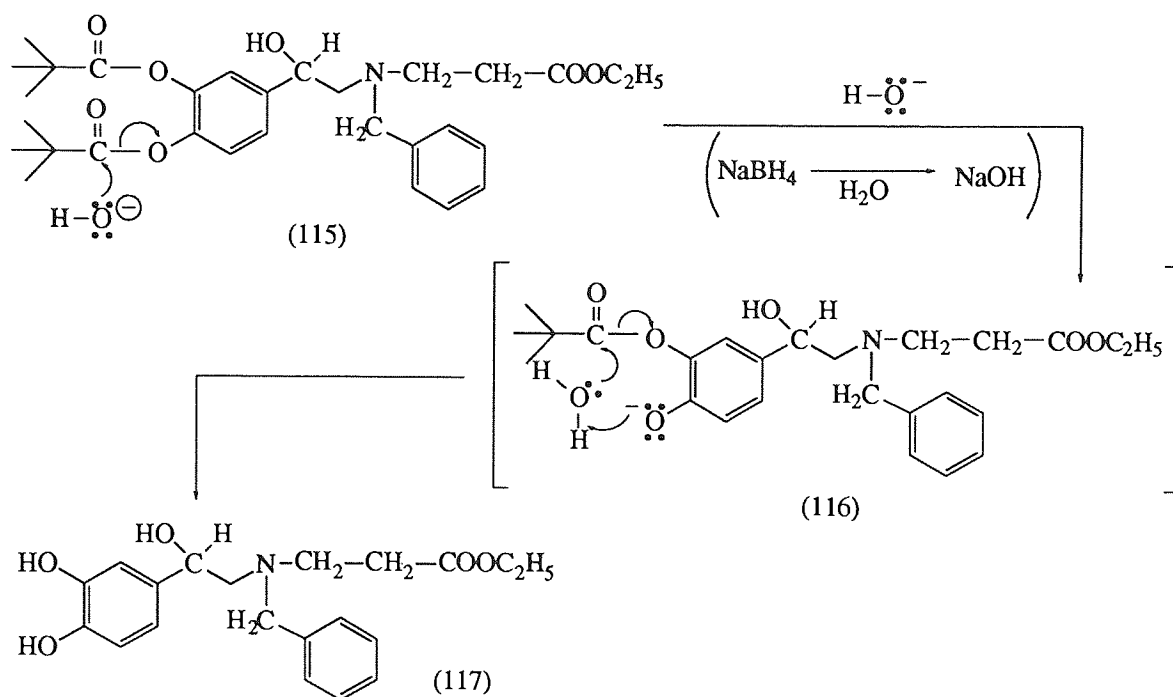
3,4-Dipivaloyloxy- α -chloroacetophenone (**113**) was coupled with ethyl *N*-benzyl-3-aminopropionate (**64**) in dry DMF, in the presence of sodium iodide and triethylamine. The product, ethyl *N*-[(3',4'-dipivaloyloxybenzoyl)methyl]-*N*-benzyl-3-amino-propionate (**114**) was isolated by flash column chromatography as a pale yellow oil in a yield of 70%. The coupling was confirmed by the disappearance of a peak in the ^1H NMR spectrum at δ_{H} 4.67 (s, 2H) for ($-\text{CO}-\text{CH}_2-\text{Cl}$) and appearance of a peak at δ_{H} 3.87 (s, 2H) for ($-\text{CO}-\text{CH}_2-\text{N}$). Other peaks in the ^1H NMR spectrum which support the formation of compound (**114**) include δ_{H} 1.34 (s, 9H) for (Bu^tCOO -), 1.36 (s, 9H) for (Bu^tCOO -) and 3.87 (s, 2H) for ($-\text{CO}-\text{CH}_2-\text{N}$). Further evidence is provided by peaks in the ^{13}C NMR spectrum for (**114**) at δ_{C} 27.1 for [$-\text{C}(\underline{\text{C}}\text{H}_3)_3$], 27.2 for [$-\text{C}(\underline{\text{C}}\text{H}_3)_3$], 39.15 for [$-\underline{\text{C}}(\text{CH}_3)_3$], 39.25 for [$-\underline{\text{C}}(\text{CH}_3)_3$], 59.6 for ($-\text{CO}-\underline{\text{C}}\text{H}_2-\text{N}$), 172.5 for ($\text{CH}_2\underline{\text{C}}\text{OO}$), 175.4 for ($\text{Bu}^t\underline{\text{C}}\text{OO}$), 175.6 for ($\text{Bu}^t\underline{\text{C}}\text{OO}$) and 196.6 for (keto $\text{C}=\text{O}$). The IR (neat) spectrum for (**114**) included peaks at 1763 cm^{-1} for ($\text{C}=\text{O}$ ester), 1734 cm^{-1} for ($\text{C}=\text{O}$ ester) and 1689 cm^{-1} for ($\text{C}=\text{O}$ keto).

Ethyl *N*-[(3',4'-dipivaloyloxybenzoyl)methyl]-*N*-benzyl-3-aminopropionate (**114**) was reduced with sodium borohydride in ethanol¹⁰⁹ to give ethyl *N*-[2'-(3'',4''-dipivaloyloxyphenyl)-2'-hydroxyethyl]-*N*-benzyl-3-aminopropionate (**115**) in a yield of 45%, data on which included δ_{H} 4.66 (dd, $J_{\text{HH}}=10.1$, $J_{\text{HH}}=3.2$ Hz, 1H) for [$-\text{C}(\text{OH})-\underline{\text{H}}$]. In the ^{13}C NMR spectrum the peak at δ_{C} 196.6 for the substrate ($\text{C}=\text{O}$) was absent giving rise to a new peak at δ_{C} 69.2 for [$-\text{C}(\text{OH})-\text{H}$].

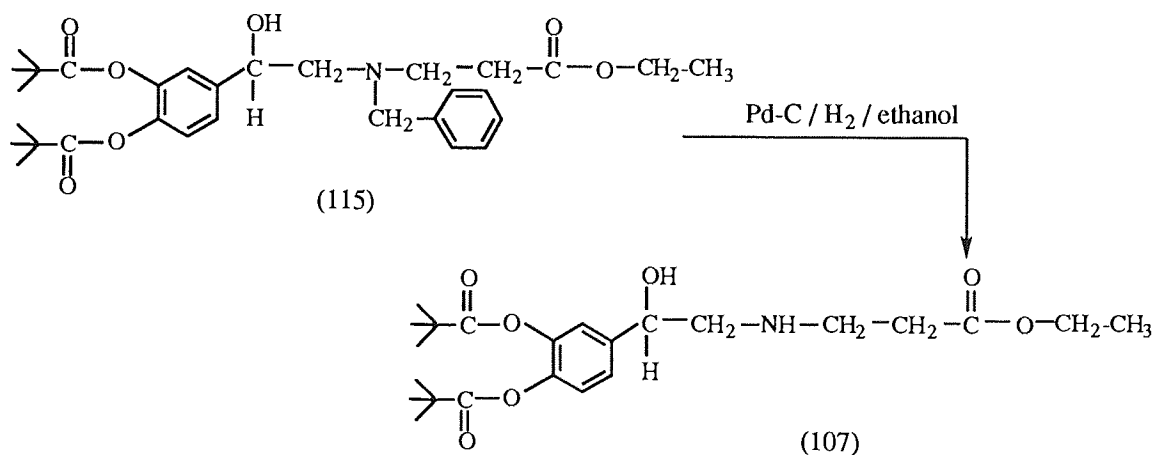


After completion of the reaction, water was added to hydrolyse the excess sodium borohydride, however the sodium hydroxide formed caused hydrolysis of the ethyl *N*-[2'-(3'',4''-dipivaloyloxyphenyl)-2'-hydroxyethyl]-*N*-benzyl-3-aminopropionate (**115**) to give the monopivaloyl derivative (**116**) which hydrolysed rapidly to give ethyl *N*-[2'-(3'',4''-dihydroxyphenyl)-2'-hydroxyethyl]-*N*-benzyl-3-aminopropionate (**117**). Removal of the second pivaloyl group is faster than removal of the first because of the ability of the *o*-hydroxyl group in the monopivaloyl compound (**116**) to act as an acid catalyst. It has been reported that hydrolysis of catechol monoacetate is 500 times faster than that for catechol diacetate and 700 times faster than the hydrolysis of phenyl acetate.¹¹⁸ It is suggested that this is due to the inductive and resonance effects of an oxygen atom in the *o*-position and the possibility of intramolecular hydrogen bonding.

In another reaction, the solvent, ethanol was removed under vacuum. The product was extracted into dichloromethane and the dichloromethane solution was washed with water to remove traces of sodium borohydride. The product (**115**) was isolated in 40% yield.



The *N*-benzyl group of ethyl *N*-[2'-(3'',4''-dipivaloyloxyphenyl)-2'-hydroxyethyl]-*N*-benzyl-3-aminopropionate (**115**) was removed by hydrogenation catalysed by 10% palladium on activated charcoal in ethanol¹⁰⁹ at atmospheric pressure and room temperature to yield ethyl *N*-[2'-(3'',4''-dipivaloyloxyphenyl)-2'-hydroxyethyl]-3-aminopropionate (**107**).



Compound (**107**) was characterised by ^1H NMR, ^1H - ^1H COSY and ^{13}C NMR spectroscopy, IR spectrometry, elemental analysis and mass spectrometry. The peaks in the ^1H NMR (CDCl_3) spectrum at δ_{H} 1.26 (t, $J_{\text{HH}}=7.1$ Hz, 3H) for (-CH₃) and δ_{H} 4.14 (q, $J_{\text{HH}}=7.1$ Hz, 2H) for (-COO-CH₂-) are for the ethyl ester. Other peaks include δ_{H} 4.67 (dd, $J_{\text{HH}}=9.1$, $J_{\text{HH}}=3.4$, 1H) for [-C(OH)-H], 2.49 (t, $J_{\text{HH}}=6.4$ Hz, 2H) for (-CH₂-COO-), 2.66 (dd, $J_{\text{gem}}=12.2$, $J_{\text{HH}}=9.1$, 1H) for [-HC(OH)-CH_AH_B-N-] and 2.84-3.00 (m, 3H) for (-HC(OH)-CH_AH_B-N-CH₂-CH₂-).

Assignments of peaks at δ_{H} 2.49, 2.66 and 2.84-3.00 were made with the help of a ^1H - ^1H COSY spectrum. The signal from [-C(OH)-H] at δ_{H} 4.67 (dd) has a cross-peak connection to the signal at δ_{H} 2.66 (dd) [-HC(OH)-CH_AH_B-N-], which is connected to the multiplet at δ_{H} 2.84-3.00 [-HC(OH)-CH_AH_B-N-]. The multiplet at 2.84-3.0 is further connected to the signal from triplet at δ_{H} 2.49 for (-CH₂-COO-) which confirm that (-N-CH₂-CH₂-) is also part of the multiplet. The ^1H - ^1H COSY spectrum is shown in Figure 2.6a and an expansion of the COSY spectrum is shown in Figure 2.6b.

Assignments in the ^{13}C NMR (CDCl_3) spectrum for (**107**) were confirmed by the ^{13}C DEPT experiment in which the quaternary carbons at δ_{C} 38.6 for [-C(CH₃)₃], 141.2, 141.5, 142.3 for (aromatic C), 172.5 for (COO ethyl ester), 175.7 (Bu^tCOO) and 175.8 (Bu^tCOO) disappeared from the spectrum. Methyl and methine carbons were phased upright [14.1 for (-CH₃), 70.6 for -HC(OH)-] and all the methylene carbons phase downwards in the spectrum. ^1H and ^{13}C NMR assignments of compound (**107**) in CDCl_3 are shown in Figure 2.7.

The IR (KBr) spectrum shows absorbances at 3506 cm^{-1} for (broad, -OH), 1759 cm^{-1} for (C=O, pivaloyl ester) and 1734 cm^{-1} for (C=O, ethyl ester). The structure (**107**) was also supported by elemental analysis and mass spectrometry (Cl, NH_3) which showed an (M + H⁺) ion at 438.2492 (M + H⁺). The mass spectrum fragmentation pattern is shown in Scheme 2.12.

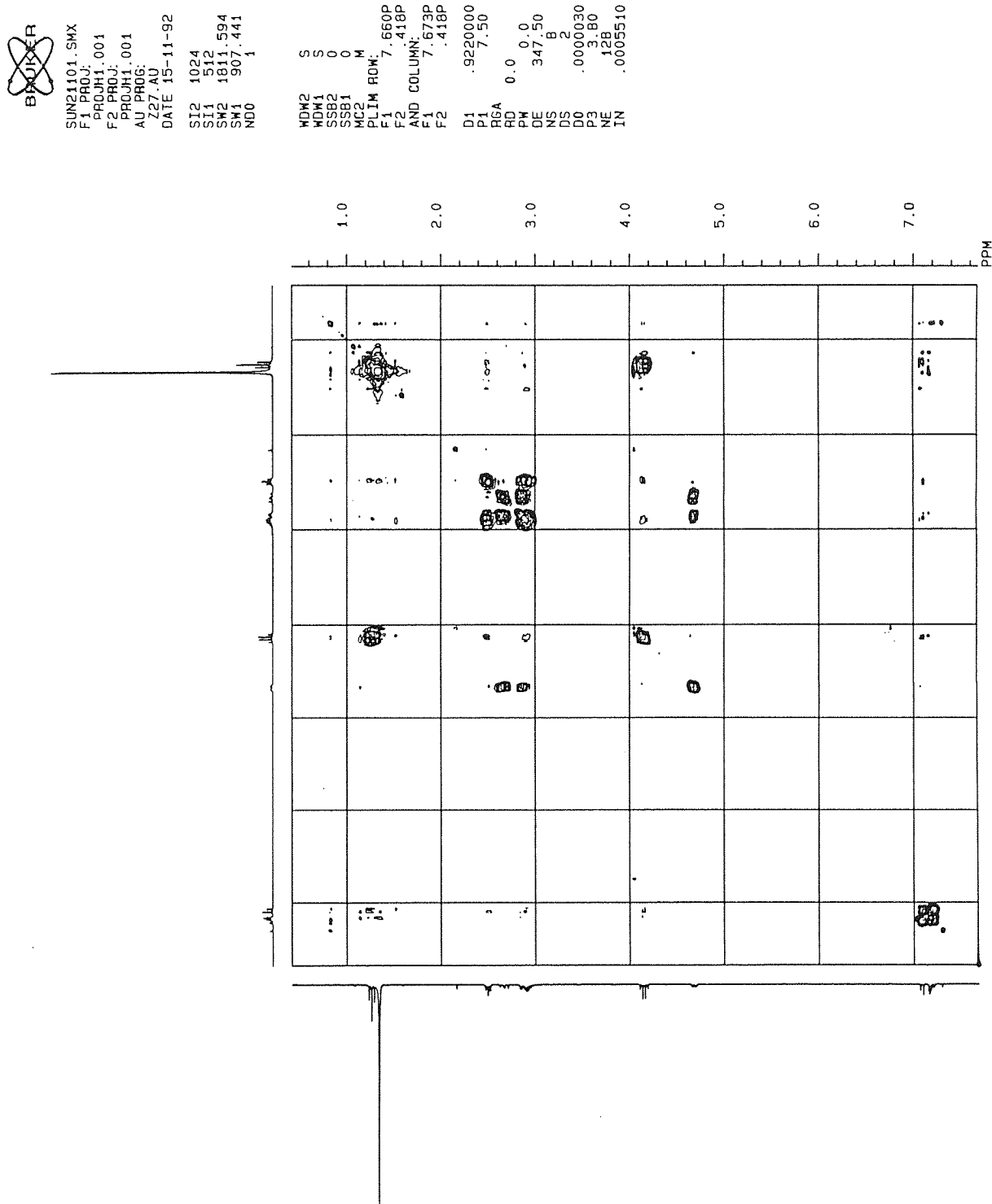


Figure 2.6a: ^1H - ^1H COSY spectrum of ethyl *N*-[2'-(3'',4''-dipivaloyloxyphenyl)-2'-hydroxyethyl]-3-aminopropionate (107)



 SUN21101.SMX

 F1 PROJ: PROJH1.001

 F2 PROJ: PROJH1.001

 AU PROG: Z27.AU

 DATE 15-11-92

 SI2 1024

 SI1 512

 SM2 1817.594

 SM1 907.441

 NDO 1

 MDW2 S

 MDW1 S

 SSB2 0

 SSB1 0

 MC2 M

 PLIM ROW: F1 4.803P

 F2 2.342P

 AND COLUMN: F1 4.896P

 F2 2.203P

 D1 .9220000

 P1 7.50

 RGA 0.0

 RD 0.0

 PW 347.50

 DE B

 NS 2

 DS .0000030

 DO 3.80

 P3 128

 NE .0005510

 IN

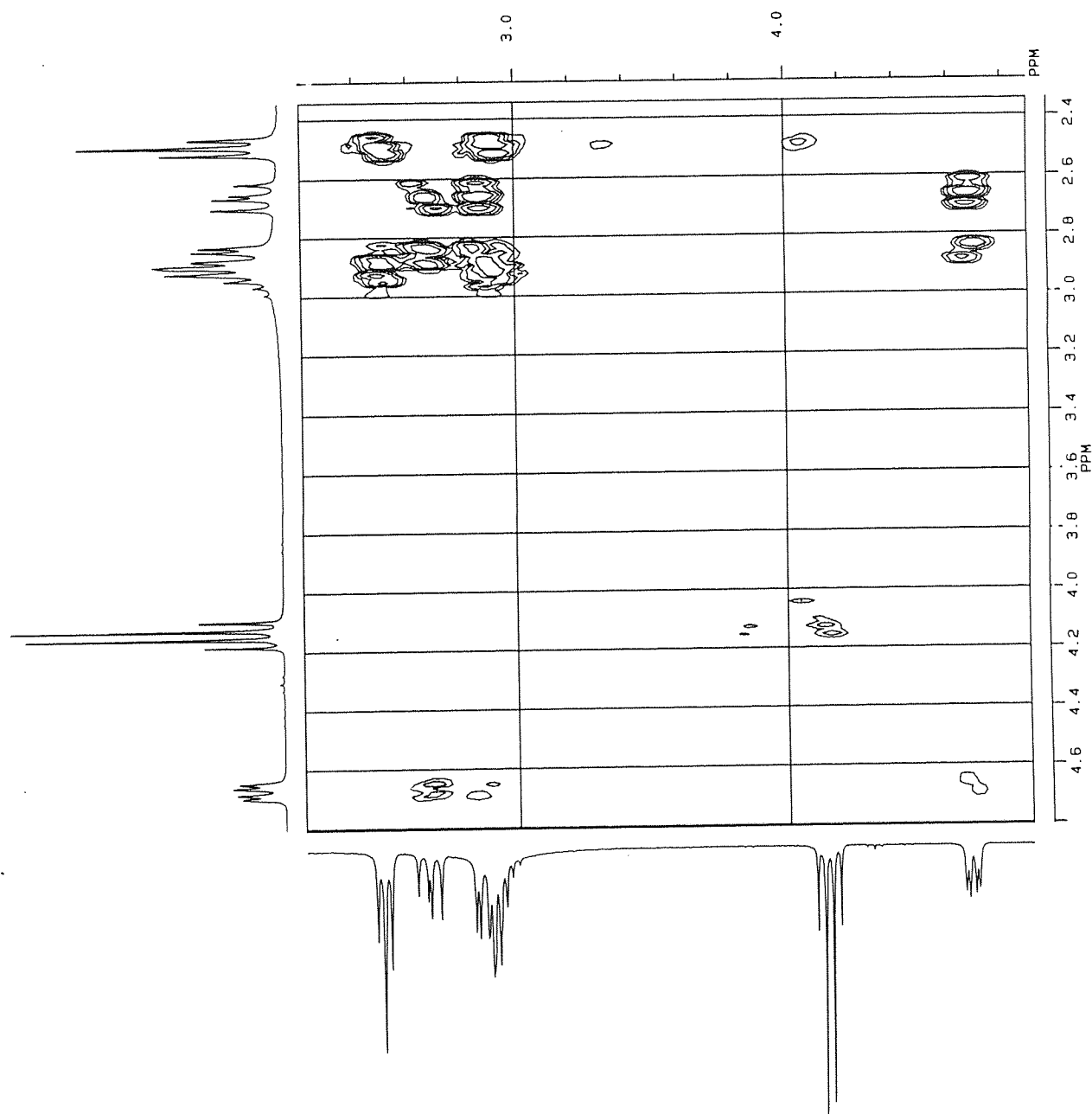
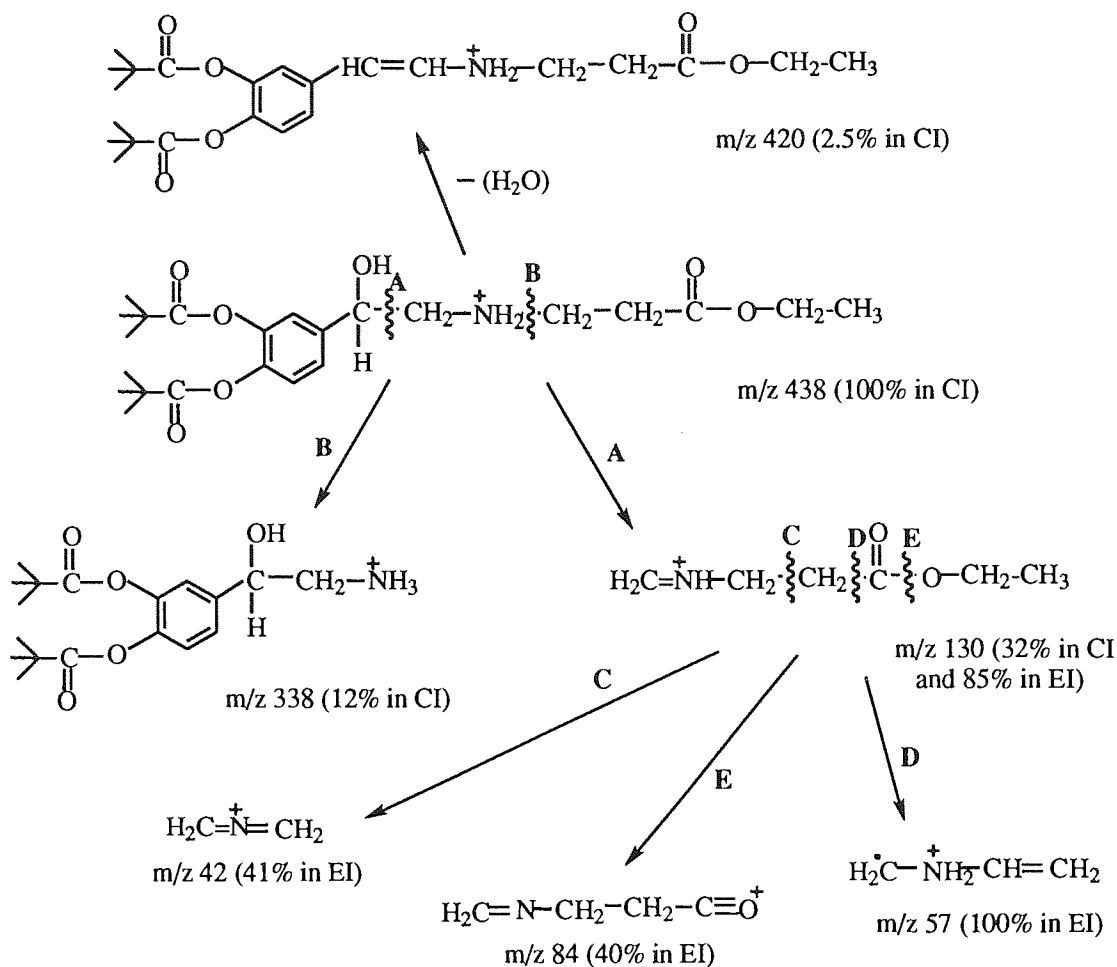


Figure 2.6b: Expansion of ^1H - ^1H COSY spectrum of ethyl *N*-[2'-(3'',4''-dipivaloyloxyphenyl)-2'-hydroxyethyl]-3-aminopropionate (**107**)



Scheme 2.12: Mass spectral fragmentation (CI, NH_3) and EI pattern of ethyl *N*-[2'-(3'',4''-dipivaloyloxyphenyl)-2'-hydroxyethyl]-3-aminopropionate (**107**)

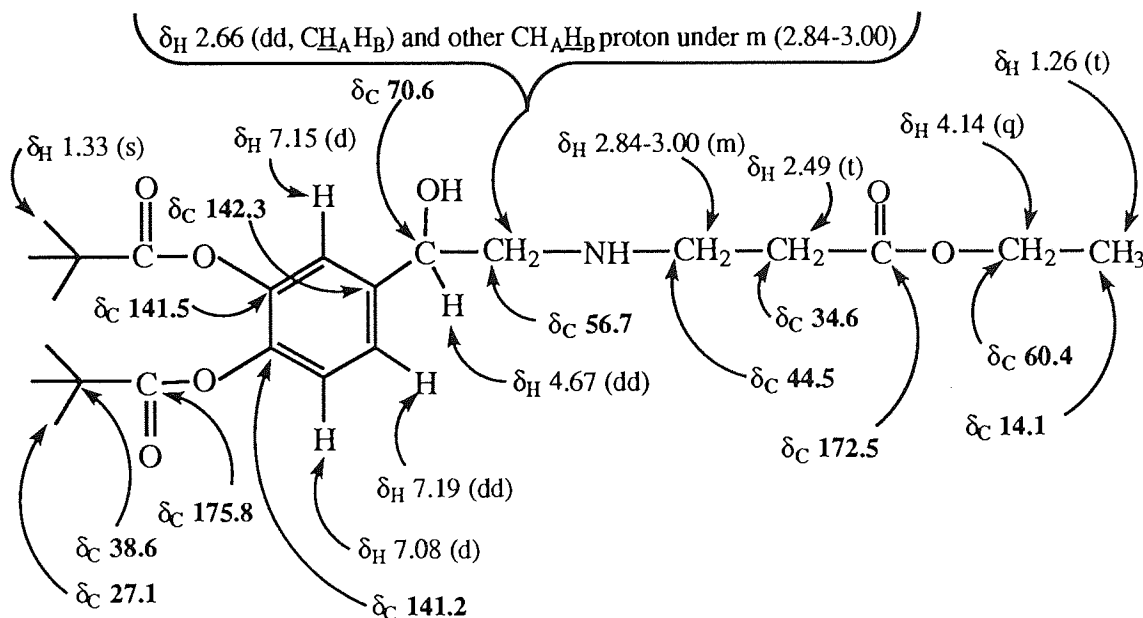


Figure 2.7: ^1H -NMR and ^{13}C -NMR assignments of ethyl *N*-[2'-(3'',4''-dipivaloyloxyphenyl)-2'-hydroxyethyl]-3-aminopropionate (**107**) in (CDCl_3). Aliphatic -OH and -NH- groups are between δ_{H} 2.2-3.4.

2.6 COMPARISON OF δ_H VALUES OBTAINED FOR DIPIVALOYL ETHYL ESTER (107), DIHYDROXY ETHYL ESTER (74, R=Et) AND DIHYDROXY ACID (74, R=H) by 1H NMR SPECTROSCOPY

The 1H NMR data for the dihydroxy ethyl ester (74, R=Et), dihydroxy acid (74, R=Et) and in dipivaloyl ethyl ester (107) are given in Table 2.1.

The ethyl ester in both the soft-drug (74, R=Et) and pro-soft-drug (107) appear approximately at the same chemical shifts [$\delta_H \sim 1.25$ ($J_{HH} \sim 7.10$, $-CH_3$) and ~ 4.20 ($J_{HH} \sim 7.10$, $-COO-CH_2-$)].

Aromatic protons in the soft-drug (74, R=Et) and its hydrolysis product (74, R=H) appears approximately at the same chemical shifts, $\delta_H \sim 6.90$ (dd, $J_{ortho} \sim 8.3$, $J_{meta} \sim 2.0$ Hz, H_6 -aromatic), $\delta_H \sim 6.97$ (d, $J_{ortho} \sim 8.3$ Hz, H_5 -aromatic) and $\delta_H \sim 7.00$ (d, $J_{meta} \sim 2.0$ Hz, H_2 -aromatic). In contrast for pro-soft-drug (107) the aromatic protons are slightly downfield due to the deshielding effect of the carbonyl of the pivaloyl groups, δ_H 7.19 (dd, $J_{ortho} = 8.3$, $J_{meta} = 1.7$ Hz, H_6 -aromatic), δ_H 7.08 (d, $J_{ortho} = 8.2$ Hz, H_5 -aromatic) and δ_H 7.15 (d, $J_{meta} = 1.7$ Hz, H_2 -aromatic).

In pro-soft-drug (107) the $-CH_2-COO-$ methylene group appears at δ_H 2.49 (t, $J_{HH} = 6.4$ Hz), the methylene group in $(-NH-CH_2-CH_2-COO)$ appears as a multiplet between δ_H 2.84-3.00, $-C(OH)-CH_AH_B-N-$ appears as doublet of doublets at δ_H 2.66 ($J_{gem} = 12.2$, $J_{HH} = 9.1$ Hz) and $[-C(OH)-CH_AH_B-N-]$ group is under the multiplet at δ_H 2.84-3.00. All of these groups in soft-drug (74, R=Et) and its hydrolysis product (74, R=H) appear approximately 0.4 ppm downfield due to protonation of the amine in the molecule (Table 2.1).

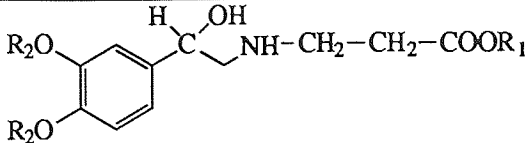
			
Protons	Dihydroxy acid HCl (74, R ₁ =R ₂ =H) in D ₂ O	Dihydroxy ethyl ester HCl (74, R ₁ =Et, R ₂ =H) in D ₂ O	Dipivaloyl ethyl ester [107, R ₁ =Et, R ₂ = -COC(CH ₃) ₃] in CDCl ₃
-COO-CH ₂ -CH ₃	—	δ 1.27 (t, J _{HH} = 7.10 Hz)	δ 1.26 (t, J _{HH} = 7.13 Hz)
-COO-CH ₂ -	—	δ 4.21 (q, J _{HH} = 7.10 Hz)	δ 4.14 (q, J _{HH} = 7.14 Hz)
-CH ₂ -COO-	δ 2.91 (t, J _{HH} = 6.6 Hz)	δ 2.89 (t, J _{HH} = 6.7 Hz)	δ 2.49 (t, J _{HH} = 6.4 Hz)
-C(OH)-CH _A H _B -N-	δ 3.22-3.42 (m) [-C(OH)-CH ₂ -N-]	δ 3.28-3.36 (m) [-C(OH)-CH ₂ -N-]	δ 2.66 (dd, J _{gem} = 12.2, J _{HH} = 9.1 Hz)
-C(OH)-CH _A H _B -N-	—	—	2.84-3.0 (peaks under the multiplet)
-NH-CH ₂ -CH ₂ -COO	δ 3.42-3.52 (m)	δ 3.36-3.52 (m)	δ 2.84-3.0 (m)
-C(OH)-H	δ 4.97 (dd, J _{HH} = 8.1, 4.9 Hz)	δ 4.96 (dd, J _{HH} = 7.9, 5.1 Hz)	δ 4.67 (dd, J _{HH} = 9.1, 3.4 Hz)
H ₆ -aromatic proton	δ 6.91 (dd, J _{ortho} = 8.3, J _{meta} = 2.0 Hz)	δ 6.88 (dd, J _{ortho} = 8.3, J _{meta} = 1.9 Hz)	δ 7.19 (dd, J _{ortho} = 8.3, J _{meta} = 1.7 Hz)
H ₅ -aromatic proton	δ 6.99 (d, J _{ortho} = 8.3 Hz)	δ 6.96 (d, J _{ortho} = 8.1 Hz)	δ 7.08 (d, J _{ortho} = 8.2 Hz)
H ₂ -aromatic proton	δ 7.00 (d, J _{meta} = 2.0 Hz)	δ 6.97 (d, J _{meta} = 2.0 Hz)	δ 7.15 (d, J _{meta} = 1.7 Hz)
R ₂ = Bu ^t CO-	-	-	δ 1.33 (s, 9H) and 1.34 (s, 9H)

Table 2.1: Chemical shifts of dipivaloyl ethyl ester (107), dihydroxy ethyl ester (74, R=Et) and dihydroxy acid (74, R=H) by ¹H NMR spectroscopy

CHAPTER THREE

SYNTHESIS OF SOFT β -ADRENOCEPTOR AGONISTS
-EXPERIMENTAL (CHEMISTRY)

3.1 INTRODUCTION

^1H NMR (250 MHz) and ^{13}C NMR (62.9 MHz) spectra were recorded on a Bruker AC-250 MHz spectrometer with TMS as the internal standard. Mass spectra were recorded at the Department of Chemistry, University of Swansea (SERC service) on a Micromass 12 instrument at 70 eV and a source temperature of 300 °C. Infra-red spectra were recorded on a Perkin-Elmer 1310 infrared spectrometer, or Unicam Mattson 2020 or 3000 FTIR Spectrometer Galaxy Systems. Melting points were measured on either a Electrothermal digital melting point apparatus, or a Kofler Reichert-Jung hot stage of Cambridge Instruments and are not corrected. TLC was performed using DC-Plastikfolien Kieselgel 60 F254 containing a fluorescent indicator. Spots were visualised under 254 nm UV light and/or with the aid of iodine. Silica gel Merck C 60-H (40-60 μm) was used for flash chromatography. Elemental analyses were recorded at Butterworth Laboratories Ltd., Middlesex.

3.1.1 Correlated spectroscopy in ^1H NMR (^1H - ^1H COSY):

By NMR, with suitable pulse sequences it is possible, in a single, rather extended experiment, to reveal all the coupling relationships in a molecule. This is then plotted in a three-dimensional plot, either as a stacked plot, or, more usually, as a contour plot. The result is called COrelated SpectroscopY (COSY).

Figure 3.1 shows the conventional ^1H spectrum and a COSY plot in the contour form 1,3-dinitrobenzene. The lines are contours from the third dimensional, representing intensity. The conventional spectrum can be seen along the diagonal, marked with a line, and the cross-peaks identify nuclei that are coupled to each other. Thus the signal from H_2 at the bottom left of the diagonal has a cross-peak connecting it (dashed lines) to the signal from $\text{H}_{4,6}$, and the signal from $\text{H}_{4,6}$ is further connected (dashed lines) by a cross-peak to the signal from H_5 .

The cross-peaks themselves contain the coupling constants, but not the full multiplicity. Whereas the signal of H_5 on the diagonal is a triplet, viewed both from the abscissa looking up or, but less clearly, from the ordinate looking to the right, the cross-peaks do not have the centre line. This also occurs with quintets, but doublets and quartets remain as doublets and quartets in the cross-peak. COSY spectra can be obtained to emphasize long range coupling. The planes used to define the contours have to be chosen wisely, if all the cross-peaks are to be displayed. Sometimes as much effort has to go into preparing data for presentation as into taking spectra.

In the case of 1,3-dinitrobenzene, the couplings are all evident and analysable in the conventional spectrum, but in more complicated cases it is very valuable to be able to see where all the couplings are without the need to carry out separate decoupling experiments for all the possible connections. Furthermore, when two (or more) signals have very similar chemical shifts, irradiation of one of the signals inevitably hits the other at the same time, and we are then unable to tell from the decoupling observed which protons are coupled. COSY spectra are not as limited in this way; as long as the signals are resolved, the cross-peaks can be associated accurately with one or the other of a closely spaced pair.

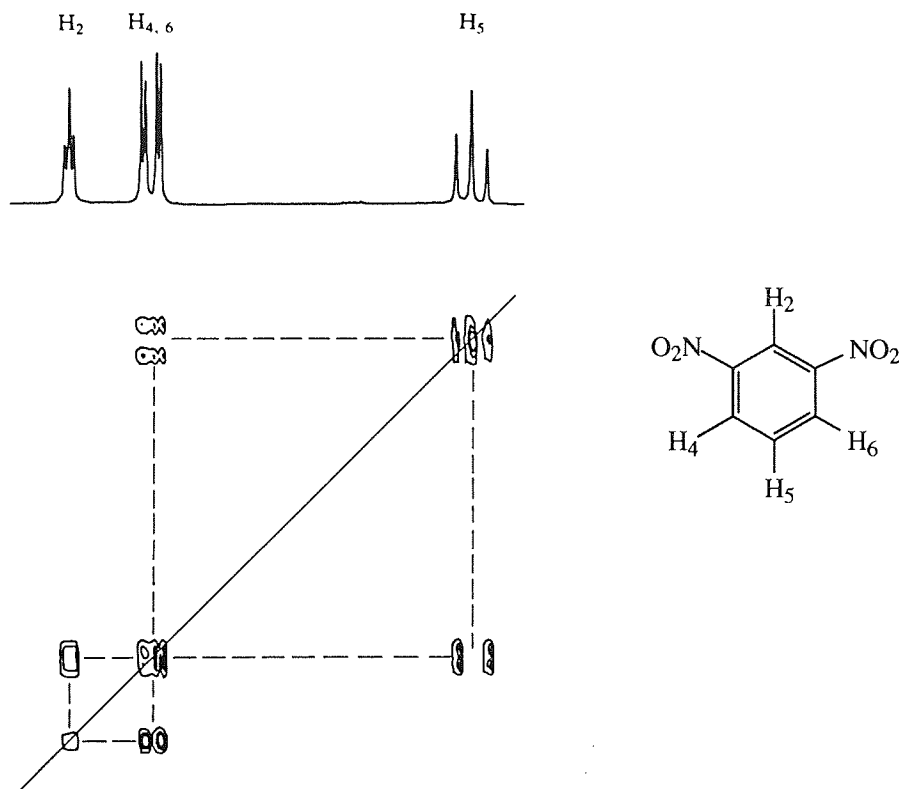


Figure 3.1: Typical COSY spectrum obtained from 1,3-dinitrobenzene.

3.1.2 Distortionless Enhancement by Polarisation Transfer in ¹³C NMR (¹³C DEPT):

The ¹³C NMR DEPT spectrum distinguishes between methyl or methine, methylene and quaternary carbon atoms. In the ¹³C NMR DEPT spectrum methyl or methine carbon peaks remain upright, methylene carbons are phased negative, whereas quaternary carbons are absent from the spectrum. Figure 3.2 [A] shows a diagram of ¹³C NMR DEPT spectra of ethyl *N*-[2'-(3'',4''-dihydroxyphenyl)-2'-hydroxyethyl]-3-aminopropionate (**74**, R= Et). In the ¹³C NMR DEPT spectrum (Figure 3.2 [B]), the methyl carbon at δ_C 14.5 (-CH₃), methine carbon at 69.5 [-C(OH)-] and aromatic C-H carbons at 115.1, 117.6 and 119.8 remain phased positive.

The methylene carbons at δ_C 31.4 ($-\underline{C}H_2-COO-$), 44.3 ($-N-\underline{C}H_2-CH_2-$), 54.3 [$-C(OH)-\underline{C}H_2-N-$] and 63.7 ($-COO-\underline{C}H_2-$) phased negative in the ^{13}C NMR DEPT spectrum. The quaternary carbons at δ_C 133.3, 145.5 and 145.6 (aromatic C) and 173.7 ($-COO-$) are absent in the ^{13}C NMR DEPT spectrum.

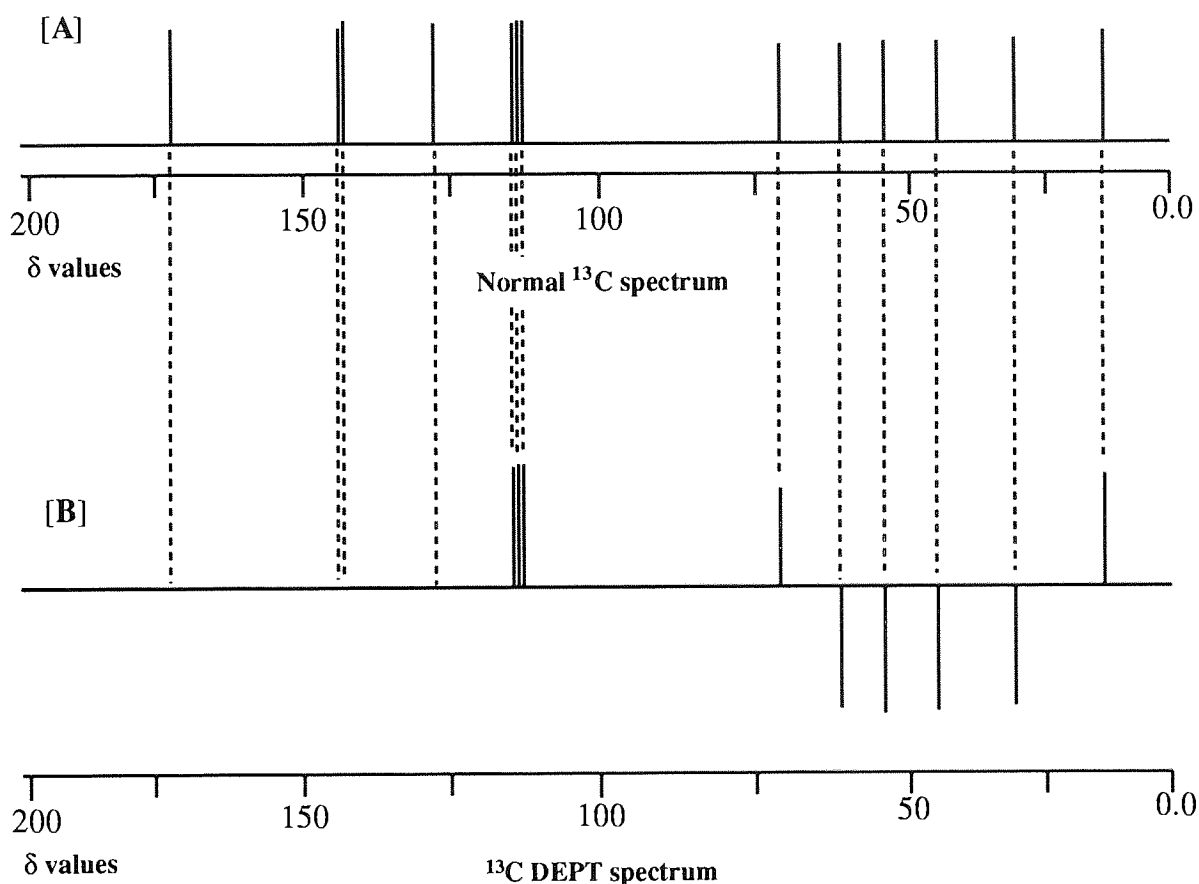
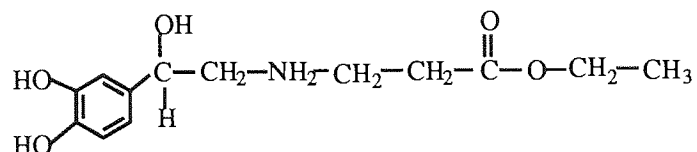


Figure 3.2: A diagram of the ^{13}C NMR and ^{13}C DEPT spectrum (D_2O) of ethyl *N*-[2'-(3',4'-dihydroxyphenyl)-2'-hydroxyethyl]-3-aminopropionate (**74**, R= Et).

3.2 SYNTHESIS OF ALKYL ESTERS OF 3-BROMOPROPIONATE

3.2.1 Propyl 3-bromopropionate (68, R= n-Pr):

A solution of 3-bromopropionyl chloride (5.0 g, 29.2 mmol) was stirred in dry dichloromethane (75 ml) in an ice bath. Anhydrous n-propanol (1.75 g, 2.2 ml, 29.2 mmol) and triethylamine (2.95 g, 4.1 ml, 29.2 mmol) were dissolved in dry dichloromethane (10 ml) and added dropwise to the reaction mixture over a period of 30 min. The reaction was further stirred at room temperature for 2 hr. Dry ether was added to precipitate the triethylammonium hydrochloride which was removed by filtration from the reaction mixture, and the filtrate was evaporated under vacuum to give an oil. The product was isolated by flash chromatography eluting with ethyl acetate-hexane (1:3, R_f 0.62) to yield a pale yellow oil (3.2 g, 16.4 mmol, 56%). No alkene was detected in the product.

^1H NMR (CDCl_3): δ 0.96 (t, $J_{\text{HH}}=7.4$ Hz, 3H, $-\text{CH}_3$), 1.68 (sextet, $J_{\text{HH}}=7.1$ Hz, 2H, $-\text{CH}_2-\text{CH}_3$), 2.92 (t, $J_{\text{HH}}=6.8$ Hz, 2H, $-\text{CH}_2-\text{COO}$), 3.59 (t, $J_{\text{HH}}=6.8$ Hz, 2H, $\text{Br}-\text{CH}_2-$) and 4.10 (t, $J_{\text{HH}}=6.7$ Hz, 2H, $-\text{COO}-\text{CH}_2-$).

^{13}C NMR (CDCl_3): δ 10.3 ($-\text{CH}_3$), 21.9 ($-\text{CH}_2-\text{CH}_3$), 25.9 ($-\text{CH}_2-\text{COO}$), 37.7 ($\text{Br}-\text{CH}_2-$), 66.5 ($-\text{COO}-\text{CH}_2-$) and 172.7 ($\text{C}=\text{O}$).

IR (neat): 1738 cm^{-1} (COO).

3.2.2 Butyl 3-bromopropionate (68, R= n-Bu):

A solution of 3-bromopropionyl chloride (5.0 g, 29.2 mmol) in dry dichloromethane (75 ml) was stirred in an ice bath. A solution of anhydrous n-butanol (2.16 g, 2.67 ml, 29.2 mmol) and triethylamine (2.95 g, 4.1 ml, 29.2 mmol) in dry dichloromethane (10 ml) was added dropwise to the reaction mixture over a period of 30 min. The reaction was further stirred at room temperature for 2 hr. Dry ether was added to precipitate the triethylammonium hydrochloride which was removed by filtration from the reaction mixture, and the filtrate was evaporated under vacuum to give an oil. The product was isolated by flash chromatography eluting with ethyl acetate-hexane (1:3, R_f 0.65) to yield a pale yellow oil (4.96 g, 23.7 mmol, 81%).

^1H NMR (CDCl_3): δ 0.88 (t, $J_{\text{HH}}=7.3$ Hz, 3H, $-\text{CH}_3$), 1.33 (appears as a sextet with an average $J_{\text{HH}}=7.4$ Hz, 2H, $-\text{CH}_2-\text{CH}_3$), 1.57 (appears as a pentet, $J_{\text{HH}}=6.9$ Hz, 2H, $-\text{CH}_2-\text{CH}_2-\text{CH}_3$), 2.86 (t, $J_{\text{HH}}=6.8$ Hz, 2H, $-\text{CH}_2-\text{COO}$), 3.52 (t, $J_{\text{HH}}=6.8$ Hz, 2H, $\text{Br}-\text{CH}_2-$) and 4.08 (t, $J_{\text{HH}}=6.5$ Hz, 2H, $-\text{COO}-\text{CH}_2-$).

^{13}C NMR (CDCl_3): δ 13.5 ($-\text{CH}_3$), 19.0 ($-\text{CH}_2-\text{CH}_3$), 25.9 ($-\text{CH}_2-\text{COO}$), 30.5 ($-\text{COO}-\text{CH}_2-\text{CH}_2-$), 37.6 ($\text{Br}-\text{CH}_2-$), 64.5 ($-\text{COO}-\text{CH}_2-$) and 170.4 ($\text{C}=\text{O}$).

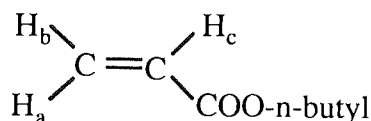
IR (neat): 1739 cm^{-1} (COO).

There is a 15% impurity of alkene ($\text{CH}_2=\text{CH}-\text{COO}-\text{CH}_2-\text{CH}_2-\text{CH}_2-\text{CH}_3$) caused by the elimination of HBr .

Data for alkene group:

δH 5.76 (dd, 1H, H_a), 6.08 (dd, 1H, H_c) and 6.37 (dd, 1H, H_b).

δC 128.5 ($\text{CH}_2=\text{CH}-\text{COO}-$) and 130.3 ($\text{CH}_2=\text{CH}-\text{COO}-$).



3.3 SYNTHESIS OF ALKYL ESTERS OF *N*-BENZYL-3-AMINOPROPIONATE

3.3.1 Methyl *N*-benzyl-3-aminopropionate¹¹⁰ (**64**, R= Me):

A solution of methyl 3-bromopropionate (5.0 g, 30 mmol), benzylamine (6.42 g, 6.5 ml, 60 mmol) and tetrahydrofuran (40 ml) was stirred at $40\text{ }^\circ\text{C}$ for one hour. Dry ether was added to precipitate the benzylammonium hydrochloride which was removed by filtration. The filtrate was evaporated under vacuum to yield an oil (4.0 g). The oil was purified by flash chromatography with ethyl acetate (R_f 0.38) as eluent to yield a viscous colourless oil (3.78 g, 19.56 mmol, 65 %).

^1H NMR (CDCl_3): δ 1.68 (s, 1H, $-\text{NH}-$), 2.52 (t, $J_{\text{HH}}=6.5\text{ Hz}$, 2H, $-\text{CH}_2-\text{COO}-$), 2.88 (t, $J_{\text{HH}}=6.5\text{ Hz}$, 2H, $-\text{N}-\text{CH}_2-\text{CH}_2-$), 3.66 (s, 3H, $-\text{OCH}_3$), 3.79 (s, 2H, $-\text{CH}_2-\text{Ph}$) and 7.21-7.30 (m, 5H, Ph).

^{13}C NMR (CDCl_3): δ 34.5 ($-\text{CH}_2-\text{COO}-$), 44.4 ($-\text{N}-\text{CH}_2-\text{CH}_2-$), 51.5 ($-\text{OCH}_3$), 53.7 ($-\text{CH}_2-\text{Ph}$), 126.9, 128.0, 128.3 (aromatic CH), 140.1 (aromatic C) and 173.1 ($\text{C}=\text{O}$).

IR (neat): 3325 cm^{-1} (N-H), 1735 cm^{-1} (COO), 1454 and 1439 cm^{-1} ($\text{C}=\text{C}$).

3.3.2 Ethyl *N*-benzyl-3-aminopropionate¹¹⁰ (**64**, R= Et):

A solution of ethyl 3-bromopropionate (5.0 g, 28 mmol), benzylamine (5.92 g, 6.0 ml, 56 mmol) and toluene (25 ml) was stirred at 40 °C for one hour. Precipitated benzylammonium hydrochloride was removed by filtration. The filtrate was evaporated under vacuum to yield an oil (4.4 g). The oil was purified by flash chromatography with ethyl acetate (R_f 0.39) as eluent to yield a viscous colourless oil (4.0 g, 19.30 mmol, 77 %).

¹H NMR (CDCl₃): δ 1.25 (t, J_{HH} =7.1 Hz, 3H, -CH₃), 1.72 (s, 1H, -NH-), 2.52 (t, J_{HH} =6.4 Hz, 2H, -CH₂-COO-), 2.90 (t, J_{HH} =6.4 Hz, 2H, -N-CH₂-CH₂-), 3.80 (s, 2H, -CH₂-Ph), 4.12 (q, J_{HH} =7.1 Hz, 2H, -COO-CH₂-), and 7.2-7.4 (m, 5H, Ph).

¹³C NMR (CDCl₃): δ 14.2 (-CH₃), 34.8 (-CH₂-COO-), 44.5 (-N-CH₂-CH₂-), 53.8 (-CH₂-Ph), 60.4 (-COO-CH₂-), 126.9, 128.1, 128.4 (aromatic C-H), 140.2 (aromatic C) and 172.8 (C=O).

3.3.3 Propyl *N*-benzyl-3-aminopropionate¹¹⁰ (**64**, R= n-Pr):

A solution of propyl 3-bromopropionate (1.4 g, 7.18 mmol), benzylamine (1.54 g, 1.6 ml, 14.4 mmol) and tetrahydrofuran (20 ml) was stirred at 40 °C for one hour. Dry ether was added to precipitate the benzylammonium hydrochloride which was removed by filtration. The filtrate was evaporated under vacuum to yield an oil (1.6 g). The oil was purified by flash chromatography with ethyl acetate (R_f 0.39) as eluent to yield a viscous colourless oil (1.46 g, 6.6 mmol, 92 %).

¹H NMR (CDCl₃): δ 0.92 (t, J_{HH} =7.4 Hz, 3H, -CH₃), 1.63 (appears as a sextet, J_{HH} =7.2 Hz, 2H, -CH₂-CH₃), 2.20 (broad s, 1H, -NH-), 2.53 (t, J_{HH} =6.4 Hz, 2H, -CH₂-COO), 2.89 (t, J_{HH} =6.4 Hz, 2H, -NH-CH₂-CH₂-), 3.79 (s, 2H, -NH-CH₂-Ph), 4.03 (t, J_{HH} =6.7 Hz, 2H, -COO-CH₂-) and 7.20-7.35 (m, 5H, Ph).

¹³C NMR (CDCl₃): δ 10.3 (-CH₃), 21.9 (-CH₂-CH₃), 34.7 (-CH₂-COO), 44.4 (-NH-CH₂-CH₂-), 53.7 (-NH-CH₂-Ph), 65.9 (-COO-CH₂-), 126.8, 128.0, 128.3 (aromatic CH), 140.1 (aromatic C) and 172.8 (C=O).

IR (neat): 3338 cm⁻¹ (N-H), 1732 cm⁻¹ (COO), 1454 and 1178 cm⁻¹ (C=C).

3.3.4 Butyl *N*-benzyl-3-aminopropionate¹¹⁰ (64, R= n-Bu):

A solution of butyl 3-bromopropionate (4.63 g, 22.1 mmol), benzylamine (4.75 g, 4.8 ml, 44.3 mmol) and tetrahydrofuran (50 ml) was stirred at 40 °C for one hour. Dry ether was added to precipitate the benzylammonium hydrochloride which was removed by filtration. The filtrate was evaporated under vacuum to yield an oil (4.5 g). The oil was purified by flash chromatography with ethyl acetate (R_f 0.40) as eluent to yield a viscous colourless oil (4.2 g, 17.8 mmol, 81 %).

¹H NMR (CDCl₃): δ 0.92 (t, J_{HH} =7.3 Hz, 3H, -CH₃), 1.36 (appears as a sextet with an average J_{HH} =7.4 Hz, 2H, -CH₂-CH₃), 1.57 (appears as a pentet with an average J_{HH} =7.1 Hz, 2H, -CH₂-CH₂-CH₃), 1.67 (broad s, 1H, -NH-), 2.52 (t, J_{HH} =6.4 Hz, 2H, -CH₂-COO), 2.89 (t, J_{HH} =6.4 Hz, 2H, -NH-CH₂-CH₂-), 3.79 (s, 2H, -NH-CH₂-Ph), 4.07 (t, J_{HH} =6.6 Hz, 2H, -COO-CH₂-) and 7.20-7.35 (m, 5H, Ph).

¹³C NMR (CDCl₃): δ 13.6 (-CH₃), 19.1 (-CH₂-CH₃), 30.6 (-CH₂-CH₂-CH₃), 34.7 (-CH₂-COO), 44.5 (-NH-CH₂-CH₂-), 53.7 (-NH-CH₂-Ph), 64.2 (-COO-CH₂-), 126.8, 128.0, 128.3 (aromatic CH), 140.1 (aromatic C) and 172.8 (C=O).

IR (neat): 3327 cm⁻¹ (N-H), 1732 cm⁻¹ (COO), 1454 and 1176 cm⁻¹ (C=C).

3.4 SYNTHESIS OF α -CHLOROACETOPHENONE ANALOGUES**3.4.1 3,4-Dihydroxy- α -chloroacetophenone¹¹¹ (75):**

A solution of catechol (55 g, 0.50 mol), chloroacetyl chloride (65g, 46 ml, 0.575 mol) and phosphorus oxychloride (4.75g, 3.0 ml, 0.031 mol) in toluene (75 ml) was heated under reflux for 40 h. The dark purple reaction mixture was filtered and the precipitate was dissolved in 10% acetic acid in water (400 ml). Charcoal was added, the solution was heated for 5 to 10 min at 80 °C and it was then filtered through celite. The filtrate was concentrated to give pale purple crystals of 3,4-dihydroxy- α -chloroacetophenone (25g, 0.134 mol, 27%), mp. 173 °C (lit. 173-175 °C).¹¹¹

¹H NMR (CDCl₃): δ 4.67 (s, 2H, -CH₂-), 6.92 (d, J_{ortho} =8.3 Hz, 1H, aromatic-H₅), 7.40 (dd, J_{meta} =2.1 Hz and J_{ortho} =8.3 Hz, 1H, aromatic-H₆), 7.52 (d, J_{meta} =2.1 Hz, 1H, aromatic-H₂) and 8.32 (broad s, 2H, -OH).

3.4.2 1,2-Diacetoxybenzene¹¹⁷ (108):

1,2-Dihydroxybenzene (1.0 g, 9.1 mmol) was dissolved in aqueous 3M sodium hydroxide solution (20 ml). Crushed ice (10-20 g) was added to the solution followed by acetic anhydride (1.85 g, 1.72 ml, 18.0 mmol). The mixture was shaken vigorously for 30 to 60 seconds. 1,2-Diacetoxybenzene separated out as a precipitate which was collected by filtration and recrystallised from ethanol, to yield crystals of diacetoxybenzene (50%), m.p. 61.5-62 °C, lit. 65 °C.¹¹⁷

¹H NMR (CDCl₃): δ 2.29 (s, 6H, -OCOCH₃) and 7.18-7.29 (m, 4H, Ph).

3.4.3 3,4-Dimethoxy- α -chloroacetophenone¹¹¹ (84):

Dimethoxybenzene (5.42 g, 5ml, 39.3 mmol) was heated under reflux with chloroacetyl chloride (6.40 g, 4.53 ml, 56.7 mmol) and phosphorus oxychloride (0.47g, 1.3 ml, 3.06 mmol) in 8 ml of toluene for 50 h. The dark brown reaction mixture was filtered, and the filtrate was concentrated under vacuum. The product was isolated by flash chromatography using ethyl acetate-hexane (1:1.5, R_f 0.25) as eluent, to give a solid, which was crystallised from ethyl acetate-hexane (mp. 98-99 °C).

¹H NMR (CDCl₃): δ 3.95 (s, 3H, -OCH₃), 3.97 (s, 3H, -OCH₃), 4.68 (s, 2H, -CH₂-Cl), 6.92 (d, J_{ortho}=8.3 Hz, 1H, H₅-aromatic), 7.54 (d, J_{meta}=2.0 Hz, 1H, H₂-aromatic) and 7.58 (dd, J_{ortho}=8.4 and J_{meta}=2.0 Hz, 1H, H₆-aromatic).

IR (KBr): 1689 cm⁻¹ (C=O), 1511 and 1465 cm⁻¹ (C=C), and 1255 cm⁻¹ (C-O-C).

3.4.4 Attempted synthesis of 3,4-dibenzyloxy- α -chloroacetophenone¹¹² (80):

To a stirred mixture of finely powdered anhydrous potassium carbonate (0.74 g, 5.36 mmol) and 3,4-dihydroxy- α -chloroacetophenone (0.5 g, 2.68 mmol) in acetone (5ml), was added benzyl bromide (0.92 g, 0.64 ml, 5.36 mmol) in acetone (5 ml). The mixture was heated under reflux for 3 h after which time the reaction mixture was cooled, filtered and evaporated under vacuum. The residue was extracted with ether, the ethereal layer was evaporated and the product isolated by flash chromatography using ethyl acetate-hexane (1:1, R_f 0.36) as eluent to give a white solid, which was recrystallised with ethyl acetate-hexane. The product was not the title compound. Instead the NMR data is consistent with a monobenzylated derivative, most likely 3-benzyloxy-4-hydroxy- α -chloroacetophenone (**81**). 3-Benzyloxy-4-hydroxy- α -bromoacetophenone (**82**), the product of halide exchange, was also formed.

^1H NMR (CDCl_3): δ 4.45 (s, 2H, $-\text{CH}_2\text{-Br}$), 4.65 (s, 2H, $-\text{CH}_2\text{-Cl}$), 5.2 (s, 2H, $-\text{O-CH}_2\text{-Ph}$), 5.78 (s, 1H, $-\text{OH}$), 6.98 (d, $J_{\text{ortho}}=8.0$ Hz, 1H, $\text{H}_5\text{-aromatic}$), 7.32-7.58 (m, 7H, aromatic).

IR (KBr): 3505 cm^{-1} (OH), 1687 cm^{-1} (C=O), 1511 and 1611 (C=C) cm^{-1} , and 1268 and 1143 cm^{-1} (C-O-C).

3.4.5 3,4-(1',1',3',3'-Tetra-*t*-butyldisiloxane)dioxy- α -chloroacetophenone¹¹⁴ (93):

A mixture of 3,4-dihydroxy- α -chloroacetophenone (1.0 g, 5.36 mmol) and 1-hydroxybenzotriazole (0.073 g, 0.536 mmol, dried overnight at 0.5 mm Hg at 25 °C) was stirred in acetonitrile (10 ml) at 65 °C. A solution of di-*t*-butyl dichlorosilane (1.26 g, 5.89 mmol) and triethylamine (2.71 g, 3.74 ml, 26.8 mmol) in acetonitrile (10 ml) was added dropwise to the reaction mixture over a period of 15 min. After 10 minutes, a white precipitate was formed and the reaction was complete within 0.5 h. The reaction mixture was partitioned between water and dichloromethane. The dichloromethane layer was dried and evaporated under vacuum to give a thick oil. Hexane was added to precipitate the impurities, which were removed by filtration and the filtrate was evaporated under vacuum. 3,4-(1',1',3',3'-Tetra-*t*-butyldisiloxane)dioxy- α -chloroacetophenone was isolated by flash chromatography eluting with ethyl acetate-hexane (1:20, R_f 0.38) to yield a colourless oil (1.14 g, 2.1 mmol, 74.5%).

^1H NMR (CDCl_3): δ 1.10 [s, 36H, $(\text{CH}_3)_3\text{C-Si}$], 4.68 (s, 2H, $-\text{CO-CH}_2\text{-Cl}$), 6.96 (d, $J_{\text{ortho}}=8.3$ Hz, 1H, $\text{H}_5\text{-aromatic}$), 7.49 (dd, $J_{\text{ortho}}=8.3$ and $J_{\text{meta}}=2.2$ Hz, 1H, $\text{H}_6\text{-aromatic}$) and 7.54 (d, $J_{\text{meta}}=2.2$ Hz, 1H, $\text{H}_2\text{-aromatic}$).

^{13}C NMR (CDCl_3): δ 21.3 [$(\text{CH}_3)_3\text{C-Si}$], 27.9 [$(\text{CH}_3)_3\text{C-Si}$], 45.7 ($-\text{CO-CH}_2\text{-Cl}$), 121.6, 121.9, 123.3 (aromatic CH), 128.7, 146.1, 151.3 (aromatic C) and 193.3 (C=O).

IR (KBr): 1698 cm^{-1} (C=O), 1509 cm^{-1} (C=C) and 1319 cm^{-1} (Si-O-C).

Elemental analysis: Calculated for $\text{C}_{24}\text{H}_{41}\text{ClO}_4\text{Si}_2$: C, 59.41; H, 8.52 %. Found: C, 60.24; H, 7.89%.

Mass spectrum (CI, NH_3): observed mass for $\text{C}_{24}\text{H}_{41}\text{ClO}_4\text{Si}_2$ m/e 485.0 (M^+ , 100% ^{35}Cl), 487 (M^+ , 45% ^{37}Cl) and 451 ($\text{M}^+ - \text{Cl}$, 50%).

3.4.6 3,4-Diphenylmethylenedioxy- α -chloroacetophenone¹¹⁶ (102):

3,4-Dihydroxy- α -chloroacetophenone (1.6 g, 8.43 mmol) was added to α,α -dichlorodiphenylmethane (2.0 g, 8.43 mmol) and heated to 170 °C with stirring. After 15 min at 170-180 °C, the reaction mixture was cooled and then extracted with hexane to remove the unreacted dichlorodiphenylmethane. The product was isolated by flash chromatography using ethyl acetate-hexane (1:1, R_f 0.68) as eluent to give 3,4-diphenylmethylenedioxy- α -chloroacetophenone as a colourless solid (2.4 g, 6.84 mmol, 81%), mp. 91.0-92.5 °C.

¹H NMR (CDCl₃): δ 4.61 (s, 2H, -CH₂-Cl), 6.94 (d, J_{ortho} =8.1 Hz, 1H, H₅-aromatic), 7.35-7.45 (m, 6H, aromatic) and 7.50-7.60 (m, 6H, aromatic).

¹³C NMR (CDCl₃): δ 45.6 (-CH₂-Cl), 125.0, 126.1, 128.3, 128.8, 129.4 (aromatic CH), 108.2, 108.4, 139.3, 147.4, 152.3 (aromatic C), 193.0 (-CO-).

IR (KBr): 1697 cm⁻¹ (C=O), 1616 and 1498 cm⁻¹ (C=C), and 1257 and 1216 cm⁻¹ (C-O-C).

3.4.7 3,4-Diacetoxy- α -chloroacetophenone¹⁰⁹ (109):

A stirred solution of 3,4-dihydroxy- α -chloroacetophenone (2.0 g, 10.7 mmol), triethylamine (2.17 g, 3 ml, 21.4 mmol) and anhydrous THF (10 ml) was cooled in an ice bath. Acetic anhydride (2.18 g, 2.0 ml, 21.4 mmol) was added dropwise to the reaction mixture over a period of 10 min. After 3 h, the solvent was removed by evaporation under vacuum and the residue was recrystallised with ethyl acetate-hexane to give 3,4-diacetoxy- α -chloroacetophenone (2.5 g, 10.5 mmol, 97%), mp. 115 °C.

¹H NMR (CDCl₃): δ 2.33 (s, 6H, -OCOCH₃), 4.67 (s, 2H, -CH₂-Cl), 7.35 (d, J_{ortho} =8.4 Hz, 1H, H₅-aromatic), 7.81 (d, J_{meta} =2.1 Hz, 1H, H₂-aromatic) and 7.86 (dd, J_{ortho} =8.5 and J_{meta} =2.1 Hz, 1H, H₆-aromatic).

IR (KBr): 1769 cm⁻¹ (C=O ester), 1706 cm⁻¹ (C=O keto), 1501 and 1422 cm⁻¹ (C=C), and 1210 cm⁻¹ (C-O-C).

3.4.8 3,4-Dipivaloyloxy- α -chloroacetophenone¹⁰⁹ (113):

A stirred solution of 3,4-dihydroxy- α -chloroacetophenone (5.4 g, 28.9 mmol) and triethylamine (5.86 g, 8.07 ml, 57.9 mmol) in anhydrous THF (50 ml) was stirred in an ice bath. Pivaloyl chloride (6.98 g, 7.13 ml, 57.9 mmol) was added dropwise to the reaction mixture over a period of 10 min. The triethylammonium hydrochloride precipitate was removed by filtration. The filtrate was evaporated under vacuum to give a solid (9.5 g). Compound (113) was purified by flash chromatography eluting with ethyl acetate-hexane (1:4, R_f 0.32) (9.0 g, 25.4 mmol, 88%), m.p. 62.5 °C.

^1H NMR (CDCl_3): δ 1.36 (s, 9H, Bu^tCOO), 1.37 (s, 9H, Bu^tCOO), 4.68 (s, 2H, $-\text{CO}-\text{CH}_2-\text{Cl}$), 7.28 (d, $J_{\text{ortho}}=8.5$ Hz, 1H, H_5 -aromatic), 7.74 (d, $J_{\text{meta}}=2.1$ Hz, 1H, H_2 -aromatic) and 7.83 (dd, $J_{\text{meta}}=2.1$ and $J_{\text{ortho}}=8.5$ Hz, 1H, H_6 -aromatic).

^{13}C NMR (CDCl_3): δ 27.1 [$-\text{C}(\underline{\text{C}}\text{H}_3)_3$], 27.2 [$-\text{C}(\underline{\text{C}}\text{H}_3)_3$], 39.2 [$-\underline{\text{C}}(\text{CH}_3)_3$], 39.3 [$-\underline{\text{C}}(\text{CH}_3)_3$], 45.7 ($-\text{CO}-\underline{\text{C}}\text{H}_2-\text{Cl}$), 123.9, 124.0, 126.7 (aromatic C-H), 132.3, 143.1, 147.4 (aromatic C), 175.3 ($\text{Bu}^t\underline{\text{C}}\text{OO}$), 175.6 ($\text{Bu}^t\underline{\text{C}}\text{OO}$) and 189.3 ($-\underline{\text{C}}\text{O}-\text{CH}_2-\text{Cl}$).

Elemental analysis: Calculated for $\text{C}_{18}\text{H}_{23}\text{O}_5\text{Cl}$: C, 60.93; H, 6.53%. Found: C, 60.62; H, 6.39%.

Mass spectrum (CI, NH_3): calculated mass for $\text{C}_{18}\text{H}_{27}\text{NO}_5\text{Cl}$ 372.15778 ($\text{M} + \text{NH}_4^+$). Observed accurate mass is 372.1578 ($\text{M} + \text{NH}_4^+$).

Mass (CI, NH_3): m/z 372 [$(\text{M} + \text{NH}_4^+)$, ^{35}Cl , 100%], 374 [$(\text{M} + \text{NH}_4^+)$, ^{37}Cl , 35%] and 338 [$(\text{M} + \text{NH}_4^+) - \text{Cl}$, 89%].

Mass spectrum (EI, NH_3): m/z 57 [$(\text{CH}_3)_3\text{C}^+$, 100%] and 85 [$(\text{CH}_3)_3\text{CC}=\text{O}^+$, 35%].

3.5 Product (53) isolated from the reaction between ethyl bromoacetate and 1-phenyl-2-aminoethanol¹⁰⁹:

A solution of ethyl bromoacetate (1.22 g, 0.81 ml, 7.28 mmol) and triethylamine (0.81 g, 1.12 ml, 8.02 mmol) in anhydrous THF (10 ml) was stirred in an ice bath. A solution of 1-phenyl-2-aminoethanol (1.0 g, 7.28 mmol) was dissolved in anhydrous THF (5 ml) and added dropwise to the reaction mixture, over a period of 15 min. The reaction was complete in 3 h and the product (53), which was formed in good yield was isolated by flash chromatography by elution with ethyl acetate (R_f 0.37) to give a colourless viscous oil. Its structure (53) was assigned by ^1H -NMR, ^1H - ^1H COSY, ^{13}C -NMR, ^{13}C -DEPT spectroscopy and elemental analysis:

^1H NMR (CDCl_3): δ 1.26 (t, $J_{\text{HH}}=7.1$ Hz, 3H, $-\text{C}^3\text{H}_3$), 1.27 (t, $J_{\text{HH}}=7.1$ Hz, 6H, $-\text{C}^{14}\text{H}_3$ and $-\text{C}^{14'}\text{H}_3$), 2.60 (dd, $J_{\text{gem}}=13.6$, $J_{\text{HH}}=10.1$ Hz, 1H, $\text{C}^4\text{-H}_a$), 2.80 (dd, $J_{\text{gem}}=12.5$, $J_{\text{HH}}=10$. Hz, 1H, $\text{C}^8\text{-H}_e$), 3.13-3.21 (m, 2H, $\text{C}^4\text{-H}_b$ and $\text{C}^8\text{-H}_f$), 3.35 (s, 2H, $-\text{OOC}-\text{CH}_2\text{-N-}$), 3.45 (d, $J_{\text{HH}}=17.3$ Hz, 1H, $\text{C}^{10}\text{-H}_a$), 3.60 (dd, $J_{\text{HH}}=18.2$, $J_{\text{HH}}=17.3$ Hz, 4H, $\text{C}^{10'}\text{-H}_b$, $\text{C}^{10'}\text{-H}_a$ and $-\text{C}^2\text{H}_2-$), 3.82 (dd, $J_{\text{HH}}=17.3$, $J_{\text{HH}}=1.6$ Hz, 1H, $\text{C}^{10}\text{-H}_b$), 4.18 (q, $J_{\text{HH}}=7.1$ Hz, 6H, $-\text{COO}-\text{CH}_2-$), 4.67 (dd, $J_{\text{HH}}=10.0$, $J_{\text{HH}}=2.9$ Hz, 1H, $\text{C}^5\text{-H}$), 5.56 (dd, $J_{\text{HH}}=10.0$, $J_{\text{HH}}=3.4$ Hz, 1H, $\text{C}^7\text{-H}$), 7.2-7.4 (m, 10H, Ph) and -OH between 4.40-4.80 (broad s, 1H),

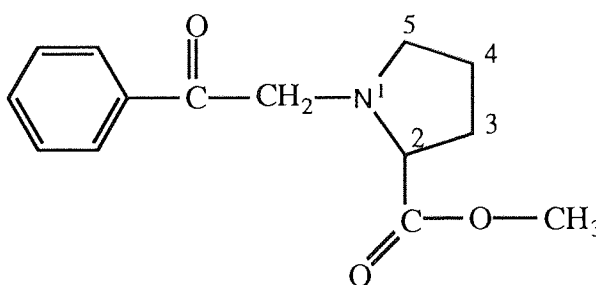
3.6 REACTIONS OF α -CHLOROACETOPHENONE WITH ESTERS OF AMINO ACIDS (EXCLUDING ESTERS OF *N*-BENZYL-3-AMINOPROPIONATE)

3.6.1 Methyl *N*-(benzoylmethyl)proline¹⁰⁹ (59):

A mixture of L-proline methyl ester (0.52 g, 4.0 mmol), triethylamine (0.45 g, 0.62 ml, 4.4 mmol) and sodium iodide (0.06 g, 0.4 mmol) were stirred in dry THF (5 ml) in an ice bath. A solution of α -chloroacetophenone (0.62 g, 4.0 mmol) in dry THF (5 ml) was added dropwise to the reaction mixture over a period of 15 min. The reaction was complete after 3 hr. The reaction mixture was filtered to remove the triethylammonium hydrochloride precipitate and the filtrate was evaporated under vacuum to give an oil. The product was isolated by flash chromatography eluting with ethyl acetate (R_f 0.75) to yield a colourless oil (0.88 g, 3.6 mmol, 88%).

^1H NMR (CDCl_3): δ 1.8-2.0 (m, 3H, $\text{C}_4\text{-H}_2$ and $\text{C}_3\text{-H}_a$), 2.10-2.22 (m, 1H, $\text{C}_3\text{-H}_b$), 2.72 (q, $J_{\text{HH}}=7.5$ Hz, 1H, $\text{C}_5\text{-H}_a$), 3.10-3.18 (m, 1H, $\text{C}_5\text{-H}_b$), 3.56-3.62 (m, 1H, $\text{C}_2\text{-H}$), 3.64 (s, 3H, $-\text{OCH}_3$), 4.02 (d, $J_{\text{gem}}=17.2$ Hz, 1H, $-\text{CO}-\underline{\text{C}}_A\text{H}_B\text{-N}$), 4.31 (d, $J_{\text{gem}}=17.2$ Hz, 1H, $-\text{CO}-\text{C}_A\underline{\text{H}}_B\text{-N}$), 7.3-7.5 (m, 3H, Ph) and 7.9-8.0 (m, 2H, Ph).

^{13}C NMR (CDCl_3): δ 23.5 (C_4), 29.4 (C_3), 51.6 ($-\text{CH}_3$), 53.0 (C_5), 58.9 (C_7), 64.2 (C_2), 128.1, 128.4, 129.8, 133.1, 135.6 (aromatic CH), 132.6 (aromatic C), 174.1 ($\text{C}=\text{O}$ ester) and 196.8 ($\text{C}=\text{O}$ keto).



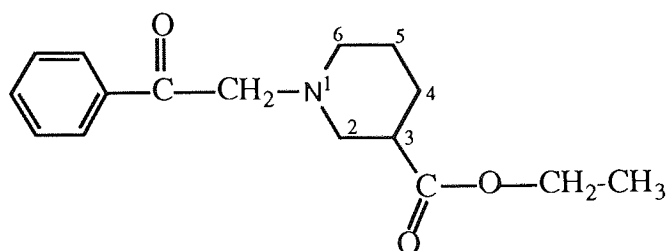
3.6.2 Ethyl *N*-(benzoylmethyl)-3-piperidine carboxylate¹⁰⁹ (61):

A mixture of ethyl 3-piperidine carboxylate (1.0 g, 6.36 mmol), triethylamine (0.71 g, 0.98 ml, 7.0 mmol) and sodium iodide (0.1 g, 6.36 mmol) were stirred in dry THF (5 ml) in an ice bath. A solution of α -chloroacetophenone (0.99 g, 6.36 mmol) in dry THF (5 ml) was added dropwise to the reaction mixture over a period of 15 min. The reaction was complete after 3 h. The precipitate of triethylammonium hydrochloride was removed by filtration from the reaction mixture, and the filtrate was evaporated under vacuum to give an oil. The product was isolated by flash chromatography eluting with ethyl acetate (R_f 0.75) to yield a colourless oil (1.55 g, 5.6 mmol, 89%).

^1H NMR (CDCl_3): δ 1.22 (t, $J_{\text{HH}}=7.15$ Hz, 3H, $-\text{CH}_3$), 1.4-1.55 (m, 1H, $\text{C}_5\text{-H}_a$), 1.6-1.8 (m, 2H, $\text{C}_5\text{-H}_b$ and $\text{C}_4\text{-H}_a$), 1.96 (m, $J_{\text{gem}}=12.55$, $J_{\text{HH}}=3.72$ Hz, 1H, $\text{C}_4\text{-H}_b$), 2.20 (dt, $J_{\text{gem}}=10.5$, $J_{\text{HH}}=3.9$ Hz, 1H, $\text{C}_6\text{-H}_a$), 2.38 (dd, $J_{\text{gem}}=J_{\text{HH}}=10.5$ Hz, 1H, $\text{C}_6\text{-H}_b$), 2.68 (tt, $J_{\text{HH}}=10.3$, $J_{\text{HH}}=3.9$ Hz, 1H, $\text{C}_3\text{-H}$), 2.8-2.9 (m, 1H, $\text{C}_2\text{-H}_a$), 3.05-3.15 (m, 1H, $\text{C}_2\text{-H}_b$), 3.78 (d, $J_{\text{HH}}=16.5$ Hz, 1H, $-\text{CO}-\underline{\text{C}}\text{H}_A\text{H}_B\text{-N-}$), 3.85 (d, $J_{\text{HH}}=16.5$ Hz, 1H, $-\text{CO}-\text{C}\underline{\text{H}}_A\text{H}_B\text{-N-}$), 4.06 (dq, $J_{\text{gem}}=10.8$ and $J_{\text{HH}}=7.2$ Hz, 1H, $-\text{COO}-\underline{\text{C}}\text{H}_A-$), 4.12 (dq, $J_{\text{gem}}=10.8$ and $J_{\text{HH}}=7.2$ Hz, 1H, $-\text{COO}-\underline{\text{C}}\text{H}_B-$), 7.35-7.6 (m, 3H, aromatic) and 7.95-8.10 (m, 2H, aromatic).

IR (neat): 1730 cm^{-1} ($\text{C}=\text{O}$ ester) and 1678 cm^{-1} ($\text{C}=\text{O}$ keto).

^{13}C NMR (CDCl_3): δ 13.9 ($-\text{CH}_3$), 24.2 (C_4), 26.3 (C_5), 41.4 (C_3), 53.6 (C_6), 55.4 (C_2), 60.1 ($-\text{COO}-\underline{\text{C}}\text{H}_2-$), 64.6 ($-\text{CO}-\underline{\text{C}}\text{H}_2\text{-N-}$), 128.2, 132.9 (aromatic CH), 135.7 (aromatic C), 172.3 ($-\text{COO}$) and 196.4 ($-\underline{\text{C}}\text{O}-\text{CH}_2\text{-N-}$).



3.6.3 Ethyl aminoethanoate (55):

Ethyl ammoniummethanoate hydrochloride (glycine ethyl ester hydrochloride, 4.0 g, 28.7 mmol) was dissolved in 10 ml of water and neutralised with aqueous ammonia to pH 8.5-9.0 (2 ml). The solution was extracted with dichloromethane and the lower organic layer was dried with anhydrous molecular sieves and then evaporated under vacuum to yield a colourless oil (2.61 g, 25.3 mmol, 88.3 %).

^1H NMR (CDCl_3): δ 1.28 (t, $J_{\text{HH}}=7.1$ Hz, 3H, $-\text{CH}_3$), 1.51 (broad s, 2H, $-\text{NH}_2$), 3.43 (s, 2H, $-\text{N}-\text{CH}_2-\text{COO}-$) and 4.18 (q, $J_{\text{HH}}=7.1$ Hz, 2H, $-\text{COO}-\text{CH}_2-$).

3.6.4 Ethyl *N*-benzoylmethyl-aminoethanoate¹⁰⁹ (56):

Ethyl aminoethanoate (1.0 g, 9.7 mmol), triethylamine (1.46 g, 2ml, 14.5 mmol) and sodium iodide (0.146 g, 0.97 mmol) were stirred in dry THF (10 ml) in an ice bath. A solution of α -chloroacetophenone (1.5 g, 9.7 mmol) in dry THF (5 ml) and added dropwise to the reaction mixture over a period of 15 min. The reaction was complete after 3 h. The reaction mixture was filtered to remove the precipitate of triethylammonium hydrochloride, and the filtrate was evaporated under vacuum to give an oil. The product was isolated by flash column chromatography eluting with ethyl acetate (R_f 0.42) to yield a colourless oil (1.85 g, 8.4 mmol, 86%).

^1H NMR (CDCl_3): δ 1.28 (t, $J_{\text{HH}}=7.2$ Hz, 3H, $-\text{CH}_3$), 2.4 (broad s, 1H, $-\text{NH}-$), 3.55 (s, 2H, $-\text{N}-\text{CH}_2-\text{COO}-$), 4.20 (q, $J_{\text{HH}}=7.2$ Hz, 2H, $-\text{COO}-\text{CH}_2-$), 4.21 (s, 2H, $-\text{CO}-\text{CH}_2-\text{N}-$), 7.45-7.6 (m, 3H, aromatic) and 7.9-8.0 (m, 2H, aromatic).

^{13}C NMR (CDCl_3): δ 14.1 ($-\text{CH}_3$), 50.2 ($-\underline{\text{C}}\text{H}_2-\text{COO}-$), 54.9 ($-\text{CO}-\underline{\text{C}}\text{H}_2-\text{N}-$), 60.7 ($-\text{COO}-\underline{\text{C}}\text{H}_2$), 127.6, 128.6, 133.4 (aromatic CH), 135.2 (aromatic C), 171.9 ($-\underline{\text{C}}\text{OO}-$) and 196.0 ($-\underline{\text{C}}\text{O}-\text{CH}_2-$).

IR (KBr): 3360 cm^{-1} (N-H), 1745 cm^{-1} (C=O ester), 1700 cm^{-1} (C=O keto), 1460 and 1380 cm^{-1} (C=C).

3.7 SYNTHESIS OF ESTERS OF *N*-(SUBSTITUTED) BENZOYLMETHYL-*N*-BENZYL-3-AMINOPROPIONATE

3.7.1 Ethyl *N*-(benzoylmethyl)-*N*-benzyl-3-aminopropionate¹⁰⁹ (65, R=Et):

A stirred mixture of ethyl *N*-benzyl-3-aminopropionate (1.0 g, 4.85 mmol), triethylamine (0.33 g, 0.45 ml, 3.23 mmol) and sodium iodide (0.049 g, 0.32 mmol) in anhydrous DMF (10 ml) was cooled in an ice bath. A solution of α -chloroacetophenone (0.5 g, 3.23 mmol) in anhydrous DMF (10 ml) and was added dropwise to the reaction mixture over a period of 15 min. The reaction was nearly complete in 3 h. The turbid reaction mixture was filtered and evaporated under vacuum to yield an oil (1.0 g). The product was isolated by flash chromatography eluting with ethyl acetate-hexane (1:5, R_f 0.25) to yield ethyl *N*-(benzoylmethyl)-*N*-benzyl-3-aminopropionate as a colourless oil (0.75 g, 2.30 mmol, 72 %).

¹H NMR (CDCl₃): δ 1.12 (t, $J_{HH}=7.1$ Hz, 3H, -CH₃), 2.51 (t, $J_{HH}=6.5$ Hz, 2H, -CH₂-COO-), 3.08 (t, $J_{HH}=6.5$ Hz, 2H, -N-CH₂-CH₂-), 3.82 (s, 2H, N-CH₂-Ph), 3.92 (s, 2H, -CO-CH₂-N-), 4.11 (q, $J_{HH}=7.1$ Hz, -COO-CH₂-), 7.22-7.58 (m, 8H, aromatic) and 7.82-7.86 (m, 2H, aromatic).

¹³C NMR (CDCl₃): δ 14.2 (-CH₃), 33.2 (-CH₂-COO-), 50.0 (-N-CH₂-CH₂-), 58.0 (-N-CH₂-Ph), 59.4 (-CO-CH₂-N-), 60.3 (-COO-CH₂-), 127.1, 128.2, 128.2, 128.3, 129.0, 133.0 (aromatic CH), 135.9, 138.5 (aromatic C), 172.4 (-COO-) and 196.0 (-CO-).

3.7.2 Ethyl *N*-[(3',4'-diacetoxybenzoyl)methyl]-*N*-benzyl-3-aminopropionate¹⁰⁹ (110):

Ethyl *N*-benzyl-3-aminopropionate (0.66 g, 3.14 mmol), triethylamine (0.21 g, 0.30 ml, 2.0 mmol) and sodium iodide (0.031 g, 0.2 mmol) were stirred in 10 ml of anhydrous DMF in an ice bath. A solution of 3,4-diacetoxy- α -chloroacetophenone (0.5 g, 2.0 mmol) in 10 ml of anhydrous DMF was added dropwise to the reaction mixture over a period of 15 min. The reaction was complete after 3 hr, the insoluble material was removed by filtration and the filtrate was evaporated under vacuum to give an oil. The ethyl *N*-[(3',4'-diacetoxybenzoyl)methyl]-*N*-benzyl-3-aminopropionate was isolated by flash chromatography eluting with ethyl acetate-hexane (1:1, R_f 0.47) to yield a colourless oil (0.74 g, 1.8 mmol, 87%).

¹H NMR (CDCl₃): δ 1.20 (t, $J_{HH}=7.1$ Hz, 3H, -CH₂-CH₃), 2.30 (s, 3H, CH₃-COO-), 2.31 (s, 3H, CH₃-COO-), 2.52 (t, $J_{HH}=6.8$ Hz, 2H, -CH₂-COO-), 3.04 (t, $J_{HH}=6.8$ Hz, 2H, -N-CH₂-CH₂-), 3.78 (s, 2H, -N-CH₂-Ph), 3.85 (s, 2H, -CO-CH₂-N-), 4.05 (q, $J_{HH}=7.1$ Hz, 2H, -COO-CH₂-), 7.24 (d, $J_{ortho}=8.4$ Hz, 1H, H₅-aromatic), 7.25-7.35 (m, 5H, Ph), 7.73 (d, $J_{meta}=2.0$ Hz, 1H, H₂-aromatic) and 7.79 (dd, $J_{ortho}=8.4$, $J_{meta}=2.0$ Hz, 1H, H₆-aromatic).

3.7.3 Ethyl *N*-[(3',4'-dimethoxybenzoyl)methyl]-*N*-benzyl-3-aminopropionate¹⁰⁹ (85):

A stirred mixture of ethyl *N*-benzyl-3-aminopropionate (2.55 g, 12.3 mmol), triethylamine (0.623 g, 6.15 mmol) and sodium iodide (0.092 g, 0.615 mmol) in anhydrous DMF (8 ml) was cooled in an ice bath. A solution of 3,4-dimethoxy- α -chloroacetophenone (1.32 g, 6.15 mmol) in anhydrous DMF (4 ml) was added dropwise to the cooled reaction mixture over a period of 15 min. The reaction was complete in 3 h. The turbid reaction mixture was filtered and evaporated under vacuum to give an oil. The ethyl *N*-[(3',4'-dimethoxybenzoyl)methyl]-*N*-benzyl-3-aminopropionate was isolated by flash chromatography eluting with ethyl acetate-hexane (1:1, R_f 0.43) to yield a colourless oil (2.0 g, 5.41 mmol, 88%) which was contaminated with some starting material (3,4-dimethoxy- α -chloroacetophenone). It was used in the next step without further purification.

¹H NMR (CDCl₃): δ 1.22 (t, $J_{\text{HH}}=7.1$ Hz, 3H, -CH₃), 2.52 (t, $J_{\text{HH}}=6.5$ Hz, 2H, -CH₂-CH₂-COO-), 3.08 (t, $J_{\text{HH}}=6.5$ Hz, 2H, -N-CH₂-CH₂-), 3.81 (s, 2H, -N-CH₂-Ph), 3.88 (s, 2H, -CO-CH₂-N-), 3.92 (s, 3H, -OCH₃), 3.94 (s, 3H, -OCH₃), 4.12 (q, $J_{\text{HH}}=7.1$ Hz, 2H, -COO-CH₂-), 6.82 (d, $J_{\text{ortho}}=8.0$ Hz, 1H, H₅-aromatic), 7.29-7.38 (m, 5H, aromatic) and 7.46-7.62 (m, 2H, aromatic).

NMR peaks for starting material (3,4-dimethoxy- α -chloroacetophenone):

¹H NMR (CDCl₃): δ 3.95 (s, 3H, -OCH₃), 3.97 (s, 3H, -OCH₃), 4.68 (s, 2H, -CH₂-Cl), 6.92 (d, $J_{\text{ortho}}=8.0$ Hz, 1H, H₅-aromatic), 7.46-7.62 (m, 2H, aromatic).

3.7.4 Ethyl *N*-{[3,4-(1',1',3',3'-tetra-*t*-butyldisiloxane)dioxybenzoyl]methyl}-*N*-benzyl-3-aminopropionate¹⁰⁹ (96):

A stirred mixture of ethyl *N*-benzyl-3-aminopropionate (0.349 g, 1.68 mmol), triethylamine (0.155 g, 0.22 ml, 1.53 mmol) and potassium iodide (0.03 g, 0.153 mmol) in anhydrous DMF (20 ml) was cooled in an ice bath. A solution of 3,4-(1',1',3',3'-tetra-*t*-butyldisiloxane)dioxy- α -chloroacetophenone (0.50 g, 1.53 mmol) in anhydrous DMF (10 ml) was added dropwise to the reaction mixture over a period of 30 min. The reaction was complete within 3 h. Dry ether was added to precipitate the triethylammonium hydrochloride which was removed by filtration. The filtrate was evaporated under vacuum to give an oil. Ethyl *N*-{[3,4-(1',1',3',3'-tetra-*t*-butyldisiloxane)dioxybenzoyl]methyl}-*N*-benzyl-3-aminopropionate was isolated by flash chromatography eluting with ethyl acetate-hexane (1:5, R_f 0.38) to yield a colourless oil (0.56 g, 0.81 mmol, 82%).

^1H NMR (CDCl_3): δ 1.10 [s, 36H, $(\text{CH}_3)_3\text{C-Si}$], 1.21 (t, $J_{\text{HH}}=7.1$ Hz, 3H, $-\text{CH}_3$), 2.52 (t, $J_{\text{HH}}=7.0$ Hz, 2H, $-\text{CH}_2\text{-COO-}$), 3.08 (t, $J_{\text{HH}}=7.0$ Hz, 2H, $-\text{N-CH}_2\text{-CH}_2\text{-}$), 3.83 (s, 2H, $-\text{N-CH}_2\text{-Ph}$), 3.89 (s, 2H, $-\text{CO-CH}_2\text{-N-}$), 4.08 (q, $J_{\text{HH}}=7.1$ Hz, 2H, $-\text{COO-CH}_2\text{-}$), 6.88 (d, $J_{\text{ortho}}=8.4$ Hz, 1H, $\text{H}_5\text{-aromatic}$), 7.21-7.33 (m, 5H, aromatic), 7.42 (dd, $J_{\text{ortho}}=8.4$, $J_{\text{meta}}=2.2$ Hz, 1H, $\text{H}_6\text{-aromatic}$) and 7.52 (d, $J_{\text{meta}}=2.2$ Hz, 1H, $\text{H}_2\text{-aromatic}$).

^{13}C NMR (CDCl_3): δ 14.1 ($-\text{CH}_3$), 21.3 [$(\text{CH}_3)_3\text{C-Si}$], 27.9 [$(\text{CH}_3)_3\text{C-Si}$], 33.2 ($-\text{CH}_2\text{-COO}$), 50.0 ($-\text{N-CH}_2\text{-CH}_2\text{-}$), 58.09 ($-\text{N-CH}_2\text{-Ph}$), 59.2 ($-\text{CO-CH}_2\text{-N-}$), 60.2 ($-\text{COO-CH}_2\text{-}$), 121.1, 121.4, 123.0, 127.0, 128.2, 128.9, 130.5, 138.8, 145.7, 150.5 (aromatic), 172.5 (COO), and 193.3 ($-\text{CO-CH}_2\text{-N-}$).

IR (neat): 1729 cm^{-1} (COO) and 1249 cm^{-1} (Si-O-C).

3.7.5 Ethyl *N*-[(3',4'-diphenylmethylenedioxy)benzoylmethyl]-*N*-benzyl-3-aminopropionate¹⁰⁹ (103, R= Et):

Ethyl *N*-benzyl-3-aminopropionate (1.54 g, 7.39 mmol), triethylamine (0.5 g, 0.7 ml, 4.93 mmol) and sodium iodide (0.07 g, 0.44 mmol) were stirred in 10 ml of anhydrous DMF in an ice bath. A solution of 3,4-diphenylmethylenedioxy- α -chloroacetophenone (1.73 g, 4.93 mmol) in 10 ml of anhydrous DMF was added dropwise to the reaction mixture over a period of 15 min. The reaction was complete within 3 hr. The reaction mixture was filtered and evaporated under vacuum to give an oil. The product, ethyl *N*-[(3',4'-diphenylmethylenedioxy)benzoylmethyl]-*N*-benzyl-3-aminopropionate was isolated by flash chromatography eluting with ethyl acetate-hexane (1:5, R_f 0.25) to yield a pale yellow colour oil (2.2 g, 4.22 mmol, 86%).

^1H NMR (CDCl_3): δ 1.15 (t, $J_{\text{HH}}=7.1$ Hz, 3H, $-\text{CH}_3$), 2.50 (t, $J_{\text{HH}}=7.0$ Hz, 2H, $-\text{CH}_2\text{-COO-}$), 3.03 (t, $J_{\text{HH}}=7.0$ Hz, 2H, $-\text{N-CH}_2\text{-CH}_2\text{-}$), 3.78 (s, 2H, $-\text{N-CH}_2\text{-Ph}$), 3.81 (s, 2H, $-\text{CO-CH}_2\text{-N-}$), 4.02 (q, $J_{\text{HH}}=7.1$ Hz, 2H, $-\text{COO-CH}_2\text{-}$), 6.84 (d, $J_{\text{ortho}}=8.0$ Hz, 1H, $\text{H}_5\text{-aromatic}$), and 7.2-7.6 (m, 17H, aromatic).

^{13}C NMR (CDCl_3): δ 14.1 ($-\text{CH}_3$), 33.2 ($-\text{CH}_2\text{-COO-}$), 50.1 ($-\text{N-CH}_2\text{-CH}_2\text{-}$), 58.1 ($-\text{N-CH}_2\text{-Ph}$), 59.4 ($-\text{CO-CH}_2\text{-N-}$), 60.3 ($-\text{COO-CH}_2\text{-}$), 117.9 [$(\text{Ph})_2\text{C-}$], 107.8, 108.2, 124.5, 126.1, 127.2, 128.2, 128.3, 129.1, 129.3, 130.7, 138.5, 139.5, 147.5, 151.2 (aromatic), 172.4 ($-\text{COO-}$) and 196.5 ($-\text{CO-CH}_2\text{-N-}$).

IR (Neat): 1730 cm^{-1} (C=O ester), 1680 cm^{-1} (C=O keto), 1493 and 1445 cm^{-1} (C=C), 1254 and 1208 cm^{-1} ($-\text{C-O-C}$).

3.7.6 Methyl *N*-[(3',4'-diphenylmethylenedioxy)benzoylmethyl]-*N*-benzyl-3-aminopropionate¹⁰⁹ (**103**, R= Me):

A mixture of methyl *N*-benzyl-3-aminopropionate (1.21 g, 6.27 mmol), triethylamine (0.58 g, 0.8 ml, 5.7 mmol) and sodium iodide (0.08 g, 0.57 mmol) in anhydrous DMF (20 ml) was stirred and cooled in an ice bath. A solution of 3,4-diphenylmethylenedioxy- α -chloroacetophenone (2.00 g, 5.7 mmol) in anhydrous DMF (10 ml) was added dropwise to the reaction mixture over a period of 15 min. The reaction mixture was complete within 3 hr. The reaction was filtered and evaporated under vacuum to give an oil. Methyl *N*-[(3',4'-diphenylmethylenedioxy)benzoylmethyl]-*N*-benzyl-3-aminopropionate was isolated by flash chromatography eluting with ethyl acetate-hexane (1:5, R_f 0.25) to yield a pale yellow oil (2.4 g, 4.73 mmol, 83%).

¹H NMR (CDCl₃): δ 2.52 (t, $J_{HH}=7.0$ Hz, 2H, -CH₂-COO-), 3.10 (t, $J_{HH}=7.0$ Hz, 2H, -N-CH₂-CH₂-), 3.78 (s, 2H, -N-CH₂-Ph), 3.80 (s, 2H, -CO-CH₂-N-), 3.62 (s, 3H, -COOCH₃), 6.86 (d, $J_{ortho}=8.0$ Hz, 1H, H₅-aromatic), and 7.2-7.8 (m, 17H, aromatic).

¹³C NMR (CDCl₃): δ 33.2 (-CH₂-COO-), 50.2 (-N-CH₂-CH₂-), 51.8 (-COOCH₃), 58.1 (-N-CH₂-Ph), 59.4 (-CO-CH₂-N-), 117.9 [(Ph)₂C-], 107.8, 108.2, 124.5, 126.1, 127.2, 128.2, 128.3, 129.1, 129.3, 130.7, 138.5, 139.5, 147.5, 151.2 (aromatic), 172.4 (-COO-) and 196.5 (-CO-CH₂-N-).

IR (neat): 1731 cm⁻¹ (-COO-), 1678 cm⁻¹ (C=O), 1495 and 1448 cm⁻¹ (C=C), 1254 and 1212 cm⁻¹ (-C-O-C).

3.7.7 Propyl *N*-[(3',4'-diphenylmethylenedioxy)benzoylmethyl]-*N*-benzyl-3-aminopropionate¹⁰⁹ (**103**, R= n-Pr):

A mixture of propyl *N*-benzyl-3-aminopropionate (2.44 g, 11.0 mmol), triethylamine (1.01 g, 1.4 ml, 10.0 mmol) and potassium iodide (0.17 g, 1.0 mmol) in anhydrous DMF (25 ml) was stirred and cooled in an ice bath. A solution of 3,4-diphenylmethylenedioxy- α -chloroacetophenone (3.51 g, 10.0 mmol) in anhydrous DMF (10 ml) and was added dropwise to the reaction mixture over a period of 30 min. The reaction was complete within 3 hr. Dry ether was added to precipitate the triethylammonium hydrochloride, which was then removed by filtration. The filtrate was evaporated under vacuum to give an oil. Propyl *N*-[(3',4'-diphenylmethylenedioxy)benzoylmethyl]-*N*-benzyl-3-aminopropionate was isolated by flash chromatography eluting with ethyl acetate-hexane (1:5, R_f 0.25) to yield a pale yellow oil (4.19 g, 7.82 mmol, 78%).

^1H NMR (CDCl_3): δ 0.79 (t, $J_{\text{HH}}=7.0$ Hz, 3H, $-\text{CH}_3$), 1.48 (sextet, 2H, $J_{\text{HH}}=7.0$ Hz, 2H, $-\text{CH}_2-\text{CH}_3$), 2.44 (t, $J_{\text{HH}}=7.0$ Hz, 2H, $-\text{CH}_2-\text{COO}-$), 2.97 (t, $J_{\text{HH}}=7.0$ Hz, 2H, $-\text{N}-\text{CH}_2-\text{CH}_2-$), 3.71 (s, 2H, $-\text{N}-\text{CH}_2-\text{Ph}$), 3.74 (s, 2H, $-\text{CO}-\text{CH}_2-\text{N}-$), 3.87 (t, $J_{\text{HH}}=6.8$ Hz, 2H, $-\text{COO}-\text{CH}_2-$), 6.76 (d, $J_{\text{ortho}}=8.1$ Hz, 1H, H_5 -aromatic) and 7.16-7.49 (m, 17H, aromatic).

^{13}C NMR (CDCl_3): δ 10.3 ($-\text{CH}_3$), 21.8 ($-\text{CH}_2-\text{CH}_3$), 33.2 ($-\text{CH}_2-\text{COO}-$), 50.1 ($-\text{N}-\text{CH}_2-\text{CH}_2-$), 58.1 ($-\text{N}-\text{CH}_2-\text{Ph}$), 59.3 ($-\text{CO}-\text{CH}_2-\text{N}-$), 65.9 ($-\text{COO}-\text{CH}_2-$), 117.9 [$(\text{Ph})_2\text{C}-$], 107.8, 108.2, 124.5, 126.1, 127.1, 128.2, 128.3, 129.0, 129.3, 130.7, 138.5, 139.5, 147.5, 151.1 (aromatic), 172.5 ($-\text{COO}-$) and 196.3 ($-\text{CO}-\text{CH}_2-\text{N}-$).

IR (Neat): 1732 cm^{-1} ($\text{C}=\text{O}$ ester), 1676 cm^{-1} ($\text{C}=\text{O}$ keto), 1493 and 1448 cm^{-1} ($\text{C}=\text{C}$) and 1254 cm^{-1} ($-\text{C}-\text{O}-\text{C}$).

3.7.8 Butyl *N*-[(3',4'-diphenylmethylenedioxy)benzoylmethyl]-*N*-benzyl-3-aminopropionate¹⁰⁹ (**103**, R= n-Bu):

Butyl *N*-benzyl-3-aminopropionate (3.69 g, 15.7 mmol), triethylamine (1.44 g, 2.0 ml, 14.3 mmol) and potassium iodide (0.237 g, 1.43 mmol) were stirred in 50 ml of anhydrous DMF in an ice bath. A solution of 3,4-diphenylmethylenedioxy- α -chloroacetophenone (5.0 g, 14.3 mmol) in anhydrous DMF (25 ml) and was added dropwise to the reaction mixture over a period of 30 min. The reaction was complete within 3 hr. Dry ether was added to precipitate the triethylammonium hydrochloride, which was then removed by filtration. The filtrate was evaporated under vacuum to give an oil. Butyl *N*-[(3',4'-diphenylmethylenedioxy)benzoylmethyl]-*N*-benzyl-3-aminopropionate was isolated by flash chromatography eluting with ethyl acetate-hexane (1:5, R_f 0.26) to yield a pale yellow oil (6.0 g, 10.9 mmol, 76%).

^1H NMR (CDCl_3): δ 0.90 (t, $J_{\text{HH}}=7.3$ Hz, 3H, $-\text{CH}_3$), 1.32 (appears as a sextet with an average $J_{\text{HH}}=7.4$ Hz, 2H, $-\text{CH}_2-\text{CH}_3$), 1.54 (appears as a pentet with an average, $J_{\text{HH}}=7.1$ Hz, 2H, $-\text{CH}_2-\text{CH}_2-\text{CH}_3$), 2.52 (t, $J_{\text{HH}}=7.0$ Hz, 2H, $-\text{CH}_2-\text{COO}-$), 3.06 (t, $J_{\text{HH}}=7.0$ Hz, 2H, $-\text{N}-\text{CH}_2-\text{CH}_2-$), 3.80 (s, 2H, $-\text{N}-\text{CH}_2-\text{Ph}$), 3.83 (s, 2H, $-\text{CO}-\text{CH}_2-\text{N}-$), 4.00 (t, $J_{\text{HH}}=6.7$ Hz, 2H, $-\text{COO}-\text{CH}_2-$), 6.85 (d, $J_{\text{ortho}}=8.1$ Hz, 1H, H_5 -aromatic) and 7.23-7.59 (m, 17H, aromatic).

^{13}C NMR (CDCl_3): δ 13.6 ($-\text{CH}_3$), 19.0 ($-\text{CH}_2-\text{CH}_3$), 30.5 ($-\text{CH}_2-\text{CH}_2-\text{CH}_3$), 33.2 ($-\text{CH}_2-\text{COO}-$), 50.1 ($-\text{N}-\text{CH}_2-\text{CH}_2-$), 58.0 ($-\text{N}-\text{CH}_2-\text{Ph}$), 59.3 ($-\text{CO}-\text{CH}_2-\text{N}-$), 64.2 ($-\text{COO}-\text{CH}_2-$), 117.9 [$(\text{Ph})_2\text{C}-$], 107.8, 108.2, 124.5, 126.1, 127.1, 128.2, 128.3, 129.0, 129.3, 130.7, 138.6, 139.5, 147.5, 151.1 (aromatic), 172.5 ($-\text{COO}-$) and 196.5 ($-\text{CO}-\text{CH}_2-\text{N}-$).

IR (neat): 1732 cm^{-1} ($\text{C}=\text{O}$ ester), 1676 cm^{-1} ($\text{C}=\text{O}$ keto), 1493 and 1446 cm^{-1} ($\text{C}=\text{C}$) and 1254 cm^{-1} ($-\text{C}-\text{O}-\text{C}$).

3.7.9 Ethyl *N*-[(3',4'-dipivaloyloxybenzoyl)methyl]-*N*-benzyl-3-aminopropionate¹⁰⁹ (114):

Ethyl *N*-benzyl-3-aminopropionate (1.93 g, 9.30 mmol), triethylamine (0.855 g, 1.2 ml, 8.45 mmol) and sodium iodide (0.127 g, 0.845 mmol) were stirred in 20 ml of anhydrous DMF in an ice bath. A solution of 3,4-dipivaloyloxy- α -chloroacetophenone (3.0 g, 8.45 mmol) in anhydrous DMF (50 ml) and was added dropwise to the reaction mixture over a period of 30 min. After 3 h, the triethylamine hydrochloride was removed by filtration. Evaporation of the filtrate under vacuum to gave an oil, which was purified by flash chromatography eluting with ethyl acetate-hexane (1:5, R_f 0.28) to give ethyl *N*-[(3',4'-dipivaloyloxybenzoyl)methyl]-*N*-benzyl-3-aminopropionate as a pale yellow oil (3.13 g, 5.96 mmol, 70%).

¹H NMR (CDCl₃): δ 1.21 (t, $J_{HH}=7.1$ Hz, 3H, -CH₃), 1.34 (s, 9H, Bu^tCOO), 1.36 (s, 9H, Bu^tCOO), 2.52 (t, $J_{HH}=7.0$ Hz, 2H, -CH₂-COO-), 3.05 (t, $J_{HH}=7.0$ Hz, 2H, -N-CH₂-CH₂-), 3.80 (s, 2H, -N-CH₂-Ph), 3.87 (s, 2H, -CO-CH₂-N-), 4.07 (q, $J_{HH}=7.1$ Hz, 2H, -COO-CH₂-), 7.17 (d, $J_{ortho}=8.4$ Hz, 1H, H₅-aromatic), 7.20-7.39 (m, 5H, Ph-), 7.69 (d, $J_{meta}=1.9$ Hz, 1H, H₂-aromatic) and 7.75 (dd, $J_{ortho}=8.4$, $J_{meta}=2.0$ Hz, 1H, H₆-aromatic).

¹³C NMR (CDCl₃): δ 14.1 (-CH₃), 27.1 [-C(CH₃)₃], 27.2 [-C(CH₃)₃], 33.2 (-CH₂-COO), 39.15 [-C(CH₃)₃], 39.25 [-C(CH₃)₃], 50.2 (-N-CH₂-CH₂-), 58.2 (-N-CH₂-Ph), 59.6 (-CO-CH₂-N-), 60.4 (-COO-CH₂-), 123.4, 123.6, 126.5, 127.3, 128.4, 129.1 (aromatic CH), 134.1, 138.4, 142.6, 146.7 (aromatic C), 172.5 (CH₂COO), 175.4 (Bu^tCOO), 175.6 (Bu^tCOO) and 196.6 (-CO-CH₂-N-).

IR (neat): 1763 cm⁻¹ (C=O ester), 1734 cm⁻¹ (C=O ester), 1689 (C=O keto), 1604 and 1481 cm⁻¹ (C=C), 1255 and 1101 cm⁻¹ (C-O-C).

3.8 SYNTHESIS OF ALKYL *N*-[(2'-HYDROXY-2'-(SUBSTITUTED) PHENYLETHYL)]-*N*-BENZYL-3-AMINOPROPIONATE

3.8.1 Ethyl *N*-(2'-hydroxy-2'-phenylethyl)-*N*-benzyl-3-aminopropionate¹⁰⁹ (66, R= Et):

To a stirred solution of ethyl *N*-(benzoylmethyl)-*N*-benzyl-3-aminopropionate (6.0 g, 18.4 mmol) in ethanol (80 ml), was added sodium borohydride (1.80 g, 46.0 mmol) in small portions over a period of 15 min. The resulting suspension was stirred at room temperature for a further 1 hr, after which time the reaction mixture was evaporated under vacuum to dryness. Water was added and the mixture was extracted with dichloromethane. The lower organic layer was dried with molecular sieves and evaporated under vacuum to give an oil (5.0 g). Ethyl *N*-(2'-hydroxy-2'-phenylethyl)-*N*-benzyl-3-aminopropionate was isolated by flash chromatography eluting with ethyl acetate (R_f 0.60) to yield a colourless oil (4.50 g, 13.75 mmol, 75%).

¹H NMR (CDCl₃): δ 1.23 (t, $J_{HH}=7.1$ Hz, -CH₃), 2.40-2.59 [m, 3H, -C(OH)H-CH_AH_B-N-CH₂-CH₂-], 2.64 [dd, $J_{gem}=13.0$, $J_{HH}=3.9$ Hz, 1H, -C(OH)-CH_AH_B-N-], 2.76 (dt, $J_{gem}=13.1$, $J_{HH}=6.5$ Hz, 1H, -N-CH_AH_B-CH₂-), 3.05 (dt, $J_{gem}=13.2$, $J_{HH}=7.4$ Hz, 1H, -N-CH_AH_B-CH₂-), 3.50 (d, $J_{gem}=13.5$ Hz, 1H, -N-CH_AH_B-Ph), 3.86 (d, $J_{gem}=13.5$ Hz, 1H, -N-CH_AH_B-Ph), 4.07 (dq, $J_{gem}=10.8$, $J_{HH}=7.1$ Hz, 1H, -COO-CH_AH_B-), 4.17 (dq, $J_{gem}=10.8$, $J_{HH}=7.1$ Hz, 1H, -COO-CH_AH_B-), 4.67 [dd, $J_{gem}=9.7$, $J_{HH}=3.8$ Hz, 1H, -C(OH)-H], 7.18-7.35 (m, 10H, aromatic) (By integration -OH is between 3.70-4.0).

¹H NMR (MeOH-d₄): δ 1.21 (t, $J_{HH}=7.2$ Hz, -CH₃), 2.48 (dt, $J_{HH}=6.6$, $J_{HH}=2.0$ Hz, 2H, -CH₂-COO), 2.63 [s, 1H, -C(OH)H-CH_AH_B-N-], 2.65 [d, $J_{HH}=1.7$ Hz, 1H, -C(OH)H-CH_AH_B-N-), 2.80 (dt, $J_{gem}=13.0$, $J_{HH}=6.3$ Hz, 1H, -N-CH_AH_B-CH₂-), 2.95 (dt, $J_{gem}=13.2$, $J_{HH}=7.1$ Hz, 1H, -N-CH_AH_B-CH₂-), 3.59 (d, $J_{HH}=13.5$ Hz, 1H, -N-CH_AH_B-Ph), 3.73 (d, $J_{HH}=13.5$ Hz, 1H, -N-CH_AH_B-Ph), 4.08 (q, $J_{HH}=1.97$, $J_{HH}=7.2$ Hz, 1H, -COO-CH_AH_B-), 4.09 (q, $J_{HH}=1.97$, $J_{HH}=7.2$ Hz, 1H, -COO-CH_AH_B-), 4.69 [dd, $J_{HH}=5.9$ and 7.2 Hz, 1H, -C(OH)-H] and 7.21-7.37 (m, 10H, aromatic).

¹³C NMR (CDCl₃): δ 14.1 (-CH₃), 32.8 (-CH₂-COO-), 49.6 (-N-CH₂-CH₂-), 58.6 (-N-CH₂-Ph), 60.6 (-COO-CH₂-), 62.8 (-HOCH-CH₂-N-), 69.9 [-C(OH)-H], 125.8, 126.1, 127.3, 128.2, 128.4, 129.0, 129.3 (aromatic C-H), 138.2 142.0 (aromatic C) and 172.5 (-COO-).

IR (neat): 3471 cm⁻¹ (OH), 1730 cm⁻¹ (COO) and 1452 cm⁻¹ (C=C).

3.8.2 Ethyl *N*-[2'-(3'',4''-dimethoxyphenyl)-2'-hydroxyethyl]-*N*-benzyl-3-aminopropionate¹⁰⁹ (**86**):

To a stirred solution of ethyl *N*-[(3',4'-dimethoxybenzoyl)methyl]-*N*-benzyl-3-aminopropionate (2.00 g, 5.42 mmol) in ethanol (30 ml), was added sodium borohydride (0.512 g, 13.6 mmol) in small portions over a period of 10 min. The resulting suspension was stirred at room temperature for 1 hr, after which time the reaction mixture was evaporated under vacuum to dryness. The residue was shaken with water and extracted with dichloromethane. The dichloromethane layer was dried with molecular sieves and evaporated under vacuum to yield an oil (1.5 g). The ethyl *N*-[2'-(3'',4''-dimethoxyphenyl)-2'-hydroxyethyl]-*N*-benzyl-3-aminopropionate (**86**) was isolated by flash chromatography with ethyl acetate-hexane (1:1, R_f 0.40) to yield a thick colourless oil (1.20 g, 3.23 mmol, 67.5%). Some 3,4-dimethoxy- α -chloroacetophenone was present in the starting material, which gives rise to 1-(3',4'-dimethoxyphenyl)-2-chloroethanol as an impurity in the product (**86**). These could not be separated by flash chromatography, therefore mixture was used in the next step without further purification.

¹H NMR (CDCl₃): δ 1.25 (t, $J_{HH}=7.14$ Hz, 3H, -CH₃), 2.49-2.65 [m, 4H, -C(OH)-CH₂-N-CH₂-CH₂-], 2.78 (dt, $J_{gem}=13.2$, $J_{HH}=6.1$ Hz, 1H, -N-CH_AH_B-CH₂-), 3.05 (dt, $J_{gem}=13.2$, $J_{HH}=7.4$ Hz, 1H, -N-CH_AH_B-CH₂-), 3.50 (d, $J_{gem}=13.5$ Hz, 1H, -N-CH_AH_B-Ph), 3.65 (d, $J_{gem}=13.5$ Hz, 1H, -N-CH_AH_B-Ph), 3.86 (s, 3H, -OCH₃), 3.87 (s, 3H, -OCH₃), 3.8-4.1 (broad s, 1H, -OH), 4.08 (dq, $J_{gem}=10.8$, $J_{HH}=7.2$ Hz, 1H, -COO-CH_AH_B-), 4.16 (dq, $J_{gem}=10.8$, $J_{HH}=7.2$ Hz, 1H, -COO-CH_AH_B-), 4.82 [dd, $J_{HH}=4.0$, $J_{HH}=8.3$ Hz, 1H, -C(OH)-H], 6.80-6.90 (m, 3H, aromatic) and 7.24-7.37 (m, 5H, aromatic).

For 1-(3',4'-dimethoxyphenyl)-2-chloroethanol

¹H NMR (CDCl₃): δ 3.49-3.72 [m, 2H, -C(OH)-CH₂-Cl], 3.84 (s, 6H, -OCH₃), 4.62 [dd, $J_{HH}=4.3$ and 9.1 Hz, 1H, -C(OH)-H], 6.80-7.37 (m, 3H, aromatic).

3.8.3 Ethyl *N*-{2'-[3'',4''-(1''',1''',3''',3'''-tetra-*t*-butyldisiloxane)dioxyphenyl]-2'-hydroxyethyl}-*N*-benzyl-3-aminopropionate¹⁰⁹ (**97**):

To a stirred solution of ethyl *N*-{[3,4-(1',1',3',3'-tetra-*t*-butyldisiloxane)dioxybenzoyl]methyl}-*N*-benzyl-3-aminopropionate (0.56 g, 0.81 mmol) in 25 ml of ethanol, was added sodium borohydride (0.076 g, 2.0 mmol) in small portions over a period of 10 min. The resulting suspension was stirred at room temperature for a further 1 hr, after which time the reaction mixture was evaporated under vacuum. Water was added to the residue and the product was extracted with dichloromethane. The dichloromethane layer was dried with molecular sieves and evaporated to yield an oil (0.55 g). The product (**97**) was purified by flash chromatography eluting with ethyl acetate-hexane (1:5, R_f 0.35) to yield a colourless oil (0.27 g, 0.39 mmol, 48%).

^1H NMR (CDCl_3): δ 1.08 [s, 18H, $(\text{CH}_3)_3\text{C-Si}$], 1.09 [s, 18H, $(\text{CH}_3)_3\text{C-Si}$], 1.24 (t, $J_{\text{HH}}=7.1$ Hz, 3H, $-\text{CH}_3$), 2.49-2.58 [m, 3H, $-\text{C}(\text{OH})-\text{CH}_2\text{H}_B\text{-N-}$, $-\text{CH}_2\text{-COO-}$], 2.66 [dd, $J_{\text{gem}}=13.5$, $J_{\text{HH}}=3.7$ Hz, 1H, $-\text{C}(\text{OH})-\text{CH}_2\text{H}_A\text{-N-}$], 2.80 (dt, $J_{\text{gem}}=13.2$, $J_{\text{HH}}=6.1$ Hz, 1H, $-\text{N-CH}_2\text{H}_A\text{-CH}_2\text{-}$), 3.05 (dt, $J_{\text{gem}}=13.2$, $J_{\text{HH}}=7.2$ Hz, 1H, $-\text{N-CH}_2\text{H}_B\text{-CH}_2\text{-}$), 3.54 (d, $J_{\text{gem}}=13.6$ Hz, $-\text{N-CH}_2\text{H}_A\text{-Ph}$), 3.86 (d, $J_{\text{gem}}=13.6$ Hz, $-\text{N-CH}_2\text{H}_B\text{-Ph}$), 3.91 (broad s, 1H, OH), 4.11 (dq, $J_{\text{gem}}=10.7$, $J_{\text{HH}}=7.1$ Hz, 1H, $-\text{COO-CH}_2\text{H}_A\text{-}$), 4.15 (dq, $J_{\text{gem}}=10.7$, $J_{\text{HH}}=7.1$ Hz, 1H, $-\text{COO-CH}_2\text{H}_B\text{-}$), 4.59 [dd, 1H, $J_{\text{gem}}=9.5$, $J_{\text{HH}}=3.7$ Hz, $-\text{C}(\text{OH})-\text{H}$], 6.74 (dd, $J_{\text{ortho}}=8.2$ Hz, $J_{\text{meta}}=1.9$, 1H, $\text{H}_6\text{-aromatic}$), 6.82 (d, $J_{\text{ortho}}=8.2$ Hz, 1H, $\text{H}_5\text{-aromatic}$), 6.85 (d, $J_{\text{meta}}=1.8$ Hz, 1H, $\text{H}_2\text{-aromatic}$) and 7.26-7.37 (m, 5H, aromatic).

^{13}C NMR (CDCl_3): δ 14.1 ($-\text{CH}_3$), 21.3 [$(\text{CH}_3)_3\text{C-Si}$], 28.0 [$(\text{CH}_3)_3\text{C-Si}$], 32.7 ($-\text{CH}_2\text{-COO}$), 49.6 ($-\text{N-CH}_2\text{-CH}_2\text{-}$), 58.6 ($-\text{N-CH}_2\text{-Ph}$), 60.6 ($-\text{COO-CH}_2\text{-}$), 62.7 ($\text{HOCH-CH}_2\text{-N-}$), 69.3 [$-\text{C}(\text{OH})\text{H-}$], 118.9, 119.3, 121.0, 127.3, 128.4, 128.9, 135.6, 144.9, 145.5 (aromatic C), 172.5 (C=O).

IR (neat): 3400 cm^{-1} (OH), 1727 cm^{-1} (COO), 1504 cm^{-1} (C=C), 1311 cm^{-1} (Si-O-Si) and 973 cm^{-1} (Si-O-C).

Elemental analysis: calculated for $\text{C}_{35}\text{H}_{54}\text{NO}_6\text{Si}_2$: C, 65.71; H, 9.04; N, 2.13%. Found: C, 64.96; H, 8.72; N, 2.23%.

Mass spectrum (CI-NH_3): 658.0 ($\text{M} + \text{NH}_4^+$, 70%). m/e 640 [$(\text{M} + \text{NH}_4^+) - \text{OH}$, 10%], 612 [$(\text{M} + \text{NH}_4^+) - \text{OEt}$, 2%], 437 [$(\text{M} + \text{NH}_4^+) - \text{CH}_2\text{-N}^+\text{H}_2\text{-CH}_2\text{-CH}_2\text{-COOC}_2\text{H}_5$, 24%], 220 ($\text{Ph-HC=CH-N}^+\text{H}_2\text{-CH}_2\text{-CH}_2\text{-COOC}_2\text{H}_5$, 100%), and 91 (tropolium ion, 24%) (Section 2.4, Scheme 2.9).

3.8.4 Methyl *N*-[2'-(3'',4''-diphenylmethylenedioxyphenyl)-2'-hydroxyethyl]-*N*-benzyl-3-aminopropionate¹⁰⁹ (**104**, R= Me):

To a stirred solution of methyl *N*-[(3',4'-diphenylmethylenedioxy)benzoylmethyl]-*N*-benzyl-3-aminopropionate (5.0 g, 9.85 mmol) in 50 ml of methanol, was added sodium borohydride (0.93 g, 24.63 mmol) in small portions over a period of 10 min. The resulting suspension was stirred at room temperature for a further 1 hr, and the reaction mixture was evaporated under vacuum. Water was added to the residue and extracted with dichloromethane. The dichloromethane layer was dried with molecular sieves and evaporated to yield an oil (4.05 g). The title compound (**104**, R=Me) was purified by flash chromatography eluting with ethyl acetate-hexane (1:5, R_f 0.24) to yield a colourless oil (3.91 g, 7.67 mmol, 78%).

^1H NMR (CDCl_3): δ 2.47-2.65 [m, 4H, $-\text{C}(\text{OH})-\text{CH}_2-\text{N}-\text{CH}_2-\text{CH}_2-$], 2.78 (dt, $J_{\text{gem}}=13.0$, $J_{\text{HH}}=6.5$ Hz, $-\text{N}-\text{CH}_A\text{H}_B-\text{CH}_2-$), 3.06 (dt, $J_{\text{gem}}=13.2$, $J_{\text{HH}}=7.5$ Hz, $-\text{N}-\text{CH}_A\text{H}_B-\text{CH}_2-$), 3.52 (d, $J_{\text{gem}}=13.5$ Hz, 1H, $-\text{N}-\text{CH}_A\text{H}_B-\text{Ph}$), 3.69 (s, 3H, $-\text{OCH}_3$), 3.87 (d, $J_{\text{gem}}=13.6$ Hz, 1H, $-\text{N}-\text{CH}_A\text{H}_B-\text{Ph}$), 3.92 (broad s, 1H, $-\text{OH}$), 4.61 [dd, $J_{\text{HH}}=4.5$, $J_{\text{HH}}=8.9$ Hz, 1H, $-\text{C}(\text{OH})-\text{H}$], 6.78 (dd, $J_{\text{ortho}}=8.0$, $J_{\text{meta}}=1.4$ Hz, 1H, H_6 -aromatic), 6.84 (d, $J_{\text{ortho}}=7.9$ Hz, 1H, H_5 -aromatic), 6.93 (d, $J_{\text{meta}}=1.3$ Hz, 1H, H_2 -aromatic), 7.25-7.43 (m, 11H, aromatic) and 7.57-7.64 (m, 4H, aromatic).

^{13}C NMR (CDCl_3): δ 32.6 ($-\text{CH}_2-\text{COO}-$), 49.5 ($-\text{N}-\text{CH}_2-\text{CH}_2-$), 51.7 ($-\text{OCH}_3$), 58.6 ($-\text{N}-\text{CH}_2-\text{Ph}$), 62.7 [$-\text{C}(\text{OH})-\text{CH}_2-\text{N}$], 69.8 [$-\text{C}(\text{OH})-\text{H}$], 106.6, 108.0, 116.6, 119.4, 126.3, 127.4, 128.2, 128.4, 128.96, 129.0, 135.9, 138.1, 140.3, 146.5, 147.2 (aromatic) and 172.9 ($-\text{COO}-$).

3.8.5 Ethyl *N*-[2'-(3",4"-diphenylmethylenedioxyphenyl)-2'-hydroxyethyl]-*N*-benzyl-3-aminopropionate¹⁰⁹ (**104**, R= Et):

To the stirred solution of ethyl *N*-[(3',4'-diphenylmethylenedioxy)benzoylmethyl]-*N*-benzyl-3-aminopropionate (2.20 g, 4.22 mmol) in 25 ml of ethanol, was added sodium borohydride (0.40 g, 10.5 mmol) in small portions over a period of 10 min. The resulting suspension was stirred at room temperature for a further one h, and the reaction mixture was evaporated under vacuum. Water was added to the residue and extracted with dichloromethane. The dichloromethane layer was dried with molecular sieves and evaporated to yield an oil. The title compound (**104**, R=Et) was purified by flash chromatography eluting with ethyl acetate-hexane (1:5, R_f 0.23) to yield a colourless oil (1.75 g, 3.34 mmol, 79%).

^1H NMR (CDCl_3): δ 1.24 (t, $J_{\text{HH}}=7.1$ Hz, 3H, $-\text{CH}_3$), 2.44-2.61 [m, 4H, $-\text{C}(\text{OH})-\text{CH}_2-\text{N}-\text{CH}_2-\text{CH}_2-$], 2.75 (dt, $J_{\text{gem}}=13.0$, $J_{\text{HH}}=6.3$, 1H, $-\text{N}-\text{CH}_A\text{H}_B-\text{CH}_2-$), 3.05 (dt, $J_{\text{gem}}=13.2$, $J_{\text{HH}}=7.5$ Hz, $-\text{N}-\text{CH}_A\text{H}_B-\text{CH}_2-$), 3.50 (d, $J_{\text{gem}}=13.5$ Hz, 1H, $-\text{N}-\text{CH}_A\text{H}_B-\text{Ph}$), 3.85 (d, $J_{\text{gem}}=13.5$ Hz, 1H, $-\text{N}-\text{CH}_A\text{H}_B-\text{Ph}$), 3.90 (broad s, 1H, $-\text{OH}$), 4.10 (dq, $J_{\text{gem}}=10.85$, $J_{\text{HH}}=7.1$ Hz, 1H, $-\text{COO}-\text{CH}_A\text{H}_B-$), 4.15 (dq, $J_{\text{gem}}=10.85$, $J_{\text{HH}}=7.15$ Hz, 1H, $-\text{COO}-\text{CH}_A\text{H}_B-$), 4.57 [dd, $J_{\text{HH}}=4.5$, $J_{\text{HH}}=8.9$ Hz, 1H, $-\text{C}(\text{OH})-\text{H}$], 6.73 (dd, $J_{\text{ortho}}=8.0$, $J_{\text{meta}}=1.4$ Hz, 1H, H_6 -aromatic), 6.79 (d, $J_{\text{ortho}}=7.9$ Hz, 1H, H_5 -aromatic), 6.87 (d, $J_{\text{meta}}=1.3$ Hz, 1H, H_2 -aromatic), 7.25-7.4 (m, 11H, Ph) and 7.52-7.58 (m, 4H, Ph).

^{13}C NMR (CDCl_3): δ 14.1 ($-\text{CH}_3$), 32.7 ($-\text{CH}_2-\text{COO}-$), 49.5 ($-\text{N}-\text{CH}_2-\text{CH}_2-$), 58.5 ($-\text{N}-\text{CH}_2-\text{Ph}$), 60.6 ($-\text{COO}-\text{CH}_2-$), 62.6 [$-\text{C}(\text{OH})-\text{CH}_2-\text{N}$], 69.7 [$-\text{C}(\text{OH})-\text{H}$], 116.6 [(Ph) $_2\text{C}$], 106.5, 108.0, 119.3, 126.2, 127.3, 128.1, 128.4, 128.9 (aromatic C-H), 135.8, 138.1, 140.2, 146.4, 147.2 (aromatic C) and 172.5 ($-\text{COO}-$).

IR (neat): 3466 cm^{-1} (broad, -OH), 1728 cm^{-1} (-COO-), 1494 and 1448 (C=C), 1250 and 1209 cm^{-1} (C-O-C).

3.8.6 Propyl *N*-[2'-(3",4"-diphenylmethylenedioxyphenyl)-2'-hydroxyethyl]-*N*-benzyl-3-aminopropionate¹⁰⁹ (**104**, R= n-Pr):

To the stirred solution of propyl *N*-[(3',4'-diphenylmethylenedioxy)benzoylmethyl]-*N*-benzyl-3-amino propionate (2.36 g, 4.41 mmol) in 40 ml of n-propanol, was added sodium borohydride (0.417 g, 11.0 mmol) in small portions over a period of 10 min. The resulting suspension was stirred at room temperature for a further one h, and the reaction mixture was evaporated under vacuum. Water was added to the residue and extracted with dichloromethane. The dichloromethane layer was dried with molecular sieves and evaporated to yield an oil (1.82 g). Compound (**104**, R=n-Pr) was purified by flash chromatography eluting with ethyl acetate-hexane (1:5, R_f 0.23) to yield a colourless oil (1.57 g, 2.92 mmol, 67%).

¹H NMR (CDCl_3): δ 0.84 (t, $J_{\text{HH}}=7.5$ Hz, 3H, -CH₃), 1.55 (sextet, $J_{\text{HH}}=7.2$ Hz, 3H, -CH₂-CH₃), 2.39-2.54 [m, 4H, -C(OH)-CH₂-N-CH₂-CH₂-], 2.68 (dt, $J_{\text{gem}}=13.1$, $J_{\text{HH}}=6.3$ Hz, -N-CH_AH_B-CH₂-), 2.95 (dt, $J_{\text{gem}}=13.2$, $J_{\text{HH}}=7.4$ Hz, -N-CH_AH_B-CH₂-), 3.42 (d, $J_{\text{gem}}=13.5$ Hz, 1H, -N-CH_AH_B-Ph), 3.77 (d, $J_{\text{gem}}=13.5$ Hz, 1H, -N-CH_AH_B-Ph), 3.70-3.96 (broad s, 1H, -OH), 3.91 (dq, $J_{\text{gem}}=10.7$, $J_{\text{HH}}=6.7$ Hz, 1H, -COO-CH_AH_B-), 4.00 (dq, $J_{\text{gem}}=10.7$, $J_{\text{HH}}=6.8$ Hz, 1H, -COO-CH_AH_B-), 4.49 [dd, $J_{\text{HH}}=9.1$, $J_{\text{HH}}=4.3$ Hz, 1H, -C(OH)-H], 6.65 (dd, $J_{\text{ortho}}=8.0$, $J_{\text{meta}}=1.4$ Hz, 1H, H₆-aromatic), 6.72 (d, $J_{\text{ortho}}=7.9$ Hz, 1H, H₅-aromatic), 6.79 (d, $J_{\text{meta}}=1.4$ Hz, 1H, H₂-aromatic), 7.16-7.32 (m, 11H, aromatic), and 7.46-7.51 (m, 4H, aromatic).

IR (neat): 3454 cm^{-1} (broad, -OH), 1734 cm^{-1} (-COO-), 1493 and 1443 (C=C), 1252 and 1209 cm^{-1} (C-O-C).

3.8.7 Butyl *N*-[2'-(3",4"-diphenylmethylenedioxyphenyl)-2'-hydroxyethyl]-*N*-benzyl-3-aminopropionate¹⁰⁹ (**104**, R= n-Bu):

To the stirred solution of butyl *N*-[(3',4'-diphenylmethylenedioxy)benzoylmethyl]-*N*-benzyl-3-amino propionate (5.0 g, 9.1 mmol) in 50 ml of n-butanol, was added sodium borohydride (0.86 g, 22.74 mmol) in small portions over a period of 10 min. The resulting suspension was stirred at room temperature for a further one h, and the reaction mixture was evaporated under vacuum. Water was added to the residue and extracted with dichloromethane. The dichloromethane layer was dried with molecular sieves and evaporated to yield an oil (3.96 g). Compound (**104**, R=n-Bu) was purified by flash chromatography eluting with ethyl acetate-hexane (1:5, R_f 0.25) to yield a colourless oil (3.77 g, 8.7 mmol, 75%).

^1H NMR (CDCl_3): δ 0.90 (t, $J_{\text{HH}}=7.3$ Hz, 3H, $-\text{CH}_3$), 1.34 (sextet, $J_{\text{HH}}=7.3$ Hz, 2H, $-\text{CH}_2-\text{CH}_3$), 1.57 (pentet, $J_{\text{HH}}=7.1$ Hz, 2H, $-\text{CH}_2-\text{CH}_2-\text{CH}_3$), 2.41-2.59 [m, 4H, $-\text{C}(\text{OH})-\text{CH}_2-\text{N}-\text{CH}_2-\text{CH}_2-$], 2.73 (dt, $J_{\text{gem}}=13.2$, $J_{\text{HH}}=6.5$ Hz, $-\text{N}-\text{CH}_A\text{H}_B-\text{CH}_2-$), 3.00 (dt, $J_{\text{gem}}=13.2$, $J_{\text{HH}}=6.1$ Hz, $-\text{N}-\text{CH}_A\text{H}_B-\text{CH}_2-$), 3.46 (d, $J_{\text{gem}}=13.5$ Hz, 1H, $-\text{N}-\text{CH}_A\text{H}_B-\text{Ph}$), 3.81 (d, $J_{\text{gem}}=13.5$ Hz, 1H, $-\text{N}-\text{CH}_A\text{H}_B-\text{Ph}$), 3.63-4.05 (broad s, 1H, $-\text{OH}$), 4.01 (dq, $J_{\text{gem}}=10.8$, $J_{\text{HH}}=6.7$ Hz, 1H, $-\text{COO}-\text{CH}_A\text{H}_B-$), 4.12 (dq, $J_{\text{gem}}=10.8$, $J_{\text{HH}}=6.7$ Hz, 1H, $-\text{COO}-\text{CH}_A\text{H}_B-$), 4.56 [dd, $J_{\text{HH}}=4.7$ and 8.7 Hz, 1H, $-\text{C}(\text{OH})-\text{H}$], 6.72 (dd, $J_{\text{ortho}}=8.1$, $J_{\text{meta}}=1.3$ Hz, 1H, H_6 -aromatic), 6.78 (d, $J_{\text{ortho}}=8.0$ Hz, 1H, H_5 -aromatic), 6.88 (d, $J_{\text{meta}}=1.2$ Hz, 1H, H_2 -aromatic), 7.23-7.36 (m, 11H, aromatic) and 7.53-7.58 (m, 4H, aromatic).

^{13}C NMR (CDCl_3): δ 13.6 ($-\text{CH}_3$), 19.0 ($-\text{CH}_2-\text{CH}_3$), 30.4 ($-\text{CH}_2-\text{CH}_2-\text{CH}_3$), 32.6 ($-\text{CH}_2-\text{COO}-$), 49.5 ($-\text{N}-\text{CH}_2-\text{CH}_2-$), 58.5 ($-\text{N}-\text{CH}_2-\text{Ph}$), 62.6 ($-\text{COO}-\text{CH}_2-$), 64.4 [$-\text{C}(\text{OH})-\text{CH}_2-\text{N}-$], 69.7 ($-\text{C}-\text{OH}$), 106.5, 107.9, 119.2, 126.2, 127.2, 128.0, 128.1, 128.3, 128.8, 128.9 (aromatic C-H), 116.5, 135.9, 138.0, 140.18, 140.2, 146.3, 147.1 (aromatic C) and 172.5 ($-\text{COO}-$).

IR (neat): 3294 cm^{-1} (OH), 1730 cm^{-1} (COO), 1448 and 1495 cm^{-1} (C=C), 1211 and 1249 cm^{-1} (C-O-C).

Elemental analysis: calculated for $\text{C}_{35}\text{H}_{37}\text{NO}_5 \cdot \text{H}_2\text{O}$: C, 73.79; H, 6.90; N, 2.46%. Found C, 73.16; H, 6.53; N, 2.44%.

Mass spectrum (CI, NH_3): Calculated mass for $\text{C}_{35}\text{H}_{38}\text{NO}_5$ is 552.275 ($\text{M}+\text{H}^+$). Observed accurate mass is 552.275 ($\text{M}+\text{H}^+$). m/e 553 [$(\text{M}+2)^+$, 28%], 236 (100%), 303 [$\text{M}^+-(\text{CH}_2-\text{NH}-\text{CH}_2-\text{CH}_2-\text{COOCH}_2-\text{CH}_2-\text{CH}_2-\text{CH}_3)$, 96%] and 108 (60%) (Section 2.4, Scheme 2.10)

3.8.8 Ethyl *N*-[2'-(3'',4''-dipivaloyloxyphenyl)-2'-hydroxyethyl]-*N*-benzyl-3-aminopropionate¹⁰⁹ (**115**):

To a stirred solution of ethyl *N*-[(3',4'-dipivaloyloxybenzoyl)methyl]-*N*-benzyl-3-aminopropionate (3.13 g, 5.96 mmol) in 100 ml of ethanol, was added sodium borohydride (0.563 g, 14.9 mmol) in small portions over a period of 10 min. The resulting suspension was stirred at room temperature for a further 1 hr, after which time the reaction mixture was evaporated under vacuum to remove ethanol (To remove excess sodium borohydride after completion of the reaction, never add water, because the formation of a tiny amount of sodium hydroxide immediately hydrolysed the pivaloyloxy ester). The residue was extracted with diethyl ether. The diethyl ether layer was dried and residue was extracted with hexane and hexane layer was evaporated to yield an oil. The title compound (**115**) was purified by flash chromatography eluting with ethyl acetate-hexane (1:2, R_f 0.25) to yield a colourless oil (1.41 g, 2.68 mmol, 45%).

^1H NMR (CDCl_3): δ 1.24 (t, $J_{\text{HH}}=7.1$ Hz, 3H, $-\text{CH}_3$), 1.32 (s, 9H, Bu^tCOO), 1.33 (s, 9H, Bu^tCOO), 2.45-2.55 [m, 3H, $-\text{C}(\text{OH})-\text{CH}_A\text{H}_B\text{-N-}$, $-\text{CH}_2\text{-COO}$], 2.67 [dd, $J_{\text{gem}}=13.0$, $J_{\text{HH}}=3.2$ Hz, 1H, $-\text{C}(\text{OH})-\text{CH}_A\text{H}_B\text{-N-}$], 2.78 (dt, $J_{\text{gem}}=13.2$, $J_{\text{HH}}=6.1$ Hz, 1H, $-\text{N-CH}_A\text{H}_B\text{-CH}_2\text{-}$), 3.05 (dt, $J_{\text{gem}}=13.2$, $J_{\text{HH}}=7.2$ Hz, 1H, $-\text{N-CH}_A\text{H}_B\text{-CH}_2\text{-}$), 3.53 (d, $J_{\text{gem}}=13.5$ Hz, $-\text{N-CH}_A\text{H}_B\text{-Ph}$), 3.86 (d, $J_{\text{gem}}=13.5$ Hz, $-\text{N-CH}_A\text{H}_B\text{-Ph}$), 4.10 (dq, $J_{\text{gem}}=10.8$, $J_{\text{HH}}=7.1$ Hz, 1H, $-\text{COO-CH}_A\text{H}_B\text{-}$), 4.17 (dq, $J_{\text{gem}}=10.8$, $J_{\text{HH}}=7.18$ Hz, 1H, $-\text{COO-CH}_A\text{H}_B\text{-}$), 4.66 [dd, 1H, $J_{\text{HH}}=3.2$, $J_{\text{HH}}=10.1$ Hz, $-\text{C}(\text{OH})-\text{H}$], 7.05 (d, $J_{\text{ortho}}=8.3$ Hz, 1H, $\text{H}_5\text{-aromatic}$), 7.08 (d, $J_{\text{meta}}=1.8$ Hz, 1H, $\text{H}_2\text{-aromatic}$) and 7.15 (dd, $J_{\text{ortho}}=8.3$, $J_{\text{meta}}=1.9$ Hz, 1H, $\text{H}_6\text{-aromatic}$) and 7.21-7.35 (m, 5H, Ph) (OH is not observed).

^{13}C NMR (CDCl_3): δ 14.1 ($-\text{CH}_3$), 27.2 [$-\text{C}(\text{CH}_3)_3$], 32.8 ($-\text{CH}_2\text{-COO}$), 39.0 [$-\text{C}(\text{CH}_3)_3$], 49.5 ($-\text{N-CH}_2\text{-CH}_2\text{-}$), 58.7 ($-\text{N-CH}_2\text{-Ph}$), 60.7 ($-\text{COO-CH}_2\text{-}$), 62.7 [$-\text{C}(\text{OH})-\text{CH}_2\text{-N-}$], 69.2 [$-\text{C}(\text{OH})-\text{CH}_2\text{-N-}$], 120.7, 123.0, 123.5, 127.4, 128.4, 129.0 (aromatic C-H), 138.0, 140.5, 141.6, 142.5 (aromatic C), 172.5 (CH_2COO), 175.7 (Bu^tCOO) and 175.9 (Bu^tCOO).

IR (neat): 3462 cm^{-1} (OH), 1759 cm^{-1} (C=O, Bu^t ester), 1732 cm^{-1} (C=O, ethyl ester), 1504 & 1479 cm^{-1} (C=C), 1255 & 1120 cm^{-1} (C-O-C).

3.9 SYNTHESIS OF ESTERS OF *N*-[(2'-HYDROXY-2'-(SUBSTITUTED) PHENYLETHYL]-3-AMINOPROPIONATE

3.9.1 Ethyl *N*-(2'-hydroxy-2'-phenylethyl)-3-aminopropionate¹⁰⁹ (50, R= Et):

A solution of ethyl *N*-(2'-hydroxy-2'-phenylethyl)-*N*-benzyl-3-aminopropionate (100 mg, 0.305 mmol) in 15 ml of ethanol was exposed to hydrogen in the presence of 10% palladium on charcoal (20 mg) at room temperature and pressure. The uptake of hydrogen ceased after 40 min. The catalyst was removed by filtration through celite and the filtrate was evaporated to dryness. The residue was recrystallised from hexane to yield a crystalline solid (20 mg, 0.084 mmol, 27%), mp. 75-77 °C.

¹H NMR (CDCl₃): δ 1.26 (t, $J_{\text{HH}}=7.1$ Hz, 3H, -CH₃), 2.3-2.6 (broad s, 2H, -OH, -NH-), 2.51 (t, $J_{\text{HH}}=6.3$ Hz, 2H, -CH₂-COO-), 2.70 [dd, $J_{\text{gem}}=12.2$, $J_{\text{HH}}=9.2$ Hz, 1H, -C(OH)-CH_AH_B-N-], 2.85-3.03 [m, 3H, -C(OH)-CH_AH_B-N-CH₂-], 4.15 (q, $J_{\text{HH}}=7.1$ Hz, 2H, -COO-CH₂), 4.70 [dd, $J_{\text{HH}}=9.0$, $J_{\text{HH}}=3.5$ Hz, 1H, -C(OH)-H] and 7.25-7.4 (m, 5H, aromatic).

¹H NMR (DMSO-d₆): δ 1.17 (t, $J_{\text{HH}}=7.1$ Hz, 3H, -CH₃), 2.42 (t, $J_{\text{HH}}=6.6$ Hz, 2H, -CH₂-COO-), 2.50 (s, 1H, -NH-), 2.60 [d, $J_{\text{HH}}=6.2$ Hz, 2H, -C(OH)-CH₂-N-], 2.77 (t, $J_{\text{HH}}=6.6$ Hz, 2H, -N-CH₂-CH₂-), 3.35 (broad s, 1H, -OH), 4.06 (q, $J_{\text{HH}}=7.1$ Hz, 2H, -COO-CH₂-), 4.59 [t, $J_{\text{HH}}=6.2$ Hz, 1H, -C(OH)-H] and 7.2-7.4 (m, 5H, aromatic).

¹³C NMR (CDCl₃): δ 14.1 (-CH₃), 34.7 (-CH₂-COO-), 44.5 (-N-CH₂-CH₂-), 56.8 [-C(OH)-CH₂-N-], 60.5 (-COO-CH₂-), 71.5 [-C(OH)-], 125.7, 127.4, 128.3 (aromatic C-H), 142.3 (aromatic C) and 172.6 (-COO-).

IR (KBr): 3428 cm⁻¹ (broad -OH), 3300 cm⁻¹ (-NH-) and 1723 cm⁻¹ (-COO-).

Elemental analysis calculated for C₁₃H₁₉NO₃: C, 65.80; H, 8.07; N, 5.90%. Found C, 65.45; H, 7.72; N, 5.74%.

Mass spectrum (CI, NH₃): calculated mass for [C₁₃H₂₀NO₃ (M+H⁺)] 238.1443. Observed accurate mass 238.1443 (M + H⁺). m/e 238 (M + H⁺, 100%), 220 [M + H⁺ - (H₂O), 11%], 192 [Ph-C(OH)H-CH₂-NH-CH₂-CH₂-C=O⁺, 2.5%], 150 [Ph-C(OH)-CH₂-N⁺H=CH₂, 5%], 130 (H₂C=N⁺H-CH₂-CH₂-COOC₂H₅, 88%), 84 (H₂C=N-CH₂-CH₂-C=O⁺, 9.0%) (Section 2.3, Scheme 2.5).

3.9.2 Methyl *N*-(2'-hydroxy-2'-phenylethyl)-3-aminopropionate¹⁰⁹ (50, R=Me):

A mixture of methyl *N*-benzyl-3-aminopropionate (3.19 g, 16.5 mmol), triethylamine (1.52 g, 2.1 ml, 15.0 mmol) and sodium iodide (0.22 g, 1.5 mmol) was stirred in 25 ml of anhydrous DMF in an ice bath. A solution of α -chloroacetophenone (2.32 g, 15.0 mmol) in 10 ml of anhydrous DMF and was added dropwise to the reaction mixture over a period of 15 min. The reaction was nearly complete in three hours. The turbid reaction mixture was filtered and evaporated under vacuum to yield an oil. The product was isolated by flash chromatography eluting with ethyl acetate-hexane (1:5, R_f 0.25) to yield methyl *N*-(benzoylmethyl)-*N*-benzyl-3-aminopropionate as a colourless oil (3.05 g, 9.79 mmol, 65%). To a stirred solution of methyl *N*-(benzoylmethyl)-*N*-benzyl-3-aminopropionate (3.0 g, 9.63 mmol) in 80 ml of methanol, was added sodium borohydride (0.91 g, 24.1 mmol) in small portions over a period of 15 min. The resulting suspension was stirred at room temperature for a further 1 hr, after which time the reaction was evaporated under vacuum to dryness. Water was added and the mixture was extracted with dichloromethane. The lower organic layer was dried with molecular sieves and evaporated under vacuum to give an oil (2.27 g, 7.26 mmol, 75%). The methyl *N*-(2'-hydroxy-2'-phenylethyl)-*N*-benzyl-3-aminopropionate was committed to the next step without further purification. A solution of methyl *N*-(2'-hydroxy-2'-phenylethyl)-*N*-benzyl-3-aminopropionate (2.27 g, 7.26 mmol) in methanol (20 ml) was exposed to hydrogen in the presence of 10% palladium on charcoal (0.23 g) at room temperature and pressure. The uptake of hydrogen ceased after 40 min. The catalyst was removed by filtration through celite and the filtrate was evaporated to dryness. The residue was recrystallised from hexane to yield a crystalline solid (1.15 g, 5.15 mmol, 70%).

¹H NMR (DMSO- d_6): δ 2.44 (t, $J_{HH}=6.6$ Hz, 2H, $-\underline{CH}_2-COO-$), 2.50 (s, 1H, $-NH-$), 2.60 [d, $J_{HH}=6.0$ Hz, 2H, $-C(OH)-\underline{CH}_2-N-$], 2.77 (t, $J_{HH}=6.6$ Hz, 2H, $-N-\underline{CH}_2-CH_2-$), 3.1-3.6 (broad s, 1H, $-OH$), 3.58 (s, 3H, $-OCH_3$), 4.59 (t, $J_{HH}=6.2$ Hz, 1H, $-C(OH)-\underline{H}$] and 7.22-7.35 (m, 5H, aromatic).

¹³C NMR (DMSO- d_6): δ 34.6 ($-\underline{CH}_2-COO-$), 44.8 ($-N-\underline{CH}_2-CH_2-$), 51.4 ($-OCH_3$), 57.6 [$-C(OH)-\underline{CH}_2-N-$], 71.6 [$-C(OH)-$], 126.1, 127.0, 128.1 (aromatic CH), 144.8 (aromatic C) and 172.9 ($-COO-$).

3.9.3 Ethyl *N*-[2'-(3'',4''-dimethoxyphenyl)-2'-hydroxyethyl]-3-aminopropionate¹⁰⁹ (87):

A solution of ethyl *N*-[2'-(3'',4''-dimethoxyphenyl)-2'-hydroxyethyl]-*N*-benzyl-3-aminopropionate (1.20 g, 3.67 mmol) in 50 ml of ethanol was hydrogenated at room temperature and pressure in the presence of 10% palladium on charcoal (0.5 g) catalyst. The uptake of hydrogen ceased after 40 min. The catalyst was removed by filtration through celite and the filtrate was evaporated to dryness. Crystallisation from ethyl acetate-hexane gave white crystals of ethyl *N*-[2'-(3'',4''-dimethoxyphenyl)-2'-hydroxyethyl]-3-aminopropionate (0.8 g, 2.7 mmol, 74 %) mp. 83-84 °C.

¹H NMR (CDCl₃): δ 1.27 (t, $J_{\text{HH}}=7.1$ Hz, 3H, -CH₃), 2.10-2.62 (broad s, 2H, -OH and -NH-), 2.52 (t, $J_{\text{HH}}=6.3$, 2H, -CH₂-COO-), 2.70 [dd, $J_{\text{gem}}=12.2$, $J_{\text{HH}}=9.2$ Hz, 1H, -C(OH)-CH_AH_B-N-], 2.88-3.02 [m, 3H, -C(OH)-CH_AH_B-N-CH₂-], 3.88 (s, 3H, -OCH₃), 3.90 (s, 3H, -OCH₃), 4.16 (q, $J_{\text{HH}}=7.1$ Hz, -COO-CH₂-), 4.66 [dd, $J_{\text{HH}}=9.2$, $J_{\text{HH}}=3.5$ Hz, 1H, -C(OH)-H], 6.84 (d, $J_{\text{ortho}}=8.2$ Hz, 1H, H₅-aromatic), 6.89 (dd, $J_{\text{ortho}}=8.3$ & $J_{\text{meta}}=1.6$ Hz, 1H, H₆-aromatic) and 6.95 (d, $J_{\text{meta}}=1.5$ Hz, 1H, H₂-aromatic).

¹³C NMR (CDCl₃): δ 14.1 (-CH₃), 34.7 (-CH₂-COO-), 44.5 (-N-CH₂-CH₂-), 55.7 [-C(OH)-CH₂-N-], 55.8 (-OCH₃), 56.8 (-OCH₃), 60.5 (-COO-CH₂-), 71.3 [-C(OH)-], 108.8, 110.9, 117.9 (aromatic CH), 134.9, 148.3 and 148.9 (aromatic C) and 172.6 (-COO-).

Elemental analysis calculated for C₁₅H₂₃NO₅: C, 60.59; H, 7.80; N, 4.71%. Found C, 59.95; H, 7.57; N, 4.69%.

IR (KBr): 3313 cm⁻¹ (-OH), 3100 cm⁻¹ (broad, -NH-), 1721 cm⁻¹ (-COO-), 1518 and 1464 (C=C), 1263 and 1023 cm⁻¹ (Ar-O-R).

Mass spectrum (CI, NH₃): observed mass for C₁₅H₂₃NO₅ 279.0 (M⁺ - H₂O).

3.9.4 Ethyl *N*-[2'-(3'',4''-diphenylmethylenedioxyphenyl)-2'-hydroxyethyl]-3-aminopropionate^{109,113} (105, R= Et):

A solution of ethyl *N*-[2'-(3'',4''-diphenylmethylenedioxyphenyl)-2'-hydroxyethyl]-*N*-benzyl-3-aminopropionate (0.2 g, 0.382 mmol) in ethyl acetate (10 ml) was hydrogenated at room temperature at 30 psi hydrogen atmosphere in the presence of 10% palladium on charcoal (20 mg) catalyst. After 48 h, the catalyst was removed by filtration through celite and the filtrate was evaporated under vacuum to dryness. The product was isolated by flash chromatography eluting with 10% ethanol in chloroform (R_f 0.42), as a colourless solid. The product was crystallized from ethyl acetate-hexane.

^1H NMR (CDCl_3): δ 1.24 (t, $J_{\text{HH}}=7.1$ Hz, 3H, $-\text{CH}_3$), 2.2-2.69 (broad s, 2H, $-\text{OH}$ and $-\text{NH}-$), 2.49 (t, $J_{\text{HH}}=6.4$ Hz, 2H, $-\text{CH}_2-\text{COO}-$), 2.65 [dd, $J_{\text{gem}}=12.2$, $J_{\text{HH}}=9.1$ Hz, 1H, $-\text{C}(\text{OH})-\text{CH}_A\text{H}_B-\text{N}-$], 2.84 [dd, $J_{\text{gem}}=12.2$, $J_{\text{HH}}=3.6$ Hz, 1H, $-\text{C}(\text{OH})-\text{CH}_A\text{H}_B-\text{N}-$], 2.8-3.0 (m, 2H, $-\text{N}-\text{CH}_2-\text{CH}_2-$), 4.12 (q, $J_{\text{HH}}=7.1$ Hz, 2H, $-\text{COO}-\text{CH}_2-$), 4.60 [dd, $J_{\text{HH}}=3.6$, $J_{\text{HH}}=9.1$ Hz, 1H, $-\text{C}(\text{OH})-\text{H}$], 6.75-6.85 (m, 2H, aromatic), 6.93 (s, 1H, aromatic), 7.3-7.45 (m, 6H, aromatic), 7.5-7.65 (m, 4H, aromatic).

^{13}C NMR (CDCl_3): δ 14.1 ($-\text{CH}_3$), 34.7 ($-\text{CH}_2-\text{COO}-$), 44.5 ($-\text{N}-\text{CH}_2-\text{CH}_2-$), 56.8 [$-\text{C}(\text{OH})-\text{CH}_2-\text{N}-$], 60.5 ($\text{COO}-\text{CH}_2-$), 71.4 [$-\text{C}(\text{OH})-$], 116.5 [$(\text{Ph})_2\text{C}-$], 106.4, 108.1, 119.2, 126.2, 128.1, 129.0, 136.3, 140.2, 146.5, 147.3 (aromatic) and 172.5 (COO).

3.9.5 Ethyl *N*-{2'-[3'',4''-(1''',1''',3''',3'''-tetra-*t*-butyldisiloxane)dioxyphenyl]-2'-hydroxyethyl}-3-aminopropionate¹⁰⁹ (**98**):

A solution of ethyl *N*-{2'-[3'',4''-(1''',1''',3''',3'''-tetra-*t*-butyldisiloxane)dioxyphenyl]-2'-hydroxyethyl}-*N*-benzyl-3-aminopropionate (0.25 g, 0.359 mmol) in 20 ml of ethanol was hydrogenated in the presence of 10% palladium on charcoal (25 mg) at room temperature and pressure. The uptake of hydrogen ceased after 40 min. The catalyst was removed by filtration through celite and the filtrate was evaporated to dryness under vacuum to remove toluene. The residue was crystallized from hexane to give the title compound (**98**) (0.075 g, 0.14 mmol, 35%).

^1H NMR (CDCl_3): δ 1.08 [s, 18H, $(\text{CH}_3)_3\text{C}-\text{Si}$], 1.09 [s, 18H, $(\text{CH}_3)_3\text{C}-\text{Si}$], 1.24 (t, $J_{\text{HH}}=7.1$ Hz, 3H, $-\text{CH}_3$), 2.76-3.26 (m, 6H, $-\text{CH}_2-\text{N}-\text{CH}_2-\text{CH}_2-$), 4.15 (q, $J_{\text{HH}}=7.1$ Hz, 2H, $-\text{COO}-\text{CH}_2-$), 5.00 [dd, 1H, $J_{\text{HH}}=9.8$, $J_{\text{HH}}=2.8$ Hz, $-\text{C}(\text{OH})-\text{H}$], 4.9-5.3 (broad s, 3H, $-\text{OH}$, $-\text{NH}-$ and some protonation), 6.85 (s, 2H, aromatic) and 6.93 (s, 1H, aromatic).

^{13}C NMR (CDCl_3): δ 14.1 ($-\text{CH}_3$), 21.4 [$(\text{CH}_3)_3\text{C}-\text{Si}$], 28.1 [$(\text{CH}_3)_3\text{C}-\text{Si}$], 32.0 ($-\text{CH}_2-\text{COO}$), 44.1 ($-\text{N}-\text{CH}_2-\text{CH}_2-$), 55.8 [$-\text{C}(\text{OH})-\text{CH}_2-\text{N}-$], 61.2 ($-\text{COO}-\text{CH}_2-$), 69.4 [$-\text{C}(\text{OH})-\text{CH}_2-\text{N}-$], 118.8, 119.3, 121.5 (aromatic C-H), 134.5, 145.5, 145.8 (aromatic C) and 171.5 ($\text{C}=\text{O}$).

3.9.6 Ethyl *N*-[2'-(3'',4''-dihydroxyphenyl)-2'-hydroxyethyl]-3-aminopropionate^{109,113} (**74**, R= Et):

A solution of ethyl *N*-[2'-(3'',4''-diphenylmethylenedioxyphenyl)-2'-hydroxyethyl]-*N*-benzyl-3-aminopropionate (0.30 g, 0.573 mmol) in 25 ml of ethanol was hydrogenated at room temperature under 60 psi hydrogen atmosphere in the presence of 10% palladium on charcoal catalyst (30 mg). After 18 h, the catalyst was removed by filtration through celite and the filtrate was evaporated under vacuum to dryness. The residue was washed with toluene to remove the byproduct diphenylmethane.

The residue was evaporated under vacuum to give ethyl *N*-[2'-(3'',4''-dihydroxyphenyl)-2'-hydroxyethyl]-3-aminopropionate as a pale pink solid. The product was highly oxygen (air) sensitive, therefore all of the filtration and concentration procedures were performed under argon. The product was dissolved in a small amount of ethanol and then dry ether was added to the solution. Dry HCl was passed through the solution until it turned yellow. The hydrochloride salt of the product (**74**, R=Et) precipitated out as a white solid and was collected by filtration. The compound was stored under argon and was protected from light (0.143 g, 0.531 mmol, 92%) mp. 156.8 °C.

^1H NMR (D_2O): δ 1.27 (t, $J_{\text{HH}}=7.1$ Hz, 3H, $-\text{CH}_3$), 2.89 (t, $J_{\text{HH}}=6.7$ Hz, 2H, $\text{CH}_2\text{-COO}$), 3.28-3.36 [m, 2H, $-\text{C}(\text{OH})\text{-CH}_2\text{-N-}$], 3.36-3.52 (m, 2H, $-\text{N-CH}_2\text{-CH}_2\text{-}$), 4.21 (q, $J_{\text{HH}}=7.1$ Hz, 2H, $-\text{COO-CH}_2\text{-}$), 4.96 (dd, $J_{\text{HH}}=7.9$, $J_{\text{HH}}=5.1$ Hz, 1H, $-\text{C}(\text{OH})\text{-H}$], 6.88 (dd, $J_{\text{ortho}}=8.3$, $J_{\text{meta}}=1.9$ Hz, 1H, $\text{H}_6\text{-aromatic}$), 6.96 (d, $J_{\text{ortho}}=8.1$ Hz, 1H, $\text{H}_5\text{-aromatic}$) and 6.97 (d, $J_{\text{meta}}=2.0$ Hz, 1H, $\text{H}_2\text{-aromatic}$). Assignments were made with the aid of a COSY spectrum.

^1H NMR ($\text{MeOH-}d_4$): δ 1.23 (t, $J_{\text{HH}}=7.1$ Hz, 3H, $-\text{CH}_3$), 2.52 (t, $J_{\text{HH}}=6.6$ Hz, 2H, $-\text{CH}_2\text{-COO-}$), 2.69 [dd, $J_{\text{gem}}=12.0$, $J_{\text{HH}}=4.8$ Hz, 1H, $-\text{C}(\text{OH})\text{-CH}_A\text{H}_B\text{-N-}$], 2.78 [dd, $J_{\text{HH}}=12.0$, $J_{\text{HH}}=8.3$ Hz, 1H, $-\text{C}(\text{OH})\text{-CH}_A\text{H}_B\text{-N-}$], 2.87 (t, $J_{\text{HH}}=6.6$ Hz, 2H, $-\text{N-CH}_2\text{-CH}_2\text{-}$), 4.11 (q, $J_{\text{HH}}=7.1$ Hz, 2H, $-\text{COO-CH}_2\text{-}$), 4.60 [dd, $J_{\text{HH}}=8.3$, $J_{\text{HH}}=4.8$ Hz, 1H, $-\text{C}(\text{OH})\text{-H}$], 6.67 (dd, $J_{\text{ortho}}=8.1$, $J_{\text{meta}}=1.9$ Hz, 1H, $\text{H}_6\text{-aromatic}$), 6.73 (d, $J_{\text{ortho}}=8.0$ Hz, 1H, $\text{H}_5\text{-aromatic}$) and 6.80 (d, $J_{\text{meta}}=1.8$ Hz, 1H, $\text{H}_2\text{-aromatic}$).

^{13}C NMR (D_2O): δ 14.5 ($-\text{CH}_3$), 31.4 ($-\text{CH}_2\text{-COO-}$), 44.3 ($-\text{N-CH}_2\text{-CH}_2\text{-}$), 54.3 [$-\text{C}(\text{OH})\text{-CH}_2\text{-N-}$], 63.7 ($-\text{COO-CH}_2\text{-}$), 69.5 [$-\text{C}(\text{OH})\text{-}$], 115.1, 117.6, 119.8 (aromatic CH), 133.3, 145.5, 145.6 (aromatic C) and 173.7 ($-\text{COO-}$).

^{13}C NMR ($\text{MeOH-}d_4$): δ 14.5 ($-\text{CH}_3$), 34.9 ($-\text{CH}_2\text{-COO-}$), 45.6 ($-\text{N-CH}_2\text{-CH}_2\text{-}$), 57.7 [$-\text{C}(\text{OH})\text{-CH}_2\text{-N-}$], 61.6 ($-\text{COO-CH}_2\text{-}$), 73.2 [$-\text{C}(\text{OH})\text{-}$], 114.2, 116.2, 118.6 (aromatic CH), 135.8, 146.0, 146.4 (aromatic C) and 174.0 ($-\text{COO-}$).

Elemental analysis calculated for $\text{C}_{13}\text{H}_{20}\text{ClNO}_5$: C, 51.06; H, 6.59; N, 4.58%. Found C, 50.92; H, 6.62; N, 4.64%.

IR (KBr): 3404 cm^{-1} (broad, $-\text{N}^+\text{H}_2\text{-}$), 3315 cm^{-1} (broad, $-\text{OH}$), 1731 cm^{-1} ($-\text{COO-}$).

Mass spectrum (FAB): calculated mass for cation $[\text{C}_{13}\text{H}_{20}\text{NO}_5]^+$ 270.13415 ($\text{M}^+ - \text{Cl}$). Accurate mass of cation found at m/e 270.13415 ($\text{M}^+ - \text{Cl}$) (Section 2.4, Scheme 2.11).

3.9.7 Methyl *N*-[2'-(3'',4''-dihydroxyphenyl)-2'-hydroxyethyl]-3-amino-propionate^{109,113} (**74**, R= Me):

A solution of methyl *N*-[2'-(3'',4''-diphenylmethylenedioxyphenyl)-2'-hydroxyethyl]-*N*-benzyl-3-aminopropionate (3.91 g, 7.68 mmol) in methanol (50 ml) was hydrogenated at room temperature under 60 psi hydrogen atmosphere in the presence of 10% palladium on charcoal catalyst (0.39 g). After 12 hr, the catalyst was removed by filtration through celite and the filtrate was evaporated under vacuum to dryness. The residue was washed with toluene to remove the by-product diphenylmethane. The residue was evaporated under vacuum to dryness to give methyl *N*-[2'-(3'',4''-dihydroxyphenyl)-2'-hydroxyethyl]-3-aminopropionate as a pale pink solid. The product was highly oxygen (air) sensitive, therefore all of the filtration and concentration manipulations were done under argon. The compound (**74**, R=Me) was stored in the dark under argon (1.82 g, 7.13 mmol, 93%).

¹H NMR (MeOH-*d*₄): δ 2.75 (broad, 2H, -CH₂-COO-), 3.04 [broad, 2H, -C(OH)-CH₂-N], 3.22 (broad, 2H, -N-CH₂-CH₂-), 3.71 (s, 3H, -OCH₃), 4.76 [broad, 1H, -C(OH)-H], 6.66-6.94 (m, 3H, aromatic).

¹³C NMR (MeOH-*d*₄): δ 31.0 (-CH₂-COO-), 44.4 (-N-CH₂-CH₂-), 50.0 (-OCH₃), 54.4 [-C(OH)-CH₂-N-], 79.5 [-C(OH)-], 114.7, 116.6, 119.7 (aromatic CH), 129.3, 147.0, 147.2 (aromatic C) and 172.4 (-COO-).

3.9.8 Propyl *N*-[2'-(3'',4''-dihydroxyphenyl)-2'-hydroxyethyl]-3-amino-propionate^{109,113} (**74**, R= n-Pr):

A solution of propyl *N*-[2'-(3'',4''-diphenylmethylenedioxyphenyl)-2'-hydroxyethyl]-*N*-benzyl-3-aminopropionate (1.57 g, 2.92 mmol) in *n*-propanol (50 ml) was hydrogenated at room temperature under 60 psi hydrogen atmosphere in the presence of 10% palladium on charcoal catalyst (157 mg). After 24 hr, the reaction mixture comprised of the starting material and propyl *N*-[2'-(3'',4''-diphenylmethylenedioxyphenyl)-2'-hydroxyethyl]-3-aminopropionate (**105**, R=Pr). The reaction mixture was subjected to a hydrogen atmosphere for a further 48 hrs, after which time the reaction mixture comprised of 10% propyl *N*-[2'-(3'',4''-diphenylmethylenedioxyphenyl)-2'-hydroxyethyl]-3-aminopropionate (**105**, R=Pr) and 90% propyl *N*-[2'-(3'',4''-dihydroxyphenyl)-2'-hydroxyethyl]-3-aminopropionate (**74**, R=Pr). The catalyst was removed by filtration through celite and the filtrate was evaporated under vacuum to dryness to give propyl *N*-[2'-(3'',4''-dihydroxyphenyl)-2'-hydroxyethyl]-3-aminopropionate with 90% purity.

^1H NMR (MeOH- d_4): δ 0.82 (t, $J_{\text{HH}}=7.5$ Hz, 3H, $-\text{CH}_3$), 1.51 (sextet, $J_{\text{HH}}=7.1$ Hz, 2H, $-\text{CH}_2-\text{CH}_3$), 2.43 (t, $J_{\text{HH}}=6.5$ Hz, 2H, $-\text{CH}_2-\text{COO}-$), 2.59 [dd, $J_{\text{gem}}=12.1$, $J_{\text{HH}}=4.8$ Hz, 1H, $-\text{C}(\text{OH})-\text{CH}_A\text{H}_B-\text{N}-$], 2.67 [dd, $J_{\text{HH}}=12.1$, $J_{\text{HH}}=8.4$ Hz, 1H, $-\text{C}(\text{OH})-\text{CH}_A\text{H}_B-\text{N}-$], 2.78 (t, $J_{\text{HH}}=6.5$ Hz, 2H, $-\text{N}-\text{CH}_2-\text{CH}_2-$), 3.91 (t, $J_{\text{HH}}=6.6$ Hz, 2H, $-\text{COO}-\text{CH}_2-$), 4.49 [dd, $J_{\text{HH}}=4.8$, $J_{\text{HH}}=8.3$ Hz, 1H, $-\text{C}(\text{OH})-\text{H}$], 6.55 (dd, $J_{\text{ortho}}=8.1$, $J_{\text{meta}}=1.9$ Hz, 1H, H_6 -aromatic), 6.61 (d, $J_{\text{ortho}}=8.0$ Hz, 1H, H_5 -aromatic) and 6.69 (d, $J_{\text{meta}}=1.8$ Hz, 1H, H_2 -aromatic).

^{13}C NMR (MeOH- d_4): δ 10.7 ($-\text{CH}_3$), 23.0 ($-\text{CH}_2-\text{CH}_3$), 34.7 ($-\text{CH}_2-\text{COO}-$), 45.6 ($-\text{N}-\text{CH}_2-\text{CH}_2-$), 57.6 ($-\text{HOCH}-\text{CH}_2-\text{N}-$), 67.3 ($-\text{COO}-\text{CH}_2-$), 73.0 [$-\text{C}(\text{OH})-$], 114.2, 116.2, 118.6 (aromatic CH), 135.8, 146.0, 146.4 (aromatic C) and 174.0 ($-\text{COO}-$).

3.9.9 Butyl *N*-[2'-(3'',4''-dihydroxyphenyl)-2'-hydroxyethyl]-3-amino-propionate^{109,113} (**74**, R= n-Bu):

Butyl *N*-[2'-(3'',4''-diphenylmethylenedioxyphenyl)-2'-hydroxyethyl]-*N*-benzyl-3-amino-propionate (3.5 g, 6.35 mmol) in *n*-butanol (50 ml) was hydrogenated at room temperature under 60 psi hydrogen atmosphere in the presence of 10% palladium on charcoal catalyst (150 mg). After 24 hr, the reaction mixture contained starting material and butyl *N*-[2'-(3'',4''-diphenylmethylenedioxyphenyl)-2'-hydroxyethyl]-3-aminopropionate (**105**, R=Bu). After hydrogenation for 96 hrs, the reaction mixture still contained 70% butyl *N*-[2'-(3'',4''-diphenylmethylenedioxyphenyl)-2'-hydroxyethyl]-3-aminopropionate (**105**, R=Bu) and 30% butyl *N*-[2'-(3'',4''-dihydroxyphenyl)-2'-hydroxyethyl]-3-aminopropionate (**74**, R=Bu). The catalyst was removed by filtration through celite and the filtrate was evaporated under vacuum to dryness to give butyl *N*-[2'-(3'',4''-dihydroxyphenyl)-2'-hydroxyethyl]-3-aminopropionate in 30% purity.

^1H NMR (DMSO- d_6): δ 0.88 (t, $J_{\text{HH}}=7.3$ Hz, 3H, $-\text{CH}_3$), 1.32 (sextet, $J_{\text{HH}}=7.4$ Hz, 2H, $-\text{CH}_2-\text{CH}_3$), 1.56 (pentet, $J_{\text{HH}}=7.04$ Hz, 2H, $-\text{CH}_2-\text{CH}_2-\text{CH}_3$), 2.80 (t, $J_{\text{HH}}=7.1$ Hz, 2H, $-\text{CH}_2-\text{COO}-$), 2.85-3.28 [m, 2H, $-\text{C}(\text{OH})-\text{CH}_2-\text{N}-$], 3.3-3.55 (m, 2H, $-\text{N}-\text{CH}_2-\text{CH}_2-$), 4.05 (t, $J_{\text{HH}}=6.5$ Hz, 2H, $-\text{COO}-\text{CH}_2-$), 4.85 [dd, $J_{\text{HH}}=7.9$ Hz, $J_{\text{HH}}=4.0$, 1H, $-\text{C}(\text{OH})-\text{H}$], 6.91 (dd, $J_{\text{ortho}}=8.1$ Hz, J_{meta} =not resolved, 1H, H_6 -aromatic), 7.04 (d, $J_{\text{ortho}}=8.0$ Hz, 1H, H_5 -aromatic), 7.07 (d, $J_{\text{meta}}=1.4$ Hz, 1H, H_2 -aromatic), 8.7 (broad s, 1H, phenolic -OH) and 9.1 (broad s, 1H, phenolic -OH).

3.9.10 Ethyl *N*-[2'-(3'',4''-dipivaloyloxyphenyl)-2'-hydroxyethyl]-3-aminopropionate¹⁰⁹ (107):

A solution of ethyl *N*-[2'-(3'',4''-dipivaloxyphenyl)-2'-hydroxyethyl]-*N*-benzyl-3-aminopropionate (0.80 g, 1.55 mmol) in ethanol (50 ml) was subjected to hydrogenation in the presence of 10% palladium on charcoal (80 mg) at room temperature and pressure. The uptake of hydrogen ceased after 40 min. The catalyst was removed by filtration through celite and the filtrate was evaporated to dryness. The residue was extracted into ether which was evaporated to dryness to yield a thick oil which on standing solidified. The solid was recrystallised from hexane to yield ethyl *N*-[2'-(3'',4''-dipivaloxyphenyl)-2'-hydroxyethyl]-3-aminopropionate (0.67 g, 1.53 mmol, 89%).

¹H NMR (CDCl₃): (Assignment were made with the aid of a COSY) δ 1.26 (t, $J_{\text{HH}}=7.13$ Hz, 3H, -CH₃), 1.33 (s, 9H, Bu^tCOO), 1.34 (s, 9H, Bu^tCOO), 2.49 (t, $J_{\text{HH}}=6.41$ Hz, 2H, -CH₂-COO-), 2.66 [dd, $J_{\text{gem}}=12.2$, $J_{\text{HH}}=9.1$ Hz, 1H, -C(OH)-CH_AH_B-N-], 2.84-3.00 [m, 3H, -C(OH)-CH_AH_B-N-, -N-CH₂-CH₂-], 4.14 (q, $J_{\text{HH}}=7.1$ Hz, 2H, -COO-CH₂-), 4.67 [dd, $J_{\text{HH}}=9.1$, $J_{\text{HH}}=3.4$ Hz, 1H, -C(OH)-H], 7.08 (d, $J_{\text{ortho}}=8.3$ Hz, 1H, H₅-aromatic), 7.15 (d, $J_{\text{meta}}=1.7$ Hz, 1H, H₂-aromatic) and 7.19 (dd, $J_{\text{ortho}}=8.3$, $J_{\text{meta}}=1.7$ Hz, 1H, H₆-aromatic). By integration OH and NH lie between 2.2 and 3.4 as very broad peaks.

¹³C NMR (CDCl₃): δ 14.1 (-CH₃), 27.1 [-C(CH₃)₃], 34.6 (-CH₂-COO), 38.6 [-C(CH₃)₃], 44.5 (-N-CH₂-CH₂-), 56.7 [-C(OH)-CH₂-N-], 60.4 (-COO-CH₂-), 70.6 [-C(OH)-], 120.6, 123.1, 123.4 (aromatic CH), 141.2, 141.5, 142.3 (aromatic C), 172.5 (CH₂COO), 175.7 (Bu^tCOO) and 175.8 (Bu^tCOO).

IR (KBr): 3506 cm⁻¹ (OH), 1759 cm⁻¹ [COO-C(CH₃)₃], 1734 cm⁻¹ (COO-C₂H₅), 1504 and 1481 cm⁻¹ (C=C), 1257 and 1113 cm⁻¹ (C-O-C).

Elemental analysis: Calculated for C₂₃H₃₆NO₇: C, 63.14; H, 8.06; N, 3.20%. Found: C, 62.94; H, 8.07; N, 3.02%.

Mass spectrum (CI, NH₃): calculated mass for C₂₃H₃₇NO₇ 438.2492 (M + H⁺). Observed accurate mass 438.2492 (M + H⁺). Mass spectrum (CI, NH₃): m/e 438 (M + H⁺, 100%), 130 (H₂C=N⁺H-CH₂-CH₂-COOC₂H₅, 32%). Mass spectrum (EI, NH₃): m/e 130 (H₂C=N⁺H-CH₂-CH₂-COOC₂H₅, 85%), 84 (H₂C=N-CH₂-CH₂-C=O⁺, 40%), 57 (H₂C=N⁺H-CH=CH₂, 100%), 42 (H₂C=N⁺=CH₂, 41%) (Section 2.5, Scheme 2.12).

3.9.11 *N*-[2'-(3'',4''-Dihydroxyphenyl)-2'-hydroxyethyl]-3-aminopropionic acid (74, R=H):

Ethyl *N*-[2'-(3'',4''-dihydroxyphenyl)-2'-hydroxyethyl]-3-aminopropionate (0.1 g, 0.327 mmol) was dissolved in 25 ml of distilled water and acidified with 0.5 ml of conc. HCl and stirred at room temperature for two days. Water was removed under vacuum to dryness and water was added again and evaporated under vacuum to remove excess of acid, to give *N*-[2'-(3'',4''-hydroxyphenyl)-2'-hydroxyethyl]-3-aminopropionic acid (74, R=H) as a hydrochloride salt (0.085 g, 0.306 mmol, 94 %).

^1H NMR (D_2O): δ 2.91 (t, $J_{\text{HH}}=6.6$ Hz, 2H, $\text{CH}_2\text{-COO}$), 3.22-3.42 [m, 2H, $\text{-C(OH)-CH}_2\text{-N-}$], 3.42-3.52 (m, 2H, $\text{-N-CH}_2\text{-CH}_2\text{-}$), 4.97 (dd, $J_{\text{HH}}=8.3$, $J_{\text{HH}}=4.9$ Hz, 1H, -C(OH)-H], 6.91 (dd, $J_{\text{ortho}}=8.3$, $J_{\text{meta}}=2.0$ Hz, 1H, $\text{H}_6\text{-aromatic}$), 6.99 (d, $J_{\text{ortho}}=8.3$ Hz, 1H, $\text{H}_5\text{-aromatic}$) and 7.0 (d, $J_{\text{meta}}=2.0$ Hz, 1H, $\text{H}_2\text{-aromatic}$).

^{13}C NMR (D_2O): δ 31.0 ($\text{-CH}_2\text{-COO-}$), 44.27 ($\text{-N-CH}_2\text{-CH}_2\text{-}$), 54.26 [$\text{-C(OH)-CH}_2\text{-N-}$], 69.45 [-C(OH)-], 115.0, 117.53, 119.77 (aromatic C-H), 133.26, 145.47, 145.41 (aromatic C) and 175.47 (-COO-).

CHAPTER FOUR

HPLC OF β -ADRENOCEPTOR AGONISTS

4.1 INTRODUCTION

This chapter is a discussion on the development of HPLC methods for the quantitative analysis of soft-drugs, prodrug and related analogues during the course of this study. HPLC is undoubtedly one of the most valuable and versatile analytical techniques currently available to the pharmaceutical scientist. Its attributes include the ability to efficiently separate and detect a wide range of molecules with varying molecular weight, polarities and thermal labilities. The technique is especially valuable in the analytical separation of groups of closely related compounds such as enantiomers, degradation products, metabolites and structural analogues. In addition, the provision of a rapid, specific, sensitive and readily quantifiable assay system makes HPLC an ideal analytical method for this purpose.

The development of a suitable assay procedure may be achieved by the modification of several variables which determine the efficient chromatographic separation of compounds. Once the basic components of the systems are assembled, selection of an appropriate column-stationary phase is the initial criterion. A number of these are available and a single stationary phase may be used for the analysis of a multitude of compounds. System selectivity and separation of individual components is however achieved by the careful choice of mobile phase. Changes in solvent composition together with selection of an appropriate UV detection wavelength are used to achieve optimal detection and resolution which may be quantified in terms of various mathematical parameters. Internal standards may be incorporated into samples to aid standardisation by minimising errors caused by fluctuation in column performance, while analyte concentrations are determined by interpolation from calibration plots which are validated in terms of their linearity. The development of HPLC methods for soft-drugs, prodrugs and analogues, described in this thesis, will be discussed in this chapter with respect to these variables.

Comprehensive accounts of the theoretical principles and practical aspects of HPLC may be found in several texts.^{119,120} Basically the system involves the delivery of the sample through an injection valve onto a solid-phase chromatographic column. A combination of partitioning and adsorption processes distribute the analyte between the solid stationary, and the liquid mobile phase, by virtue of their physicochemical characteristics and results in separation and elution of the analyte through a detection device where they may be quantified.

The HPLC system used may be quantified by a number of mathematical parameters which define chromatographic performance in terms of retention and resolution. Figure 4.1 illustrates a typical HPLC chromatogram for a two-component mixture where t_0 , t_A and t_B are the retention times of a solvent front or unretained solute, component A and component B respectively; t_0 is commonly recognised as the first disturbance in the baseline, usually observed as the solvent front.

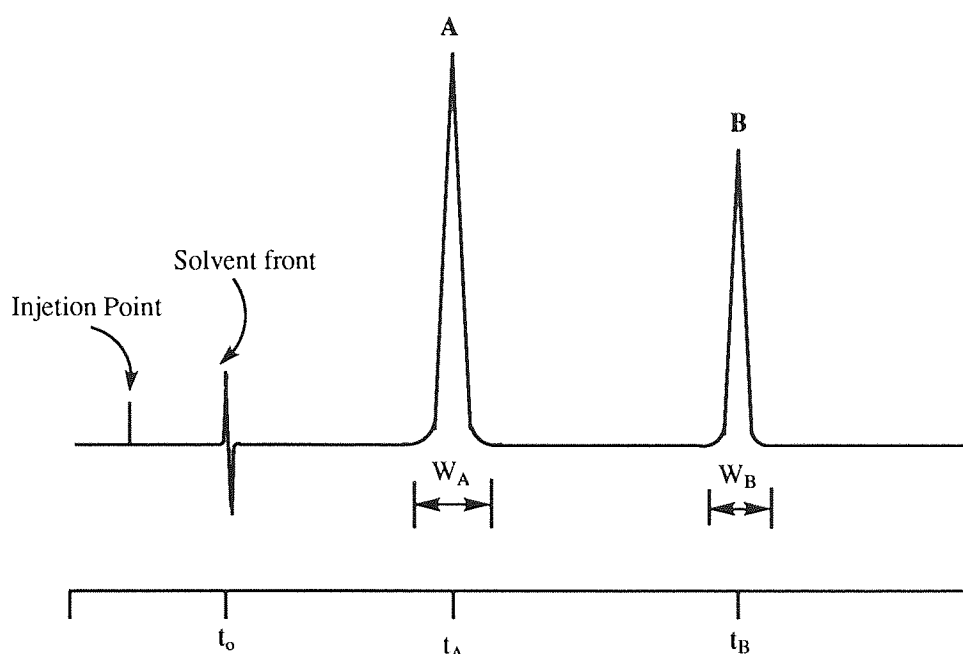


Figure 4.1: Typical HPLC chromatogram of a two-component mixture.

Mathematical parameters in HPLC	Formula	Typical value
Column capacity factor (k') (a measure of sample retention)	$k_A' = \frac{(t_A - t_0)}{t_0}$	1 - 10
Number of theoretical plates (N) (per metre of column length)	$N_A = 16 \left(\frac{t_A}{W_A} \right)^2$	2,500 - 10,000 m^{-1}
Column length (L) in cm	L	10 - 25 cm
Efficiency (H) (height equivalent to theoretical plates)	$H = \frac{L}{N}$	25 - 100 μm
The resolution (R_S), of a system is a measure of the efficiency of the separation of different components	$R_S = \frac{2(t_B - t_A)}{(W_A + W_B)}$	$R_S = 1.0$, satisfactory separation with $\sim 2\%$ overlap $R_S = 1.5$, total separation

Table 4.1: Mathematical parameters and their typical values in HPLC.

Mathematical parameters which can be calculated for a typical HPLC chromatogram are given in Table 4.1. A value of less than 1 for the column capacity factor indicates inadequate separation from the solvent front, whilst large values of k' , greater than 10, are associated with long retention times and broadened peaks. Columns with large N values will produce narrow peaks and better resolution than those with lower N values.

4.2 MATERIALS

Alkyl *N*-[2'-(3'',4''-dihydroxyphenyl)-2'-hydroxyethyl]-3-aminopropionates (**74**, R=Et, Pr), ethyl *N*-[2'-(3'',4''-dipivaloyloxyphenyl)-2'-hydroxyethyl]-3-aminopropionate (**107**) and alkyl *N*-(2'-phenyl-2'-hydroxyethyl)-3-aminopropionates (**50**, R=Me, Et) were synthesized as described in chapter three.

All other chemicals and solvents were purchased from Aldrich, Lancaster and Fisons and were used as received. HPLC grade solvents were used for the preparation of HPLC mobile phases whilst other chemicals were either Analar or reagent grade as appropriate.

4.3 INSTRUMENTATION (High-performance liquid chromatography)

High-performance liquid chromatography (HPLC) analyses were performed using a system constructed from an Altex 100A dual reciprocating, solvent-metering pump delivering mobile phases, typically at a flow rate of 1 ml min⁻¹, to a stainless-steel column (10 cm x 4.6 mm; column length x internal diameter) packed with 5 μ m Hyposil-ODS (Shandon, UK) reversed-phase material. Samples were introduced through a Rheodyne 7120 injection valve fitted with a 10 μ l, 20 μ l or 100 μ l loop as appropriate, UV detection was accomplished with a Pye Unicam LC variable UV wavelength detector equipped with an 8 μ l flow cell and sensitivity setting ranging from 0.08 to 1.28 AUFS. Chromatograms were recorded using a Gallenkamp Euroscribe chart recorder operating at a chart speed of 15 cm h⁻¹.

All pH measurements were undertaken using a Philips CD 660 Digital pH meter (3 decimal place display) or a WPA CD 660 Digital pH meter (2 decimal place display) in conjunction with a Gallenkamp combination glass electrode calibrated with Colourkey[®] buffer solutions (BDH Ltd).

A range of electronic balances; Sartorius 1601 MP8 and analytic A200S (four decimal place) instruments were used for accurate weighing purposes. A Kerry laboratory sonicator was employed where sonication was required as an aid to dissolution or solvent de-gassing.

4.4 EXPERIMENTAL

The UV spectrum of compounds were recorded on a Philips PU 8730 UV/VIS spectrometer in CHCl₃ to determine λ_{\max} values.

4.5 RESULTS AND DISCUSSION

4.5.1 Selection of UV wavelength

The use of a UV detector to monitor the presence and concentration of analyte separated on the chromatographic column requires a preliminary knowledge of the UV absorption characteristics of the compounds of interest. Hence, the UV spectra of soft-drugs (**74**, R= Et, Pr), prodrug (**107**) and their analogues (**50**, R= Me, Et) were initially studied in the range 200-350 nm. Two examples are illustrated in Figures 4.2 and 4.3. All compounds were found to have a maximum absorption at 210 nm and 255 nm, but 210 nm wavelength was chosen for the HPLC analysis due to sensitivity.

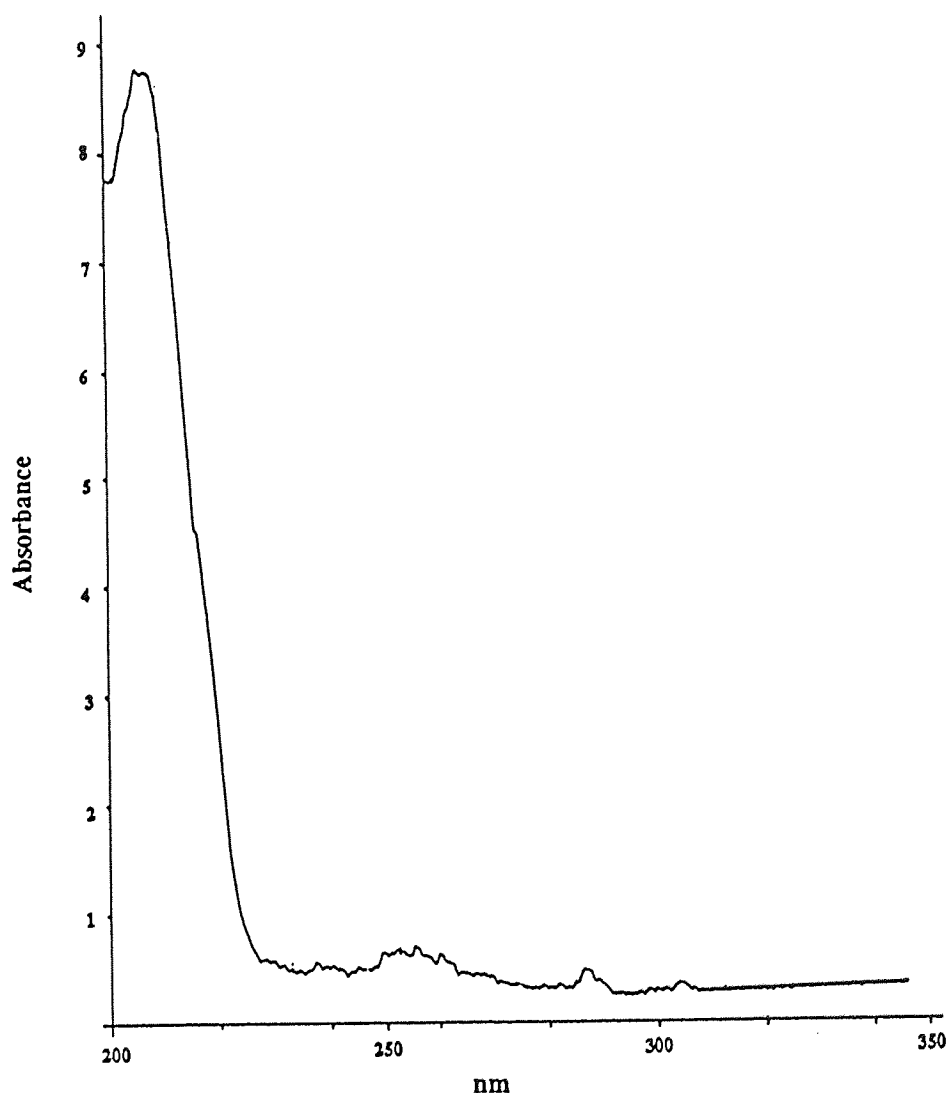


Figure 4.2: UV spectrum of ethyl *N*-[2'-(3',4'-dihydroxyphenyl)-2'-hydroxyethyl]-3-aminopropionate (**74**, R=Et) in chloroform (200-350 nm).

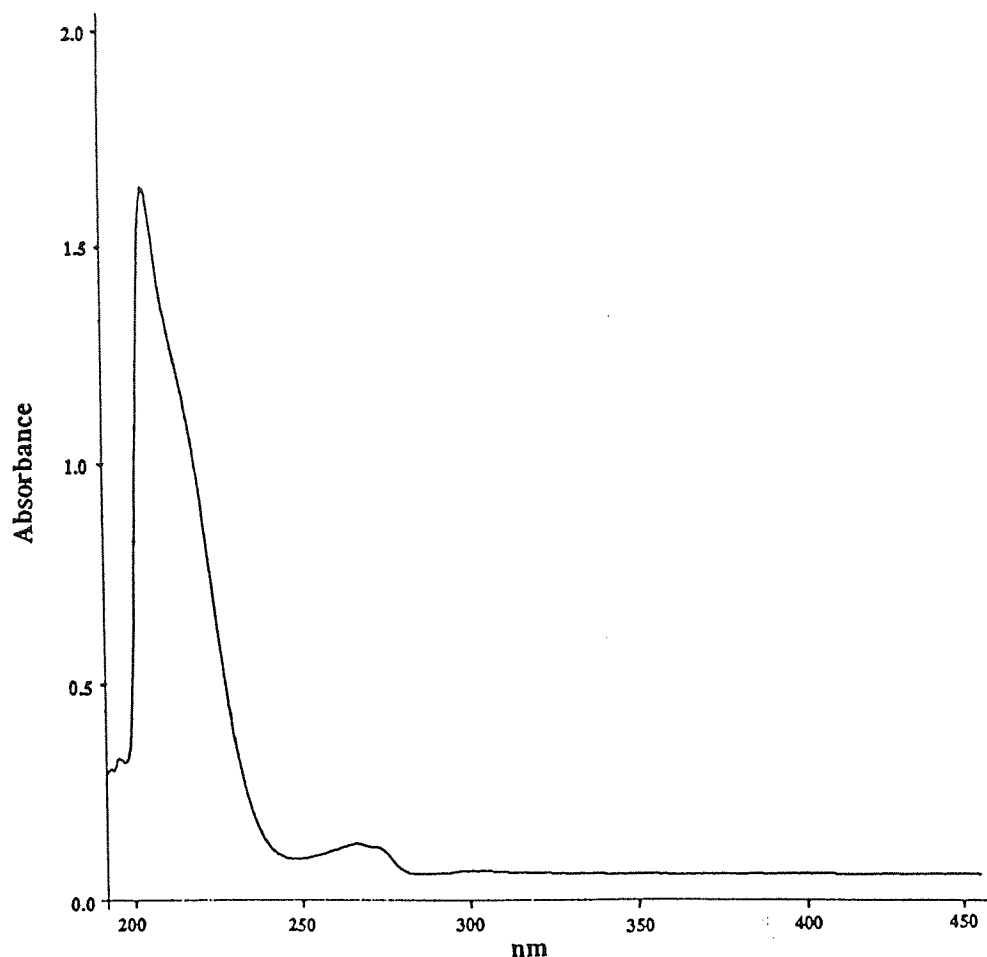


Figure 4.3: UV spectrum of ethyl *N*-[2'-(3',4''-dipivaloyloxyphenyl)-2'-hydroxyethyl]-3-aminopropionate (107) in chloroform (190-450 nm).

4.5.2 Choice of stationary phase

Analytical separations were performed by HPLC using a stainless steel column packed with 5 μ m Hypersil-ODS reversed-phase material. The hydrophobic alkyl-bonded phase permits the use of highly polar mobile phases. The surface silanol groups are modified with hydrocarbon derivatives to yield a non-polar surface coating. This process is termed reversed-phase chromatography and enables the separation of polar compounds which would not be eluted from normal phase systems. The octadecylsilane (ODS-C₁₈) bonded phase is probably the most widely used.

Silica-based bonded phases are prone to degradation at extreme pH's. Consequently, they were operated between the suggested guidelines of pH 2.5 and 7.0. At low pH values (pH < 2.5) there may be loss of bonded phase, whereas at higher pH values (pH > 7) the silica particles are prone to dissolution.

4.5.3 Choice of mobile phase

The soft-drugs and their analogues contain amino groups in the structure which give broad tailing peaks. This was dramatically improved by the addition of diethylamine (0.1% v/v) to the mobile phase at pH 3.0. Adjusting the mobile phase to pH =3 ensures that the samples are in a protonated form and added base reduces acidic and basic silanol interactions. Consequently, all mobile phases were acidified to a pH 3.0 with orthophosphoric acid to improve chromatography.

The prodrug (**107**) gave a very long retention time with a broad peak. Chromatography was improved by the addition of tetrabutylammonium hydroxide (0.1% v/v), which decreased the retention time and sharpened the peak. The strong base interacts with the polar regions of the silica and allows the amine to elute quickly, therefore the retention time of the amine decreases and the peak is sharpened.

Dissolved gases can cause deterioration in chromatography by degassing in the detector flow-cell or by the formation of UV-absorbing complexes with solvents.¹²¹ To minimise these problems, mobile phases were degassed by vacuum filtration or sonication prior to HPLC analyses.

4.5.4 Analysis of soft-drugs, their prodrugs and their analogues

The soft β -adrenoceptor agonists and their analogues used in this work were generally analysed using mobile phases consisting of varying concentrations of acetonitrile in distilled water and 0.1% diethylamine or 0.1% tetrabutylammonium hydroxide, adjusted to a final pH of 3.0 with orthophosphoric acid. A flow rate of 1 ml min^{-1} was employed and the column eluant was usually measured spectrophotometrically at 210 nm. Sample injection volumes were typically 10 μl but were increased up to 100 μl according to the specific experimental conditions. Similarly, sensitivity settings ranged from 0.08 to 1.28 AUFS.

During the development of suitable systems for these compounds, the effect of varying acetonitrile concentrations (4-30%) on their retention time and resolution was investigated. Examples of the resulting chromatograms for soft-drugs (**74**, R= Et, Pr), pro-soft-drug (**107**) and their analogues (**50**, R= Et, Me) are shown in Figures 4.4, 4.5, 4.6, 4.8, and 4.10. Calculations of resolution (R_S) between adjacent peaks, values of t_R , k' , N and H quantifying the chromatographic efficiency of these systems are summarised in Tables 4.2, 4.3, 4.5, 4.7, and 4.9. The values of these parameters were useful indicators in choosing a mobile phase for the compounds.

The final selection of a solvent system was also dependent on the specific experimental conditions which determined whether a particular substance was to be analysed separately or in conjunction with other analogues, metabolites, degradation or reaction products. Subtle variations in the column performance amongst different columns were also occasionally noticeable; these occurred rarely and were usually negligible. However, analysis of compounds with capacity factors close to 1 or those resolving close to other peaks sometimes necessitated minor changes in the solvent composition with different columns for efficient chromatography. As a result of these factors, different mobile phases were employed for analysis of the same compound (e.g., prodrug, **107**) under varying test procedures. The solvent systems and conditions used for these compounds are summarised in Table 4.11.

In these instances, the highest acetonitrile concentration which could be employed was 30%, allowing sufficient resolution of prodrug (**107**) from intermediate (*N*-[2'-(3",4"-dipivaloyloxyphenyl)-2'-hydroxyethyl]-3-aminopropionic acid, (**120**) and *N*-[2'-(3",4"-dihydroxyphenyl)-2'-hydroxyethyl]-3-aminopropionic acid (**74**, R=H) (see chapter six, Section 6.1). In contrast, the soft-drug (**74**, R=Et) and its analogues were analysed using a mobile phase with a lower acetonitrile content of 4% v/v. Quantification of sample peak responses was achieved by way of calibration measurements. These were performed for the test compounds during each assay procedure, under the conditions of that particular experiment and in an appropriate concentration range. The validity of this technique was assessed by examining the linearity of the calibration curve of peak height against compound concentration.

4.5.4.1 Choice of mobile phase for alkyl *N*-(2'-hydroxy-2'-phenylethyl)-3-aminopropionates (**50**, R= Et, Me)

Mobile phase using methanol:

A series of mobile phases with 30, 40 and 50% of methanol in distilled water were prepared, with 0.1% diethylamine and the pH adjusted to 3.0 with orthophosphoric acid. The values of t_R , k' , N , H and resolution (R_S) between adjacent peaks quantifying the chromatographic efficiency of these systems are summarised in Table 4.1. It was found that 30% methanol in water is a satisfactory mobile phase for methyl *N*-(2'-hydroxy-2'-phenylethyl)-3-aminopropionate (**50**, R= Me) with a retention time of 4.1 min (Table 4.2). 40% Methanol in water is appropriate for ethyl *N*-(2'-hydroxy-2'-phenylethyl)-3-aminopropionate (**50**, R= Et) with a retention time of 7.0 min (Table 4.2). The HPLC chromatogram of ethyl *N*-(2'-hydroxy-2'-phenylethyl)-3-aminopropionate (**50**, R= Et) and methyl *N*-(2'-hydroxy-2'-phenylethyl)-3-aminopropionate (**50**, R= Et) are shown in Figures 4.4 and 4.5 respectively.

$ \begin{array}{c} \text{OH} \\ \\ \text{C}_6\text{H}_5 - \text{C} - \text{CH}_2 - \text{NH} - \text{CH}_2 - \text{CH}_2 - \text{COO-R} \\ \\ \text{H} \end{array} $ (50)						
Compounds	MeOH (%)	t_R (min)	k'	N (m^{-1})	H (μm)	R_s from Acid (R=H)
Methyl ester (50, R= Me)	30	4.1	1.93	332	301	1.86
	40	3.2	1.28	113	885	0.67
Ethyl ester (50, R= Et)	30	7.0	4.0	306	327	4.0
	40	4.2	2.0	282	354	2.88
Acid (50, R= H)	30	2.8	1.0	502	200	-
	40	2.4	0.71	1475	68	-

Table 4.2: Chromatographic data for ethyl *N*-(2'-hydroxy-2'-phenylethyl)-3-aminopropionate (50, R= Et) and methyl *N*-(2'-hydroxy-2'-phenylethyl)-3-aminopropionate (50, R= Me) in 30 and 40% methanol in water mobile phase. Flow rate is 1 ml min^{-1} .

With high concentrations of methanol, peaks are broad with tailing; this was avoided by using acetonitrile, which can be used in lower concentrations.

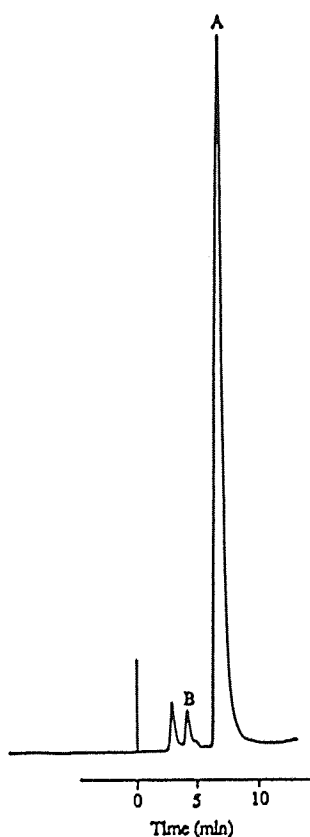


Figure 4.4: HPLC chromatogram of [A= ethyl *N*-(2'-hydroxy-2'-phenylethyl)-3-aminopropionate (50, R= Et)] in 40% methanol in water mobile phase [B= acid; (50, R= H)].

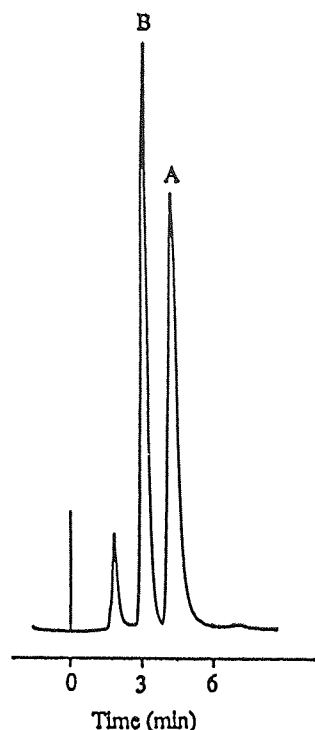


Figure 4.5: HPLC chromatogram of [A= methyl *N*-(2'-hydroxy-2'-phenylethyl)-3-aminopropionate (**50**, R= Me)] in 30% methanol in water mobile phase [B= acid; (**50**, R= H)].

Mobile phase using acetonitrile:

A series of mobile phases with 10, 15 and 20% acetonitrile in water were prepared, with 0.1% diethylamine and the pH adjusted to 3.0 with orthophosphoric acid. Acetonitrile (15%) in water was found to be the best mobile phase for ethyl *N*-(2'-hydroxy-2'-phenylethyl)-3-aminopropionate (**50**, R= Et) with t_R 8.8 min [t_R acid (R= H), 1.6 min] and resolution between the ester and the acid is $R_S = 5.54$ (Table 4.3). The HPLC traces of ethyl *N*-(2'-hydroxy-2'-phenylethyl)-3-aminopropionate (**50**, R= Et) are shown in Figure 4.7.

$\text{C}_6\text{H}_5-\underset{\text{H}}{\overset{\text{OH}}{\text{C}}}-\text{CH}_2-\text{NH}-\text{CH}_2-\text{CH}_2-\text{COO}-\text{R}$ <div style="text-align: right;">(50)</div>						
Compounds	W_A (min)	t_R (min)	k'	N (m^{-1})	H (μm)	R_S from Acid (R= H)
Ethyl ester (50 , R= Et)	2.2	8.8	5.7	2,560	40	5.54
Acid (50 , R= H)	0.4	1.6	0.2	2,560	40	

Table 4.3: Chromatographic data for ethyl *N*-(2'-hydroxy-2'-phenylethyl)-3-aminopropionate (**50**, R= Et) and acid (**50**, R= H) in 15% acetonitrile in water mobile phase. Flow rate is 1 ml min^{-1} .

A calibration graph was plotted with different concentrations of ethyl *N*-(2'-hydroxy-2'-phenylethyl)-3-aminopropionate (**50**, R= Et) against peak height; the graph was linear ($R^2=0.997$) and calibration statistics are shown in Table 4.4 and Figure 4.6.

Concentration (μM)	Mean peak height (cm)	Standard deviation (σ_{n-1})	Coefficient of variation (cv%)
210.7	24.92	0.104	0.418
189.6	21.57	0.076	0.354
168.6	20.02	0.076	0.382
147.5	17.17	0.076	0.445
126.4	15.63	0.076	0.489
105.4	12.30	0.050	0.407
84.3	10.32	0.126	1.219
63.2	7.18	0.076	1.064
42.1	5.22	0.104	1.994
21.1	2.52	0.076	3.031

Table 4.4: Statistical data for ethyl *N*-(2'-hydroxy-2'-phenylethyl)-3-aminopropionate (**50**, R=Et), showing standard deviation and coefficient of variation in calibration curve ($n=3$).

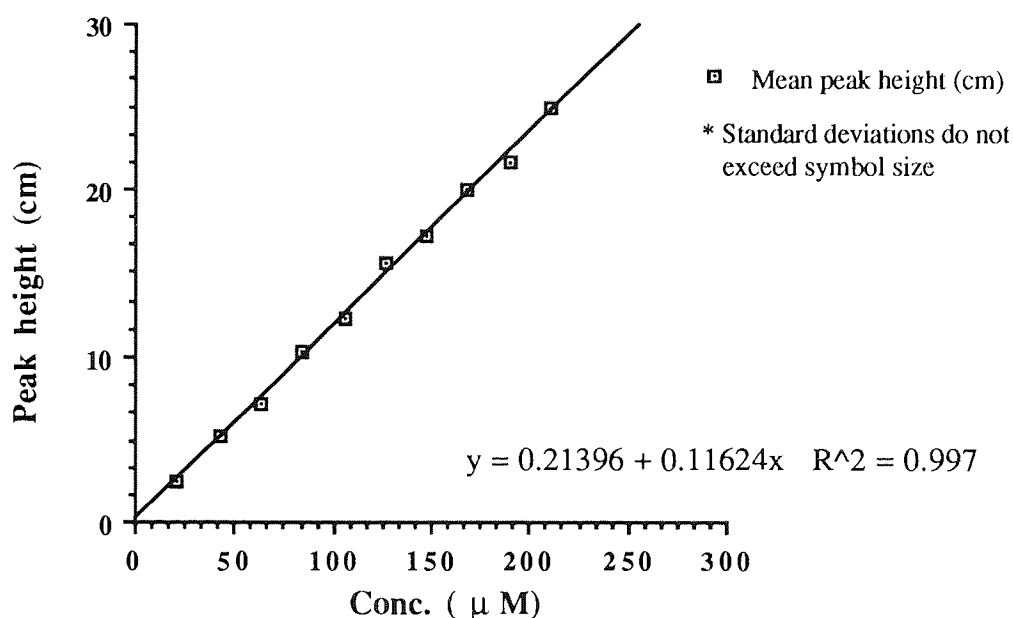


Figure 4.6: Calibration graph for ethyl *N*-(2'-hydroxy-2'-phenylethyl)-3-aminopropionate (**50**, R=Et) in 15% acetonitrile in water mobile phase.

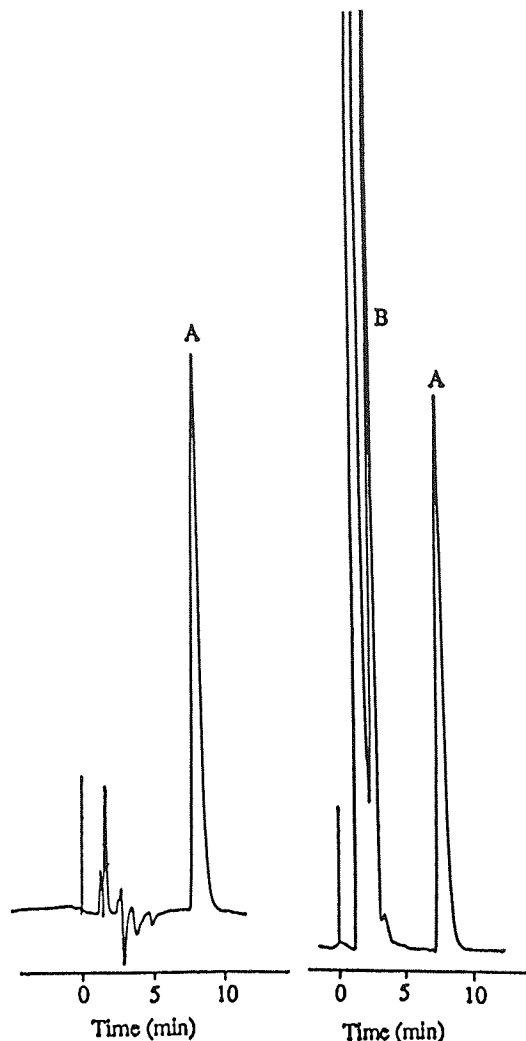


Figure 4.7: HPLC chromatogram of ethyl *N*-(2'-hydroxy-2'-phenylethyl)-3-aminopropionate (**50**, R=Et) in 15% acetonitrile in water mobile phase [B= acid; (**50**, R= H)].

4.5.4.2 Choice of mobile phase for ethyl *N*-[2'-(3'',4''-dihydroxyphenyl)-2'-hydroxyethyl]-3-aminopropionate (**74**, R= Et)

A series of mobile phases with 4, 5, 10, 15 and 20% acetonitrile in water were prepared, with 0.1% diethylamine and the pH adjusted to 3.0 with orthophosphoric acid. Acetonitrile (4%) in water was found to be the best mobile phase for ethyl *N*-[2'-(3'',4''-dihydroxyphenyl)-2'-hydroxyethyl]-3-aminopropionate (**74**, R= Et) with t_R 8.8 min [t_R acid (R= H), 2.4 min] and the resolution R_S (ester : acid)= 4.92 (Table 4.5). The HPLC traces of ethyl *N*-[2'-(3'',4''-dihydroxyphenyl)-2'-hydroxyethyl]-3-aminopropionate (**74**, R= Et) are shown in Figure 4.8.

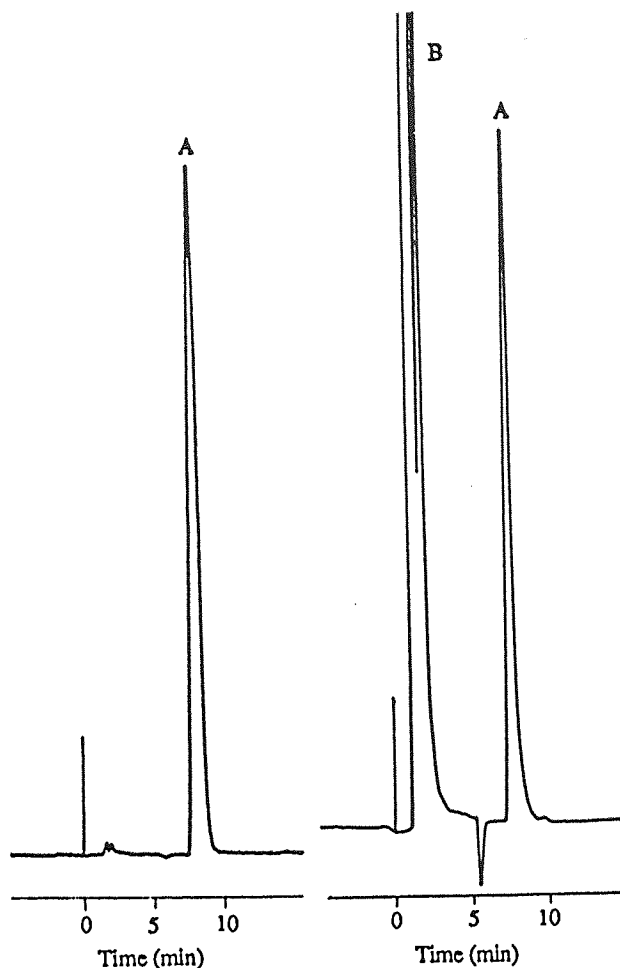


Figure 4.8: HPLC chromatogram of [A= ethyl *N*-[2'-(3",4"-dihydroxyphenyl)-2'-hydroxyethyl]-3-aminopropionate (**74**, R= Et)] in 4% acetonitrile mobile phase [B= acid; (**74**, R= H)].

$ \begin{array}{c} \text{HO} \\ \\ \text{HO}-\text{C}_6\text{H}_3-\text{C}-\text{CH}_2-\text{NH}-\text{CH}_2-\text{CH}_2-\text{COO-R} \\ \\ \text{H} \end{array} $ (74)						
Compound	W_A (min)	t_R (min)	k'	N (m^{-1})	H (μm)	R_S from Acid (R=H)
Ethyl ester (74 , R= Et)	2.2	8.8	4.5	2,560	40	4.92
Acid (74 , R= H)	0.8	2.4	0.5	2,560	40	

Table 4.5: Chromatographic data for ethyl *N*-[2'-(3",4"-dihydroxyphenyl)-2'-hydroxyethyl]-3-aminopropionate (**74**, R= Et) in 4% acetonitrile mobile phase.
Flow rate is 1 ml min^{-1} .

A calibration graph was plotted with different concentrations (20-175 μM) of ethyl *N*-[2'-(3",4"-dihydroxyphenyl)-2'-hydroxyethyl]-3-aminopropionate (**74**, R= Et) against peak height and the graph was linear ($R^2=0.999$). Calibration statistics are shown in Table 4.6 and Figure 4.9.

Concentration (μM)	Mean peak height (cm)	Standard deviation (σ_{n-1})	Coefficient of variation (cv%)
176.6	21.97	0.205	0.934
157.0	19.53	0.247	1.263
137.4	17.56	0.093	0.529
117.7	15.02	0.104	0.693
98.1	12.65	0.061	0.483
78.5	10.16	0.093	0.915
58.9	7.75	0.061	0.788
39.3	5.34	0.140	2.622
19.6	2.29	0.042	1.818

Table 4.6: Statistical data for ethyl *N*-[2'-(3",4"-dihydroxyphenyl)-2'-hydroxyethyl]-3-aminopropionate (74, R= Et), showing standard deviation and coefficient of variation in calibration curve (n=3).

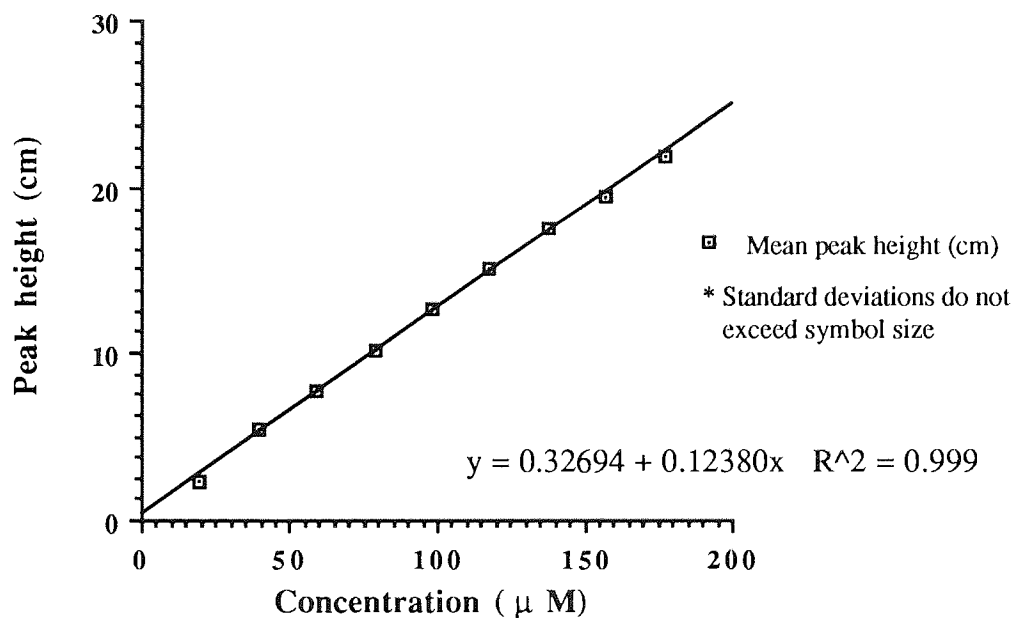


Figure 4.9: Calibration graph for ethyl *N*-[2'-(3",4"-dihydroxyphenyl)-2'-hydroxyethyl]-3-aminopropionate (74, R= Et) in 4% acetonitrile in water mobile phase.

4.5.4.3 Choice of mobile phase for ethyl *N*-[2'-(3'',4''-dipivaloyloxyphenyl)-2'-hydroxyethyl]-3-aminopropionate (**107**)

Ethyl *N*-[2'-(3'',4''-dipivaloyloxyphenyl)-2'-hydroxyethyl]-3-aminopropionate (**107**) and intermediates *N*-[2'-(3'',4''-dipivaloyloxyphenyl)-2'-hydroxyethyl]-3-aminopropionic acid (**120**), ethyl *N*-[2'-(3'',4''-dihydroxyphenyl)-2'-hydroxyethyl]-3-aminopropionate (**74**, R=Et) and dihydroxy acid (**74**, R=H) could not be monitored simultaneously due to large differences in polarity of the compounds (Chapter five, Section 5.3.7). Despite manipulation of the mobile phase with ion-pairing agents, the retention times of the polar ethyl *N*-[2'-(3'',4''-dihydroxyphenyl)-2'-hydroxyethyl]-3-aminopropionate (**74**, R=Et) and *N*-[2'-(3'',4''-dihydroxyphenyl)-2'-hydroxyethyl]-3-aminopropionic acid (**74**, R=H) could not be increased sufficiently to allow separation from the solvent front, whilst maintaining acceptable chromatography of the better retained and late-eluting triester (**107**). The mobile phase consisting of 30% acetonitrile in water with 0.1% v/v tetrabutylammonium hydroxide, adjusted to pH 3.0 with orthophosphoric acid was used to separate triester (**107**) and dipivaloyl acid (**120**) from ethyl *N*-[2'-(3'',4''-dihydroxyphenyl)-2'-hydroxyethyl]-3-aminopropionate (**74**, R=Et) and dihydroxy acid (**74**, R=H). The retention time for triester (**107**) was 9.4 min and that for dipivaloyl acid (**120**), 5.4 min. The resolution R_S [triester (**107**) : dipivaloyl acid (**120**)] was 1.54 (Table 4.7). The HPLC trace of ethyl *N*-[2'-(3'',4''-dipivaloyloxyphenyl)-2'-hydroxyethyl]-3-amino propionate (**107**) is shown in Figure 4.10.

A mobile phase comprising 4% acetonitrile in water with 0.1% v/v diethylamine, adjusted to pH 3.0 with orthophosphoric acid was used to separate ethyl *N*-[2'-(3'',4''-dihydroxyphenyl)-2'-hydroxyethyl]-3-aminopropionate (**74**, R=Et) and dihydroxy acid (**74**, R=H) which are formed from the hydrolysis of triester (**107**).

Compound	W_A (min)	t_R (min)	k'	N (m^{-1})	H (μm)	R_S from Dipivaloyl acid (R= H)
Triester (107 , R= Et)	3.6	9.4	5.96	1,091	91	1.54
Dipivaloyl acid (120)	1.6	5.4	3.0	1,823	55	

Table 4.7: Chromatographic data for ethyl *N*-[2'-(3'',4''-dipivaloyloxyphenyl)-2'-hydroxyethyl]-3-aminopropionate (**107**) in 30% acetonitrile in water mobile phase. Flow rate is 1 ml min^{-1} .

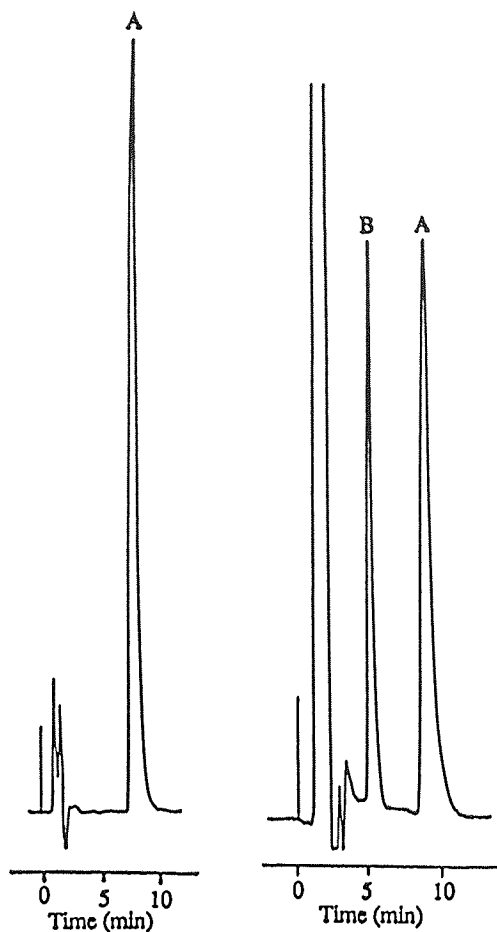


Figure 4.10: HPLC chromatogram of [A= ethyl *N*-[2'-(3'',4''-dipivaloyloxyphenyl)-2'-hydroxyethyl]-3-aminopropionate (**107**)] in 30% acetonitrile mobile phase [B=dipivaloyl acid; (**120**, R= H)].

A calibration graph was plotted with different concentrations (5-120 μM) of ethyl *N*-[2'-(3'',4''-dipivaloyloxyphenyl)-2'-hydroxyethyl]-3-aminopropionate (**107**) against peak height. The graph was linear ($R^2=0.997$) and calibration statistics are shown in Table 4.8 and Figure 4.11.

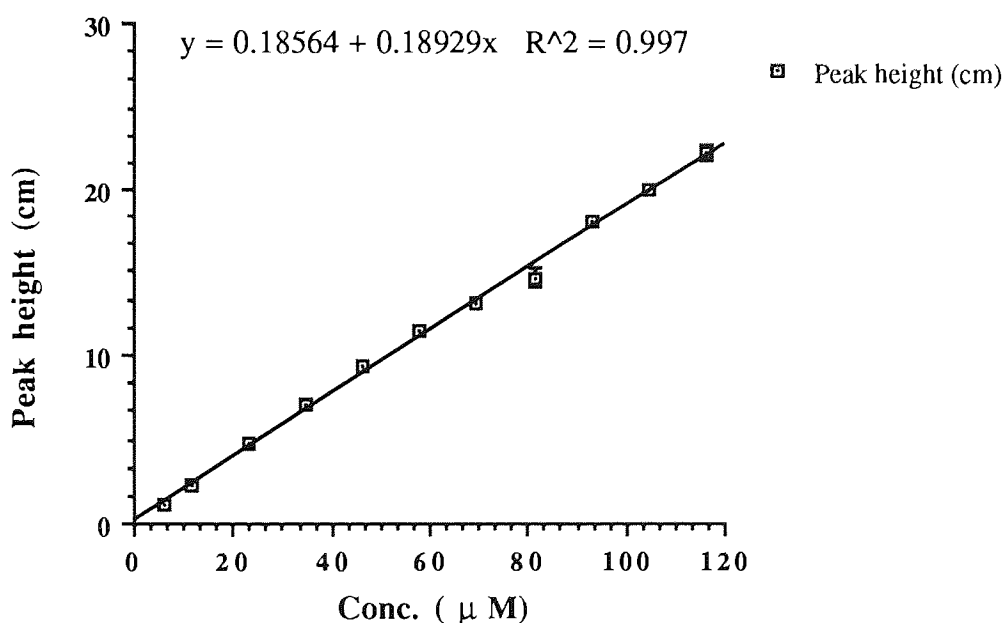


Figure 4.11: Calibration graph for ethyl *N*-[2'-(3'',4''-dipivaloyloxyphenyl)-2'-hydroxyethyl]-3-aminopropionate (**107**) in 30% acetonitrile in water mobile phase.

Concentration (μM)	Mean peak height (cm)	Standard deviation (σ_{n-1})	Coefficient of variation (cv%)
116.0	22.30	0.436	1.955
104.4	20.03	0.208	1.039
92.8	18.03	0.379	2.100
81.2	14.67	0.503	3.431
69.6	13.07	0.643	4.919
58.0	11.50	0.265	2.301
46.4	9.27	0.153	1.648
34.8	7.03	0.153	2.173
23.2	4.72	0.076	1.618
11.6	2.25	0.050	2.222
5.8	1.08	0.029	2.673

Table 4.8: Statistical data for ethyl *N*-[2'-(3",4"-dipivaloyloxyphenyl)-2'-hydroxyethyl]-3-aminopropionate (**107**), showing standard deviation and coefficient of variation in calibration curve ($n=3$).

4.5.4.4 Choice of mobile phase for propyl *N*-[2'-(3",4"-dihydroxyphenyl)-2'-hydroxyethyl]-3-aminopropionate (**74**, $R= n\text{-Pr}$)

A series of mobile phases with 5, 10, 15 and 20% acetonitrile in water were prepared, with 0.1% diethylamine and the pH adjusted to 3.0 with orthophosphoric acid. Acetonitrile (10%) in water was found to be the best mobile phase for propyl *N*-[2'-(3",4"-dihydroxyphenyl)-2'-hydroxyethyl]-3-aminopropionate (**74**, $R= \text{Pr}$) with t_{R} 9.4 min. The t_{R} for the acid (**74**, $R=H$) was 1.6 min. The resolution R_{S} (ester : acid) was 4.33 (Table 4.9). The HPLC trace of propyl *N*-[2'-(3",4"-dihydroxyphenyl)-2'-hydroxyethyl]-3-amino propionate (**74**, $R= \text{Pr}$) is shown in Figure 4.12.

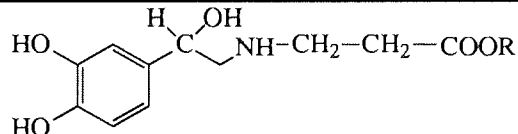
						
Compound	W_{A} (min)	t_{R} (min)	k'	N (m^{-1})	H (μm)	R_{S} from Acid ($R= H$)
Propyl ester (74 , $R= \text{Pr}$)	2.8	9.4	5.71	1,803	56	4.33
Acid (74 , $R= H$)	0.8	1.6	0.14	640	158	

Table 4.9: Chromatographic data for propyl *N*-[2'-(3",4"-dihydroxyphenyl)-2'-hydroxyethyl]-3-aminopropionate (**74**, $R= \text{Pr}$) in 10% acetonitrile in water. Flow rate is 1 ml min^{-1} .

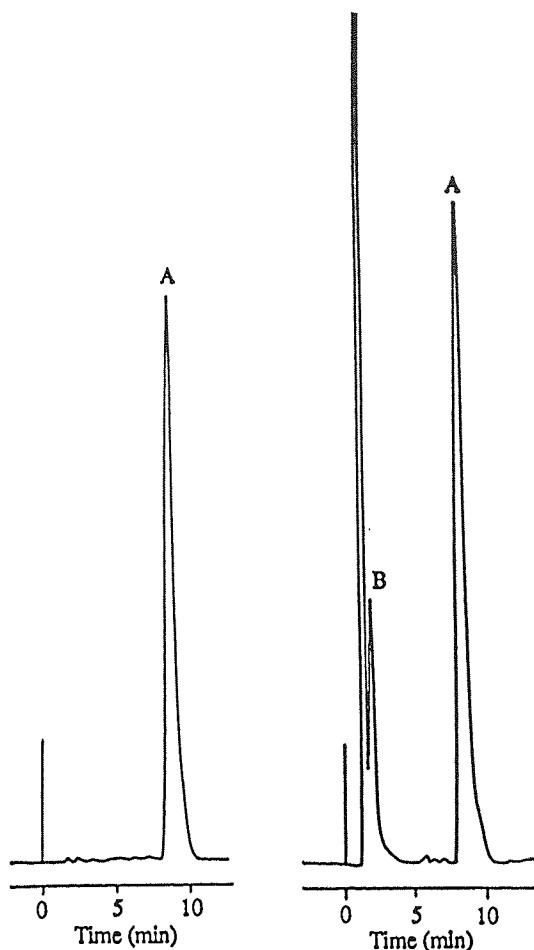


Figure 4.12: HPLC chromatogram of [A= propyl *N*-[2'-(3'',4''-dihydroxyphenyl)-2'-hydroxyethyl]-3-aminopropionate (**74**, R= Pr)] in 10% acetonitrile mobile phase [B= acid; (**74**, R= H)].

A calibration graph was plotted with different concentrations (20-190 μM) of propyl *N*-[2'-(3'',4''-dihydroxyphenyl)-2'-hydroxyethyl]-3-aminopropionate (**74**, R= Pr) against peak height. The graph was linear ($R^2=0.999$) and calibration statistics are shown in Table 4.10 and Figure 4.13.

Concentration (μM)	Mean peak height (cm)	Standard deviation (σ_{n-1})	Coefficient of variation (cv%)
190.8	23.58	0.104	0.441
171.7	21.30	0.050	0.235
152.6	19.15	0.150	0.783
133.5	17.10	0.132	0.774
114.5	14.72	0.093	0.631
76.3	10.35	0.100	0.968
57.2	8.00	0.090	1.120
38.2	5.49	0.036	0.657
19.1	2.87	0.031	1.064

Table 4.10: Statistical data for propyl *N*-[2'-(3'',4''-dihydroxyphenyl)-2'-hydroxyethyl]-3-aminopropionate (**74**, R= Pr), showing standard deviation and coefficient of variation in calibration curve ($n=3$).

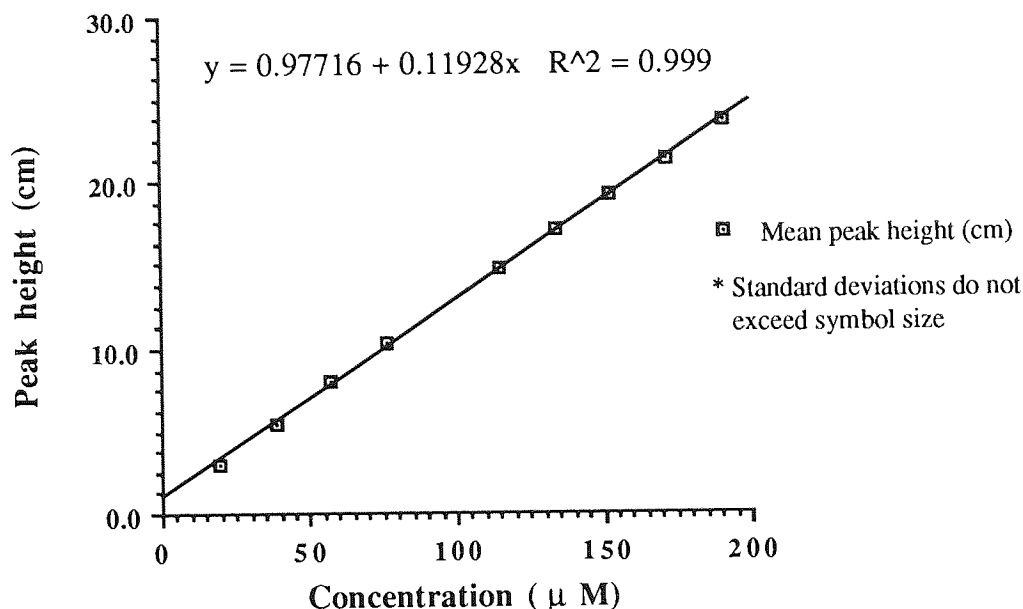


Figure 4.13: Calibration graph for propyl *N*-[2'-(3',4''-dihydroxyphenyl)-2'-hydroxyethyl]-3-aminopropionate (74, R= Pr) in 10% acetonitrile in water.

4.6 SUMMARY

Suitable reversed-phase HPLC methods for the assay of the compounds under study were developed. These enabled sensitive and specific analysis under a range of experimental conditions, allowing separation of compounds from their hydrolysis products and subsequent quantification. These methods, as techniques for quantitative analysis, were validated in terms of linearity of calibration plots with respect to analyte concentration. The linear regression correlation coefficients (R^2) of these plots were determined to be ≥ 0.997 , thus validating the assay procedure for each compound. The different solvent systems used for soft β -adrenoceptor agonist, prodrug of soft β -adrenoceptor agonist and their analogues are summarised in Table 4.11.

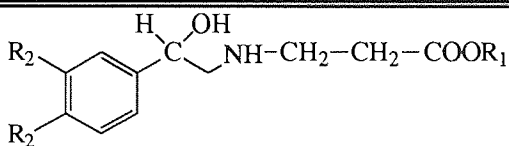
			
Compounds	Mobile phase	Sensitivity (AUFS)	Retention time (t_R) (min)
Methyl ester (50) ($R_1 = \text{Me}$, $R_2 = \text{H}$)	30% CH_3OH / water with 0.1% diethylamine and pH adjusted to 3.0 with orthophosphoric acid	0.16	t_R (ester)= 4.1 min t_R [acid, ($R_1 = R_2 = \text{H}$)]= 2.8 min
Ethyl ester (50) ($R_1 = \text{Et}$, $R_2 = \text{H}$)	15% CH_3CN / water with 0.1% diethylamine and pH adjusted to 3.0 with orthophosphoric acid	0.16	t_R (ester)= 8.8 min t_R [acid, ($R_1 = R_2 = \text{H}$)]= 1.6 min
Dihydroxy ethyl ester (74) ($R_1 = \text{Et}$, $R_2 = -\text{OH}$)	4% CH_3CN / water with 0.1% diethylamine and pH adjusted to 3.0 with orthophosphoric acid	0.16	t_R (ester)= 8.8 min t_R [acid, ($R_1 = \text{H}$, $R_2 = \text{OH}$)]= 2.4 min
Dihydroxy propyl ester (74) ($R_1 = \text{Pr}$, $R_2 = -\text{OH}$)	10% CH_3CN / water with 0.1% diethylamine and pH adjusted to 3.0 with orthophosphoric acid	0.32	t_R (ester)= 9.4 min t_R [acid, ($R_1 = \text{H}$, $R_2 = \text{OH}$)]= 1.6 min
Dipivaloyl ethyl ester (107) [$R_1 = \text{Et}$, $R_2 = -\text{OCOC}(\text{CH}_3)_3$]	30% CH_3CN / water with 0.1% tetrabutyl ammonium hydroxide and pH adjusted to 3.0 with orthophosphoric acid.	0.16	t_R (ester)= 9.4 min t_R [acid, ($R_1 = \text{H}$, $R_2 = -\text{OCOC}(\text{CH}_3)_3$)]= 5.4 min

Table 4.11: HPLC solvent systems used for soft β -adrenoceptor agonist, prodrug of soft β -adrenoceptor agonist and their analogues.
Loop size in all experiments is 20 μl .

CHAPTER FIVE

DEGRADATION KINETICS OF SOFT β -ADRENOCEPTOR AGONISTS

5.1 INTRODUCTION

As β -agonists are known to possess anti-inflammatory and anti-proliferative properties, a therapeutic benefit in inflammatory dermatitis of an acute or chronic nature, and in inflammatory proliferative disease such as psoriasis, could be anticipated. For a β -adrenoceptor agonist to be useful clinically in the treatment of inflammatory and proliferative skin disease, it is a pre-requisite that activity be restricted to the percutaneous layers, and that no untoward cardiovascular effects occur as a consequence of systemic absorption.

The 'soft-drug' approach to drug design, as discussed earlier (Section 1.4.3, page 59), involves the predictable *in vivo* detoxification of an active drug after therapeutic activity, in order to minimize systemic toxicity. In contrast, the prodrug concept involves the controlled *in vivo* bioactivation of a previously inactive species, prior to eliciting a pharmacological response.⁸⁷

Esterification is commonly the means used to modify the lipophilicity of drug derivatives, thereby furnishing a prodrug which has ideal characteristics for partitioning into the stratum corneum and which therefore permeates the skin more readily than the parent drug. Reversion to the parent drug is facilitated by enzyme-catalysed ester cleavage, a process which can exploit the significant metabolic capacity of the skin.^{122,123} The presence of carboxylic acid and hydroxyl groups in drug molecules, together with the abundance of cutaneous hydrolytic enzymes, makes esterification an excellent prodrug type for the dermal delivery of many drugs.

Although esterification is perhaps the most common form of prodrug derivatization, it is by no means exhaustive. The skin is recognised as a highly active metabolic organ and cutaneous enzymes other than esterases, which can metabolize a wide range of endogenous and exogenous substances have been identified.^{124,125,126} Consequently, enzyme-labile derivatives other than esters, which are able to utilize this vast range of cutaneous enzyme activities for bioactivation have been considered.¹²⁷ A variety of topical drugs have been the subject of such prodrug modifications in order to improve their penetration profile and/or localize drug action within the skin (Table 5.1).

Taking this idea into consideration, soft-drugs (**74**, R= Me, Et) were synthesized as potential antipsoriatic agents. Such soft-drugs (**74**) are hydrophilic and may be expected to show poor penetration across the membrane (see Chapter seven, Section 7.3.1), therefore lipophilic pro-soft-drugs (**107**) have been synthesized.

Bio-conversion mechanism/Parent drug	Prodrug derivatives	Therapeutic use
Chemical hydrolysis		
5-Fluorouracil	<i>N</i> -Mannich bases	Psoriasis ^{128,129}
Indomethacin	<i>N,N</i> -Dialkylhydroxy amine deriv.	Anti-inflammatory ¹³⁰
6-Mercaptopurine	<i>N</i> -Mannich bases	Psoriasis ¹³¹
Theophylline	<i>N</i> -Mannich bases	Psoriasis ¹²⁸
Enzymatic hydrolysis		
Aspirin and salicylic acid	Methylthiomethyl and methylsulfinylmethyl esters	Anti-inflammatory _132,133
Diflurocortolone	Valerate ester	Anti-inflammatory ¹³⁴ Anti-proliferative ¹³⁵
Dithranol	Triacetate	Psoriasis ¹³⁶
5-Fluorouracil	<i>N</i> -Acyloxymethyl derivatives	Psoriasis ¹³⁷
Hydrocortisone	Spirothiazolidine derivatives	Anti-inflammatory ¹³⁸ Anti-proliferative ^{139,140}
6-Mercaptopurine	Bis(acyloxymethyl) derivatives	Psoriasis ¹⁴¹
6-Mercaptopurine	Acyloxymethyl derivatives	Psoriasis ¹⁴²
Metronidazole	Aliphatic esters	Anti-microbial ¹⁴³
Vidarabine	5'-Valerate ester	Anti-viral ^{144,145,146}
Vidarabine	5'-Monoesters	Anti-viral ¹⁴⁷
Enzymatic oxidation		
Theophylline	Acyloxymethyl derivatives	Psoriasis ¹⁴⁸
Enzymatic reduction		
Cromolyn	Pivaloyloxymethyl nitrate derivative	Anti-inflammatory ¹⁴⁹

Table 5.1: Examples of prodrugs developed for topical use.

In the context of present definitions of prodrug and soft-drug, the pivaloyl ester derivative (107) of (74) may be regarded as a pro-soft-drug designed to enhance the topical bioavailability of the parent drug. Figure 5.1 illustrates a simplified scheme for the postulated hydrolysis of the triester (107). It was found that k_1 is very high in the enzyme hydrolysis with PLCE and k_2 is very small or negligible ($k_1 \gg k_2$), whereas in chemical hydrolysis k_2 is very high compared to k_1 ($k_2 \gg k_1$) (see Chapter six, Section 6.4).

To meet our design constraints, the pro-soft-drug (A) is required to undergo hydrolysis to the soft-drug (B) after penetrating the epidermal barrier, a bioactivation process which should be facilitated in the presence of skin esterases. Metabolism of the active entity (B) to the inactive species (C) subsequent to exerting a pharmacological response is the next requirement. For this strategy to be satisfied, k_1 must be greater than k_2 , such that the dominant pathway follows the following kinetic model ($A \rightarrow B \rightarrow C$; $k_1 \gg k_2$) as in the enzyme hydrolysis, see Chapter Six, Section 6.4).

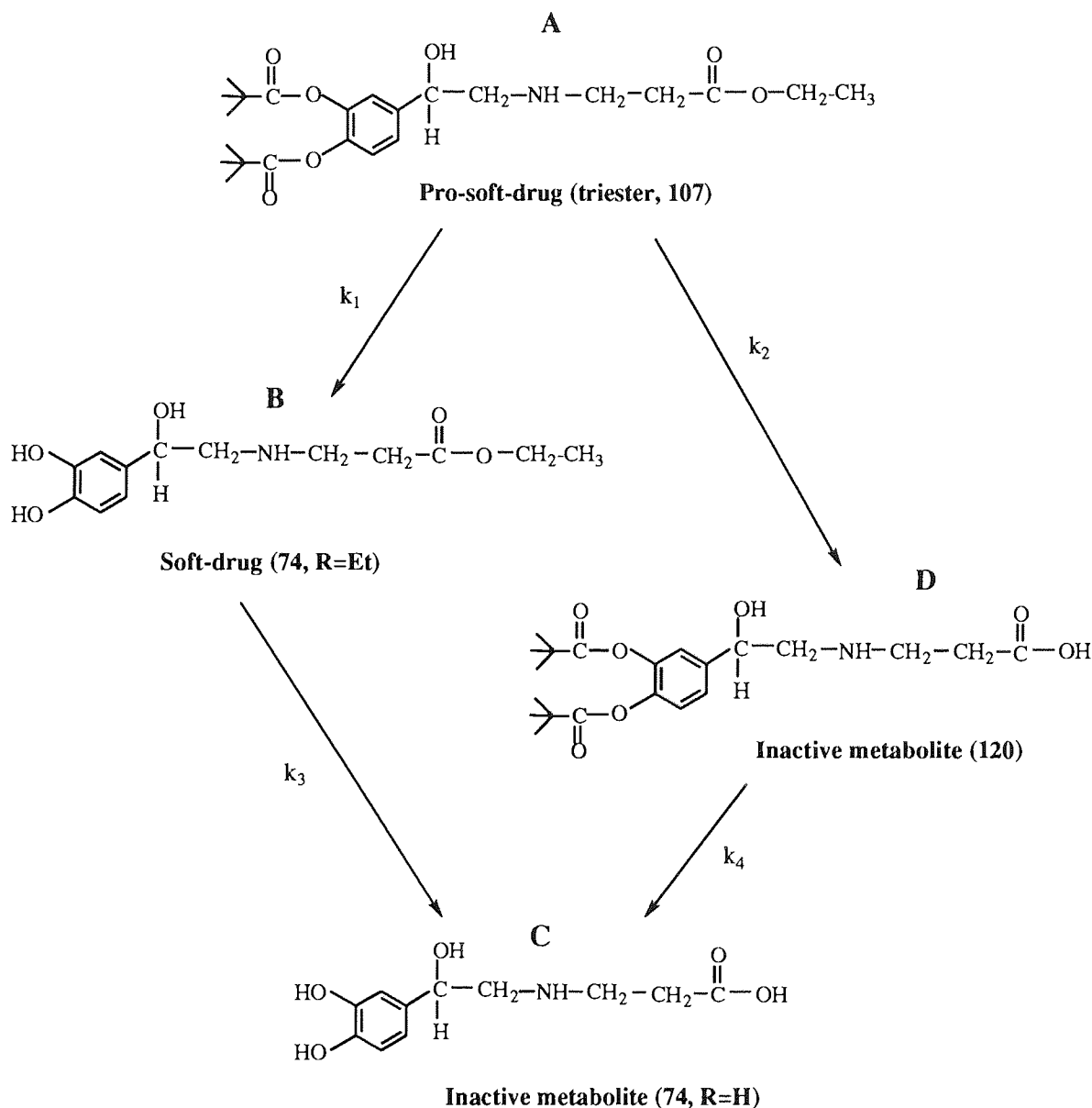


Figure 5.1: Postulated hydrolysis pathway of triester (107)

The complexity of this series of events, the progression of which is dependent upon a multitude of pharmacokinetic and physicochemical parameters involving drug (pro-soft-drug, soft-drug, metabolite), vehicle and membrane is self-evident. Theoretical studies, mathematically modelling the concurrent penetration and metabolism of drugs in the skin^{150,151,152} could serve to facilitate the rational evaluation of topical prodrug delivery in such instances. A prior understanding of the factors governing the transport and metabolism of biologically labile compounds is, however, a prerequisite.

In the current study, the ester soft-drug and prodrug of the β -adrenoceptor agonists and their analogues were investigated for susceptibility to chemical and enzymatic hydrolysis using *in vitro* models, namely isolated enzyme system, in order to assess their soft-drug and pro-soft-drug potential.

5.2 EXPERIMENTAL

5.2.1 Chemical hydrolysis of ethyl *N*-[2'-(3'',4''-dihydroxyphenyl)-2'-hydroxyethyl]-3-aminopropionate (74, R= Et), ethyl *N*-[2'-(3'',4''-dipivaloyloxyphenyl)-2'-hydroxyethyl]-3-aminopropionate (107) and the unsubstituted phenyl- analogue (50, R= Et) from pH 2.0-11.0 at 50 °C.

Chemical hydrolyses were conducted from pH 2.0 to 11.0 in phosphate-citrate buffer at 50 °C (pH-rate profile). Ethyl *N*-[2'-(3'',4''-dipivaloyloxyphenyl)-2'-hydroxyethyl]-3-aminopropionate (107) (50 μ g/ml solution) and unsubstituted phenyl- analogue (50, R=Et) require 10% acetonitrile in phosphate-citrate buffer to solubilize the esters. The hydrochloride salt of (74, R= Et) is freely soluble in phosphate-citrate buffer, therefore it does not require acetonitrile. Chemical hydrolysis of the soft-drug HCl (74, R= Et) and the pro-soft-drug (107) were also carried out at pH 7.4 at 37 °C to allow comparison with enzyme hydrolysis at 37 °C. The phosphate-citrate buffer from pH 2.0 to 8.0 were McIlvaine's buffer¹⁵³ (Appendix, Table 5.1A) and those at pH 9.0 and 10.0 were prepared with sodium carbonate and sodium-bicarbonate.¹⁵⁴ The final pH values are adjusted by the addition of phosphoric acid.

Samples (0.5 ml) are withdrawn at appropriate time intervals during the experiment and 20 μ l aliquots were analysed by HPLC. Concentrations of ester were calculated from a calibration line prepared from standards chromatographed under the same conditions.

5.2.2 Enzyme hydrolysis of ethyl *N*-[2'-(3",4"-dihydroxyphenyl)-2'-hydroxyethyl]-3-aminopropionate (**74**, R= Et) and ethyl *N*-[2'-(3",4"-dipivaloyloxyphenyl)-2'-hydroxyethyl]-3-aminopropionate (**107**) with porcine liver carboxyesterase at pH 7.4 at 37 °C.

The porcine liver carboxyesterase used in the hydrolysis studies was commercially available purified carboxylic ester hydrolase (from Sigma Chemicals), available as suspension in 3.2 M ammonium sulphate solution adjusted to pH 8.0. Each mg of protein was equivalent to 230 Units, where each unit was capable of hydrolysing 1 μ l of ethyl butyrate per minute at pH 8.0 and at 25 °C. The esterase solution contained 11.0 mg of protein per ml of solution and it was diluted as appropriate with distilled water, prior to use.

Reaction mixtures consisting of the esters are protection from light and air (under argon gas, because catechols can undergo oxidation) with constant stirring at 37 °C.

A reaction mixture consisting of 164.0 μ M ethyl *N*-[2'-(3",4"-dihydroxyphenyl)-2'-hydroxyethyl]-3-aminopropionate (**74**, R= Et) in 10 ml of phosphate-citrate buffer (pH 7.4) was maintained at 37 °C. The reaction was initiated by the addition of porcine liver carboxyesterase (i) 31 U (ii) 253 U which was previously incubated at 37 °C. Hydrolysis was monitored by HPLC (20 μ l sample being injected).

A reaction mixture consisting of 80.0 μ M ethyl *N*-[2'-(3",4"-dipivaloyloxyphenyl)-2'-hydroxyethyl]-3-aminopropionate (**107**) in 10 ml of phosphate-citrate buffer (pH 7.4) was maintained at 37 °C. Porcine liver carboxyesterase (i) 5.06 U (ii) 6.29 U was added to the reaction mixture and the reaction mixture was analysed by HPLC (20 μ l sample was injected).

In all experiments, 0.5 ml samples were withdrawn at appropriate time intervals during the experiment and were analysed by HPLC. The concentration of ester was calculated from a calibration line prepared from standards assayed under the same conditions. Experiments were performed in duplicate together with controls, omitting the esterase solutions.

5.2.3 Determination of dissociation constant (pK_a value) of ethyl *N*-[2'-(3'',4''-dipivaloyloxyphenyl)-2'-hydroxyethyl]-3-aminopropionate (107) and their analogues (50, R=Et, Me) by potentiometric titrations.

Initially, the pK_a of ephedrine HCl in water and 10% acetonitrile and of ephedrine base, in 10% acetonitrile in water, were determined as a check on method performance. Ephedrine HCl was dissolved in distilled water, the solution was then titrated with 0.1 M KOH (ephedrine base was titrated with 0.1 M HCl); the pH of the solution was determined by pH meter. Solutions were similarly prepared and titrated as follows:

Methyl *N*-(2'-phenyl-2'-hydroxyethyl)-3-aminopropionate HCl (50, 129.92 mg, R= Me) in 40 ml of distilled water was titrated with 0.1 M KOH.

Ethyl *N*-(2'-phenyl-2'-hydroxyethyl)-3-aminopropionate (50, 19.50 mg, R= Et) in 10 ml of distilled water was titrated with 0.1 M HCl.

Ethyl *N*-[2'-(3'',4''-dipivaloyloxyphenyl)-2'-hydroxyethyl]-3-aminopropionate HCl (107, 180.80 mg) in 22 ml of distilled water was titrated with 0.1 M KOH.

All end-points were determined potentiometrically.

5.2.4 Determination of degradation profile of ethyl *N*-[2'-(3'',4''-dipivaloyloxyphenyl)-2'-hydroxyethyl]-3-aminopropionate (107) in chemical [pD 8.57 (pH 8.17)] and enzyme medium (porcine liver carboxyesterase, pH 7.4) at 37 °C.

A reaction mixture consisting of 80.0 μ M ethyl *N*-[2'-(3'',4''-dipivaloyloxyphenyl)-2'-hydroxyethyl]-3-aminopropionate (107) in 10 ml of phosphate-citrate buffer (pH 7.4) was maintained at 37 °C. Porcine liver carboxyesterase 6.29 U was added to the reaction mixture and the reaction mixture was analysed by HPLC using a mobile phase of 30% acetonitrile in water. The same experiment was repeated using 4% acetonitrile in water as the mobile phase in order to identify the hydrolysis products.

5.3 RESULTS AND DISCUSSION

5.3.1 Chemical hydrolysis of ethyl *N*-(2'-hydroxy-2'-phenylethyl)-3-amino propionate (**50**, R= Et) in phosphate-citrate buffer containing 10% acetonitrile from pH 2.0 to 11.0 at 50 °C

Initially, the hydrolyses were conducted in phosphate-citrate buffer at pH 5.0 at 50 °C, however, a first-order kinetic model was not followed due to the poor solubility of the compound in phosphate-citrate buffer. Because the compound is lipophilic, it is not freely soluble and it exists as a suspension in the buffer; sampling errors caused much deviation (Figure 5.2).

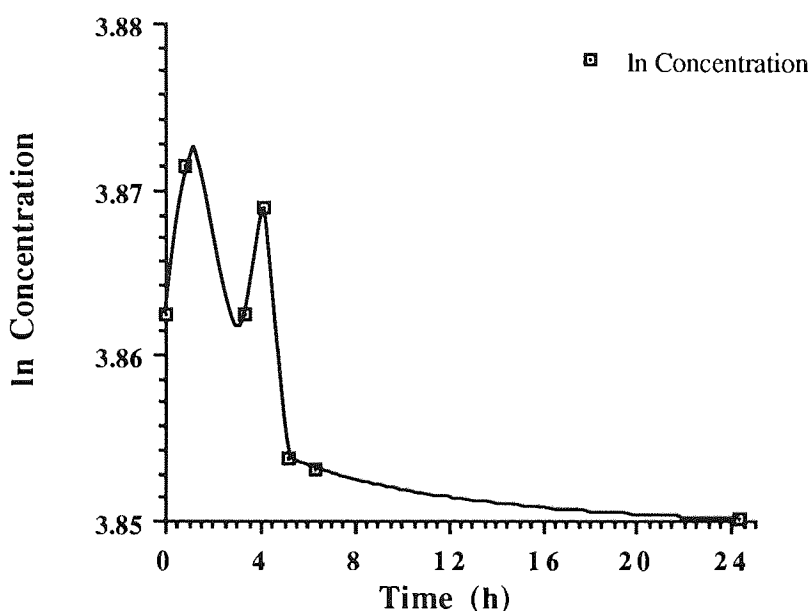


Figure 5.2: Chemical hydrolysis of ethyl *N*-(2'-hydroxy-2'-phenylethyl)-3-aminopropionate (**50**, R=Et) in phosphate-citrate buffer pH 5.0 without any co-solvent. The compound was not fully soluble in phosphate-citrate buffer.

To overcome this problem 10% acetonitrile was added as a co-solvent to solubilize the compound. Figure 5.3 shows the first-order plots of ethyl *N*-(2'-hydroxy-2'-phenylethyl)-3-amino propionate (**50**, R=Et), under the new conditions at different pH values at 50 °C; the pH rate-profile is shown in Figure 5.7 [A]. Hydrolysis of ethyl *N*-(2'-hydroxy-2'-phenylethyl)-3-amino propionate (**50**, R=Et) was acid-base catalysed. The pH rate-profile was U-shape, suggesting there is also a solvent catalytic effect. The ethyl *N*-(2'-hydroxy-2'-phenylethyl)-3-amino propionate (**50**, R=Et) was most stable at pH 4.1 with a half-life of 438 h. Rate constants and correlation coefficients at different pH values are shown in Table 5.2.

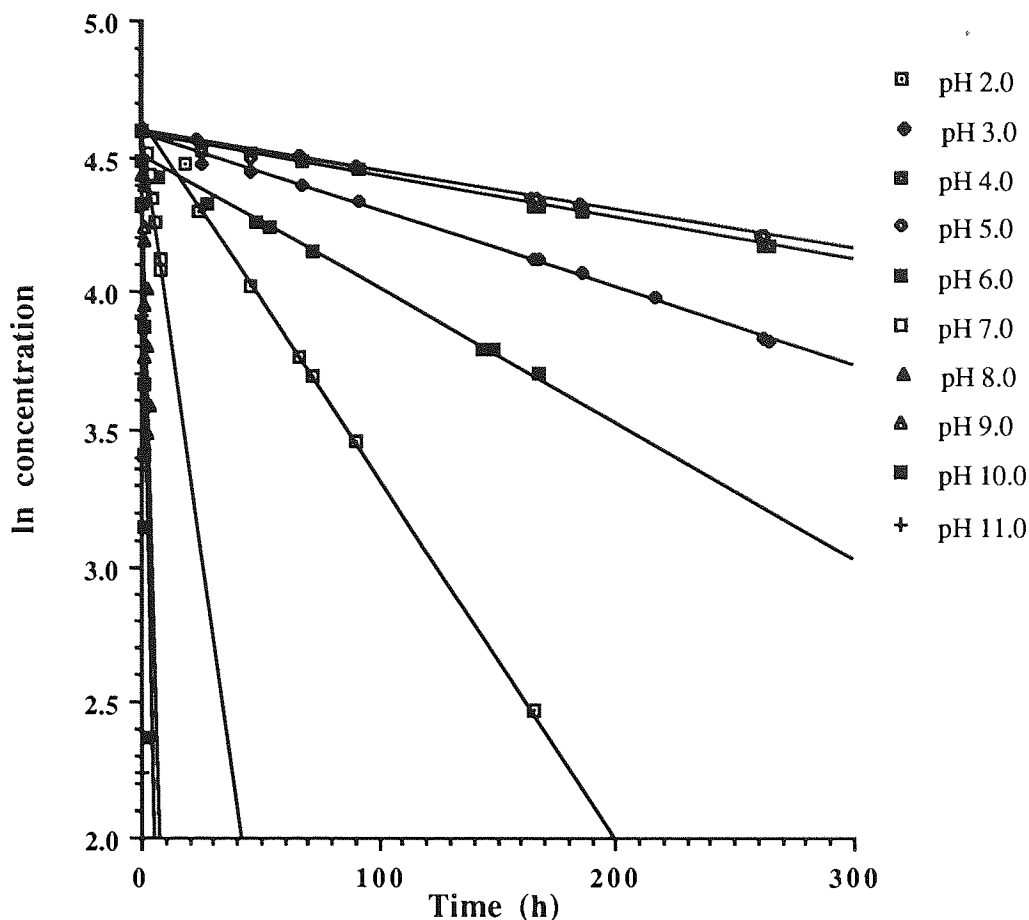


Figure 5.3: Chemical hydrolysis of ethyl *N*-(2'-hydroxy-2'-phenylethyl)-3-aminopropionate (**50**, R= Et) in phosphate-citrate buffer pH 2.0 to 11.0 in 10% acetonitrile in water at 50 °C.

pH	First Experiment			Second Experiment		
	k (h ⁻¹)	cc (r ²)	log k	k (h ⁻¹)	cc (r ²)	log k
2.0	0.0119	0.999	-1.9242	0.0112	0.996	-1.9512
3.0	0.0028	0.997	-2.5467	0.0029	0.996	-2.5446
4.0	0.0016	0.996	-2.8002	0.0016	0.998	-2.7987
5.0	0.0015	0.992	-2.8349	0.0015	0.996	-2.8336
6.0	0.0049	0.983	-2.3078	0.0050	0.998	-2.3034
7.0	0.0629	0.997	-1.2010	0.0645	0.999	-1.1904
8.0	0.3350	1.000	-0.4750	0.3789	0.996	-0.4215
9.0	0.4895	0.994	-0.3102	0.3808	1.000	-0.4193
10.0	1.0807	1.000	0.0337	1.0998	1.000	0.0413
11.0	5.9466	0.999	0.7743	6.0178	0.999	0.7794

Table 5.2: Rate constants of ethyl *N*-(2'-hydroxy-2'-phenylethyl)-3-amino propionate (**50**, R= Et) from pH 2.0 to 11.0 in 10% acetonitrile in water at 50 °C.

5.3.2 Chemical hydrolysis of ethyl *N*-[2'-(3'',4''-dihydroxyphenyl)-2'-hydroxyethyl]-3-aminopropionate hydrochloride (74, R=Et) in phosphate-citrate buffer containing 10% acetonitrile from pH 2.0 to 11.0 at 50 °C

Chemical hydrolysis of ethyl *N*-[2'-(3'',4''-dihydroxyphenyl)-2'-hydroxyethyl]-3-aminopropionate hydrochloride (74, R= Et) was carried out from pH 2.0 to 11.0 in phosphate-citrate buffer at 50 °C.

Figure 5.4 shows the first-order plots of ethyl *N*-[2'-(3'',4''-dihydroxyphenyl)-2'-hydroxyethyl]-3-aminopropionate hydrochloride (74, R= Et) at different pH values and the pH rate-profile is shown in Figure 5.8 [A]. Hydrolysis of ethyl *N*-[2'-(3'',4''-dihydroxyphenyl)-2'-hydroxyethyl]-3-aminopropionate hydrochloride (74, R= Et) was acid-base catalysed. The pH rate-profile was U-shape, suggesting, again, that there is also a solvent catalytic effect. The ethyl *N*-[2'-(3'',4''-dihydroxyphenyl)-2'-hydroxyethyl]-3-aminopropionate hydrochloride (74, R= Et) was most stable at pH 3.7 with a half-life of 295 h. Rate constants and correlation coefficients at different pH values are shown in Table 5.3.

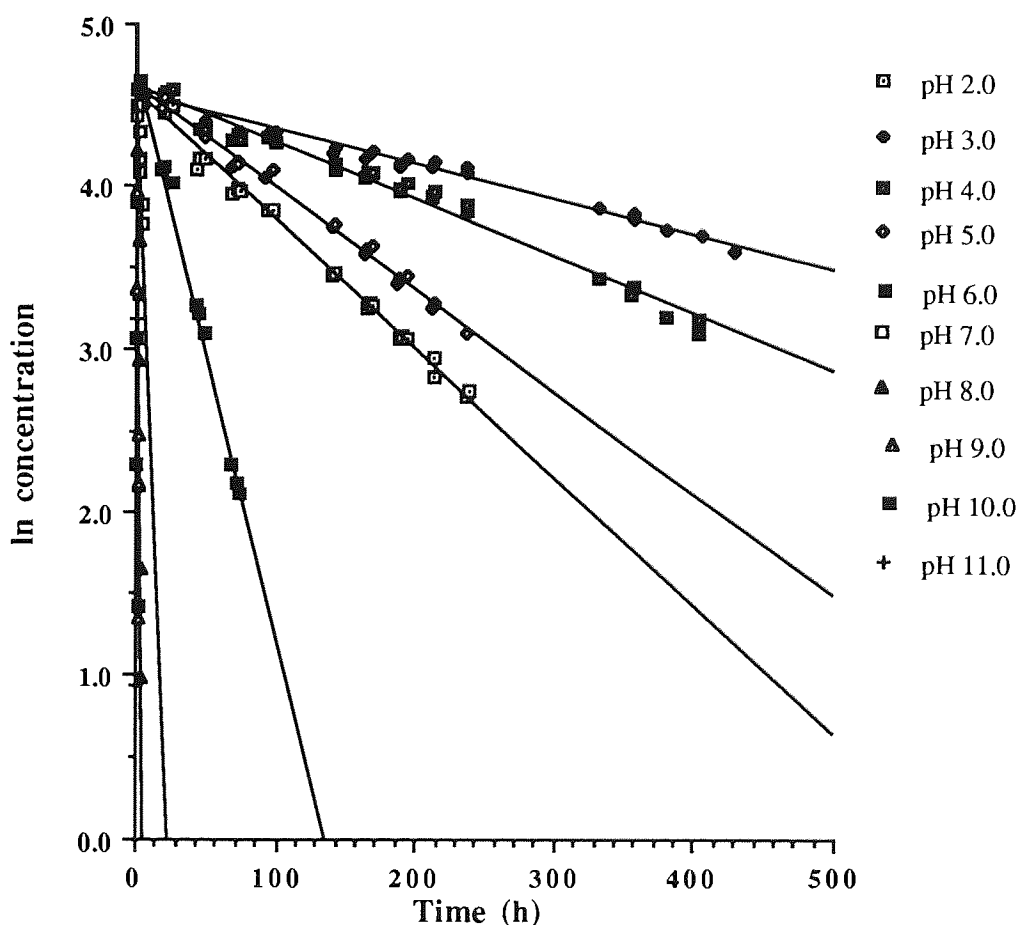


Figure 5.4: Chemical hydrolysis of ethyl *N*-[2'-(3'',4''-dihydroxyphenyl)-2'-hydroxyethyl]-3-aminopropionate (74, R= Et) in phosphate-citrate buffer pH 2.0 to 11.0 at 50 °C.

pH	k (h ⁻¹)	Correlation coefficient (r ²)	log k
2.0	0.0079	0.993	-2.1023
3.0	0.0021	0.972	-2.6746
4.0	0.0026	0.980	-2.5901
5.0	0.0063	0.992	-2.2034
6.0	0.0348	0.992	-1.4581
7.0	0.2016	0.998	-0.6954
8.0	0.9363	0.996	-0.0286
9.0	1.4404	0.996	0.1585
10.0	3.2538	0.995	0.5124
11.0	10.807	0.992	1.0337

Table 5.3: Rate constants of ethyl *N*-[2'-(3",4"-dihydroxyphenyl)-2'-hydroxyethyl]-3-aminopropionate (**74**, R= Et) from pH 2.0 to 11.0 in 10% acetonitrile in water at 50 °C.

5.3.3 Chemical hydrolysis of ethyl *N*-[2'-(3",4"-dipivaloyloxyphenyl)-2'-hydroxyethyl]-3-aminopropionate hydrochloride (**107**) in phosphate citrate buffer containing 10% acetonitrile from pH 2.0 to 11.0 at 50 °C

Hydrolysis of ethyl *N*-[2'-(3",4"-dipivaloyloxyphenyl)-2'-hydroxyethyl]-3-aminopropionate (**107**) was carried out in phosphate-citrate buffer at pH 9.0 at 50 °C without any solvent. The first-order plot does not give a straight line due to the insolubility of the compound in the phosphate-citrate buffer. Different solvents were used to evaluate the solubility of ethyl *N*-[2'-(3",4"-dipivaloyloxyphenyl)-2'-hydroxyethyl]-3-aminopropionate (**107**). By monitoring the linearity of the first-order hydrolysis plot (Figure 5.5), 10% acetonitrile in water was considered suitable.

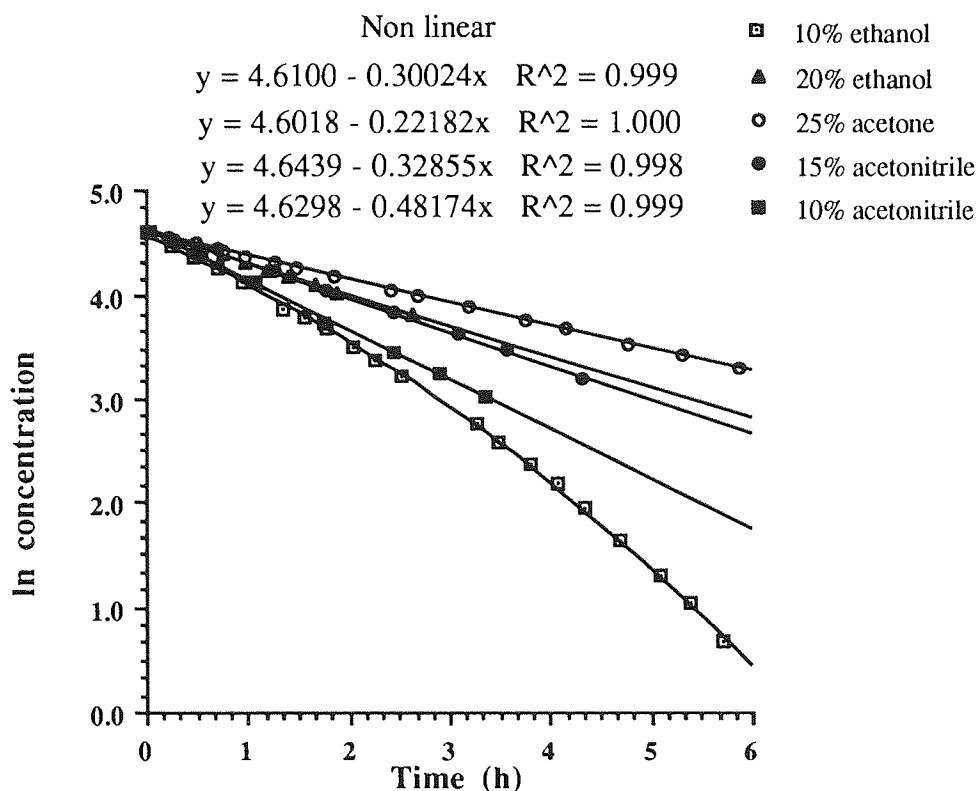


Figure 5.5: Hydrolysis of ethyl *N*-[2'-(3",4"-dipivaloyloxyphenyl)-2'-hydroxyethyl]-3-aminopropionate (**107**) in different solvents included in phosphate-citrate buffer at pH 9.0 at 50 °C.

Using 10% acetonitrile in aqueous buffer, Figure 5.6 shows the first order plots of ethyl *N*-[2'-(3",4"-dipivaloyloxyphenyl)-2'-hydroxyethyl]-3-aminopropionate (**107**) at different pH values at 50 °C. The pH rate-profile is shown in Figure 5.9 [A]. Hydrolysis of ethyl *N*-[2'-(3",4"-dipivaloyloxyphenyl)-2'-hydroxyethyl]-3-aminopropionate (**107**) was catalysed by both acid and base. The pH rate-profile was, again, U-shaped. The ethyl *N*-[2'-(3",4"-dipivaloyloxyphenyl)-2'-hydroxyethyl]-3-aminopropionate (**107**) was most stable at pH 4.0 with a half-life of 560 h. Rate constants and correlation coefficients at different pH values are shown in Table 5.4.

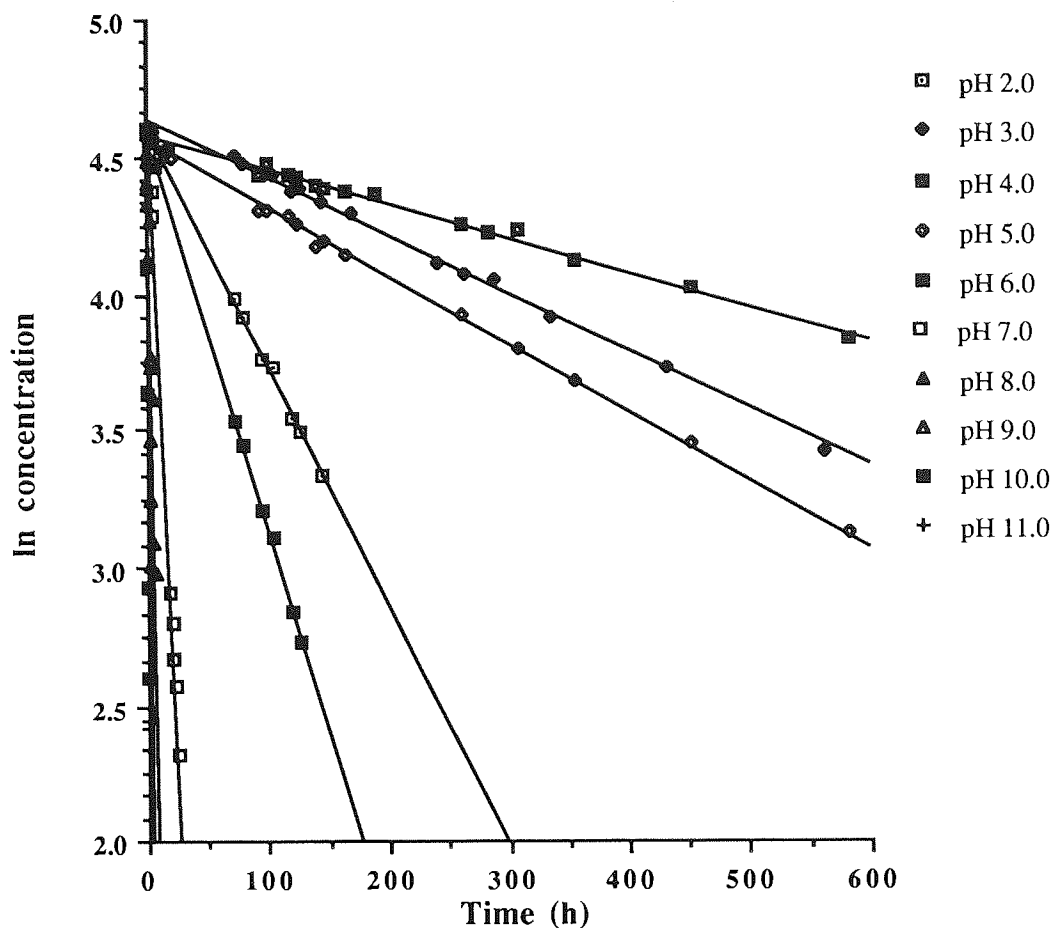


Figure 5.6: Chemical hydrolysis of ethyl *N*-[2'-(3',4'-dipivaloyloxyphenyl)-2'-hydroxyethyl]-3-aminopropionate (**107**) in aqueous phosphate-citrate buffer, pH 2.0 to 11.0 containing 10% acetonitrile at 50 °C.

pH	k (h^{-1})	Correlation coefficient (r^2)	$\log k$
2.0	0.0087	0.999	-2.0580
3.0	0.0021	0.996	-2.6766
4.0	0.0012	0.991	-2.9079
5.0	0.0025	0.995	-2.6103
6.0	0.0146	0.999	-1.8359
7.0	0.0986	0.999	-1.0063
8.0	0.2811	0.999	-0.5512
9.0	0.4817	0.999	-0.3172
10.0	1.9082	0.999	0.2806
11.0	13.308	1.000	1.1241

Table 5.4: Rate constants of ethyl *N*-[2'-(3',4'-dipivaloyloxyphenyl)-2'-hydroxyethyl]-3-aminopropionate (**107**) from pH 2.0 to 11.0 in 10% acetonitrile in water at 50 °C.

5.3.4 Calculation of rate-constants (pH rate-profile) and pK_a

5.3.4.1 Calculation of rate-constants and pK_a for ethyl *N*-(2'-hydroxy-2'-phenylethyl)-3-aminopropionate (50, $R=Et$)

The hydrolysis of an ester as a function of pH may be modelled by equation 5.1:

$$k_{obs} = k_1 [H_3O^+] + k_2 [H_2O] + k_3 [HO^-] \quad \dots\dots\dots Eq. 5.1$$

where k_{obs} is the observed first-order rate constant, and k_1 , k_2 and k_3 are the second order rate constants for the individual reactions involving proton-, solvent- and hydroxide-ion catalysis respectively.

There is, typically, a U- or V- shaped dependence of $\log(k_{obs})$ on pH, and a pH of minimum degradation rate (pH_{min}) may be identified. This occurs when the acid-catalysed rate [$\log(k_{obs}) = \log(k_1) - pH$] and the base-catalysed rate [$\log(k_{obs}) = \log(k_3 K_w) + pH$] are equal, thus:

$$pH_{min} = 0.5 \times \log \left(\frac{k_1}{k_3 K_w} \right) \quad \dots\dots\dots Eq.5.2$$

When a basic group is present, the degradation is more complex as both neutral and protonated forms may undergo reaction. In this case, the overall degradation rate (k_{obs}) is given by:

$$k_{obs} = \alpha \{k_1[H_3O^+] + k_2[H_2O] + k_3[HO^-]\} + (1-\alpha) \{k_4[H_3O^+] + k_5[H_2O] + k_6[HO^-]\} \dots Eq. 5.3$$

Where k_1 , k_2 and k_3 are the second order rate constants for the individual reactions of the protonated base involving proton, solvent and hydroxide ion catalysis respectively, and k_4 , k_5 and k_6 are the corresponding constants for the reaction involving the free base. The first component, thus, models degradation of the protonated form and is important at low pH, while the second component models degradation of the free base and is important at higher pH values. The fraction protonated (α) is dependent upon the pK_a (K_a) of the base and pH ($[H_3O^+]$) of the solution:

$$\alpha = \frac{[H_3O^+]}{K_a + [H_3O^+]} \quad \dots\dots\dots Eq. 5.4$$

The contributions of the various terms are dependent upon pH as $[H_3O^+]$, $[HO^-]$ and the fraction of the protonated base change. The pH-dependence of the hydrolysis of ethyl *N*-(2'-hydroxy-2'-phenylethyl)-3-aminopropionate (**50**, R=Et) is shown in Figure 5.7 [A]. This shows a U-shaped profile at moderate pH values but a discontinuity, typical of the involvement of an ionisation process, at higher values.

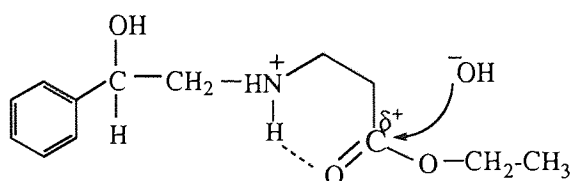
To obtain the individual rate constants for the degradation, the data were fitted, by non-linear regression to equation 5.3 ($k_4=k_5=0$) using programs NONREG and FIGP. Iteration was rapid and yielded the values recorded in Table 5.5.

Parameter	Value ($l\ mol^{-1}\ h^{-1}$)
k_1	1.0278
k_2	0.001197
k_3	670,056
k_6	5289.0
K_a	1.231×10^{-8}
pK_a	7.91

Table 5.5: Individual rate constants and pK_a calculated by NONREG and FIGP programs in the hydrolysis of ethyl *N*-(2'-hydroxy-2'-phenylethyl)-3-aminopropionate (**50**, R= Et).

The pK_a of ethyl *N*-(2'-hydroxy-2'-phenylethyl)-3-aminopropionate (**50**, R=Et) estimated from non-linear regression is 7.91. Thus, at pH values lower than this, the majority of the compound is in the protonated form. Degradation at acidic pH values involves the protonated species undergoing proton (k_1) and hydroxide ion (k_3) catalysed reactions. The intersection of these two curves is rather flat and suggests that a small solvent-catalysed component (k_2) is also present. As the pH increases, the concentration of the free base grows at the expense of the protonated form, and hydroxide catalysis (k_6) of the free base becomes dominant. It is unlikely that an acid-catalysed component (k_4) is present at such high pH values and the involvement of significant solvent catalysis (k_5) at the high degradation rates observed is also unlikely.

Hydroxide ion catalysed hydrolysis (k_3) is very fast because the protonated amine may assist hydrolysis of the ethyl ester by forming an intramolecular hydrogen bond.



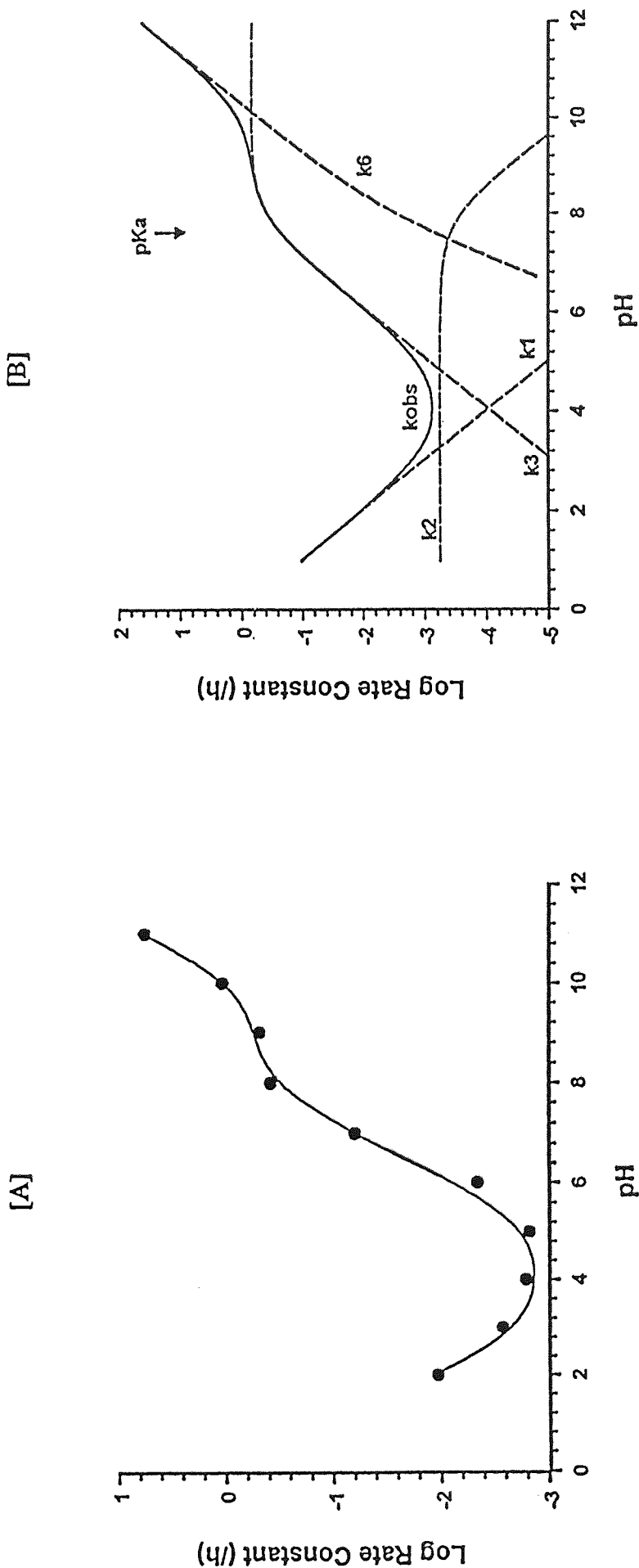


Figure 5.7: Hydrolysis rate constants of ethyl N-(2-hydroxy-2-phenylethyl)-3-aminopropionate (50, R=Et) dependent upon pH. [A] experimentally determined rate constants (k_{obs}). [B] Theoretical pH rate-profile calculated from equation 5.3 using k_1 , 1.0278; k_2 , 0.001197; k_3 , 670,056; k_6 , 5289.0 ($l \text{ mol}^{-1} \text{ h}^{-1}$) and K_a , 1.231×10^{-8} . Contribution of component rate constants (dashed line) to the observed rate constant (solid line).

The pK_a of 7.91, estimated from non-linear regression, is in reasonable agreement with that determined by direct titration (7.76) and indicates that satisfactory convergence was achieved. Moreover, the pH of minimum rate of degradation calculated from these data using equation 5.2 is $pH_{\min} = 4.1$; a value which is in agreement with that obtained by inspection of the plot (Figure 5.7). To confirm the analysis, the individual contribution of each of the reactions (k_1 , k_2 , k_3 , k_6 , K_a) to the observed degradation rate are displayed in Figure 5.7 [B]. Summation of the individual contributions yield the observed curve; the calculated lines indeed parallel the observed plot closely showing that a reliable analysis has been undertaken.

5.3.4.2 Calculation of rate constants and pK_a for ethyl *N*-[2'-(3'',4''-dihydroxyphenyl)-2'-hydroxyethyl]-3-aminopropionate (74, R=Et)

Data from the hydrolysis of ethyl *N*-[2'-(3'',4''-dihydroxyphenyl)-2'-hydroxyethyl]-3-aminopropionate (74, R=Et) were also analysed by non-linear regression to equation 5.3 ($k_4=k_5=0$) using programs NONREG and FIGP and the individual rate constants are shown in Table 5.6. This shows a U-shaped profile at moderate pH values but, again, there is discontinuity, typical of the involvement of an ionisation process, at higher values (Figure 5.8 [A]). The pK_a of ethyl *N*-[2'-(3'',4''-dihydroxyphenyl)-2'-hydroxyethyl]-3-aminopropionate (74, R=Et) has been measured to be 7.40. Thus, at pH values lower than this, most of the molecule is in the protonated form.

Parameter	Value ($l\ mol^{-1}\ h^{-1}$)
k_1	0.5289
k_2	0.002189
k_3	2.6085×10^6
k_6	11905.6
K_a	1.806×10^{-8}
pK_a	7.74

Table 5.6: Individual rate constants and pK_a calculated by NONREG and FIGP programs in the hydrolysis of ethyl *N*-[2'-(3'',4''-dihydroxyphenyl)-2'-hydroxyethyl]-3-aminopropionate (74, R=Et).

The pK_a estimated from non-linear regression, was 7.74, and the pH of minimum rate of degradation calculated from these data using equation 5.2 is $pH_{\min} = 3.8$; a value which is in agreement with that obtained by inspection of the plot. To confirm the analysis, the individual contribution of each of the reactions (k_1 , k_2 , k_3 , k_6 , K_a) to the observed degradation rate are displayed in Figure 5.8 [B]. Summation of the individual contributions yielded the observed curve; the calculated lines again parallel the observed plot closely showing that a reliable analysis has been undertaken.

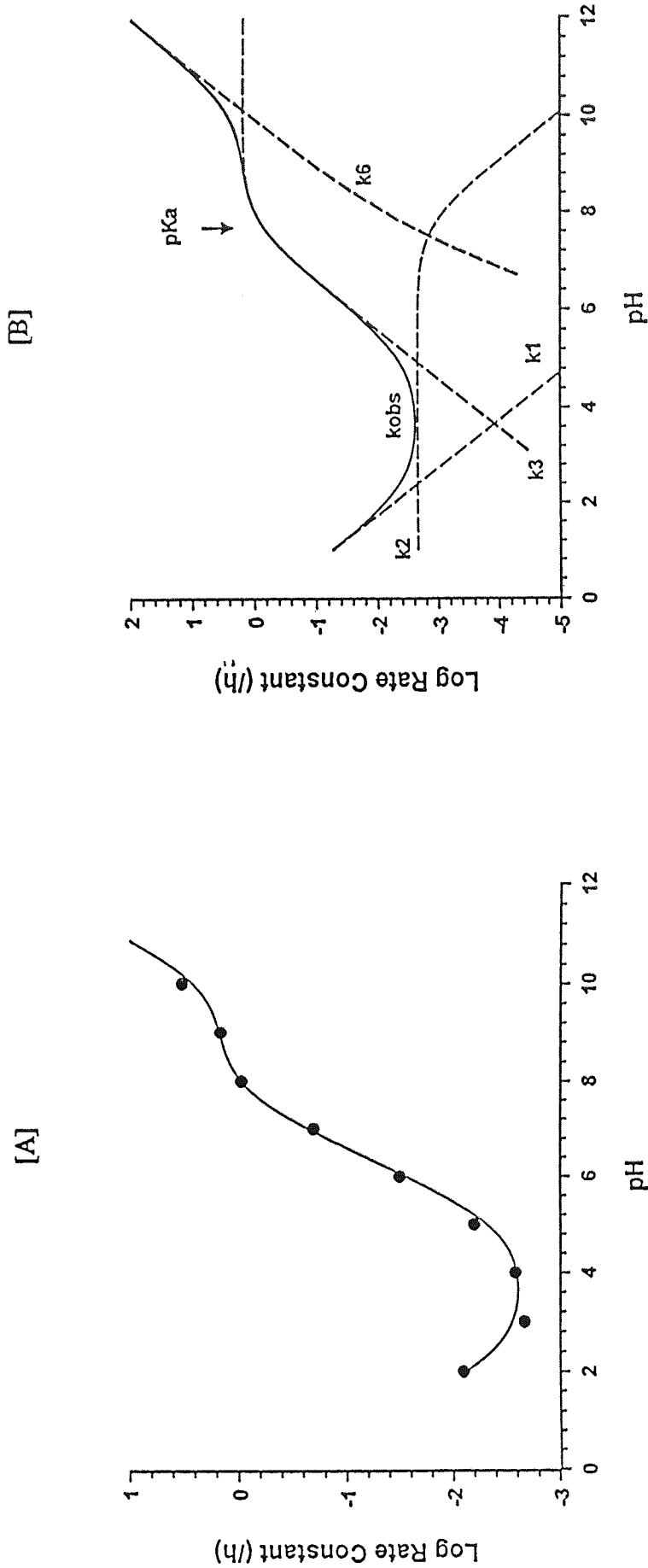


Figure 5.8: Hydrolysis rate constants of ethyl N-[2-(3'', 4''-dihydroxyphenyl)-2'-hydroxyethyl]-3-aminopropionate (74, R=Et) dependent upon pH. [A] experimentally determined rate constants (k_{obs}). [B] Theoretical pH rate-profile calculated from equation 5.3 using k_1 , 0.5289; k_2 , 0.002189; k_3 , 2.6085×10^6 ; k_6 , 11905.6 ($l \text{ mol}^{-1} \text{ h}^{-1}$) and K_a , 1.806×10^{-8} . Contribution of component rate constants (dashed line) to the observed rate constant (solid line).

5.3.4.3 Calculation of rate constants and pK_a for ethyl *N*-[2'-(3'',4''-dipivaloyloxyphenyl)-2'-hydroxyethyl]-3-aminopropionate (107)

In the same way as that described in Sections 5.3.4.1 and 5.3.4.2, the hydrolysis data of ethyl *N*-[2'-(3'',4''-dipivaloyloxyphenyl)-2'-hydroxyethyl]-3-aminopropionate (107) was analysed and individual rate constants are shown in Table 5.7. The pK_a of ethyl *N*-[2'-(3'',4''-dipivaloyloxyphenyl)-2'-hydroxyethyl]-3-aminopropionate (107) has been measured to be 7.40. Thus, at pH values lower than this, most of the compound exists in the protonated form.

Parameter	Value ($l\ mol^{-1}\ h^{-1}$)
k_1	0.7927
k_2	0.001105
k_3	1.3656×10^6
k_6	14922.6
K_a	3.972×10^{-8}
pK_a	7.40

Table 5.7: Individual rate constants and pK_a calculated by NONREG and FIGP programs in the hydrolysis of ethyl *N*-[2'-(3'',4''-dipivaloyloxyphenyl)-2'-hydroxyethyl]-3-aminopropionate (107).

The pK_a of 7.40, estimated from non-linear regression, is in excellent agreement with that determined by direct titration (7.43) and indicates that satisfactory convergence was achieved. The pH of minimum rate of degradation calculated from these data using equation 5.2 is $pH_{min} = 4.0$; a value which is in agreement with that obtained by inspection of the pH-rate profile plot (Figure 5.9). To confirm the analysis, the individual contribution of each of the reactions (k_1 , k_2 , k_3 , k_6 , K_a) to the observed degradation rate are displayed in Figure 5.9 [B].

The reactions of (50, R=Et), (74, R=Et) and (107) all involve hydrolysis of the ethyl ester group. Small differences are apparent between the corresponding rate constants, however, the overall picture is consistent and comparable between the three analogues.

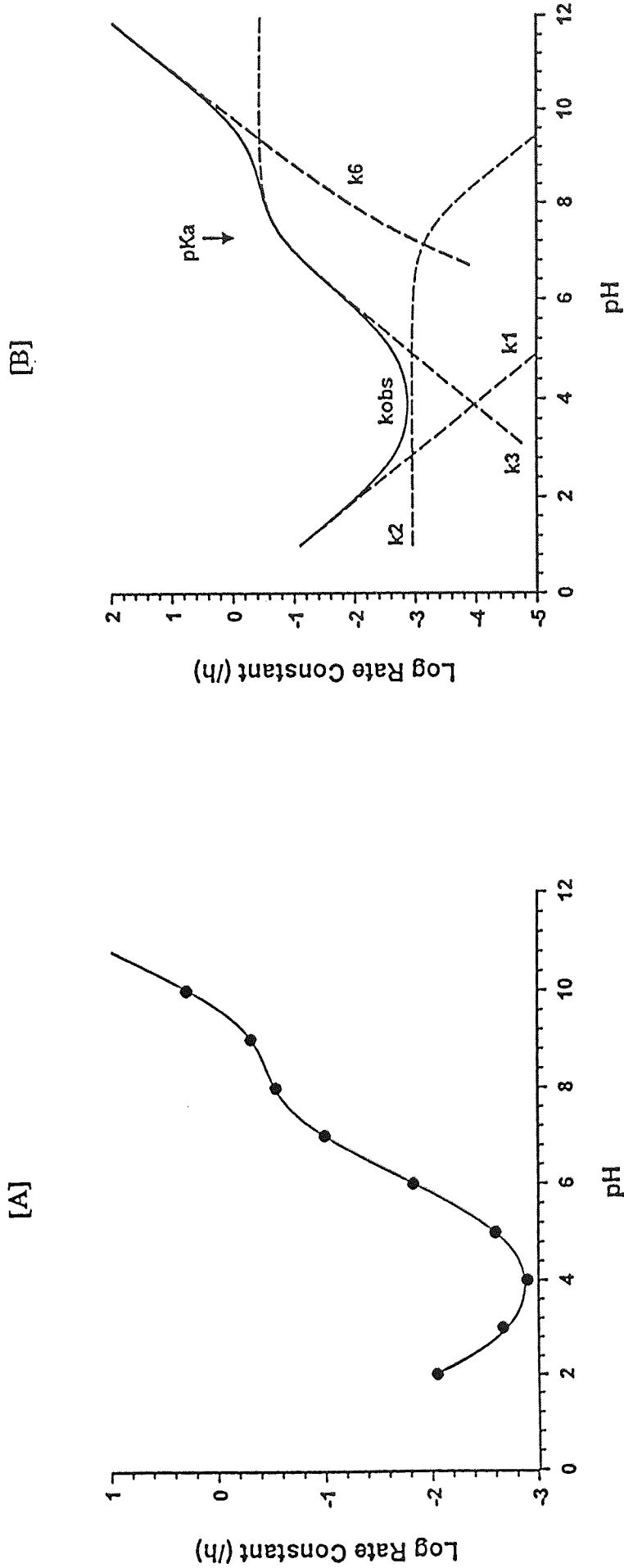


Figure 5.9: Hydrolysis rate constants of ethyl N-[2-(3',4'-dipivaloyloxyphenyl)-2-hydroxyethyl]-3-aminopropionate (107) dependent upon pH. [A] experimentally determined rate constants (k_{obs}). [B] Theoretical pH rate-profile (line) calculated from equation 5.3 using k_1 , 0.7927; k_2 , 0.001105; k_3 , 1.3656×10^6 ; k_6 , 14922.6 ($l \text{ mol}^{-1} \text{ h}^{-1}$) and K_a , 3.972×10^{-8} . Contribution of component rate constants (dashed line) to the observed rate constant (solid line).

5.3.5 Enzyme hydrolysis of β -adrenoceptor agonists with porcine liver carboxyesterase in phosphate-citrate buffer at pH 7.4 and 37 °C:

When an enzyme (E) is mixed with a large excess of substrate (S), there is an initial period, known as the pre-steady state, during which the concentrations of enzyme-bound intermediates (ES) build up to their steady state levels. Once the intermediates reach their steady state concentrations, the reaction rate changes relatively slowly with time. Steady-state kinetics are important to understand metabolism because it measures the catalytic activity of an enzyme.



The rate of the enzyme-catalysed reaction is dependent upon the concentration of both enzyme and substrate. If the concentration of substrate is in excess, the reaction rate increases linearly with increasing enzyme concentration. For a fixed concentration of enzyme, increasing substrate concentration increases the rate of the reaction in a non-linear relationship until the maximum rate occurs. This relationship is described by the Michaelis-Menten equation (Equation 5.5).

$$v = \frac{V_{max} [S]}{K_M + [S]} \quad \dots\dots\dots\text{Eq. 5.5}$$

Where v is the initial rate of the reaction ($-\delta S/\delta t$), $[S]$ is the substrate concentration, V_{max} is the maximum reaction rate and K_M is the Michaelis constant, equal to the substrate concentration at which the reaction rate is half its maximum value. The parameters V_{max} and K_M are determined to indicate substrate capacity and affinity often by using a range of substrate concentrations at one concentration of enzyme. The integrated Michaelis-Menten equation takes the form Equation 5.6

$$\ln [S]_t + \frac{[S]_t}{K_M} = \ln [S]_0 + \frac{[S]_0}{K_M} - \frac{V_{max} t}{K_M} \quad \dots\dots\dots\text{Eq 5.6}$$

Where S_0 is the initial concentration and S_t is the concentration at time t . The non-linear equation approximates to a the zero-order case when $[S]_0 \gg K_M$ ($v=V_{max}$) and to a first-order case when $K_M \gg [S]_0$ ($v=k[S]$; where the first order rate constant $k=V_{max}/K_M$).

5.3.5.1 Enzymatic hydrolysis of ethyl *N*-[2'-(3'',4''-dihydroxyphenyl)-2'-hydroxyethyl]-3-aminopropionate HCl (74, R=Et) in phosphate-citrate buffer at pH 7.4 and 37 °C with PLCE.

The enzymatic hydrolysis of ethyl *N*-[2'-(3'',4''-dihydroxyphenyl)-2'-hydroxyethyl]-3-aminopropionate HCl (74, R=Et) was found to follow a first-order model ($K_m \gg S_0$). Little difference was observed between the rate of chemical and enzymatic degradation in the presence of 31 units of porcine liver carboxyesterase, however rapid degradation was seen when 253 units of enzyme was used. The half-life of ethyl *N*-[2'-(3'',4''-dihydroxyphenyl)-2'-hydroxyethyl]-3-aminopropionate HCl (74, R=Et) (164.0 μ M) in 10 ml phosphate-citrate buffer at pH 7.4 and 37 °C with 253 units of porcine liver carboxyesterase was 0.59 h ($k = 1.1722 \text{ h}^{-1}$, $r^2 = 0.996$, Figure 5.10, Table 5.8).

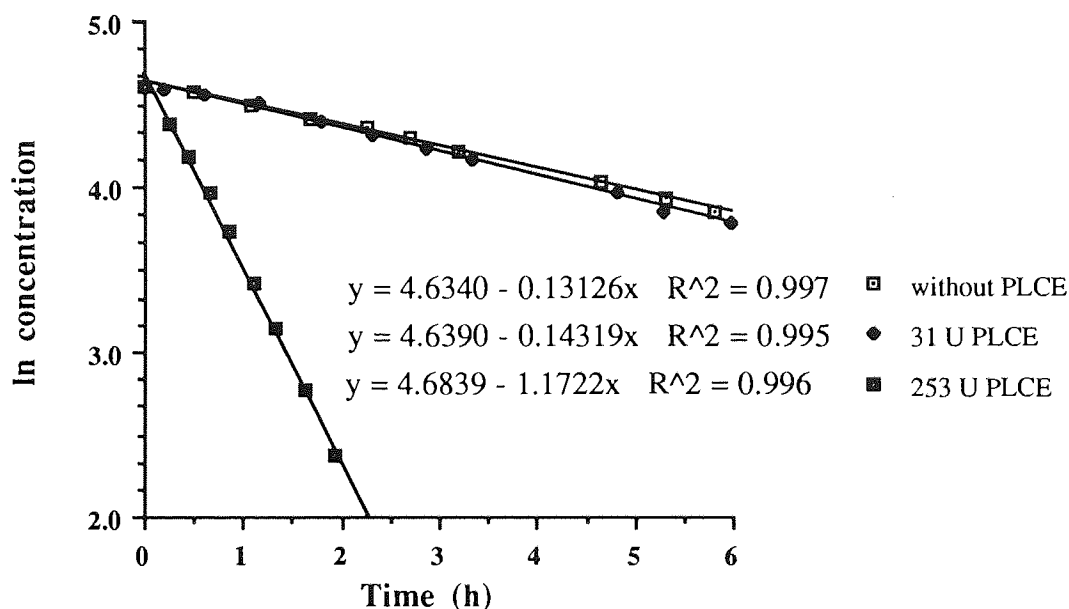


Figure 5.10: Enzyme hydrolysis of ethyl *N*-[2'-(3'',4''-dihydroxyphenyl)-2'-hydroxyethyl]-3-aminopropionate (74, R=Et) with and without PLCE at pH 7.4 and 37 °C.

PLCE (Units)	Conditions	rate constant (h^{-1})	$t_{1/2}$ (h)
No enzyme	Hydrolysis at 37 °C in phosphate citrate buffer pH 7.4 without enzyme	0.13126	5.28
31	Enzyme was added to 164.0 μ M ester at pH 7.4 at 37 °C	0.14319	4.84
253	Enzyme was added to 164.0 μ M ester at pH 7.4 at 37 °C	1.17220	0.59

Table 5.8: Enzyme hydrolysis of ethyl *N*-[2'-(3'',4''-dihydroxyphenyl)-2'-hydroxyethyl]-3-aminopropionate (74, R=Et) with and without PLCE at pH 7.4 and 37 °C.

5.3.5.2 Enzymatic hydrolysis of ethyl *N*-[2'-(3'',4''-dipivaloyloxyphenyl)-2'-hydroxyethyl]-3-aminopropionate HCl (**107**) in phosphate-citrate buffer at pH 7.4 and 37 °C with PLCE.

The enzyme hydrolysis of ethyl *N*-[2'-(3'',4''-dipivaloyloxyphenyl)-2'-hydroxyethyl]-3-aminopropionate HCl (**107**) was conducted in an aqueous phosphate-buffer containing 10% acetonitrile at pH 7.4 to ensure the solubility of pro-soft-drug (**107**). Figure 6.2 shows a typical HPLC chromatogram for the hydrolysis of pro-soft-drug (**107**) with no formation of intermediate product (**120**, peak B). In contrast, the chemical hydrolysis gave intermediate product (**120**, peak B) (Figure 6.1) (Chapter six explains the degradation of pro-soft-drug (**107**) in chemical and enzyme medium).

The enzymatic hydrolysis of ethyl *N*-[2'-(3'',4''-dipivaloyloxyphenyl)-2'-hydroxyethyl]-3-aminopropionate HCl (**107**, 80.0 μ M) in 20 ml phosphate-citrate buffer pH 7.4 at 37 °C was carried out with 5.06 U, 6.29 U and 12.58 U of porcine liver carboxyesterase (PLCE) and without PLCE. Plots again followed a simple first-order model and results were shown in Table 5.9 and graphs are shown in Figures 5.11 and 5.12.

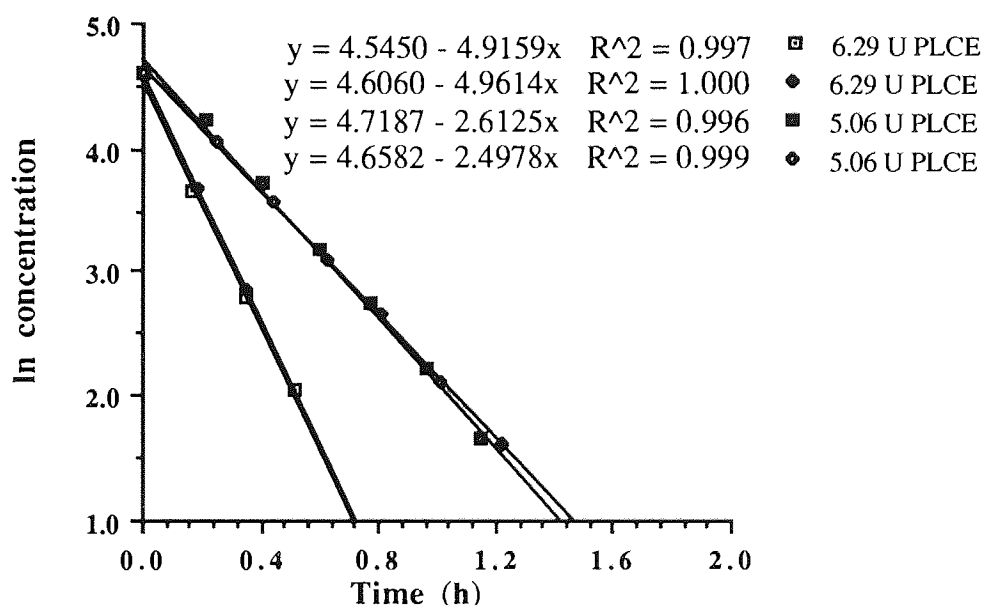


Figure 5.11: Hydrolysis of ethyl *N*-[2'-(3'',4''-dipivaloyloxyphenyl)-2'-hydroxyethyl]-3-aminopropionate (**107**, 80 μ M) in buffer solution at pH 7.4 and 37 °C with PLCE.

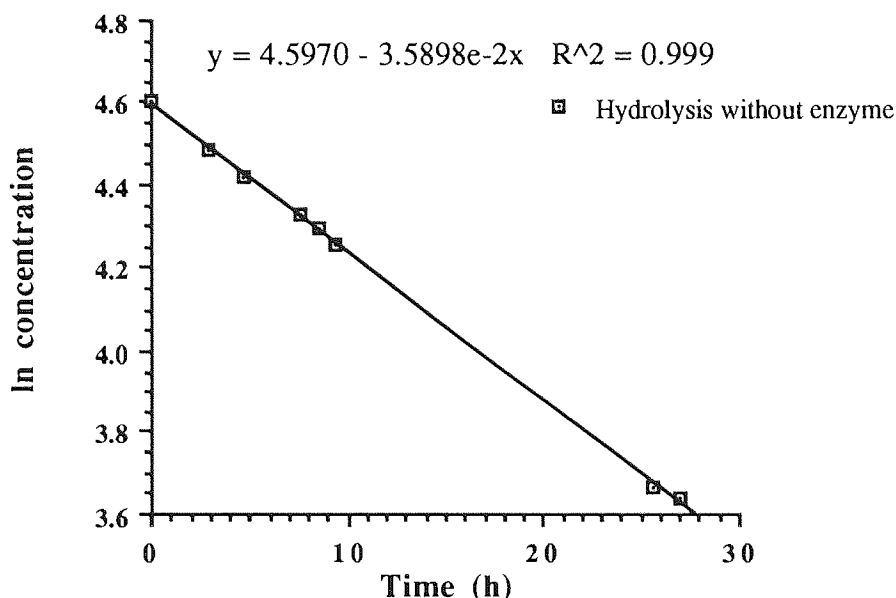


Figure 5.12: Enzyme hydrolysis of ethyl *N*-[2'-(3',4'-dipivaloyloxyphenyl)-2'-hydroxyethyl]-3-aminopropionate HCl (107) without PLCE at pH 7.4 and 37 °C.

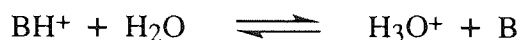
PLCE (Units)	Conditions	Rate constant (h^{-1})	$t_{1/2}$ (h)
No enzyme	Hydrolysis at 37 °C in buffer pH 7.4 (10% CH_3CN) without enzyme	3.5898×10^{-2}	19.31
5.06 U	Enzyme was added to 80 μM compound in buffer pH 7.4 (10% CH_3CN) at 37 °C	2.4978	0.28
5.06 U	Enzyme was added to 80 μM compound in buffer pH 7.4 (10% CH_3CN) at 37 °C	2.6125	0.27
6.29 U	Enzyme was added to 80 μM compound in buffer pH 7.4 (10% CH_3CN) at 37 °C	4.9614	0.14
6.29 U	Enzyme was added to 80 μM compound in buffer pH 7.4 (10% CH_3CN) at 37 °C	4.9159	0.14
12.58 U	Enzyme was added to 80 μM compound in buffer pH 7.4 (10% CH_3CN) at 37 °C	9.7347	0.071

Table 5.9: Hydrolysis data of ethyl *N*-[2'-(3',4'-dipivaloyloxyphenyl)-2'-hydroxyethyl]-3-aminopropionate (107, 80 μM) in buffer solution pH 7.4 at 37 °C with PLCE.

5.3.6 Determination of dissociation constants (pK_a)

The dissociation constant (K_a) is used to measure the relative strengths of acids or bases, and it allows the proportions of the different ionic species present at any chosen pH to be calculated.

For bases the ionization is



and

$$K = \frac{[H_3O^+][B]}{[BH^+][H_2O]}$$

The concentration ionization constant, K_a^c , is defined for bases as

$$K_a^c = K[H_2O] = \frac{[H_3O^+][B]}{[BH^+]} \quad \dots\dots\dots\text{Eq. 5.7}$$

in which square brackets denote the concentration of each ionic species. To yield convenient numbers (rather than negative powers of ten) equation 5.7 is generally used in the following form, in which pK_a is the negative logarithm of the ionization constant:

$$pK_a = -\log_{10} K_a \quad \dots\dots\dots\text{Eq. 5.8}$$

The pK_a values of the model and soft-drugs were determined potentiometrically in (a) water and (b) 10% acetonitrile in water. The values obtained are summarized in Table 5.11. The accuracy of this methodology was assessed by determining the pK_a for the hydrochloride salt of ephedrine (9.468 ± 0.039), a value for which is available in the literature (9.60)¹⁵⁵. The results shows that the experimental value is within $\pm 0.13\%$ of those quoted in the literature, suggesting a similar range of accuracy for model compound and soft-drugs.

5.3.6.1 Determination of ionization constant (pK_a) of ethyl *N*-(2'-phenyl-2'-hydroxyethyl)-3-aminopropionate (50, R=Et)

The pK_a value of ethyl *N*-(2'-phenyl-2'-hydroxyethyl)-3-aminopropionate (50, R=Et) was measured by potentiometric titration with 0.1 M HCl and data were analysed with program PKA using the model described by equation 5.9.

$$pK_a = pH + \log \left(\frac{a - [H_3O^+] + [HO^-]}{b + [H_3O^+] + [HO^-]} \right) \quad \dots\dots\dots \text{Eq.5.9}$$

Where a and b are the stoichiometric concentrations of the weak conjugate acid $[BH^+]$ and base $[B]$ respectively. A typical plot is displayed in Figure 5.13 and a typical titration run in Table 5.10.

HCl (ml)	pH	$[H_3O^+]$	$a=[NH^+]$	$b=[N:]$	pK_a
0.2	8.17	6.761E-9	1.869E-3	5.792E-3	7.679
0.3	7.98	1.047E-8	2.778E-3	4.813E-3	7.741
0.4	7.80	1.585E-8	3.670E-3	3.851E-3	7.779
0.5	7.59	2.570E-9	4.546E-3	2.907E-3	7.784
0.6	7.35	4.467E-8	5.405E-3	1.980E-3	7.786
0.7	7.01	9.772E-8	6.250E-3	1.069E-3	7.777

Table 5.10: Potentiometric titration of ethyl *N*-(2'-phenyl-2'-hydroxyethyl)-3-aminopropionate (50, R=Et) (19.5 mg) with HCl (0.1 M). (End-point 0.82 ml, mean pK_a value= 7.760 \pm 0.038).

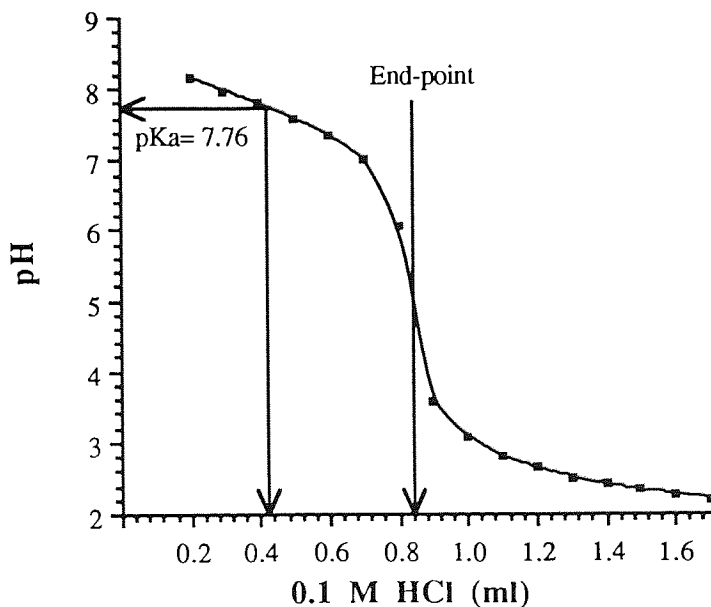


Figure 5.13: Potentiometric titration run of ethyl *N*-(2'-phenyl-2'-hydroxyethyl)-3-aminopropionate (50, R=Et) with 0.1 M HCl.

The pK_a of ethyl *N*-(2'-hydroxy-2'-phenylethyl)-3-aminopropionate (**50**, R=Et) has been measured to be 7.760 ± 0.038 . Thus, at pH values lower than this, the majority of the molecule is in the protonated form as indicated by equation 5.4

5.3.6.2 Determination of ionization constant (pK_a) of methyl *N*-(2'-hydroxy-2'-phenylethyl)-3-aminopropionate (50**, R=Me)**

The methyl *N*-(2'-hydroxy-2'-phenylethyl)-3-aminopropionate hydrochloride (**50**, R=Me) was titrated potentiometrically with 0.1 M KOH and the data were analysed with program PKA. The pK_a value was found to be 7.768 ± 0.06 (Appendix V, Table 5.1A). The pK_a value calculated by NONREG and FIGP programmes was found to be 7.91.

5.3.6.3 Determination of ionization constant (pK_a) of ethyl *N*-[2'-(3'',4''-dipivaloyloxyphenyl)-2'-hydroxyethyl]-3-aminopropionate (107**)**

The ethyl *N*-[2'-(3'',4''-dipivaloyloxyphenyl)-2'-hydroxyethyl]-3-aminopropionate HCl (**107**) was titrated potentiometrically with 0.1 M KOH and the data were analysed with the PKA program. The pK_a value was found to be 7.427 ± 0.194 (Appendix V, Table 5.2A). The pK_a value calculated by NONREG and FIGP programmes was found to be 7.40.

5.3.6.4 Determination of ionization constant (pK_a) of ephedrine base and hydrochloride salt in water and 10% MeCN in water

The hydrochloride salt of ephedrine in water and 10% acetonitrile in water were titrated potentiometrically with 0.1 M KOH and the data were analysed with the PKA program. The pK_a value of ephedrine in water was found to be 9.371 ± 0.092 (Appendix V, Table 5.3A) and 9.468 ± 0.039 (Appendix V, Table 5.4A) in 10% acetonitrile in water. The results show that the experimental values for K_a is within $\pm 0.13\%$ of those quoted in the literature (9.60). The difference might be due to the temperature (all the titrations were performed at 22 °C) and method. Addition of organic solvent (acetonitrile) increases the pK_a value of ephedrine.

The ephedrine base in 10% acetonitrile in water was titrated potentiometrically with 0.1 M HCl and the data were analysed with the PKA program. The pK_a value of ephedrine in 10% acetonitrile in water was found to be 9.396 ± 0.124 (Appendix V, Table 5.5A).

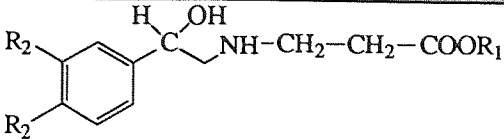
			
Compound	Solvent	Experimental value	pK _a Values from NONREG and FIGP
Ephedrine HCl	water	9.371 ± 0.092	9.60 (Literature value) ¹⁵⁵
Ephedrine HCl	10% MeCN in water	9.468 ± 0.039	
Ephedrine base	10% MeCN in water	9.396 ± 0.124	
Methyl ester HCl (50, R ₁ = Me, R ₂ = H)	10% MeCN in water	7.768 ± 0.060	---
Ethyl ester (50, R ₁ = Et, R ₂ = H)	10% MeCN in water	7.760 ± 0.038	7.91
Dipivaloyl ethyl ester HCl (107, R ₁ = Et, R ₂ =Bu ^t COO ⁻)	10% MeCN in water	7.4275 ± 0.194	7.40
Dihydroxy ethyl ester (74, R ₁ = Et, R ₂ = -OH)	---	---	7.74

Table 5.11: The pK_a values of analogue (50, R₁=Me, R₂=H), analogue (50, R₁=Et, R₂=H), pro-soft-drug (107, R₁=Et, R₂=Bu^tCOO⁻). Calculated by potentiometric titration (PKA programme) and NONREG and FIGP programs.

5.3.7 Determination of degradation profile of ethyl *N*-[2'-(3",4"-dipivaloyloxyphenyl)-2'-hydroxyethyl]-3-aminopropionate (**107**) in enzyme medium (PLCE) at pH 7.4 and 37 °C.

The enzymatic hydrolysis of ethyl *N*-[2'-(3",4"-dipivaloyloxyphenyl)-2'-hydroxyethyl]-3-aminopropionate HCl (**107**, 80.0 μ M) in 20 ml phosphate-citrate buffer pH 7.4 at 37 °C was carried out with 6.29 U of porcine liver carboxyesterase (PLCE). The hydrolysis was monitored by HPLC analysis with 30% acetonitrile in water, pH 3.0 as the mobile phase. The pro-soft-drug (**107**) was rapidly hydrolysed [first-order hydrolysis with a first-order rate constant of 4.9654 h⁻¹ ($r^2= 1.000$, $t_{1/2}=0.14$ hrs) (Figure 5.14)], to give an unknown product [later identified as dihydroxy ethyl ester (**74**, R=Et)], which eluted with the solvent front in the HPLC chromatogram. The intermediate product (peak B in Figure 6.2) was not detected by HPLC.

To identify the product from enzymatic hydrolysis, the experiment was repeated except that the reaction was monitored by HPLC eluting with 4% acetonitrile in water, pH 3.0. The rapid appearance of ethyl *N*-[2'-(3",4"-dihydroxyphenyl)-2'-hydroxyethyl]-3-aminopropionate HCl (**74**, R=Et) (t_R 8.8 min, Section 4.5.4.2) was indicated. Figure 5.14 shows the enzymatic hydrolysis of the pro-soft-drug (**107**) eluting with 30% acetonitrile in water as the mobile phase. When the hydrolysis of the pro-soft-drug (**107**) with porcine liver carboxyesterase was completed, as indicated by the disappearance of the triester peak by HPLC using a mobile phase of 30% acetonitrile in water, the reaction mixture was analysed with 4% acetonitrile in water. Plots were constructed from data collected after the complete disappearance of the pro-soft-drug (**107**) to reveal the degradation of the intermediate soft-drug (**74**, R=Et). This showed that the soft-drug (**74**, R= Et) ($t_R= 8.8$ min), which hydrolyses further to dihydroxy acid (**74**, R= H) proceeds also with first-order kinetics with a first-order rate constant of 0.090901 h⁻¹ ($r^2= 0.994$, $t_{1/2}=7.625$ hrs) (Figure 5.14). Figure 5.15 shows the hydrolysis profile of the pro-soft-drug (**107**). Appendix 5.6A [I] shows the enzymatic hydrolysis of pro-soft-drug (**107**) eluting with 30% acetonitrile in water and Appendices 5.6A [II] and 5.7A shows the formation of soft-drug (**74**, R= Et) from pro-soft-drug (**107**) eluting with 4% acetonitrile in water.

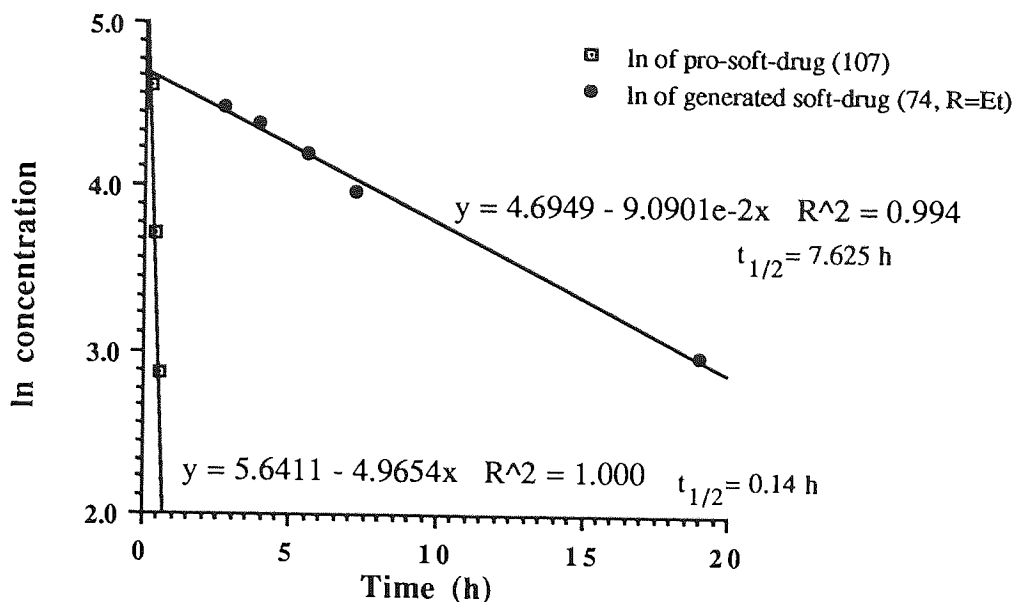


Figure 5.14: Half-lives of pro-soft-drug (107) and *in situ* generated soft-drug (74, R=Et) in enzyme hydrolysis in buffer containing 10% acetonitrile at pH 7.4 and 37 °C.

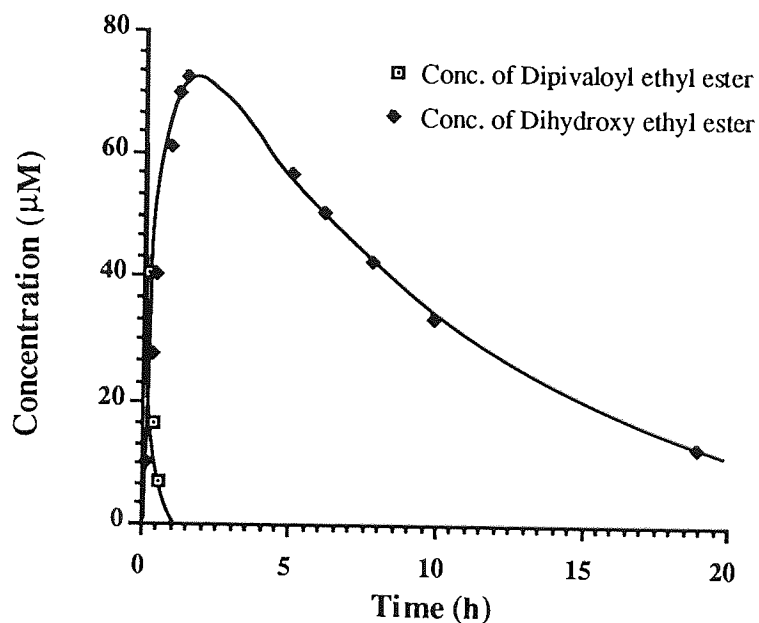


Figure 5.15: Kinetic profile of pro-soft-drug (107) and *in situ* generated soft-drug (74, R=Et) in enzyme hydrolysis in buffer containing 10% acetonitrile at pH 7.4 and 37 °C.

The same experiment was repeated under the same conditions. The pro-soft-drug (107) was rapidly hydrolysed [first-order hydrolysis with a first-order rate constant of 4.9164 h^{-1} ($r^2 = 0.997$, $t_{1/2} = 0.14$ hrs) (Figure 5.16)]. Figure 5.16 shows the enzymatic hydrolysis of pro-soft-drug (107) in 30% acetonitrile in water mobile phase. When the hydrolysis of the pro-soft-drug (107) with porcine liver carboxyesterase was completed, as indicated by the disappearance of the triester peak by HPLC using a mobile phase of 30% acetonitrile in water, the reaction mixture was analysed with 4% acetonitrile in water. Again data were collected after disappearance of the pro-soft-drug (107).

These showed that the generated soft-drug (74, R= Et) ($t_R = 8.8$ min), which hydrolysed further to dihydroxy acid (74, R= H) is also a first-order hydrolysis with a first-order rate constant of 0.091423 h^{-1} ($r^2 = 1.000$, $t_{1/2} = 7.582$ hrs) (Figure 5.16). Figure 5.17 shows the hydrolysis profile of pro-soft-drug (107). Appendix 5.8A [I] shows the enzymatic hydrolysis of pro-soft-drug (107) eluting with 30% acetonitrile in water and Appendices 5.8A [II] and 5.9A shows the formation of soft-drug (74, R= Et) from pro-soft-drug (107) eluting with 4% acetonitrile in water.

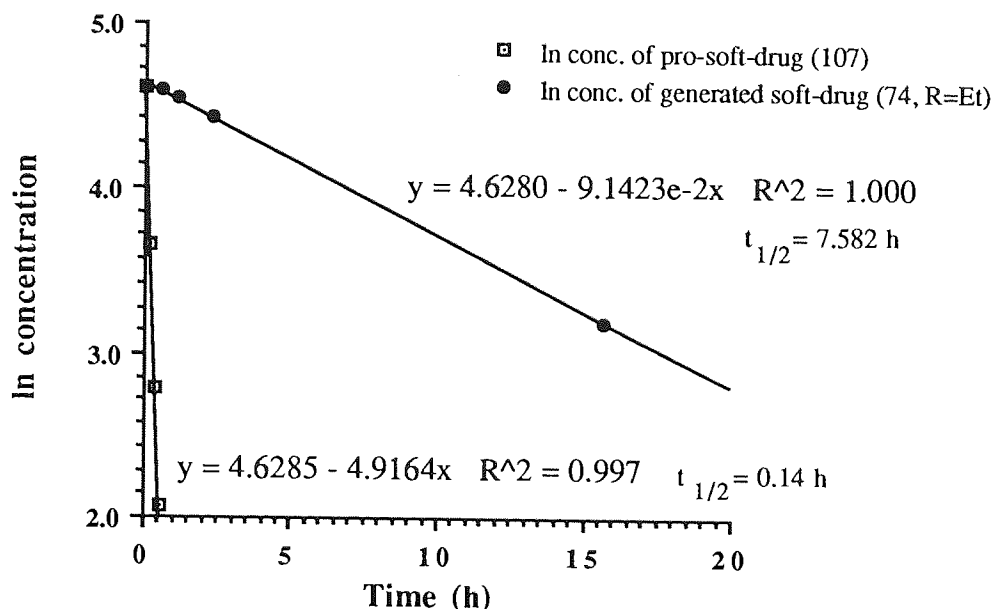


Figure 5.16: Half-lives of pro-soft-drug (107) and *in situ* generated soft-drug (74, R=Et) in enzyme hydrolysis in buffer containing 10% acetonitrile at pH 7.4 and 37 °C.

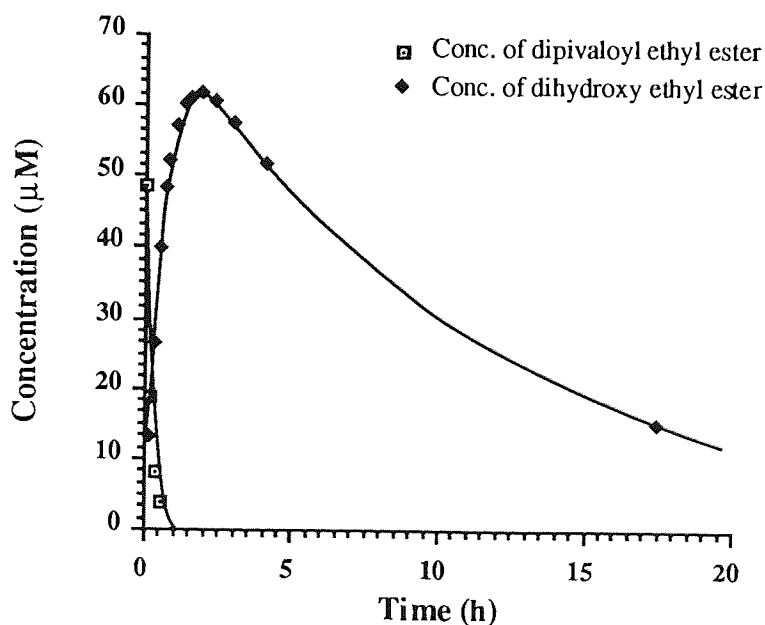


Figure 5.17: Kinetic profile of pro-soft-drug (107) and *in situ* generated soft-drug (74, R=Et) in enzyme hydrolysis in buffer containing 10% acetonitrile at pH 7.4 and 37 °C.

The hydrolysis of the pro-soft-drug (**107**) with porcine liver carboxyesterase is very rapid and generates the soft-drug (**74**, R=Et) as the major intermediate. Under these conditions, the hydrolysis of the pivaloyl ester is much faster than that of the ethyl ester in pro-soft-drug (**107**) (Figure 5.18) probably because the more lipophilic pivaloyl group has more favourable interactions with the enzyme than the less lipophilic ethyl ester in the proximity of an amino residue.

In contrast, in the chemical hydrolysis, the ethyl ester is hydrolysed faster than the pivaloyl group probably because of steric hindrance of the pivaloyl group. Table 5.12 shows the alkaline and enzymatic hydrolysis of various benzoate esters in the homologues series; progression up the homologous series increases the rate of ester hydrolysis, because the lipophilic esters interact more effectively with the enzyme.

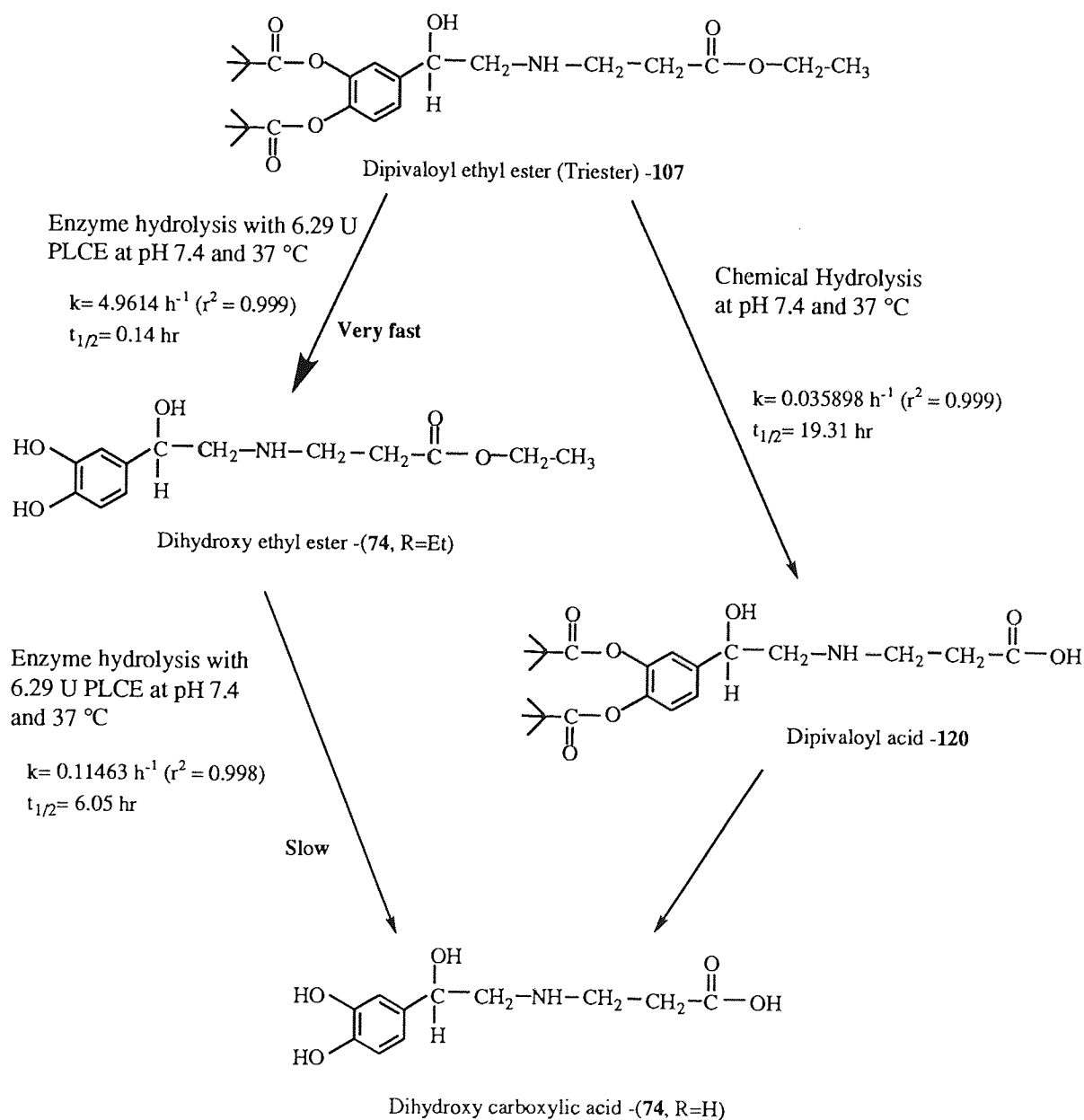
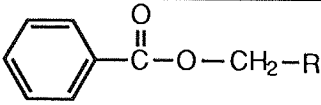


Figure 5.18: Chemical and enzymatic hydrolysis of pro-soft-drug (**107**)

Bundgaard and Nielsen^{105,106} have suggested glycolamide esters as useful prodrug functions for drugs with carboxylic acid groups, combining high stability in aqueous solution together with a high susceptibility towards enzymatic hydrolysis. The most important structural requirement for this profile appears to be the presence of two substituents on the amide nitrogen, *N,N*-disubstituted glycolamide esters being much more readily hydrolysed in plasma than either mono- or unsubstituted glycolamide esters (Table 5.12).

					
Compound No.	R	σ^* for R	kOH ($M^{-1} \text{ min}^{-1}$)	80% human plasma	
				k (min^{-1})	$t_{1/2}$ (min)
1	H	0.49	13.6	6.4×10^{-3}	108
2	-CH ₃	0.00	6.59	3.3×10^{-3}	210
3	-C ₂ H ₅	-0.10	5.52	1.5×10^{-2}	46
4	-C ₃ H ₇	-0.12	4.50	1.7×10^{-2}	40
5	-C ₄ H ₉	-0.25	5.33	2.9×10^{-2}	24
6	-C ₆ H ₅	0.75	13.0	3.7×10^{-2}	19
7	-CH ₂ C ₆ H ₅	0.27	4.63	4.7×10^{-2}	15
8	-COO ⁻	-1.06	6.28	$< 10^{-4}$	> 100 h
9	-COOCH ₃	2.00	70.1	2.0×10^{-1}	3.5
10	-COOC ₂ H ₅	2.26	60.3	4.4×10^{-2}	16
11	-COOCH ₂ C ₆ H ₅	-	55.7	2.7×10^{-1}	2.6
12	-CONH ₂	1.68	69.9	1.7×10^{-2}	40
13	-CON(CH ₃) ₂	1.94	19.2	> 5.0	< 8 s
14	-SCH ₃	1.56	24.4	3.1×10^{-2}	22
15	-SOCH ₃	2.88	274	5.9×10^{-1}	1.2
16	-SO ₂ CH ₃	3.68	592	5.8×10^{-1}	1.2
17	-CH ₂ N(CH ₃) ₂	0.49	9.83	> 8.0	< 5 s
18	-CH ₂ N(CH ₃) ₃ ⁺	1.90	95.1	> 8.0	< 5 s

σ^* = Taft polar substituent parameter

Table 5.12: Rate data for the alkaline and enzymatic hydrolysis of various benzoate esters at 37 °C.⁸⁷

5.4 CONCLUSIONS

The soft-drug (**74**, R=Et), pro-soft-drug (**107**) and unsubstituted phenyl analogue (**50**, R=Et) are most stable at pH 4.0 with half-lives of 295, 560 and 438 hrs, respectively. The pK_a values of the pro-soft-drug (**107**), analogue (**50**, R=Et) and (**50**, R=Me) were found to be 7.427 ± 0.194 , 7.760 ± 0.038 and 7.768 ± 0.060 respectively. The pK_a of 7.40 (for pro-soft-drug **107**), estimated from non-linear regression, is in excellent agreement with that determined by direct titration (7.43) and indicates that satisfactory convergence was achieved. Moreover, the pH of minimum rate of degradation calculated from these data using equation 5.2 is $pH_{\min} = 4.0$; a value which is in agreement with that obtained by inspection of the plot (Figure 5.9).

The hydrolysis of the pro-soft-drug (**107**) with porcine liver carboxyesterase is very rapid and generated the soft-drug (**74**, R=Et) as the major intermediate. The esterase catalysed hydrolysis at the pivaloyl ester is much faster than that at the ethyl ester and indicates the possibility that the pro-soft-drug (**107**) will undergo metabolic activation and deactivation in the required manner *in vivo*.

CHAPTER SIX

DEGRADATION PATHWAYS OF SOFT β -ADRENOCEPTOR AGONISTS

6.1 INTRODUCTION

The chemical hydrolysis of ethyl *N*-[2'-(3",4"-dipivaloyloxyphenyl)-2'-hydroxyethyl]-3-aminopropionate (**107**) was monitored over the pH range 2.0 to 11.0 by HPLC. Compound (**107**) had a retention time of 9.4 min and unknown product (B) had a retention time of 5.4 min (HPLC trace shown in Figure 6.1). In the enzymatic hydrolysis, ethyl *N*-[2'-(3",4"-dipivaloyloxyphenyl)-2'-hydroxyethyl]-3-aminopropionate (**107**) was hydrolysed rapidly, with very little formation of the unknown product (B)(HPLC trace shown in Figure 6.2). The hydrolytic pathways of this pro-soft-drug are complex and are illustrated in Scheme 6.1. It is possible, that ethyl *N*-[2'-(3",4"-dipivaloyloxyphenyl)-2'-hydroxyethyl]-3-aminopropionate (**107**) may be hydrolysed *via* the formation of 4-pivaloyl ethyl ester (**118**) and/or 3-pivaloyl ethyl ester (**119**) which degrade to the dihydroxy ethyl ester (**74**). Alternatively hydrolysis may proceed *via* the formation of dipivaloyl carboxylic acid (**120**) with subsequent degradation to the 4-pivaloyl carboxylic acid (**121**) and/or 3-pivaloyl carboxylic acid (**122**), which ultimately gives dihydroxy carboxylic acid (**74**, R=H) (Scheme 6.1). For ethyl *N*-[2'-(3",4"-dipivaloyloxyphenyl)-2'-hydroxyethyl]-3-aminopropionate (**107**) to be used as a prodrug, it is a prerequisite that triester (**107**) should undergo hydrolysis *via* the initial formation of either the 4-pivaloyl ethyl ester (**118**) and/or 3-pivaloyl ethyl ester (**119**) with further hydrolysis to the dihydroxy ethyl ester (**74**), to retain activity.

Hydrolysis studies of ethyl *N*-[2'-(3",4"-dipivaloyloxyphenyl)-2'-hydroxyethyl]-3-aminopropionate (**107**) using ^1H NMR spectroscopy were carried out to investigate:

- the identification of unknown hydrolysis product (B, $t_{\text{R}} = 5.4$ min)
- product from and mechanism of the chemical hydrolysis of the triester (**107**)
- product from and mechanism of the esterase-catalysed hydrolysis of the triester (**107**)

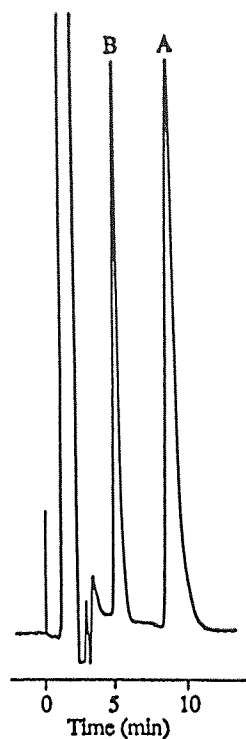


Figure 6.1: HPLC chromatogram shows the formation of unknown peak [B= dipivaloyl carboxylic acid (120)] in the chemical hydrolysis of ethyl *N*-[2'-(3",4"-dipivaloyloxyphenyl)-2'-hydroxyethyl]-3-aminopropionate (107, A) at pH 4.0 after 582 hours.

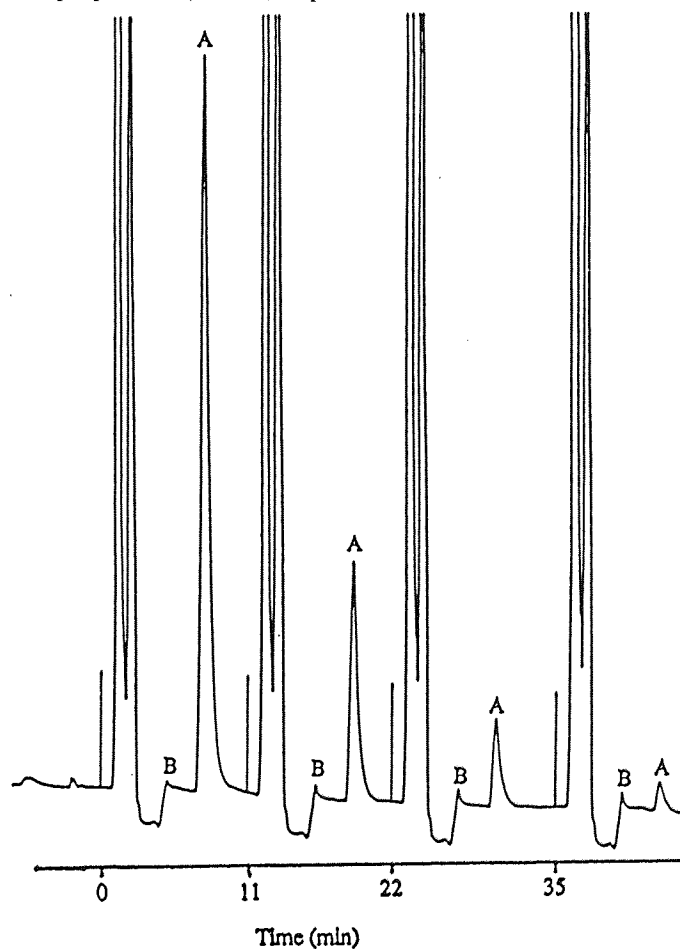
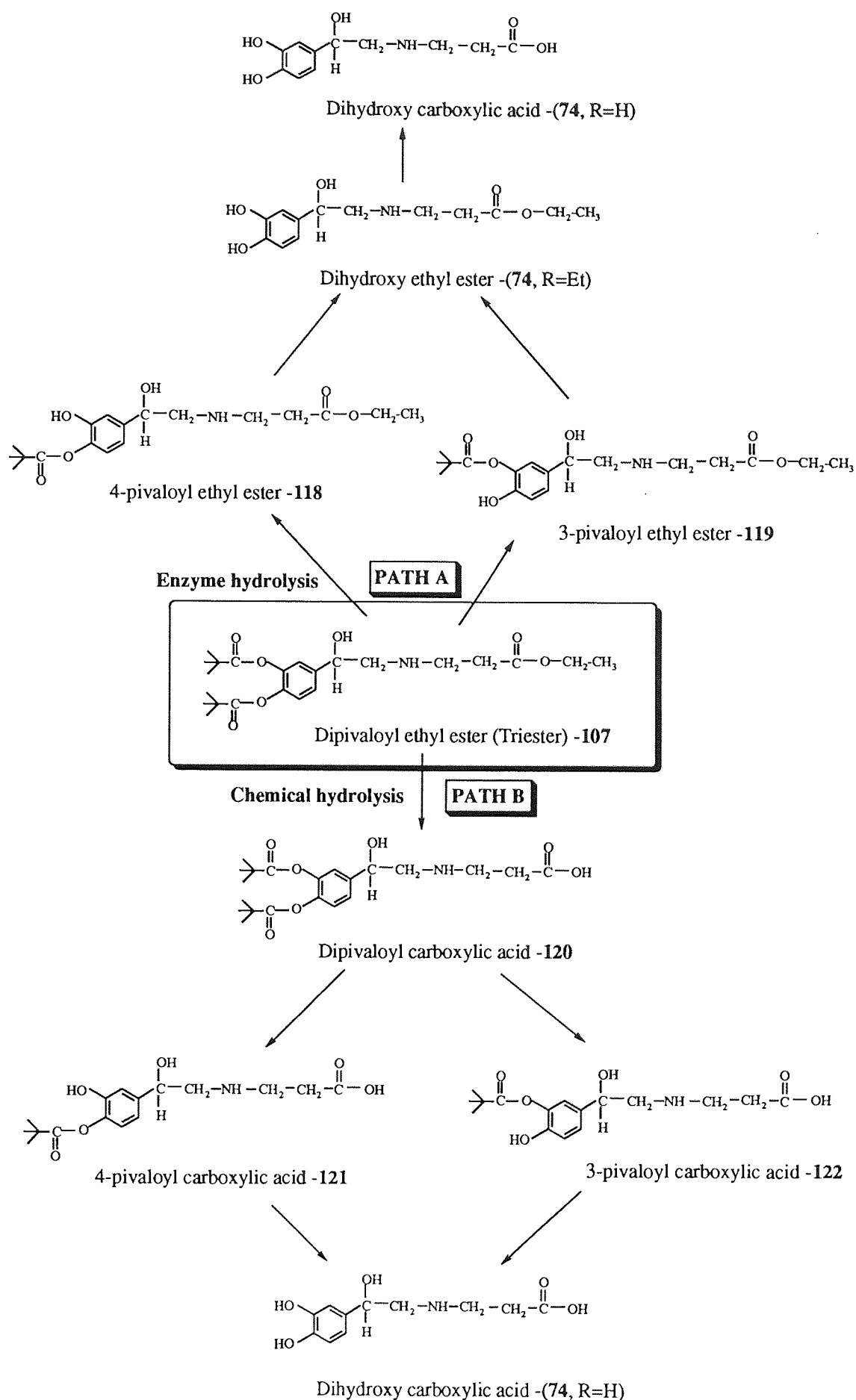


Figure 6.2: HPLC chromatogram shows very little or no formation of unknown peak [B= dipivaloyl carboxylic acid (120)] in the esterase catalysed hydrolysis of ethyl *N*-[2'-(3",4"-dipivaloyloxyphenyl)-2'-hydroxyethyl]-3-aminopropionate (107, A).



Scheme 6.1: Possible routes of hydrolysis of ethyl *N*-[2'-(3,4'-dipivaloyloxyphenyl)-2'-hydroxyethyl]-3-aminopropionate (107).

6.2 EXPERIMENTAL

Preparation of buffer pD 8.57 (pH 8.17)

The buffer of pD 8.57 (pH 8.17) was made with potassium dihydrogen phosphate and potassium hydroxide in D₂O. Potassium dihydrogen phosphate (100 mg) was dissolved in D₂O (10 ml) and evaporated to dryness under high vacuum at 50 °C. This was repeated three times such that most of the hydrogen atoms in the potassium dihydrogen phosphate were replaced with deuterium. The same procedure was used for potassium hydroxide in D₂O. The pH 8.17 buffer was made with potassium dihydrogen phosphate and potassium hydroxide, which is equivalent to a pD of 8.57 at 22 °C. This was calculated according to the method of Fife and Bruce,¹⁵⁶ using the following equation.

$$\text{pD} = \text{pH meter reading} + \frac{4.29 \times 10^2}{T^\circ \text{K}} - 1.04 \dots \text{Eq. 6.1}$$

Chemical hydrolysis studies of triester (107) and ethyl ester (74) by ¹H-NMR spectroscopy

A solution of ethyl *N*-[2'-(3'',4''-dipivaloyloxyphenyl)-2'-hydroxyethyl]-3-amino propionate (**107**, 5 mM) in potassium phosphate buffer (0.1 mol dm⁻³, D₂O, pD 8.57)-CD₃CN (8:2, v/v) (0.5 ml) was monitored over 300 hrs by ¹H NMR spectroscopy at 37 °C.

A solution of ethyl *N*-[2'-(3'',4''-dihydroxyphenyl)-2'-hydroxyethyl]-3-aminopropionate (**74**, 5 mM) in potassium phosphate buffer (0.1 mol dm⁻³, D₂O, pD 8.57)-CD₃CN (9:1, v/v) (0.5 ml) was monitored over 30 hrs by ¹H NMR spectroscopy at 37 °C.

Chemical hydrolysis studies of triester (107) and ethyl ester (74) by HPLC

A solution of ethyl *N*-[2'-(3'',4''-dipivaloyloxyphenyl)-2'-hydroxyethyl]-3-aminopropionate (**107**, 105.5 μ M) in phosphate-citrate buffer pH 8.0 (6.96 g disodium hydrogen phosphate Na₂HPO₄.12H₂O and 0.0589 g citric acid C₆H₈O₇.H₂O in 100 ml water) containing 10% acetonitrile at 50 °C was monitored with time by HPLC. The mobile phase was aqueous acetonitrile (30%) containing 0.1% tetrabutylammonium hydroxide with the pH adjusted to 3.0 with orthophosphoric acid. When 80% of the triester had been converted to the intermediate, the reaction was cooled and extracted successively with hexane (2 x 20 ml), diethyl ether (2 x 20 ml), chloroform (2 x 20 ml) and ethyl acetate (2 x 20 ml). Each extract was analysed by HPLC and ¹H-NMR spectroscopy.

The chemical hydrolysis of ethyl *N*-[2'-(3'',4''-dihydroxyphenyl)-2'-hydroxyethyl]-3-aminopropionate (**74**, 163.5 μ M) in phosphate-citrate buffer pH 7.4 (6.80 g disodium hydrogen phosphate Na₂HPO₄.12H₂O and 0.0585 g citric acid C₆H₈O₇.H₂O in 100 ml water) containing 10% acetonitrile at 37 °C was monitored by HPLC.

6.3 RESULTS AND DISCUSSION

6.3.1 Chemical hydrolysis studies of ethyl *N*-[2'-(3'',4''-dipivaloyloxyphenyl)-2'-hydroxyethyl]-3-aminopropionate (**107**) at pD 8.57 (pH 8.17) and 37 °C by $^1\text{H-NMR}$ spectroscopy

6.3.1.1 Products from and mechanism of chemical hydrolysis

The solution of ethyl *N*-[2'-(3'',4''-dipivaloyloxyphenyl)-2'-hydroxyethyl]-3-aminopropionate (**107**, 105.5 μM) in phosphate-citrate buffer pH 8.0 containing 10% acetonitrile at 50 °C was monitored with time by HPLC. The mobile phase was aqueous acetonitrile (30%) containing 0.1% tetrabutylammonium hydroxide with the pH adjusted to 3.0 with orthophosphoric acid. When 80% of the triester had been converted to the intermediate, the reaction was cooled and extracted successively with hexane (2 x 20 ml), diethyl ether (2 x 20 ml), chloroform (2 x 20 ml) and ethyl acetate (2 x 20 ml). Each extract was analysed by HPLC and $^1\text{H-NMR}$ spectroscopy.

The hexane extract shows the presence of only ethyl *N*-[2'-(3'',4''-dipivaloyloxyphenyl)-2'-hydroxyethyl]-3-aminopropionate (**107**), whereas the diethyl ether and ethyl acetate extracts contained little material by $^1\text{H-NMR}$ spectroscopy. By HPLC, the chloroform extract contained the majority of the intermediate (peak B). $^1\text{H-NMR}$ spectrum of the chloroform extract showed that the peaks were absent for an ethyl ester, however there was a large signal for the pivaloyl ester, δ_{H} 1.25 (s). Integration of this suggests that the intermediate could be the dipivaloyloxy carboxylic acid (**120**). Further evidence was sought by monitoring the hydrolysis of ethyl *N*-[2'-(3'',4''-dipivaloyloxyphenyl)-2'-hydroxyethyl]-3-aminopropionate (**107**) by $^1\text{H-NMR}$ spectroscopy.

By $^1\text{H-NMR}$ spectroscopy, the triester (**107**) gave peaks at δ_{H} 1.15 (3H, t, $J_{\text{HH}}=7.15$ Hz) and 4.05 (2H, q, $J_{\text{HH}}=7.1$ Hz) for the ethyl ester, and peaks at δ_{H} 1.25 (9H, s) and 1.26 (9H, s) for the pivaloyl esters. Details of the aromatic protons are given in Table 6.1. The reference peak of d_3 -acetonitrile appears at 1.95 (quintet). The $^1\text{H-NMR}$ assignment for (**107**) is given in Figure 6.3. The $^1\text{H-NMR}$ spectrum is shown in Figure 6.4a with an expansion of the aromatic protons in Figure 6.4b.

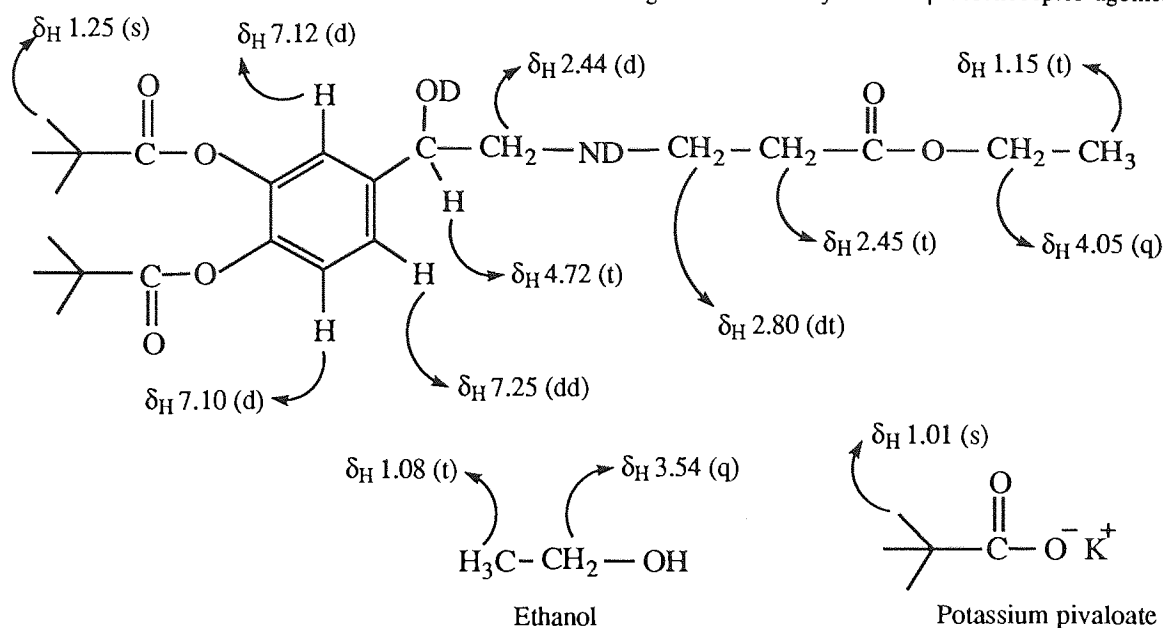


Figure 6.3: Assignments of ethyl *N*-[2'-(3'',4''-dipivaloyloxyphenyl)-2'-hydroxyethyl]-3-aminopropionate (**107**) by $^1\text{H-NMR}$ [D_2O , pD 8.57- CD_3CN (8:2, v/v)].

The hydroxyl and -NH- groups are exchanged with D_2O . $^1\text{H-NMR}$ assignments of the hydrolysis products, ethanol and potassium pivaloate are also given.

Aromatic protons	H ₂ -aromatic (δ)	H ₅ -aromatic (δ)	H ₆ -aromatic (δ)
Triester (107)	7.12, d ($J_{\text{meta}}=1.9$ Hz)	7.10, d ($J_{\text{ortho}}=8.3$ Hz)	7.25, dd ($J_{\text{ortho}}=8.4$ and $J_{\text{meta}}=2.0$ Hz)
Intermediate (120) (Dipivaloyl acid)	7.21, d ($J_{\text{meta}}=2.0$ Hz)	7.17, d ($J_{\text{ortho}}=8.4$ Hz)	7.32, dd ($J_{\text{ortho}}=8.2$ and $J_{\text{meta}}=2.0$ Hz)
Dihydroxy acid (74 , R=H)	6.82, d ($J_{\text{meta}}=1.5$ Hz)	6.80, d ($J_{\text{ortho}}=8.3$ Hz)	6.73, dd ($J_{\text{ortho}}=8.3$ and $J_{\text{meta}}=1.8$ Hz)

Table 6.1: Chemical shifts and coupling constants of aromatic protons in catechol derivatives.

The hydrolysis of the pivaloyl ester of ethyl *N*-[2'-(3'',4''-dipivaloyloxyphenyl)-2'-hydroxyethyl]-3-aminopropionate (**107**) was monitored by the formation of potassium pivaloate in the ^1H NMR spectrum at δ_{H} 1.01. The hydrolysis of the ethyl ester of (**107**) was monitored by the formation of ethanol in the ^1H NMR spectrum at δ_{H} 1.08 (3H, t, $J_{\text{HH}}=7.1$ Hz, - CH_3) and 3.54 (2H, q, $J_{\text{HH}}=7.1$ Hz, - CH_2 -). Hydrolysis of the ethyl ester occurs first in potassium phosphate buffer pD 8.57 (pH 8.17) to give the dipivaloyl carboxylic acid (**120**), which gave in the $^1\text{H-NMR}$ spectrum peaks at δ_{H} 1.26 (9H, s) and 1.27 (9H, s) for pivaloyl esters. The $^1\text{H-NMR}$ assignments of (**120**) are shown in Figure 6.5. The $^1\text{H-NMR}$ spectra of (**107**) after 24 h and 70 h hydrolysis are shown in Figures 6.7a and 6.8a respectively. The expansion of the aromatic protons are shown in Figures 6.7b and 6.8b and the δ values are recorded in Table 6.1.

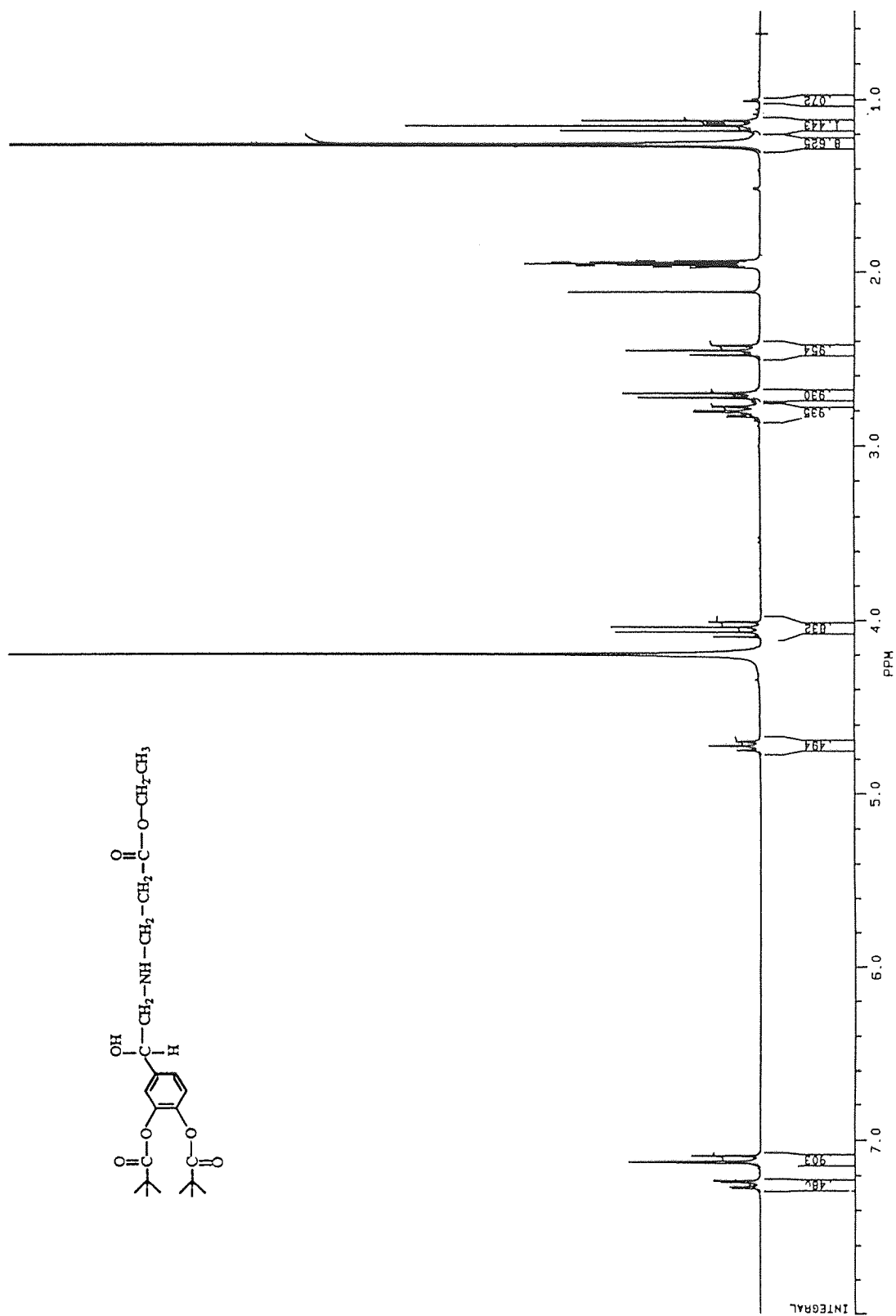


Figure 6.4a: $^1\text{H-NMR}$ spectrum of ethyl *N*-[2'-(3',4'-dipivaloyloxyphenyl)-2'-hydroxyethyl]-3-aminopropionate (**107**) in buffer pH 8.57 (pH 8.17) in 20% CD_3CN in D_2O .

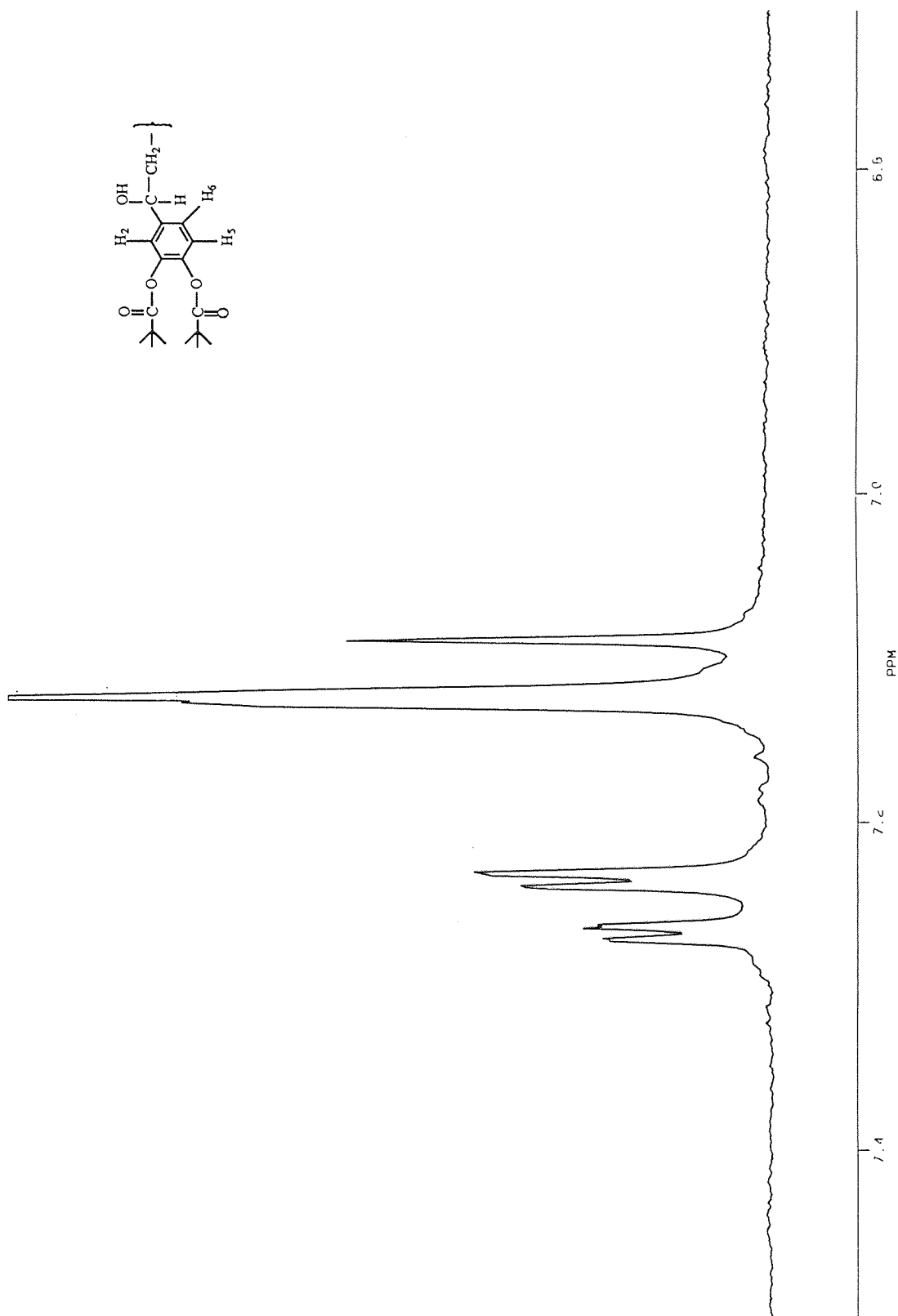


Figure 6.4b: Expansion of aromatic region of ethyl *N*-[2'-(3'',4'')-dipivaloyloxyphenyl]-2'-hydroxyethyl]-3-aminopropionate (107) in buffer pD 8.57 (pH 8.17) in 20% CD₃CN in D₂O.

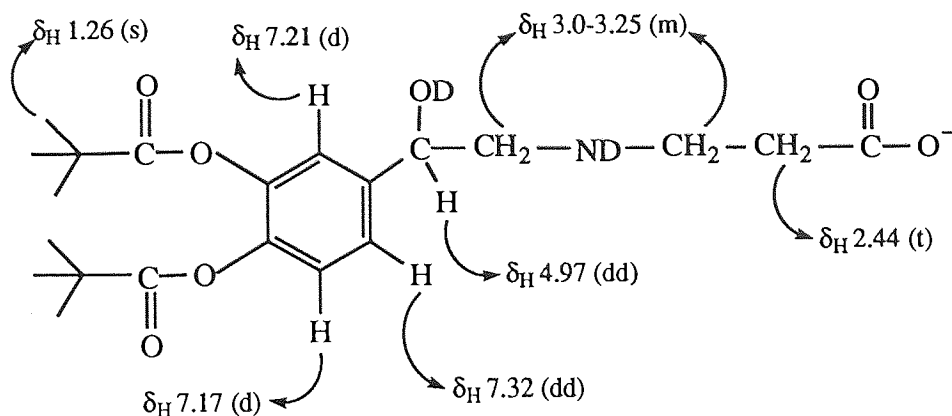


Figure 6.5: Assignments of *N*-[2'-(3'',4''-dipivaloyloxyphenyl)-2'-hydroxyethyl]-3-aminopropionic acid (**120**) by $^1\text{H-NMR}$ [D_2O , pD 8.57- CD_3CN (8:2, v/v)].

Under these conditions, the hydrolysis of the pivaloyloxy esters of ethyl *N*-[2'-(3'',4''-dipivaloyloxyphenyl)-2'-hydroxyethyl]-3-aminopropionate (**107**) was not observed owing to the higher reactivity of the ethyl ester, presumably because of steric hindrance of the pivaloyl groups. The dipivaloyl carboxylic acid (**120**) showed slow hydrolysis of the first pivaloyloxy group with removal of the 3- and 4-pivaloyloxy groups presumably occurring at similar rates.¹⁵⁷ The second pivaloyloxy group undergoes a rapid hydrolysis, principally because of the ability of the *o*-hydroxyl group in the monopivaloyl compound to act as an acid catalyst and also because of less steric hindrance in (**121**, **122**) when compared with dipivaloyl carboxylic acid (**120**), to form the dihydroxy carboxylic acid (**74**, R=H)(Scheme 6.2). The dihydroxy acid (**74**, R=H) gave a peak in the $^1\text{H-NMR}$ spectrum at δ_{H} 2.47 (2H, t, $J_{\text{HH}}=6.6$ Hz) for $-\text{CH}_2-\text{COO}^-$. The full $^1\text{H-NMR}$ assignments of (**74**, R=H) are shown in Figure 6.6 and the $^1\text{H-NMR}$ spectrum, with a 2:1 ratio of dihydroxy acid (**74**, R=H): dipivaloyl acid (**120**) is shown in Figure 6.9a. The aromatic protons are expanded in Figure 6.9b and are listed in Table 6.1.

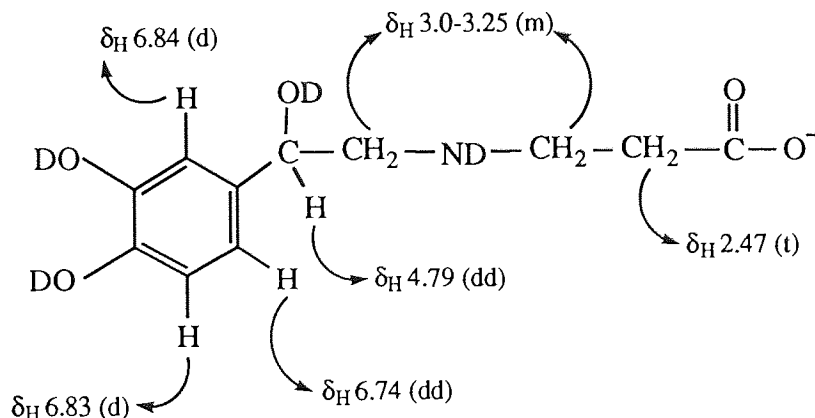
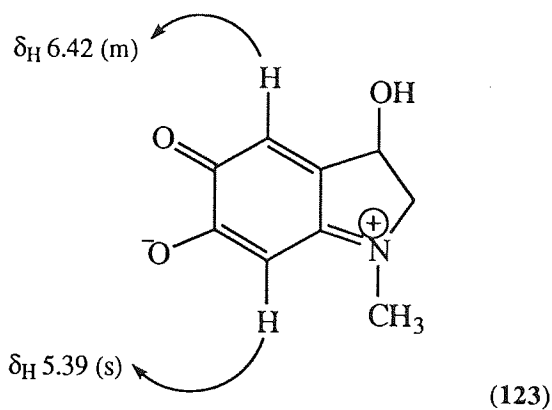


Figure 6.6: Assignments of *N*-[2'-(3'',4''-dihydroxyphenyl)-2'-hydroxyethyl]-3-aminopropionic acid (**74**, R=H) by $^1\text{H-NMR}$ [D_2O , pD 8.57- CD_3CN (8:2, v/v)].

Potassium pivaloate was also formed, as shown by the peak in the ^1H NMR spectrum (D_2O , buffer pD 8.57) at δ 1.01 (s, 9H). There was a small amount ($< 5\%$) of the aminochrome oxidation product (**125**, Scheme 6.4) at δ_{H} 5.45-5.60 (m) and 6.00-6.40 (m). The literature value of the adrenochrome (**123**) (oxidation product from epinephrine) zwitterionic mesomeric structure, appears in the ^1H NMR ($\text{DMSO-}d_6$) spectrum at δ_{H} 5.39 (s, 1H, H₅-aromatic) and 6.42 (m, 1H, H₂-aromatic).¹⁵⁸



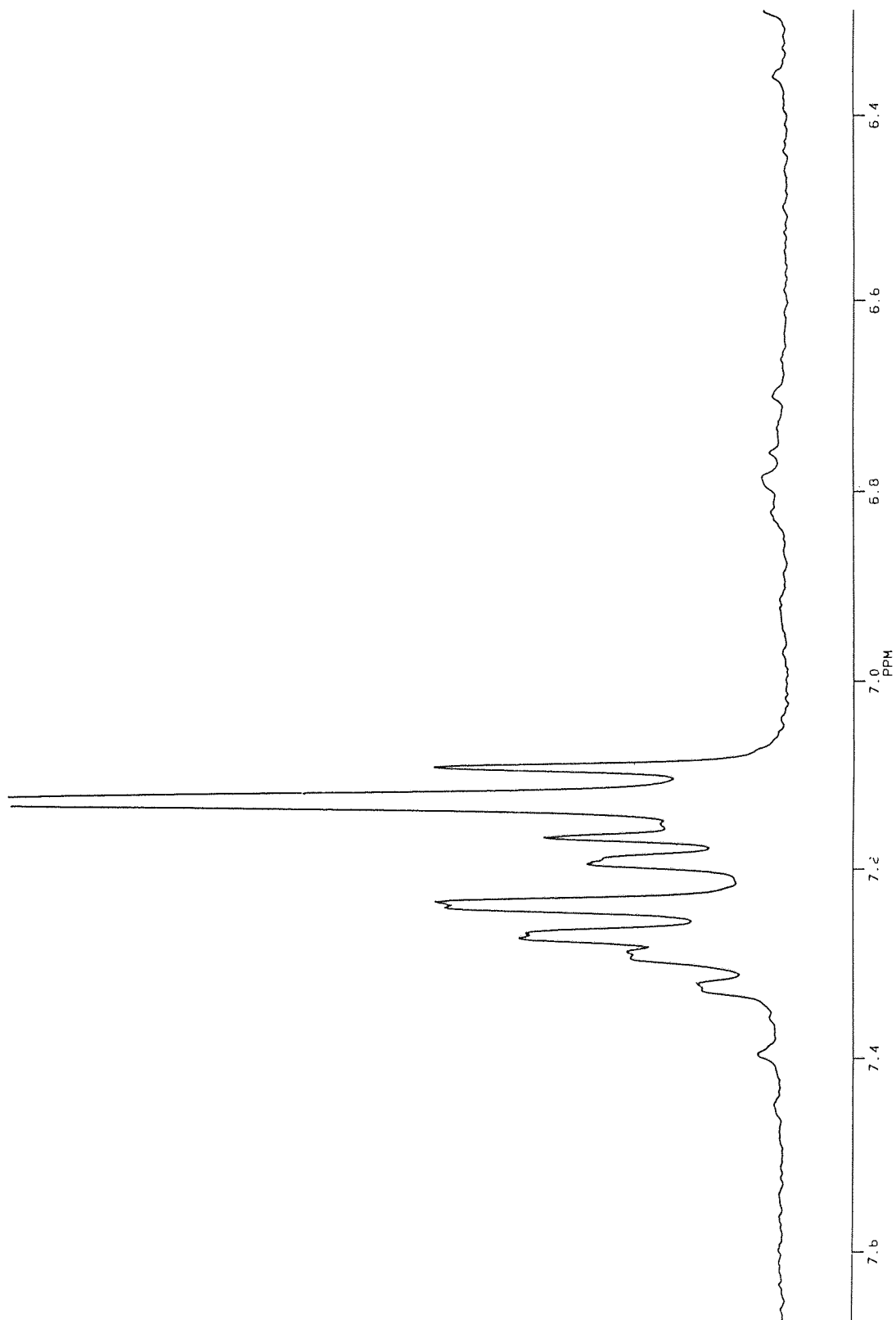


Figure 6.7b: Expansion of aromatic region of ethyl *N*-[2'-(3',4'-divaloyloxyphenyl)-2'-hydroxyethyl]-3-aminopropionate (**107**) in buffer pD 8.57 (pH 8.17) in 20% CD_3CN in D_2O after 24 hrs.

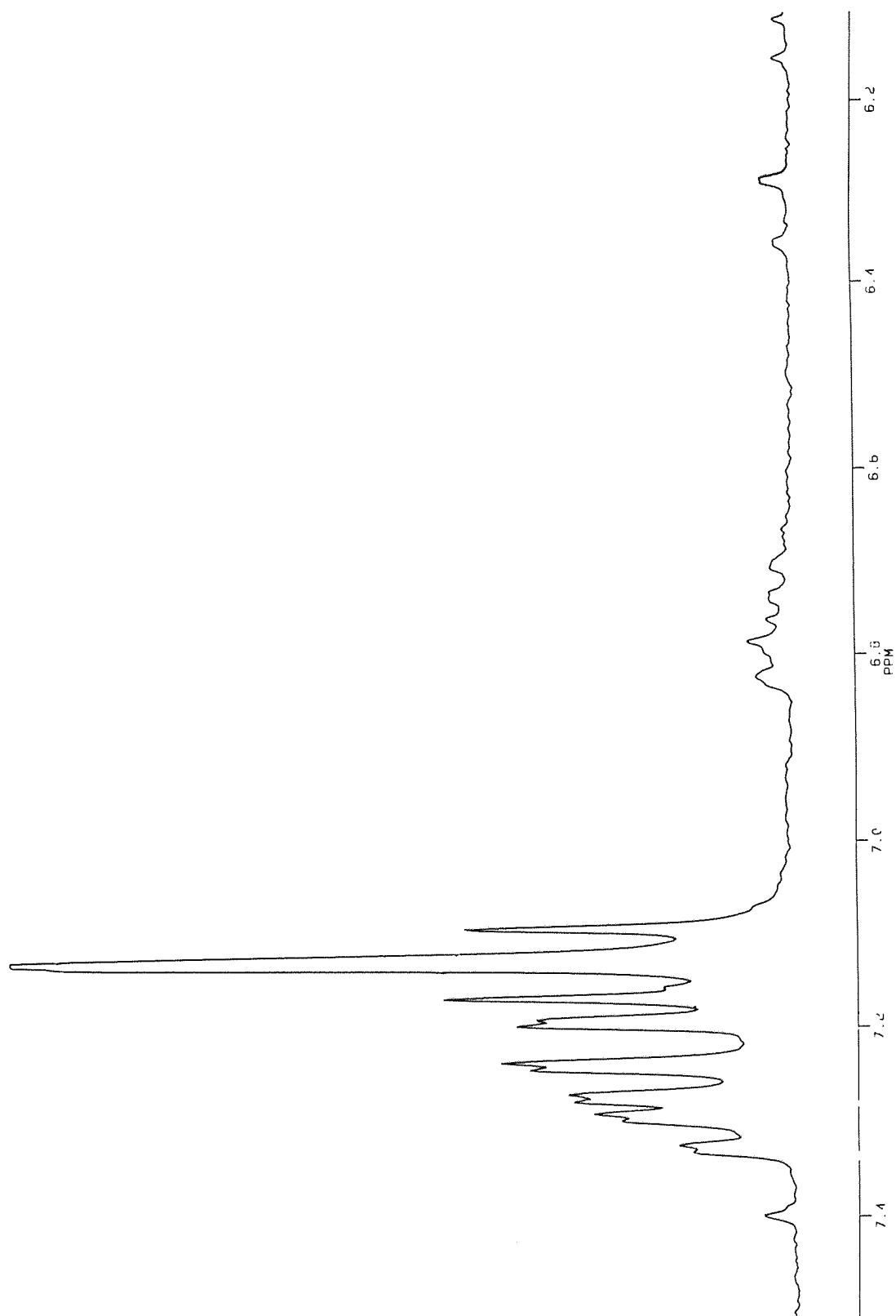


Figure 6.8b: Expansion of aromatic region of ethyl *N*-[2'-(3",4"-divaloyloxyphenyl)-2'-hydroxyethyl]-3-aminopropionate (**107**) in buffer pD 8.57 (pH 8.17) in 20% CD₃CN in D₂O after 70 hrs.

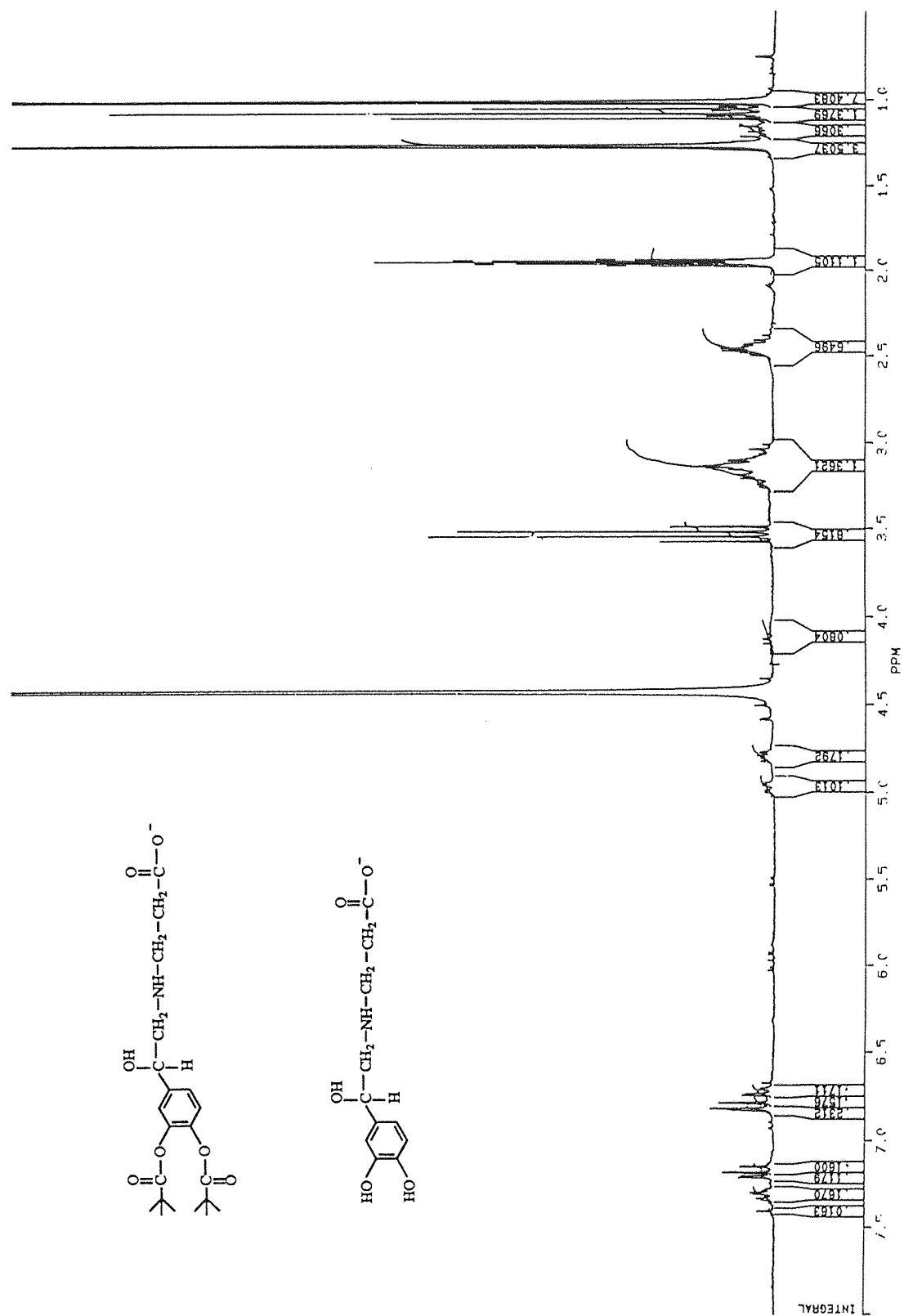


Figure 6.9a: $^1\text{H-NMR}$ spectrum of ethyl *N*-[2'-(3,4"-dipivaloyloxyphenyl)-2'-hydroxyethyl]-3-aminopropionate (107) in buffer pH 8.57 (pH 8.17) in 20% CD_3CN in D_2O after 300 hrs.

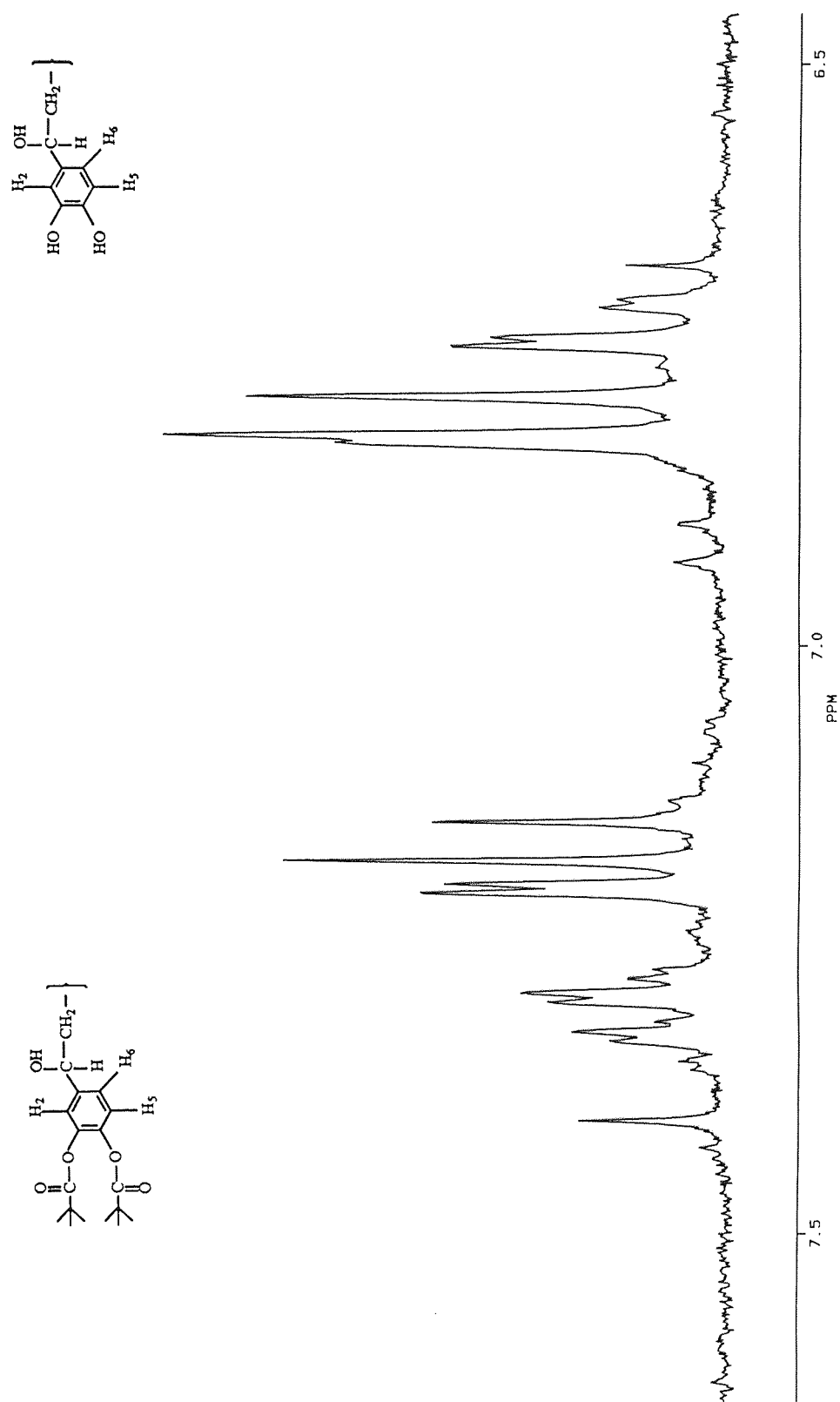


Figure 6.9b: Expansion of aromatic region of ethyl *N*-[2'-(3'',4'')-dipivaloyloxyphenyl]-2'-hydroxyethyl]-3-aminopropionate (107) in buffer pD 8.57 (pH 8.17) in 20% CD₃CN in D₂O after 300 hrs.

If the monopivaloyl compounds (**118**, **119**) had been the first formed metabolites, then the chemical shift for the aromatic protons would have been shifted up-field relative to ethyl *N*-[2'-(3'',4''-dipivaloyloxyphenyl)-2'-hydroxyethyl]-3-aminopropionate (**107**). To confirm that the $^1\text{H-NMR}$ peaks in Figure 6.9b at δ_{H} 7.21 (d), 7.17 (d) and 7.32 (dd) were for the dipivaloyl acid (**120**) and peaks at δ_{H} 6.73 (dd), 6.80 (d) and 6.82 (d) were due to dihydroxy acid (**74**, R=H), chemical hydrolysis of ethyl *N*-[2'-(3'',4''-dihydroxyphenyl)-2'-hydroxyethyl]-3-aminopropionate (**74**, R=Et) was studied under the same $^1\text{H-NMR}$ conditions. It was revealed (Table 6.3) that the aromatic protons for the dihydroxy ethyl ester (**74**, R=Et) and dihydroxy acid (**74**, R=H) appear at the same chemical shifts as these compounds assigned from the hydrolysis of the triester (**107**)(Table 6.1).

For early time points (10 h), the ethyl *N*-[2'-(3'',4''-dipivaloyloxyphenyl)-2'-hydroxyethyl]-3-aminopropionate (**107**) : ethanol ratio by integration matches with the ratio of ethyl *N*-[2'-(3'',4''-dipivaloyloxyphenyl)-2'-hydroxyethyl]-3-aminopropionate (**107**) : dipivaloyloxy acid (**120**) in the aromatic region. Together with the fact that very little potassium pivaloate was formed in comparison to ethanol, suggests that the first formed product was the dipivaloyloxy acid (**120**). Further, in Figure 6.9a, the ethyl ester (δ_{H} 4.05 for $-\text{COO}-\text{CH}_2$) was totally hydrolysed but the pivaloyl ester (δ_{H} 1.26 for Bu^tCOO) was still intact in the intermediate, confirming that the metabolite giving rise to peak [B] in the HPLC trace was indeed dipivaloyl acid (**120**).

Table 6.2 shows the changes in the $^1\text{H-NMR}$ peak area for the % of ethyl *N*-[2'-(3",4"-dipivaloyloxyphenyl)-2'-hydroxyethyl]-3-aminopropionate (**107**), dipivaloyloxy acid (**120**) and dihydroxy acid (**74**, R=H) with time (Appendix VI shows full calculation).

Time (h)	% of (107)	% of (120)	% of (74 , R=H)	ln [% of (107)]
0.10	99.09	0.91	0.00	4.605
0.85	94.84	4.40	0.76	4.552
1.85	93.87	4.93	1.20	4.542
3.85	92.51	6.02	1.47	4.527
5.85	91.05	7.55	1.41	4.511
8.60	89.20	9.07	1.73	4.491
23.0	81.52	13.62	4.85	4.401
24.0	80.79	14.35	4.86	4.392
26.0	76.51	17.91	5.59	4.337
28.0	79.19	14.68	6.13	4.372
30.0	72.09	21.57	6.34	4.278
32.0	72.62	20.88	6.50	4.285
34.0	76.28	16.98	6.73	4.334
36.0	69.98	22.37	7.65	4.248
38.0	71.33	20.52	8.15	4.267
40.0	68.92	22.62	8.46	4.233
42.0	68.93	22.71	8.37	4.233
44.0	65.00	26.75	8.25	4.174
48.15	67.43	23.40	9.17	4.211
49.65	65.48	25.07	9.45	4.182
70.15	58.26	28.91	12.84	4.065
300.0	8.98	23.13	67.89	2.194

Table 6.2: Calculation of % of ethyl *N*-[2'-(3",4"-dipivaloyloxyphenyl)-2'-hydroxyethyl]-3-aminopropionate (**107**) and hydrolysis product *N*-[2'-(3",4"-dipivaloyloxyphenyl)-2'-hydroxyethyl]-3-aminopropionic acid (**120**) and *N*-[2'-(3",4"-dihydroxyphenyl)-2'-hydroxyethyl]-3-aminopropionic acid (**74**, R=H) by integration in $^1\text{H-NMR}$.

The data in table 6.2 was used to plot the ln-concentration of triester (**107**) against time (Figure 6.10a). Degradation followed a first order model (Equation 6.2) and the rate constant for the hydrolysis of ethyl *N*-[2'-(3",4"-dipivaloyloxyphenyl)-2'-hydroxyethyl]-3-aminopropionate (**107**) to the dipivaloyl carboxylic acid (**120**) at pH 8.17 (pD 8.57) and 37 °C is $7.477 \times 10^{-3} \text{ h}^{-1}$ with a half-life of 92.0 h.

$$\ln A_t = \ln A_0 - kt \quad \text{.....Eq. 6.2}$$

A value of $7.8605 \times 10^{-3} \text{ h}^{-1}$ with a half-life of 88.0 h was obtained when an extended time point (300 h) was included in the data (Figure 6.10b). In contrast, the HPLC studies were performed at 50 °C, in the presence of only 10% acetonitrile which increases the rate constant k to 0.281 h^{-1} ($t_{1/2} = 2.47 \text{ hr}$). 20% Acetonitrile was used in the NMR studies (because NMR needs more compound than HPLC therefore more acetonitrile was used to solubilise the triester) which decreased the rate of hydrolysis.

The chemical hydrolysis of ethyl *N*-[2'-(3'',4''-dipivaloyloxyphenyl)-2'-hydroxyethyl]-3-aminopropionate (**107**) to the dihydroxy acid (**74**, R=H) was slow (Figure 6.11). After 70 hrs, only 13% of ethyl *N*-[2'-(3'',4''-dipivaloyloxyphenyl)-2'-hydroxyethyl]-3-aminopropionate (**107**) was converted to the dihydroxy acid (**74**, R=H) (Figure 6.11a). After 300 h, only 9% ethyl *N*-[2'-(3'',4''-dipivaloyloxyphenyl)-2'-hydroxyethyl]-3-aminopropionate (**107**) was present, along with 23% of the dipivaloyl acid (**120**) and 68% of the dihydroxy acid (**74**, R=H) (Figure 6.11b).¹⁰³ These values may slightly underestimate the true rates of triester conversion, since a small amount of the dihydroxy acid formed was oxidised to the aminochrome.¹⁵⁸ This was assumed to occur because the solution became pink as time increased.

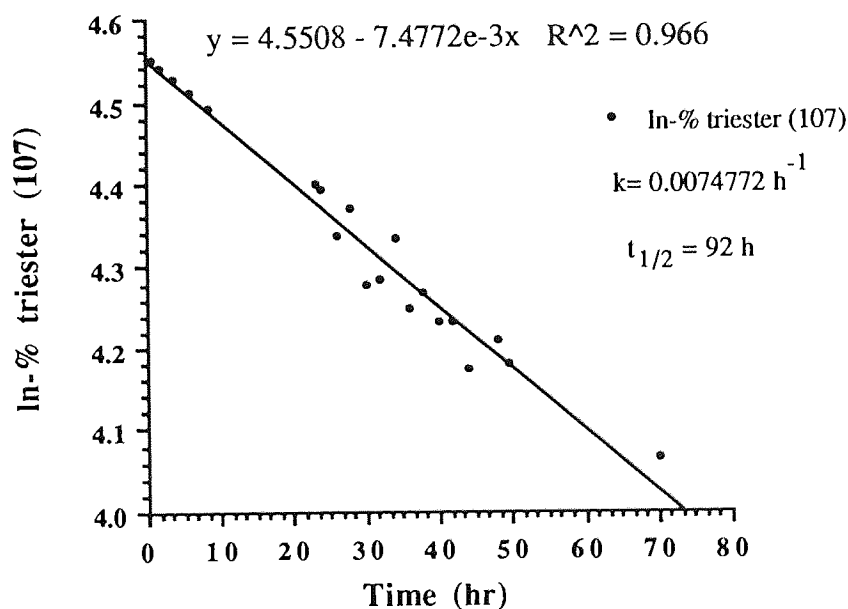


Figure 6.10a: Hydrolysis of triester (**107**) in potassium phosphate buffer (pD 8.57) in 20% acetonitrile at 37 °C by ^1H -NMR spectroscopy over 70 hrs.

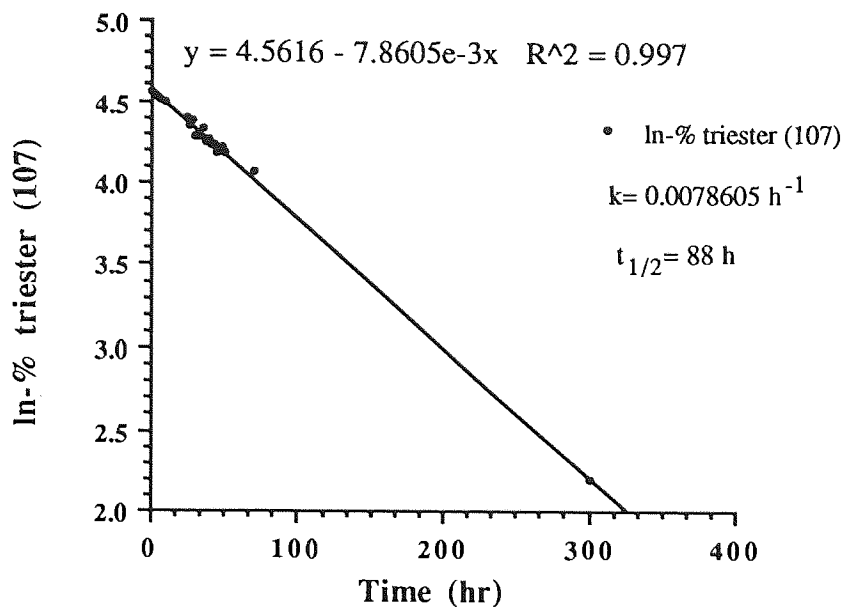


Figure 6.10b: Hydrolysis of triester (107) in potassium phosphate buffer (pD 8.57) in 20% acetonitrile at 37 °C by $^1\text{H-NMR}$ spectroscopy over 300 hrs.

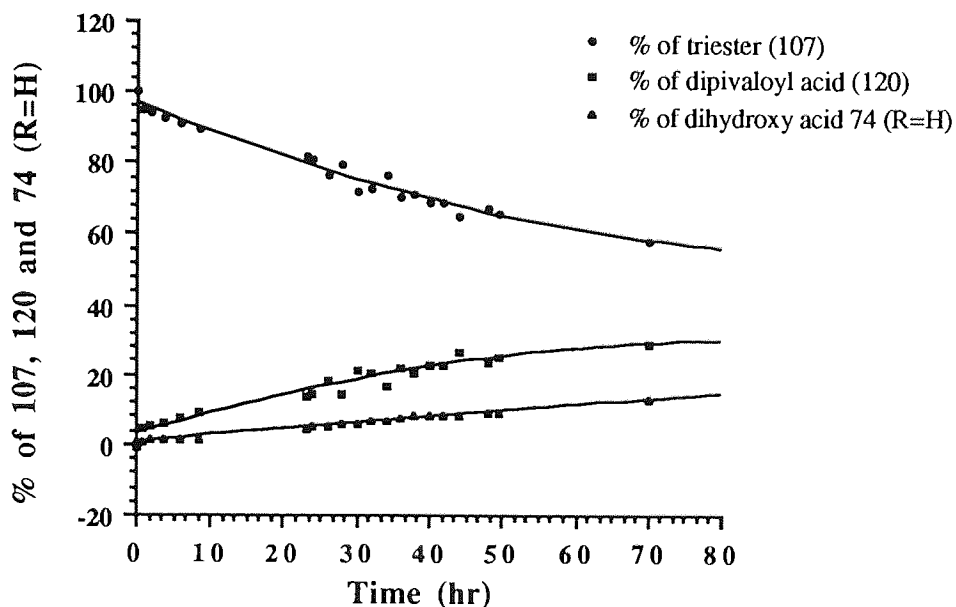
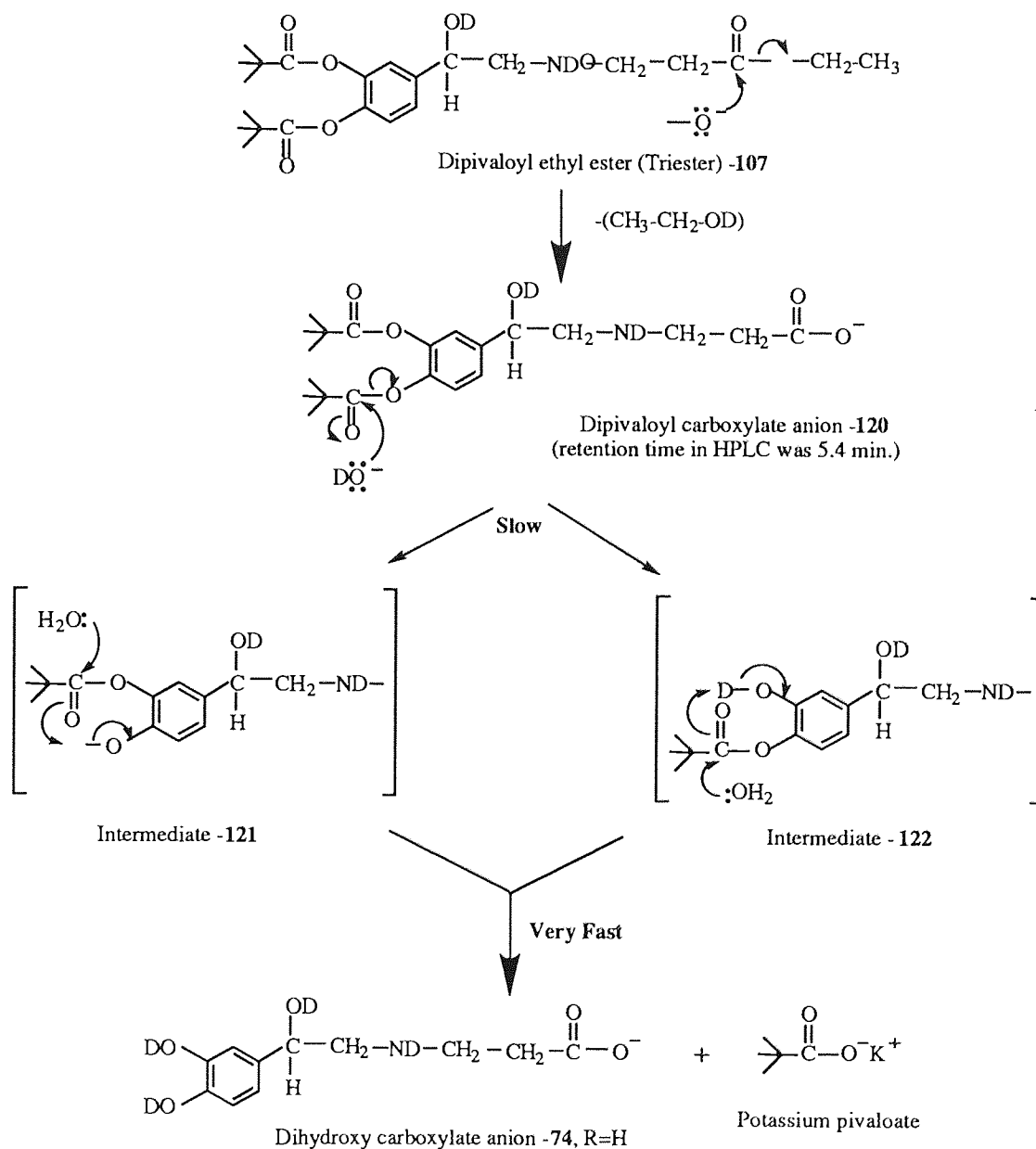


Figure 6.11a: Hydrolysis of triester (107): formation of the dipivaloyloxy acid (120) and the dihydroxy acid (74, R=H). After 70 h the proportions of (107), (120) and (74, R=H) were 58, 29 and 13% respectively by $^1\text{H-NMR}$ spectroscopy.

Conclusion

The chemical hydrolysis of the pro-soft-drug (**107**) proceeds *via* hydrolysis of the ethyl ester (path B). However, the dipivaloyl acid product (**120**) is not active as a β -adrenoceptor agonist, therefore reaction by chemical hydrolysis does not lead to the required soft-drug. Hydrolysis of the pivaloyl esters in (**107**) needs to be faster than the hydrolysis of the ethyl group to give the soft-drug (**74**, R=Et). If the ethyl ester were also hydrolysed faster than the pivaloyl ester under physiological condition, then the prodrug of the soft-drug (**74**, R=Et) would indeed be unsuitable. To see how the drug is hydrolysed in a biological system, the hydrolysis of the pro-soft-drug (**107**) was monitored in an enzymatic medium.



Scheme 6.2: Mechanism of chemical hydrolysis of triester (**107**) in potassium phosphate buffer in D_2O (pH 8.17, pD 8.57)-acetonitrile (8:2 v/v) at 37 °C by 1H -NMR spectroscopy. Triester hydrolysed to dihydroxy acid (**74**, R=H) by the formation of intermediate dipivaloyloxy acid (**120**, t_R = 5.4 min in HPLC). The pink colour is due to oxidation of the hydrolysis product into aminochrome (**125**, **126**).

6.3.1.2 *Products from and mechanism of hydrolysis of ethyl N-[2'-(3",4"-dipivaloyloxyphenyl)-2'-hydroxyethyl]-3-aminopropionate (107) in phosphate-citrate buffer at pH 7.4 and 37 °C, containing 10% acetonitrile in the presence of porcine liver carboxyesterase*

Enzyme hydrolysis studies of triester (107) by HPLC

The reaction mixture consisted of triester [107, (50 μ M)] in 20 ml of phosphate-citrate buffer at pH 7.4 containing 10% acetonitrile. Porcine liver carboxyesterase (0.5 ml, 6.29 U) was added and the reaction mixture was incubated at 37 °C with constant stirring. The mixture was protected from light and air (under argon gas) and was monitored by HPLC at regular time intervals. By HPLC, the triester peak disappears rapidly with no formation of intermediate dipivaloyl acid (120). The reaction is first order and the data was fit to the first order equation (6.2) which gives a straight line with $k = 4.9159 \text{ h}^{-1}$ ($r^2 = 0.997$, $t_{1/2} = 0.14 \text{ h}$). The reaction was monitored 4 times over 5 half-lives (Figure 6.12). The HPLC traces (Figure 6.2) eluting with 30% acetonitrile in water shows no formation of dipivaloyl acid (120) in the enzyme hydrolysis.

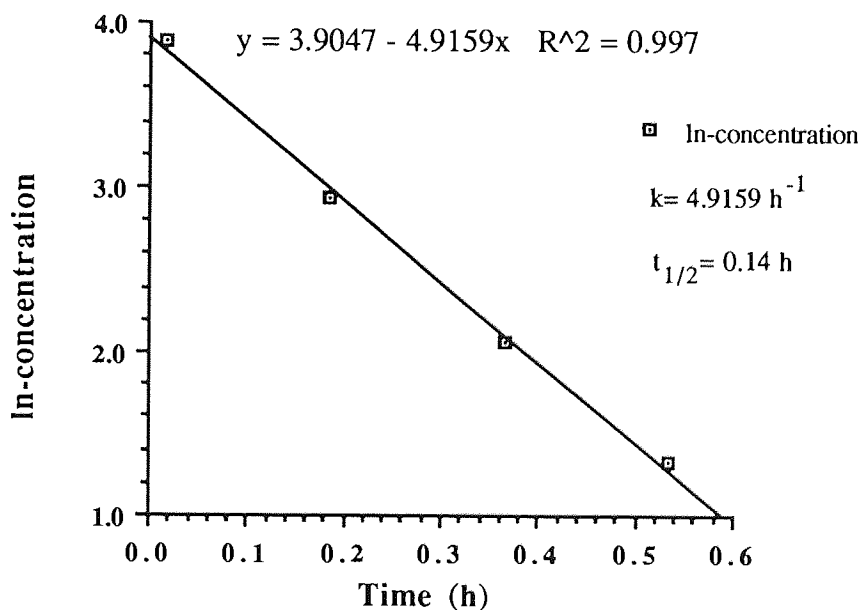


Figure 6.12: Enzyme hydrolysis of triester (107) in 10% acetonitrile in phosphate-citrate buffer at pH 7.4 and 37 °C with 6.29 U of porcine liver carboxyesterase.

When the hydrolysis of the triester (**107**) with porcine liver carboxyesterase was complete, as indicated by the disappearance of the triester peak by HPLC using a mobile phase of 30% acetonitrile in water, the reaction mixture was analysed with 4% acetonitrile in water. This showed that the triester yielded the dihydroxy ethyl ester (**74**, R= Et) ($t_R = 8.8$ min) as the sole product, which further degrades to the dihydroxy acid (**74**, R= H). This is also a first order hydrolysis with a k value of $9.1423 \times 10^{-2} \text{ h}^{-1}$ ($r^2 = 1.000$, $t_{1/2} = 7.582$ hrs) (Figure 6.13 and Scheme 6.3). It shows that with porcine liver carboxyesterase the hydrolysis of the pivaloyl ester is much faster than hydrolysis of the ethyl ester for triester (**107**). The soft-drug dihydroxy ethyl ester (**74**, R= Et) is the major intermediate in enzyme hydrolysis (Scheme 6.4). In enzyme hydrolysis the reaction proceeds in the required way thus the dipivaloyl ethyl ester (**107**) can be used as a pro-soft-drug.

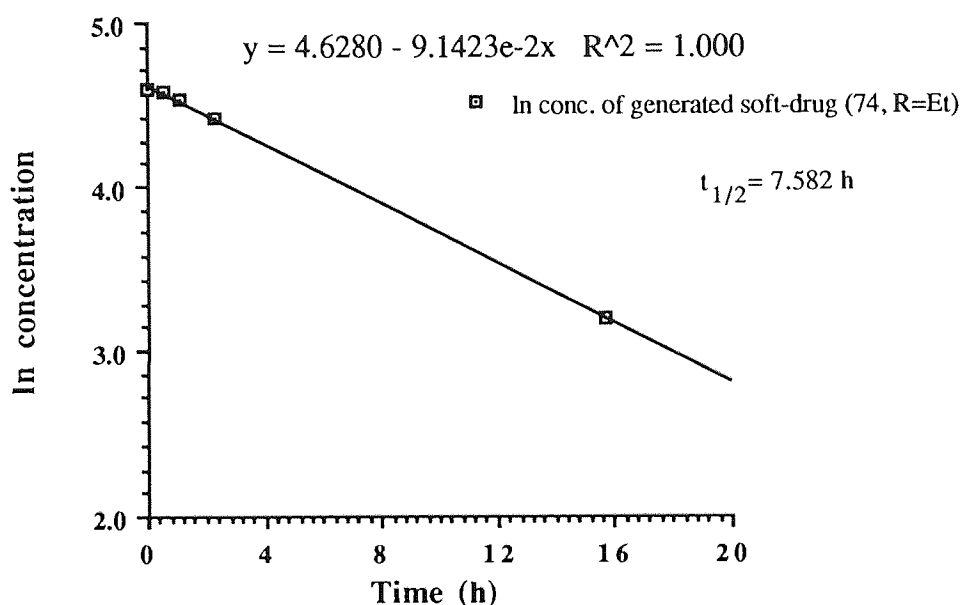
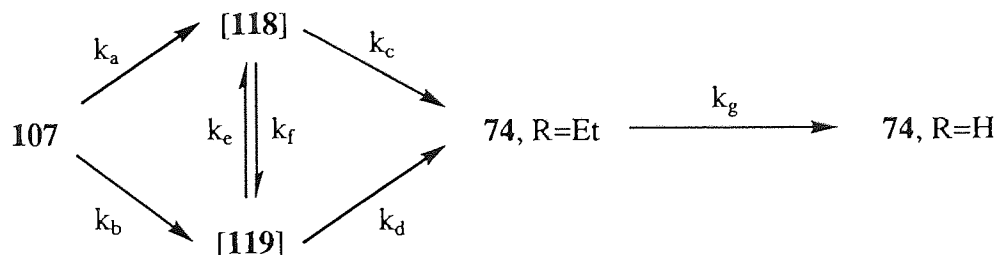
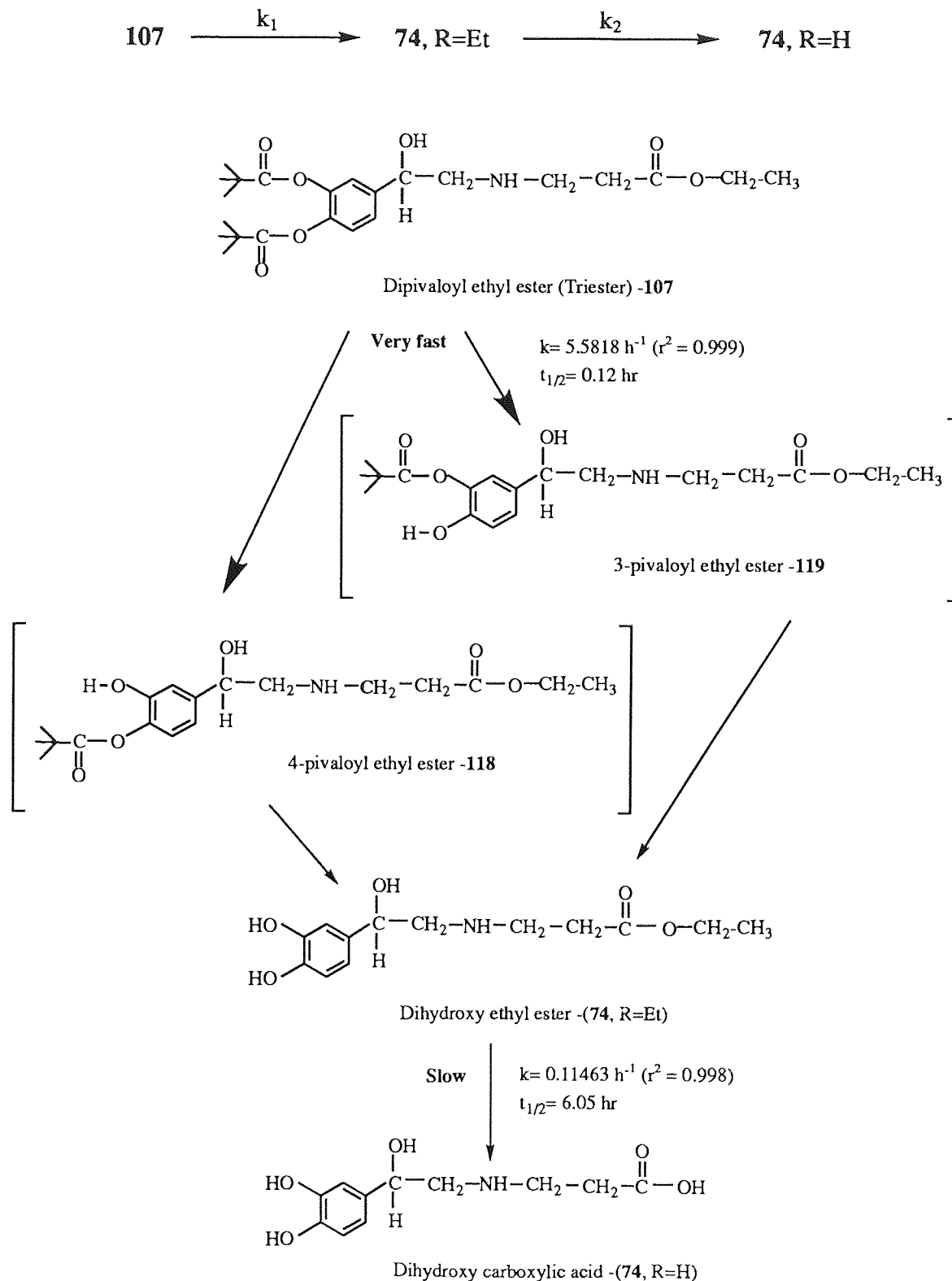


Figure 6.13: Half-life of dihydroxy ethyl ester (**74**, R= Et) formed in the reaction mixture by the hydrolysis of triester HCl (**107**) in 10% acetonitrile in phosphate-citrate buffer at pH 7.4 at 37 °C with 6.29 U of porcine liver carboxyesterase.

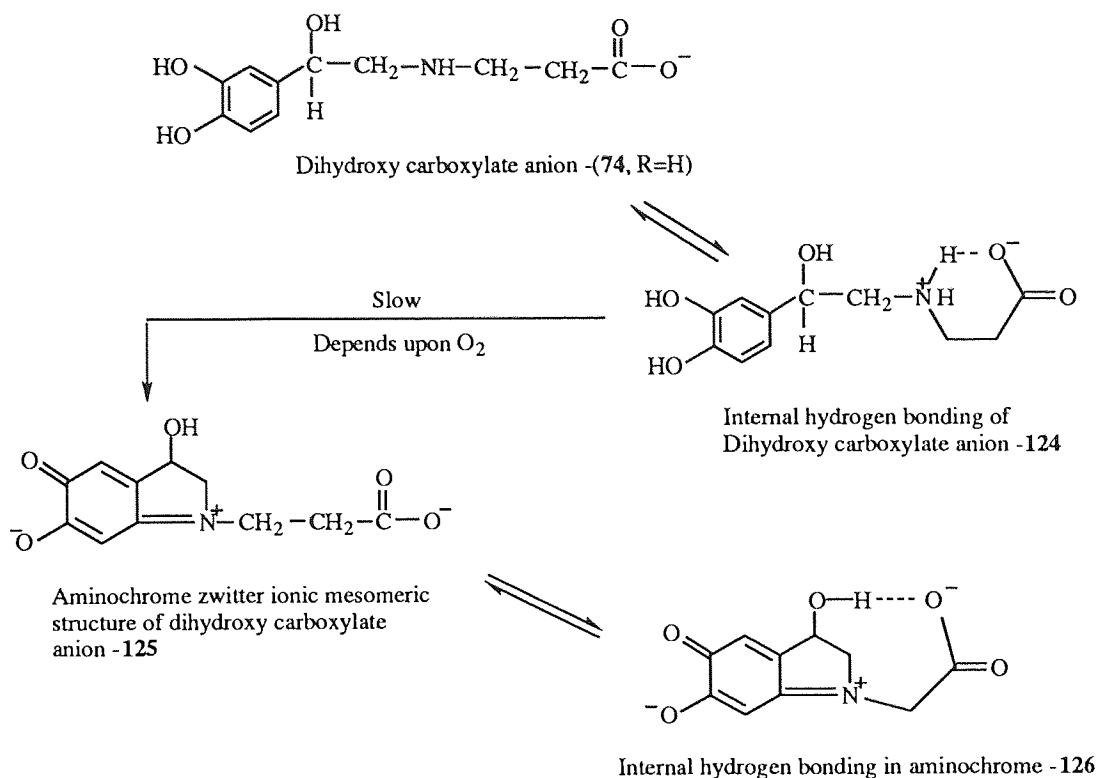
A full kinetic scheme for the enzymatic degradation may be expressed as:



The rate constant for the disappearance of the triester (**107**) [$k_1 = k_a + k_b$] is much smaller [$k_1 \ll (k_c + k_d)$] than that for the degradation of the monopivaloyl residues [$k_c + k_d$] and becomes rate-determining in the formation of the soft-drug (**74**, R=Et). Hence, the overall degradation is closely modelled by a three-compartment sequential pathway ($k_2 = k_g$):



Scheme 6.3: Hydrolysis of triester HCl (**107**) in phosphate-citrate buffer (10% acetonitrile) pH 7.4 at 37 °C with 6.29 U of porcine liver carboxyesterase by HPLC analysis.



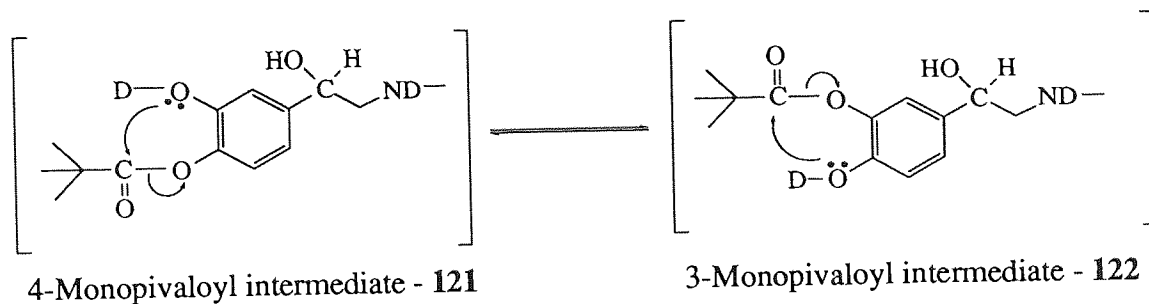
Scheme 6.4: Oxidation of dihydroxy acid (74, R=H).
The pink colour is due to oxidation of the hydrolysis product into aminochrome (125, 126).

6.3.1.3 Rearrangement of catechol esters in ethyl *N*-[2'-(3'',4''-dipivaloyloxyphenyl)-2'-hydroxyethyl]-3-aminopropionate (107)

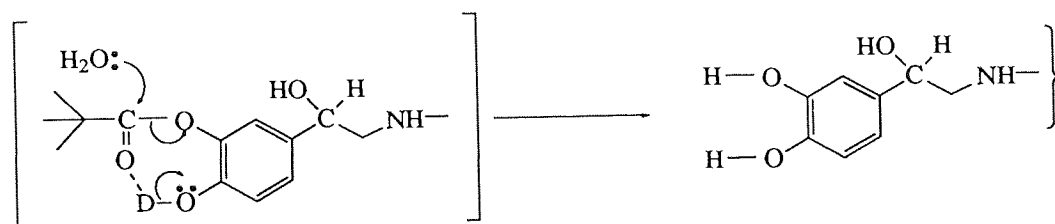
In the chemical hydrolysis of triester (107), the ethyl ester was hydrolysed much faster than the pivaloyl group, to form the dipivaloyl acid (120, t_R , 5.4 min). The first pivaloyl group then presumably cleaves to form the intermediates (121) and (122) which will be in rapid equilibrium with one another (Scheme 6.5).^{104,159-161} The individual isomers cannot be detected by HPLC or ¹H-NMR spectroscopy because the rate of acyl migration is faster than the rate of hydrolysis at 37 °C.^{104,159-161} The rate of hydrolysis of the dipivaloyloxy acid (120) to form the intermediates (121, 122) is slow due to steric hindrance. However, the rate of hydrolysis of the intermediates (121, 122) is very fast to form the dihydroxy acid (74, R=H) (in one reference, the hydrolysis of catechol monoacetate to catechol was shown to be 500-700 times faster than the hydrolysis of catechol diacetate to catechol).¹¹⁸ The rapid acyl migration and hydrolysis is due to the existence of a neighbouring hydroxyl group.^{104,159-161} Two factors may contribute to this difference in the rate constants:

- the inductive effect and the resonance effects of an oxygen atom in the ortho- position, and
- the possibility of intramolecular hydrogen bonding of pivaloyl group.

Consequently, base-catalysed hydrolysis through hydrogen bonding with the neighbouring hydroxyl group must be the main reason why the intermediates (121 and 122) undergo rapid hydrolysis to the dihydroxy acid (74, R=H) (Scheme 6.6).



Scheme 6.5: Rearrangement of the pivaloyloxy group in the catechol ring. Isomeric degradation intermediates are not detected by HPLC or $^1\text{H-NMR}$ spectroscopy.



Scheme 6.6: Intramolecular hydrogen bonding with neighbouring hydroxyl group assists the rapid hydrolysis of mono pivaloyl group in catechol. Neighbouring group assistance in dipivaloyloxy catechol is not available.

6.3.2 Chemical hydrolysis studies of ethyl *N*-[2'-(3'',4''-dihydroxyphenyl)-2'-hydroxyethyl]-3-aminopropionate (**74**, R= Et) at pD 8.57 (pH 8.17) and 37 °C by ^1H -NMR spectroscopy

A solution of ethyl *N*-[2'-(3'',4''-dihydroxyphenyl)-2'-hydroxyethyl]-3-aminopropionate (**74**, 5 mM) in potassium phosphate buffer {0.1 mol dm⁻³, D₂O [pD 8.57 (pH 8.17)]}-CD₃CN (9:1, v/v) was monitored by ^1H NMR spectroscopy at 37 °C. The ethyl *N*-[2'-(3'',4''-dihydroxyphenyl)-2'-hydroxyethyl]-3-aminopropionate (**74**, R= Et) gave peaks at δ 1.14 (t, $J_{\text{HH}}=7.15$ Hz, 3H) and 4.07 (q, $J_{\text{HH}}=7.15$ Hz, 2H) for the ethyl ester, and 2.65 (t, $J_{\text{HH}}=6.7$ Hz, 2H) for $-\text{CH}_2\text{-COO-}$. The aromatic protons are recorded in Table 6.3 and the reference peak of d₃-acetonitrile appears at 1.95 (quintet). The full ^1H -NMR assignment of (**74**, R= Et) is shown in Figure 6.14 and the ^1H -NMR spectrum is shown in Figure 6.15a with an expansion of the aromatic protons in Figure 6.15b.

The hydrolysis of ethyl *N*-[2'-(3'',4''-dihydroxyphenyl)-2'-hydroxyethyl]-3-aminopropionate (**74**, R= Et) was monitored by the formation of ethanol in the ^1H -NMR spectrum at δ_{H} 1.08 (t, $J_{\text{HH}}=7.1$ Hz, 3H) and 3.54 (q, $J_{\text{HH}}=7.1$ Hz, 2H). Hydrolysis of the ethyl ester (**74**, R= Et) gave the dihydroxy acid (**74**, R=H). The ^1H -NMR assignments of (**74**, R=H) are given in Figure 6.6 and in Table 6.3. The formation of ethanol may be seen in the ^1H -NMR spectrum (Figure 6.16).

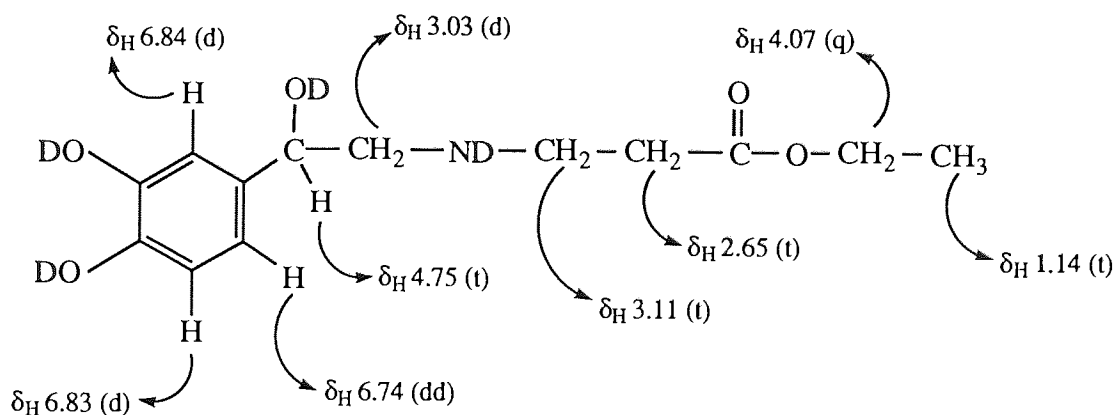


Figure 6.14: Assignments of ethyl *N*-[2'-(3'',4''-dihydroxyphenyl)-2'-hydroxyethyl]-3-aminopropionate (**74**, R= Et) in ^1H -NMR [D₂O, pD 8.57-CD₃CN (9:1, v/v)].

Aromatic protons	H ₂ -aromatic (δ)	H ₅ -aromatic (δ)	H ₆ -aromatic (δ)
Dihydroxy ethyl ester (74, R= Et)	6.84, d (J _{meta} =2.0 Hz)	6.83, d (J _{ortho} =7.9 Hz)	6.74, dd (J _{ortho} =8.1 and J _{meta} =2.0 Hz)
3,4-Dihydroxy acid (74, R=H)	6.82, d (J _{meta} =1.5 Hz)	6.80, d (J _{ortho} =8.3 Hz)	6.73, dd (J _{ortho} =8.3 and J _{meta} =1.85 Hz)

Table 6.3: Chemical shift and coupling constants of aromatic protons of ethyl *N*-[2'-(3",4"-dihydroxyphenyl)-2'-hydroxyethyl]-3-aminopropionate (74, R= Et) and dihydroxy acid (74, R=H).

Table 6.4 shows the proportions of ethyl *N*-[2'-(3",4"-dihydroxyphenyl)-2'-hydroxyethyl]-3-aminopropionate (74, R= Et) and dihydroxy acid (74, R=H), calculated from the ¹H-NMR peak areas with time.

Time (min)	% of (74, R=Et)	% of (74, R=H)	ln [% of (74, R=Et)]
0	93.38	6.62	4.537
66	85.93	14.07	4.454
141	82.13	17.88	4.408
216	77.09	22.91	4.345
291	73.78	26.22	4.301
366	66.82	33.18	4.202
441	64.01	35.99	4.159
516	60.22	39.78	4.098
591	55.77	44.23	4.021

Table 6.4: Calculation of % of ethyl *N*-[2'-(3",4"-dihydroxyphenyl)-2'-hydroxyethyl]-3-aminopropionate (74) and hydrolysis product *N*-[2'-(3",4"-dihydroxyphenyl)-2'-hydroxyethyl]-3-aminopropionic acid (74, R=H) by integration in ¹H-NMR.

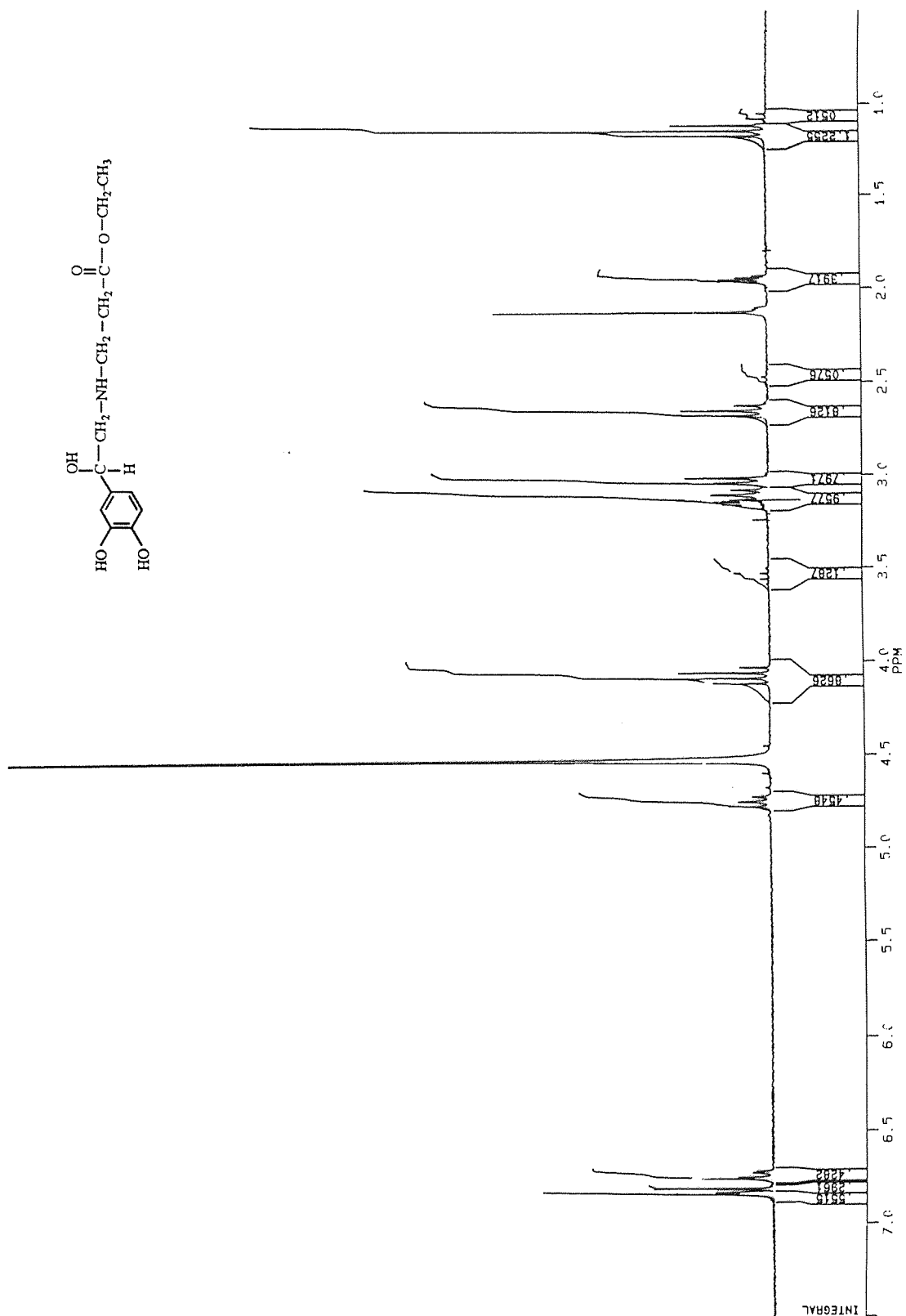


Figure 6.15a: $^1\text{H-NMR}$ spectrum of ethyl *N*-[2'-(3,4"-dihydroxyphenyl)-2'-hydroxyethyl]-3-aminopropionate (74, R= Et) in buffer pD 8.57 (pH 8.17) in 10% CD_3CN in D_2O .

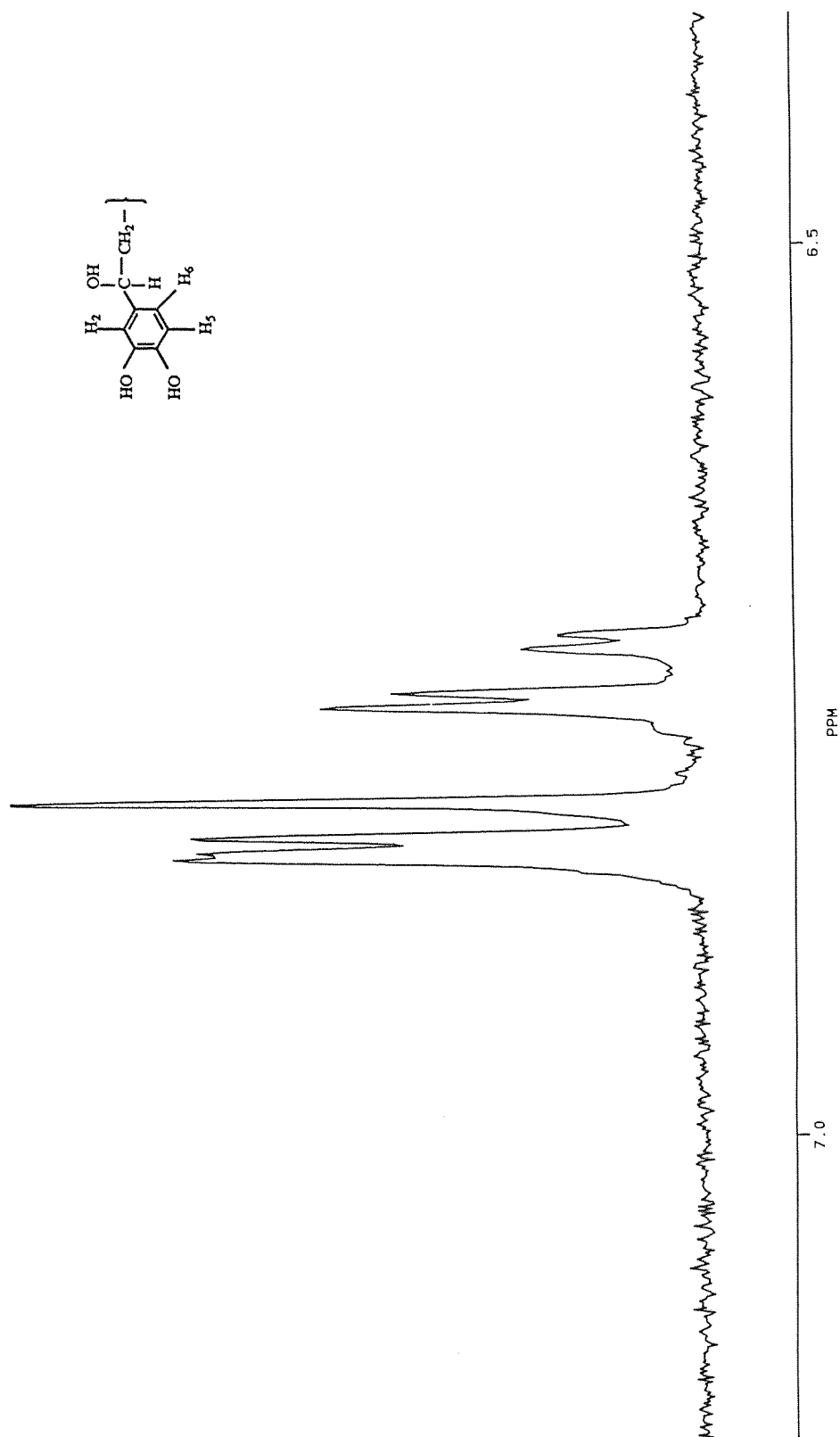


Figure 6.15b: Expansion of aromatic region of ethyl *N*-[2'-(3",4"-dihydroxyphenyl)-2'-hydroxyethyl]-3-aminopropionate (**74**, R= Et) in buffer pD 8.57 (pH 8.17) in 10% CD₃CN in D₂O.

The rate constant for the hydrolysis of ethyl *N*-[2'-(3'',4''-dihydroxyphenyl)-2'-hydroxyethyl]-3-aminopropionate (**74**, R= Et) to the dihydroxy acid (**74**, R=H) at pH 8.17 (pD 8.57) and 37 °C is $5.0648 \times 10^{-2} \text{ h}^{-1}$ with a half-life of 13.7 h (Figure 6.17).

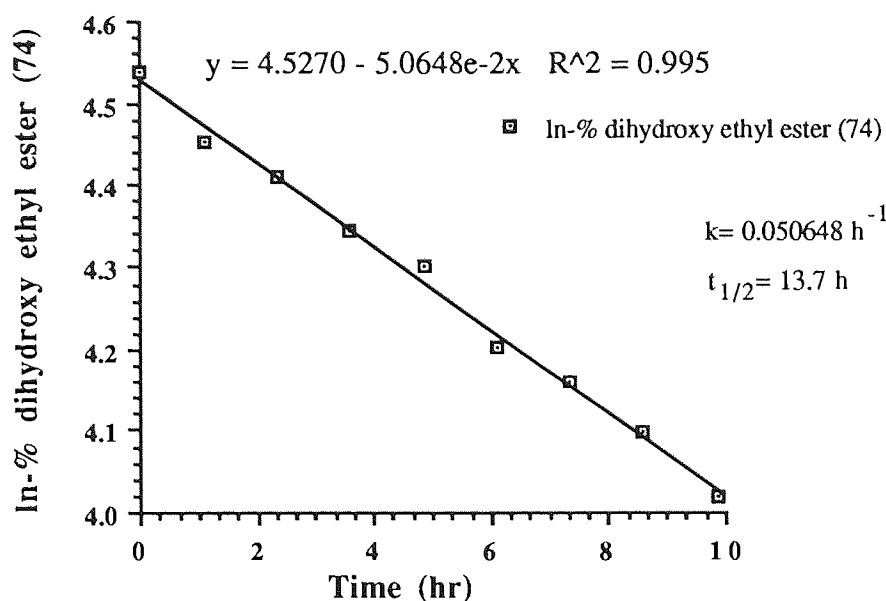


Figure 6.17: Hydrolysis of ethyl *N*-[2'-(3'',4''-dihydroxyphenyl)-2'-hydroxyethyl]-3-aminopropionate (**74**, R= Et) at pH 8.17 (pD 8.57) in potassium phosphate buffer in 10% acetonitrile at 37 °C by $^1\text{H-NMR}$ spectroscopy.

Figure 6.18 shows the percentage of ethyl *N*-[2'-(3'',4''-dihydroxyphenyl)-2'-hydroxyethyl]-3-aminopropionate (**74**, R= Et) converted. At pH 8.17 (pD 8.57) after 10 hrs, 56% dihydroxy ethyl ester (**74**, R= Et) was found as dihydroxy acid (**74**, R=H). Scheme 6.6 shows the chemical hydrolysis of the dihydroxy ethyl ester (**74**, R= Et).

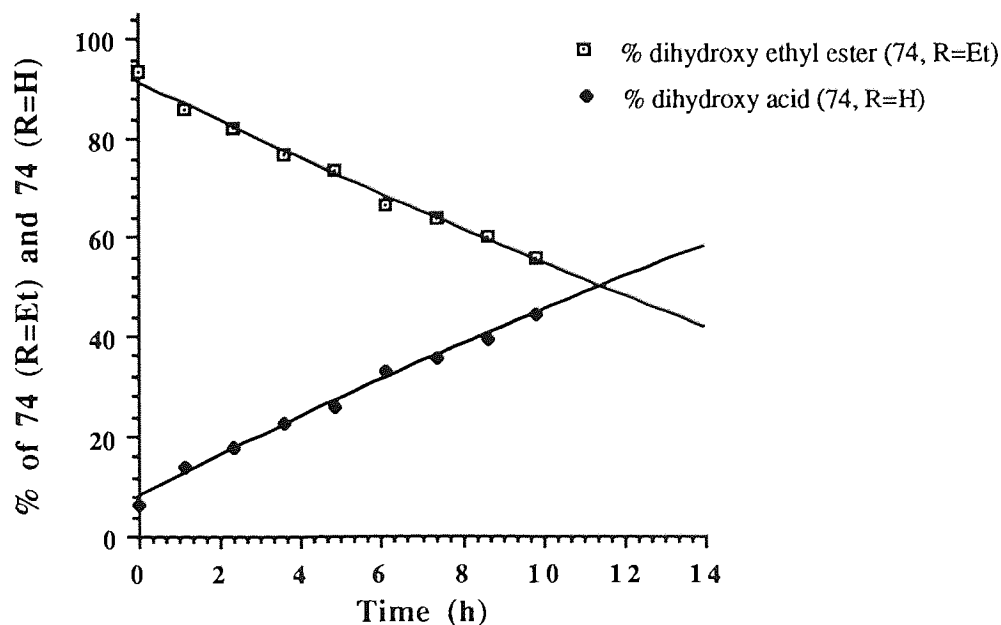
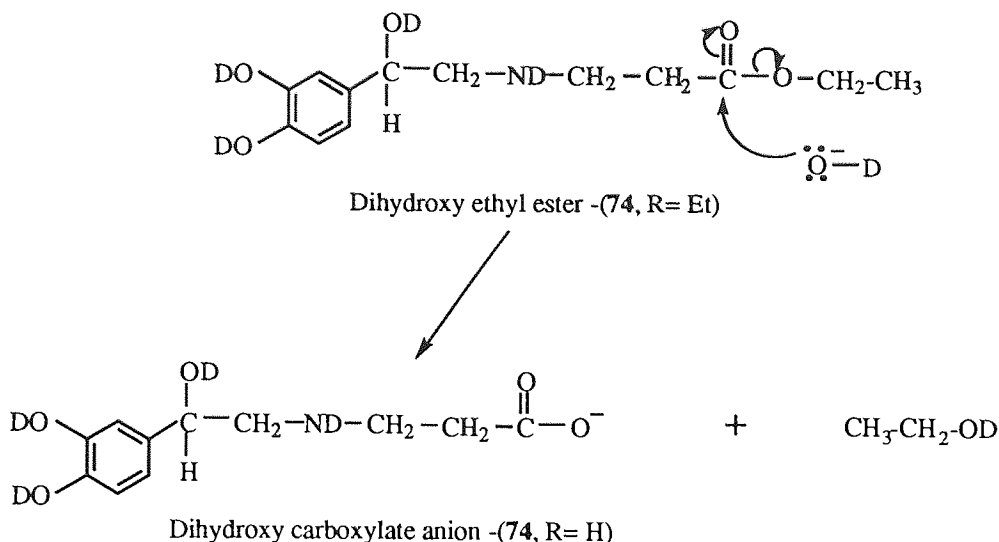


Figure 6.18: Hydrolysis of ethyl *N*-[2'-(3'',4''-dihydroxyphenyl)-2'-hydroxyethyl]-3-aminopropionate (**74**, R= Et) in pH 8.17 (pD 8.57) and formation of dihydroxyacid (**74**, R=H) in potassium phosphate buffer in 10% acetonitrile at 37 °C by $^1\text{H-NMR}$ spectroscopy.



Scheme 6.7: Mechanism of chemical hydrolysis of dihydroxy ethyl ester (74, R= Et) in potassium phosphate buffer (10% acetonitrile) at pH 8.17 (pD 8.57) and 37 °C by ¹H-NMR spectroscopy.

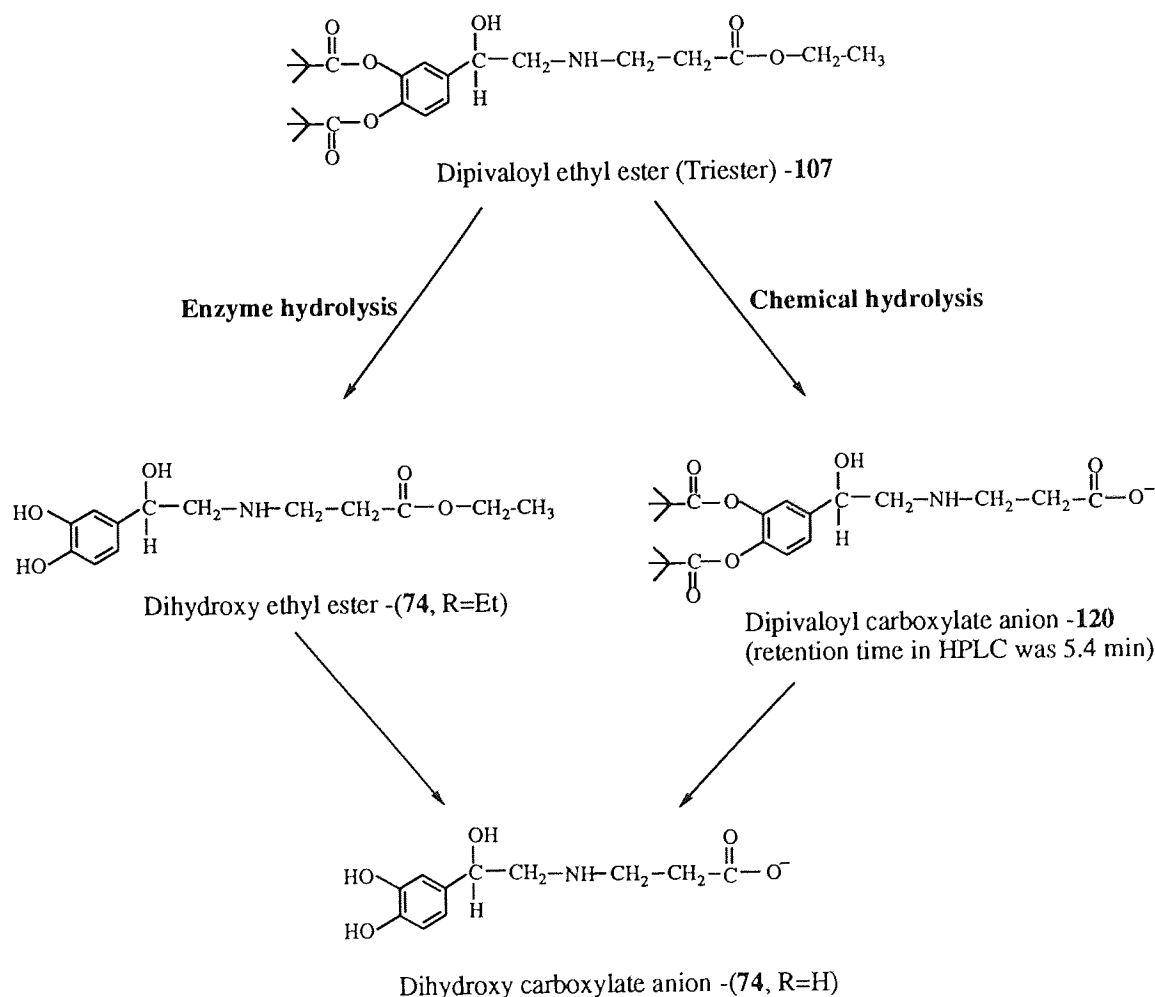
6.4 CONCLUSIONS

In conclusion, the chemical hydrolysis of the triester (107) proceeded *via* the formation of dipivaloyl acid (120). The first pivaloyl group is hydrolysed slowly presumably to form competitively either of the intermediates (121, 122), which are in rapid equilibrium with one another. They are not detected either by HPLC or ¹H-NMR spectroscopy, probably due to a very high rate of hydrolysis to the dihydroxy acid (113).

In contrast, the enzyme hydrolysis of the triester (107) proceeded *via* the formation of dihydroxy ethyl ester (74, R= Et) and there is very little or no formation of dipivaloyl acid (120) (Figure 6.2). The hydrolysis of the pivaloyl ester is some 50 times faster than the hydrolysis of ethyl ester of (107) in the presence of PLCE.

In the chemical hydrolysis, the ethyl ester is hydrolysed faster than the pivaloyl ester probably because of steric hindrance of pivaloyl group. In contrast, the pivaloyl ester is hydrolysed faster than the ethyl ester in enzyme hydrolysis probably because the more lipophilic pivaloyl group interacts better with the enzyme than the less lipophilic ethyl ester in the proximity of an amino residue. Table 5.12 shows the alkaline and enzymatic hydrolysis of various benzoate esters in a homologous series; progression up the series increases the hydrolysis rates in the presence of esterase, because the lipophilic esters interact more effectively with the enzyme.

For ethyl *N*-[2'-(3'',4''-dipivaloxyphenyl)-2'-hydroxyethyl]-3-aminopropionate (**107**) to be used as a pro-soft-drug, it is a prerequisite that triester (**107**) should undergo hydrolysis *via* the formation of 4-monopivaloyl ethyl ester (**118**)/3-monopivaloyl ethyl ester (**119**) to yield the soft-drug dihydroxy ethyl ester (**74**). This is because the generation of the acid function at the carboxylate end of the molecule makes the compound inactive (Section 8.3). It has been found that in the enzyme system, hydrolysis of the triester (**107**) proceeded *via* the formation of the dihydroxy ethyl ester (**74**, R=Et) and there is very little or no formation of the dipivaloyl acid (**120**) (Figure 6.2). This is the required degradation mode for the pro-soft-drug (**107**), which is less sensitive to oxidation and more lipophilic to enable absorption through the skin more rapidly than soft-drug (**74**, R=Et). Pro-soft-drug (**107**) can then be hydrolysed to give the active soft-drug (**74**, R=Et). There is thus a good prospect that triester (**107**) has the appropriate kinetic features to enable it to be evaluated further as a drug for the treatment of psoriasis.



Scheme 6.8: Major products in the chemical and enzyme hydrolysis of triester (**107**).

CHAPTER SEVEN

PERCUTANEOUS ABSORPTION STUDIES OF SOFT β -ADRENOCEPTOR
AGONISTS

7.1 INTRODUCTION

The predominant physiological factors which influence percutaneous absorption are site, condition, age, metabolic potential, vascularization and racial variation of the treated skin.^{162,163} In clinical practice, it is usually not possible to exercise any control over these biological variables. Optimization of topical delivery is, therefore, most frequently achieved by manipulating the physicochemical parameters of the dosage form. The main characteristics of the permeant which influences its absorption are partition coefficient, diffusivity and concentration.

The biopharmaceutics of topical drug delivery is concerned with the release of the active therapeutic agent from a vehicle, and penetration through the skin to its site of action. For drug delivery to diseased skin, the purpose is to produce a local therapeutic response by achieving an appropriate drug level at the particular skin site.^{164,165} The therapeutic response, in terms of onset, duration and magnitude, depends on the relative efficiency of three sequential events: release of the drug from the topical vehicle, penetration of the drug through the skin barriers and production of the desired pharmacological response by the drug.

Skin penetration can be tested *in vitro* using a diffusion cell equipped with animal, human or silicone membrane and this procedure can give a good indication of the penetration potential of the drug under study.

Diffusion is a process of mass transfer of individual molecules of a substance, brought about by random molecular motion and associated with a concentration gradient. The transport or flow of molecules through the barrier is a particularly convenient way to study diffusion and at steady-state the process is described by Fick's first law of diffusion:

$$J = - D \frac{\delta C}{\delta x} \quad \dots\dots\dots\text{Eq 7.1}$$

where, J is the rate of mass transfer per unit area of surface (the Flux), C is the concentration of the diffusing substance, x is the distance in cm of the movement perpendicular to the surface of the barrier, $\delta C/\delta x$ is the concentration gradient across the membrane and D is the diffusion coefficient. The flux of the substance corresponds to the slope of the steady-state diffusion curve in Figure 7.1

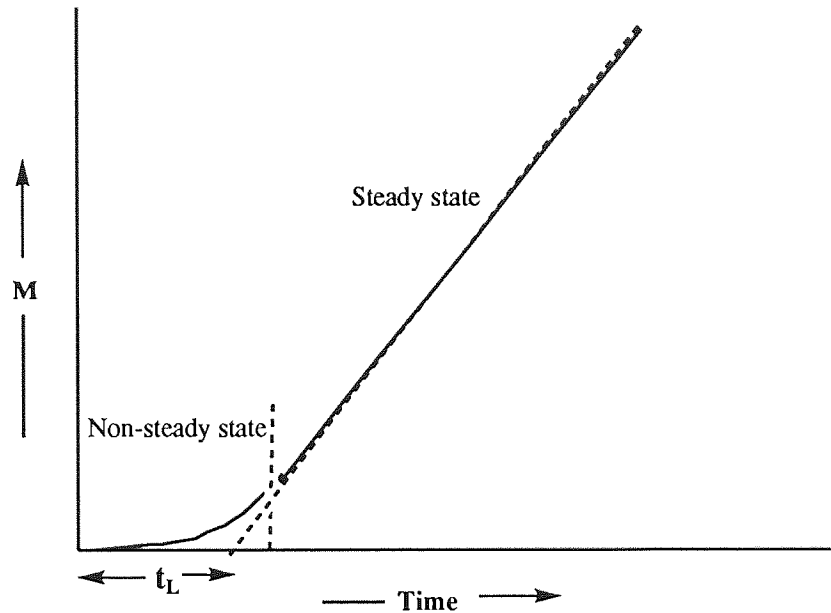


Figure 7.1: The time course for absorption for the simple flux obtained by plotting the cumulative amount of diffusant crossing unit area of membrane (M) as a function of time. Steady state is achieved when the plot becomes linear; extrapolation of the linear portion to the time axis yields the lag time (t_L).

However, the stratum corneum is not simply an inert structure barrier to diffusion but one with an affinity for the applied solute. Hence, the drug concentration at the skin surface will not be the same as in the formulation but will be related to it according to the membrane-vehicle partition coefficient (P) which is defined as an index of the relative affinity of the solute for the stratum corneum and vehicle. Equation 7.1 can therefore be expressed as:

$$J = \frac{DP (C_d - C_r)}{h} \dots\dots\dots \text{Eq 7.2}$$

where $\delta C = (C_d - C_r)$ is the concentration difference across the membrane, C_d is the concentration of diffusant in the donor compartment, C_r is the concentration of diffusant in the receiving compartment and h is the membrane thickness.

P, D and h may be combined into a single proportionality constant:

$$K_p = \frac{DP}{h} \dots\dots\dots \text{Eq 7.3}$$

where K_p represents the permeability coefficient. Substitution into equation 7.2 gives:

$$J = K_p \delta C \dots\dots\dots \text{Eq 7.4}$$

Provided that the depletion in the donor compartment is negligible and sink conditions apply, δC approximates to C_d , since the applied concentration is essentially constant and the drug concentration in the receptor phase remains effectively zero, thus:

$$J = K_p C_d \quad \dots\dots\dots \text{Eq 7.5}$$

The establishment of steady-state diffusion, described by equation 7.5, is preceded by the period (non-steady state) where the flux of the drug gradually increases as it equilibrates within the membrane (Figure 7.1). By extrapolating the linear region of this plot to the x-axis, a lag time (t_L) can be defined, which is dependent upon the membrane diffusion coefficient (D) and the thickness of the membrane (h):

$$t_L = \frac{h^2}{6D} \quad \dots\dots\dots \text{Eq 7.6}$$

The time taken to achieve steady-state diffusion is considered to be approximately 2.7 times the lag time.¹⁶² As values of t_L for different penetrants can vary from a few minutes to many hours, this early phase of absorption is clearly of clinical relevance.

7.2 EXPERIMENTAL

7.2.1 Preparation of membranes

The silicone rubber membrane (dimethyl polysiloxane, Silastic® Medical grade 500-3, Dow Corning, 0.010 inch thick) was used in the permeation studies. The membrane was rinsed in distilled water to remove surface deposits and subsequently cut into rectangular pieces of appropriate size, prior to mounting onto diffusion cells. The largely lipoidal nature of the stratum corneum has implications for the use of simple lipid membranes such as Silastic to mimic skin, which have found widespread use in permeation studies.¹⁶⁶ From a range of synthetic membranes used to study the permeation of salicylic acid, Silastic yielded a flux closest to that of excised human skin.¹⁶⁷

7.2.2 Franz-type diffusion cells

Franz-type diffusion cells¹⁶⁸ as shown in Figure 7.2, were employed during the course of the permeation studies. The membrane was mounted between the two halves of the diffusion cell, comprising an upper donor chamber and a lower receptor chamber, thereby offering a surface area of approximately 2.0 cm² for diffusion. The two halves of the cell were secured with Parafilm and held together by a spring clamp. The receptor compartment, which had a capacity to hold 20 to 30 ml of fluid, could be sampled *via* a side-arm. This sampling port was sealed with a small rubber stopper in between sampling to prevent evaporation of the receptor solution. Uniform mixing of the drug in the receiving compartment was achieved by a small teflon-coated magnetic stirring bar driven by an external motor. The receptor cell was maintained at 37 °C by a thermostated water pump which circulated water through a jacket surrounding the cell body. This resulted in a donor compartment (and skin surface) temperature of 32 ± 1 °C. The donor compartment could be sealed with a perspex lid to minimise evaporation of the donor fluid during the permeation study.

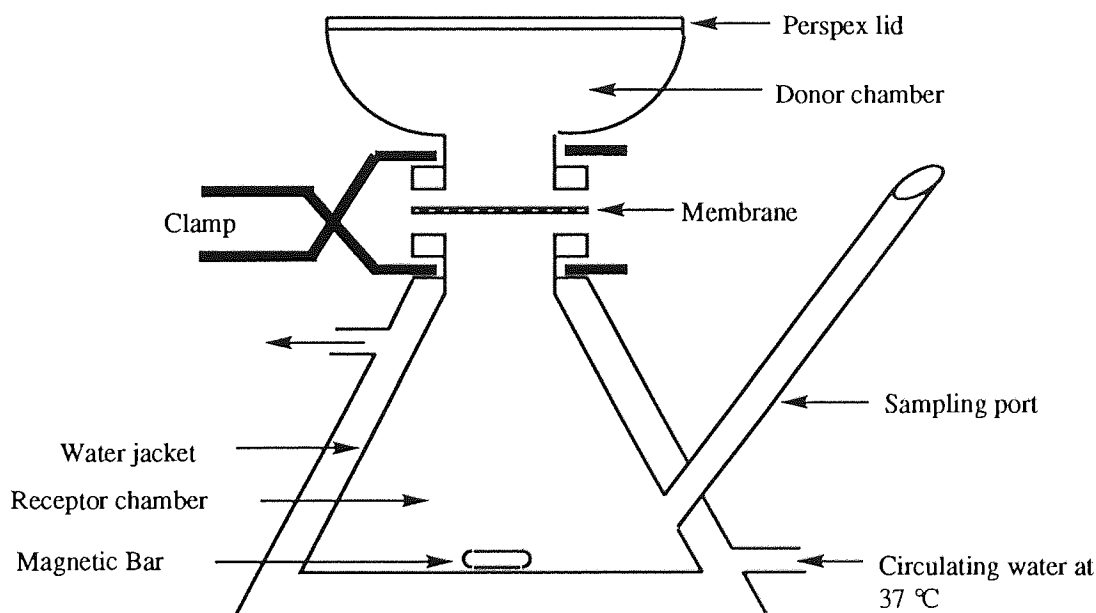


Figure 7.2: Schematic representation of a Franz-type diffusion cell.

7.2.3 Preparation of test vehicles

The choice of a suitable receptor medium is also important. For the duration of these permeation studies, the receptor phase employed was chosen to resemble the drug-free donor vehicle. This was most commonly a vehicle composed of 10% propylene glycol in buffer (pH 2.0-8.0). The prime objective of a receptor medium is to provide an effective sink for the penetrant and thus maintain a favourable driving force for absorption.

This criterion is considered to be met, provided the concentration of the penetrant in the receptor phase does not exceed 10% of its saturated solubility in the donor compartment. Non-buffered 10% v/v propylene glycol in water and buffered 10% v/v propylene glycol in water were used as test vehicles during the permeation studies. The buffered 10% v/v propylene glycol solutions (pH 2.0-8.0) of constant ionic strength were prepared from the phosphate-citrate (McIlvaine) buffers (Appendix, Table 5.1A). The pH values were adjusted as required with sodium hydroxide or phosphoric acid to give the values pH 2.0 - 8.0. To the membrane surface of the donor phase was added a solution of drug in ethanol. After 5 minutes, during which time the ethanol had evaporated, 0.5 ml of phosphate-citrate buffer in 10% propylene glycol at different pH (2.0-8.0) was added over the membrane. The donor compartment was protected from air by keeping it under argon gas.

7.2.4 Permeation procedure

The receptor compartments were filled with the chosen vehicle (20-30 ml), which had been maintained at 37 °C and degassed by sonication to minimise volume changes and prevent accumulation of air bubbles at the membrane-receptor fluid interface. The membrane was allowed to equilibrate with the receptor solution for 30 min., at which time any air bubbles which had collected in the vicinity of the membrane were removed *via* the sampling port by carefully tilting the cell assembly. Ethyl *N*-[2'-(3",4"-dipivaloyloxyphenyl)-2'-hydroxyethyl]-3-aminopropionate (**107**) (500 mg) was dissolved in ethanol (10 ml) to make a stock solution of 50 mg/ml. The stock solution (100 μ l) was added over the membrane (10.55 μ M). After 5 minutes when the ethanol had evaporated, 0.5 ml of phosphate-citrate buffer in 10% propylene glycol was added.

Samples of the receptor compartment (1 ml) were removed every hour and analysed by HPLC. After withdrawal of each sample, the receptor fluid was replenished with an equivalent volume of the drug-free vehicle.

All permeation studies were performed in triplicate and were protected from light and air for the duration of the study. The concentration of the permeant in the receptor compartment at each sampling point was determined by HPLC (30% acetonitrile in water was used as a mobile phase in HPLC and 20 μ l volume was injected in HPLC). The amount of drug penetrating the membrane per unit area was calculated by the volume of the receptor compartment and the area of the membrane available for diffusion, which varies for each cell. The cumulative amount of drug penetrated per unit area was calculated by MT-CALC.¹⁶⁹ A plot of the cumulative amount penetration per unit area as a function of time yielded the steady-state flux (slope) (J) and the lag time (t_L).

7.3 RESULTS AND DISCUSSION

7.3.1 Percutaneous absorption of ethyl *N*-[2'-(3'',4''-dihydroxyphenyl)-2'-hydroxyethyl]-3-aminopropionate (74, R=Et)

Initial permeation experiments of ethyl *N*-[2'-(3'',4''-dihydroxyphenyl)-2'-hydroxyethyl]-3-aminopropionate (74, R=Et) were performed with the solution at pH 6.5 in the donor compartment and pH 3.0 in the receiving compartment each containing 10% propylene glycol in water. These showed very irregular absorption; the profile was linear up to 3.0 h after which the rate of transport of drug fell rapidly (Figure 7.3 and Appendix 7.1A). The colour of the drug in the donor compartment changed to purple. The colour is due to degradation of drug by oxidation of the catechol ring. Further, the drug is hydrophilic, a factor which will limit the rate of transport through the Silastic membrane. This led to the synthesis of the lipophilic derivative (107).

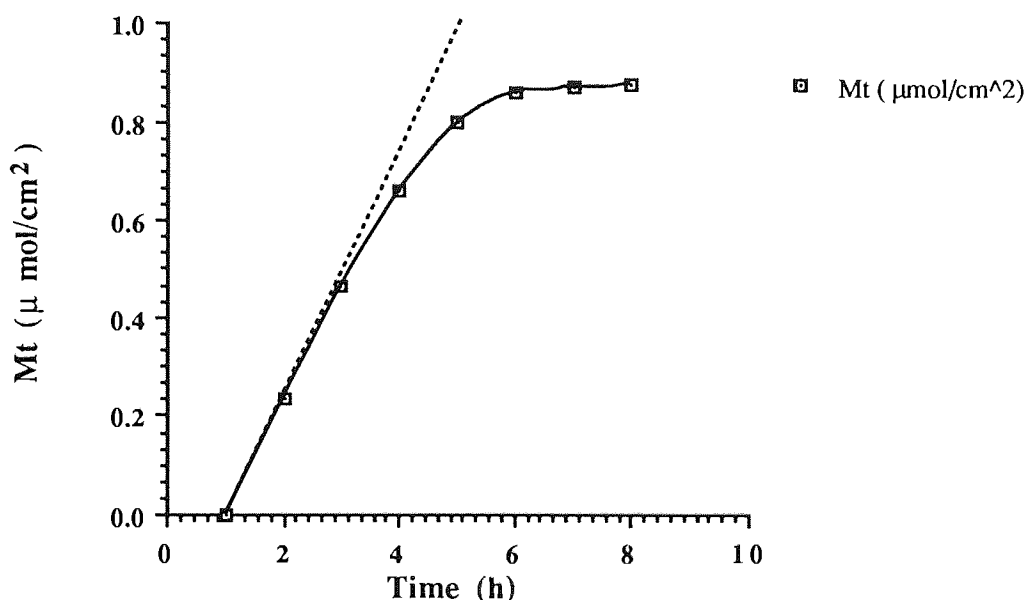


Figure 7.3: Transport of ethyl *N*-[2'-(3'',4''-dihydroxyphenyl)-2'-hydroxyethyl]-3-aminopropionate (74, R=Et) through the silicone membrane at pH 6.5 in the donor compartment. Receiving compartment contains 10% propylene glycol in water at pH 3.0.

In contrast, there was no transport of ethyl *N*-[2'-(3'',4''-dihydroxyphenyl)-2'-hydroxyethyl]-3-aminopropionate (74, R=Et) at pH 3.0 in the donor compartment. Here, virtually all of the amine is in the protonated form, a species which has little affinity for the membrane.

7.3.2 Percutaneous absorption of ethyl *N*-[2'-(3'',4''-dipivaloyloxyphenyl)-2'-hydroxyethyl]-3-aminopropionate (**107**)

The initial permeation experiment of ethyl *N*-[2'-(3'',4''-dipivaloyloxyphenyl)-2'-hydroxyethyl]-3-aminopropionate (**107**) at pH 7.0 in the donor compartment into a receiver containing 10% propylene glycol in distilled water (pH 6.5) showed an initial lag phase followed by non-linear transport with a steadily falling rate (Figure 7.4 and Appendix 7.2A). The drug in the receiving fluid slowly developed a light purple colouration. This is due to slow hydrolysis of the pivaloyl esters followed by degradation of drug by oxidation. This is because the drug (**107**) was not stable at pH 6.5. Therefore, the pH of the receiving fluid was reduced to pH 3.0, a pH at which the drug was stable (Section 5.3.3).

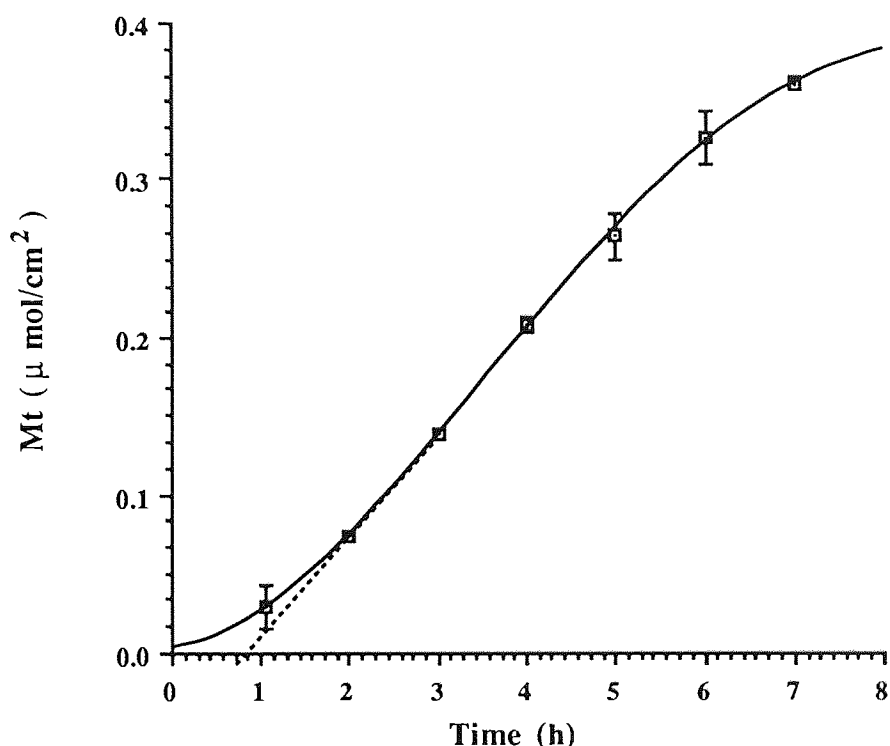


Figure 7.4: Transport of ethyl *N*-[2'-(3'',4''-dipivaloyloxyphenyl)-2'-hydroxyethyl]-3-aminopropionate (**107**) through the silicone membrane in 10% propylene glycol in water at pH 6.5 in receiving compartment (pH 7.0 in the donor compartment).

The permeation studies of ethyl *N*-[2'-(3'',4''-dipivaloyloxyphenyl)-2'-hydroxyethyl]-3-aminopropionate (**107**) at pH 7.0 (non-buffered) in the donor compartment and receiving compartment containing 10% propylene glycol in distilled water (pH 3.0) showed that steady-state flux was obtained (Figure 7.5), due to the increased stability of the drug at the reduced receiving pH. The mean flux is $8.673 \times 10^{-2} (\pm 0.005) \mu\text{mol}/\text{cm}^2/\text{h}$ and mean lag time is $0.65 (\pm 0.13)$ h.

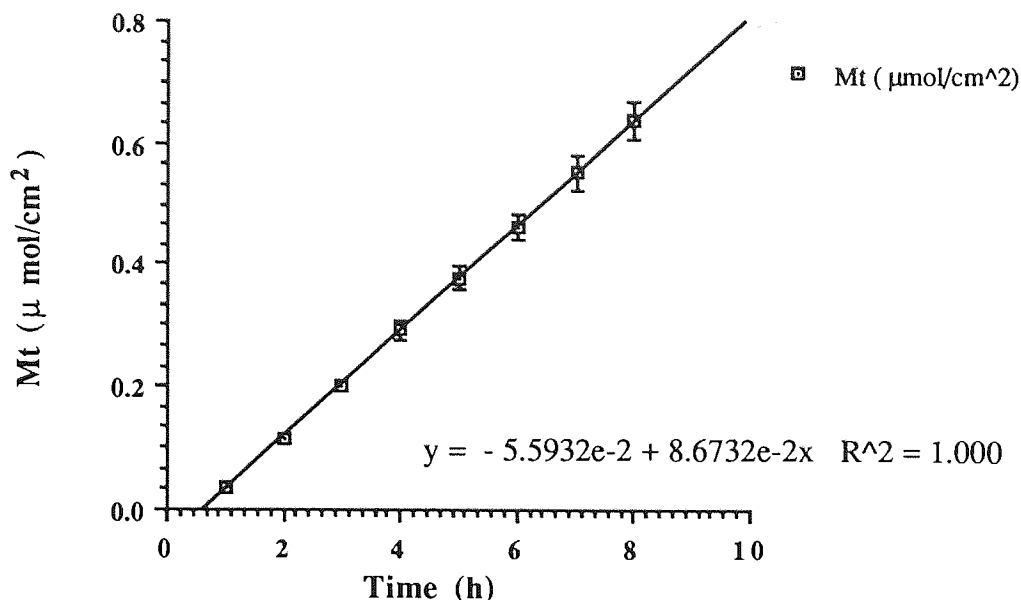


Figure 7.5: Transport of ethyl *N*-[2'-(3",4"-dipivaloyloxyphenyl)-2'-hydroxyethyl]-3-aminopropionate (**107**) through the silicone membrane in 10% propylene glycol in water at pH 3.0 in receiving compartment (pH 7.0 in the donor compartment). The mean flux was $8.6732 \times 10^{-2} (\pm 0.005) \mu\text{mol}/\text{cm}^2/\text{h}$ and mean lag time was $0.65 (\pm 0.13)$ h.

In initial investigations, the permeation of the ethyl *N*-[2'-(3",4"-dipivaloyloxyphenyl)-2'-hydroxyethyl]-3-aminopropionate (**107**) in 10% propylene glycol (pH 3.0, 5.0 and 7.0, all non-buffered) across the silicone membrane was examined. Steady-state fluxes and lag times were determined and are shown in Figure 7.6 and Table 7.1. (See Appendix 7.3A).

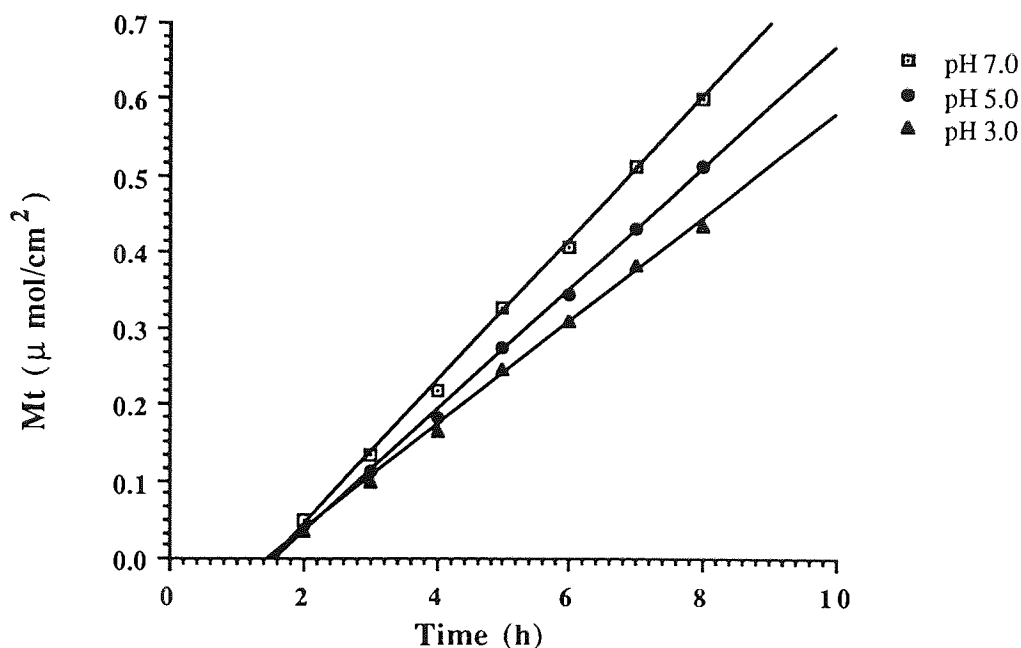


Figure 7.6: Permeation of ethyl *N*-[2'-(3",4"-dipivaloyloxyphenyl)-2'-hydroxyethyl]-3-aminopropionate (**107**) across the silicone membrane at different pH (non-buffered) in 10% propylene glycol in water in the donor compartment.

pH	Flux ($\mu\text{moles}/\text{cm}^2/\text{h}$)	Lag time (h)
3.0	0.068436	1.64
5.0	0.079579	1.61
7.0	0.092911	1.55

Table 7.1: Permeation data for ethyl *N*-[2'-(3'',4''-dipivaloyloxyphenyl)-2'-hydroxyethyl]-3-aminopropionate (**107**) across the silicone membrane at different pH (non-buffered) in 10% propylene glycol in water in the donor compartment.

These data clearly illustrate the effect of pH on the membrane transport with increased transport at higher pH values. A series of experiments were conducted to assess the effect of buffered pH on the percutaneous absorption of ethyl *N*-[2'-(3'',4''-dipivaloyloxyphenyl)-2'-hydroxyethyl]-3-aminopropionate (**107**, 10.55 μM) from buffered 10% propylene glycol in water (pH 2.0-8.0). The cumulative transport and fluxes at different pH values are shown in Figures 7.7 and 7.8.

7.3.2.1 Percutaneous absorption of ethyl N-[2'-(3'',4''-dipivaloyloxyphenyl)-2'-hydroxyethyl]-3-aminopropionate (107) at buffered pH 3.0-8.0 in 10% propylene glycol in water.

The penetration profiles and corresponding data of ethyl *N*-[2'-(3'',4''-dipivaloyloxyphenyl)-2'-hydroxyethyl]-3-aminopropionate (**107**) at buffered pH 3.0-5.0 are presented in Figure 7.7 and from pH 6.0-8.0 in Figure 7.8. (See Appendix 7.4A-7.9A).

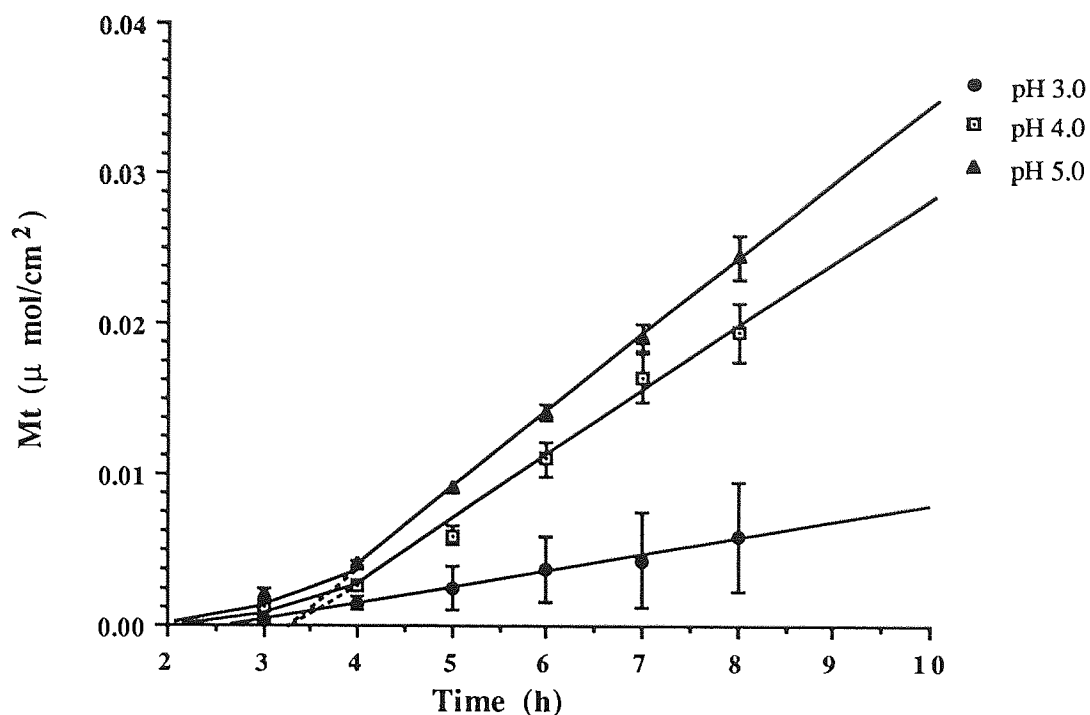


Figure 7.7: Silicone membrane transport of ethyl *N*-[2'-(3'',4''-dipivaloyloxyphenyl)-2'-hydroxyethyl]-3-aminopropionate (107) at buffered pH 3.0-5.0 in 10% propylene glycol in water in the donor compartment.

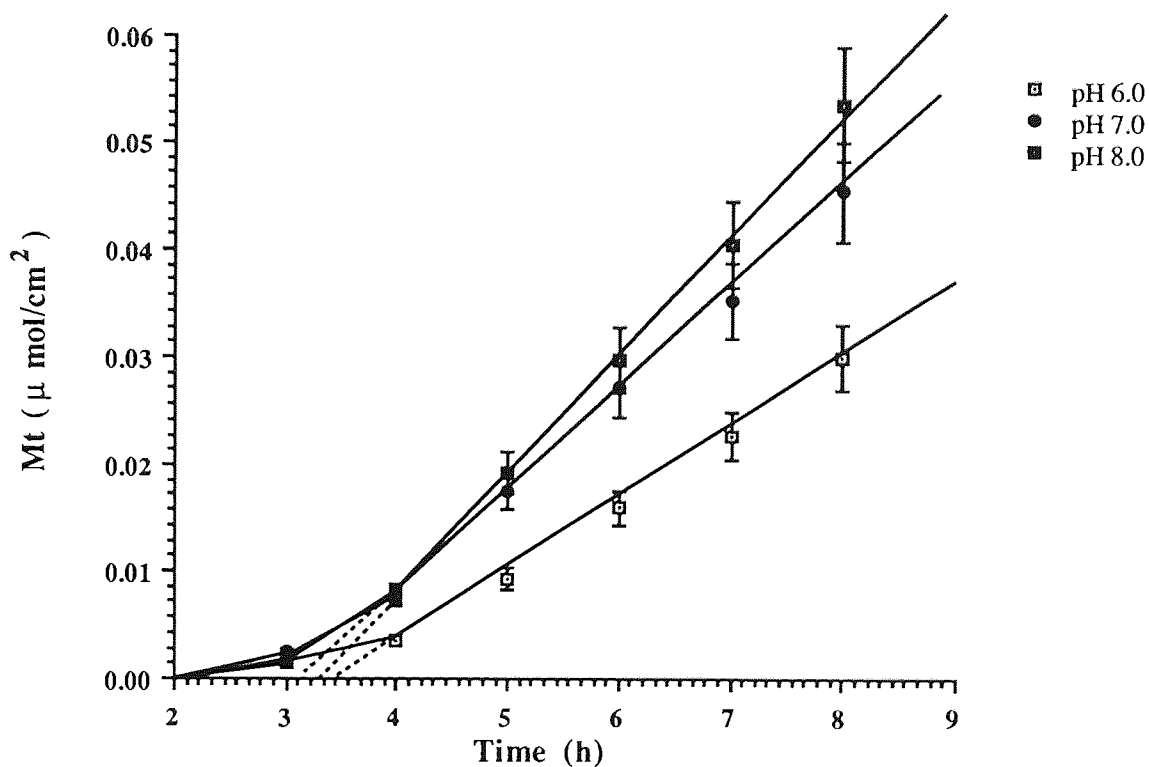


Figure 7.8: Silicone membrane transport of ethyl *N*-[2'-(3'',4''-dipivaloyloxyphenyl)-2'-hydroxyethyl]-3-aminopropionate (107) at buffered pH 6.0-8.0 in 10% propylene glycol in water in the donor compartment.

Table 7.2 shows the mean flux (J), permeability coefficient (K_p) and lag time (t_L) of ethyl *N*-[2'-(3",4"-dipivaloyloxyphenyl)-2'-hydroxyethyl]-3-aminopropionate (**107**) at buffered pH (2.0-8.0) in 10% propylene glycol in water.

pH	Flux (J) ($\mu\text{mol}/\text{cm}^2/\text{h}$) (\pm s.d.)	Permeability coefficient (K_p) (cm^2/h) (\pm s.d.)	lag time (t_L) (h) (\pm s.d.)
3.0	1.0067×10^{-3} ($\pm 3.83 \times 10^{-4}$)	9.5418×10^{-5} ($\pm 3.63 \times 10^{-5}$)	2.56 (± 0.20)
4.0	4.3167×10^{-3} ($\pm 4.07 \times 10^{-4}$)	4.0916×10^{-4} ($\pm 3.86 \times 10^{-5}$)	3.14 (± 0.05)
5.0	5.4369×10^{-3} ($\pm 4.76 \times 10^{-5}$)	5.1535×10^{-4} ($\pm 4.51 \times 10^{-6}$)	1.80 (± 0.2)
6.0	6.7400×10^{-3} ($\pm 4.53 \times 10^{-4}$)	6.3886×10^{-4} ($\pm 4.30 \times 10^{-5}$)	3.18 (± 0.03)
7.0	9.1076×10^{-3} ($\pm 1.11 \times 10^{-3}$)	8.6328×10^{-4} ($\pm 1.05 \times 10^{-4}$)	2.92 (± 0.19)
8.0	1.0569×10^{-2} ($\pm 9.72 \times 10^{-4}$)	1.0018×10^{-3} ($\pm 9.20 \times 10^{-5}$)	3.08 (± 0.07)

Table 7.2: Silicone membrane transport data of ethyl *N*-[2'-(3",4"-dipivaloyloxyphenyl)-2'-hydroxyethyl]-3-aminopropionate (**107**) at different buffered pH in 10% propylene glycol in water in the donor compartment.

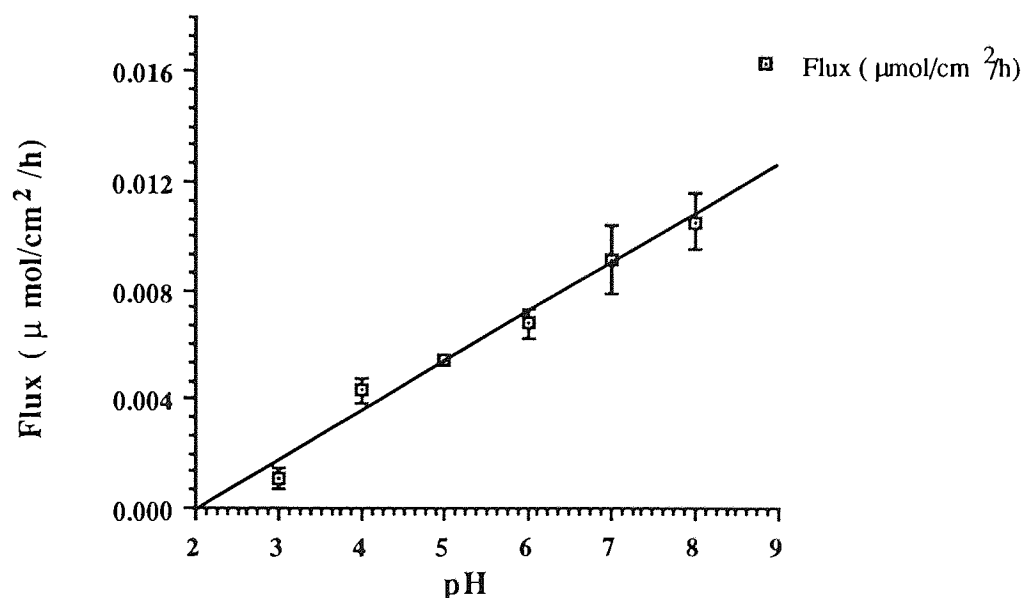


Figure 7.9: Silicone membrane transport of ethyl *N*-[2'-(3",4"-dipivaloyloxyphenyl)-2'-hydroxyethyl]-3-aminopropionate (**107**) at different buffered pH in 10% propylene glycol in water in the donor compartment.

A plot of the observed flux against the pH of the donor compartment shows that transport is enhanced at higher pH values (Figure 7.9). Partitioning into the membrane is favoured by the undissociated form of the drug, the ratio of which increases with increasing pH for basic drugs such as ethyl *N*-[2'-(3",4"-dipivaloyloxyphenyl)-2'-hydroxyethyl]-3-aminopropionate (107). The percentage of base ionized at a given pH can be calculated from Equation 7.7. Table 7.3 shows the percentage of ionized ethyl *N*-[2'-(3",4"-dipivaloyloxyphenyl)-2'-hydroxyethyl]-3-aminopropionate (107) at different pH (pK_a of 107 is 7.43, see Section 5.3.6).

$$\% \text{ Ionized} = \frac{100}{1 + 10^{(pH - pK_a)}} \quad \dots\dots\dots \text{Eq. 7.7}$$

pH	% of unionized (107)	Flux ($\mu\text{mol}/\text{cm}^2/\text{h}$)
2.0	0.001	-
3.0	0.004	1.0067×10^{-3}
4.0	0.037	4.3167×10^{-3}
5.0	0.372	5.4369×10^{-3}
6.0	3.602	6.7400×10^{-3}
7.0	27.203	9.1076×10^{-3}
8.0	78.889	1.0569×10^{-2}

Table 7.3: Percentage of ionized and unionized ethyl *N*-[2'-(3",4"-dipivaloyloxyphenyl)-2'-hydroxyethyl]-3-aminopropionate (107) at different buffered pH in 10% propylene glycol in water in the donor compartment.

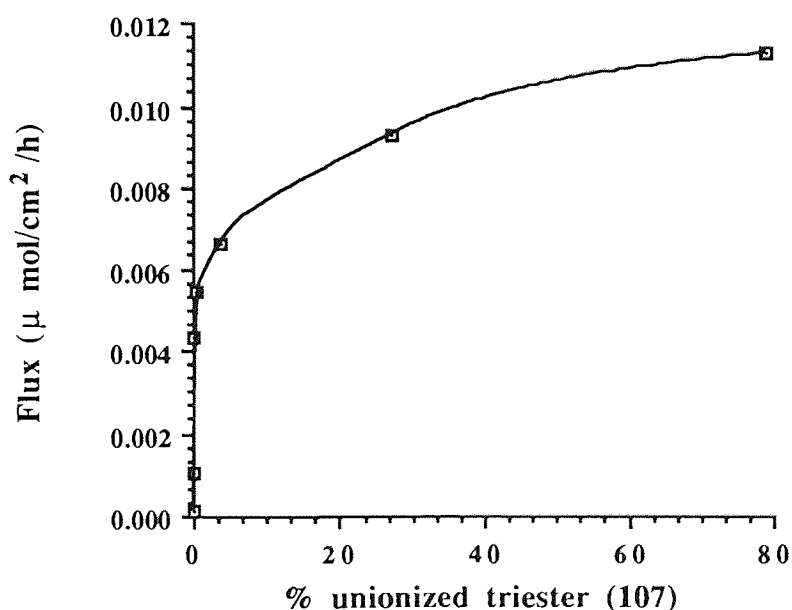


Figure 7.10: Permeation of ethyl *N*-[2'-(3",4"-dipivaloyloxyphenyl)-2'-hydroxyethyl]-3-aminopropionate (107) increases as the percentage of unionized triester increases in the donor compartment.

A plot of flux as a function of the fraction of drug in the unionised form (Figure 7.10) suggests that the protonated form does not penetrate the membrane, although it does not show the expected linear relationship.

7.4 CONCLUSIONS

The penetration of ethyl *N*-[2'-(3",4"-dihydroxyphenyl)-2'-hydroxyethyl]-3-amino propionate (**74**, R=Et) and ethyl *N*-[2'-(3",4"-dipivaloyloxyphenyl)-2'-hydroxyethyl]-3-aminopropionate (**107**) through the silastic membrane was investigated. Ethyl *N*-[2'-(3",4"-dihydroxyphenyl)-2'-hydroxyethyl]-3-aminopropionate (**74**, R=Et) was poorly absorbed through the membrane because of its hydrophilicity and its rapid oxidation at the catechol group. This led to the synthesis of the more lipophilic derivative (**107**) with dipivaloyl protection of the catechol group. Compound (**107**) has a better penetration profile due to the lipophilic pivaloyl groups and to the greater stability towards oxidation.

According to the simple form of the pH-partition hypothesis, only unionised molecules pass across lipid membranes in significant amounts.¹⁷⁰ Ionised species do not have favourable free energies for transfer to lipid phases. Weak acids and weak bases are dissociated to different degrees, depending on the pH and the pK_a of the diffusant. Thus, the fraction of the unionised drug in the applied phase determines the effective membrane gradients, and this fraction is a function of pH.

At high values of pH, at which the drug was substantially in the unionized form, the flux value was maximal. Decreasing the pH increased the fraction of ionized drug and resulted in a decrease in flux. However, at pH values higher than 6.0, the drug begins to degrade at measurable rates. Therefore pH 6.0 is optimal for its formulation because at that pH there is a fine balance between flux and the stability of the drug.

CHAPTER EIGHT

BIOLOGICAL ACTIVITY OF SOFT-DRUGS AND PRO-SOFT-DRUG

8.1 INTRODUCTION

8.1.1 Effect of β -adrenoceptor agonists on trachea

β -Adrenoceptor agonists cause the relaxation of smooth muscle which contains β_2 receptors. Therefore β -adrenoceptor agonists (isoprenaline) are given to relieve bronchospasm.⁸⁵

8.1.2 Effect of β -adrenoceptor agonists on heart

β -Adrenoceptor agonists increase the rate and force of the heart beat by interacting with β_1 receptors. β -Adrenoceptor agonists increase the frequency of heart beat (positive chronotropic response) and force of contraction (positive inotropic effect).⁸⁵ The positive chronotropic and inotropic actions produced by the β -adrenoceptor agonists are accompanied by an increase in glycogenolysis by the activation of adenylate cyclase-cyclic AMP system. The positive inotropic effect is also mediated by c-AMP. The c-AMP activates a kinase enzyme that in turn activates some mechanism that makes more Ca^{2+} available for the contractile proteins. Cyclic-AMP is also thought to mediate the increase in Ca^{2+} flux through the membrane during the action potential.

8.2 EXPERIMENTAL

8.2.1 Guinea pig trachea

The trachea was dissected from a guinea pig (300-400 g) and opened into a sheet by making a longitudinal incision opposite to the smooth muscle. Alternate cuts were made through the tissue and the strip so formed was mounted in an organ bath maintained at 37 °C and bathed in physiological salt solution (PSS) of the following composition (mM): NaCl 118.5, KCl 4.75, CaCl_2 2.5, KH_2PO_4 1.2, NaHCO_3 25, $\text{MgSO}_4 \cdot 7\text{H}_2\text{O}$ 1.17 and dextrose 11.6. The tissues were gassed with 95% O_2 /5% CO_2 . The tissue was mounted under a resting tension of 2 g and all contractions were recorded *via* Pioden isometric transducers by means of UF1 transducers from Ormed, preamplified to a BBC flatbed recorder connected to a MacLab. Tissues were pre-contracted with acetylcholine (10^{-5} M) and the effect of the experimental compounds and of isoprenaline were determined as relaxations of the pre-contracted tissues.

8.2.2 Guinea pig atria

The heart was dissected from guinea pigs (300-400 g), cleared of fat and the atria were separated from the ventricular mass. The atria were mounted separately in organ baths under 1 gram tension, bathed in PSS and gassed with 95% O₂/5% CO₂ at 37 °C. The right atria was used to record chronotropic responses and the left atria was driven through a bipolar electrode at 60 V, 6 msec pulse, 1Hz, with supramaximal voltage to record inotropic responses.

All results are presented as the mean and standard error of the mean of at least 6 observations.

8.3 RESULTS AND DISCUSSION

The soft-drug (**74**, R=Et) caused a concentration dependent relaxation of the pre-contracted guinea pig trachea, similar to that produced by the β -adrenoceptor agonist isoprenaline (Figure 8.1). Propranolol (10⁻⁶ M) caused a competitive antagonism of the responses to the soft-drug characterised by a parallel displacement of the dose-response curve to the right with no change in the maximum response (Figure 8.2). A similar concentration dependent relaxation of the pre-contracted trachea was observed with the propyl analogue of the soft-drug (**74**, R=Pr). The dihydroxy acid (**74**, R=H) also caused a dose dependent relaxation of the pre-contracted tracheas but was significantly less potent than the soft-drug (**74**, R=Et) (Figure 8.3). Thus the maximum response of the acid was attained at a concentration of 3 x 10⁻⁴ M whereas with the soft-drug the maximum response was achieved at a concentration of 10⁻⁵ M (Figure 8.4). The soft-drug (**74**, R=Pr) had a similar potency to that of the soft-drug (**74**, R=Et) (Table 8.1, graph not shown). The soft-drugs (**74**, R=Et and Pr) were slightly less potent than isoprenaline but significantly more potent than the parent acid.

Compound	ED ₅₀
Isoprenaline	2.68 (\pm 0.37) x 10 ⁻⁷ M (n=25)
Soft drug (74 , R=Et)	4.07 (\pm 0.49) x 10 ⁻⁷ M (n=9)
Soft drug (74 , R=Et) with propranolol 10 ⁻⁶ M	8.8 (\pm 0.9) x 10 ⁻⁶ M
Soft drug (74 , R=Pr)	6.52 x 10 ⁻⁷ M
Dihydroxy acid (74 , R=H)	2.95 (\pm 0.9) x 10 ⁻⁵ M (n=6)

Table 8.1: The ED₅₀ of isoprenaline, soft drugs (**74**, R=Et, Pr), soft drug (**74**, R=Et) with propranolol and metabolite (**74**, R=H).

Both the soft-drugs (74, R=Et and Pr) were full agonists on the pre-contracted guinea pig trachea and produced maximum responses that were not significantly different from the maximum response achieved with the potent β -adrenoceptor agonist isoprenaline. The maximum response to the dihydroxy acid (74, R=H) was significantly less than that to either isoprenaline or the soft drug (74, R=Pr) ($p < 0.01$) (Figure 8.4).

The pro-soft-drug (107) had little activity on the pre-contracted guinea pig ileum but at high concentrations ($> 10^{-5}$ M) it produced slowly developing relaxations. This is consistent with *in vitro* results which show that the dipivaloyl groups are hydrolysed more readily than the ethyl ester to produce the active soft-drug (74, R=Et).

On the isolated atria of the guinea pig, the soft-drug (74, R=Et) produced a positive inotropic and chronotropic response similar to that observed with isoprenaline. Again the dihydroxy acid (74, R=H) showed activity only at high concentrations. As with the guinea pig trachea, the soft drug was a full agonist on the atria but was less potent than isoprenaline.

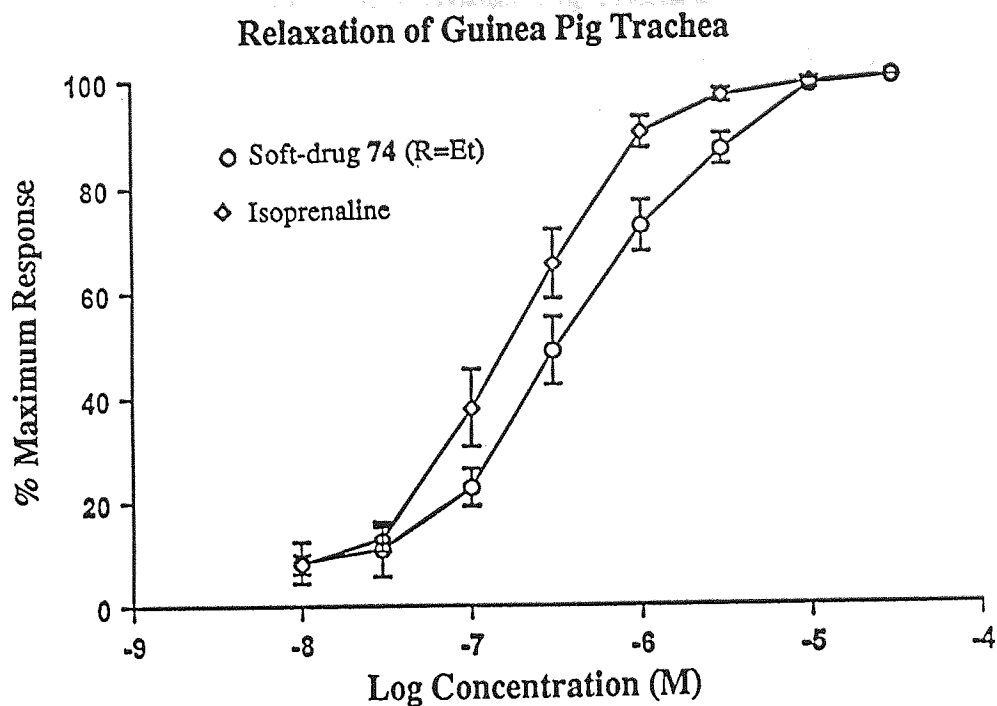


Figure 8.1: The soft-drug (74, R=Et) was a full agonist on the trachea preparations but was less potent than isoprenaline [ED_{50} of $4.07 (\pm 0.49) \times 10^{-7}$ M compared with $2.68 (\pm 0.37) \times 10^{-7}$ M for isoprenaline].

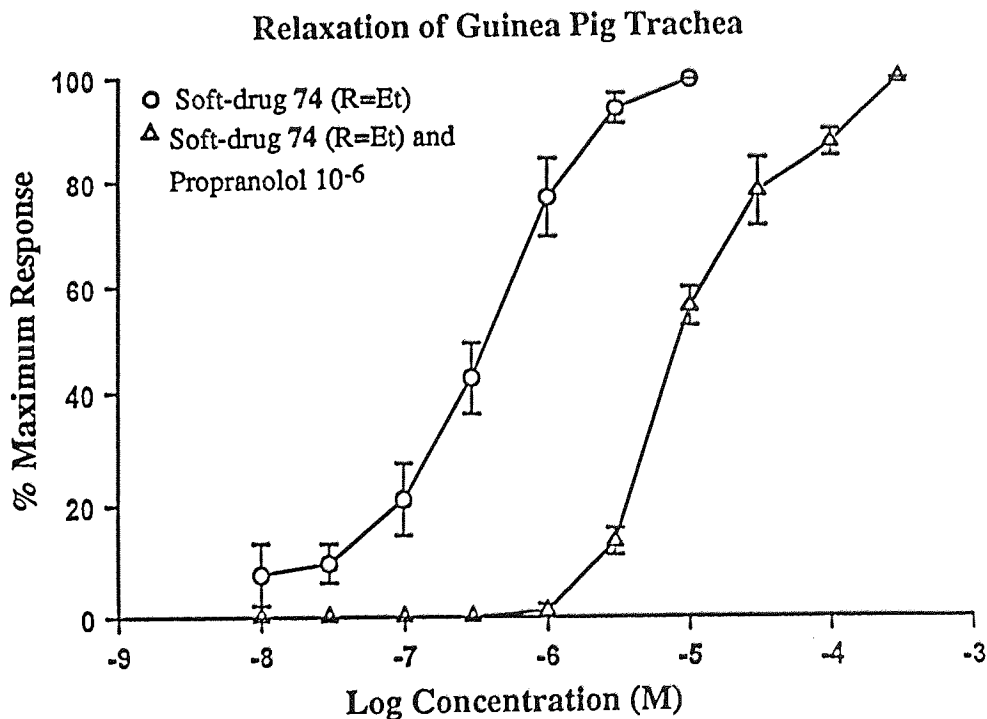


Figure 8.2: Responses to the soft-drug (74, R=Et) was competitively antagonised by propranolol (10^{-6} M) and, in the presence of propranolol, the ED_{50} of the drug was $8.8 (\pm 0.9) \times 10^{-6}$ M.

Relaxation of Guinea Pig Trachea

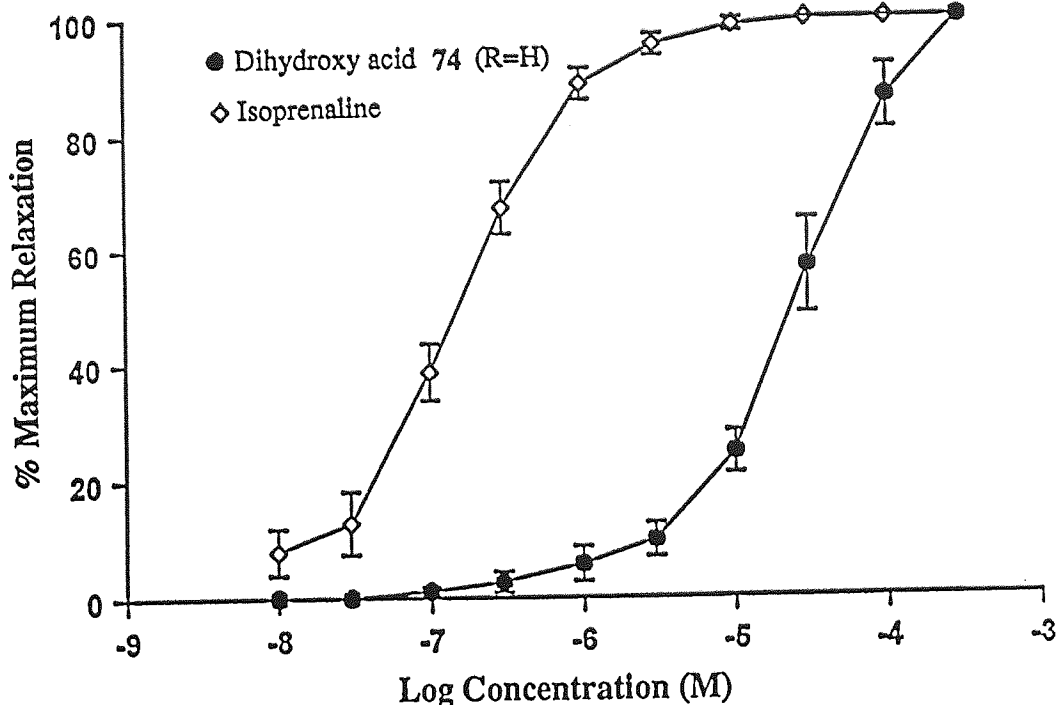


Figure 8.3: The maximal response of acid (74, R=H) was significantly less than the agonist (74, R=Et) and was attained at a concentration of 3×10^{-4} M, whereas with the soft drug the maximum response was achieved at a concentration of 10^{-5} M [ED₅₀ of $2.95 (\pm 0.9) \times 10^{-5}$ M].

Maximum Relaxation of Guinea Pig Trachea

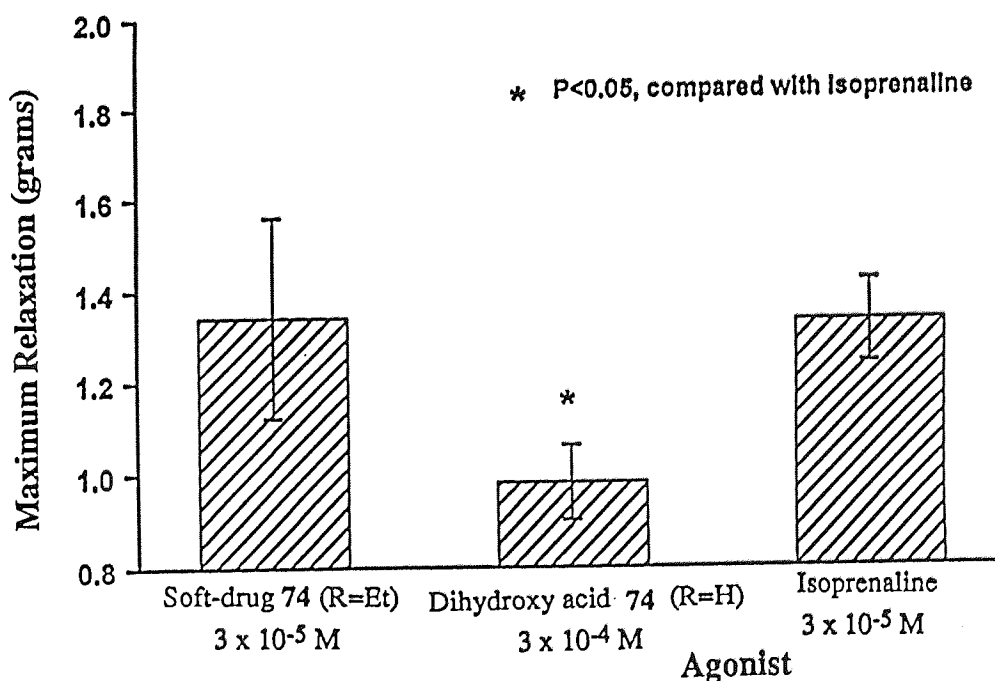


Figure 8.4: The maximum relaxation of guinea pig trachea by soft-drug (74, R=Et) at a concentration of 3×10^{-5} M, isoprenaline at a concentration of 3×10^{-5} M and dihydroxy acid (74, R=H) at a concentration of 3×10^{-4} M.

CHAPTER NINE

CONCLUSION

CONCLUSION

Psoriasis is characterised by epidermal proliferation and inflammation resulting in the appearance of elevated erythematous plaques. The clinical manifestation of psoriasis is marked by extensive scaling and a thickened epidermis, therefore, an uncontrolled cellular proliferation of epidermal cells is regarded as the primary disorder in psoriasis. A defect in the cyclic nucleotide system in the epidermis, reflected by an imbalance in the ratio of c-AMP to c-GMP, has been proposed to play a central role in the pathogenesis of psoriasis. Normal human epidermis contains approximately 0.2-0.4 pmol of cyclic-AMP/ μg of DNA. Cyclic-GMP is also present in the dermis but in much smaller amounts, ranging from 5 to 7 fmol/ μg of DNA, and shows a statistically significant two-fold increase in the lesional epidermis. When the epidermal cell surface receptors are stimulated by β -adrenergic agonists, intracellular ATP is transformed into c-AMP thus restoring the c-AMP/c-GMP levels. Therefore, the topical application of β -adrenoceptor agonists may be beneficial in psoriasis. For example, the topical application of 0.1% isoprenaline sulphate was found to significantly decrease the elevated glycogen content and scaliness and cause remission of psoriasis.

Based on the above discussion, anti-psoriatic drugs may possibly be developed due to their influence on the cyclic nucleotides in three ways (Figure 1.2):

- * stimulation of adenylate cyclase,
- * administration of c-AMP or dibutyl c-AMP,
- * inhibition of c-AMP-degradation by phosphodiesterases.

The simultaneous use of more than one of the above mentioned pathways may provide a greater possibility of success.

Cyclic-AMP or its lipophilic analogue dibutyl c-AMP can be administered to increase the c-AMP level, but both are short lived and quickly hydrolyse by phosphodiesterase (PDE) to AMP. Inhibitors of cyclic nucleotide phosphodiesterase such as papaverine and Ro 20-1724 [4-(3'-butoxy-4'-methoxybenzyl)-2-imidazolidinone] have also been shown to be beneficial in psoriasis. Papaverine inhibits both cyclic-AMP-phosphodiesterase (c-AMP-PDE) and c-GMP-PDE whereas Ro 20-1724 inhibits c-AMP-PDE only, but both agents improve psoriasis lesions.

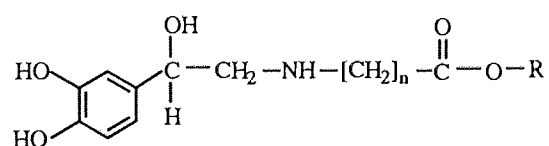
Another option is to activate the adenylate cyclase enzyme, which catalyses the production of intracellular c-AMP. It may be possible, therefore, to develop a new therapeutic approach in psoriasis *via* the stimulation of adenylate cyclase by β -adrenoceptor agonists.

For a β -adrenoceptor agonist to be useful clinically in the treatment of inflammatory and proliferative skin disease, it is a pre-requisite that activity be restricted to the percutaneous layers, and that no untoward cardiovascular effects occur as a consequence of systemic absorption. As the drug enters into the blood stream, it needs to be hydrolysed or metabolised into an inactive moiety.

To test this hypothesis, we have prepared a series of β -adrenoceptor agonists for topical delivery. To limit systemic effects, we have adopted the soft-drug approach. The *N*-substituent of β -adrenoceptor agonists can accommodate a broad range of structures, so, here, we have used the alkoxycarbonyl ethyl group. Based on the structure activity relationship, β -adrenoceptor activity can be terminated in two ways:

- * Loss of the basic centre at nitrogen (eg. -NH- to -N-CO-)
- * Dramatic polarity change in the *N*-substitution

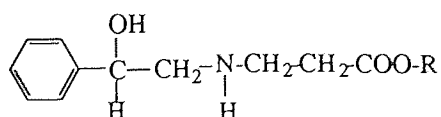
Based on this idea, a carboxylate ester group was introduced one or two carbon atoms distant from the amino group. Such derivatives should hydrolyse to give a carboxylate anion in the blood, which we believe will be devoid of β -adrenoceptor activity (see section 1.3.3, Figure 1.5). The first part of this project sets out to explore the synthesis of β -adrenoceptor agonists with the general structure (49, $n=1$ or 2):



(49, $n=1$ or 2)

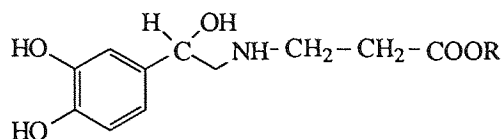
However, compound (49, $n=1$) was not synthesised due to the instability of the compound which may react to give a 6-membered cyclic lactone, suggesting that compounds of structure type ($n=1$) are not stable. The attempted synthesis of this class of compound was terminated and, for subsequent syntheses, the chain length between the amino and carboxylate groups was increased to two carbon atoms.

The catechol group is nucleophilic as well as been prone to oxidation in the presence of light and air, which may make the chemistry complex. Therefore, prior to the incorporation of the catechol group, which is important for β -adrenergic activity, the synthesis of model compounds (50, $R=Me, Et$), without the 3,4-dihydroxy substituents, were considered.



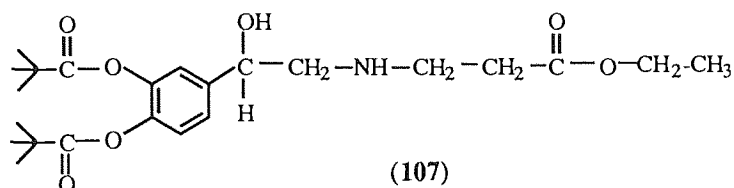
(50, $R=Me, Et$)

Having successfully prepared two amino acid esters (**50**, R=Me, Et) as model compounds, the catechol derivatives with 3,4-dihydroxy substituents (**74**, R= Me, Et, Pr, Bu) were synthesised.



(74)

The increased polarity of the dihydroxy acid (**74**, R=H), expected after metabolic conversion of the soft-drug (**74**, R=Et), should eliminate agonist activity. Further, to prevent oxidation and enhance topical delivery we have sought to esterify the catechol hydroxyl groups to produce a pro-soft-drug (**107**), which generates the soft-drug (**74**, R=Et) in enzymic systems.

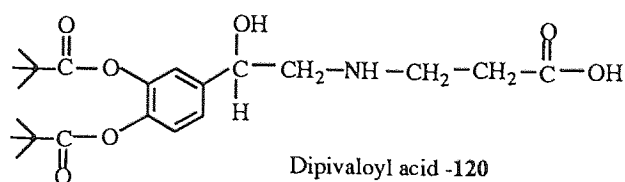


(107)

Before these compounds were studied further to evaluate their biological response, their stability in chemical and enzyme media was determined.

In chemical hydrolysis, the soft-drug (**74**, R=Et), pro-soft-drug (**107**) and phenyl analogue (**50**, R=Et) are most stable at pH 4.0 with half-lives of 295, 560 and 438 hrs, respectively. The pK_a values of the pro-soft-drug (**107**) and phenyl analogues (**50**, R=Et) and (**50**, R=Me) were found to be 7.427 ± 0.194 , 7.760 ± 0.038 and 7.768 ± 0.060 respectively. The pK_a of 7.40 for the pro-soft-drug (**107**), estimated from the hydrolysis data by non-linear regression, is in excellent agreement with that determined by direct titration (7.43) and indicates that satisfactory convergence was achieved. Moreover, the pH of minimum rate of degradation calculated from these data using equation 5.2 is $pH_{min} = 4.0$; a value which is in agreement with that obtained by inspection of the plot (Figure 5.9).

The chemical hydrolysis of the pro-soft-drug (**107**) proceeded *via* the formation of dipivaloyloxy acid (**120**). In contrast, in the presence of porcine liver carboxyesterase the hydrolysis of the pivaloyl group in the pro-soft-drug (**107**) was much more rapid than the hydrolysis of the ethyl ester, and the esterase-catalysed hydrolysis of the pro-soft drug (**107**) proceeded *via* the formation of the soft-drug (**74**, R= Et). This mode of degradation of the pro-soft drug (**107**) to give active the soft drug (**74**, R= Et) is the required route. The pro-soft-drug (**107**), therefore, has the appropriate kinetic features to enable it to be evaluated further as a drug for the treatment of psoriasis.



After establishing the stability and hydrolysis path in chemical and enzyme media, permeation through a membrane was assessed using Franz-type diffusion cells. The soft-drug (**74**, R=Et) was poorly transported across the membrane; it was also air-sensitive due to oxidation of the catechol group. The transport of the pro-soft-drug (**107**) over the donor pH range 3-8 increased with pH as, at lower values, the largely protonated species was not transported. However, above pH 7, chemical degradation is rapid so that a donor pH of 5-6 may be optimum for a formulation.

Subsequently, these compounds were tested for their β -adrenergic agonist activity by *in vitro* measurement of the chronotropic and inotropic responses in the guinea pig atria and relaxation of guinea pig trachea precontracted with acetylcholine (10^{-5} M). The soft-drug (**74**, R=Et) was a full agonist on the tracheal preparation but was less potent than isoprenaline [ED_{50} of $4.07 (\pm 0.49) \times 10^{-7}$ M compared with $2.68 (\pm 0.37) \times 10^{-7}$ M for isoprenaline, $p < 0.05$]. Responses of soft-drug (**74**, R=Et) were competitively antagonised by propranolol (10^{-6} M) and, in the presence of propranolol, the ED_{50} of the drug was $8.8 (\pm 0.9) \times 10^{-6}$ M. The soft-drug (**74**, R=Et) produced an increase in force and rate of the isolated atrial preparation. The soft-drug (**74**, R=Pr) was equally potent with an ED_{50} of 6.52×10^{-7} M.

In contrast, at equivalent doses, the dihydroxy acid (**74**, R=H) showed no activity; only a marginal effect was observed on the tracheal preparation. The maximal response of acid (**74**, R=H) was significantly less than the agonist (**74**, R=Et) with an ED_{50} of $2.95 (\pm 0.9) \times 10^{-5}$ M.

For the pro-soft-drug (**107**), responses were of slow onset in both preparations, with a slowly developing relaxation of the tracheal preparation at high concentrations (10^{-5} M). This is consistent with *in vitro* results where the dipivaloyl groups are hydrolysed more readily than the ethyl ester to give the active soft-drug (**74**, R=Et). These results confirm the validity of the pro-soft-drug approach to the delivery of β -adrenoceptor agonists and suggest that as *in vitro* assessment may now be appropriate.

REFERENCES

1. Roenigk Jr., H. H. and Maibach, H. I., *Psoriasis*, Marcel Dekker, New York, 1985.
2. Van Scott, E. J. and Ekel, T. M., *Arch. Dermatol.*, **88**, 373-381 (1963).
3. Bauer, F. W., Cell kinetics. In: Mier PD, van de kerhof PCM (eds) *Textbook of psoriasis*. Churchill Livingstone, Edinburgh, pp 100-112 (1986).
4. Voorhees, J. J., "Psoriasis as a possible defect of the adenyl cyclase c-AMP cascade", *Arch. Dermatol.*, **118**, 862-868 (1982).
5. Goodwin, P.; Hamilton, S. and Fry, L., "A comparison between DNA synthesis and mitosis in uninvolved and involved psoriatic epidermis and normal epidermis", *Br. J. Dermatol.*, **89**, 613-618, (1973).
6. Ragaz, A. and Ackerman, A.B., "Evolution, maturation and regression of lesion in psoriasis", *Am. J. Dermatopath.*, **1**, 199-214 (1979).
7. Hammarstrom, S.; Hamberg, M. and Samuelsson, B., "Increased contractions of nonesterified arachidonic acid, 12-L-hydroxy-5,8,10,14-eicosatetraenoic acid, prostaglandin E₂ and prostaglandin F_{2α} in epidermis of psoriasis", *Proc. Natl. Acad. Sci. USA*, **72**, 974-986 (1975).
8. Adachi, K.; Yoshikawa, K.; Halprin, K. M. and Levine, V., "Prostaglandins and cyclic-AMP in epidermis", *Br. J. Dermatol.*, **92**, 381-388 (1975).
9. Anderson, W. B. and Jaworski, C. J., "Modulation of adenylate cyclase activity of fibroblasts by the free fatty acids and phospholipids", *Arch. Biochem. Biophys.*, **180**, 374-383 (1977).
10. Das, N. S.; Chowdary, T. N.; Sobhanadri, C. and Rao, K. V., "The effect of topical isoprenaline on psoriatic skin", *Br. J. Dermatol.*, **99**, 197-200, (1978).
11. Bilski, A. J.; Evans, J. R. and Harrison, M. P., "Lipoidal anti-inflammatory prodrugs as local targeting agents", *Biochem. Soc. Trans.*, **14**, 388-391, (1986).
12. Voohees, J. J.; Marcelo, C. L., and Duel, E. A., "Cyclic AMP, cyclic GMP and glucocorticoids as potential metabolic regulators of epidermal proliferation and differentiation", *J. Invest. Dermatol.* **65**, 179, (1975).

13. Royer, E.; Chaintreul, J.; Meynadier, J. and Michiel, B., "Cyclic AMP and cyclic GMP production in normal and psoriatic epidermis", *Dermatologica*, **165**, 533-543, (1982).
14. Sotherland, E. W. and Rall, T. W., "The relation of adenosine-3',5'-phosphate and phosphorylase to the action of catecholamine and other hormones", *Pharmacol. Rev.*, **12**, 265-299 (1960).
15. DeLange, R. J.; Kemp, R. G.; Dickson, W. R.; Cooper, R. A. and Krebs, E. G., "Activation of skeletal muscle phosphorylase kinase by adenosine triphosphate and adenosine-3',5'-monophosphate", *J. Biol. Chem.*, **243**, 2200-2208 (1968).
16. Powell, J. A.; Duell, E. A. and Voorhees, J. J., "Beta adrenergic stimulation of endogenous epidermal cyclic AMP formation", *Arch. Dermatol.*, **104**, 359-365, (1971).
17. Duell, E. A. and Voorhees, J. J., "Control of epidermal growth. In Biochemistry and Physiology of the skin. L.A. Goldsmith (ed.). Oxford University Press, New York, pp. 241-268, (1983).
18. Halprin, K. M. and Ohkawara, A., "Carbohydrate metabolism in psoriasis: an enzymatic study", *J. Invest. Dermatol.* **46**, 51-68, (1966).
19. Harris, R. R. and Mackenzie, I. C., "The effect of α - and β -adrenergic agonists and cyclic adenosine 3',5'-monophosphate on epidermal metabolism", *J. Invest. Dermatol.*, **77**, 337-340, (1981).
20. Raab, W. P., "Cyclic nucleotides and prostaglandins in psoriasis", *Int. Clin. Pharm. Ther. Toxicol.* **18**, 212-224, (1980).
21. Gaylarde, P.; Brock, A. and Sarkany, T., "Psoriasiform changes in guinea-pig skin from propranolol", *Clin. Exp. Dermatol.* **3**, 157-159, (1978).
22. Wiley, H. E. and Weinstein, G. D., "Abnormal proliferation of uninvolved psoriatic epidermis", *J. Invest. Dermatol.*, **73**, 545-547, (1979).
23. Tutton, P. J. M. and Helme, R. D., "The influence of adrenoceptor activity on crypt cell proliferation in the rat jejunum", *Cell Tis Kin*, **7**, 125-136, (1974).

24. Winchurch, R. A. and Mardiney Jr., M. R., "The effect of adrenergic agonists and blockers on antigen-induced DNA synthesis *in vitro*", *Biomed.*, **26**, 36-42, (1977).
25. Voohrees, J. J. and Duell, E. A., "Psoriasis as a possible defect of adenylyl cyclase cyclic AMP cascade—a defective chalone mechanism", *Archives of Dermatology*, **104**, 352, (1971).
26. Rusin, L. J.; Duell, E. A. and Voorhees, J. J., "Papaverine and Ro 20-1724 Inhibit Cyclic Nucleotide Phosphodiesterase Activity and Increase Cyclic AMP Levels in Psoriatic Epidermis In Vitro", *J. Invest. Dermatol.*, **71**, 154-156, (1978).
27. Jorde, W. and Schata, M., "Inhibitory effect of β -adrenergic stimulant on the histamine reaction in human skin", *Arzneim. Forsch.* **26**, 2103-2105, (1976).
28. Gronneberg, R.; Strandberg and Hagermark, O., "Cutaneous responses to allergen after pre-treatment with β -adenoceptor stimulating and blocking agents", *Allergy*, **35**, 409-412, (1980).
29. Seely, R. J. and Glenn, E. M., "Salbutamol as a topical antiinflammatory drug", *Proc. Soc. Exp. Biol. Med.* **159**, 223-225, (1978).
30. Rassner, G., "Enzyme der Epidermis", *Arch. Dermatol. Forsch.*, **244**, 48-52, (1972).
31. Hammar, H., "Glyceraldehyde phosphate dehydrogenase and glucose-6-phosphate dehydrogenase activities in psoriasis and neurodermatitis and the effect of dithranol", *J. Invest. Dermatol.*, **54**, 121-125, (1970).
32. de Groot, A. C. and Nater, J. P., "Contact allergy to dithranol", *Contact Dermatitis*, **7**, 5-8, (1981).
33. Goeckerman, W. H., "Treatment of psoriasis", *Northwest. Med.*, **24**, 229-231 (1925).
34. Parrish, J. A. and Morrison, W. L., "Therapy of psoriasis by tar photosensitisation", *J. Invest. Dermatol.*, **70**, 111-112, (1978).
35. Elks, J., "Steroid structure and steroid activity", *Br. J. Dermatol. Supplement*, **12**, 3-13, (1976).

36. Fried, J. and Sabo, E. F., "Synthesis of 17- α -hydrocorticosterone and its 9 α -helo derivatives from 11-epi-17 α -hydroxycorticosterone", *J. Am. Chem. Soc.*, **75**, 2273-2274 (1953).
37. Alani, M. D. and Alani, S. D., "Allergic contact dermatitis to corticosteroids", *Ann. Allergy*, **30**, 181-185, (1972).
38. Nieboer, C. and Verburgh, C. A., "Psoriasis treatment with vitamin D₃ analogue MC 903", *Br. J. Dermatol.*, **126**, 302-303 (1992).
39. Zackheim, H. S., "Treatment of psoriasis with 6-aminonicotinamide", *Arch. Dermatol.*, **111**, 880-882 (1975).
40. Herkin, H. and Lange, K., Antimetabolite action on the pentose phosphate pathway in the central nervous system induced by 6-aminonicotinamide. In *Central Nervous System-Studies on Metabolic Regulation and Function*. E. Genazzani and H. Herkin (Eds.). Spring Verlag, pp 41-54, (1974).
41. Krieglstein, J. and Stock, R., "Decreased glycolytic flux rate in the isolated perfused rat brain after pre-treatment with 6-aminonicotinamide", *Naunyn Schmiedebergs Arch. Pharmacol.*, **290**, 323-327, (1975).
42. Matschke, G. H. and Fagerstone, K. A., "Teratogenic effect of 6-aminonicotinamide in mice", *J. Toxicol. Environ. Health*, **3**, 735-743, (1977).
43. Epstein, W. L.; Fukuyama, K. and Epstein, J. H., "Early effects of ultraviolet light on DNA synthesis in human skin *in vivo*", *Arch. Dermatol*, **100**, 84, (1969).
44. Sakuntabhai, A.; Sharpe, G. R. and Farr, P.M., "Improved efficiency and efficacy of PUVA for psoriasis with twice weekly treatment", *Br. J. Dermatol. (Supplement)*, **125**, 28 (1991).
45. Murphy, G. M.; Logan, R. A.; Lovell, C. R.; Morris, R. W.; Hawk, J. L. M. and Magnus, I. A., "Prophylactic PUVA and UVB therapy in polymorphic light eruption - a controlled trial", *Br. J. Dermatol.*, **116**, 531-538 (1987).
46. Addo, H. A. and Sharma, S. C., "UVB phototherapy and photochemotherapy (PUVA) in the treatment of polymorphic light eruption and solar urticaria", *Br. J. Dermatol.*, **116**, 539-547 (1987).

47. Thomson, A. W.; Nalesnik, M. A.; Rilo, H. R.; Woo, J.; Carroll, P. B.; Van Thiel D. H., "ICAM-1 and E-selection expression in lesional biopsies of psoriasis patients responding to systemic FK 506 therapy", *Autoimmunity*, **15**, 215-223 (1993).
48. Gubner, R.; August, S. and Ginsberg, V., "Therapeutic suppression of tissue reactivity: effect of aminopterin in rheumatoid arthritis and psoriasis", *Am. J. Med. Sci.*, **221**, 176-182 (1951).
49. Stern, R. S.; Fierler, S. and Parrish, J. A., "Methotrexate used for psoriasis and the risk of noncutaneous or cutaneous malignancy", *Cancer*, **50**, 869-872, (1982).
50. Leavell, U. W. and Yarbrow, J. W., *Arch. Dermatol.*, **102**, 144 (1970).
51. Yarbrow, J. W.; Kennedy, B. J. and Barnum, L. P., "Hydroxyurea inhibition of DNA synthesis in ascites tumor", *Proct. Natl. Acad. Sci.* **53**, 1033-1035, (1965).
52. Dahl, M. G. C. and Comaish, J. S., "Long-term effects of hydroxyurea in psoriasis", *Br. Med. J.*, **4**, 585-587, (1972).
53. Horton, J. J. and Wells, R. S., "Razoxane: a review of 6 years' therapy in psoriasis", *Br. J. Dermatol.*, **109**, 669-673 (1983).
54. Demis, D. J.; Brown, C. S. and Crosby, W. H., "Thioguanine in the treatment of certain autoimmune, immunologic and related diseases", *Am. J. Med.*, **37**, 195-205 (1964).
55. Calabresi, P. and Parks, R. E. Jr., "Chemotherapy of neoplastic disease." In *The Pharmacological Basis of Therapeutics*. L.S. Goodman and A. Gilman (Eds.) Macmillan, pp 1248-1307, (1975).
56. Wolbach, S. B. and Howe, P. R., "Tissue changes following deprivation of fat soluble A-vitamin", *J. Exp. Med.*, **42**, 753-778 (1925).
57. Harris, L. J.; Innes, J. R. M. and Griffith, A. S., "On the pathogenesis of avitaminosis A: vitamin A as the anti-keratinising factor", *Lancet*, **2**, 614-617 (1932).
58. Stuetgen, G., "Zur lokalbehandlung von keratosen mit vitamin-A-Saure", *Dermatologica*, **124**, 65-80 (1962).

59. Schumacher, A. and Stuetgen, G., "Vitamin-A-saure bei hyperkeratosen, epithelialen tumoren und akne. orale und lokale anwendung", *Dtsch. Med. Wochenschr.*, **96**, 1547-1551 (1971).
60. Bischoff, R.; De Jong, E. M. G. J.; Rulo, H. F. C.; Sendagorta, E.; Czarnetzki, B. M. and Van De Kerkhof, P. C. M., "Topical application of 13-cis-retinoic acid in the treatment of chronic plaque psoriasis", *Clin. Exp. Dermatol.*, **17**, 9-12 (1992).
61. Dierlich, E. and Orfanos, C. E., "Epidermale zelloproliferation under oraler retinoid-therapy bei psoriasis. Autoradiographisch befunde an befallener und nicht-befallener haut", *Arch. Dermatol. Res.*, **264**, 169-177, (1979).
62. Lands, A. M.; Arnold, A.; McAuliff, J. P.; Luduena, F. P. and Brown, T. G., "Differentiation of receptor systems activated by sympathomimetic amines", *Nature*, **214**, 597-598 (1967).
63. Hedberg, A.; Minneman, K. P. and Molinoff, P. B., "Differential Distribution of Beta-1 and Beta-2 Adrenergic Receptors in Cats and Guinea-Pig Heart", *J. Pharmacol. Exp. Ther.*, **212**, 503-508 (1980).
64. Heitz, A.; Schwartz, J. and Velly, J., " β -Adrenoceptors of the human myocardium: Determination of β_1 and β_2 subtypes by radioligand binding", *Br. J. Pharmacol.*, **80**, 711-717 (1983).
65. Purdy, R. E.; Stupecky, G. L. and Coulombe, P. R., "Further Evidence for a Homogeneous Population of Beta-1-adrenoceptors in Bovine Coronary Artery", *J. Pharmacol. Exp. Ther.*, **245**, 67-71 (1988).
66. Strader, C. D.; Sigal, I. S. and Dixon, R. A. F., "Mapping the Functional Domains of the β -adrenergic Receptor", *Am. J. Respir. Cell Mol. Biol.*, **1**, 81-86 (1989).
67. Strader, C. D.; Sigal, I. S.; Candelore, M. R.; Rands, E.; Hill, W. S. and Dixon, R.A.F., "Conserved aspartic acid residues of 79 and 113 of the β -adrenergic receptor have different roles in receptor function", *J. Biol. Chem.*, **263**, 10267-10271 (1988).
68. Strader, C. D.; Candelore, M. R.; Hill, W. S.; Sigal, I. S. and Dixon, R. A. F., "Identification of two serine residues involved in agonist activation of the β -adrenergic receptor", *J. Biol. Chem.*, **264**, 13572-13578 (1989).

69. Strader, C. D.; Sigal, I. S. and Dixon, R. A. F., "Structural basis of β -adrenergic receptor function", *FASEB J.*, **3**, 1825-1832 (1989).
70. Frielle, T.; Daniel, K. W.; Caron, M. G. and Lefkowitz, R. J., "Structural basis of β -adrenergic receptor subtype specificity studied with chimeric β_1/β_2 -adrenergic receptors", *Proc. Natl Acad. Sci. USA*, **85**, 9494-9498 (1988).
71. Dixon, R. A. F., *Proteins*, **6**, 267-274 (1989).
72. Tota, M. R. and Strader, C. D., "Characterization of the binding domain of the β -adrenergic receptor with the fluorescent antagonist carazolol", *J. Biol. Chem.*, **265**, 16891-16897 (1990).
73. Triggle, D. J. and Triggle, C. R., *Chemical Pharmacology of The Synapse*, Chapter III, Academic, London, 1976.
74. Weinstock, L. M.; Mulvey, D. M. and Tull, R., "Synthesis of β -adrenergic blocking agent Timolol from optically active precursors", *J. Org. Chem.*, **41**, 3121-3124 (1976).
75. Easson, L. H. and Stedman, E., *Biochem. J.*, **27**, 1257 (1933).
76. Larsen, A. A., "Catecholamine chemical species at the adrenergic receptors", *Nature*, **224**, 25-27 (1969).
77. Lands, A. M. and Brown, T. G., In "Drugs Affecting the Peripheral Nervous System", (A. Burger, ed.), vol. **1**, Dekker, New York, 399 (1967).
78. Lands, A. M.; Nash, V. L; McCarthy, H. M.; Granger, H. R. and Dertinger, B. L., "The pharmacology of *N*-alkyl homologues of epinephrine", *J. Pharmac. exp. Ther.* **90**, 110-119 (1947).
79. Lands, A. M.; Nash, V. L; Dertinger, B. L.; Granger, H. R. and McCarthy, H. M., "The pharmacology of compounds structurally related to hydroxytyramine", *J. Pharmac. exp. Ther.* **92**, 369-380 (1948).
80. Lands, A. M.; Arnold, A.; McAuliff, J. P.; Luduena, F. P. and Brown, T. G., "Differentiation of receptor systems activated by sympathomimetic amines", *Nature*, **214**, 597-598 (1967).

81. Pratesi, P., Grana, E. and Villa, L., *Jl. Farm. Ed. Sci.*, **26**, 379 (1971).
82. Bloom, B. M. and Goldman, I. M., In "Advances in Drug Research." (N.J. Harper and A.B. Simmonds, eds.), vol 3, p 121. Academic Press, London and New York (1966).
83. i. Manfred, E. Wolff, In "*Burger's Medicinal Chemistry 4th Ed.*", part III, p 261. John Wiley & Sons, New York (1981).
ii. Nishikawa, M.; Kanno, M.; Kuriki, H.; Sugihara, H.; Motohashi, M., Itoh, K.; Miyashita, O.; Oka, Y. and Sanno, Y., "Selective β -adrenoceptor activities of tetrahydronaphthalene derivatives", *Life Sci.*, **16**, 305-314 (1975).
84. Irwin, W. J. and Belaid, K. A., "Drug Delivery by Ion Exchange. Part I, II and III", *Drug Develop. Ind. Pharm.*, **13**, 2017-2031, 2033-2045 and 2047-2066 (1987).
85. Bowman, W. C. and Rand, M. J., *Textbook of Pharmacology*, 2nd Ed., Blackwell Scientific Publications, Oxford, p 11.26 (1980).
86. Bodor, N., "Novel approaches to the design of safer drugs: Soft drugs and site specific chemical delivery systems", *Advances in Drug Research*, **13**, 255-331 (1984).
87. Bundgaard, H. (Ed.), *Design of Prodrugs*, Elsevier Science Publishers, Amsterdam (1985).
88. Daehne, E.; Frederiksen, E.; Gundersen, Lund, F.; Morch, P.; Petersen, H. J.; Roholt, K.; Tybring, L. and Godtfredsen, W. O., "Acyloxymethyl esters of ampicillin", *J. Med. Chem.*, **13**, 607-612 (1970).
89. Clyton, J. P.; Cole, M.; Elson, S. W. and Ferres, H., "BRL.8988 (talampicillin), a well-absorbed oral form of ampicillin", *Antimicrobiol. Agents Chemother.*, **5**, 670-671 (1974).
90. Bodin, N. O.; Ekstrom, B.; Forsgren, U.; Jalar, L. P.; Migni, L.; Ramsey, C. H. and Sioberg, B., "Bacampicillin: a new orally well-absorbed derivative of ampicillin", *Antimicrobiol. Agents Chemother.*, **8**, 518-525 (1975).

91. Wei, C. P.; Anderson, J. P. and Leopold, I., "Ocular absorption and metabolism of the topically applied epinephrine and a dipivaloyl ester of epinephrine", *Invest. Ophthalmol. Vis. Sci.*, **17**, 315-321 (1978).
92. Krogsgaard-Larsen, P. (Ed.) and Bundgaard, H. (Ed.), *A Textbook of Drug Design and Development*, Harwood Academic Publishers, Oxford, In Chapter 5 (Design and application of prodrugs), p 112-191 (1991).
93. Chowdhary, M. E. H. and Chacon, C., "Depot Fluphenazine and Flupenthixol in the treatment of stabilized schizophrenics. A double-blind comparative trial", *Comprehensive Psychiatry*, **21**, 135-139 (1980).
94. Kohler, C.; Tolman, E.; Wooding, W. and Ellenbogen, L., "A review of the effect of fenbufen and a metabolite, biphenylacetic acid, on platelet biochemistry and fenbufen", *Arzneim. Forsch.*, **30**, 702-707 (1980).
95. Chiccarelli, F. S.; Eisner, H. J. and Van Lear, G. E., "Disposition and metabolism of fenbufen in several laboratory animals", *Arzneim. Forsch.*, **30**, 707-716 (1980).
96. Yu, C. D.; Fox, J. L.; Ho, N. F. H. and Higuchi, W. I., "Physical model evaluation of topical prodrug delivery - Simultaneous transport and bioconversion of Vidarabine-5'-valerate I: Physical model development", *J. Pharm. Sci.*, **68**, 1341-1346 (1979).
97. Boyle, E. A.; Freeman, P. C.; Mangan, F. R. and Thomson, M. J., "Nabumetone [BRL 14777, 4-(6-methoxy-2-naphthyl)-butan-2-one]: a new anti-inflammatory agent", *J. Pharm. Pharmacol.*, **34**, 562-569 (1982).
98. Haddock, R. E.; Jeffery, D. J.; Lloyd, J. A. and Thawley, A. R., "Metabolism of nabumetone (BRL 14777) by various species including man", *Xenobiotica*, **14**, 327-337 (1984).
99. Wermuth, C. G., In *Drug Design: Fact or Fantasy?*, Jolles, J. and Woolbridge, K. R. H. (eds.), Academic Press Inc., New York, pp 47 (1984).
100. Mandell, A. I.; Stentz, F. and Kitabaldi, A. E., "Dipivaloyl epinephrine: A new prodrug in the treatment of glaucoma", *Ophthalmology*, **85**, 268-275 (1978).
101. Wei, C. P.; Anderson, J. A. and Leopold, I. H., "Ocular absorption and metabolism of topically applied epinephrine and dipivaloyl ester of epinephrine", *Invest Ophthalmol Vis Sci*, **17**, 315-321 (1978).

102. Anderson, J. A.; Richman, J. B. and Mindel, J. S., "Effects of echothiophate on enzymatic hydrolysis of dipivefrin", *Arch. Ophthalmol.*, **102**, 913-916 (1984).
103. Mindel, J. S.; Cohen, G.; Barker, A. and Lewis, D. E., "Enzymatic and non-enzymatic hydrolysis of D,L-dipivefrin", *Arch. Ophthalmol.*, **102**, 457-460 (1984).
104. Ihara, M.; Nakajima, S.; Hisaka, A. and Tsuchiya, Y., "Hydrolysis and acyl migration of a catechol monoester of L-dopa: L-3-(3-Hydroxy-4-pivaloyloxyphenyl)alanine", *J. Pharm. Sci.*, **79** (8), 703-708 (1990).
105. Nielson, N. M. and Bundgaard, H., "Esters of *N,N*-disubstituted 2-hydroxyacetamides as a novel highly biolabile prodrug type for carboxylic acid agents", *J. Med. Chem.*, **30**, 451-454 (1987).
106. Nielson, N. M. and Bundgaard, H., "Glycolamide esters are biolabile prodrugs of carboxylic acid agents: Synthesis, bioconversion and physicochemical properties", *J. Pharm. Sci.*, **77**, 285-298 (1988).
107. March, J. (ed.), *Advanced Organic Chemistry: reaction, mechanism and structure*, 4th edition, John Wiley & Sons, Inc., New York, p 397 (1992).
108. Scheuing, G. and Thoma, O., "Isopropylaminomethyl-(3,4-dioxyphenyl) carbinol", *United States Patent No. 2,308,232* (1943).
109. i. Lunts, L. H. C. and Toon P., "4-Hydroxy- α' -aminomethyl-*m*-xylene- α' , α^3 -diols", *United States Patent No. 3,644,353* (1972).
ii. Thoma, O. and Zeile, K., "1-(3,5-Dihydroxy-phenyl)-1-hydroxy-2-isopropyl-aminoethane and salts thereof", *United States Patent No. 3,341,594* (1967).
iii. Bockmühl, M.; Ehrhart, G. and Stein, L., "Process of preparing compounds of the 1-phenyl-2-aminoalcohols-1 series hydroxylated in the phenyl nucleus", *United States Patent No. 1,948,162* (1934).
iv. Collin, D. T.; Hartley, D.; Jack, D.; Lunts, L. H. C.; Press, J. C.; Ritchie, A. C. and Toon, P., "Saligenin analogs of sympathomimetic catecholamines", *J. Med. Chem.*, **13**, 674-680 (1970).
110. John, A. K. and Freeman, H. M., "The preparation of some α -benzylamino- β , β -dialkoxypropionic acid derivatives", *J. Am. Chem. Soc.*, **72**, 1236-1239 (1950).

111. Remizov, A. L., "Synthesis of some derivatives of adrenaline. I Synthesis of *dl*-adrenaline and its analogs", *Zhur. Obshchei Khim.*, **28**, 2530-2538 (1958).
112. Buchi, G.; Foulkes, D. M., Kurono, M., Mitchell, G. F. and Schneider, R. S., "The total synthesis of racemic aflatoxin B₁", *J. Am. Chem. Soc.*, **89**, 6745-6753 (1967).
113. McOmie, J. F. W., *Protective groups in organic chemistry*, Plenum press, London, 1973.
114. Trost, B. M. and Caldwell, C. G., "The di *t*-butylsilylene protecting group for diols", *Tetrahedron Lett.*, **22**, 4999-5002 (1981).
115. Collington, E. W.; Finch, H. and Smith, I. J., "Selective deprotection of alcoholic and phenolic silyl ethers", *Tet. Letts.*, **26**, 681-684 (1985).
116. Leonard, J., "Plant polyphenols. IV. Experiments on the synthesis of 3,3'- and 4,4'-di-O-methylellagic acid", *J. Am. Chem. Soc.*, **81**, 4606-4610 (1959).
117. Furniss, B. S.; Hannaford, A. J.; Smith, P. W. G. and Tatchell, A. R. (eds.), *Vogel's: Textbook of practical organic chemistry*, 5th edition, Longman Scientific and technical, Essex, p 1248 (1989).
118. Hansen, B., "Kinetics of the alkaline hydrolysis of catechol monoacetate and some derivatives", *Acta Chem. Scand.*, **17**, 1375-1379 (1963).
119. Knox, J. H.; Done, J. N.; Fell, A. F.; Gilbert, M. T.; Pryde A. and Wall, R. A., *High Performance Liquid Chromatography*, Edinburgh University Press, Edinburgh, (1978).
120. Fong, G. W. and Lam, S. K., *HPLC in the pharmaceutical industry*, volume 47, Marcel Dekker, Inc., New York, (1991).
121. Bakalayer, S. R.; Bradley, M. P. T. and Honganen, R., "The role of dissolved gases in high performance liquid chromatography", *J. Chromatography*, **158**, 277-293 (1978).
122. Bucks, D. A. W., "Skin structure and metabolism: Relevance to the design of cutaneous therapeutics", *Pharm. Res.*, **1**, 148-153 (1984).

123. Hadgraft, J., Prodrugs and skin absorption. In: Bundgaard, H. (ed.). *Design of Prodrugs*. Elsevier Science Publishers, Amsterdam (1985).
124. Kappus, H., Drug metabolism in the skin. In: Greaves M. W. and Shuster, S. (eds.), *Handbook of Experimental Pharmacology, 87/1 Pharmacology of the skin II.*, Springer-Verlag, Berlin, 123-163 (1989).
125. Noonan, P. K. and Waster, R. C., Cutaneous metabolism of xenobiotics. In: Bronaugh, R. L. and Maibach, H. I. (eds), *Percutaneous absorption. Mechanism-Methodology Drug Delivery*, Marcel Dekker, New York, 65-85 (1985).
126. Pannatier, A.; Jenner, P; Testa, B. and Etter, J. C., "The skin as a drug-metabolising organ", *Drug Metab. Rev.*, **8**, 319-343 (1978).
127. Chan, S. Y. and Li Wan Po, A., "Prodrugs for dermal delivery", *Int. J. Pharm.*, **55**, 1-16 (1989).
128. Sloan, K. B; Koch, S. A. M. and Siver, K. G., "Mannich base derivatives of theophylline and 5-fluorouracil: synthesis, properties and topical delivery characteristics", *Int. J. Pharm.*, **21**, 251-264 (1984).
129. Sloan, K. B; Sheretz, E. F. and McTiernan, R. G., "The effect of structure of Mannich base prodrugs on their ability to deliver theophylline and 5-fluorouracil through hairless mouse skin", *Int. J. Pharm.*, **44**, 87-96 (1988).
130. Sloan, K. B; Selk, S.; Haslam, J.; Caldwell, L. and Duel, E. A., "Acyloxyamines as prodrugs of anti-inflammatory carboxylic acids for improved delivery through skin", *J. Pharm. Sci.*, **73**, 1734-1737 (1984).
131. Siver, K. G. and Sloan, K. B., "The effect of structure of Mannich base prodrugs of 6-mercaptopurine on their ability to deliver 6-mercaptopurine through hairless mouse skin", *Int. J. Pharm.*, **48**, 195-206 (1988).
132. Loftsson, T. and Bodor, N., "Improved delivery through biological membranes IX: Kinetic and mechanism of hydrolysis of methylsulfinylmethyl 2-acetoxybenzoate and related aspirin prodrugs", *J. Pharm. Sci.*, **70**, 750-755 (1981).
133. Loftsson, T. and Bodor, N., "Improved delivery through biological membranes IX: Percutaneous absorption and metabolism of methylsulfinylmethyl 2-acetoxybenzoate and related aspirin prodrugs", *J. Pharm. Sci.*, **70**, 756-758 (1981).

134. Täuber, U. and Toda, T., "Biotransformation von Difluocortolnivalerianat in der Haut von Ratte, Meerschweinchen und Mensch", *Arzneim Forsch*, **26**, 1484-1487 (1976).
135. Täuber, U., "Metabolism of drugs on and in the skin. In: Brandau R, Lippold BH (eds), *Dermal and Transdermal Absorption*. Wissenschaftliche Verlagsgesellschaft, Stuttgart, 133-151 (1982).
136. Wiegrebe, W.; Retzow, A.; Plumier, E.; Ersoy, N.; Garber, A.; Faro, H. P. and Kunert, R., "Dermal absorption and metabolism of the antipsoriatic drug dithranol triacetate", *Arzneim-Forsch Drug Res.*, **34**, 48-51 (1984).
137. Møllgaard, B.; Hoelgaard, A. and Bundgaard, H., "Prodrugs as drug delivery systems XXIII. Improved dermal delivery of 5-fluorouracil through human skin via N-acyclomethyl prodrug derivatives", *Int. J. Pharm.*, **12**, 153-162 (1982).
138. Bodor, N., "Designing safer drugs based on the soft-drugs approach", *Trends in Pharmacol. Sci.*, **3**, 53-58 (1982).
139. Bodor, N. and Sloan, K. B., "Improved delivery through biological membranes XII. The effect of the incorporation of biphasic solubilizing group into prodrugs of steroids", *Int. J. Pharm.*, **15**, 235-250 (1983).
140. Bodor, N.; Sloan, K. B.; Little R. J.; Selk, S. H. and Caldwell, L., "Soft drugs 4. 3-Spirothiazolidines of hydrocortisone and its derivatives", *Int. J. Pharm.*, **10**, 307-321 (1982).
141. Waranis, R. P. and Sloan, K. B., "Effects of vehicles and prodrug properties and their interactions on the delivery of 6-mercaptopurine through skin: bisacycloxymethyl-6-mercaptopurine prodrugs", *J. Pharm. Sci.*, **76**, 587-595 (1987).
142. Waranis, R. P. and Sloan, K. B., "Effects of vehicles and prodrug properties and their interactions on the delivery of 6-mercaptopurine through skin: S⁶-acycloxymethyl-6-mercaptopurine prodrugs", *J. Pharm. Sci.*, **77**, 210-215 (1988).
143. Johansen, M.; Møllgaard, B.; Wotton, P.; Larsen, C. and Hoelgarrd, A., "In vitro evaluation of dermal prodrug delivery - transport and bioconversion of a series of aliphatic esters of metronidazole", *Int. J. Pharm.*, **32**, 199-206 (1986).

144. Yu, C. D.; Fox, J. L.; Ho, N. F. H. and Higuchi, W. I., "Physical model evaluation of topical prodrug delivery - simultaneously transport and bioconversion of vidarabine-5'-valerate I & II.", *J. Pharm. Sci.*, **68**, 1341-1357 (1979).
145. Yu, C. D.; Higuchi, W. I.; Ho, N. F. H.; Fox, J. L. and Flynn, G. L., "Physical model evaluation of topical prodrug delivery - simultaneously transport and bioconversion of vidarabine-5'-valerate III. Permeability differences of vidarabine and *n*-pentanol in components of hairless mouse skin", *J. Pharm. Sci.*, **68**, 770-772 (1980).
146. Yu, C. D.; Fox, J. L.; Ho, N. F. H. and Higuchi, W. I., "Physical model evaluation of topical prodrug delivery - simultaneously transport and bioconversion of vidarabine-5'-valerate IV. Distribution of esterase and deaminase enzymes in hairless mouse skin", *J. Pharm. Sci.*, **69**, 772-775 (1980).
147. Higuchi, W. I.; Gordon, N. A.; Fox, J. L. and Ho, N. F. H., "Transdermal delivery of prodrugs", *Drug Dev. Ind. Pharm.*, **9**, 691-706 (1983).
148. Sloan, K. B. and Bodor, N., "Hydroxymethyl and acycloxymethyl prodrugs of theophylline: enhanced delivery of polar drugs through skin", *Int. J. Pharm.*, **12**, 299-313 (1982).
149. Bodor, N.; Zupan, J. and Selk, S., "Improved delivery through biological membranes VII. Dermal delivery of cromoglycic acid (Cromolyn) *via* its prodrugs", *Int. J. Pharm.*, **7**, 63-75 (1980).
150. Ando, H. Y.; Ho, N. F. H. and Higuchi, W. I., "Skin as an active metabolizing barrier I: Theoretical analysis of topical bioavailability", *J. Pharm. Sci.*, **66**, 1525-1528 (1977).
151. Guy, R. H. and Hadgraft, J., "Percutaneous metabolism with saturable enzyme kinetics", *Int. J. Pharm.*, **11**, 187-197 (1982).
152. Guy, R. H. and Hadgraft, J., "Pharmacokinetics of percutaneous absorption with concurrent metabolism", *Int. J. Pharm.*, **20**, 43-51 (1984).
153. Elving, P. J.; Markowitz, J. M. and Rosenthal, I., "Preparation of buffer system of controlled ionic strength", *Anal. Chem.*, **28**, 1179-1180 (1956).

154. Perrin, D. D. and Dempsey, B., *Buffers for pH and Metal Ion Control*, Chapman and Hall, London (1974).
155. Albert, A. and Serjeant, E. P., *The determination of ionization constants*, 3rd edn., Chapman and Hall, London (1984).
156. Fife, T. H. and Bruice, T. C., "The temperature dependence of the δ pD correction for the use of the glass electrode in D₂O", *J. Phys. Chem.*, **65**, 1079-1080 (1961).
157. Wall, G. M.; Kenny, J. C.; Fan, T. Y. and Schafer, C., "Analysis of 3- and 4-monopivaloyl epinephrine, degradation products in dipivefrin hydrochloride drug substances and ophthalmic formulations", *J. Pharm. Biomed. Anal.*, **10**, 465-471 (1992).
158. Powell, W. S.; Heacock, R. A.; Smith, D. G. and McInnes, A. G., "The chemistry of aminochromes. Part XVI. Proton magnetic resonance spectroscopy", *Can. J. Chem.*, **51**, 776-779 (1973).
159. Shalitin, Y. and Bernhard, S. A., "Neighboring group effects on ester hydrolysis. I. neighboring hydroxyl groups", *J. Am. Chem. Soc.*, **86**, 2291-2292 (1964).
160. Fuller, E. J., "Catalysis by catechol monoanion", *J. Am. Chem. Soc.*, **85**, 1777-1780 (1963).
161. Capon, B. and Ghosh, B. C., "The mechanism of the hydrolysis of phenyl salicylate and catechol monobenzoate in the presence and absence of borate ions", *J. Chem. Soc. (B)*, 4720-478 (1966).
162. Barry, B. W., *Dermatological formulations: percutaneous absorption*, Marcel Dekker, New York (1983).
163. Siddiqui, O., "Physicochemical, physiological and mathematical considerations in optimising percutaneous absorption of drugs", *Crit. Rev. Ther. Drug Carrier Systems*, **6**, 1-38, (1989).
164. Guy, R. H; Maibach, H. I. and Shah, V. P., "The bioavailability of dermatological and other topically administered drugs", *Pharm. Res.*, **3**, 253-262 (1986).

165. Hadgraft, J. Formulation of anti-inflammatory agents. In Hensby, C. and Lowe, N. J. (eds.), *Pharmacology and the skin, Vol 2. Nonsteroidal Anti-inflammatory Drugs*. Karger, Basel, 21-43 (1989).
166. Houk, J. and Guy, R. H., "Membrane models for skin penetration studies", *Chem. Rev.*, **88**, 455-457 (1988).
167. Nacht, S. and Yeung, D., Artificial membranes and skin permeability. In: Bronaugh, R. L. and Maibach, H. I. (eds.), *Percutaneous Absorption. Mechanisms-Methodology-Drug Delivery*. Marcel Dekker, New York, 373-386 (1985).
168. Franz, T. J., "Percutaneous absorption. On the relevance of *in vitro* data", *J. Invest. Dermatol.*, **64**, 190-195 (1975).
169. MT-CALC (a basic programme by W. J. Irwin, Department of Pharmaceutical and Biological Sciences, Aston University, Aston Triangle, Birmingham B4 7ET, UK.).
170. Barry, B. W. (ed.), *Dermatological Formulations: Percutaneous Absorption*, volume 18, Marcel Dekker, Inc., New York, p 72 (1983).

APPENDICES

APPENDIX FOR CHAPTER FIVE:

pH	Disodium hydrogen Phosphate in grams (Na ₂ HPO ₄ · 12H ₂ O)	Citric acid in grams (C ₆ H ₈ O ₇ · H ₂ O)	Potassium chloride in grams to make buffer of ionic strength 1M
2.2	0.143	2.060	3.72
3.0	1.470	1.670	3.14
4.0	2.760	1.290	2.55
5.0	3.690	1.020	1.82
6.0	4.520	0.774	1.16
7.0	5.890	0.370	0.544
8.0	6.960	0.059	-

Amounts are dissolved in distilled water and final volume are made up to 100 ml

Table 5.1A: Preparation of McIlvine buffers

KOH (ml)	pH	[H ₃ O ⁺]	a=[NH ⁺]	b=[N:]	pK _a
0.4	6.77	1.6982E-11	1.1392E-04	9.9010E-03	7.831
0.8	7.11	7.7625E-11	1.0300E-03	1.9608E-03	7.830
1.2	7.32	4.7863E-11	9.2287E-03	2.9126E-03	7.821
1.6	7.48	3.3113E-10	8.1784E-03	3.8462E-03	7.808
2.0	7.62	2.3988E-10	7.1482E-03	4.7619E-03	7.796
2.4	7.74	1.8197E-10	6.1373E-03	5.6604E-03	7.775
2.8	7.86	1.3804E-10	5.1454E-03	6.5421E-03	7.756
3.0	7.91	1.2303E-10	4.6563E-03	6.9767E-03	7.734
3.4	8.02	9.5499E-10	3.6918E-03	7.8341E-03	7.693
3.8	8.14	7.2443E-10	2.7448E-03	8.6758E-03	7.640

Table 5.2A: Potentiometric titration of methyl *N*-[2'-phenyl-2'-hydroxyethyl]-3-aminopropionate HCl (50, R=Me, 129.92 mg) with KOH (0.1 M) in 10% acetonitrile in water. [End-point 2.64 ml, mean pK_a value= 7.768 ± 0.06]

KOH (ml)	pH	[H ₃ O ⁺]	a=[NH ⁺]	b=[N:]	pK _a
0.2	6.31	4.8978E-07	1.6282E-02	9.0090E-04	7.567
0.4	6.41	3.8905E-07	1.5243E-02	1.7857E-03	7.341
0.6	6.52	3.0200E-07	1.4223E-02	2.6549E-03	7.249
0.8	6.64	2.2909E-07	1.3222E-02	3.5088E-03	7.216
1.0	6.79	1.6218E-07	1.2237E-02	4.3478E-03	7.239
1.2	6.96	1.0965E-07	1.1269E-02	5.1724E-03	7.298
1.4	7.14	7.2444E-08	1.0318E-02	5.9829E-03	7.377
1.6	7.36	4.3652E-08	9.3835E-03	6.7797E-03	7.501
1.8	7.61	2.4547E-08	8.4643E-03	7.5630E-03	7.659
2.0	7.87	1.3490E-08	7.5604E-03	8.3333E-03	7.828

Table 5.3A: Potentiometric titration of ethyl *N*-[2'-(3",4"-dipivaloyloxyphenyl)-2'-hydroxyethyl]-3-aminopropionate HCl (107, 180.80 mg) with KOH (0.1 M) in 10% acetonitrile in water. [End-point 1.72 ml, mean pK_a value= 7.4275 ± 0.194]

KOH (ml)	pH	[H ₃ O ⁺]	a=[NH ⁺]	b=[N:]	pK _a
0.6	8.59	2.5704E-09	9.1366E-03	1.1858E-03	9.478
1.0	8.86	1.3804E-09	8.2806E-03	1.9608E-03	9.487
1.4	9.01	9.7724E-10	7.4379E-03	2.7237E-03	9.448
1.8	9.14	7.2443E-10	6.6083E-03	3.4749E-03	9.421
2.2	9.26	5.4954E-10	5.7914E-03	4.2146E-03	9.401
2.6	9.37	4.2658E-10	4.9869E-03	4.9430E-03	9.377
3.0	9.48	3.3113E-10	4.1945E-03	5.6604E-03	9.354
3.4	9.57	2.6915E-10	3.4141E-03	6.3670E-03	9.305
3.8	9.67	2.1380E-10	2.6452E-03	7.0632E-03	9.252
4.2	9.79	1.6218E-10	1.8876E-03	7.7491E-03	9.191

Table 5.4A: Potentiometric titration of ephedrine HCl (105.35 mg) with KOH (0.1 M) in water. [End-point 2.55 ml, mean pK_a value= 9.371 ± 0.092].

KOH (ml)	pH	[H ₃ O ⁺]	a=[NH ⁺]	b=[N:]	pK _a
0.1	7.85	1.4125E-08	9.7804E-03	1.9960E-04	9.540
0.3	8.31	4.8978E-09	9.3439E-03	5.9642E-04	9.505
0.5	8.55	2.8184E-09	8.9109E-03	9.9010E-04	9.504
0.7	8.69	2.0417E-09	8.4813E-03	1.3807E-03	9.478
1.1	8.92	1.2023E-09	7.6321E-03	2.1526E-03	9.470
1.3	9.01	9.7724E-10	7.2125E-03	2.5341E-03	9.464
1.7	9.16	6.9183E-10	6.3830E-03	3.2882E-03	9.448
1.9	9.23	5.8884E-10	5.9730E-03	3.6609E-03	9.443
2.1	9.29	5.1286E-10	5.5662E-03	4.0307E-03	9.430
2.5	9.40	3.9811E-10	4.7619E-03	4.7619E-03	9.400

Table 5.5A: Potentiometric titration of ephedrine HCl (100.85 mg) with KOH (0.1 M) in 10% acetonitrile in water.
 [End-point 1.85 ml, mean pK_a value= 9.468 ± 0.039]

HCl (ml)	pH	[H ₃ O ⁺]	a=[NH ⁺]	b=[N:]	pK _a
0.2	10.41	3.8905E-11	3.9841E-04	9.6678E-03	9.025
0.4	10.28	5.2481E-11	7.9365E-04	9.2326E-03	9.214
0.6	10.16	6.9183E-11	1.1858E-03	8.8009E-03	9.289
0.8	10.07	8.5114E-11	1.5748E-03	8.3726E-03	9.344
1.0	9.98	1.0471E-10	1.9608E-03	7.9476E-03	9.372
1.2	9.91	1.2303E-10	2.3438E-03	7.5259E-03	9.403
1.4	9.84	1.4454E-10	2.7237E-03	7.1075E-03	9.423
1.6	9.76	1.7378E-10	3.1008E-03	6.6924E-03	9.426
1.8	9.71	1.9498E-11	3.4749E-03	6.2804E-03	9.453
2.0	9.64	2.2909E-11	3.8462E-03	5.8716E-03	9.456
2.2	9.58	2.6303E-11	4.2146E-03	5.4660E-03	9.467
2.4	9.51	3.0903E-10	4.5802E-03	5.0635E-03	9.466
2.6	9.44	3.6308E-10	4.9430E-03	4.6640E-03	9.465
2.8	9.40	3.9811E-10	5.3030E-03	4.2675E-03	9.494
3.0	9.31	4.8978E-10	5.6604E-03	3.8741E-03	9.475
3.2	9.25	5.6234E-10	6.0150E-03	3.4836E-03	9.487
3.4	9.17	6.7608E-10	6.3670E-03	3.0960E-03	9.483
3.6	9.09	8.1283E-10	6.7164E-03	2.7113E-03	9.484
3.8	9.00	1.0000E-09	7.0632E-03	2.3295E-03	9.482
4.0	8.90	1.2589E-09	7.4074E-03	1.9505E-03	9.480
4.2	8.76	1.7378E-09	7.7491E-03	1.5743E-03	9.452
4.4	8.59	2.5704E-09	8.0882E-03	1.2008E-03	9.418
4.6	8.34	4.5709E-09	8.4249E-03	8.3014E-04	9.346
4.8	7.83	1.4791E-08	8.7591E-03	4.6215E-04	9.108

Table 5.6A: Potentiometric titration of ephedrine (83.5 mg) with HCl (0.1 M) in 10% acetonitrile in water.
[End-point 4.90 ml, mean pK_a value= 9.396 ± 0.124].

[I]			[II]	
Enzymatic hydrolysis of pro-soft-drug (107) [mobile phase is 30% MeCN in water]			Generation of <i>In Situ</i> soft-drug (74, R=Et) by the enzymatic hydrolysis of pro-softdrug (107) [mobile phase is 4% MeCN in water]	
Time (h)	Conc. (μM)	In conc.	Time (h)	Conc. (μM)
0.01667	-		0.15833	9.969
0.20833	40.670	3.705	0.33333	27.444
0.39167	16.421	2.799	0.48333	40.389
0.55833	7.163	1.969	0.88333	60.710
			1.17500	69.327
			1.50000	71.933
			2.33333	63.596
			5.03333	56.301
			6.1500	50.289
			7.83333	42.273
			9.53333	33.456
			21.3333	12.614

Table 5.7A: Enzymatic hydrolysis of ethyl *N*-[2'-(3",4"-dipivaloyloxyphenyl)-2'-hydroxyethyl]-3-aminopropionate HCl (107) with 6.29 U of PLCE at pH 7.4. Hydrolysis was monitored by HPLC using 30% acetonitrile in water as mobile phase [I]. The same experiment was repeated and monitored in 4% acetonitrile in water [II].

Time (h)	Conc. (μM)	In conc.
0.000	63.596	4.153
2.700	56.301	4.031
3.817	50.289	3.918
5.500	42.273	3.744
7.200	33.456	3.510
19.00	12.614	2.535

Table 5.8A: Enzymatic hydrolysis of *in situ* generated soft-drug (74, R=Et) by the enzymatic hydrolysis of pro-soft-drug (107) [mobile phase is 4% MeCN in water].

[I]			[II]	
Enzymatic hydrolysis of pro-soft-drug (107) [mobile phase is 30% MeCN in water]			Generation of <i>in situ</i> soft-drug (74, R=Et) by the enzymatic hydrolysis of pro-softdrug (107) [mobile phase is 4% MeCN in water]	
Time (h)	Conc. (μM)	In conc.	Time (h)	Conc. (μM)
0.01667	48.486	3.881	0.200	13.015
0.18333	18.826	2.935	0.358	26.241
0.36667	7.8440	2.060	0.525	39.668
0.53333	3.7960	1.334	0.708	48.285
			0.867	51.933
			1.100	57.103
			1.333	59.949
			1.550	60.710
			1.900	61.512
			2.417	60.550
			2.983	57.464
			4.150	51.652
			17.55	15.019

Table 5.9A: Enzymatic hydrolysis of ethyl *N*-[2'-(3",4"-dipivaloyloxyphenyl)-2'-hydroxyethyl]-3-aminopropionate HCl (107) with 6.29 U of PLCE at pH 7.4. Hydrolysis was monitored by HPLC using 30% acetonitrile in water as mobile phase [I]. The same experiment was repeated and monitored in 4% acetonitrile in water [II].

Time (h)	Conc. (μM)	In conc.
0.0000	61.512	4.119
0.5167	60.550	4.103
1.0833	57.464	4.051
2.2500	51.652	3.945
15.650	15.019	2.709

Table 5.10A: Enzymatic hydrolysis of *in situ* generated soft-drug (74, R=Et) by the enzymatic hydrolysis of pro-soft-drug (107) [mobile phase is 4% MeCN in water].

APPENDIX FOR CHAPTER SIX:

1	2	3	4	5	6	7	8
Time (h)	COOCH ₂ (107)* at δ 4.05 (q)	O-CH ₂ (EtOH)* at δ 3.54 (q)	Pivalic ester in (107)* at δ 1.25 (s)	Potassium Pivaloate* at δ 1.0068 (s)	CH ₃ CN* at δ 1.95 (quintet)	-COOCH ₂ of (107)= $\frac{2}{6}$	-OCH ₂ of (EtOH)= $\frac{3}{6}$
0	0.832	0.000	8.625	0.072	-	-	-
0.10	1.787	0.000	15.643	0.144	2.308	0.774	0.000
0.85	0.886	0.048	7.833	0.060	1.148	0.772	0.042
1.85	1.77	0.115	15.629	0.190	2.266	0.781	0.051
3.85	0.84	0.068	7.779	0.116	1.097	0.766	0.062
5.85	1.677	0.164	15.638	0.222	2.143	0.783	0.077
8.60	3.237	0.392	31.266	0.552	3.379	0.958	0.116
22.98	3.014	0.681	38.185	1.948	3.858	0.781	0.177
23.98	3.06	0.729	38.601	1.975	4.044	0.757	0.180
25.98	3.98	1.224	38.842	2.299	4.412	0.902	0.277
27.98	3.237	0.849	37.806	2.471	4.05	0.799	0.210
29.98	3.473	1.346	38.37	2.598	4.455	0.780	0.302
31.98	3.54	1.334	38.589	2.683	4.511	0.785	0.296
33.98	3.29	1.021	37.701	2.723	4.026	0.817	0.254
35.98	3.33	1.428	38.127	3.158	4.424	0.753	0.323
37.98	3.344	1.343	37.694	3.341	4.463	0.749	0.301
39.98	1.651	0.745	18.897	1.747	2.217	0.745	0.336
41.98	1.669	0.753	19.216	1.755	2.218	0.752	0.339
43.98	1.437	0.773	19.504	1.752	2.256	0.637	0.343
48.15	1.111	0.537	14.781	1.493	1.642	0.677	0.327
49.65	2.253	1.187	29.189	3.048	3.404	0.662	0.349
70.15	1.904	1.365	28.016	4.125	3.396	0.561	0.402
300.0	0.080	0.815	3.504	7.408	1.110	0.0724	0.734

* Integration value in ¹H-NMR spectrum

Table 6.1A: Calculation of % of ethyl *N*-[2'-(3",4"-dipivaloyloxyphenyl)-2'-hydroxyethyl]-3-aminopropionate (107) and hydrolysis products *N*-[2'-(3",4"-dipivaloyloxyphenyl)-2'-hydroxyethyl]-3-aminopropionic acid (120) and *N*-[2'-(3",4"-dihydroxyphenyl)-2'-hydroxyethyl]-3-aminopropionic acid (74, R=H) by integration in ¹H-NMR.

9	10	11	12	13	14	15	16
pivaloyl ester (107+120) $= \frac{4}{6}$	pivalic acid \propto (74, R=H) $= \frac{5}{6}$	Total OCH ₂ $= 7 + 8$	(107) $= \frac{7}{11}$	% (107)= 12×100	ln (107)	total pivaloyl ester= 9 + 10	(107+120) $= \frac{9}{15}$
-	-	-	-	-	-	-	-
6.778	0.062	0.774	1.000	100.000	4.605	6.840	0.991
6.823	0.052	0.814	0.948	94.840	4.552	6.875	0.992
6.897	0.084	0.832	0.939	93.870	4.542	6.981	0.988
7.091	0.106	0.828	0.925	92.512	4.527	7.197	0.985
7.297	0.104	0.860	0.910	91.047	4.511	7.401	0.986
9.253	0.163	1.074	0.892	89.199	4.491	9.416	0.983
9.898	0.505	0.958	0.815	81.524	4.401	10.403	0.951
9.545	0.488	0.937	0.808	80.790	4.392	10.033	0.951
8.804	0.521	1.179	0.765	76.506	4.337	9.325	0.944
9.335	0.610	1.009	0.792	79.187	4.372	9.945	0.939
8.613	0.583	1.082	0.721	72.089	4.278	9.196	0.937
8.554	0.595	1.081	0.726	72.618	4.285	9.149	0.935
9.364	0.676	1.071	0.763	76.284	4.334	10.040	0.933
8.618	0.714	1.076	0.700	69.981	4.248	9.332	0.923
8.446	0.749	1.050	0.713	71.333	4.267	9.195	0.919
8.524	0.788	1.081	0.689	68.918	4.233	9.312	0.915
8.664	0.791	1.091	0.689	68.928	4.233	9.455	0.916
8.645	0.777	0.980	0.650	65.000	4.174	9.422	0.918
9.002	0.909	1.004	0.674	67.430	4.211	9.911	0.908
8.575	0.895	1.011	0.655	65.480	4.182	9.470	0.905
8.250	1.215	0.963	0.583	58.255	4.065	9.465	0.872
3.155	6.671	0.807	0.090	8.975	2.194	9.826	0.321

Table 6.1B: Calculation of % of (107) and hydrolysis products (120) and (74, R=H) by integration in ¹H-NMR.

17	18	19	20	21	22
$\% (107+120)$ $= 16 \times 100$	$(74, R=H)$ $\infty = \frac{10}{15}$	$\% (74, R=H) =$ 18×100	$(120 +$ $74, R=H) = \frac{8}{11}$	$\% (120 +$ $74, R=H)$ $= 20 \times 100$	$\% (120)$ $= 21 - 19$
	-	-	-	-	-
99.094	0.009	0.906	0.000	0.000	-0.906
99.244	0.008	0.756	0.052	5.160	4.403
98.797	0.012	1.203	0.061	6.130	4.927
98.527	0.015	1.473	0.075	7.488	6.015
98.595	0.014	1.405	0.090	8.953	7.548
98.269	0.017	1.731	0.108	10.801	9.070
95.146	0.049	4.854	0.185	18.476	13.622
95.136	0.049	4.864	0.192	19.210	14.346
94.413	0.056	5.587	0.235	23.494	17.907
93.866	0.061	6.134	0.208	20.813	14.679
93.660	0.063	6.340	0.279	27.911	21.572
93.497	0.065	6.503	0.274	27.382	20.879
93.267	0.067	6.733	0.237	23.716	16.983
92.349	0.077	7.651	0.300	30.019	22.367
91.854	0.081	8.146	0.287	28.667	20.521
91.538	0.085	8.462	0.311	31.082	22.620
91.634	0.084	8.366	0.311	31.072	22.706
91.753	0.082	8.247	0.350	35.000	26.753
90.828	0.092	9.172	0.326	32.570	23.398
90.549	0.095	9.451	0.345	34.520	25.069
87.163	0.128	12.837	0.417	41.745	28.908
32.109	0.679	67.891	0.910	91.025	23.133

Table 6.1C: Calculation of % of (107) and hydrolysis products (120) and (74, R=H) by integration in $^1\text{H-NMR}$.

1	2	3	4	5	6	7	8	9
Time (min)	-CH ₂ -COO (74, R=Et)*	-CH ₂ -COO (74, R=H)*	CH ₃ CN*	$\frac{2}{4} \times 100$	$\frac{3}{4} \times 100$	% of (74, R=Et) = $\frac{5}{5+6} \times 100$	% of (74, R=H)	ln % of (74, R=Et)
0	0.8126	0.0576	0.3917	207.455	14.705	93.381	6.619	4.537
66	0.7621	0.1248	0.4175	182.539	29.892	85.929	14.071	4.454
141	0.7645	0.1664	0.4250	179.882	39.153	82.125	17.875	4.408
216	0.6820	0.2027	0.4142	164.655	48.938	77.088	22.912	4.345
291	0.6604	0.2347	0.4205	157.051	55.815	73.779	26.221	4.301
366	0.5956	0.2957	0.4144	143.726	71.356	66.824	33.176	4.202
441	0.5811	0.3267	0.4264	136.280	76.618	64.012	35.988	4.159
516	0.2798	0.1848	0.2161	129.477	85.516	60.224	39.776	4.098
591	0.4688	0.3718	0.3999	117.229	92.973	55.770	44.230	4.021
1800	0.0000	5.7210	3.6670	-	156.013	0.000	100.00	-

* Integration in ¹H-NMR spectrum

Table 6.2A: Calculation of % of ethyl *N*-[2'-(3",4"-dihydroxyphenyl)-2'-hydroxyethyl]-3-aminopropionate (74, R=Et) and hydrolysis product *N*-[2'-(3",4"-dihydroxyphenyl)-2'-hydroxyethyl]-3-aminopropionic acid (74, R=H) by integration in ¹H-NMR.

APPENDIX FOR CHAPTER SEVEN:

Time (h)	Mt (μmol/cm ²)		
	cell-1	cell-2	cell-3
1	0.0420	0.0287	0.0161
2	0.0743	0.0783	0.0675
3	0.1410	0.1512	0.1249
4	0.2031	0.2308	0.1922
5	0.2790	0.2738	0.2413
6	0.3095	0.3421	0.3271
7	0.3566	0.3817	0.3445

Table 7.1A: Transport of ethyl *N*-[2'-(3",4"-dipivaloyloxyphenyl)-2'-hydroxyethyl]-3-aminopropionate (107) through the silicone membrane in 10% propylene glycol in water at pH 6.5 in receiving compartment.

Time (h)	Mt ($\mu\text{mol}/\text{cm}^2$)		
	cell-1	cell-2	cell-3
1	0.0377	0.0442	0.0291
2	0.1091	0.1222	0.1084
3	0.1877	0.2121	0.2038
4	0.2694	0.2952	0.3081
5	0.3528	0.3814	0.3968
6	0.4372	0.4686	0.4845
7	0.5304	0.5478	0.5824
8	0.6172	0.6308	0.6678
Flux	0.083273	0.084404	0.092520

Table 7.2A: Transport of ethyl *N*-[2'-(3",4"-dipivaloyloxyphenyl)-2'-hydroxyethyl]-3-aminopropionate (**107**) through the silicone membrane in 10% propylene glycol in water at pH 3.0 in receiving compartment [mean flux is $0.086732 \pm 0.005 \mu\text{mol}/\text{cm}^2/\text{h}$].

Time (h)	Mt ($\mu\text{mol}/\text{cm}^2$)		
	pH 3.0	pH 5.0	pH 7.0
1	0.0000	0.0000	0.0000
2	0.0361	0.0411	0.0491
3	0.0980	0.1111	0.1327
4	0.1646	0.1829	0.2196
5	0.2470	0.2751	0.3272
6	0.3108	0.3449	0.4067
7	0.3845	0.4338	0.5122
8	0.4351	0.5147	0.6009
Flux	0.068436	0.079579	0.092911

Table 7.3A: Cumulative transport data for ethyl *N*-[2'-(3",4"-dipivaloyloxyphenyl)-2'-hydroxyethyl]-3-aminopropionate (**107**) across the silicone membrane at different pH in the donor compartment [flux in ($\mu\text{mol}/\text{cm}^2/\text{h}$)].

Time (h)	Mt ($\mu\text{mol}/\text{cm}^2$)		
	cell-1	cell-2	cell-3
3	0.0003	0.0005	0.0005
4	0.0013	0.0017	0.0015
5	0.0018	0.0032	0.0020
6	0.0027	0.0048	0.0033
7	0.0028	0.0059	0.0036
8	0.0041	0.0077	0.0052
Flux ($\mu\text{mol}/\text{cm}^2/\text{h}$)	8.886×10^{-4}	1.4343×10^{-3}	6.971×10^{-4}
K_p (cm^2/h)	8.4227×10^{-5}	1.3595×10^{-4}	6.6076×10^{-5}
lag time (h)	2.50	2.80	2.40

Table 7.4A: Silicone membrane transport data of ethyl *N*-[2'-(3",4"-dipivaloyloxyphenyl)-2'-hydroxyethyl]-3-aminopropionate (**107**) at buffered pH 3.0 in 10% propylene glycol in water in the donor compartment.

Time (h)	Mt ($\mu\text{mol}/\text{cm}^2$)		
	cell-1	cell-2	cell-3
3	0.0010	0.0014	0.0013
4	0.0025	0.0030	0.0027
5	0.0054	0.0064	0.0061
6	0.0100	0.0119	0.0109
7	0.0146	0.0180	0.0168
8	0.0177	0.0210	0.0185
Flux ($\mu\text{mol}/\text{cm}^2/\text{h}$)	4.230×10^{-3}	3.9600×10^{-3}	4.7600×10^{-3}
K_p (cm^2/h)	4.0095×10^{-4}	3.7536×10^{-4}	4.5118×10^{-4}
lag time (h)	3.20	3.15	3.10

Table 7.5A: Silicone membrane transport data of ethyl *N*-[2'-(3",4"-dipivaloyloxyphenyl)-2'-hydroxyethyl]-3-aminopropionate (**107**) at buffered pH 4.0 in 10% propylene glycol in water in the donor compartment.

Time (h)	Mt ($\mu\text{mol}/\text{cm}^2$)		
	cell-1	cell-2	cell-3
1	0.0117	-	-
2	0.0207	0.0227	0.0217
3	0.0246	0.0260	0.0287
4	0.0312	0.0311	0.0316
5	0.0364	0.0383	0.0402
6	0.0414	0.0433	0.0436
7	0.0473	0.0474	0.0501
8	0.0528	0.0556	0.0538
Flux ($\mu\text{mol}/\text{cm}^2/\text{h}$)	5.3964×10^{-3}	5.4893×10^{-3}	5.4250×10^{-3}
K_p (cm^2/h)	5.1151×10^{-4}	5.2030×10^{-4}	5.1420×10^{-4}
lag time (h)	1.60	1.80	2.0

Table 7.6A: Silicone membrane transport data of ethyl *N*-[2'-(3",4"-dipivaloyloxyphenyl)-2'-hydroxyethyl]-3-aminopropionate (**107**) at buffered pH 5.0 in 10% propylene glycol in water in the donor compartment.

Time (h)	Mt ($\mu\text{mol}/\text{cm}^2$)		
	cell-1	cell-2	cell-3
3	0.0015	0.0014	0.0015
4	0.0035	0.0036	0.0043
5	0.0085	0.0101	0.0096
6	0.0141	0.0178	0.0172
7	0.0211	0.0244	0.0263
8	0.0283	0.0317	0.0307
Flux ($\mu\text{mol}/\text{cm}^2/\text{h}$)	6.9500×10^{-3}	7.0500×10^{-3}	6.2200×10^{-3}
K_p (cm^2/h)	6.5877×10^{-4}	6.6825×10^{-4}	5.8957×10^{-4}
lag time (h)	3.15	3.20	3.20

Table 7.7A: Silicone membrane transport data of ethyl *N*-[2'-(3",4"-dipivaloyloxyphenyl)-2'-hydroxyethyl]-3-aminopropionate (**107**) at buffered pH 6.0 in 10% propylene glycol in water in the donor compartment.

Time (h)	Mt ($\mu\text{mol}/\text{cm}^2$)		
	cell-1	cell-2	cell-3
3	0.0033	0.0015	0.0017
4	0.0090	0.0062	0.0124
5	0.0175	0.0174	0.0206
6	0.0261	0.0282	0.0293
7	0.0329	0.0375	0.0416
8	0.0420	0.0488	0.0507
Flux ($\mu\text{mol}/\text{cm}^2/\text{h}$)	9.7514×10^{-3}	9.7486×10^{-3}	7.8229×10^{-3}
K_p (cm^2/h)	9.2430×10^{-4}	9.2404×10^{-4}	7.4151×10^{-4}
lag time (h)	2.90	3.10	2.75

Table 7.8A: Silicone membrane transport data of ethyl *N*-[2'-(3",4"-dipivaloyloxyphenyl)-2'-hydroxyethyl]-3-aminopropionate (**107**) at buffered pH 7.0 in 10% propylene glycol in water in the donor compartment.

Time (h)	Mt ($\mu\text{mol}/\text{cm}^2$)		
	cell-1	cell-2	cell-3
3	0.0015	0.0015	0.0013
4	0.0086	0.0072	0.0104
5	0.0205	0.0180	0.0223
6	0.0323	0.0274	0.0283
7	0.0439	0.0370	0.0423
8	0.0585	0.0487	0.0554
Flux ($\mu\text{mol}/\text{cm}^2/\text{h}$)	1.06340×10^{-2}	1.15060×10^{-2}	9.5657×10^{-3}
K_p (cm^2/h)	1.0080×10^{-3}	1.0906×10^{-3}	9.0670×10^{-4}
lag time (h)	3.00	3.15	3.10

Table 7.9A: Silicone membrane transport data of ethyl *N*-[2'-(3",4"-dipivaloyloxyphenyl)-2'-hydroxyethyl]-3-aminopropionate (**107**) at buffered pH 8.0 in 10% propylene glycol in water in the donor compartment.

POSTERS PRESENTED:

1. Poster and oral presentation at The UK Association of Pharmaceutical Scientists Conference in April, 1993 at Exeter University, Exeter, UK entitled
"SYNTHESIS AND PRELIMINARY STABILITY STUDIES OF SOFT-DRUGS AS β -ADRENOCEPTOR AGONISTS FOR THE TREATMENT OF PSORIASIS". Hardyal Singh Gill, Sally Freeman, William J. Irwin.
2. Poster presented at the 208th American Chemical Society National Meeting at Washington D.C., August 21-25, 1994 in the Medicinal Chemistry Division, entitled
"SYNTHESIS AND STABILITY STUDIES OF SOFT-DRUGS AS β -ADRENOCEPTOR AGONISTS FOR THE TREATMENT OF PSORIASIS". Hardyal Singh Gill, Sally Freeman, William J. Irwin.
3. Poster presented at the 131st British Pharmaceutical Conference at London, 16-19 September, 1994, entitled
" β -ADRENERGIC ACTIVITY OF SOFT DRUGS FOR THE TOPICAL TREATMENT OF PSORIASIS". Hardyal Singh Gill, Keith. A. Wilson, Sally Freeman, William J. Irwin.